



**HAL**  
open science

# Cationic amphipathic peptoid oligomers as antimicrobial peptide mimics

Radhe Shyam

► **To cite this version:**

Radhe Shyam. Cationic amphipathic peptoid oligomers as antimicrobial peptide mimics. Organic chemistry. Université Clermont Auvergne [2017-2020], 2018. English. NNT : 2018CLFAC048 . tel-02060354

**HAL Id: tel-02060354**

**<https://theses.hal.science/tel-02060354v1>**

Submitted on 7 Mar 2019

**HAL** is a multi-disciplinary open access archive for the deposit and dissemination of scientific research documents, whether they are published or not. The documents may come from teaching and research institutions in France or abroad, or from public or private research centers.

L'archive ouverte pluridisciplinaire **HAL**, est destinée au dépôt et à la diffusion de documents scientifiques de niveau recherche, publiés ou non, émanant des établissements d'enseignement et de recherche français ou étrangers, des laboratoires publics ou privés.



**UNIVERSITE CLERMONT AUVERGNE**

**ECOLE DOCTORALE DES SCIENCES FONDAMENTALES**

**THESE**

présentée pour obtenir le grade de

**DOCTEUR D'UNIVERSITE**

*Spécialité : Chimie organique, minérale et industrielle*

Par **SHYAM Radhe**

**CATIONIC AMPHIPATHIC PEPTOID OLIGOMERS  
AS ANTIMICROBIAL PEPTIDE MIMICS**

Date de soutenance le 18 Mai 2018 devant la Commission d'Examen :

**Rapporteurs :**

Mme Céline DOUAT, Chargé de Recherche CNRS, CBMN, Université de Bordeaux

M. Philippe KAROYAN, Professeur, LBM, Université Pierre et Marie Curie

**Examineurs :**

Mme Christiane FORESTIER, Professeur, LMGE, Université Clermont Auvergne

M. Francesco De RICCARDIS, Professeur, Université de Salerne

Mme. Sophie FAURE, Chargé de Recherche CNRS, ICCF, Université Clermont Auvergne (directeur de thèse)

M. Claude TAILLEFUMIER, Professeur, ICCF, Université Clermont Auvergne (co-directeur de thèse)



**To my life teacher, my late dad Vedpal Kashwan: as I owe it all to you.**

*Many thanks!*

## Acknowledgments

A very special gratitude goes out to the French Ministry of Higher Education and Research, and ANR ARCHIPEP project grant ANR Blanc - SIMI 7 2013 of the French Agence Nationale de la Recherche for helping and providing the funding for this work.

I would like to thank the former director of ICCF Dr. A. M. Delort and the current director Dr. Fabrice Leroux and assistant director L. Hecquet of ICCF for giving me this opportunity to conduct my thesis at ICCF.

I am indebted to my supervisor Dr. Sophie Faure for her constant support and appraisal. This work would not have been possible without the guidance of Dr. Sophie, with whom I have developed a special relationship during the period of this thesis. She has shown me, by her example, what a good scientist (and person) should be. I remember during the initial months of the thesis, she went to great lengths to make the things easier for me. I would like to thank my co-supervisor Dr. Claude Taillefumier for the leadership and help during the thesis.

Special thanks go towards the members of CBRV. I would like thank Dr C. Forestier, and N. Charbonnel for the guidance in antimicrobial studies, Dr D. Balestrino and L. Nakusi-Ollivier for the assistance in cell selectivity assays.

I am also grateful to the following people: With a special mention to M. Lereboure for mass spectrometry analysis (UCA START), A. Kriznik for circular dichroism experiments (SCBIM, FR 3209 BMCT of Université de Lorraine), Aurilie Job for the aid in HPLC and specially Cassandra Perez for her contribution in synthesis. Christelle Blavignac- Centre Imagerie Cellulaire Santé (CICS UCA) for SEM and Anne-Marie Gélinaud- 2Matech for FEGSEM studies.

I am very happy to thank Dr. Céline Douat and Pr. Philippe Karoyan for accepting to evaluate my thesis manuscript. Also, I would like to thank Pr. Francesco De Riccardis and Pr. Christiane Forestier for being a part of the Jury to examine my thesis.

The peptoid group was a great opportunity for me to learn and evolve my personal growth. It was pleasuring to spend my time working and chatting with the group members: Dr Oliver Roy, Dr Geoffrey Dumonteil, Maha Rzeigui and specially Dr Gaetano Angilici. Overall, the bigger team formerly SEESIB and now COM has played a significant part in my growth and development.



Various lunches and tea/coffee time were celebrated in their company. Dr Arnaud Gautier, Dr Federico Cisnetti and Dr Kevin Fauche were very accommodating. The good times spent at Nota bene in the company of these and others were fun. I still remember the days when I was exceptionally terrible at understanding French (I still am :p) but the members of the team made it an enjoyable journey.

There are few people outside the group who were part of my journey and I made good friends with them for life. You guys are the best investment outside the thesis time. Many thanks to the fellow members of lunch group; Dr Alexander Lowe, Laura Sivet, Dr. Joana Szala-Bilnik, Dr Barbara Liborio, Dr Sven Plappert, Dr Fernando Lepre, Fernando Hevia, Tarek Moufawad, (soon to be Dr) Darius Yeadon and specially Dr Emilie Bordes (stay awesome).

To my flatmates; Antoine Tavin and Luca Terray, I have a special place for you in my heart forever. It was remarkable that we guys met and developed an amicable relationship during these years. I would also like to thank the people outside ICCF who made this voyage worthwhile; Dr Gunjita Singh, Dr Nolwenn Wirgot and Dr Juliette Maurice. This would not have been possible if you guys would not have helped me at various stages emotionally. Thank you for energising my dreams. Moreover, the friends I made at Clermont Ferrand are going to stay forever. Thank you to Meghana Upadhyaya, Indira Tegri, Anas Ait Hamou, Tasnuva Chowdhury and Sinja Klenk

In the end, I am grateful to my sister and mummy; Savita and Santosh, who have provided me through moral and emotional support in my life. I am also grateful to other family members and friends who have supported me along the way.

I am sorry to have forgotten few names, but you know that I am grateful to all those with whom I have had the pleasure to work and enjoy during this thesis.

## List of Abbreviations

EARS-Net	European Antimicrobial Resistance Surveillance Network
ACD	Acid Citrate Dextrose
ACPC	( <i>R,R</i> )- <i>Trans</i> -2-aminocyclopentane Carboxylic Acid
aetm	1-aminoethyl- 1,2,3-triazolylmethyl
aetm+	1-aminoethyl-3-methyl-1,2,3-triazolium methyl
AMPs	Antimicrobial Peptides
AP	( <i>R</i> )- $\beta$ -amino D-Proline
APC	( <i>3R,4S</i> )- <i>Trans</i> -4-aminopyrrolidine-3-Carboxylic Acid
ATCC	American Type Cell Culture
ATP	Adenosine Triphosphate
Boc	Tert-butyloxycarbonyl
BSA	Bovine Serum Albumin
btm	1-Benzyl-1,2,3-triazolylmethyl
btm+	(Benzyltriazolium)methyl
Cbz	Carboxybenzyl
CD	Circular Dichroism
CFU	Colony Forming Units
chtm	1-Cyclohexylmethyl-1,2,3-triazolylmethyl
chtm+	1-Cyclohexylmethyl-3-methyl-1,2,3-triazolium methyl
CICS	Centre Imagerie Cellulaire Santé
CLSI	Clinical and Laboratory Standard Institute
CuAAC	Copper-Catalysed Alkyne-Azide Cycloaddition
CV	Crystal Violet
CY	Cytotoxicity
DBU	1,8-diazobicyclo[5.4.0]undec-7-ene
DCC	Dicyclohexylcarbodiimide
DIC	<i>N,N'</i> -diisopropylcarbodiimide
DMSO	Dimethyl Sulfoxide
DSC	Differential Scanning Calorimetry
EPS	Extracellular Polymeric Substances
FBS	Foetal Bovine Serum
FC	Flash Chromatography
FEGSEM	Field Emission Gun Scanning Electron Microscopy
G	Guanidinium
gLys	1,1-dimethyl- 4-aminobutyl
HC	Haemolytic Activity
HDMS	Hexamethyldisilazane
HeLA	Henrietta Lacks
HLeu	Homoleucine
HLys	Homolysine
HPLC	High-Pressure Liquid Chromatography
hRBC	Human Red Blood Cells
HRMS	High-Resolution Mass Spectra
HVal	Homovaline
ID	Inhibitory Dose
IR	Infrared Spectra
LCMS	Liquid Chromatography Mass Spectroscopy
MBC	Minimum Bactericidal Concentration
MBHA	Methylbenzhydrylamine

MFC	Minimal Fungicidal Concentrations
MHB	Muller Hinton Broth
MIC	Minimum Inhibitory Concentration
MRSA	Methicillin-Resistant <i>Staphylococcus Aureus</i>
MTT	3-[4,5-Dimethylthiazol-2-yl]-2,5- diphenyltetrazolium bromide
NADH	Nicotinamide Adenine Dinucleotide
NLys	<i>N</i> -(4-aminobutyl)glycine
NMR	Nuclear Magnetic Resonance
Nrch	( <i>R</i> )- <i>N</i> -(1-cyclohexylethyl)glycine
Nrpe	( <i>R</i> )- <i>N</i> -(1-phenylethyl)glycine
Ns1npe	( <i>S</i> )- <i>N</i> -(1-naphthylethyl)glycine
Ntbu	<i>N</i> tertbutyl
OD	Optical Density
PBS	Phosphate Buffered Saline
Pg	Protecting Groups
PPI	Polyproline Type I
QSAR	Quantitative Structure–Activity Relationship
RAISIN	Réseau d'Alerte, d'Investigation et de Surveillance des Infections Nosocomiales
s1tbe	( <i>S</i> )-(1-tert-butylethyl)
SAR	Structure and Activity Relationship
SEM	Scanning Electron Microscopy
SMH	Shai-Matsuzaki-Huang Model
spe	( <i>S</i> )-phenylethyl
SPOT	Synthetic Peptide Arrays on Membrane Supports
SPPS	Solid-Phase Peptide Synthesis
SPSS	Solid Phase Submonomer Synthesis
ssb	( <i>S</i> )- <i>N</i> -(sec-butyl)glycine
T	Thiourea
TEM	Transmission Electron Microscopy
TLC	Thin Layer Chromatography
<i>trans</i> -ACHC	<i>Trans</i> -2-aminocyclohexane Carboxylic Acid
U	Urea
XRD	X-Ray Diffraction

## TABLE OF CONTENTS

General Introduction .....	6
Chapter I <b>Literature Review and Objectives</b> .....	7
1    Natural Antimicrobial peptides .....	8
1.1    Introduction .....	8
1.2    Classification .....	8
1.3    Cell selectivity .....	9
1.4    Mode of action .....	10
1.5    Therapeutic potential of AMPs.....	13
2    Cationic amphipathic antimicrobial mimetics.....	15
3.1 $\beta$ -Peptides .....	16
3.2    Oligourea, $\gamma^4$ -peptides.....	20
3.3    Arylamides and Arylureas .....	22
3    Cationic amphipathic peptoids with antimicrobial activities .....	23
3.1    Peptoid-type family .....	24
3.2    Brief history of the development of synthetic methodology for peptoids .....	25
3.3    Examples of peptoids in development for pharmacological applications .....	27
3.4    PPI-type helical structure of peptoids.....	29
3.5    Correlation between linear peptoid structure and antimicrobial activity .....	32
3.6    Cyclic peptoids .....	41
3.7    Peptide-peptoid hybrids .....	46
3.8    Short Peptoids with antimicrobial activities .....	50
4    Objectives of this work .....	50
4.1    Family I: Replacement of <i>Nspe</i> by <i>Ntbu</i> residues .....	55
4.2    Family II: Replacement of <i>Nspe</i> by <i>Ntbu</i> and <i>NLys</i> by a triazolium-type side chain. ....	55
4.3    Family III: Replacement of <i>NLys</i> by a triazolium-type side chains.....	56
Chapter II <b>Solution-phase synthesis of cationic amphiphilic peptoid oligomers</b> .....	60
Introduction: The concept of Synthesis.....	59
1    General overview of the solution-phase synthesis .....	60
2    Synthesis of the ( <i>NLys-Ntbu-Ntbu</i> ) <sub>n</sub> peptoid family IA .....	63

2.1	Submonomer synthesis of key trimer building-block.....	63
2.2	Block coupling study using H-(NLys(Boc)-Ntbu-Ntbu)-OBn trimer.....	69
2.3	Block coupling study using H-(NLys(Cbz)-Ntbu-Ntbu)-OEt trimer.....	71
2.4	Access to cationic amphiphilic peptoids.....	73
3	Synthesis of (NgLys-Ntbu-Ntbu) <sub>n</sub> peptoid family 1B.....	76
3.1	Synthesis of $\alpha$ -gem-dimethylated primary amine.....	76
3.2	Synthesis of the trimer H-(NgLys(Pg)-Ntbu-Ntbu)-OR derivatives.....	78
3.3	Conclusion.....	79
4	Synthesis of (Nxtm <sup>+</sup> -Ntbu-Ntbu) <sub>n</sub> peptoid family II.....	79
4.1	Synthesis of hexamer Ac-(Nem-Ntbu-Ntbu) <sub>2</sub> -OEt.....	80
4.2	Post-functionalization of the hexamer Ac-(Nem-Ntbu-Ntbu) <sub>2</sub> -OEt.....	81
5	Structural and conformational insights.....	85
5.1	Conformational study of family I oligomers.....	85
5.2	Conformational study of family II oligomers.....	87
6	Conclusion.....	88
6.1	Family I.....	88
6.2	Family II.....	88
	<b>Chapter III Solid-phase synthesis of cationic amphiphilic peptoid oligomers.....</b>	<b>91</b>
1	General overview of the solid-phase synthesis.....	90
2	Synthetic strategy.....	92
3	Conventional and microwave-assisted solid-phase submonomer synthesis (SPSS).....	94
3.1	Resin selection and synthesis of reference peptoids.....	94
3.2	Synthesis of model hexamer H-(Nem-Nspe-Nspe) <sub>2</sub> -NH <sub>2</sub> .....	96
4	Triazolium formation model study.....	99
4.1	Solution phase strategy.....	99
4.2	Solid phase strategy.....	100
5	Synthesis of 1,2,3-triazolium-based oligomers.....	104
5.1	Series A.....	104
5.2	Series B.....	106
5.3	Series C.....	107

6	Structural and conformational insights Family III .....	109
6.1	NMR study .....	109
6.2	Circular dichroism study .....	111
7	Conclusion:.....	113
	 <b>Chapter IV Biological evaluation of cationic amphipathic peptoids.....</b>	<b>116</b>
	Introduction .....	115
1	Selection and design of oligomers: .....	115
1.1	Solubility of peptoid oligomers .....	116
1.2	Peptide control .....	117
2	Selection of bacteria .....	117
2.1	Gram-negative bacteria <i>Escherichia coli</i> .....	117
2.2	Gram-negative bacteria <i>Pseudomonas aeruginosa</i> .....	117
2.3	Gram-positive bacteria <i>Staphylococcus aureus</i> .....	118
2.4	Gram-positive bacteria <i>Enterococcus faecalis</i> .....	118
2.5	Gram Staining.....	118
3	Determination of antimicrobial activity .....	119
3.1	Minimal Inhibitory Concentration.....	119
3.2	Minimal Bactericidal Concentration .....	121
3.3	Antibacterial activities of the selected peptoids .....	121
3.4	Broad spectrum activity assessment.....	124
3.5	Conclusion .....	125
4	Anti-biofilm studies.....	126
4.1	Selection of bacteria .....	127
4.2	Crystal Violet staining technique .....	127
4.3	Colony forming unit plate counting method.....	129
5	Cell selectivity assays.....	130
5.1	Haemolytic activity: .....	130
5.2	Cell Viability: .....	131
5.3	Results of cell selectivity assays.....	131
6	Microscopy.....	134
6.1	Mode of action hypothesis.....	137

Conclusion and perspectives .....	140
<b>Chapter V Experimental Section</b> .....	148
1 General Information .....	146
2 Solution Phase General procedures .....	147
3 Solid Phase General Procedures .....	149
4 Experimental procedures and compounds characterisations chapter II .....	151
5 Experimental procedures and compounds characterisations Chapter III .....	175
6 General information Biological assays .....	217
7 Antimicrobial activity .....	217
7.1 Bacterial cell culture: .....	217
7.2 Minimum inhibitory concentration (MIC) measurement: .....	218
7.3 Minimal Bactericidal Concentration (MBC) measurement: .....	219
8 Preventive Anti-Biofilm activity .....	221
8.1 Growing the biofilm: .....	221
8.2 Crystal-violet staining .....	221
8.3 Colony forming units (CFU) enumeration: .....	222
9 Cell selectivity tests .....	222
9.1 Haemolytic assays .....	222
9.2 Cytotoxic assays: .....	224
10 Scanning Electron Microscopy (SEM) Imaging .....	227
10.1 Supplementary images from Microscopy .....	228
Bibliography .....	232
Summary in French .....	244

# **General Introduction**



## General Introduction

The occurrence of antimicrobial resistance in Europe varies depending on the microorganism, the antimicrobial agent, and the geographical region. The high levels and increasing trends of antimicrobial resistance in Gram-negative bacteria in Europe highlighted by European Antimicrobial Resistance Surveillance Network (EARS-Net) surveillance results illustrate the continuous loss of effective antimicrobial therapy and emphasise the need for comprehensive response strategies targeting all health sectors.<sup>1</sup> The new drug discovery and development rates are slowing in the field of antibiotics. Therefore, the problem of antimicrobial resistance calls for new therapeutic strategies. The traditional antibiotic drug discovery process and development have reached their limits thus there is a real necessity for new types of antimicrobials. Since pharmaceutical companies have left the field, academic researchers and biotech companies are exploring new strategies such as therapeutic antibodies, immune modulators, probiotics, bacteriophage-based therapies, and antimicrobial peptides. The natural antimicrobial peptides (AMPs) have shown ground breaking potential for using them as antimicrobial agents. They show broad spectrum antimicrobial activity which makes them potent candidates for replacing conventional antibiotics. However, their high manufacturing cost and their low stability hamper their therapeutic use. Naturally occurring AMPs need then to be optimized or modified to exhibit potent antimicrobial activity together with a good therapeutic profile. A possible solution is the development of peptidomimetic systems exhibiting antimicrobial mechanism of parent AMPs with enhanced proteolytic stability and bioavailability. Peptoids i.e. *N*-substituted glycine oligomers are particularly promising peptidomimetics to reach this purpose.

---

<sup>1</sup> European Centre for Disease Prevention and Control, 'Antimicrobial Resistance Surveillance in Europe 2016. Annual Report of the European Antimicrobial Resistance Surveillance Network (EARS-Net)', *European Centre for Disease Prevention and Control* (2017), 1–88.

Chapter I  
**Literature Review and Objectives**

# 1 Natural Antimicrobial peptides

## 1.1 Introduction

Every day we are regularly invaded by a horde of diverse microorganisms. Nonetheless, during evolution, our bodies armed themselves with innate immune defence system which allows us to counter probable pathogens. The AMPs are part of the innate immunity of various organisms ranging from basic unicellular organisms to the highly sophisticated mammals. Usually, most of the organisms contain multiple AMPs from several classes in their host defence system. AMPs play an active role in defence of the organism. They exhibit a broad range of antimicrobial and immunological properties. They are potent towards a broad spectrum of pathogens, including Gram-negative and Gram-positive bacteria, fungi, protozoa, and viruses.<sup>2,3,4</sup>

## 1.2 Classification

More than 3000 natural AMPs peptides produced by living organisms have been identified.<sup>5,6</sup> They have a vast diversity of structures and activity profiles which makes them difficult to classify. Typically, AMPs have diverse structures: they are linear or cyclic, cationic, or anionic, often short (less than 50 residues), and structured in  $\alpha$ -helical,  $\beta$ -strand, loop, or extended.<sup>7</sup> Antimicrobial peptides can be divided into different classes based on their amino acid composition, their net charge, or their three-dimensional structure. The major type of AMPs processes in between 12 to 50 amino acids and is composed of hydrophobic residues in a proportion  $>50\%$  and two or more positively charged residues. The underlying structural principle common to these classes of AMPs is the capacity to adopt an amphipathic shape based on the spatial arrangement of hydrophobic and cationic amino acids side-chains in distinct areas of the molecule.<sup>8</sup>

---

<sup>2</sup>C. D. Fjell; J. A. Hiss; R. E. W. Hancock; and G. Schneider, 'Designing Antimicrobial Peptides: Form Follows Function', *Nature Reviews Drug Discovery*, Vol. 11 (Nature Publishing Group, **2012**), 37–51.

<sup>3</sup>R. E. W. Hancock and H. G. Sahl, 'Antimicrobial and Host-Defense Peptides as New Anti-Infective Therapeutic Strategies', *Nature Biotechnology*, Vol. 24 (Nature Publishing Group, **2006**), 1551–7.

<sup>4</sup>K. V. R. Reddy; R. D. Yedery; and C. Aranha, 'Antimicrobial Peptides: Premises and Promises', *International Journal of Antimicrobial Agents*, Vol. 24 (Elsevier, **2004**), 536–47.

<sup>5</sup>M. Brahmachary; S. P. T. Krishnan; J. L. Y. Koh; A. M. Khan; S. H. Seah; T. W. Tan; V. Brusica; and V. B. Bajic, 'ANTIMIC: A Database of Antimicrobial Sequences.', *Nucleic Acids Research*, 32 (**2004**), D586-9.

<sup>6</sup>Z. Wang and G. Wang, 'The Antimicrobial Peptide Database', *Nucleic Acids Research*, 32 (**2004**), D590–2.

<sup>7</sup>A. Tossi; L. Sandri; and A. Giangaspero, 'Amphipathic, Alpha-Helical Antimicrobial Peptides.', *Biopolymers*, 55 (**2000**), 4–30.

<sup>8</sup>M. Zasloff, 'Antimicrobial Peptides of Multicellular Organisms', *Nature*, Vol. 415 (**2002**), 389–95.

In our view, the quite convenient way to classify AMPs is based on their secondary structure (Figure 1).<sup>9,10</sup> Structurally they can be divided into four groups, *i.e.* (A)  $\alpha$ -helical (e.g., the mammals cathelicidins and frog magainins); (B)  $\beta$ -sheet (e.g., human  $\alpha$ - and,  $\beta$ -defensins); (C)  $\alpha\beta$  for peptides incorporating both  $\alpha$ -helix and  $\beta$ -strand secondary structures (e.g., insect heliomicin) and (D) non- $\alpha\beta$  or extended peptides that do not adopt  $\alpha$ -helix and/or  $\beta$ -sheet structures (e.g., bovine indolicidin).

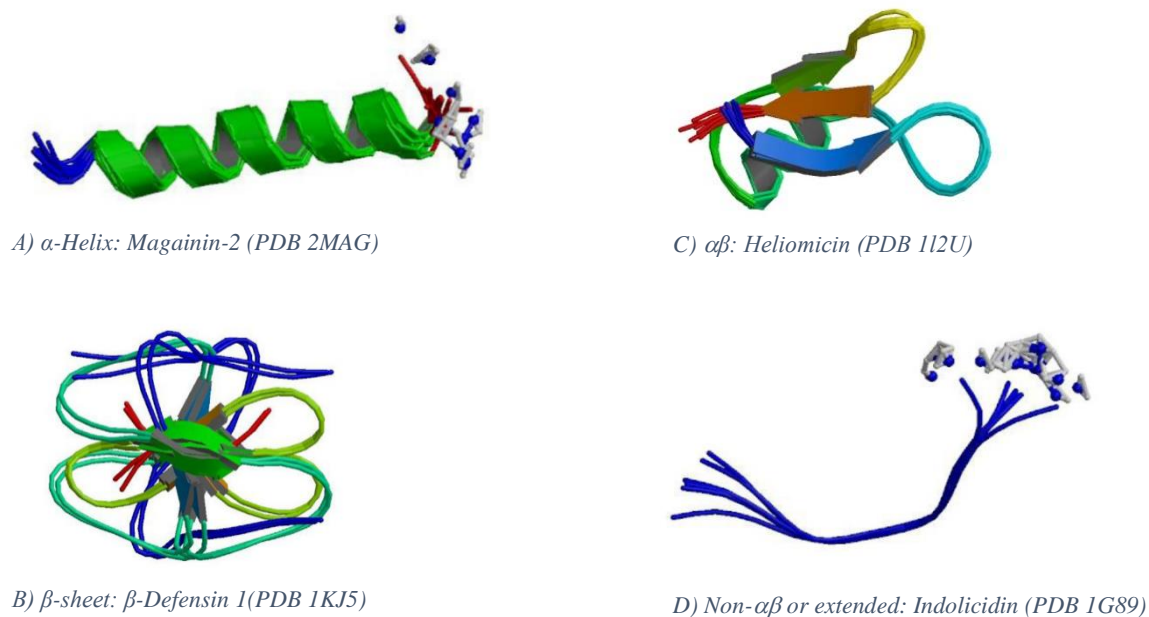


Figure 1 Different classes of AMPs based on their structure.

In this chapter, we will focus on  $\alpha$ -helical amphipathic peptides, the main classes of AMPs.

### 1.3 Cell selectivity

Essential differences occur between the composition of prokaryotic and eukaryotic cellular membrane. This composition feature serves as the “Achilles heel” of the microbial world that may signify targets for antimicrobial peptides.<sup>8</sup> AMPs target this inherent difference between the eukaryotic and the prokaryotic cell’s membrane. The surface of the bacterial cell membrane is organised in a way that the outermost exposed layer is densely populated with acidic phospholipids

<sup>9</sup>B. M. Peters; M. E. Shirtliff; and M. A. Jabra-Rizk, ‘Antimicrobial Peptides: Primeval Molecules or Future Drugs?’, Hiten D. Madhani (ed.), *PLoS Pathogens*, 6 (2010), e1001067.

<sup>10</sup> G. Wang; Xia Li; and Michael Zasloff, *Antimicrobial Peptides: Discovery, Design and Novel Therapeutic Strategies* (CABI, 2010).

such as phosphatidylglycerol and cardiolipin. It contrasts with eukaryotic cell membrane; composed of zwitterionic phospholipids (Figure 2).<sup>11,12</sup>

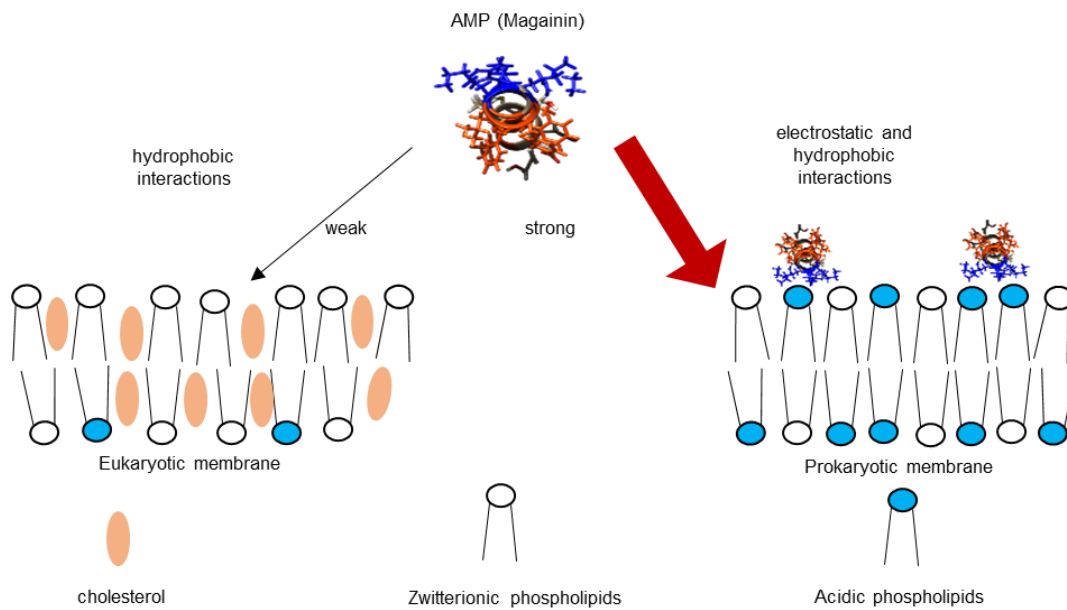


Figure 2 Basis of selectivity for the membrane targets of AMPs (Modified from Matsuzaki 1999)<sup>11</sup>

This marked difference contributes to the selectivity of AMPs that interact with the negatively charged phospholipids of the bacterial cell membrane leading to the penetration of the AMP that leads to the physical disruption of the membrane and/or the interaction of AMP with intracellular targets.

#### 1.4 Mode of action

Despite numerous studies and the constant development of new biophysical techniques, the understanding of the exact mechanism of action at the molecular level remains to be elucidated in detail. The widely accepted mode of action is described in this section. Most of the AMPs stay unstructured in the free solution, but fold into their final helical conformation upon interaction with the surface of the bacterial membrane. They contain both hydrophilic and hydrophobic amino acid residues, which are aligned along each side of the helix.<sup>13</sup> This amphipathic nature appears upon

<sup>11</sup>K. Matsuzaki, 'Control of Cell Selectivity of Antimicrobial Peptides', *Biochimica et Biophysica Acta - Biomembranes*, 1788 (2009), 1687–92.

<sup>12</sup>K. Matsuzaki, 'Why and How Are Peptide-Lipid Interactions Utilized for Self-Defense? Magainins and Tachyplesins as Archetypes', *Biochimica et Biophysica Acta - Biomembranes*, Vol. 1462 (Elsevier, 1999), 1–10.

<sup>13</sup>M. R. Yeaman and N. Y. Yount, 'Mechanisms of Antimicrobial Peptide Action and Resistance.', *Pharmacological Reviews*, 55 (2003), 27–55.

structuration and allows partition into the membrane lipid bilayer. This makes the ability to associate with membranes as a characteristic feature of AMPs.<sup>14</sup> The mechanisms of action of AMPs are represented in the Shai-Matsuzaki-Huang (SMH) model (Figure 3).<sup>15,16</sup> Once they have folded into their final secondary structure, AMPs can make their way inside the cell by permeabilization and perform a diverse set of antimicrobial actions by acting on cytoplasmic targets.

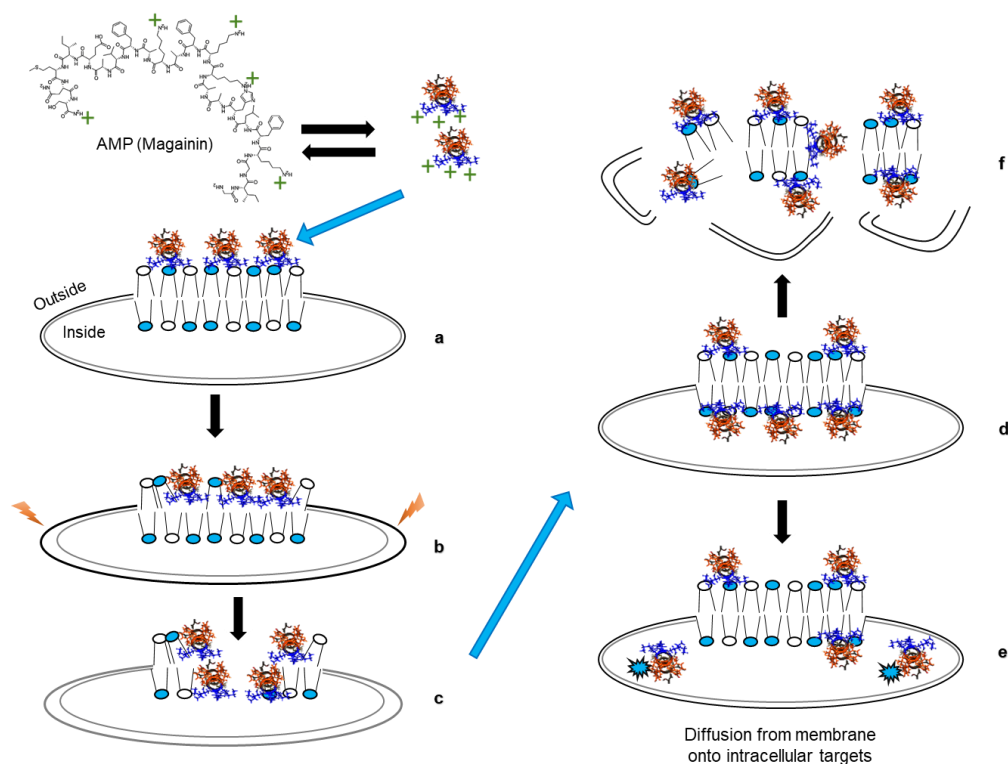


Figure 3 The Shai-Matsuzaki-Huang model of the mechanism of action of an antimicrobial peptide. An  $\alpha$ -helical peptide is depicted. **a**, Carpeting of the outer leaflet with peptides. **b**, Integration of the peptide into the membrane and thinning of the outer leaflet. The surface area of the outer leaflet expands relative to the inner leaflet, resulting in strain within the bilayer (jagged arrows). **c**, Phase transition and 'wormhole' formation. Transient pores form at this stage. **d**, Transport of lipids and peptides into the inner leaflet. **e**, Diffusion of peptides onto intracellular targets (in some cases). **f**, Collapse of the membrane into fragments and physical disruption of the target cell's membrane. Lipids with blue headgroups are acidic, or negatively charged. Lipids with white headgroups have no net charge (Modified from Zasloff 2002).<sup>8</sup>

<sup>14</sup>R. E. W. Hancock and A. Rozek, 'Role of Membranes in the Activities of Antimicrobial Cationic Peptides', *FEMS Microbiology Letters*, 206 (2002), 143–9.

<sup>15</sup>Y. Shai, 'Mechanism of the Binding, Insertion and Destabilization of Phospholipid Bilayer Membranes by  $\alpha$ -Helical Antimicrobial and Cell Non-Selective Membrane-Lytic Peptides', *Biochimica et Biophysica Acta - Biomembranes*, Vol. 1462 (1999), 55–70.

<sup>16</sup>L. Yang; T. M. Weiss; R. I. Lehrer; and H. W. Huang, 'Crystallization of Antimicrobial Pores in Membranes: Magainin and Protegrin', *Biophysical Journal*, 79 (2000), 2002–9.

After the first interaction with cell membrane followed by cell permeabilization, AMPs induce the cell lysis by pore formation which effluxes the essential ions and nutrients. However, the mechanism and pathway of membrane permeation varies from one AMP to another but once they are inside the cell, they can cause severe damage by inhibiting the core processes of the cell, i.e. central dogma.<sup>17</sup> It is believed that they disrupt replication, transcription and translation which thereby leads to the failure of the protein folding machinery and inhibits the biosynthesis of cellular membrane. AMPs can also disrupt the mitochondrial functions by inhibiting the cellular respiration and effluxing Adenosine Triphosphate (ATP) and Nicotinamide adenine dinucleotide (NADH) outside the mitochondrial membrane (Figure 4).<sup>18</sup>

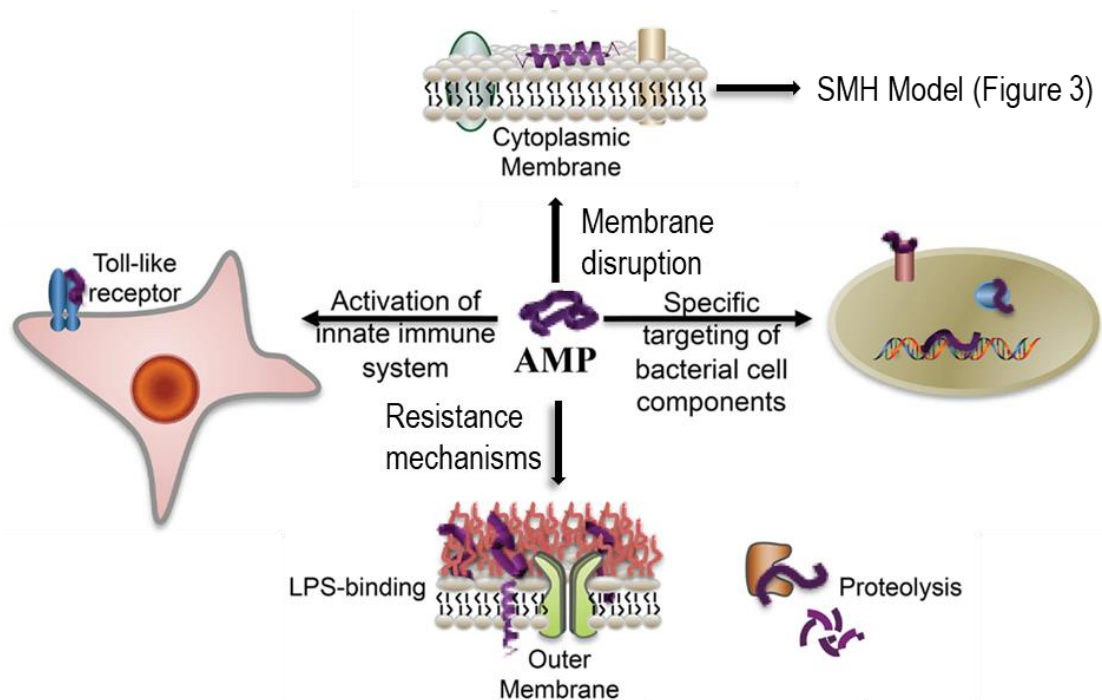


Figure 4 Mode of action of AMPs<sup>19</sup>

AMPs play a significant role in the activation of immune system. The bioactivity of AMPs is the dual ability to mediate both pro- and anti-inflammatory responses and help bridge innate and adaptive immunity by influencing the initiation and polarisation of antigen-specific adaptive

<sup>17</sup>M. Mahlapuu; J. Håkansson; L. Ringstad; and C. Björn, 'Antimicrobial Peptides: An Emerging Category of Therapeutic Agents', *Frontiers in Cellular and Infection Microbiology*, 6 (2016), 194.

<sup>18</sup>D. A. Phoenix; S. R. Dennison; and F. Harris, 'Cationic Antimicrobial Peptides', *Antimicrobial Peptides* (Wiley-VCH Verlag GmbH & Co. KGaA, 2013), 39–81.

<sup>19</sup>E. N. G. Marsh; B. C. Buer; and A. Ramamoorthy, 'Fluorine—a New Element in the Design of Membrane-Active Peptides', *Molecular BioSystems*, 5 (2009), 1143.

responses.<sup>20</sup> Unlike conventional antibiotics, AMPs appear to have the ability to enhance the immunity by functioning as immunomodulators.<sup>21</sup> Moreover, they are also known for the upregulation of gene expression in eukaryotic cells. For example, the reducing of signalling by bacterial molecules like lipopolysaccharide and lipoteichoic acid.<sup>22</sup>

### 1.5 Therapeutic potential of AMPs

Due to the growing bacterial resistance to conventional antibiotics, the broad spectrum of activity of AMPs and their ability to kill multi-resistant microorganisms have attracted attention for the development of alternative strategies. Indeed, their intrinsic properties make them promising candidates. First, their primary mechanism of action by disruption of the bacterial cell membrane implies low emergence of resistance.<sup>23,24</sup> This makes AMPs strong candidates for the development of novel therapeutic strategies.

However, specificity and effectiveness of an antimicrobial peptide depend on the right balance between its hydrophobicity and its charge: if it is too hydrophobic, it will incline to have an unwanted cytotoxic or hemolytic activity.<sup>25</sup> Natural AMPs having the right balance are very rare. Besides, their exploitation as novel therapeutics was also hampered by poor proteolytic stability and pharmacokinetics, and high manufacturing cost compared to small molecules.<sup>26,27</sup> Even if natural peptides can exhibit appealing properties such as high selectivity and potency associated with good safety and tolerability profiles, they are generally not directly suitable for therapeutic application due to poor pharmacokinetic properties. But, natural peptides are excellent starting

---

<sup>20</sup>M. Hemshekhar; V. Anaparti; and N. Mookherjee, 'Functions of Cationic Host Defense Peptides in Immunity', *Pharmaceuticals*, Vol. 9 (Multidisciplinary Digital Publishing Institute, **2016**), 40.

<sup>21</sup>S. C. Mansour; O. M. Pena; and R. E. W. Hancock, 'Host Defense Peptides: Front-Line Immunomodulators', *Trends in Immunology*, Vol. 35 (Elsevier, **2014**), 443–50.

<sup>22</sup>R. E. Hancock, 'Cationic Peptides: Effectors in Innate Immunity and Novel Antimicrobials', *The Lancet Infectious Diseases*, 1 (**2001**), 156–64.

<sup>23</sup>A. Peschel and H. G. Sahl, 'The Co-Evolution of Host Cationic Antimicrobial Peptides and Microbial Resistance', *Nature Reviews Microbiology*, Vol. 4 (**2006**), 529–36.

<sup>24</sup>J. O'Neill, 'Tackling Drug-Resistant Infections Globally: Final Report and Recommendations', *Review on Antimicrobial Resistance* (**2016**), 84.

<sup>25</sup>R. M. Dawson; M. A. Fox; H. S. Atkins; and C. Q. Liu, 'Potent Antimicrobial Peptides with Selectivity for Bacillus Anthracis over Human Erythrocytes', *International Journal of Antimicrobial Agents*, 38 (**2011**), 237–42.

<sup>26</sup>A. Moore, 'The Big and Small of Drug Discovery. Biotech versus Pharma: Advantages and Drawbacks in Drug Development', *EMBO Reports*, 4 (**2003**), 114–7.

<sup>27</sup>K. Fosgerau and T. Hoffmann, 'Peptide Therapeutics: Current Status and Future Directions', *Drug Discovery Today*, Vol. 20 (Elsevier Current Trends, **2015**), 122–8.



point for the development of therapeutics by structure-based design strategies with constant efforts in improving the physicochemical, pharmacological, and pharmacokinetic properties.

A huge number of synthetic AMPs have been prepared and studied. Sequence modification can lead to peptides with enhanced stability and availability thus a higher potency in human media.<sup>28</sup> Several strategies could be used to improve peptide stability: identification of proteolytically active amide position then modification of the sequence or stabilisation of the secondary structure (sequence optimisation, cyclisation, stapling...). Few of the AMPs, which are in commercial development phase are listed in the Table 1 along with their pharmacological application.<sup>29</sup> The potential of AMPs as suitable alternatives to conventional antibiotics used in swine and poultry industries has also been explored.<sup>30</sup>

Table 1 Development of antimicrobial peptides of animal origin

Mode of use	Peptide	Application	Stage
Topical	Pexiganan (MSI-78)	Infected diabetic foot ulcers	Phase III*
Topical	Omiganan (MBI-226)	Catheter infection, Rosacea	Phase III
Topical	OP145 (P60.4Ac)	Chronic otitis media	Phase II
Oral	Histatin analogue (P-113)	Gingivitis	Phase II
Oral	Isegranin (IB-367)	Oral mucositis	Phase III
Systematic	Heliomycin	Antifungal	Preclinical
Systematic	BPI <sup>#</sup>	Meningococcal meningitis	Phase III

\* not approved by FDA, pending additional studies, <sup>#</sup>BPI, bacterial permeability increasing protein.<sup>31</sup>

<sup>28</sup> A. de Breij; M. Riool; R. A. Cordfunke; N. Malanovic; L. de Boer; R. I. Koning; E. Ravensbergen; M. Franken; T. van der Heijde; B. K. Boekema; P. H. S. Kwakman; N. Kamp; A. El Ghalbzouri; K. Lohner; S. A. J. Zaat; J. W. Drijfhout; and P. H. Nibbering, 'The Antimicrobial Peptide SAAP-148 Combats Drug-Resistant Bacteria and Biofilms', *Science Translational Medicine*, 10 (2018), eaan4044.

<sup>29</sup> P. Kosikowska and A. Lesner, 'Antimicrobial Peptides (AMPs) as Drug Candidates: A Patent Review (2003–2015)', *Expert Opinion on Therapeutic Patents*, Vol. 26 (2016), 689–702.

<sup>30</sup> S. Wang; X. Zeng; Q. Yang; and S. Qiao, 'Antimicrobial Peptides as Potential Alternatives to Antibiotics in Food Animal Industry', *International Journal of Molecular Sciences*, Vol. 17 (Multidisciplinary Digital Publishing Institute, 2016), 603.

<sup>31</sup> R. M. Epand, *Host Defense Peptides and Their Potential as Therapeutic Agents*, Richard M. Epand (ed.) (Springer International Publishing, 2016).

Another way to circumvent therapeutic weaknesses of natural AMPs is to develop peptidomimetics exhibiting antimicrobial activity of parent AMPs with enhanced proteolytic stability and bioavailability. To reach this aim, synthetic molecules have been designed to mimic the cationic amphipathic helical structures of native AMPs which is the key determinant of their antibacterial activity by membrane permeation. For the last ten years, this issue has been of major interest for chemists working in the foldamer field.

## 2 Cationic amphipathic antimicrobial mimetics

Cationic amphipathic antimicrobial mimetics offer the possibility of development of alternative therapeutic approach to combat antimicrobial resistance.<sup>32</sup> Peptidomimetic or proteomimetic systems exhibiting the antimicrobial mechanism of parent AMPs with enhanced proteolytic stability and bioavailability have been widely explored during the last decade. Indeed, they are awaited to display extended stability in the presence of biological matrices, a critical issue for natural and synthetic AMPs. These mimetics have shown promising results as they exploit the untapped potential of AMPs by eliminating their unwanted disadvantages and embracing their advantages.<sup>33</sup> In this section, we will discuss the biomimicry of cationic antimicrobial peptides using foldamers. Foldamers are artificial folded molecular architectures mimicking the structures and functions of biopolymers such as proteins or nucleic acids.<sup>34</sup> Specifically, peptidomimetics but also a few proteomimetics with potent antimicrobial activity, adaptable design, and expedient optimisation via assembly by standard solid-phase procedures will be discussed. The main classes of peptidomimetics that have been successfully explored to date are  $\beta$ -peptides, oligoureas, peptoids and peptoid/peptide hybrids (Figure 5). Arylamides and arylureas which can be considered as proteomimetics, have also been used to design cationic amphipathic structures.<sup>35</sup>

---

<sup>32</sup> B. Mojsoska and H. Jenssen, 'Peptides and Peptidomimetics for Antimicrobial Drug Design', *Pharmaceuticals*, Vol. 8 (Multidisciplinary Digital Publishing Institute, **2015**), 366–415.

<sup>33</sup> N. Molchanova; P. R. Hansen; and H. Franzyk, 'Advances in Development of Antimicrobial Peptidomimetics as Potential Drugs', *Molecules*, Vol. 22 (Multidisciplinary Digital Publishing Institute, **2017**), 1430.

<sup>34</sup> S. H. Gellman, 'Foldamers: A Manifesto', *Accounts of Chemical Research*, 31 (**1998**), 173–80.

<sup>35</sup> G. J. Gabriel and G. N. Tew, 'Conformationally Rigid Proteomimetics: A Case Study in Designing Antimicrobial Aryl Oligomers', *Org. Biomol. Chem.*, 6 (**2008**), 417–23.

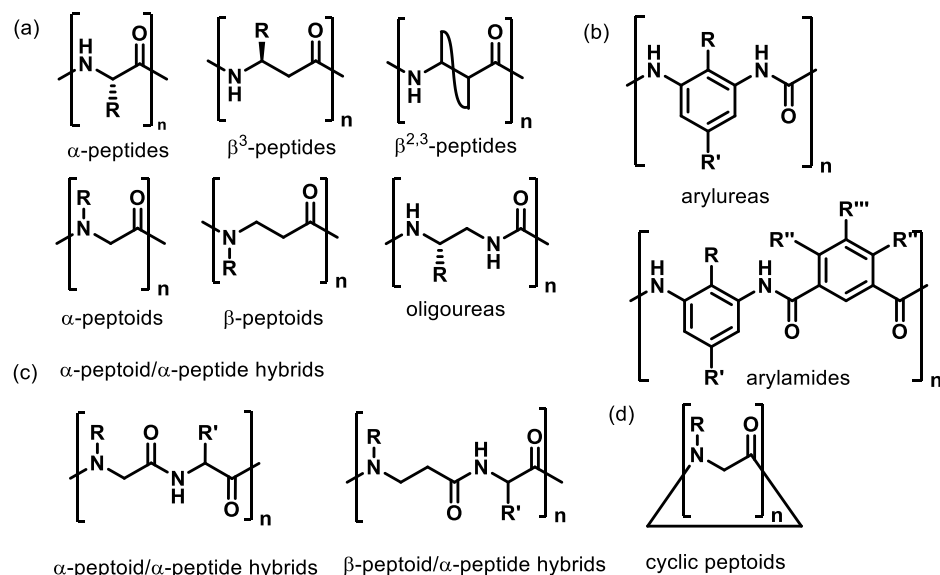


Figure 5 Structure of peptidomimetics and proteomimetics used to design cationic amphipathic AMP mimetics

The principal strategy was to exploit the foldameric properties of these oligoamides to construct (stable) helical amphipathic structure capable to interact with bacterial membrane.

## 2.1 $\beta$ -Peptides

In 1996, the Seebach's<sup>36,37</sup> and Gellman's<sup>38</sup> groups, have reported at the same time  $\beta$ -peptides with more stable helical secondary structures than their parent  $\alpha$ -peptides. Indeed,  $\beta$ -Peptides incorporating  $\beta^3$ -amino acids or the constrained alicyclic  $\beta$ -amino acid *trans*-2-aminocyclohexane carboxylic acid (*trans*-ACHC), were shown to adopt in solution a stable 14-helix also named 3<sub>14</sub>-helix with a 3-residues geometric repeat (Figure 6).

<sup>36</sup>G. Guichard and D. Seebach, 'Solid-Phase Synthesis of  $\beta$ -Oligopeptides', *CHIMIA International Journal for Chemistry*, 51 (1997), 315–8.

<sup>37</sup> D. Seebach; M. Overhand; F. N. M. Kühnle; B. Martinoni; L. Oberer; U. Hommel; and H. Widmer, ' $\beta$ -Peptides: Synthesis by Arndt-Eistert Homologation with Concomitant Peptide Coupling. Structure Determination by NMR and CD Spectroscopy and by X-Ray Crystallography. Helical Secondary Structure of a  $\beta$ -Hexapeptide in Solution and Its Stability towards  $Pe^+$ ', *Helvetica Chimica Acta*, 79 (1996), 913–41.

<sup>38</sup> D. H. Appella; L. A. Christianson; I. L. Karle; D. R. Powell; and S. H. Gellman, ' $\beta$ -Peptide Foldamers: Robust Helix Formation in a New Family of  $\beta$ -Amino Acid Oligomers', *Journal of the American Chemical Society*, 118 (1996), 13071–2.

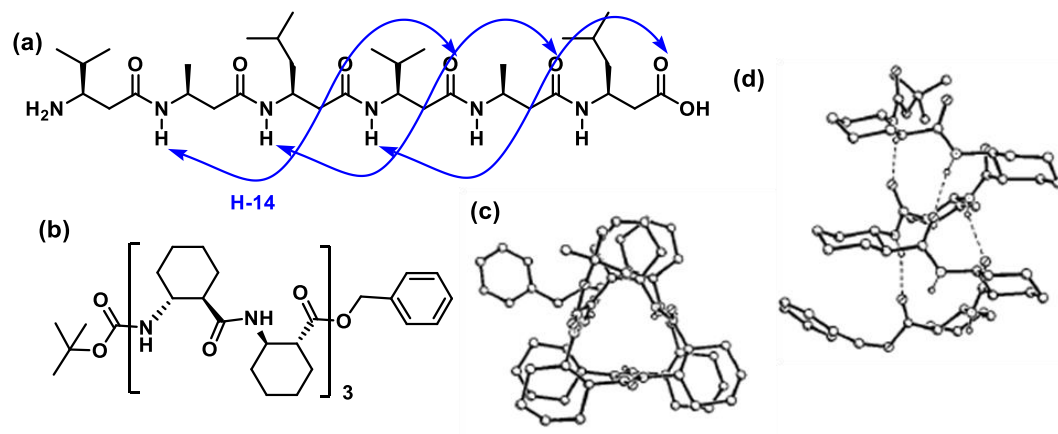


Figure 6 Structure of  $\beta$ -peptides featuring 14-helix structure (a)  $\beta^3$ -peptide hexamer from Seebach, (b) trans-ACHC hexamer from Gellman and X-ray structure of trans-ACHC hexamer (c) top view and (d) side view.<sup>38</sup>

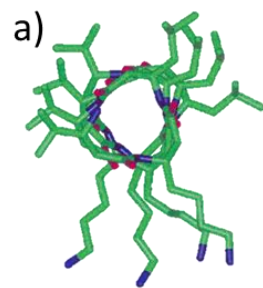
$\beta$ -peptides possess the same mode of structuration than peptides by intramolecular hydrogen bonding between NH and carbonyl from the backbone. Later, it was shown that other type of helical structures such as 12-helix, 10-helix and 8-helix could be obtained using more constrained  $\beta$ -amino acids.<sup>39</sup> These oligoamides, especially alicyclic  $\beta$ -peptides, possess a better stability and resistance to cleavage by peptidases compared to  $\alpha$ -peptides, which opens the door for developing  $\beta$ -peptides as candidates for useful drugs.<sup>40</sup>

In 1999, the DeGrado's group reported the synthesis and biological evaluation of the first  $\beta$ -peptides featuring an amphipathic cationic helical structure mimicking AMPs.<sup>41</sup> Taking advantage of the 3-residues geometric repeat of the 14-helix, amphipathic helix has been constructed using  $\beta^3$ -homovaline ( $\beta^3$ -HVal) and  $\beta^3$ -homoleucine ( $\beta^3$ -HLeu) as hydrophobic residues and  $\beta^3$ -homolysine ( $\beta^3$ -HLys) as cationic residue (Figure 7). The antibacterial activity of longer oligomers (dodecamer) were promising but the haemolysis of human red blood cells revealed a poor selectivity of these  $\beta$ -peptides.

<sup>39</sup> P. Le Grel and G. Guichard, 'Foldamers Based on Remote Intrastrand Interactions', *Foldamers: Structure, Properties, and Applications* (Wiley-VCH Verlag GmbH & Co. KGaA, 2007), 35–74.

<sup>40</sup>Gellman, *op. cit.*; D. Seebach and J. L. Matthews, ' $\beta$ -Peptides: A Surprise at Every Turn', *Chemical Communications* (1997), 2015–22.

<sup>41</sup> Y. Hamuro; J. P. Schneider; and W. F. DeGrado, 'De Novo Design of Antibacterial  $\beta$ -Peptides', *Journal of the American Chemical Society*, 121 (1999), 12200–1.



b) Peptide	Haemolysis	MIC	Selectivity
<i>Fmoc-(β<sup>3</sup>-HVal-β<sup>3</sup>-HLys- β<sup>3</sup>-HLeu)<sub>3</sub>-OH</i>	6.3	15	0.42
<i>Fmoc-(β<sup>3</sup>-HVal-β<sup>3</sup>-HLys- β<sup>3</sup>-HLeu)<sub>4</sub>-OH</i>	0.31	1.5	0.21
<i>H-(β<sup>3</sup>-HVal-β<sup>3</sup>-HLys- β<sup>3</sup>-HLeu)<sub>3</sub>-OH</i>	86	41	2.1
<i>H-(β<sup>3</sup>-HVal-β<sup>3</sup>-HLys- β<sup>3</sup>-HLeu)<sub>4</sub>-OH</i>	4.2	2.1	2.0
<i>H-(β<sup>3</sup>-HLeu-β<sup>3</sup>-HLys- β<sup>3</sup>-HLeu)<sub>4</sub>-OH</i>	2.6	1.7	1.5

Figure 7 Antibacterial  $\beta$ -peptides developed by DeGrado (a) Molecular model of the amphiphilic  $\beta$ -peptide  $H-(\beta^3\text{-HVal-}\beta^3\text{-HLys-}\beta^3\text{-HLeu})_4\text{-OH}$  and (b) Antimicrobial activity (MIC) in  $IC_{50}$  ( $\mu\text{M}$ ), hemolytic activities in  $HD_{50}$  ( $\mu\text{M}$ ) and selectivity in  $HD_{50}/IC_{50}$ .

More work was done on this type of  $\beta^3$ -peptides by the Seebach's group, which supported the belief that the activity and selectivity of AMPs mimetics is dependant on the side-chain composition of the helix.<sup>42</sup> Unfortunately their study concluded that this class of  $\beta^3$ -peptides had no real future as antibiotic due to their limited spectrum of activity.

Gellman's group have further developed an amphiphilic version of the 12-helix  $\beta$ -peptide using (*R,R*)-*trans*-2-aminocyclopentane carboxylic acid (ACPC) as hydrophobic residue and (*3R,4S*)-*trans*-4-aminopyrrolidine-3-carboxylic acid (APC) or (*R*)- $\beta$ -amino D-proline (AP) as cationic residue (Figure 8).<sup>43,44</sup> A 17-mer showed comparable antimicrobial activities to that of the magainin against four species of bacteria including the methicillin-resistant strain *Staphylococcus aureus* 5332 and possessed weaker haemolytic activity compared to magainin, melittin and previously reported  $\beta^3$ -peptides.<sup>38</sup> Additionally, the influence of the net charge and the amphipathic character on their antimicrobial activity was studied and showed that 40% cationic face is best for activity and facial amphipathicity was also necessary for optimal biological activity.

<sup>42</sup>P. I. Arvidsson; J. Frackenhohl; N. S. Ryder; B. Liechty; F. Petersen; H. Zimmermann; G. P. Camenisch; R. Woessner; and D. Seebach, 'On the Antimicrobial and Hemolytic Activities of Amphiphilic Beta-Peptides.', *Chembiochem*, 2 (2001), 771–3.

<sup>43</sup>E. A. Porter; X. Wang; H. S. Lee; B. Weisblum; and S. H. Gellman, 'Non-Haemolytic Beta-Amino-Acid Oligomers.', *Nature*, 404 (2000), 565.

<sup>44</sup>E. A. Porter; B. Weisblum; and S. H. Gellman, 'Mimicry of Host-Defense Peptides by Unnatural Oligomers: Antimicrobial  $\beta$ -Peptides', *Journal of the American Chemical Society*, 124 (2002), 7324–30.

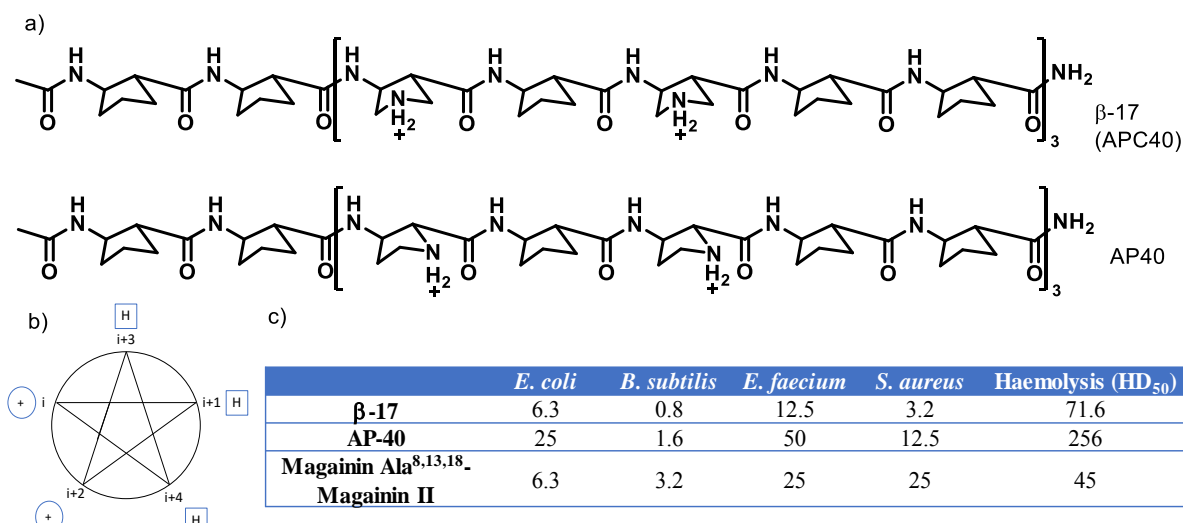


Figure 8 Antibacterial  $\beta$ -peptides developed by Gellman (a) Structure of a 17-mers  $\beta$ -17 (APC40) and AP40, (b) Axial projection of the  $\beta$ -peptide 12-helix (2.5 residues per turn): H for hydrophobic residue and + for cationic residue and (c) anti-bacterial (minimum inhibitory concentration (MIC)) and haemolytic activity of the  $\beta$ -peptide compared to magainin Ala<sup>8,13,18</sup>-Magainin II amide.

The Gellman's group has also studied the potential of 14 helix  $\beta$ -peptide incorporating the alicyclic amino acid ACHC and  $\beta^3$ -aminoacid residues.<sup>45</sup> The nonamer (ACHC- $\beta^3$ Val- $\beta^3$ Lys)<sub>3</sub> showed promising antifungal activity against *Candida albicans* and a low haemolytic activity (5% at the MIC) (Figure 9).

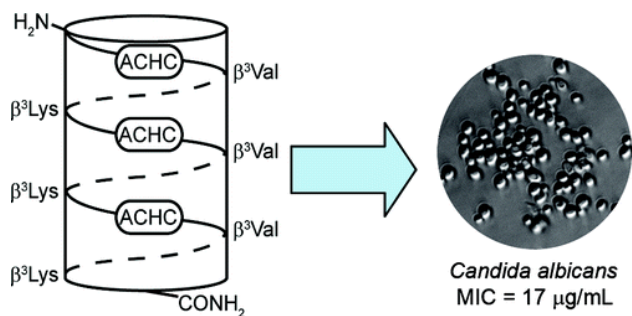


Figure 9 Antifungal activity of 14-helical  $\beta$ -peptides against *C. albicans*<sup>45</sup>

<sup>45</sup>A. J. Karlsson; W. C. Pomerantz; B. Weisblum; S. H. Gellman; and S. P. Palecek, 'Antifungal Activity from 14-Helical  $\beta$ -Peptides', *Journal of the American Chemical Society*, 128 (2006), 12630–1.

Further studies of the group reported that this type of oligomers displayed antibacterial activities against a panel of bacterial strains (*E. coli*, *B. subtilis*, *S. aureus*, *E. faecalis*).<sup>46</sup> However, best selectivity indexes (SI = HC<sub>10</sub>/MIC<sub>MRSA</sub>) were obtained using  $\beta$ -peptides incorporating  $\alpha,\alpha,\beta,\beta$ -tetra methyl  $\beta$ -amino acid residues rather than the ACHC residues.<sup>47</sup>

## 2.2 Oligourea and $\gamma^4$ -peptides

*N,N'*-linked oligoureas are peptidomimetic foldamers that are formerly  $\gamma^4$ -peptides where the  $\alpha$ CH<sub>2</sub> has been replaced by a NH (Figure 10). The Guichard's group showed that oligourea oligomers carrying proteinogenic side chains form a right-handed 2.5-helix with a pitch of 5.1 Å and stabilized by 12- and 14-membered H-bonded rings.<sup>48</sup>

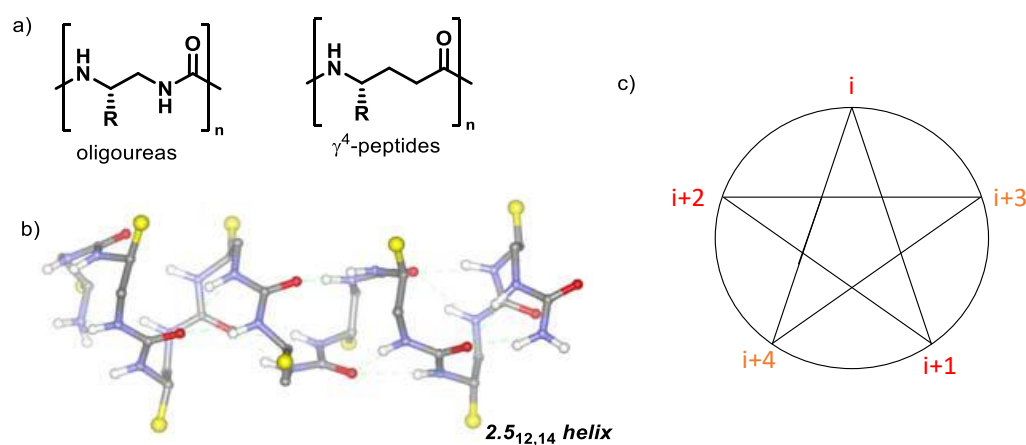


Figure 10 (a) Chemical structures of aliphatic oligoureas and  $\gamma^4$ -peptides, (b) helical structure of oligoureas and (c) helical wheel representation illustrating the spatial orientation of side chains (Modified from Aude Violette 2006).<sup>49</sup>

The same group worked on developing bioactive oligoureas based on their tendency to form (P)-2.5<sub>12,14</sub>-helix in solution. The design of cationic amphiphilic architectures was done by introduction of cationic lysine side chains in different position. They observed that these cationic amphiphilic oligoureas (7-9 residues short) show *in vitro* antibacterial activity against Gram-negative and

<sup>46</sup> B. P. Mowery; A. H. Lindner; B. Weisblum; S. S. Stahl; and S. H. Gellman, 'Structure-Activity Relationships among Random Nylon-3 Copolymers That Mimic Antibacterial Host-Defense Peptides', *Journal of the American Chemical Society*, 131 (2009), 9735–45.

<sup>47</sup> R. Liu; X. Chen; S. Chakraborty; J. J. Lemke; Z. Hayouka; C. Chow; R. A. Welch; B. Weisblum; K. S. Masters; and S. H. Gellman, 'Tuning the Biological Activity Profile of Antibacterial Polymers via Subunit Substitution Pattern', *Journal of the American Chemical Society*, 136 (2014), 4410–8.

<sup>48</sup> V. Semetey; D. Rognan; C. Hemmerlin; R. Graff; J.-P. Briand; M. Marraud; and G. Guichard, 'Stable Helical Secondary Structure in Short-Chain *N,N'*-Linked Oligoureas Bearing Proteinogenic Side Chains', *Angewandte Chemie International Edition*, 41 (2002), 1893–5.

Gram-positive bacteria including methicillin-resistant *Staphylococcus aureus* (MRSA) with promising membrane selectivity (Figure 11).<sup>49</sup>

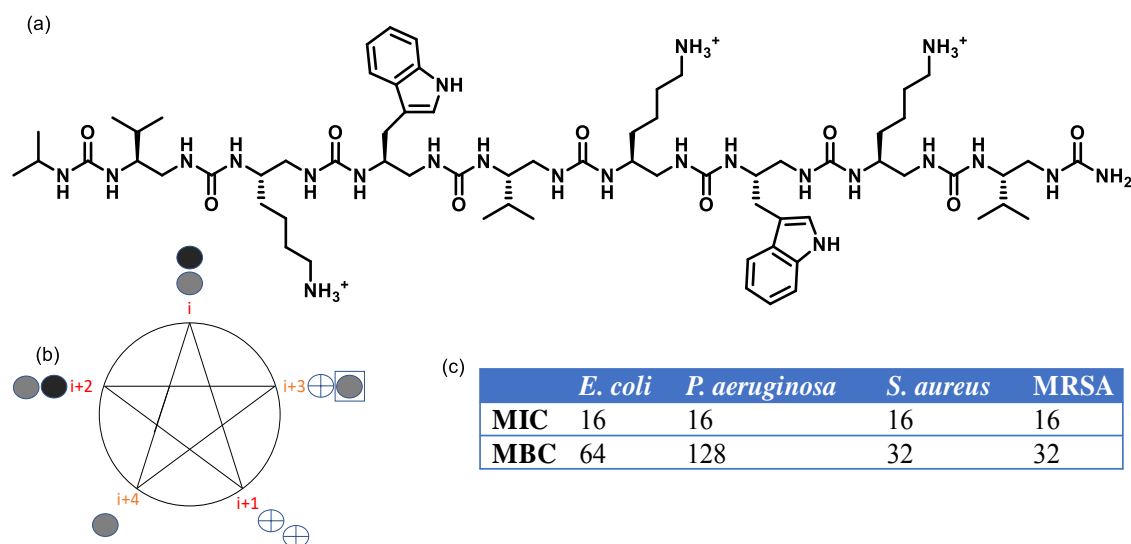


Figure 11 (a) Chemical structure of a urea octamer, (b) its helical wheel representation where cationic side chains are represented by a plus sign and aliphatic or aromatic side chains by a grey circle and (c) MIC and Minimum bactericidal concentration (MBC) in  $\mu\text{g/ml}$ .

To better understand structure-property relationships and to gain insight into the mechanisms of membrane disruption, Guichard's group undertook detailed comparative studies of oligoureas, their  $\gamma^4$ -peptide counterparts, and various mixed amide/urea oligomers bearing identical side chains.<sup>50</sup> They showed that the modification of oligourea to have more hydrophobic content (substituting *iPr* for *iBu* side chains) gave the most potent antibacterial oligourea with MIC and MBC values of 8 and 32  $\text{mg}\cdot\text{mL}^{-1}$  on *S. aureus*, respectively. Furthermore, they synthesised and evaluated mixed oligourea/ $\gamma^4$ -peptides for their antibacterial and anti-fungal activity. One of the hybrid oligomers showed good activity against both bacteria and fungi, with MIC and minimal fungicidal concentrations (MFC) ranging from 16–64  $\mu\text{g ml}^{-1}$ .

The results also point to heterogeneous helical urea/amide backbones, which may become advantageous in the development of more potent yet less cytotoxic antimicrobial helical foldamers

<sup>49</sup>A. Violette; S. Fournel; K. Lamour; O. Chaloin; B. Frisch; J. P. Briand; H. Monteil; and G. Guichard, 'Mimicking Helical Antibacterial Peptides with Nonpeptidic Folding Oligomers', *Chemistry and Biology*, 13 (2006), 531–8.

<sup>50</sup>P. Claudon; A. Violette; K. Lamour; M. Decossas; S. Fournel; B. Heurtault; J. Godet; Y. Mély; B. Jamart-Grégoire; M. C. Averlant-Petit; J. P. Briand; G. Duportail; H. Monteil; and G. Guichard, 'Consequences of Isostructural Main-Chain Modifications for the Design of Antimicrobial Foldamers: Helical Mimics of Host-Defense Peptides Based on a Heterogeneous Amide/urea Backbone', *Angewandte Chemie - International Edition*, 49 (2010), 333–6.



for *in vivo* applications. A recent study focused on the effect of urea linkages on the antibacterial activities and the selectivity.<sup>51</sup> To this aim, one urea linkage (U) was replaced at selected positions by a thiourea (T) or guanidinium (G) surrogates (Figure 12). Hybrid oligomers incorporating thiourea or guanidinium showed increased potency compared to oligoureas.

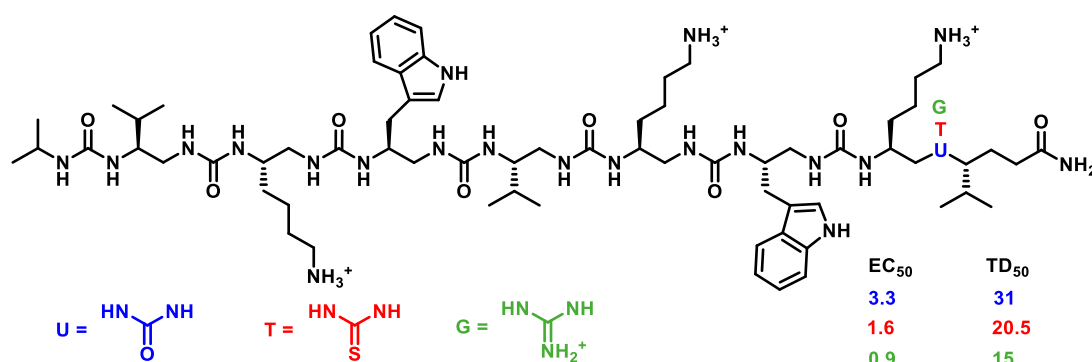


Figure 12 Structure of hybrid oligomers containing urea, thiourea and guanidinium linkages and their activity against *Bacillus anthracis* germinated spores (Effector concentration EC<sub>50</sub> in  $\mu\text{g/ml}$ ) and cytotoxicity on RAW 264.7 cell line (Toxic dose TD<sub>50</sub> in  $\mu\text{g/ml}$ ).

### 2.3 Arylamides and Arylureas

Arylamides and arylureas are proteomimetic foldamers. In 2002, Tew and De Grado developed aromatic oligoamides designed to exhibit facial amphiphilic nature thanks to an internal NH $\cdots$ S hydrogen bonding (Figure 13). Their aim was to show that to mimic AMPs function, helical structure is not needed, only facial amphiphathy is mandatory. This first generation of antimicrobial arylamide gave promising antimicrobial activities but they were highly haemolytic.<sup>52,53</sup> However great improvement in potency and selectivity were made by conformational restriction of the arylamide skeleton thanks to an intramolecular hydrogen bonds network along the backbone when R<sup>2</sup> are ether groups (Figure 13).<sup>54</sup>

<sup>51</sup> S. Antunes; J. P. Corre; G. Mikaty; C. Douat; P. L. Goossens; and G. Guichard, 'Effect of Replacing Main-Chain Ureas with Thiourea and Guanidinium Surrogates on the Bactericidal Activity of Membrane Active Oligourea Foldamers', *Bioorganic and Medicinal Chemistry*, 25 (2017), 4245–52.

<sup>52</sup>G. N. Tew; D. Liu; B. Chen; R. J. Doerksen; J. Kaplan; P. J. Carroll; M. L. Klein; and W. F. DeGrado, 'De Novo Design of Biomimetic Antimicrobial Polymers.', *Proceedings of the National Academy of Sciences of the United States of America*, 99 (2002), 5110–4.

<sup>53</sup>D. Liu; S. Choi; B. Chen; R. J. Doerksen; D. J. Clements; J. D. Winkler; M. L. Klein; and W. F. DeGrado, 'Nontoxic Membrane-Active Antimicrobial Arylamide Oligomers', *Angewandte Chemie - International Edition*, 43 (2004), 1158–62.

<sup>54</sup> S. Choi; A. Isaacs; D. Clements; D. Liu; H. Kim; R. W. Scott; J. D. Winkler; and W. F. DeGrado, 'De Novo Design and in Vivo Activity of Conformationally Restrained Antimicrobial Arylamide Foldamers', *Proceedings of the National Academy of Sciences*, 106 (2009), 6968–73.

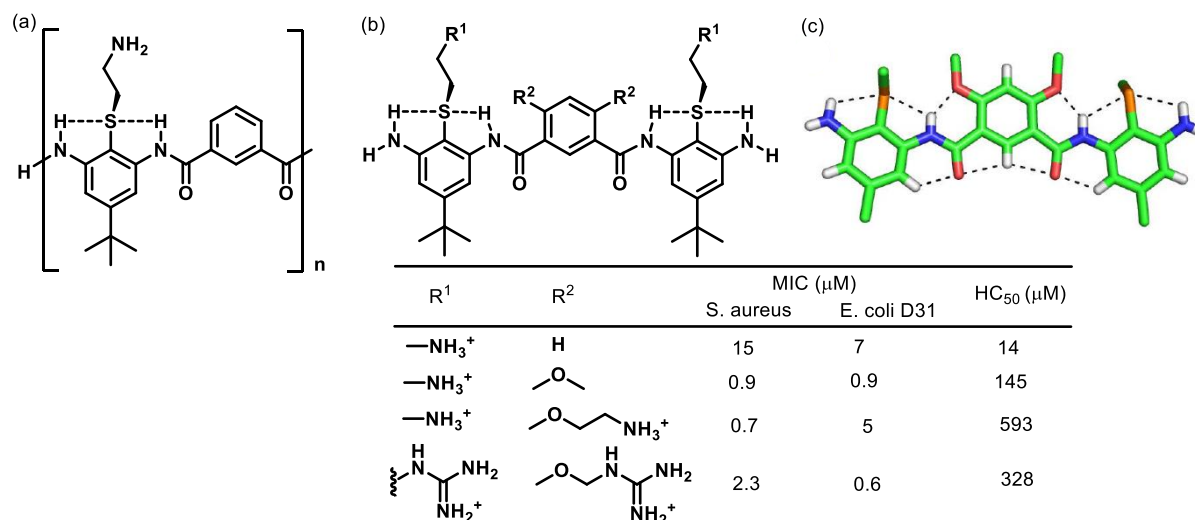


Figure 13 (a) Generic structure of arylamides developed by Tew and De Grado, (b) The effect of backbone restriction and cationic side chain modification on activity against *Staphylococcus aureus* and *Escherichia coli* and haemolytic activity, and (c) X-ray crystal structure showing the network of hydrogen bonds restricting arylamide flexibility.

Furthermore, a study on a novel series of aromatic ureas also with internal NH...S hydrogen bonding showed that decreasing the hydrophobicity is expected to generate more selective oligomers.<sup>55</sup> Further, the Tew's group focused on non oligoamide compounds such as phenylene ethynylene oligomers to mimic AMPs.<sup>56</sup>

Another class of peptidomimetics widely explored to construct AMPs mimics is peptoids. Cationic antimicrobial peptidomimetics based on peptoid family will be developed individually in section 3.

### 3 Cationic amphipathic peptoids with antimicrobial activities

In this section, a general overview of peptoids; their nature, their synthesis, their structuration and their biological potential will be presented. Then we will focus on the design of cationic amphiphilic AMP mimics using peptoids.

<sup>55</sup>H. Tang; R. J. Doerksen; and G. N. Tew, 'Synthesis of Urea Oligomers and Their Antibacterial Activity.', *Chemical Communications (Cambridge, England)*, 0 (2005), 1537–9.

<sup>56</sup>G. N. Tew; D. Clements; H. Tang; L. Arnt; and R. W. Scott, 'Antimicrobial Activity of an Abiotic Host Defense Peptide Mimic', *Biochimica et Biophysica Acta (BBA) - Biomembranes*, 1758 (2006), 1387–92.

### 3.1 Peptoid-type family

Peptoids were introduced by Chiron corporation, a biotechnology company at the end of the eighties and developed first by Zuckermann at Berkeley, University of California.<sup>57,58</sup> Peptoids have a backbone like peptides with the side chains attached to the amide nitrogen instead of the alpha-carbon (Figure 14 a, b).

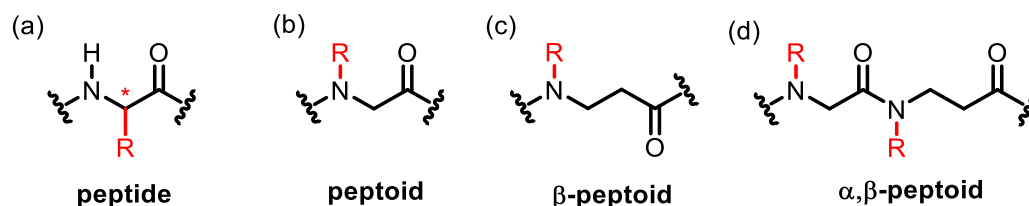


Figure 14: a) Peptide, b) ( $\alpha$ -)Peptoid (Zukermann 1992), c)  $\beta$ -peptoid (Hamper 1998), d)  $\alpha,\beta$ -peptoid (Taillefumier 2009)

This modification imparts protease resistance as well as an achiral backbone. Based on the work of Zuckermann, Hamper *et al.* introduced  $\beta$ -peptoids by analogy with  $\beta$ -peptides (Figure 14 c).<sup>59</sup> Thereafter, our group synthesised  $\alpha,\beta$ -alternating peptoids. (Figure 14 d).<sup>60</sup>

Peptoids are a class of peptidomimetics that are perfect candidates for use as therapeutic agents due to their increased bioavailability compared to peptides (*i.e.* resistance to protease degradation) and low immune response.<sup>61</sup> There are several reasons for the peptoids to be the perfect candidates for therapeutic applications. First, peptoids are structurally very close to peptides as they are simple regioisomers. This property keeps the amide-based backbone, the chemical diversity, and the spacing of the side chains conserved; which gives the ability to easily adapt the peptide-supported synthetic methods for the synthesis of peptoids. In preliminary experiments, Zuckermann *et al.* performed modelling studies to compare peptide and peptoid monomers which showed that

<sup>57</sup>R. J. Simon; R. S. Kania; R. N. Zuckermann; V. D. Huebner; D. A. Jewell; S. Banville; S. Ng; L. Wang; S. Rosenberg; and C. K. Marlowe, 'Peptoids: A Modular Approach to Drug Discovery.', *Proceedings of the National Academy of Sciences of the United States of America*, 89 (1992), 9367–71.

<sup>58</sup>R. J. Simon; P. A. Bartlett; and D. V. Santi, 'Modified Peptide and Peptide Libraries with Protease Resistance, Derivatives Thereof and Methods of Producing and Screening Such' (US6075121A Patent, 2000).

<sup>59</sup>B. C. Hamper; S. A. Kolodziej; A. M. Scates; R. G. Smith; and E. Cortez, 'Solid Phase Synthesis of Beta-Peptoids: N-Substituted Beta-Aminopropionic Acid Oligomers.', *The Journal of Organic Chemistry*, 63 (1998), 708–18.

<sup>60</sup>T. Hjelmgaard; S. Faure; C. Caumes; E. De Santis; A. a Edwards; and C. Taillefumier, 'Convenient Solution-Phase Synthesis and Conformational Studies of Novel Linear and Cyclic Alpha,beta-Alternating Peptoids.', *Organic Letters*, 11 (2009), 4100–3.

<sup>61</sup>R. N. Zuckermann, 'Peptoid Origins.', *Biopolymers*, 96 (2011), 545–55.

peptoids are more flexible than peptides, due to the presence of tertiary backbone amides leading to the *cis/trans* isomerism of the *N,N*-disubstituted amide linkage (Figure 15).<sup>62,63</sup>

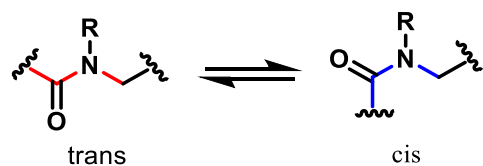


Figure 15 *cis/trans* isomerism of peptoid *N,N*-disubstituted amides

The flexibility of peptoid oligomers is such that a peptoid composed of  $n$  monomers can exist in an equilibrium mixture of  $2^{n-1}$  configurational isomers, or  $2^n$  if the *N*-terminal amino acid is acetylated. Another consequence of changing the point of side-chain connectivity is that the chiral centre on the  $\alpha$ -carbon and the hydrogen bond donor (the NH group) are lost. The stability of peptoids against proteases was tested *in vitro* by the same group.<sup>64</sup> They prepared peptides from D-amino acids and homologous peptoid oligomers and incubated them with protease enzymes from each major class. All peptides composed of L-amino acids were readily cleaved by the appropriate enzymes, while homologous peptides composed of D-amino acids and *N*-substituted glycine oligomers were not cleaved. They also found that the peptoids were more stable than the peptides composed of D-amino acids in the follow-up study.<sup>65</sup> These analogues showed both high proteolytic stability against peptidases tested and affinities for target enzymes identical to parent peptides.

### 3.2 Brief history of the development of synthetic methodology for peptoids

The first peptoids were synthesised at a small start-up company called Protos Corp. The group envisioned a direct analogy to the well-established Merrifield method of solid-phase peptide synthesis (SPPS).<sup>66</sup> Using this methodology (Figure 16 a) the first long peptoid oligomers ( $\approx$  ten

---

<sup>62</sup>R. N. Zuckermann; J. M. Kerr; S. B. H. H. Kent; W. H. Moos; W. H. Moosf; and S. B. H. H. Kent, 'Efficient Method for the Preparation of Peptoids [Oligo(*N*-Substituted Glycines)] by Submonomer Solid-Phase Synthesis', *Journal of the American Chemical Society*, 114 (1992), 10646–7.

<sup>63</sup>Q. Sui; D. Borchardt; and D. L. Rabenstein, 'Kinetics and Equilibria of *Cis/trans* Isomerization of Backbone Amide Bonds in Peptoids', *Journal of the American Chemical Society*, 129 (2007), 12042–8.

<sup>64</sup>S. M. Miller; R. J. Simon; S. Ng; R. N. Zuckermann; J. M. Kerr; and W. H. Moos, 'Proteolytic Studies of Homologous Peptide and *N*-Substituted Glycine Peptoid Oligomers', *Bioorganic and Medicinal Chemistry Letters*, 4 (1994), 2657–62.

<sup>65</sup>S. M. Miller; R. J. Simon; S. Ng; R. N. Zuckermann; J. M. Kerr; and W. H. Moos, 'Comparison of the Proteolytic Susceptibilities of Homologous L-amino Acid, D-amino Acid, and *N*-substituted Glycine Peptide and Peptoid Oligomers', *Drug Development Research*, 35 (1995), 20–32.

<sup>66</sup>G. B. Fields and R. L. NOBLE, 'Solid Phase Peptide Synthesis Utilizing 9-fluorenylmethoxycarbonyl Amino Acids', *International Journal of Peptide and Protein Research*, 35 (1990), 161–214.

residues) were synthesized with good efficiency. Once the peptoids were recognised as active therapeutic candidates, the next logical step was to synthesise peptoid libraries by automated combinatorial synthesis.<sup>67</sup> There were two serious hurdles in the fast and cost-efficient synthesis of peptoids by combinatorial approach. First, the prior preparation of large amounts of Fmoc-protected monomers which is very time consuming. Second, once interesting biological activity is identified in a combinatorial library, it can be very difficult to identify active compounds in the library (a process called deconvolution).<sup>61</sup>

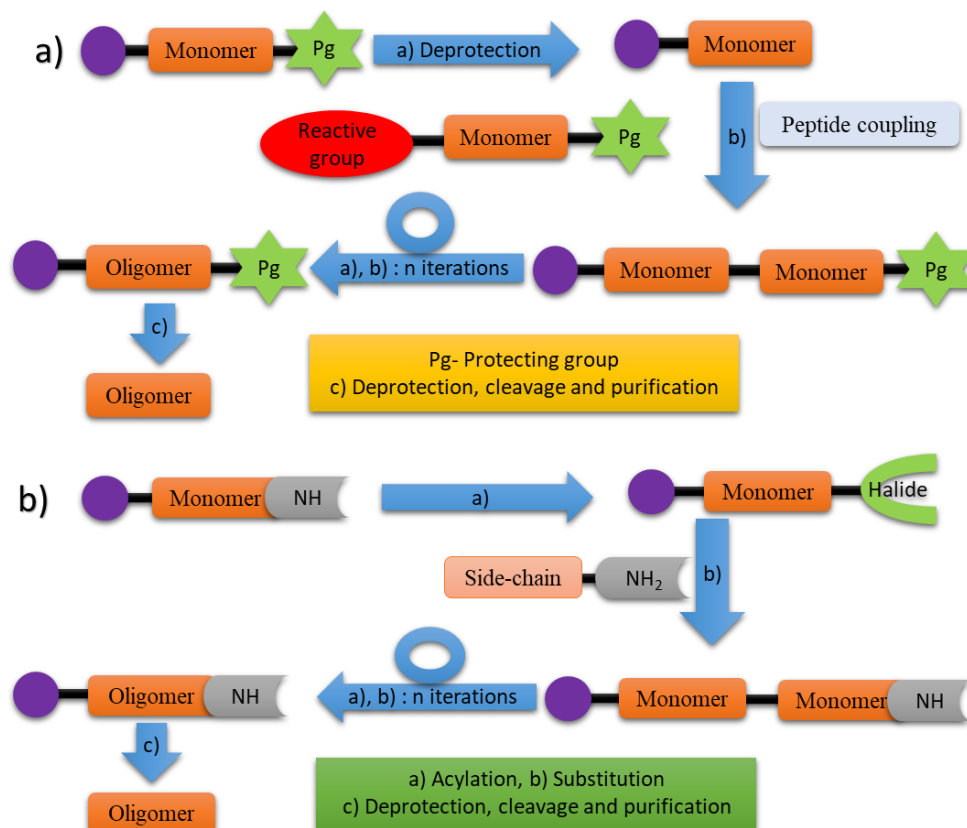


Figure 16 General scheme of synthesis of peptoid oligomer on solid support (a) Monomer synthesis, (b) Submonomer synthesis.

Therefore, the Zuckermann group quickly developed a more efficient method of supported synthesis adapted to peptoids, which they called "Submonomer solid phase synthesis" (Figure 16 b).<sup>62</sup> In the submonomer approach, the acylation is carried out first followed by substitution by a primary amine to add peptoid residues to the expanding chain, in an iterative manner that is particularly adapted to the solid phase synthesis. The submonomer synthetic approach will be dealt in detail in the following chapter.

<sup>67</sup>R. N. Zuckermann; J. M. Kerr; M. A. Siani; and S. C. Banville, 'Design, Construction and Application of a Fully Automated Equimolar Peptide Mixture Synthesizer', *International Journal of Peptide and Protein Research*, 40 (1992), 497–506.

### 3.3 Examples of peptoids in development for pharmacological applications

To highlight the potential of peptoids as future drugs, we expose in this section, a few examples of peptoids undergoing development which can be used for the treatment of diseases.

#### 3.3.1 Hybrid peptoids for enhanced bacterial selectivity and anti-inflammatory activity

Recently, a group in Korea designed hybrid peptide (PapMA) from papiliocin and magainin joined by a proline hinge, which showed good antibacterial activity but proved to be cytotoxic to mammalian cells.<sup>68</sup> To decrease cytotoxicity of PapMA, they designed a lysine (Lys) peptoid analogue, PapMA-k, which retained high antimicrobial activity but displayed cytotoxicity lower than that of PapMA. They also showed anti-inflammatory activity by inhibition of nitric oxide and inflammatory cytokine production in RAW264.7 macrophages. Consequently, PapMA and PapMA-k are potent peptide antibiotics with antimicrobial and anti-inflammatory activity, with PapMA-k displaying enhanced bacterial selectivity.

#### 3.3.2 Peptoids as therapeutics and detection agents in protein misfolding diseases

The peptoid ligand HQP09 shows promising in vitro results by specific binding to expanded polyglutamine proteins. Besides, it shows potential for the treatment of Huntington's disease (HD) by exerting Ca<sup>2+</sup> stabilizing and neuroprotective effects in HD mice.<sup>69</sup> The peptoid IAM1 and its dimer have been shown to selectively bind to both A $\beta$ 40 and A $\beta$ 42, as well as to inhibit A $\beta$  aggregation.<sup>70</sup> Furthermore, in a new study, a peptoid-based mimic (JPT1) of the peptide KLVFF (residues 16–20 of A $\beta$ ) was tested for its ability to modulate A $\beta$  aggregation (Scheme 1). JPT1 was found to modulate A $\beta$ 40 aggregation, specifically decreasing lag time to  $\beta$ -sheet aggregate formation as well as the total number of fibrillar,  $\beta$ -sheet structured aggregates formed.<sup>71</sup> The same group recently developed two new variants of JPT1 to study the effect of aromatic side chain placement (JPT1s) and chiral side chain (JPT1a). The results of this study provide a better

---

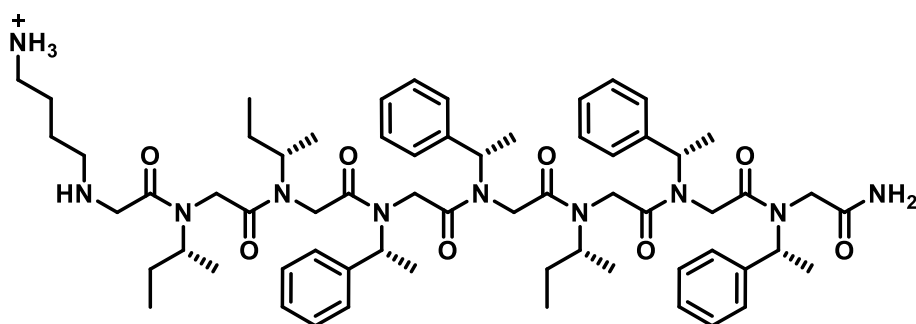
<sup>68</sup>A. Shin; E. Lee; D. Jeon; Y. G. Park; J. K. Bang; Y. S. Park; S. Y. Shin; and Y. Kim, 'Peptoid-Substituted Hybrid Antimicrobial Peptide Derived from Papiliocin and Magainin 2 with Enhanced Bacterial Selectivity and Anti-Inflammatory Activity', *Biochemistry*, 54 (2015), 3921–31.

<sup>69</sup>X. Chen; J. Wu; Y. Luo; X. Liang; C. Supnet; M. W. Kim; G. P. Lotz; G. Yang; P. J. Muchowski; T. Kodadek; and I. Bezprozvanny, 'Expanded Polyglutamine-Binding Peptoid as a Novel Therapeutic Agent for Treatment of Huntington's Disease', *Chemistry and Biology*, 18 (2011), 1113–25.

<sup>70</sup>Y. Luo; S. Vali; S. Sun; X. Chen; X. Liang; T. Drozhzhina; E. Popugueva; and I. Bezprozvanny, 'A $\beta$ 42-Binding Peptoids as Amyloid Aggregation Inhibitors and Detection Ligands', *ACS Chemical Neuroscience*, 4 (2013), 952–62.

<sup>71</sup>J. P. Turner; T. Lutz-Rechtin; K. A. Moore; L. Rogers; O. Bhave; M. A. Moss; and S. L. Servoss, 'Rationally Designed Peptoids Modulate Aggregation of Amyloid-Beta 40', *ACS Chemical Neuroscience*, 5 (2014), 552–8.

understanding for how peptoids interact with A $\beta$  and its aggregates. This improved understanding of the aggregation pathway will allow for rational design of Alzheimer's disease therapeutics.<sup>72</sup>



Scheme 1 Structure of peptoid JPT1 with  $\alpha$  chiral aliphatic and aromatic side chains to induce formation of a stable helical secondary structure.

### 3.3.3 Peptoids as vehicles of gene therapy

Transfection is the process of intentionally transferring the foreign gene into a eukaryotic cell. Viral or non-viral methods can mediate it; however, the chemical methods are popular due to their inexpensive nature. The most popular being calcium phosphate and calcium chloride salt solutions, for example via liposomes or polycationic lipids.<sup>73</sup>

Murphy *et al.* synthesised cationic peptoids such as (*N*benzyl-*N*benzyl-*N*aminoethyl)<sub>12</sub> and (*N*aminoethyl-*N*phenylethyl-*N*phenylethyl)<sub>12</sub> that has been found to be a good transfection agent in the same way as cationic lipids. These peptoids has the advantage of being stable in serum concerning lipids and can be used as vectors for gene delivery.<sup>74</sup> Huang *et al.* synthesised a small library of lipitoids (peptoid-phospholipid conjugates). These lipitoids led to a more active and stable compound in the serum than cationic lipids.<sup>75</sup>

Gene therapy promises to prevent and treat many diseases. Even though viruses are the best vectors for DNA delivery in gene therapy, there are many drawbacks to their use in therapeutic

---

<sup>72</sup>J. P. Turner; S. E. Chastain; D. Park; M. A. Moss; and S. L. Servoss, 'Modulating Amyloid- $\beta$  Aggregation: The Effects of Peptoid Side Chain Placement and Chirality', *Bioorganic and Medicinal Chemistry*, 25 (2017), 20–6.

<sup>73</sup>K. Kamimura; T. Suda; G. Zhang; and D. Liu, 'Advances in Gene Delivery Systems', *Pharmaceutical Medicine*, 25 (2012), 293–306.

<sup>74</sup>J. E. Murphy; T. Uno; J. D. Hamer; F. E. Cohen; V. Dwarki; and R. N. Zuckermann, 'A Combinatorial Approach to the Discovery of Efficient Cationic Peptoid Reagents for Gene Delivery.', *Proceedings of the National Academy of Sciences of the United States of America*, 95 (1998), 1517–22.

<sup>75</sup>C.-Y. Y. Huang; T. Uno; J. E. Murphy; S. Lee; J. D. Hamer; J. A. Escobedo; F. E. Cohen; R. Radhakrishnan; V. Dwarki; and R. N. Zuckermann, 'Lipitoids--Novel Cationic Lipids for Cellular Delivery of Plasmid DNA in Vitro.', *Chemistry & Biology*, 5 (1998), 345–54.

applications, such as uncertainties about safety. So, the methods quoted above investigate the structural requirement of cationic peptoids for efficient nontoxic DNA transfer to cells.

### 3.4 PPI-type helical structure of peptoids

After the successful synthesis of long oligomers, the next question was to discover the new set of rules which can govern the folding of a non-natural polymer in the absence of hydrogen bonding and chirality. The collaborative group from Profs. Cohen and Dill sought out to mimic peptide secondary structure: helices and sheets. Using molecular mechanics calculations, an octamer of (*S*)-*N*-(phenylethyl)glycine was predicted to form a right-handed helix with *cis* amide bonds and three residues per turn, similar to polyproline type I helix of proline-rich peptides (Figure 17).<sup>76</sup>

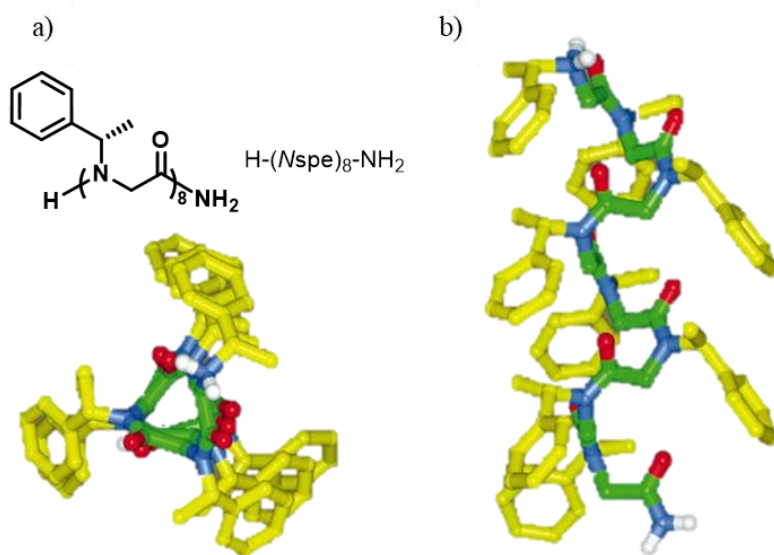


Figure 17 Molecular modelling of a peptoid octamer containing bulky chiral *S*-1-phenylethyl side chains (yellow), a) top view; b) side view.

Later on, the helical structure was demonstrated by NMR studies of a peptoid pentamer with the same chiral aromatic side chains. The Zuckermann's group further demonstrated that long peptoids could form helical structure using circular dichroism and 2D NMR.<sup>77</sup> Precisely, peptoids containing aromatic  $\alpha$ -chiral side chains adopt a polyproline type-I like helix, which has three monomers per

<sup>76</sup>P. Armand; K. Kirshenbaum; A. Falicov; R. L. Dunbrack; K. a Dill; R. N. Zuckermann; and F. E. Cohen, 'Chiral N-Substituted Glycines Can Form Stable Helical Conformations', *Folding and Design*, 2 (1997), 369–75.

<sup>77</sup>P. Armand; K. Kirshenbaum; R. A. Goldsmith; S. Farr-Jones; A. E. Barron; K. T. V Truong; K. A. Dill; D. F. Mierke; F. E. Cohen; R. N. Zuckermann; and E. K. Bradley, 'NMR Determination of the Major Solution Conformation of a Peptoid Pentamer with Chiral Side Chains', *Proceedings of the National Academy of Sciences of the United States of America*, 95 (1998), 4309–14.



turn and displays a  $\sim 6$  Å helical pitch. Differential scanning calorimetry (DSC) experiments showed that the calorimetric enthalpy of structure deformation in peptoid helices ( $\Delta H_{\text{cal}} = 1.1$  kcal/mol per residue) was comparable to that of  $\alpha$ -helical peptides ( $\Delta H_{\text{cal}} = 1.1$ -1.13 kcal/mol per residue). It was established that the helical conformations were exceptionally stable and could persist with even very short main-chain lengths.<sup>78</sup>

The group also focused on fundamental studies on the helix structural requirements and peptoid helix stability. In the first study, they focused on sequence requirements for the formation of stable peptoid helices.<sup>79</sup> The group compared more than 30 different heterooligomers consisting of mixed chiral and achiral side chains. It was observed that composition of at least 50%  $\alpha$ -chiral aromatic residues is necessary for the formation of stable helical structure in hexameric sequences for this family of peptoids. Moreover, an  $\alpha$ -chiral aromatic monomer was placed on the carboxy terminus, and sequences were designed periodically to maximise the number of “aromatic faces” on the peptoid helix. In a follow-up study, the group studied the effects of chain length, concentration, and temperature on secondary structure of peptoid homooligomers with a length ranging from 3 to 20 (*R*)-*N*-(1-phenylethyl)glycine (*Nrpe*) monomers.<sup>80</sup> They found that the oligo-*Nrpe* secondary structures are stable up to 75°C and the helices of peptoids become length-independent for chains longer than 12 residues. Finally, they studied the peptoid oligomers with  $\alpha$ -chiral aliphatic side chains like (*R*)-*N*-(1-cyclohexylethyl)glycine (*Nrch*).<sup>81</sup> They showed that peptoid oligomers with  $\alpha$ -chiral aliphatic side chains adopt helices like both the polyproline type I helix and the helical structure adopted by peptoids with  $\alpha$ -chiral aromatic side chains. As shown from the X-ray crystal structure in the Figure 18, the *Nrch* pentamer adopts a left-handed helix. The results from CD and 2D-NMR suggested that these  $\alpha$ -chiral aliphatic oligomers mostly adopt a repetitive helical structure with *cis*-amide bonds at long chain lengths.

---

<sup>78</sup>K. Kirshenbaum; A. E. Barron; R. A. Goldsmith; P. Armand; E. K. Bradley; K. T. V Truong; K. A. Dill; F. E. Cohen; and R. N. Zuckermann, ‘Sequence-Specific Polypeptoids: A Diverse Family of Heteropolymers with Stable Secondary Structure’, *Proceedings of the National Academy of Sciences of the United States of America*, 95 (1998), 4303–8.

<sup>79</sup>C. W. Wu; T. J. Sanborn; K. Huang; R. N. Zuckermann; and A. E. Barron, ‘Peptoid Oligomers with  $\alpha$ -Chiral, Aromatic Side Chains: Sequence Requirements for the Formation of Stable Peptoid Helices’, *Journal of the American Chemical Society*, 123 (2001), 6778–84.

<sup>80</sup>C. W. Wu; T. J. Sanborn; R. N. Zuckermann; and A. E. Barron, ‘Peptoid Oligomers with  $\alpha$ -Chiral, Aromatic Side Chains: Effects of Chain Length on Secondary Structure’, *Journal of the American Chemical Society*, 123 (2001), 2958–63.

<sup>81</sup>C. W. Wu; K. Kirshenbaum; T. J. Sanborn; J. A. Patch; K. Huang; K. A. Dill; R. N. Zuckermann; and A. E. Barron, ‘Structural and Spectroscopic Studies of Peptoid Oligomers with  $\alpha$ -Chiral Aliphatic Side Chains’, *Journal of the American Chemical Society*, 125 (2003), 13525–30.

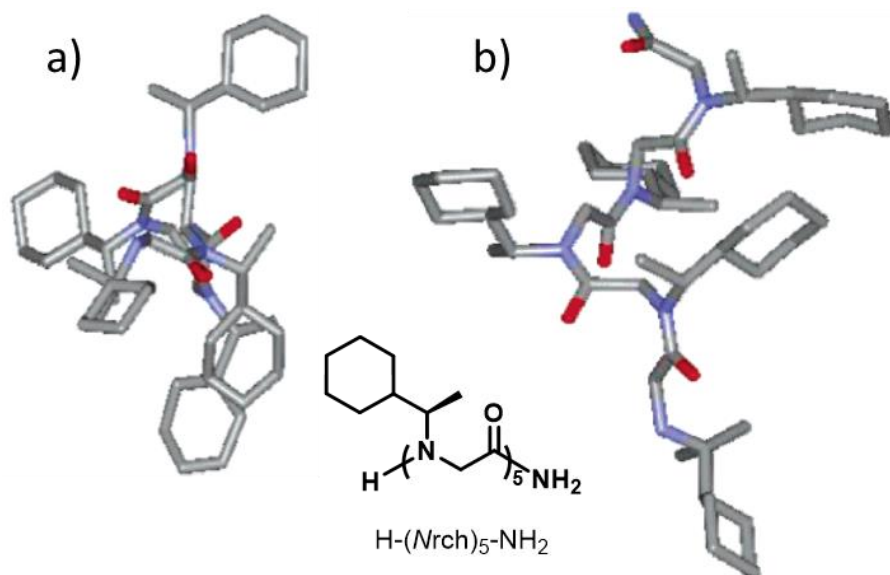


Figure 18 X-ray crystal structures of (R)-N-(1-cyclohexylethyl)glycine pentamer: a) top view; b) side view.

Peptoid helices have shown extreme stability even in 8M urea solution without denaturation and in temperatures up to 70°C.<sup>82</sup> Also, this study provided evidence for the stabilization of this type of helical structure by steric factors as peptoid secondary structure was highly insensitive to solvent environment and thermal agitations. The Yoon's group<sup>83</sup> investigated the effect of position-specific placement of  $\alpha$ -chiral aromatic monomers (*Nspe* and *Nrpe*) on the peptoid secondary structure using CD signatures.

The Blackwell's group<sup>84</sup> reported the synthesis and detailed structural analysis of a homo-oligomer series of (S)-N-(1-naphthylethyl)glycine (*Ns1npe*) peptoid by X-ray crystallography, NMR spectroscopy, and CD spectroscopy. They revealed that an *Ns1npe* peptoid monomer, dimer, trimer, and tetramer each adopt structures with all cis-amide bonds, with dihedral angles like those observed in polyproline type I (PPI) peptide helices and in peptoids with  $\alpha$ -chiral *spe* side chains (Figure 19, a).

<sup>82</sup>T. J. Sanborn; C. W. Wu; R. N. Zuckermann; and A. E. Barron, 'Extreme Stability of Helices Formed by Water-Soluble Poly-N-Substituted Glycines (Polypeptoids) with  $\alpha$ -Chiral Side Chains', *Biopolymers*, 63 (2002), 12–20.

<sup>83</sup>H.-M. Shin; C.-M. Kang; M.-H. Yoon; and J. Seo, 'Peptoid Helicity Modulation: Precise Control of Peptoid Secondary Structures via Position-Specific Placement of Chiral Monomers', *Chem. Commun.*, 50 (2014), 4465–8.

<sup>84</sup>J. R. Stringer; J. A. Crapster; I. A. Guzei; and H. E. Blackwell, 'Extraordinarily Robust Polyproline Type I Peptoid Helices Generated via the Incorporation of  $\alpha$ -Chiral Aromatic N -1-Naphthylethyl Side Chains', *Journal of the American Chemical Society*, 133 (2011), 15559–67.

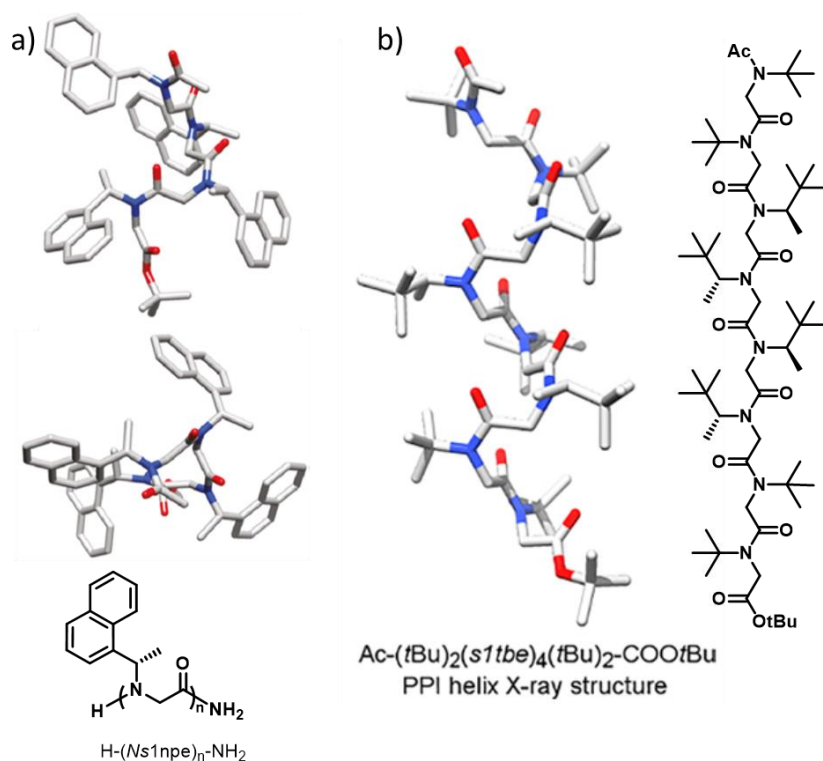


Figure 19 X-ray crystal structures of a) *Ns1npe* tetramer; b) *Ac-(tBu)<sub>2</sub>(s1tbe)<sub>4</sub>(tBu)<sub>2</sub>-COObu* octamer (CCDC: 1561295)

Recently our group developed conformationally homogeneous peptoid PPI helices composed exclusively of *N*-alkyl glycine monomers and of defined handedness.<sup>85</sup> The group has developed a new aliphatic chiral side chain (*S*)-(1-tert-butylethyl) (*s1tbe*) favouring the *cis* conformation based on side chain steric hindrance. The homooligomers formed by *Ns1tbe* can adopt dihedral angles consistent with those of PPI peptide and peptoid helices (Figure 19, b). The group also studied the folding properties of oligomers incorporating both tert-butyl (*tbu*) and *s1tbe* side chains. This work led to the longest oligomer solved in the solid state by X-ray crystallography.

### 3.5 Correlation between linear peptoid structure and antimicrobial activity

It was noticed that some cationic AMPs interact with the polyanionic surface of lipopolysaccharides by disrupting the outer membrane and later pass through the cytoplasmic membrane by self-promoted uptake.<sup>86</sup> Numerous properties of the cationic AMPs can influence

<sup>85</sup> O. Roy; G. Dumonteil; S. Faure; L. Jouffret; A. Kriznik; and C. Taillefumier, 'Homogeneous and Robust Polyproline Type I Helices from Peptoids with Nonaromatic  $\alpha$ -Chiral Side Chains', *Journal of the American Chemical Society*, 139 (2017), 13533–40.

<sup>86</sup> Y. Rosenfeld and Y. Shai, 'Lipopolysaccharide (Endotoxin)-Host Defense Antibacterial Peptides Interactions: Role in Bacterial Resistance and Prevention of Sepsis', *Biochimica et Biophysica Acta - Biomembranes*, Vol. 1758 (Elsevier, 2006), 1513–22.

their binding affinities for diverse sites on lipopolysaccharides such as molecular size, net charge, hydrophobicity, and overall steric bulk.<sup>87</sup> Therefore, it becomes important to study the structure and activity relationship (SAR) of the peptoids designed to mimic natural AMPs. Several groups have been studying the SAR of peptoids and have come up with interesting insights about the variations in different charge density distribution, overall hydrophobicities, steric hinderance, size of oligomers, etc. In this section we will go through the works of various groups to understand the SAR of designed antimicrobial peptoids.

### 3.5.1 Cationic amphipathic peptoid oligomers developed by the Barron's Group

Based on the threefold periodicity of the PPI-like helix of  $\alpha$ -peptoid, Barron's group at Stanford University in California designed cationic amphipathic oligomers mimicking the antimicrobial peptide Magainin-2 isolated from the skin of *Xenopus* frogs. Indeed, the cationic amphipathic helix was built by periodic incorporation of a cationic side chain every three residues, the remaining positions being occupied by the aromatic  $\alpha$ -chiral (*S*)-phenylethyl (*spe*) side chain which plays a dual role: hydrophobic group and PPI-like helix inducer. The resulting oligomers are structured and have a facial amphipathicity that allows to have comparable activity and selectivity to AMPs reported in the literature. They synthesised oligomers comprising of *N*-(4-aminobutyl)glycine (*Nlys*),  $\alpha$ -chiral (*S*)-*N*-(sec-butyl)glycine (*Nssb*), and  $\alpha$ -chiral aromatic (*S*)-*N*-(1-phenylethyl)glycine (*Nspe*) monomers. The oligomer H-(*NLys*-*Nspe*-*Nspe*)<sub>4</sub>-NH<sub>2</sub> showed potent antimicrobial properties for *E. coli* and *B. Subtilis* and good selectivity (Table 2, Figure 20).<sup>88</sup>

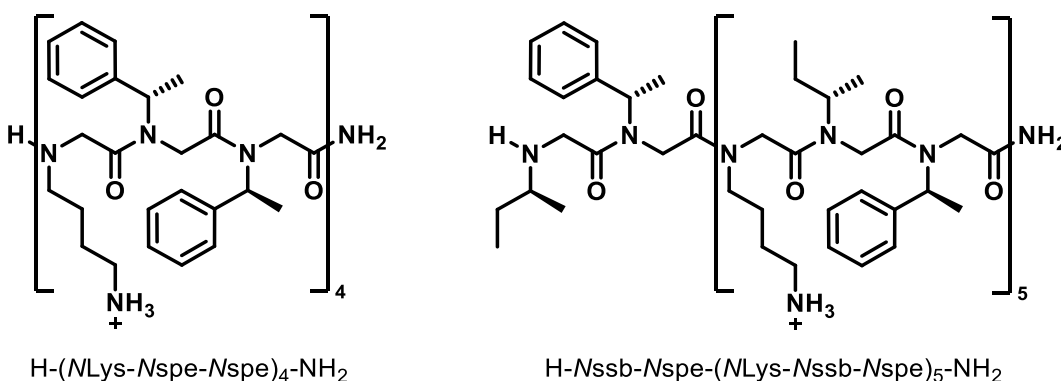


Figure 20 Structure of Peptoid Mimics of Magainin-2 peptide.

<sup>87</sup>H. Jenssen; P. Hamill; and R. E. W. Hancock, 'Peptide Antimicrobial Agents', *Clinical Microbiology Reviews*, Vol. 19 (American Society for Microbiology, **2006**), 491–511.

<sup>88</sup>J. A. Patch and A. E. Barron, 'Helical Peptoid Mimics of Magainin-2 Amide', *Journal of the American Chemical Society*, 125 (**2003**), 12092–3.

Table 2 Antibacterial and hemolytic activities of selected peptoids.

Oligomer	<i>E. coli</i> MIC	<i>B. subtilis</i> MIC	Haemolysis at <i>E. coli</i> MIC
<b>H-(NLys-Nspe-Nspe)<sub>4</sub>-NH<sub>2</sub></b>	5.4 μM	0.82 μM	1.4%
<b>H-Nssb-Nspe-(NLys-Nssb-Nspe)<sub>5</sub>-NH<sub>2</sub></b>	19 μM	1.4 μM	1.2%

In a more recent study from the same group, cationic amphiphilic peptoids of different sizes were synthesized as potential AMPs (Figure 21). Furthermore, the group reported a SAR based on a panel of 15 peptoids derived from the oligomers by varying hydrophobicity, chain length, amphipathicity and overall charge (Table 3). They concluded that the stereospecific interactions are not involved in the mechanism, the ratio of charge to hydrophobicity should be high to exhibit better cell selectivity. Helicity was found to be detrimental for haemolytic activities but has no real impact on antimicrobial activities since peptoids with weak CD signals kill bacteria with the same efficiency as those with intense CD spectra (characteristic of secondary structuration).<sup>89</sup>

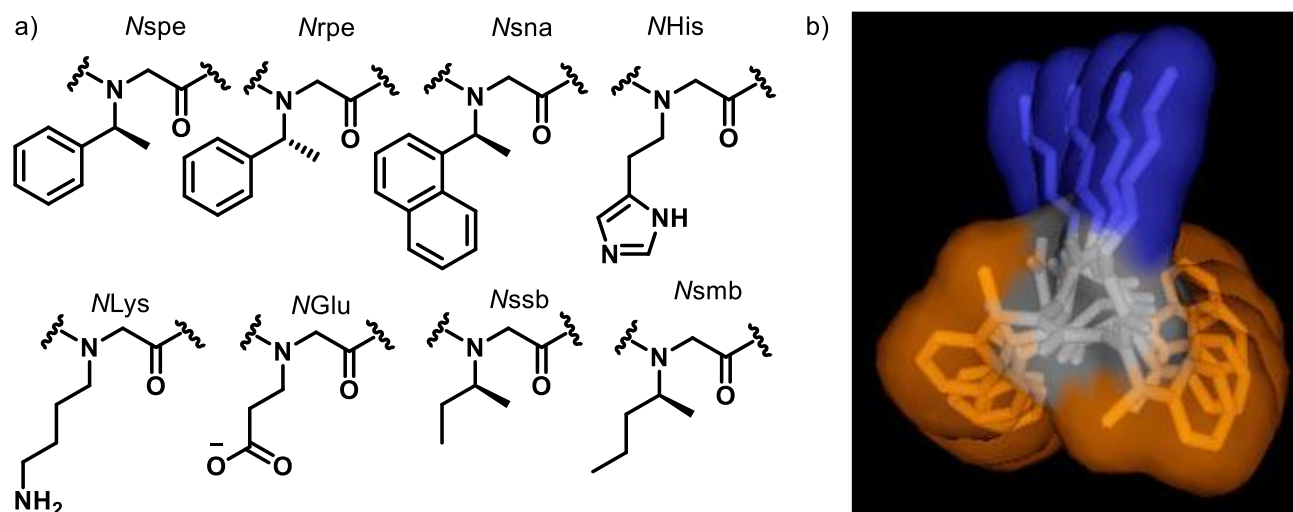


Figure 21 a) Structure of side chains employed for the design of AMP mimics b) Helicoidal antimicrobial peptoid mimicking Magainin-2<sup>89</sup>

Selectivity of the peptoids was evaluated using A549 lung epithelial cells. It shows that the metabolic inhibitory dose (ID) of these selected peptoids **1**, **6** (Table 3) compared favourably to that of pexiganan and melittin; ampetoids **7**, **8** with MICs <7 μM, had ID<sub>10</sub> ten and twenty times that of pexiganan.

<sup>89</sup>N. P. Chongsiriwatana; J. A. Patch; A. M. Czyzewski; M. T. Dohm; A. Ivankin; D. Gidalevitz; R. N. Zuckermann; and A. E. Barron, 'Peptoids That Mimic the Structure, Function, and Mechanism of Helical Antimicrobial Peptides.', *Proceedings of the National Academy of Sciences of the United States of America*, 105 (2008), 2794–9.

Table 3 Antibacterial, hemolytic and cell cytotoxicity activities of ampetoids and AMPs

Variant class		Sequence	<i>E. coli</i> MIC*	<i>B. subtilis</i> MIC*	HD <sub>10</sub> /HD <sub>50</sub> ** ( $\mu$ M)	ID <sub>10</sub> /ID <sub>50</sub> # ( $\mu$ M)
<b>Basis</b>	<b>1</b>	H-(NLys-Nspe-Nspe) <sub>4</sub> -NH <sub>2</sub>	3.5	0.88	21/100	4.01/8.94
	<b>2</b>	H-(NLys-Nssb-Nspe) <sub>4</sub> -NH <sub>2</sub>	31	3.9	>120/>120	N/A
<b>Chirality</b>	<b>3</b>	H-(NLys-Nrpe-Nrpe) <sub>4</sub> -NH <sub>2</sub>	3.5	0.88	16/86	N/A
<b>Length</b>	<b>4</b>	H-(NLys-Nspe-Nspe) <sub>2</sub> -NH <sub>2</sub>	27	27	>220/>220	N/A
	<b>5</b>	H-(NLys-Nspe-Nspe) <sub>3</sub> -NH <sub>2</sub>	9.1	1.2	>150/>150	N/A
	<b>6</b>	H-(NLys-Nspe-Nspe) <sub>5</sub> -NH <sub>2</sub>	5.5	1.4	3/19	1.57/2.96
<b>Hydrophobicity</b>	<b>7</b>	H-(NLys-Nspe-Nspe-NLys-Nspe-NHis) <sub>2</sub> -NH <sub>2</sub>	3.5	6.9	>110/>110	42.3/100
	<b>8</b>	H-NLys-(Nspe) <sub>2</sub> -NLys-Nspe-L-Pro-(NLys-Nspe-Nspe) <sub>2</sub> -NH <sub>2</sub>	3.1	1.6	63/>110	22.6/38.6
<b>Charge</b>	<b>9</b>	H-(NGlu-Nspe-Nspe) <sub>4</sub> -NH <sub>2</sub>	>219	>219	>110/>110	N/A
<b>Amphipathicity</b>	<b>10</b>	H-(Nlys) <sub>4</sub> -(Nspe) <sub>8</sub> -NH <sub>2</sub>	6.9	1.7	18/73	N/A
<b>AMPs</b>		Pexiganan	3.1	1.6	73/>200	1.83/4.08
		Melittin	1.6	0.78	2/6	0.49/0.71

\*MIC ( $\mu$ M), \*\*HD<sub>10</sub> and HD<sub>50</sub> are the concentrations of the compounds at which they cause 10% and 50% haemolysis of human erythrocytes, respectively, #10% metabolic inhibitory dose (ID<sub>10</sub>) and 50% inhibitory dose (ID<sub>50</sub>).

Peptoids **1** and **8** were studied for their antimicrobial properties to kill adherent bacteria.<sup>90</sup> Barron's group synthesized the peptoids with a peptoid spacer chain to allow mobility and an adhesive peptide moiety for smooth immobilization onto substrata. Substrata modified with Peptoid **8** exhibited increased bacterial adhesion, and a significant percentage of the adherent bacteria had compromised membranes, indicating that the surface-immobilised amphipathic peptoids can interact with the bacteria.

In a recent development, the Barron's group incorporated various hydrophobic or cationic residues to improve the selectivity of the previously developed peptoid H-(NLys-Nspe-Nspe)<sub>4</sub>-NH<sub>2</sub>. They carried out antibacterial and selectivity evaluation on the new peptoids. It was measured that one of the new analogue showed better selectivity while maintaining the antibacterial activity.<sup>91</sup> It was

<sup>90</sup> A. R. Statz; J. P. Park; N. P. Chongsiriwatana; A. E. Barron; and P. B. Messersmith, 'Surface-Immobilised Antimicrobial Peptoids.', *Biofouling*, 24 (2008), 439–48.

<sup>91</sup> J. Lee; D. Kang; J. Choi; W. Huang; M. Wadman; A. E. Barron; and J. Seo, 'Effect of Side Chain Hydrophobicity and Cationic Charge on Antimicrobial Activity and Cytotoxicity of Helical Peptoids', *Bioorganic and Medicinal Chemistry Letters*, 28 (2018), 170–3.

interesting to note the remarkable selectivity displayed by the peptoid H-(NLys-Nspe-Nspe)<sub>4</sub>-NLys-NH<sub>2</sub> by the addition of only one additional Nlys group to the nonamer reference (Table 4).

Table 4 Antibacterial, haemolytic and cytotoxicity values of peptoids

Compounds	<i>E. coli</i> MIC*	<i>B. subtilis</i> MIC*	HD <sub>10</sub> /HD <sub>50</sub> **	LC <sub>50</sub> <sup>#</sup> Jurkat	LC <sub>50</sub> <sup>#</sup> MRC5
<b>H-(NLys-Nspe-Nspe)<sub>4</sub>-NH<sub>2</sub></b>	1.6	0.8	9.1/63.4	2.21	8.0
<b>H-(NLys-Nspe-Nspe)<sub>4</sub>-Nlys-NH<sub>2</sub></b>	1.6	0.4	19.5/>200	5.04	10.0
<b>H-(NLys-Nspe-Nspe)<sub>3</sub>-Nlys-NH<sub>2</sub></b>	1.6	0.8	>200/>200	28.9	80.5

\*MIC (μM); \*\*HC<sub>10</sub> and HC<sub>50</sub> are the concentrations of the compounds at which they cause 10% and 50% haemolysis of rat erythrocytes, respectively. <sup>#</sup>LC<sub>50</sub>: 50% lethal concentration.

### 3.5.2 Peptoids rich in lysine and tryptophan side chains developed by the Jenssen's Group

The Jenssen's group studied the structure-activity relationship by investigating the effects of increasing hydrophobicity, single monomer substitution and chain length variation. In this study, peptoid oligomers were not designed to form helical secondary structures. On the contrary, according to the nature of the side chains employed, a high flexibility of the oligomers can be expected. Accordingly, the design was not based on the threefold periodicity of the PPI-helix of α-peptoids. The group also studied various 8-9 residue long cationic amphipathic peptoids with net charge of +4 and various sequence patterns of hydrophobic and cationic residues. A library of 22 peptoids were prepared and they found that the oligomers H-(Nlys)<sub>4</sub>-(NTrp)<sub>4</sub>-Nile-NH<sub>2</sub> (**A**) and H-(NLys-NTrp-(NLys)<sub>2</sub>-(NTrp)<sub>2</sub>-NLys-Ntrp-Npm)-NH<sub>2</sub> (**B**) showed high selectivity ratios (HC<sub>10</sub>/MIC) of 4-32 and 8-64, respectively (Table 5, Figure 22).<sup>92</sup>

Table 5 in vitro antibacterial, haemolytic, and cytotoxic activities of selected compounds

Peptoid	Minimum inhibitory concentration MIC (μg/ml)						Selectivity ratio* HC <sub>10</sub> <sup>#</sup> /MIC	Cytotoxicity (μg/ml) IC <sub>50</sub>
	<i>S. aureus</i>		<i>E. coli</i>		<i>P. aeruginosa</i>			
	ATCC 29213	C623 MRSA	ATCC 25922	63103 ESBL	PAO1	H1027 MDR		
<b>A</b>	8	8	32	8	32	4	32-4	110
<b>B</b>	8	8	16	16	32	4	64-8	104

<sup>#</sup>HC<sub>10</sub>: the concentrations of the compounds at which they cause 10% haemolysis; \*selectivity ratio is defined as quotient of 10 % haemolysis and the highest and lowest MIC of the bacterial strains

<sup>92</sup>B. Mojsoska; R. N. Zuckermann; and H. Jenssen, 'Structure-Activity Relationship Study of Novel Peptoids That Mimic the Structure of Antimicrobial Peptides.', *Antimicrobial Agents and Chemotherapy*, 59 (2015), 4112–20.

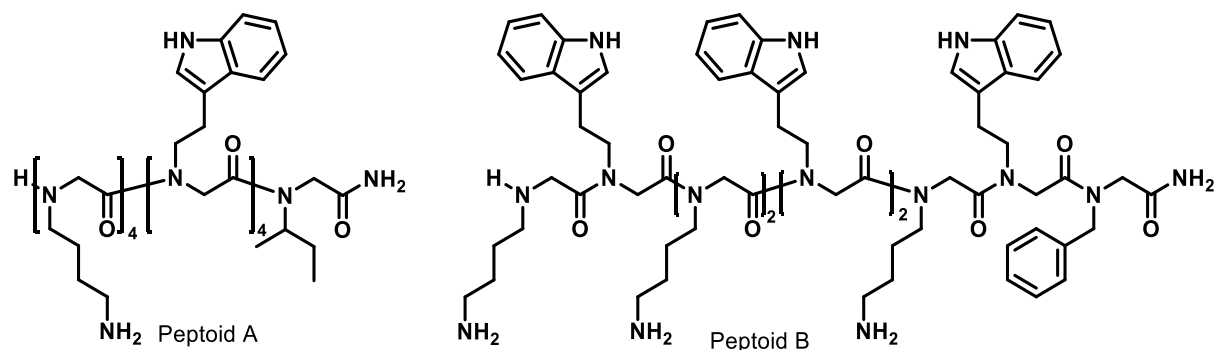


Figure 22 Chemical structure of peptoid A and peptoid B

To confirm the mode of action of these peptoids, a follow-up study was performed and suggested that these peptoids act via a mechanism involving both membrane disruption and probable intracellular targets against *E. coli*.<sup>93</sup> They observed changes in membrane morphology of bacteria upon treatment with peptoids using dye leakage assays (Figure 23). The rate of bacterial lysis was measured by calcein leakage from lipid vesicles mimicking bacterial membranes. Higher degree of bacterial lysis through membrane damage was observed for peptoid A. The peptoid A led to a substantial decrease in DNA per cell mass, at faster rate compared to that of ciprofloxacin. The authors assumed that besides the peptoids effect on the outer membrane, they enter the cytoplasm and bind to internal targets thus inhibiting central dogma.

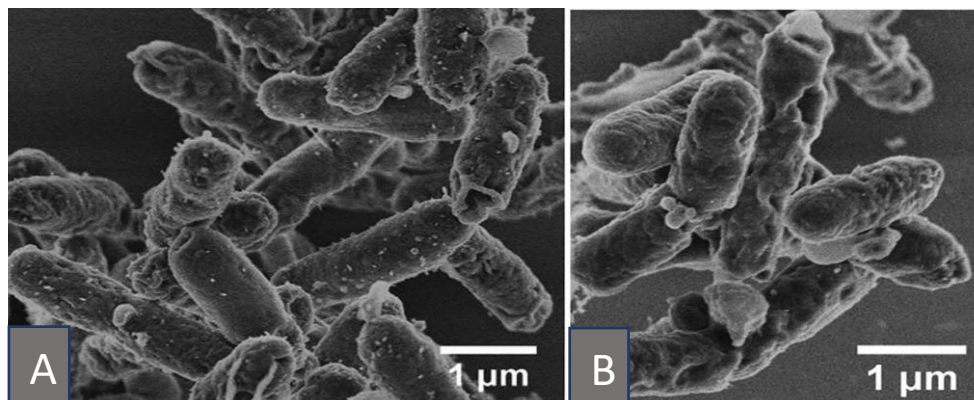


Figure 23 Scanning electron micrographs of *E. coli* ATCC 25922 exposed to peptoids A and B at  $4 \times \text{MIC}$  for 4 hours.<sup>93</sup>

### 3.5.3 Development of a QSAR model for antimicrobial activity prediction

A collaborative work between the Barron's and Hancock's groups was carried out to accurately correlate structure of antimicrobial peptoids with their antimicrobial activity. They developed a

<sup>93</sup>B. Mojsoska; G. Carretero; S. Larsen; R. V. Mateiu; and H. Jenssen, 'Peptoids Successfully Inhibit the Growth of Gram Negative *E. Coli* Causing Substantial Membrane Damage', *Scientific Reports*, 7 (2017), 1–12.



quantitative structure–activity relationship (QSAR) model capable to predict the antimicrobial activities of peptoids.<sup>94</sup> To this aim, 27 peptoid sequences were studied using several *in silico*, *in vitro*, and *in vivo* techniques. The model was based on 10 chemical descriptors: six are directly connected with the charge and the last four are related to molecular shape, surface area, and potential energy (Table 6, Figure 24).

Table 6 The ten major descriptors used to build the predictive model.<sup>94</sup>

Descriptor	Description	Category
<b>PEOE_VSA_FPPOS</b>	Fractional positive polar van der Walls surface area	Partial charge
<b>Q_VSA_FNEG</b>	Fractional negative van der Walls surface area	Partial charge
<b>PEOE_VSA+2</b>	Sum of $v_i$ where $q_i$ is in the range [0.0, 0.15]	Partial charge
<b>Q_RPC+</b>	Relative positive partial charge	Partial charge
<b>Q_VSA_FPOL</b>	Fractional polar van der Walls surface area	Partial charge
<b>FASA_H</b>	Fractional ASA_H calculated as ASA_H/ASA	Conformation dependent charge
<b>E_nb</b>	Value of potential energy with all bonded terms disabled	Potential energy
<b>glob</b>	Globularity; 1 = a sphere, 0 = a two-/one- dimensional object	Surface area, volume & shape
<b>VAdjEq</b>	Vertex adjacency information (equality)	Atom- & bond- counts
<b>SMR_VSA3</b>	Sum of $v_i$ such that $R_i$ is in [0.35, 0.39]	Subdivided surface areas

<sup>94</sup>A. M. Czyzewski; H. Jenssen; C. D. Fjell; M. Waldbrook; N. P. Chongsiriwatana; E. Yuen; R. E. W. W. Hancock; and A. E. Barron, 'In Vivo, in Vitro, and in Silico Characterization of Peptoids as Antimicrobial Agents', *PLoS ONE*, 11 (2016), 1–17.

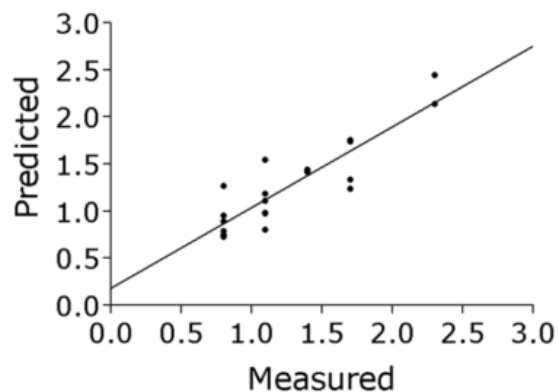


Figure 24 Illustrates predicted and measured log (MIC in  $\mu\text{M}$ ) for the peptoids in the generated QSAR model.<sup>94</sup>

The most active compound was still the dodecamer H-(NLys-Nspe-Nspe)<sub>4</sub>-NH<sub>2</sub> reported in the original article from Barron.<sup>88</sup> Indeed this dodecamer was more active than the synthetic AMPs (MSI-78 and MX-226) and showed MICs  $\leq 8 \mu\text{g/mL}$  for 19 out of the 20 multi drug resistant (MDR) bacterial strains. In vivo studies were conducted on a murine model with invasive *S. aureus*, the oligomer H-(NLys-Nspe-Nspe)<sub>4</sub>-NH<sub>2</sub> (conc. 4 mg/kg) was able to reduce colony forming units by two log orders in the peritoneum membrane without causing any medium-term toxicity and mortality. The study not only puts emphasis on the analogous behaviour of peptoids and AMPs, but also establishes the effectiveness of computer models to enable the rational design of future generations of peptoids.

#### 3.5.4 Cationic amphipathic peptoid oligomers developed by the Cobb's group

Another parameter that has been considered essential for the rational design of the biologically active molecules is hydrophobicity.<sup>95</sup> However, for larger molecules like peptoids, it becomes difficult to use average hydrophobicity as a useful predictive tool for rational design. Typically, average hydrophobicity is measured by RP-HPLC retention time values,<sup>92,89</sup> but recently the Cobb's group used the partitioning experiments in octanol and phosphate buffered saline (PBS), to determine the log D values for a series of peptoids.<sup>96</sup> They compared the values of log D and average hydrophobicities determined by HPLC experiments, and found out that the log D values have an advantage over the later as a predictive tool in the rational design of the therapeutically active peptoids (Figure 25). This study shows that the log D values may be a better tool than HPLC

<sup>95</sup>Y. C. Tang and C. M. Deber, 'Hydrophobicity and Helicity of Membrane-Interactive Peptides Containing Peptoid Residues', *Biopolymers*, 65 (2002), 254–62.

<sup>96</sup>H. L. Bolt; C. E. J. Williams; R. V. Brooks; R. N. Zuckermann; S. L. Cobb; and E. H. C. Bromley, 'Log D versus HPLC Derived Hydrophobicity: The Development of Predictive Tools to Aid in the Rational Design of Bioactive Peptoids', *Biopolymers*, 108 (2017), 1–7.

retention time to characterised peptoid oligomers hydrophobicity, but more data is required to further probe the potential application of using log D values as predictive tools in the future.

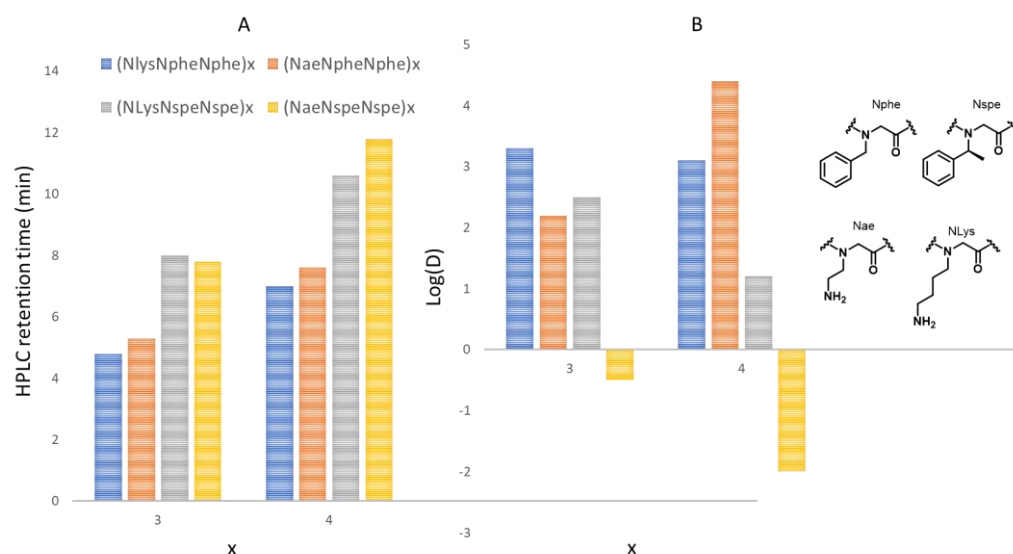


Figure 25 Comparison of average and folded hydrophobicities for peptoid sequences with different lengths, containing either chiral (Nspe) or achiral (Nphe) residues and containing either shorter (Nae) or longer (NLys) positive side chains: (A) reverse phase HPLC retention times and (B) log D values.

Results from actual studies of peptoid-type mimetics of AMPs clearly suggest that peptoids are a promising class of antimicrobial agents but the toxicity data is often limited to the haemolytic activities. To correlate toxicity profiles and antibacterial activities, a large library of cationic peptoids, composed of 18 published and 26 new sequences incorporating 12 different monomers (4 cationic and 8 hydrophobic peptoid residues, Figure 26), have been studied.<sup>97</sup> All sequences were designed using the threefold periodicity of the PPI-like helix of  $\alpha$ -peptoids to get amphiphilic architectures.

<sup>97</sup> H. L. Bolt; G. A. Eggimann; C. A. B. Jahoda; R. N. Zuckermann; G. J. Sharples; and S. L. Cobb, 'Exploring the Links between Peptoid Antibacterial Activity and Toxicity', *Med. Chem. Commun.*, 8 (2017), 886–96.

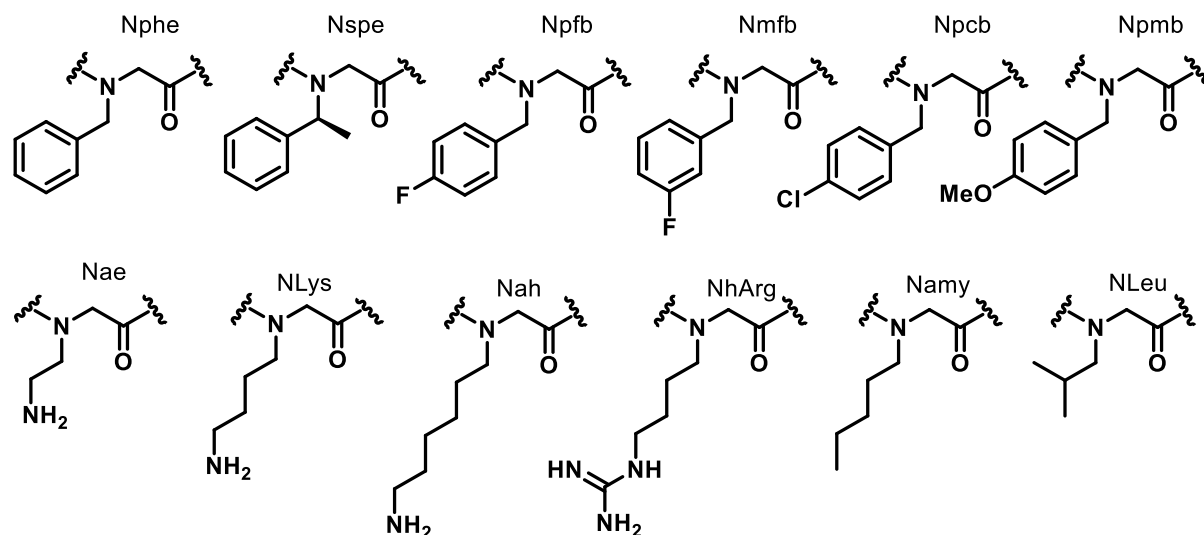


Figure 26 Different peptoid monomers utilized in the study<sup>97</sup>

The toxicity of each ampetoid was assessed against two mammalian cell lines HaCaT and HepG2 and correlated with MIC against two Gram-negative bacteria (*Escherichia coli* and *Pseudomonas aeruginosa*) and two Gram-positive bacteria (*Staphylococcus aureus* and *epidermidis*). As already observed in previous studies, peptoids were more active on Gram-positive bacteria due to their single-unit lipid membrane. Concerning Gram-negative bacteria, *P. aeruginosa* proved to be more resistant than *E. coli* upon peptoid exposition. This low activity on *P. aeruginosa* could be attributed to the special lipid composition of its membrane and/or its ability to form biofilms. It was observed that the introduction of several chiral aromatic *Nspe* residue has a detrimental effect on toxicity. Besides, since many peptoids incorporating only achiral residues exhibited potent activities with low toxicity to mammalian cells, the helical structuration does not appear to be required for antimicrobial properties. It was also noticed that fluorine substitution on aromatic side chains enhanced activity. According to the authors, peptoids having potent activity against bacteria and negligible toxicity on mammalian cells may indicate that cell membrane disruption is not the only mechanism involved.

### 3.6 Cyclic peptoids

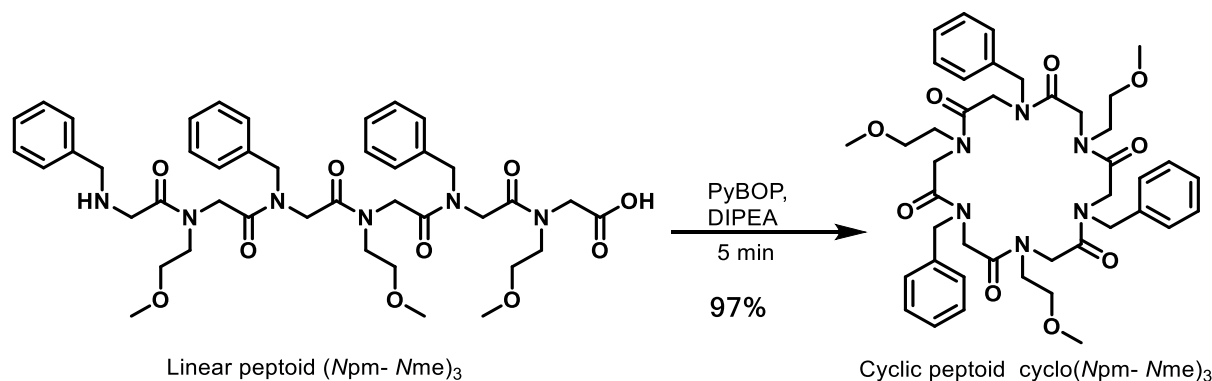
Macrocycles are a promising but perhaps underexploited class of potential therapeutic compounds.<sup>98</sup> A simple solution to rigidify the structures and to constrain them spatially is the

<sup>98</sup>E. M. Driggers; S. P. Hale; J. Lee; and N. K. Terrett, 'The Exploration of Macrocycles for Drug Discovery - An Underexploited Structural Class', *Nature Reviews Drug Discovery*, Vol. 7 (2008), 608–24.

cyclization. Cyclic peptoids could allow the presentation of pharmacophores in space in a manner required for optimal interaction with a receptor.<sup>99</sup>

### 3.6.1 Conformational structure of cyclic peptoids

The Kirshenbaum group reported in 2007 that peptoids can undergo highly efficient head-to-tail macrocyclization reactions. This study has shown that cyclization is mostly effective from pentamer to 20 mers. They were successfully able to convert linear oligomers to macrocyclic products in the presence of PyBOP within 5 minutes at room temperature with yields higher than 85%.<sup>100</sup> Also, there was striking difference in the cyclic conversion efficiency of the peptoid and its corresponding peptide. For instance, the cyclic conversion of the hexapeptoid (*Npm-Nme*)<sub>3</sub> was twice efficient (yield of 97% determined by HPLC) than its corresponding peptide (*Hse*<sup>(Me)</sup>-*Phe*)<sub>3</sub> (Scheme 2).



Scheme 2 Conversion of a linear hexapeptoid (*Npm-Nme*)<sub>3</sub> into its cyclic counterpart.

This cyclisation efficiency can easily be explained by the fact that linear peptoids in solution can explore a larger conformational space than peptides. Numerous studies in model peptide sequences have shown that incorporation of *N*-alkylated amino acid residues can support intramolecular cyclization.<sup>101</sup> The higher proportion of *cis* rotamer as compared to *trans* rotamer on the tertiary amide bonds permits the formation of turns facilitating the macrocyclization.<sup>102</sup>

<sup>99</sup>B. Yoo; S. B. Y. Shin; M. L. Huang; and K. Kirshenbaum, 'Peptoid Macrocycles: Making the Rounds with Peptidomimetic Oligomers', *Chemistry - A European Journal*, 16 (2010), 5527–37.

<sup>100</sup>S. B. Y. Shin; B. Yoo; L. J. Todaro; and K. Kirshenbaum, 'Cyclic Peptoids', *Journal of the American Chemical Society*, 129 (2007), 3218–25.

<sup>101</sup>J. Blankenstein and J. Zhu, 'Conformation-Directed Macrocyclization Reactions', *European Journal of Organic Chemistry*, 2005 (2005), 1949–64.

<sup>102</sup>G. Scherer; M. L. Kramer; M. Schutkowski; U. Reimer; and G. Fischer, 'Barriers to Rotation of Secondary Amide Peptide Bonds', *Journal of the American Chemical Society*, 120 (1998), 5568–74.

It was further established that introduction of the covalent constraint improves conformational ordering, allowing for the crystallization of a cyclic peptoid hexamer (Figure 27). Moreover, the crystal analysis of these macrocycles has shown that the peptoid skeleton appears to be a suitable candidate for spatially defined arrangement of pharmacophores. Certainly, the skeleton is superimposable with  $\beta$ -turns structure.<sup>100</sup> It is evident from the crystal structure of the cyclic peptoid that the side chains are projected on either side of the skeletal plane.

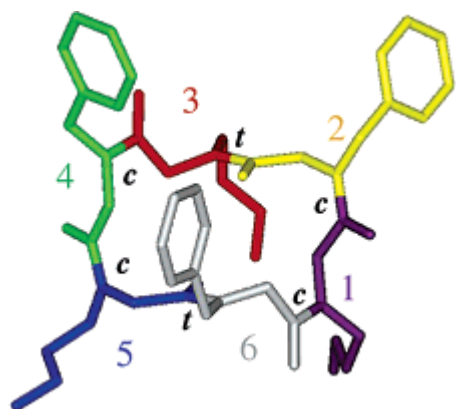


Figure 27 Crystal structure of cyclic hexapeptoid showing the projection of side chains.<sup>100</sup>

Shortly thereafter, Izzo and De Riccardis reported three cyclic peptoids bearing benzyloxyethyl side chains, of varied sizes: cyclotrimer, cyclotetramer, and cyclohexamer.<sup>103,104</sup> They found out that the cyclic trimer and tetramer adopt a unique conformation in solution by using proton NMR, molecular modelling, and X-ray diffraction (XRD). The cyclic trimer takes a crown conformation with all amide bonds in *cis* form and  $\alpha$   $C_3$  axis of symmetry. The cyclic tetramer has an alternation of *cis* and *trans* amides and a centre of symmetry. But, the hexamer is less rigid in solution and exists in equilibrium between different conformations. However, the addition of cations ( $Na^+$ ,  $NH_4^+$  or  $PhCH_2NH_3^+$ ) in the solution medium helps it to form a single complexed conformation, the lowest in energy according to the calculations, with all the amides in *trans* and a  $S_6$  axis of symmetry (Figure 28).

<sup>103</sup> N. Maulucci; I. Izzo; G. Bifulco; A. Aliberti; C. De Cola; D. Comegna; C. Gaeta; A. Napolitano; C. Pizza; C. Tedesco; D. Flot; and F. De Riccardis, 'Synthesis, Structures, and Properties of Nine-, Twelve-, and Eighteen-Membered N-Benzyloxyethyl Cyclic  $\alpha$ -Peptoids', *Chemical Communications*, 0 (2008), 3927.

<sup>104</sup> D. Comegna; M. Benincasa; R. Gennaro; I. Izzo; and F. De Riccardis, 'Design, Synthesis and Antimicrobial Properties of Non-Hemolytic Cationic  $\alpha$ -Cyclopeptoids', *Bioorganic & Medicinal Chemistry*, 18 (2010), 2010–8.

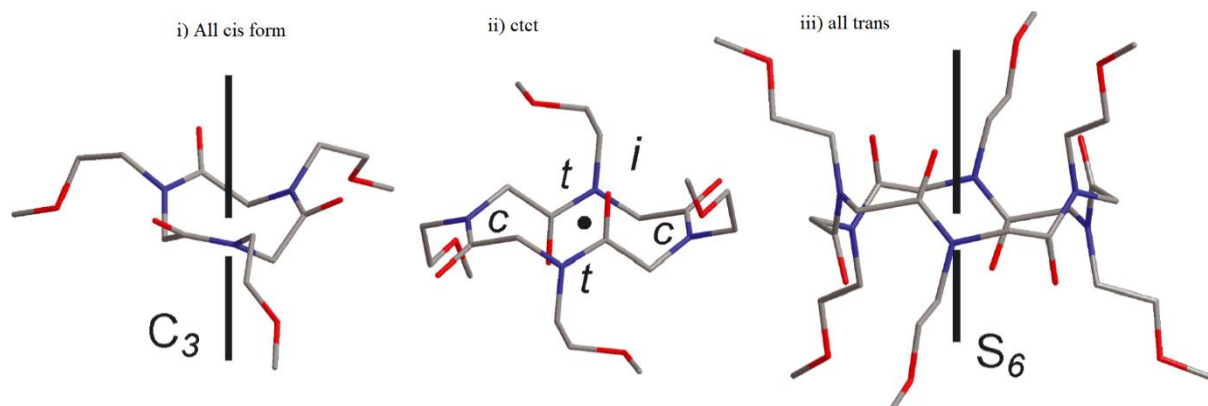


Figure 28 Predicted lowest energy conformations of cyclic peptoids having benzyloxyethyl side chains: i) cyclotrimer, ii) cyclotetramer, iii) cyclohexamer<sup>103</sup>

### 3.6.2 Design of cationic amphiphilic cyclic peptoids

According to the X-ray structure of peptoid cyclohexamer, the construction of cationic amphiphilic architectures could be done by introduction of hydrophobic and cationic side chains in an alternative manner. Kirshenbaum and co-workers synthesized a series of cyclic short peptoid sequences that contain cationic and hydrophobic side chains, and investigated the effect of head-to-tail cyclisation on the antimicrobial activity.<sup>105</sup> Fifteen cyclic peptoids (6–10 residues) were compared to the corresponding acetylated linear peptoid (Figure 29). This study showed that cyclisation and increasing length generally improved antimicrobial activity. Besides most of these cyclic compounds revealed non-haemolytic toward human red blood cells. Best MIC values were obtained against *Bacillus subtilis* (0.5  $\mu\text{g}/\text{mL}$  for cyclopeptoid C8) and MIC values for *Escherichia coli* and *Staphylococcus aureus* were modest with 7.8  $\mu\text{g}/\text{mL}$  as the best value. In another study where they synthesised and evaluated 26 cyclic peptoids containing cationic aminopropyl groups and many hydrophobic residues, better activities against *S. aureus* were obtained.<sup>106</sup> Nine of the cyclopeptoids were very active against MRSA (MICs  $\leq 3.9$   $\mu\text{g}/\text{mL}$ ).

<sup>105</sup>M. L. Huang; S. B. Y. Shin; M. A. Benson; V. J. Torres; and K. Kirshenbaum, 'A Comparison of Linear and Cyclic Peptoid Oligomers as Potent Antimicrobial Agents', *ChemMedChem*, 7 (2012), 114–22.

<sup>106</sup>M. L. Huang; M. A. Benson; S. B. Y. Shin; V. J. Torres; and K. Kirshenbaum, 'Amphiphilic Cyclic Peptoids That Exhibit Antimicrobial Activity by Disrupting Staphylococcus Aureus Membranes', *European Journal of Organic Chemistry* (2013), 3560–6.

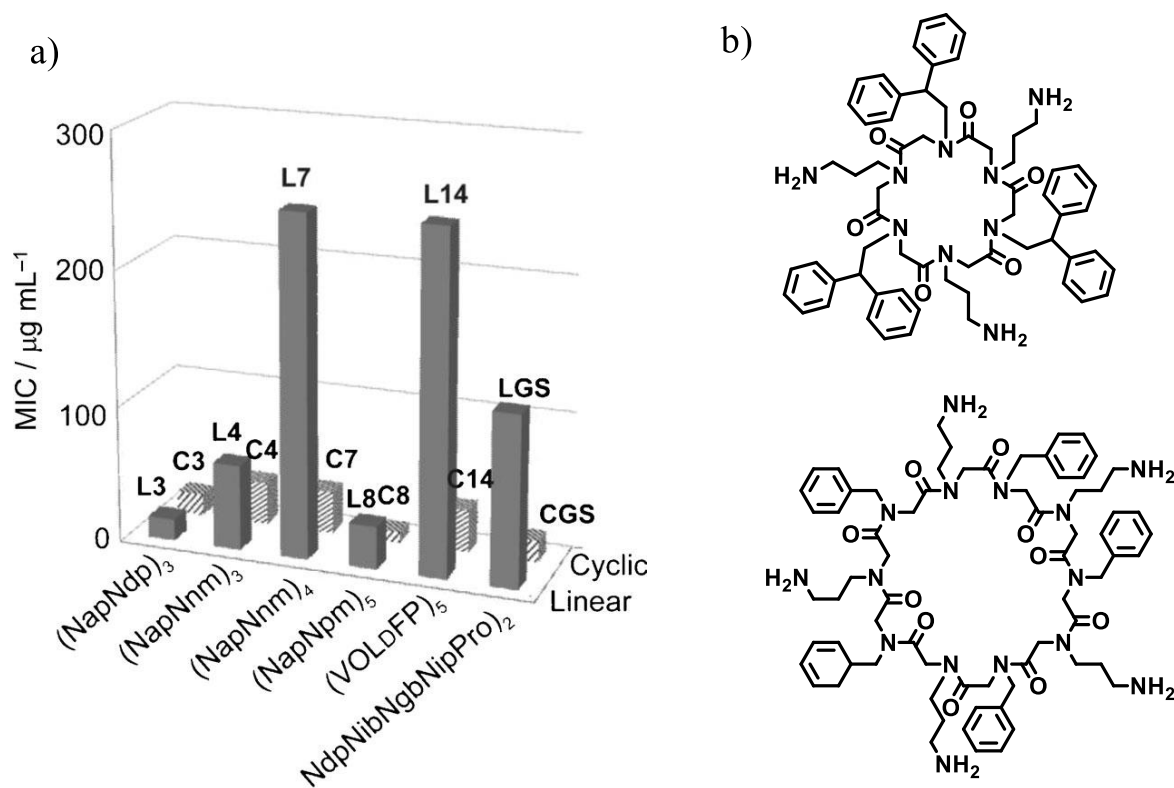


Figure 29 a) Antimicrobial activity against *E. coli* for six cyclic peptoids and their linear counterparts; Nap: N-(3-aminopropyl)glycine; Ndp: N-(2,2-diphenylethyl)glycine; Nnm: N-(1-naphthylmethyl)glycine; Npm: N-(phenylmethyl)glycine; Nib: N-(isobutyl)glycine; Ngb: N-(4-guanidinobutyl)glycine; Nip: N-(isopropyl)glycine;<sup>105</sup> and b) Structures of the most potent cyclic peptoids

The emergence in antimicrobial resistance by using cyclic peptoid C3 was also assessed on clinical strains of both methicillin-resistant and methicillin-sensitive *S. aureus*. This study showed that no change in MIC was observed over 21 days, indicating the absence of the development of antimicrobial resistance.<sup>105</sup>

The same group also studied the mechanism of action of these molecules. It was observed by electron microscopy experiments that these cyclopeptoids target and damage the cytoplasmic membrane through formation of pores (Figure 30).<sup>106</sup>

They went further to study the membrane interactions of linear and cyclic versions by using scanning electron microscopy on bacterial cells, and high-resolution X-ray scattering and epifluorescence microscopy on Langmuir monolayers of anionic lipids. They found that cyclisation



of antimicrobial peptoids (Nap-Ndp)<sub>3</sub> and (Nap-Nnm)<sub>3</sub> increases the membrane activity and suggested this can be related to the reduced conformational flexibility of the cyclic peptoids.<sup>107</sup>

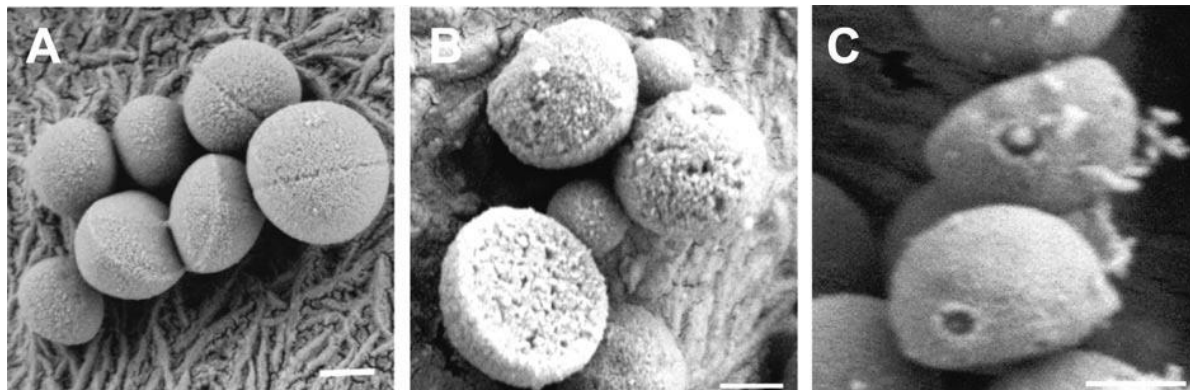


Figure 30 Membrane damage caused by cyclic peptoid oligomers: Untreated MRSA USA300 cells (A); MRSA USA300 cells incubated with C3 at its MIC (3.9 µg/mL) for 1 h (C) or 18 h (B)<sup>106</sup>

### 3.7 Peptide-peptoid hybrids

Another strategy to improve the therapeutic profile of peptides is the design of chimeras incorporating both natural amino acid and peptidomimetic residues.  $\alpha$ - or  $\beta$ -peptoid residues have been mixed with  $\alpha$ -amino acids to give rise to novel backbone sequence.<sup>108</sup> One way to design hybrid peptide-peptoid oligomers is the replacement of one or several residues by *N*-substituted glycine residues at specific position of a peptide sequence in order to increase stability, increase selectivity or affinity. This strategy was first employed by Goodman's group in the eighties.<sup>109</sup> In the field of antibacterial development, the Hansen group used a positional scanning combinatorial library to identify lysine-peptoid hybrid oligomers with high antibacterial activity against *E. coli* and *S. aureus* and low haemolytic activity.<sup>110</sup> Another way is to build new type of sequence of alternated peptide and peptoid residues in order to study the backbone preferences and the properties of these novel oligoamides. Herein, we will focus on this type of peptide-peptoid hybrids.

---

<sup>107</sup>K. Andreev; M. W. Martynowycz; A. Ivankin; M. L. Huang; I. Kuzmenko; M. Meron; B. Lin; K. Kirshenbaum; and D. Gidalevitz, 'Cyclization Improves Membrane Permeation by Antimicrobial Peptoids', *Langmuir*, 32 (2016), 12905–13.

<sup>108</sup> C. A. Olsen, 'Peptoid-Peptide Hybrid Backbone Architectures', *ChemBioChem*, Vol. 11 (Wiley-Blackwell, 2010), 152–60.

<sup>109</sup> M. Goodman; G. Melacini; and Y. Feng, 'Collagen-like Triple Helices Incorporating Peptoid Residues', *Journal of the American Chemical Society*, 118 (1996), 10928–9.

<sup>110</sup> T. S. Ryge and P. R. Hansen, 'Potent Antibacterial Lysine-Peptoid Hybrids Identified from a Positional Scanning Combinatorial Library', *Bioorganic and Medicinal Chemistry*, 14 (2006), 4444–51.

In the context of antimicrobial compounds, these type of hybrid oligomers have been mainly studied by Danish researchers.<sup>33</sup> The first generation of hybrid peptide-peptoid oligomers has been introduced by Olsen and co-workers.<sup>111</sup> Sequences were constructed by alternating repeats of  $\alpha$ -amino acids and chiral *N*-alkyl alanine (i.e.  $\beta$ -peptoid) residues. Unlike peptoids, this heteromeric backbone may adopt secondary structure stabilized by intramolecular hydrogen bonds. In order to elaborate cationic amphipathic architectures, lysine or arginine were used as cationic amino acids and  $\alpha$ -chiral *N*spe or achiral *N*Bn peptoid residues as hydrophobic counterparts (Figure 31). Synthesis of oligomers up to 16 residues long was achieved by SPPS of block dimer and conformational preferences were studied by circular dichroism. Significant chain-length effect on CD spectra was observed suggesting that hydrogen bonding contributes to the stabilization of a secondary structure present in solution.

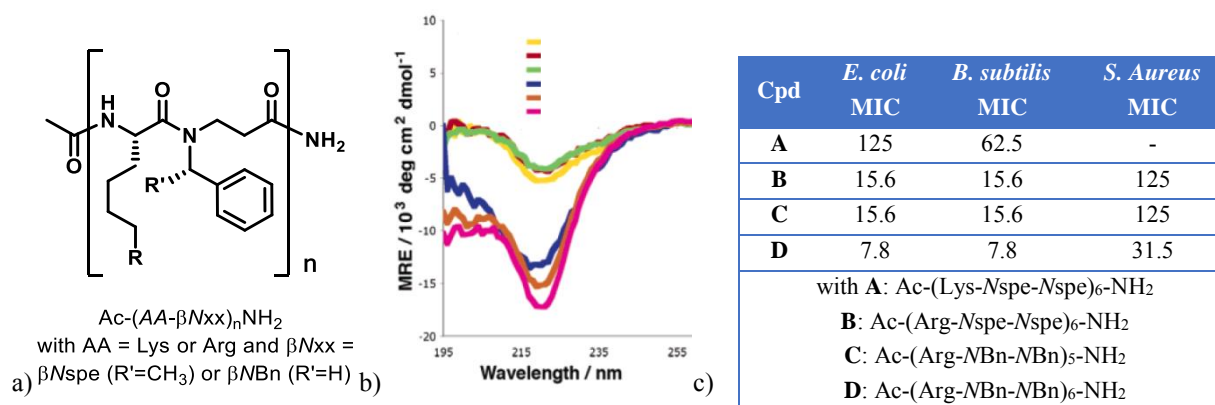


Figure 31 a) Structure of cationic amphipathic  $\alpha$ -peptide/ $\beta$ -peptoid hybrid oligomers developed by Olsen (*spe* for (*S*)-1-phenylethyl and *Bn* for benzyl), b) CD spectra at 60  $\mu$ M of oligomers Ac-(Arg-*N*Bn-*N*Bn)<sub>n</sub>-NH<sub>2</sub> with n = 6 (yellow curve) n = 7 (red curve), n = 8 (green curve) and Ac-(Arg-*N*spe-*N*spe)<sub>n</sub>-NH<sub>2</sub> with n = 6 (blue curve) n = 7 (orange curve), n = 8 (pink curve); and c) Antimicrobial activities MIC in  $\mu$ g/mL.

Antimicrobial tests showed that guanidinium-functionalized hybrids were more potent than lysine-functionalized one but could in certain case be accompanied by a concomitant increase in toxicity towards mammalian cells. It was also observed that the less structured oligomers according to CD experiments were more active than the structured ones. Larger library of these chimeras were further studied.<sup>112</sup>

<sup>111</sup> C. A. Olsen; G. Bonke; L. Vedel; A. Adersen; M. Witt; H. Franzyk; and J. W. Jaroszewski, ' $\alpha$ -Peptide/ $\beta$ -Peptoid Chimeras', *Organic Letters*, 9 (2007), 1549–52.

<sup>112</sup> C. A. Olsen; H. L. Ziegler; H. M. Nielsen; N. Fridomdt-Møller; J. W. Jaroszewski; and H. Franzyk, 'Antimicrobial, Hemolytic, and Cytotoxic Activities of  $\beta$ -Peptoid- Peptide Hybrid Oligomers: Improved Properties Compared to Natural AMPs (ChemBioChem (2010) 11, (152-160))', *ChemBioChem*, Vol. 11 (Wiley-Blackwell, 2010), 1630.

In the same group, Franzyk and co-workers extensively studied hybrid sequence  $\alpha$ -peptide/ $\alpha$ -peptoid and  $\alpha$ -peptide/ $\beta$ -peptoid. Comparative study of antimicrobial activities in function of the backbone nature was performed (Figure 32).<sup>113</sup>

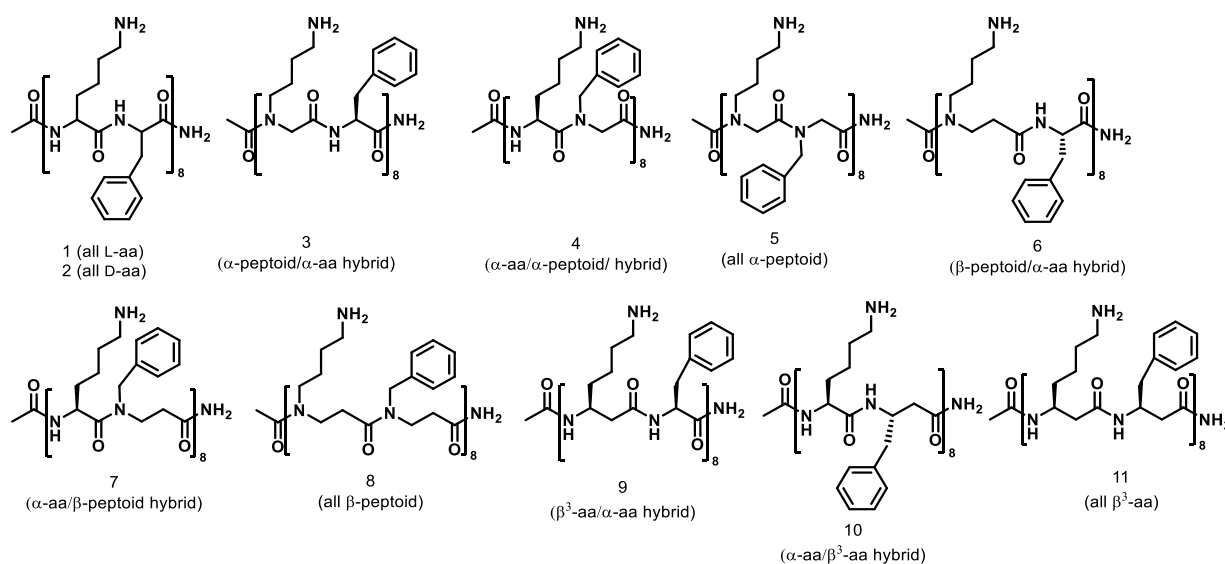


Figure 32 Structure of peptides and of peptide-peptoid hybrids studied by Franzyk and coworkers.<sup>113</sup>

This study compared antibacterial activity against MDR *E. coli* strains and other bacteria, cytotoxicity, and protease stability for the different backbones with identical side chains decoration and sequence length (18 residues). Hybrid oligomers revealed more potent on *E. coli* strains than  $\alpha$ - or  $\beta$ -peptide and  $\alpha$ -peptoids but were all inactive against MRSA. Hybrids containing  $\alpha$ - or  $\beta$ -peptoid were non-haemolytic ( $HA_{10} > 128 \mu\text{M}$ ) resulting in a higher therapeutic index than  $\alpha$ - and  $\beta$ -peptides. However, the  $\alpha$ -peptide/ $\beta$ -peptoid hybrids revealed more toxic against HeLa cells than other peptoid-containing peptidomimetics. The following study was focused on side chains nature for the cationic counterpart (ammonium or guanidinium) and for the hydrophobic counterpart (achiral or  $\alpha$ -chiral aromatic side chains).<sup>114</sup>

Peptide-peptoid hybrids represent a promising class of peptidomimetics to develop antibacterial agents with high activities and good pharmacological profiles.

<sup>113</sup> R. D. Jahnsen; N. Frimodt-Møller; and H. Franzyk, 'Antimicrobial Activity of Peptidomimetics against Multidrug-Resistant Escherichia Coli: A Comparative Study of Different Backbones', *Journal of Medicinal Chemistry*, 55 (2012), 7253–61.

<sup>114</sup> R. D. Jahnsen; A. Sandberg-Schaal; K. J. Vissing; H. M. Nielsen; N. Frimodt-Møller; and H. Franzyk, 'Tailoring Cytotoxicity of Antimicrobial Peptidomimetics with High Activity against Multidrug-Resistant Escherichia Coli', *Journal of Medicinal Chemistry*, 57 (2014), 2864–73.

A Chinese group has successfully designed medium-length hybrid peptoid-peptide oligomers (9-mer) using a strategy combining statistical design, structural analysis, and experimental test.<sup>115</sup> The QSAR predictor was generated by integration of descriptors derived from the principal component analysis of hundreds of constitutional, topological, geometrical, and physicochemical properties of 10 selected natural amino acids and 8 *N*-substituted glycine residues (Table 7).

Table 7 The 10 natural and 8 *N*-substituted amino acids used as building blocks of hybrid oligomers.

Amino Acid	Class (Natural)	Amino acid	Class (N-substituted)
<b>Lysine</b>	Positively charged	<b>NLys</b> <i>N</i> -(4-aminobutyl)glycine	Positively charged
<b>Arginine</b>	Positively charged	<b>MHis</b> <i>N</i> -(methylimidazole)glycine	Positively charged
<b>Leucine</b>	Hydrophobic	<b>Nsna</b> (S)- <i>N</i> -(1-naphthylethyl)glycine	Hydrophobic
<b>Isoleucine</b>	Hydrophobic	<b>Nspe</b> (S)- <i>N</i> -(phenylethyl)glycine	Hydrophobic
<b>Alanine</b>	Hydrophobic	<b>Nssb</b> (S)- <i>N</i> -(sec-butyl)glycine	Hydrophobic
<b>Glycine</b>	Neutral	<b>Nsmb</b> (S)- <i>N</i> -(1-methylbutyl)glycine	Hydrophobic
<b>Cystine</b>	Hydrophobic	<b>Nme</b> <i>N</i> -(methoxyethyl)glycine	Polar
<b>Valine</b>	Hydrophobic	<b>Ntfe</b> <i>N</i> -(2,2,2-trifluoroethyl)glycine	Polar
<b>Serine</b>	Polar		
<b>Tryptophan</b>	Hydrophobic		

A library of hybrid peptide-peptoid oligomers with known antibacterial activities was then used to develop, optimize, and validate the QSAR models. The most relevant QSAR predictor was used for virtual high-throughput screening of 26496 hybrid peptoid-peptide oligomers.

<sup>115</sup> H. Lin; T. Yan; L. Wang; F. Guo; G. Ning; and M. Xiong, ‘Statistical Design, Structural Analysis, and in Vitro Susceptibility Assay of Antimicrobial Peptoids to Combat Bacterial Infections’, *Journal of Chemometrics*, 30 (2016), 369–76.

### 3.8 Short Peptoids with antimicrobial activities

Goodson et al., first evaluated short tripeptoids for their antimicrobial properties from a combinatorial library of 845 molecules.<sup>116</sup> The compound CHIR29498 (Figure 33, a) with a dehydroabiethylamine moiety showed broad spectrum activity against both Gram-negative and Gram-positive bacteria (MICs between 3-12  $\mu\text{g/mL}$ ). It showed 15% haemolysis at 100 $\mu\text{M}$ . For the *in vivo* studies, intraperitoneal (IP) injection of tripeptoid (10mg/kg) was given to the mice with IP injection of  $10^8$  colony forming units (CFU) of *S. aureus*. The mice showed protection for five days.

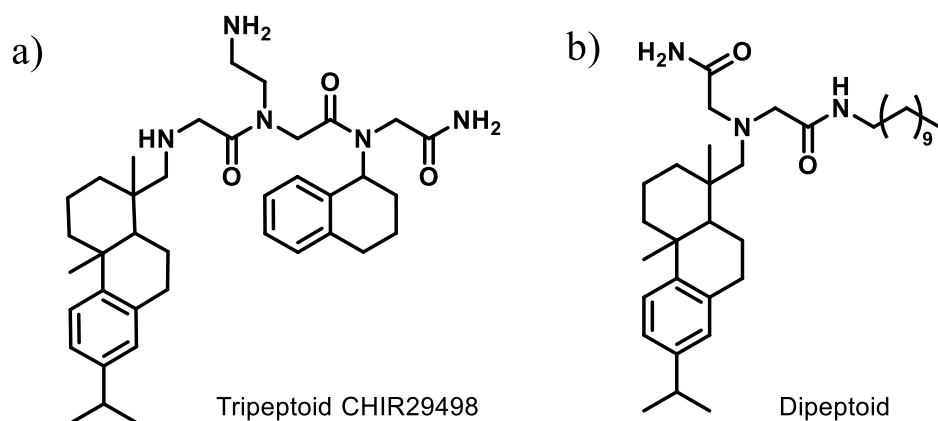


Figure 33 a) The structure of tripeptoid CHIR29498 with a dehydroabiethylamine moiety; b) Structure of dipeptoids with both dehydroabiethylamine and undecylamine residues.

Stefan Bräse et al. went further to explore the shorter dipeptoids.<sup>117</sup> They used synthetic peptide arrays on membrane supports (SPOT-synthesis) to get a library of 96 dipeptoids, out of which 29 dipeptoids showed antimicrobial activity against MRSA (25 $\mu\text{M}$ ). The key to the success of these dipeptoids is the presence of large nonpolar residues like undecylamine and dehydroabiethylamine (Figure 33, b).

## 4 Objectives of this work

As we have seen in the above literature review on the development of peptoid oligomers mimicking AMPs, the various studies seem to show that the helical folding of the peptoids is not required to get potent antimicrobial activities. But in addition, the sequences with higher propensities to adopt helical structure proved to be more toxic than more flexible one. This last point is likely to be due

<sup>116</sup> B. Goodson; A. Ehrhardt; S. Ng; J. Nuss; K. Johnson; M. Giedlin; R. Yamamoto; W. H. Moos; A. Krebber; M. Ladner; M. B. Giacona; C. Vitt; and J. Winter, 'Characterization of Novel Antimicrobial Peptoids.', *Antimicrobial Agents and Chemotherapy*, 43 (1999), 1429–34.

<sup>117</sup> A. C. Schneider; D. Fritz; J. K. Vasquez; S. B. L. Vollrath; H. E. Blackwell; and S. Bräse, 'Microwave-Facilitated SPOT-Synthesis of Antibacterial Dipeptoids', *ACS Combinatorial Science*, 19 (2017), 715–37.

to the nature of the side-chains employed to induce helical folding. Indeed, it was observed that the introduction of several  $\alpha$ -chiral bulky aromatic spe ((*S*)-phenylethyl) group in a sequence often has a detrimental effect on haemolytic activity and cytotoxicity.

In a broader context, to date, all potentially biologically relevant peptoid oligomers designed to adopt helical structures were built using a high concentration (> 50%) of  $\alpha$ -chiral bulky aromatic side chains, especially spe and to a lesser extend s1npe ((*S*)-naphthylethyl) group. However, the nature and the number of these amide controllers hamper the development of these foldamers as drug candidates as pointed out in a recent review from AstraZeneca: “Peptoids have witnessed a wealth of applications based on screening of large libraries, but libraries of helical peptoids have not enjoyed a similar success. This is most probably due to the limited physicochemical diversity available in terms of chiral bulky side chain validated as helix inducers. Indeed, phenethyl residues are by far the most studied helicity inducers in peptoids and this imposes constraints in terms of the achievable physicochemical properties, including hydrophobicity and solubility. Moreover, there is limited availability in terms of chemical diversity among these inducers, e.g., phenyl substituents, implying a limitation in terms of structure activity studies”<sup>118</sup>

Conscious of these serious drawbacks, our group has been working since last ten years at improving foldameric properties of peptoids by the development of specific side-chains capable of governing the *cis/trans* amide isomerism through local side chain-backbone interactions. Indeed, the PPI-like helix can be generated using side chains which stabilise the *cis* conformation of the backbone amides through steric and/or electronic interactions (see section 3.1, Figure 34).

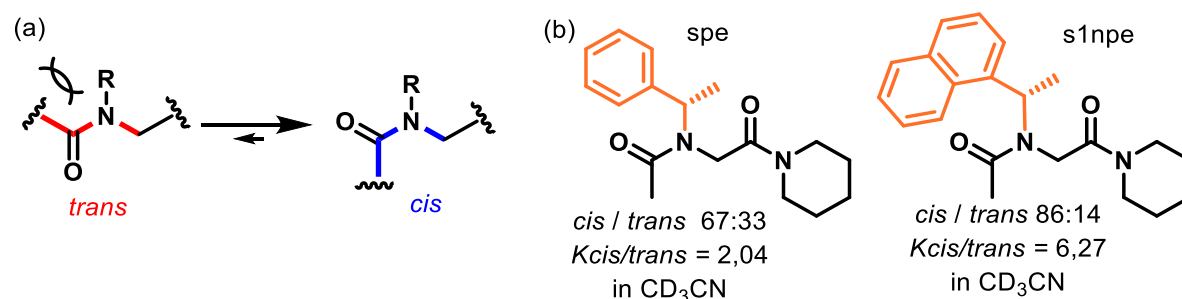


Figure 34 (a) *cis/trans* isomerism of *N,N*-disubstituted amide of the peptoid backbone and (b) Monomeric models with the (*S*)-phenylethyl (spe) and the (*S*)-1-naphthylethyl (s1npe) side chains and corresponding *cis/trans* ratios in  $CD_3CN$  determined by NMR experiments.<sup>119</sup>

<sup>118</sup> R. Gopalakrishnan; A. I. Frolov; L. Knerr; W. J. Drury; and E. Valeur, ‘Therapeutic Potential of Foldamers: From Chemical Biology Tools to Drug Candidates?’, *Journal of Medicinal Chemistry*, 59 (2016), 9599–621.

<sup>119</sup> B. C. Gorske; J. R. Stringer; B. L. Bastian; S. A. Fowler; and H. E. Blackwell, ‘New Strategies for the Design of Folded Peptoids Revealed by a Survey of Noncovalent Interactions in Model Systems’, *Journal of the American Chemical Society*, 131 (2009), 16555–67.

It is important to note that the *spe* side chain commonly employed as helix inducer, has only a slight effect to promote *cis* amide conformation (*cis/trans* ratio 67:33 for the monomer). It is the reason why it is now well admitted that peptoids containing *Nspe* residues do not present homogeneous PPI-type helix in solution, and moreover with short oligomers. The overall homogeneity and stability of the helical conformation are improved by using strong *cis*-amide inducers. In the last years, we have introduced the best *cis*-directing side chains reported to date, the *tert*-butyl (*tbu*)<sup>120</sup> and the triazolium-based side chains.<sup>121</sup> Recently, our group also reported the potential of the non-aromatic  $\alpha$ -chiral side chain (*S*)-*N*-(1-*tert*-butylethyl)glycine (*s1tbe*) to promote homogeneous and robust Polyproline Type I Helices.<sup>85</sup> However, this PhD work was done before this finding, thus the *s1tbe* side chain was not used for the design of the amphipathic cationic oligomers.

The *tert*-butyl side chain exerts a total *cis* amide control via steric effects, independently of the solvent used (Figure 35 (a)). Despite the absence of chirality, it was shown by NMR, crystallography, and molecular modelling that the helical conformation was stabilised by a network of intramolecular CO(*i*)...HC(*i*-*n*) (*n*= 1, 2, 3) H-bond and *i*/*i*+3 *tBu*...*tBu* London interaction (Figure 35 (b,c)).<sup>122</sup>

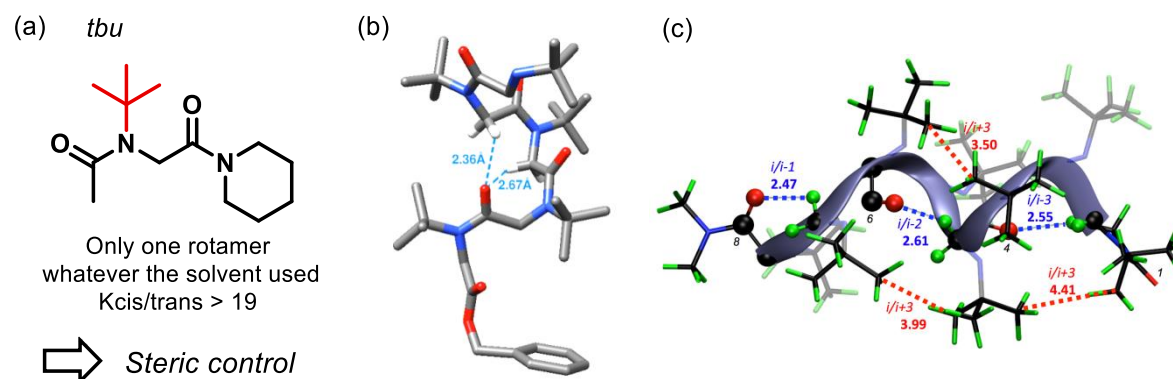


Figure 35 (a) Monomeric model carrying the *tert*-butyl (*tbu*) side chain and corresponding *cis/trans* ratios determined by NMR experiments ;(b) X-ray structure of a *NtBu* pentamer (X-ray CCDC: 1445400); (c) 50 ns free MD simulation snapshot of an *NtBu* octamer. Distance is given in Å. Index of residues involved in CO...HC are marked in italic.<sup>122</sup>

<sup>120</sup> O. Roy; C. Caumes; Y. Esvan; C. Didierjean; S. Faure; and C. Taillefumier, ‘The *Tert*-Butyl Side Chain: A Powerful Means to Lock Peptoid Amide Bonds in the *Cis* Conformation’, *Organic Letters*, 15 (2013), 2246–9.

<sup>121</sup> C. Caumes; O. Roy; S. Faure; and C. Taillefumier, ‘The Click Triazolium Peptoid Side Chain: A Strong *Cis*-Amide Inducer Enabling Chemical Diversity’, *Journal of the American Chemical Society*, 134 (2012), 9553–6.

<sup>122</sup> G. Angelici; N. Bhattacharjee; O. Roy; S. Faure; C. Didierjean; L. Jouffret; F. Jolibois; L. Perrin; and C. Taillefumier, ‘Weak Backbone CH ... O=C and Side Chain *tBu* ... *tBu* London Interactions Help Promote Helix Folding of Achiral *NtBu* Peptoids’, *Chem. Commun.*, 52 (2016), 4573–6.

The *cis*-directing effect of the triazolium was studied in monomeric peptoid model carrying 1-(benzyltriazolium)methyl ( $R' = \text{H}$ ,  $\text{btm}^+$ ) or 1-(benzyltriazolium)ethyl ( $R' = \text{Me}$ ,  $\text{bte}^+$ ) (Figure 36). The electron deficient triazolium ring enables a strong  $n \rightarrow \pi^*$  Ar donation from the oxygen of the carbonyl ( $\text{O}_{i-1}$ ) to the antibonding orbital of triazolium ring on residue  $i$ . This electronic interaction is responsible for a major *cis* conformation in different solvents. Additionally, a non-classical  $\text{CH} \cdots \text{O}$  hydrogen-bonding between the triazolium CH and same residue  $\text{C}=\text{O}$  amide carbonyl was also observed in  $\text{CDCl}_3$  and can act cooperatively with the  $n \rightarrow \pi^*$  Ar delocalisation to promote the *cis*-amide conformation (Figure 36 (b)).

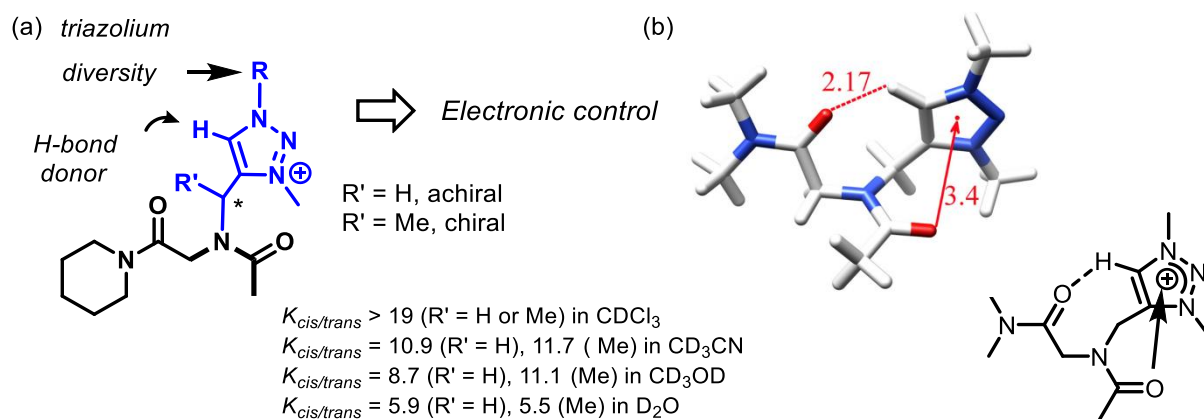


Figure 36 (a) The monomeric model carrying triazolium-type side chain and corresponding *cis/trans* ratios in various solvents determined by NMR experiments; (b) Low-energy conformation of a triazolium-type model calculated at the B3LYP/6-31G+\* level.

In addition to its exceptional *cis*-promoting effect, the triazolium side chain allows for the introduction of a wide variety of substituents (R group), this chemical diversity being crucial for their applications as peptidomimetic, foldamers or materials. Due to its *cis*-directing effect and its accessible chemical diversity, the introduction of triazolium side chain is of great interest for stabilising the structure of oligoamides for diverse applications. In the context of antimicrobial cationic amphipathic peptoids design, this positively-charged side chain may enable to target bacterial membrane while promoting helical folding of the amphipathic oligomer. Indeed, despite the huge number of amphipathic cationic peptoid oligomers studied, the chemical diversity of the cationic pendant groups was limited to date to positively charged proteinogenic side chain equivalents, *i.e.* ammonium, guanidinium and imidazolium moieties (see section 3.5). These side chains bring the positive charge but do not exert any role on the folding of the oligomers into amphipathic architecture. We hypothesise that the use of cationic side chain involved in the stabilisation of the helix together with hydrophobic helix inducer may provide short amphiphilic oligomers with interesting antimicrobial properties. Certainly, the use of *cis*-directing side-chain at each position of the oligomer should enable the formation of homogenous amphipathic helical structure even for short sequence. Indeed, no clear rationale for the charge distribution and controlled secondary structure has been established. Previous studies have not really scrutinised



the influence of the helical structure on biological properties. The aim of this PhD work is to unveil the potential of *cis*-directing side-chains developed in our group to construct robust cationic amphipathic helical architectures with potent and selective antimicrobial activities (Figure 37).

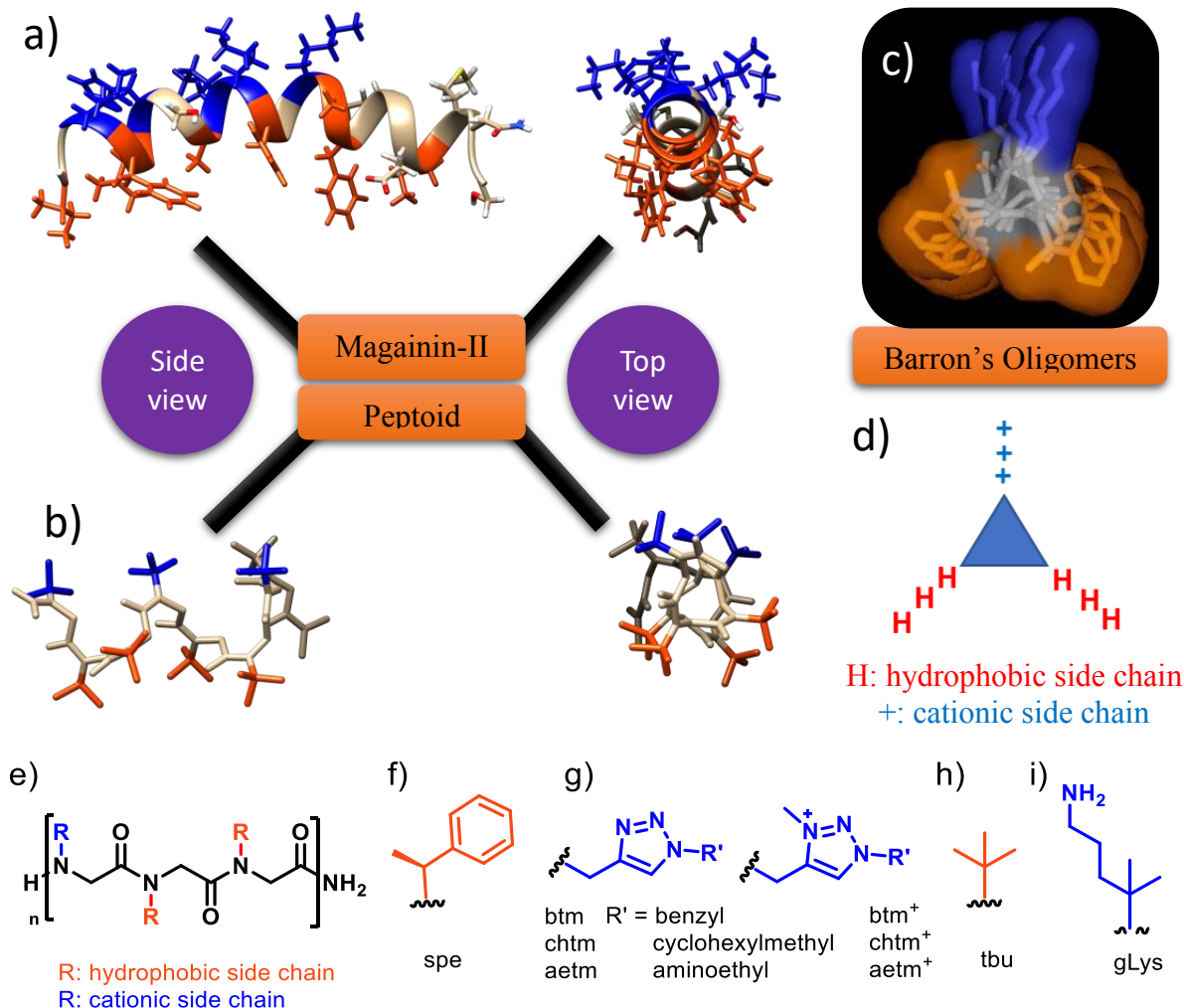


Figure 37 (a) NMR structure of magainin-2 with side and end-on representations (PDB 2MAG): The  $\alpha$ -helix is strongly amphipathic with lysine and histidine (in blue) being located on the opposite side to the nonpolar face with phenylalanine and (iso)leucine (in orange) residues; (b) Secondary structure of a Ntbu hexamer by molecular modelling; (c) Top view of helical peptoid oligomer  $H-(N\text{Lys}-N\text{spe}-N\text{spe})_n-\text{NH}_2$  developed by Barron;<sup>89</sup> (d) Schematic representation of amphipathic helical structure of peptoids; (e) Generic structure of amphipathic peptoid oligomers and various side chains studied in the present work: (f) spe for (S)-(1-phenylethyl); (g) btm for 1-benzyl-1,2,3-triazolylmethyl and btm<sup>+</sup> for 1-benzyl-3-methyl-1,2,3-triazolium methyl, chtm for 1-cyclohexylmethyl-1,2,3-triazolylmethyl and chtm<sup>+</sup> for 1-cyclohexylmethyl-3-methyl-1,2,3-triazolium methyl, aetm for 1-aminoethyl-1,2,3-triazolylmethyl and aetm<sup>+</sup> for 1-aminoethyl-3-methyl-1,2,3-triazolium methyl; (h) tbu for tert-butyl; (i) gLys for 1,1-dimethyl-4-aminobutyl.

To reach this aim, various families of cationic amphipathic peptoid oligomers mimicking the amphiphilic helical structure of magainin, have been designed (Figure 37 a). The structures of these oligomers are closely related to those developed by Barron (Figure 37 c,d and see section 3.5). Indeed, these cationic amphipathic peptoids ( $N\text{Lys}-N\text{spe}-N\text{spe}$ )<sub>n</sub> have proved to be potent antimicrobial in various biological tests.<sup>89</sup> In order to study the influence of recently developed *cis*-

inducing side chains (hydrophobic or cationic) on the antibacterial activities as well as on the selectivity for bacteria over mammalian cells, we designed three families of peptoid oligomers presented in the following sections.

#### 4.1 Family I: Replacement of *Nspe* by *Ntbu* residues

The first approach was to replace hydrophobic *Nspe* residues with the strong *cis* inducing *Ntbu* residue (Figure 38). In family I, the first series is based on the repetition of two *Ntbu* and one *NLys* residues (Series A). The second series is based on the additional modification of *NLys* to *NgLys*,  $\alpha$ -*gem*-dimethylated *NLys* equivalent (Series B). The  $\alpha$ -*gem*-dimethylated side chain could be regarded as a functionalised tert-butyl side chain. Through steric effect, this side chain induces complete *cis* geometry of the backbone amide.

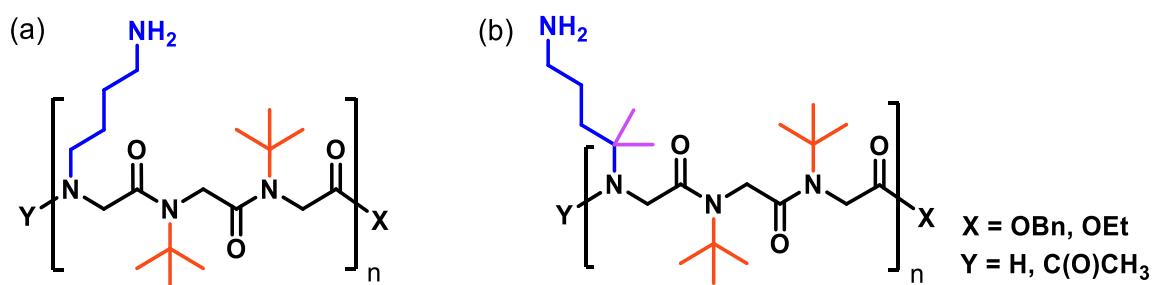


Figure 38 Structures of Family I (a) Series A:  $Y-(NLys-Ntbu-Ntbu)_n-X$ ; (b) Series B:  $Y-(NgLys-Ntbu-Ntbu)_n-X$  with *Ntbu* for *N*-(tert-butyl)glycine and *NgLys* for *N*-(1,1-dimethyl-4-aminobutyl)glycine residues.

#### 4.2 Family II: Replacement of *Nspe* by *Ntbu* and *NLys* by a triazolium-type side chain.

The second family is based on the replacement of the cationic *NLys* with 1,2,3-triazolium-type side chains while keeping the tert-butyl side chain as hydrophobic pendant group (Figure 39). The substitution of the *NLys* by 1,2,3-triazolium-type cationic group gives us the advantage of both controlling the *cis* amide geometry and bringing cationic residue to create amphiphilic helical architecture. The triazolium could be substituted by a hydrophobic group (Series A) or an amino group (Series B).

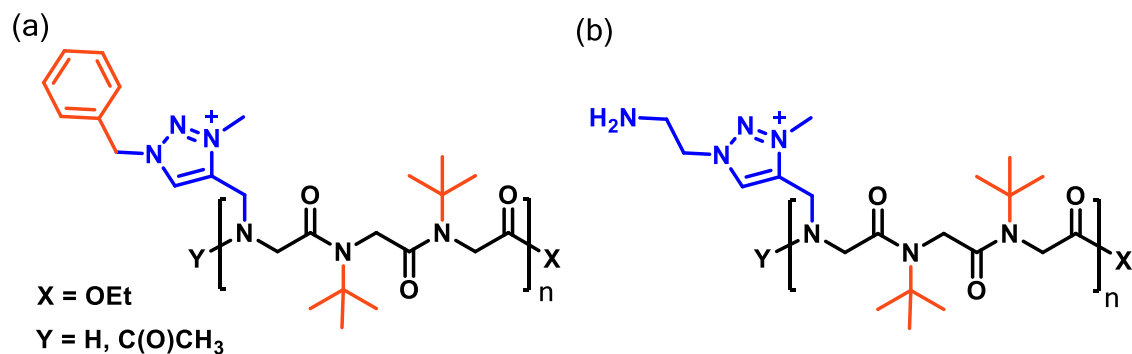


Figure 39 Structures of Family II (a) Series A:  $Y-(\text{Nbtm}^+-\text{Ntbu}-\text{Ntbu})_n\text{-X}$ ; and (b) Series B:  $Y-(\text{Naetm}^+-\text{Ntbu}-\text{Ntbu})_n\text{-X}$  with  $\text{Nbtm}^+$  for  $N$ -(1-benzyl-3-methyl-1,2,3-triazolium methyl)glycine,  $\text{Ntbu}$  for  $N$ -(tert-butyl)glycine and  $\text{Naetm}^+$  for  $N$ -(1-aminoethyl-3-methyl-1,2,3-triazolium methyl)glycine residues.

#### 4.3 Family III: Replacement of *N*Lys by a triazolium-type side chains.

The third family is based on the retention of *N*spe residues employed by Barron as hydrophobic group and helix promoter and the introduction of various 1,2,3-triazolium-type side chains as cationic group (Figure 40). This study may enable to unveil the potential of the triazolium moiety as a cationic counterpart to develop efficient and selective AMP mimetics.

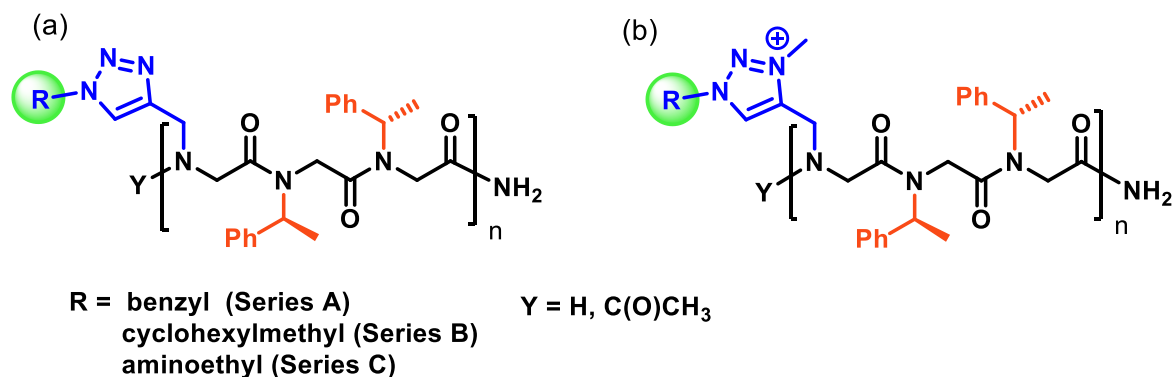


Figure 40 Structures of Family III (a) incorporating triazole-type residues:  $Y-(\text{Nxtm}-\text{Nspe}-\text{Nspe})_n\text{-NH}_2$  and (b) incorporating triazolium-type residues:  $Y-(\text{Nxtm}^+-\text{Nspe}-\text{Nspe})_n\text{-NH}_2$  with  $\text{Nbtm}$  for  $N$ -(1-benzyl-1,2,3-triazolylmethyl)glycine,  $\text{Nbtm}^+$  for  $N$ -(1-benzyl-3-methyl-1,2,3-triazolium methyl)glycine,  $\text{Nchtm}$  for  $N$ -(1-cyclohexylmethyl-1,2,3-triazolylmethyl)glycine,  $\text{Nchtm}^+$  for  $N$ -(1-cyclohexylmethyl-3-methyl-1,2,3-triazolium methyl)glycine,  $\text{Naetm}$  for  $N$ -(1-aminoethyl-1,2,3-triazolylmethyl)glycine and  $\text{Naetm}^+$  for  $N$ -(1-aminoethyl-3-methyl-1,2,3-triazolium methyl)glycine.

Three series of peptoid oligomers carrying 1,2,3-triazole or 1,2,3-triazolium side-chains were designed depending on the substituent on triazole/triazolium: a cyclohexylmethyl for series A ( $\text{Nchtm}$  or  $\text{Nchtm}^+$  residues), a benzyl for series B ( $\text{Nbtm}$  or  $\text{Nbtm}^+$  residues) and an aminoethyl for series C ( $\text{Naetm}$  or  $\text{Naetm}^+$  residues).

Family III, series A:  $\text{H}-(\text{Nchtm}-\text{Nspe}-\text{Nspe})_n\text{-NH}_2$  and  $\text{H}-(\text{Nchtm}^+-\text{Nspe}-\text{Nspe})_n\text{-NH}_2$

Family III, series B:  $\text{H}-(\text{Nbtm}-\text{Nspe}-\text{Nspe})_n\text{-NH}_2$  and  $\text{H}-(\text{Nbtm}^+-\text{Nspe}-\text{Nspe})_n\text{-NH}_2$

Family III, series C:  $H-(Naetm-Nspe-Nspe)_n-NH_2$  and  $H-(Naetm^+-Nspe-Nspe)_n-NH_2$

According to previous studies on cationic amphipathic peptoids, we will study oligomers of 6, 9 or 12 residues long. Depending of the oligomer length, the net positive charge of the peptoids ranges from +2 to +8.

The present work will be divided into three chapters, two dedicated to the solution or solid-phase synthesis of targeted oligomers and one chapter devoted to the biological evaluation of these amphiphilic peptoids.

Chapter II deals with the development and optimisation of solution-phase synthesis methods for peptoids incorporating tert-butyl side chain (Families I and II).

Chapter III deals with the preparation of oligomers from the third family, using solid-phase submonomer synthesis. New oligomers with both cationic and hydrophobic nature will be synthesised on support using various side chains. Conventional and microwave-based synthesis on support will be studied to obtain 1,2,3-triazolium-based peptoids.

Finally, chapter IV will describe the biological evaluation of the various families of cationic amphipathic oligomers. The study will include antibacterial, anti-biofilm, haemolytic and cell viability studies. To better understand the mode of action of these peptoids, microscopic imaging of the bacteria treated with selected peptoid oligomers will be presented.

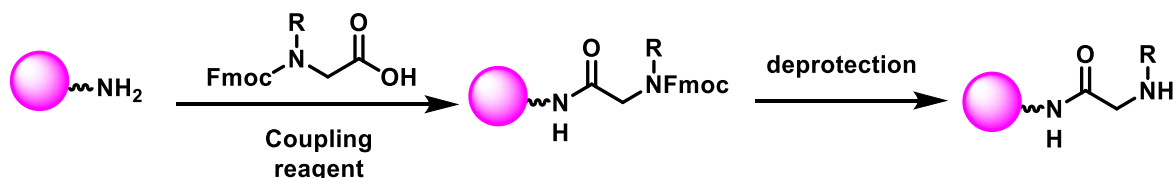
## **CHAPTER II**

# **Solution-phase synthesis of cationic amphiphilic peptoid oligomers**

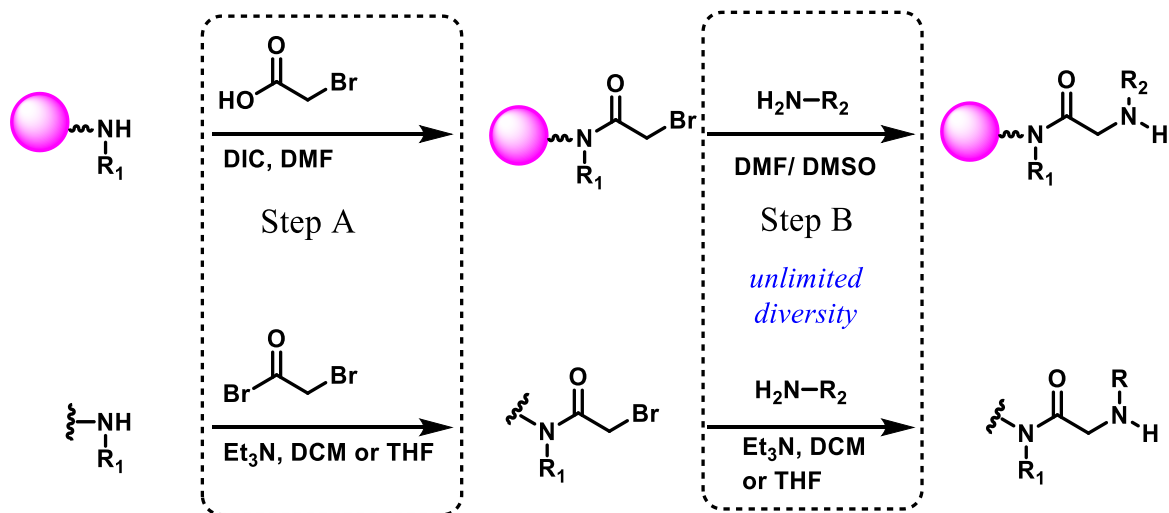
## Introduction: The concept of Synthesis

There are innumerable references for the synthesis of peptoids on a solid support.<sup>62</sup> It is possible because the synthesis of peptoids on the solid support is very efficient and it allows to obtain long oligomers up to 48 residues<sup>123</sup> very fast. Solid-phase peptoid synthesis gives the advantage for structural diversity by exploiting a submonomer protocol instead of peptide synthesis monomer strategy that necessitates the preparation of Fmoc protected monomers and involves the difficult coupling of secondary amines (Scheme 3).<sup>57</sup>

### Solid-phase monomer strategy



### Submonomer strategy (solid-phase or solution)



Scheme 3 Comparison of the monomer and submonomer synthesis of peptoid oligomers

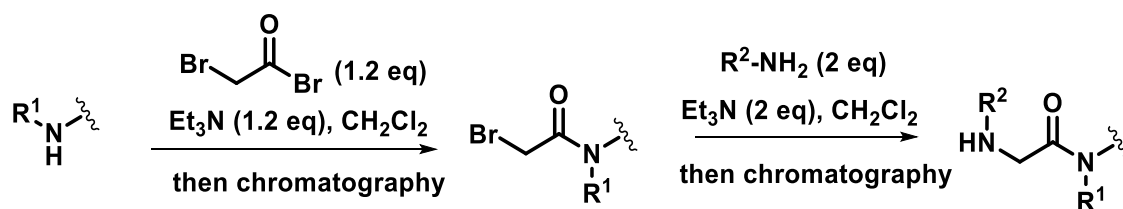
In the submonomer strategy, the peptoid residues are created in two steps by acylation of the *N*-terminus of the peptoid, ensued by reaction of the acylated intermediate with an applicable primary amine. The use of primary amine thus enables the introduction of a huge diversity of side chains

<sup>123</sup> J. E. Murphy; T. Uno; J. D. Hamer; F. E. Cohen; V. Dwarki; and R. N. Zuckermann, 'A Combinatorial Approach to the Discovery of Efficient Cationic Peptoid Reagents for Gene Delivery.', *Proceedings of the National Academy of Sciences of the United States of America*, 95 (1998), 1517–22.

on peptoids.<sup>124</sup> The main limitation to solid-phase synthesis is the inability to yield a large amount of the final compound. Another issue with the solid-phase synthesis of peptoids, is the introduction of bulky side-chain such as the naphthylethyl or tert-butyl. Therefore, it becomes necessary to find an answer to the question of producing large quantities of peptoids and oligomers incorporating bulky side chains. This led to the shift towards solution-phase synthesis which can produce gram-scale quantities of the final product. To briefly compare the solid-phase and solution-phase synthesis, the main difference is the skeleton elongation: acylation step. In solution, this is accomplished by reaction of the secondary amine with an acid halide rather than by coupling bromoacetic acid using a coupling reagent (Scheme 3).

## 1 General overview of the solution-phase synthesis

A solution-phase submonomer method to access peptoids was early reported by Zuckermann at the same time as the solid-phase submonomer method in 1992.<sup>62</sup> The field was established at that time which leads to the development of innovative strategies for the synthesis of peptoid oligomers. The submonomer synthesis has rapidly become the method of choice to access peptoids. In the original publication, Zuckermann transposed solid-phase submonomer method to solution using bromoacetic bromide and triethylamine in dichloromethane for the acylation step and 2 equivalents of primary amine and triethylamine in dichloromethane for the substitution step (Scheme 4).

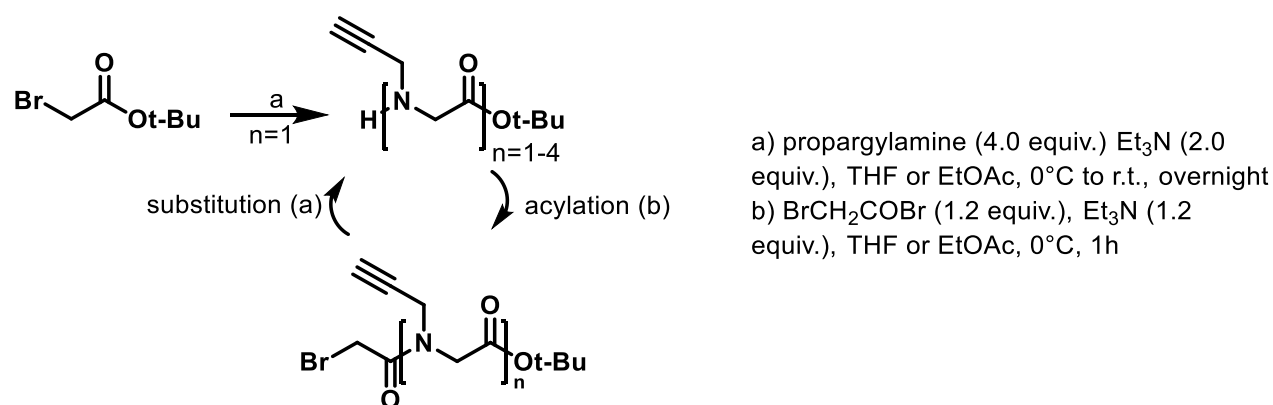


Scheme 4 Solution-phase synthesis of peptoids reported by Zuckermann<sup>62</sup>

The solution-phase submonomer version was by far less employed than the supported one since it is very costly in time due to the intermediates purification at each step. However, the solution-phase synthesis enables the access to large amount of compounds and in recent years several groups have begun to use it for specific purposes.

<sup>124</sup> A. S. Culf and R. J. Ouellette, 'Solid-Phase Synthesis of N-Substituted Glycine Oligomers ( $\alpha$ -Peptoids) and Derivatives', *Molecules*, 15 (2010), 5282–335.

The Taillefumier's group has worked on improving solution-phase submonomer methodology which enabled them to synthesise large scale of peptoids.<sup>125</sup> Their main purpose was to adapt experimental conditions to limit as possible chromatographic purifications (Scheme 5). Instead of halogenated solvent originally employed, tetrahydrofuran or ethyl acetate was used in both acylation and substitution steps, which is very important as it leads to the precipitation of the formed triethylamine ammonium salts. These salts can then be easily removed by filtration. These ammonium salts must be carefully removed since trace amounts of ammonium salts can form undesired by-products if continuously returned to the iterative synthesis. After filtration, the solvent is removed by evaporation offering pure enough bromoacetamide intermediates to proceed the substitution step. This solvent change reduces the number of chromatography operations to one per peptoid residue. Moreover, chromatographic purification could also be omitted after the substitution step if a volatile primary amine is used. Indeed, the excess of amine is readily eliminated during evaporation when ebullition point is below 100°C, otherwise, a chromatography is necessary after the substitution step.



Scheme 5 Modified solution-phase synthesis of  $\alpha$ -peptoids using volatile primary amine

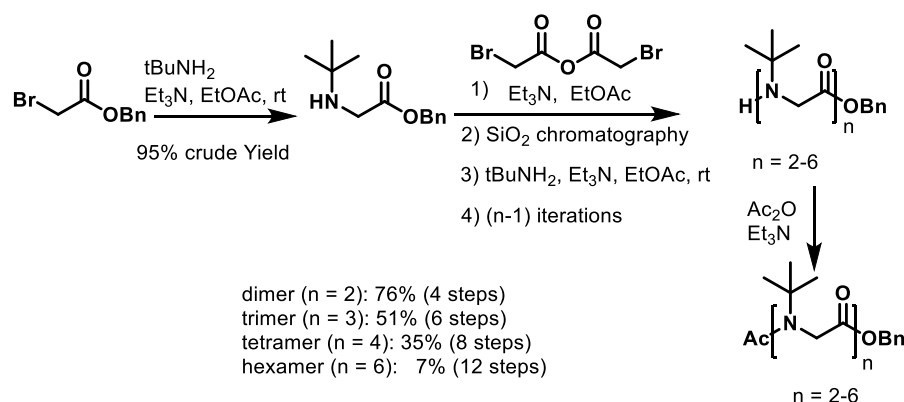
These optimised conditions were then used to synthesise  $\alpha$ -peptoid made up of four units ( $\alpha$ -tetrapeptoid) in 41% yield in 7 steps starting from tertbutyl bromoacetate and using propargyl amine as primary amines (Scheme 5). Procedures were also optimized to access  $\beta$ - and  $\alpha,\beta$ -peptoids. Long peptoid oligomers can be obtained by blockwise peptide coupling of short oligomers using conventional reagents such as HATU or EDCI.<sup>60</sup> It was further modified to suit the needs for chemical diversity. Though this method limits the choice of side chains to volatile amines, it is still possible to use side chains that serve as entries to more complex structures by post-modification. This submonomer solution-phase protocol is cost and time efficient and proved

<sup>125</sup> C. Caumes; T. Hjelmgaard; R. Remuson; S. Faure; and C. Taillefumier, 'Highly Convenient Gram-Scale Solution-Phase Peptoid Synthesis and Orthogonal Side-Chain Post-Modification', *Synthesis*, 2 (2011), 257–64.



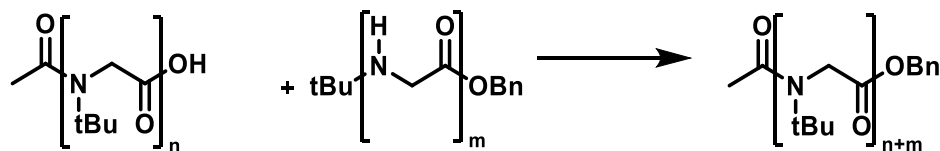
to be a valuable alternative to solid-phase synthesis to access peptoid oligomers in large scale or to synthesise oligomers with very bulky side-chains.

Indeed, when the group has developed the tertbutyl side-chain, the solid-phase synthesis was not applicable at all and modification of the solution-phase procedure was needed.<sup>120</sup> The previously optimized conditions for the substitution-acylation iterations furnished only modest yields in bromoacetamides, around 60%. It was then found that replacing bromoacetyl bromide with freshly prepared bromoacetic anhydride produced better yields (Scheme 6). This milder acylating agent provided a cleaner reaction, however, a quick chromatography on silica gel is necessary after the acylation step. Since the tertbutyl amine has a boiling point of 46°C, it can be easily removed after the substitution step by evaporation. Therefore, with these optimized conditions, chromatography is needed only once by iteration.



Scheme 6 Synthesis of Ntbu glycine oligomers by solution-phase submonomer method using bromoacetic anhydride

Longer Ntbu glycine oligomers can be accessed by a blockwise peptide coupling of short oligomers.<sup>122</sup> To perform this challenging coupling involving a secondary amine carrying a tertbutyl group, conventional coupling methods were ineffective. But it was found that pentafluorophenyl activated ester-based methods enable this difficult *N,N*-disubstituted amide formation when 1,8-diazobicyclo[5.4.0]undec-7-ene (DBU) is used as a base instead of the weakest diisopropyl ethyl amine (DIPEA) (Scheme 7, Table 8).



Scheme 7 Block coupling method to access long Ntbu oligomers

Table 8 Optimised conditions for coupling

n	m	Coupling reagent	Oligomer length (n+m)	Yield %
6	2	PFP-O-TFA <sup>a</sup>	8	68
5	5	PFP-O-TFA	10	73
10	5	PFP-O-TFA	15	10
10	5	FDPP	15	52

<sup>a</sup>Conditions: (i) PFP-O-TFA (1.5 equiv.), pyridine (1.5 equiv.), DCM, TA, (ii) DBU (3 equiv.), DCM, RT; <sup>b</sup>Conditions: FDPP (Pentafluorophenyl diphenylphosphinate) (1.2 equiv.), DBU (3 equiv.), DCM, RT.

In this research project, these optimized conditions will be used to access cationic amphiphilic oligomers incorporating the tertbutyl side chain, i.e. the families I and II (see section 4.1, 4.2 Chapter I):

Family I, series A: H-(NLys-Ntbu-Ntbu)<sub>n</sub>-NH<sub>2</sub>

Family I, series B: H-(NgLys-Ntbu-Ntbu)<sub>n</sub>-NH<sub>2</sub>

Family II, series A: H-(Nbtm<sup>+</sup>-Ntbu-Ntbu)<sub>n</sub>-NH<sub>2</sub>

Family II, series B: H-(Naetm<sup>+</sup>-Ntbu-Ntbu)<sub>n</sub>-NH<sub>2</sub>

## 2 Synthesis of the (NLys-Ntbu-Ntbu)<sub>n</sub> peptoid family IA

To synthesise the first family, we planned to synthesise the NLys-Ntbu-Ntbu trimer by solution phase submonomer protocol then access longer oligomers by block coupling.

### 2.1 Submonomer synthesis of key trimer building-block

For the preparation of the trimer block, we have studied different synthetic pathway depending on the protecting groups used at the N- and C- terminal positions and of the NLys side chain (Figure 41).

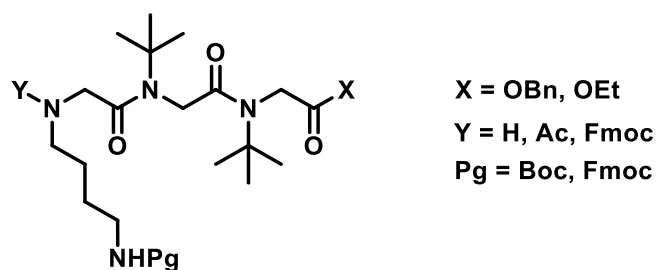
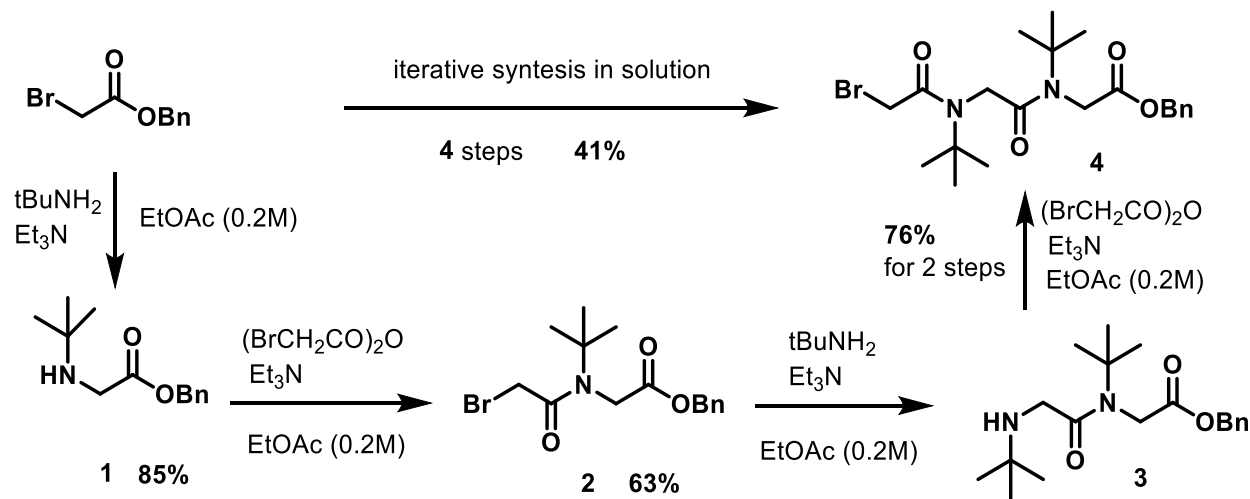


Figure 41 Structure of the NLys-Ntbu-Ntbu trimer block

### 2.1.1 Synthesis of H-NLys(Boc)-Ntbu-Ntbu-OBn trimer block starting from benzyl bromoacetate

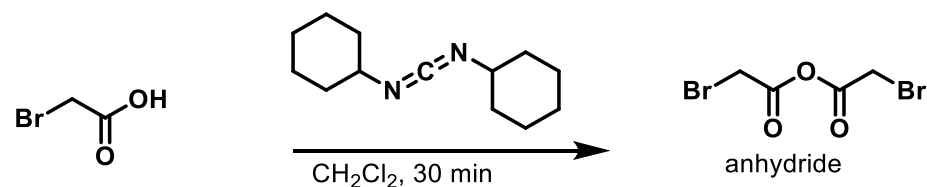
In the first synthetic strategy, we kept the acid moiety protected by a benzyl group then we studied the best combination of orthogonal protection of the amines (*N*-terminal and *N*Lys amino group).

First, the trimer block was synthesised by using solution-phase iterative synthesis starting from benzyl bromoacetate and using bromoacetic anhydride as acylating agent and the volatile tert-butylamine as a primary amine (Scheme 8).<sup>120</sup>



Scheme 8 Synthesis of tert-butyl based oligomer using benzyl bromoacetate

For the synthesis of the bromoacetic anhydride, a modified version of Calas *et al* method was employed.<sup>126</sup> The dicyclohexylcarbodiimide (DCC) was used as coupling reagent in dichloromethane. After 30 min of reaction, the formed urea was eliminated by filtration and the anhydride was directly used in the acylation step without further purification (Scheme 9).

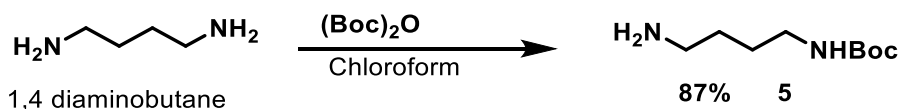


Scheme 9 Generation of bromoacetic anhydride

<sup>126</sup> B. Calas; J. Mery; and J. Parello, 'Synthesis of the Fragment 14-21 of the Amino Acid', *Tetrahedron*, 41 (1985), 5331-9.

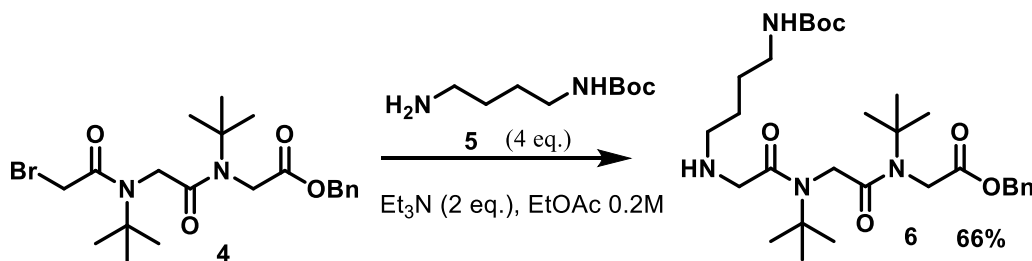
The bromoacetamide derivative **4** was thus obtained in 4 steps from benzyl bromoacetate with a global yield of 41%.

To introduce the *N*Lys residue, a monoprotected diamine is needed. The diamine **5** mono-protected with a tert-butyloxycarbonyl (Boc) group was synthesised starting from commercially available 1,4-diaminobutane by using the optimised conditions available in the literature (Scheme 10).<sup>127</sup> This reaction also produces diprotected diamine as a minor product. This is taken into consideration for yield determination by calculating the percentage of mono protected product based on proton NMR experiment.



Scheme 10 Synthesis of 1-N-Boc-1,4-diaminobutane **5**

The trimer **6** was synthesised by substitution of bromoacetamide **4** using four equivalents of monoprotected diamine **5** (Scheme 11). This reaction was optimised to obtain the trimer **6** with a yield of 66%.



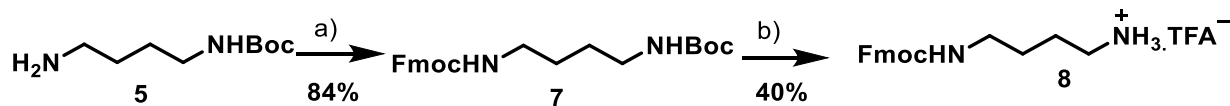
Scheme 11 Formation of the trimer block *H*-*N*Lys(Boc)-*N*tbu-*N*tbu-OBn

### 2.1.2 Synthesis of key trimer building-block *H*-*N*Lys(Fmoc)-*N*tbu-*N*tbu-OBn starting from benzyl bromoacetate

Since the *N*tbu peptoid residue revealed sensitive to acidic conditions, the selective deprotection of the Boc-protected amine may be difficult. It was thus decided to use fluorenylmethyloxycarbonyl (Fmoc) group instead of Boc as protecting group, even, though this strategy will be expensive as compared to the Boc strategy.

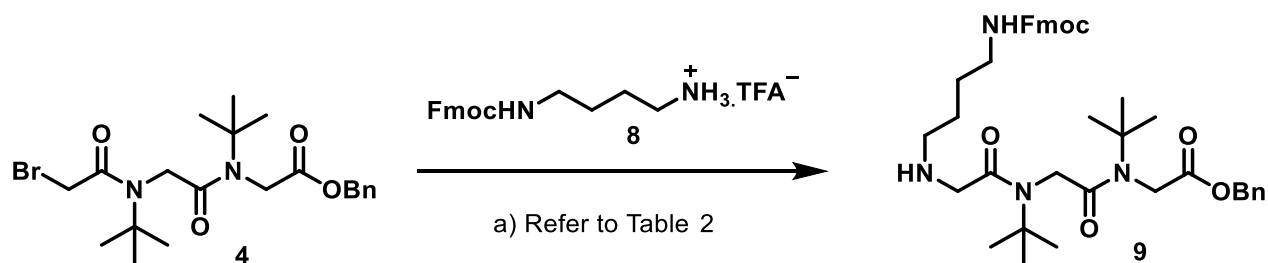
<sup>127</sup>C. Schmuck and J. Dudaczek, 'Ion Pairing between the Chain Ends Induces Folding of a Flexible Zwitterion in Methanol', *European Journal of Organic Chemistry*, 3 (2007), 3326–30.

To access the mono Fmoc-protected diamine, the free amine of previously prepared compound **5**, was protected using fluorenylmethoxycarbonyl chloride by a method described in the literature (Scheme 12).<sup>128</sup> The Boc group was then removed using trifluoroacetic acid to furnish the mono-Fmoc-1,4-diaminobutane **8** as an ammonium salt.<sup>129</sup>



Scheme 12 Synthesis of 1-N-Fmoc-1,4-diaminobutane; conditions: a) FmocCl (1.05 equiv.), NaHCO<sub>3</sub>(aq.), DCM, 25°C, 18 hr b) DCM/TFA (1:1), 0°C, 2 hr

To perform the substitution step (Scheme 13), the fast optimization of the reaction conditions was carried out and is presented in Table 9.



Scheme 13 Synthesis of trimer (NLys(Fmoc)-NtBu-NtBu)-OBn

Table 9 Optimisation of the substitution step to form the trimer H-NLys(Fmoc)-NtBu-NtBu-OBn **9**

	Conditions	Yield
<b>1</b>	Et <sub>3</sub> N (2 equiv.), THF (anhy.), 25°C, 18 hr	31%
<b>2</b>	DIPEA (2+2 equiv.), THF (anhy.), 25°C, 18 hr	50%*
<b>3</b>	DIPEA (4+2 equiv.), EtOAc, r.t., 18 hr	45%

\* not pure

First, classical conditions using 2 equiv. of triethylamine were used as a base furnishing the trimer with a modest yield of 31%. More equivalents of the base may be needed to both generate the free amine of compound **8** and to perform the substitution step. We thus decided to use the Hünig's base

<sup>128</sup>L. A. Carpino and G. Y. Han, '9-Fluorenylmethoxycarbonyl Amino-Protecting Group', *The Journal of Organic Chemistry*, 37 (1972), 3404–9.

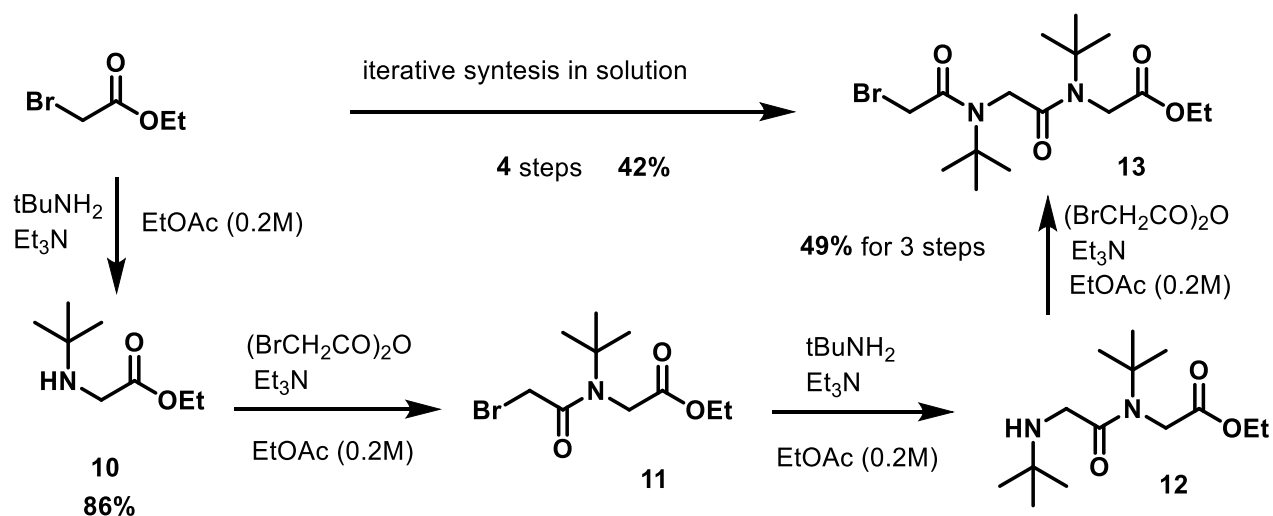
<sup>129</sup>D. M. Shendage; R. Fröhlich; and G. Haufe, 'Highly Efficient Stereoconservative Amidation and Deamidation of  $\alpha$ -Amino Acids', *Organic Letters*, 6 (2004), 3675–8.

DIPEA since the liberation of the primary amine with the 2 first equivalents leads to the precipitation of a salt that could be removed. Subsequently, the salt was filtered and 2 more equiv. of DIPEA were added followed by addition of the bromoacetamide **4**. The trimer building block **9** was thus synthesised with a yield of 50% but with low purity. A purer compound has been obtained by replacement of the solvent with ethyl acetate.

### 2.1.3 Synthesis of key trimer building block H-MLys(Cbz)-NtBu-MtBu-OEt starting from ethyl bromoacetate

In the second synthetic strategy, we kept the acid group protected as an ethyl ester and the MLys side chain amino group was orthogonally protected using carboxybenzyl (Cbz) group. The Cbz group was selected because its cleavage is easier compared to the cleavage of the Fmoc group that usually necessitate purification of the free amine before to be used.

First, the trimer block was synthesised as before by using iterative synthesis in solution phase starting from ethyl bromoacetate and using bromoacetic anhydride as acylating agent and the volatile tert-butylamine as primary amine (Scheme 14).

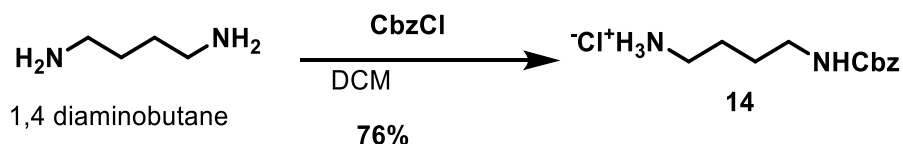


Scheme 14 Synthesis of tert-butyl based oligomer using ethyl bromoacetate

Using optimized conditions, the bromoacetyl amide derivative **13** was obtained with a global yield of 42% from ethyl bromoacetic acid.

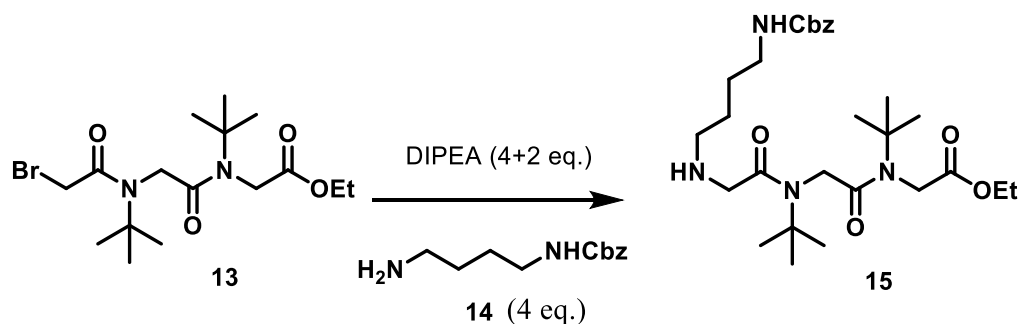
The diamine **14** mono-protected by a carboxybenzyl (Cbz) group was synthesised by using optimised conditions available in the literature (Scheme 15).<sup>130</sup> The yield is calculated based on the proportion of mono- and diprotected diamine determined by analysis of the proton NMR spectra.

<sup>130</sup> J. He; J. Bawiec; W. Liu; G. B. Liang; and L. Yang, 'Substituted Bicyclic Amines for the Treatment of Diabetes' (Google Patents, 2010).



Scheme 15 Synthesis of 1-N-Cbz-1,4-diaminobutane

Optimization of the substitution step was carried out (Scheme 16, Table 10).



Scheme 16 Formation of the H-NLys(Cbz)-Ntbu-Ntbu-OEt trimer 15

Table 10 Optimisation of the substitution step using the 1-N-Cbz-1,4-diaminobutane as primary amine

Entry	Conditions	Yield
1	Et <sub>3</sub> N (2 equiv.), EtOAc (0.2 M), 25°C, 18 hr	X
2	DIPEA (3+2 equiv.), THF (anhy.), 25°C, 18 hr	64% <sup>a</sup>
3	DIPEA (3+2 equiv.), EtOAc (0.2 M), 25°C, 18 hr	52%
4	DIPEA (4+2 equiv.), EtOAc (0.2 M), 25°C, 18 hr	63%

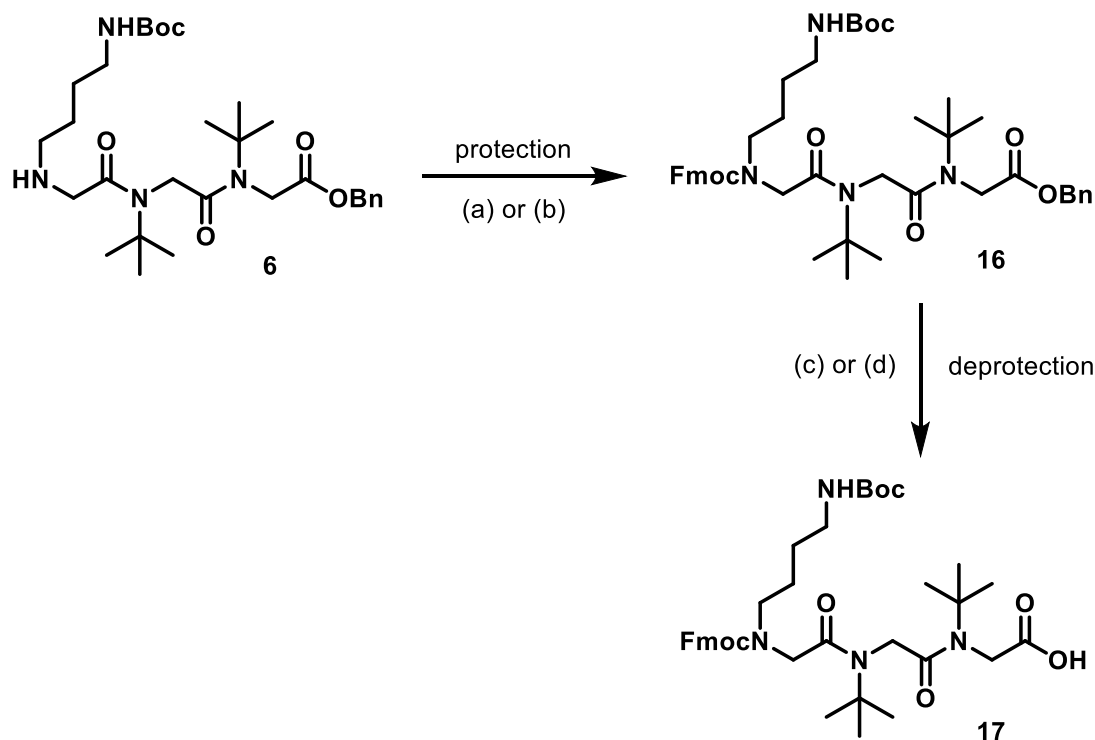
<sup>a</sup>not pure

Standard conditions using triethylamine as the base didn't provide the expected trimer. The diisopropylethylamine gave best results. After subsequent trials, the best yield was obtained by using first four equivalents of DIPEA to generate the free amine and later two more equivalents for the reaction of substitution. Besides, it was found that 0.2 M concentration in ethyl acetate at room temperature serves as the best medium for the reaction to occur. The trimer H-NLys(Cbz)-Ntbu-Ntbu-OEt **15** was thus obtained with a yield of 63%.

## 2.2 Block coupling study using H-(NLys(Boc)-Ntbu-Ntbu)-OBn trimer

### 2.2.1 Synthesis of the acid partner for block coupling

To perform the block coupling strategy, the preparation of the trimer block with a free acid at the C-terminus and a protected amine at the N-terminus was necessary. This trimer building block has been synthesized starting from trimer **6** by Fmoc protection of the amino group then cleavage of the benzyl ester by hydrogenolysis (Scheme 17, Table 11).



Scheme 17 Synthesis of the free acid trimer **17** for the block coupling strategy

Table 11 Selection of best conditions for protection and deprotection of trimer block

Entry	Conditions	Solvent system	Time	Yield
<b>a)</b>	FmocCl (1.05 equiv.), Et <sub>3</sub> N (2 equiv.)	THF (anhy.), 0°C	1 hr	94%
<b>b)</b>	FmocCl (1.05 equiv.), NaHCO <sub>3</sub> (0.4 M)	1,4-dioxane, 0°C -> rt	4 hr	78%
<b>c)</b>	H <sub>2</sub> , Pd/C 10%	MeOH (anhy.), rt	18 hr	93%
<b>d)</b>	H <sub>2</sub> , Pd/BaSO <sub>4</sub> 10%	THF/EtOH (abs.) (5:2), rt	72 hr	100%

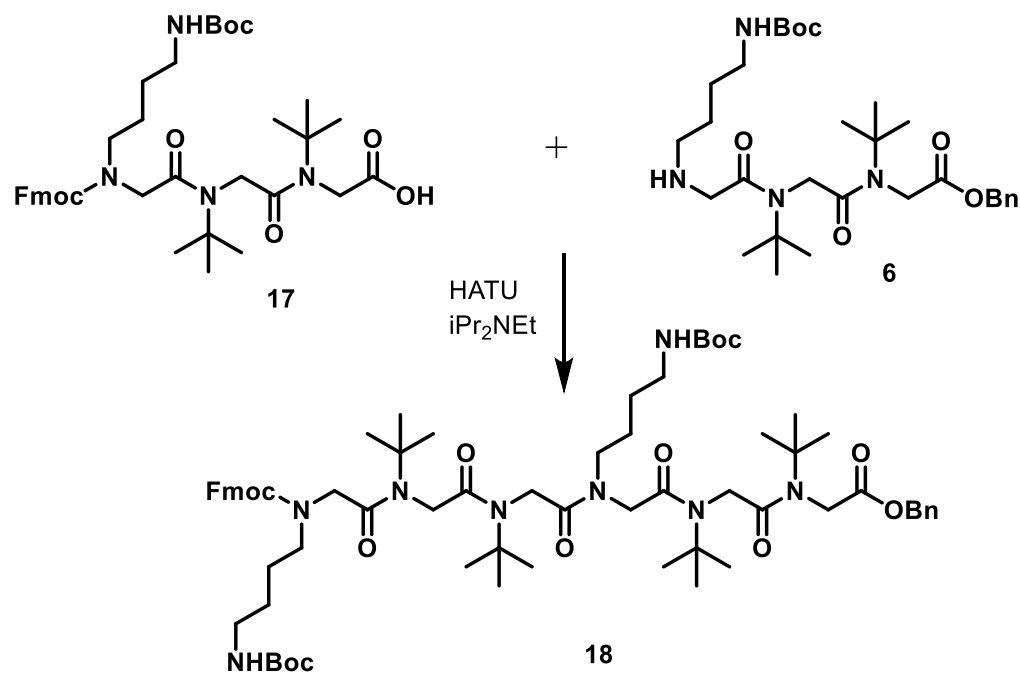
For the Fmoc protection, the method (a) in organic solvent was preferred at the method (b) conducted in aqueous media as it gave better yield. For the benzyl ester cleavage, two Palladium catalysts were tested. First, the classical one, palladium on carbon in anhydrous methanol with hydrogen at atmospheric pressure for 18 hours, gave a good yield of 93%. However, the second



method using palladium on barium sulphate as catalyst worked out better and gave 100% yield of pure acid **17**; though it takes three days to complete.

### 2.2.2 Coupling using 3+3 strategy

According to our previous studies,<sup>131</sup> the coupling reaction was done using the uronium salt HATU as a coupling agent and the diisopropylethylamine as a base (Scheme 18, Table 12).



Scheme 18 Synthesis of hexamer **18** by 3+3 block coupling

Table 12 3+3 Block coupling optimization

Entry	Acid <sup>a</sup> <b>17</b>	R group	HATU (equiv.)	DIPEA (equiv.)	Solvent	Amine <b>6</b> (equiv.)	Yield in hexamer
<b>1</b>	(c)	Fmoc	1.2	5.0	DCM/DMF 4:1 (0.3 M)	1.0	50% <sup>b</sup>
<b>2</b>	(c)	Fmoc	1.6	5.0	DCM/DMF 4:1 (0.3 M)	1.1	10%
<b>3</b>	(d)	Fmoc	1.2	5.0	DCM/DMF 4:1 (0.3 M)	1.0	73%

<sup>a</sup>The acid is generated by method c) Pd/C, H<sub>2</sub> or d) Pd/BaSO<sub>4</sub> 10%, H<sub>2</sub>; <sup>b</sup> Problem of reproducibility was encountered.

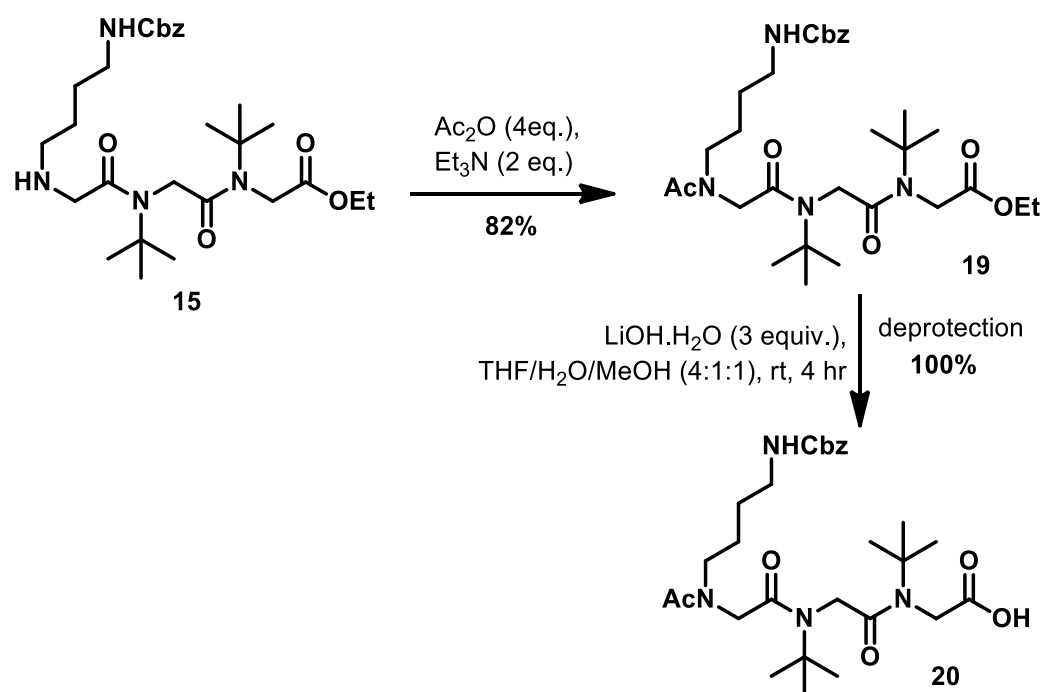
<sup>131</sup> E. De Santis; T. Hjelmgaard; C. Caumes; S. Faure; B. D. Alexander; S. J. Holder; G. Siligardi; C. Taillefumier; and A. A. Edwards, 'Effect of Capping Groups at the N- and C-Termini on the Conformational Preference of A, $\beta$ -Peptoids', *Org. Biomol. Chem.*, 10 (2012), 1108–22.

Using previously reported protocol, the hexamer **18** was obtained with a yield of 50% (entry 1). However, the coupling reaction failed to be reproduced. Subsequently, the equivalents of the coupling agent and of the amine partner **6** were increased. However, it gave poorer yield (entry 2 versus entry 1). Fortunately, it was observed that when the generation of the acid **17** was done by using palladium on barium sulphate (method d), the coupling 3+3 efficiently produced the hexamer **18** in 73% yield.

## 2.3 Block coupling study using H-(Nlys(Cbz)-Ntbu-Ntbu)-OEt trimer

### 2.3.1 Synthesis of the acid partner for block coupling

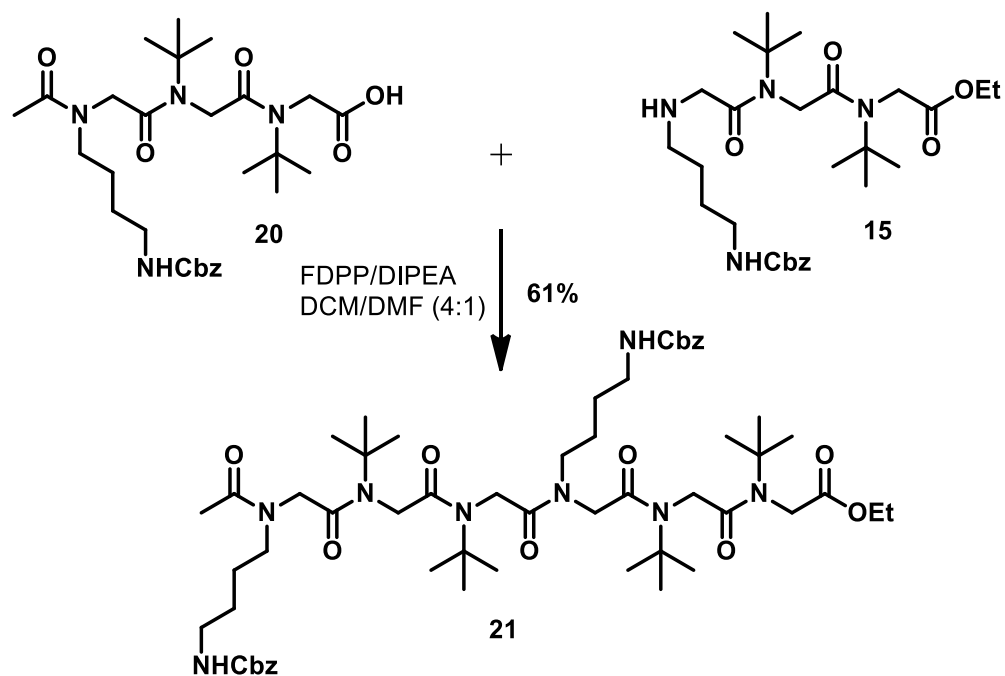
To prepare the trimer blocks for the coupling, the free acid at the C-terminus and a capped amine at the N-terminal was required. The trimer building block was synthesized by first capping the free N-terminal with acetyl group starting from trimer **15** and then cleavage of the ethyl ester by hydrolysis using lithium hydroxide (Scheme 19). The acid partner **20** was thus obtained in 100% yield and used without further purification.



Scheme 19 Synthesis of the free acid trimer **20** for the block coupling strategy

### 2.3.2 Block coupling using 3+3 strategy

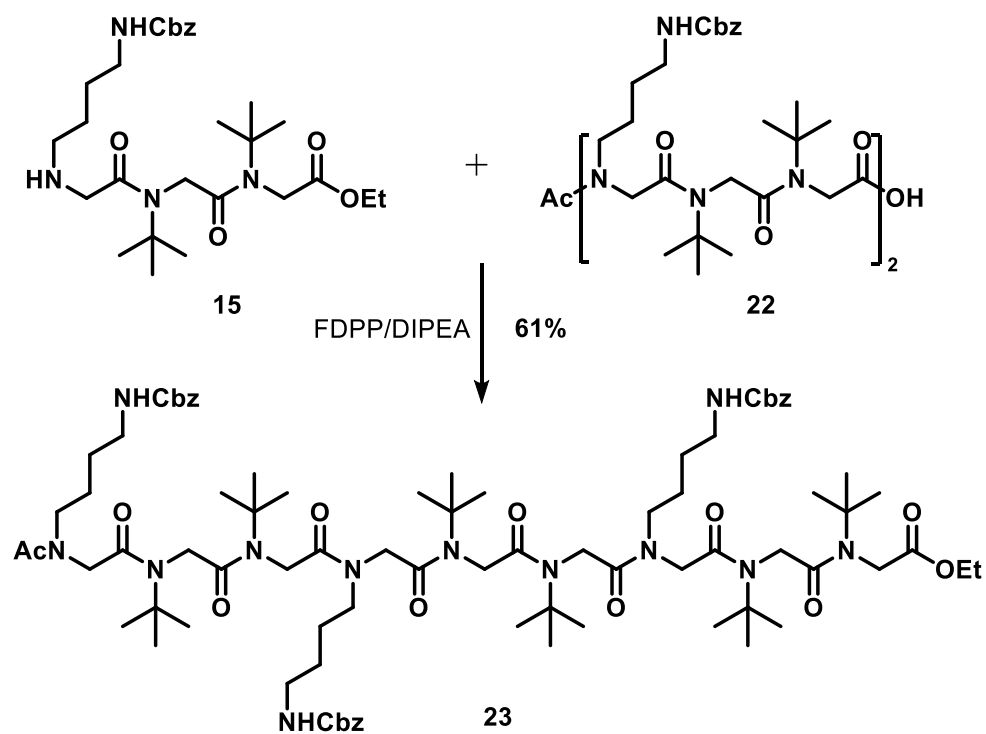
To perform the 3+3 coupling, we first tried the method using HATU and DIPEA<sup>131</sup> but it did not provide the required hexamer. After this failure, we tried different coupling agents. It was found that the pentafluorophenyl diphenylphosphinate (FDPP) leads to the construction of hexamer **21** in 61% yield (Scheme 20).



Scheme 20 3+3 Block coupling to form the hexamer 21

### 2.3.3 Block coupling using 6+3 strategy

Same conditions were used to achieve the 6+3 block coupling (Scheme 21).



Scheme 21 6+3 block coupling to form the nonamer 23.

The free acid **22** was obtained from hexamer **21** by using the same strategy as discussed before. The nonamer **23** was obtained with a yield of 61%. However, this coupling proved to be difficult to conduct and very pure substrates **22** and **15** must be employed to furnish the nonamer in a pure form. The 9+3 block coupling was also tested but failed to generate the dodecamer. Another method which could be used to produce the dodecamer is the 6+6 block coupling. However, to use the 6+6 coupling, the hexamer should be built by submonomer approach rather than 3+3 block coupling approach.

## 2.4 Access to cationic amphiphilic peptoids

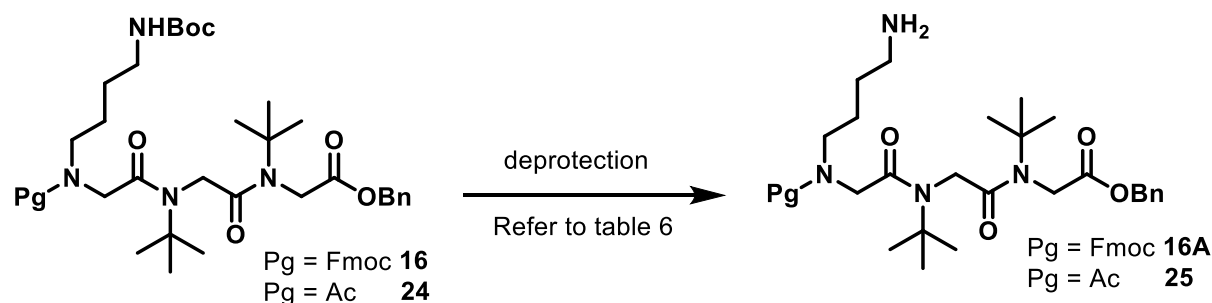
To access the therapeutic potential of these peptoids, they must present free amine side chains to play the role of the cationic group in these amphiphilic structures.

Three Protecting groups (Pg) were used for the synthesis of the R-(NLys(Pg)-Ntbu-Ntbu)<sub>n</sub>-X peptoids: Boc, Cbz and Fmoc groups. We will discuss the deprotection strategies used to remove the first two protecting groups for which peptoid oligomers of 6 and 9 residues have been obtained.

### 2.4.1 Deprotection of Boc-protected NLys residues

We employed different methods quoted in the literature for the deprotection of Boc group. The presence of tert-butyl group as a side chain in these oligomers can be a problem as it gets cleaved in acidic conditions. However, the kinetic of cleavage of the Boc group should be faster compared to the tert-butyl one and we had hoped to find conditions that enable selective deprotection. Below, we will discuss the various approaches and what we learned from it about tert-butyl based peptoids.

The study of the deprotection was performed on trimeric models: the trimer **16** (Fmoc-NLys(Pg)-Ntbu-Ntbu-OBn) and the trimer **24** (Ac-NLys(Pg)-Ntbu-Ntbu-OBn) obtained by capping of the trimer **15** with an acetyl group. As described below in Scheme 22, the removal of the protecting group will expose the cationic part of the oligomer. The various conditions tested are presented in Table 13.



Scheme 22 Deprotection of Ac-(NLys(Boc)-Ntbu-Ntbu)-OBn

Table 13 Selected methods for the removal of Boc group.

Entry	Starting material	Conditions
1	16	TFA/DCM (1:1), 0°C, 40 min
2	24	TFA/DCM (1:1), 0°C, 40 min
3	24	TFA/DCM (1:5), 0°C, 40 min
4	24	CAN (0.2equiv.), CH <sub>3</sub> CN, (reflux, 2 hr×3)
5	24	1M HCl in EtOAc (gassed), 25°C, 4 hr

Under standard TFA/DCM conditions in proportion 1:1 at 0°C (entry 1), the formation of several different compounds was observed. Two fractions were obtained by column chromatography. The first fraction being the monomer of trimer **16** which was confirmed by proton NMR that provides a hint for fragmentation of the oligomer. The second fraction was analysed by LC/MS showing five peaks. The desired unprotected oligomer showed low relative proportion. In the same conditions, trimer **24** gave two compounds (entry 2). The NMR showed that there was a loss of a tert-butyl side chain from the compound. The separation by chromatography was not possible since both compounds had similar  $R_f$ . Decreasing the TFA proportion did not show better selectivity (entry 3). The method described in entry 4 using Cerium ammonium nitrate<sup>132</sup> in acetonitrile under reflux conditions wasn't conclusive. We observed the total conversion of **24** into a single compound more polar in TLC. In the proton NMR, we observed a loss of the acetyl group and Lys side chain that seems to indicate a cleavage of the oligomer. Finally, a mild acidic non-aqueous solution of HCl dissolved in ethyl acetate<sup>133,134</sup> was used to deprotect the amino group at room

<sup>132</sup> J. R. Hwu; M. L. Jain; S. C. Tsay; and G. H. Hakimelahi, 'Ceric Ammonium Nitrate in the Deprotection of Tert-Butoxycarbonyl Group', *Tetrahedron Letters*, 37 (1996), 2035–8.

<sup>133</sup> F. S. Gibson; S. C. Bergmeier; and H. Rapoport, 'Selective Removal of an N-BOC Protecting Group in the Presence of a Tert-Butyl Ester and Other Acid-Sensitive Groups', *Journal of Organic Chemistry*, 59 (1994), 3216–8.

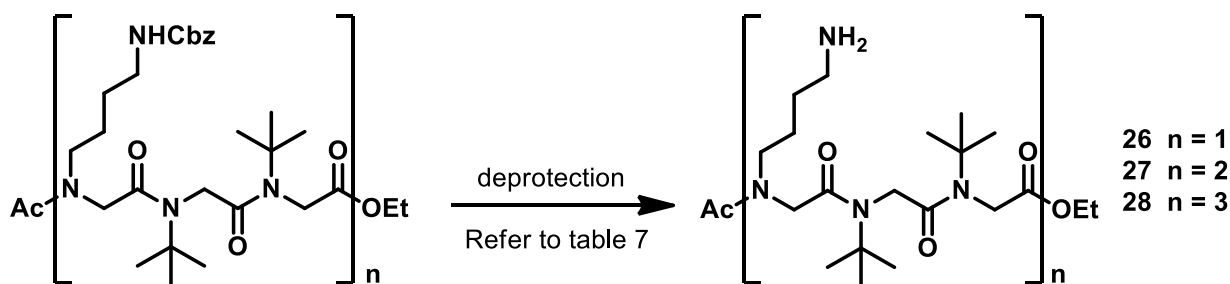
<sup>134</sup> G. L. Stahl; R. Walter; and C. W. Smith, 'General Procedure for the Synthesis of Mono-N-Acylated 1,6-Diaminohexanes', *Journal of Organic Chemistry*, 43 (1978), 2285–6.

temperature for four hours. This method also failed to give the deprotected compound. Rather it was found by LC/MS analysis the presence of the dimer H-Ntbu-Ntbu-OBn.

During this study, we were confronted with the inherent instability of these type of oligomers carrying tert-butyl side chains. So, after subsequent efforts to selectively remove the Boc group, it was decided to use a Cbz group to protect the NLys peptoid residue.

#### 2.4.2 Deprotection of Cbz-protected NLys residues

To cleave the Cbz group from the trimer Ac-(NLys(Cbz)-Ntbu-Ntbu)<sub>n</sub>-OEt, palladium on carbon or palladium on barium sulphate methods were used; both worked well to produce the free amino group on NLys side chain (Scheme 23, Table 14).



Scheme 23 Deprotection of Ac-(NLys(Cbz)-Ntbu-Ntbu)-OEt

Table 14 Deprotection of the Cbz-protected amine group.

Entry	Substrate	Conditions	Solvent system	Time	Yield
1	19 n = 1	Pd/C 10%	MeOH (anhy.)	18 hr	79%
2	19 n = 1	Pd/BaSO <sub>4</sub> 10%	THF/EtOH (abs.) (5:2)	72 hr	87%
3	21 n = 2	Pd/C 10%	MeOH (anhy.)	18 hr	84%
4	23 n = 3	Pd/C 10%	MeOH (anhy.)	18 hr	X

\*Not pure

Deprotection of the Cbz group proved to be an easy task, thereby making this family of cationic amphiphilic peptoids accessible to test their antimicrobial potency. Deprotection of the oligomer **23** did not provide the expected compound. Therefore, only the hexamer of the series A of family I was generated from the peptoid **21** (Table 14).

According to the biological results obtained for the hexamer of **27** (see chapter IV), the synthesis of the longer oligomers of Ac-(NLys-Ntbu-Ntbu)<sub>n</sub>-OEt family has not been optimized.

### 3 Synthesis of (NgLys-Ntbu-Ntbu)<sub>n</sub> peptoid family 1B

The family IB differs from family IA only by the replacement of the *MLys* peptoid residue by a  $\alpha$ -*gem*-dimethylated *MLys* residue (*N*-(1,1-dimethyl-4-aminobutyl)glycine; *NgLys*) (Figure 42). The *gem*-dimethyl side chain should as the tert-butyl group, locked the amide conformation in *cis*.

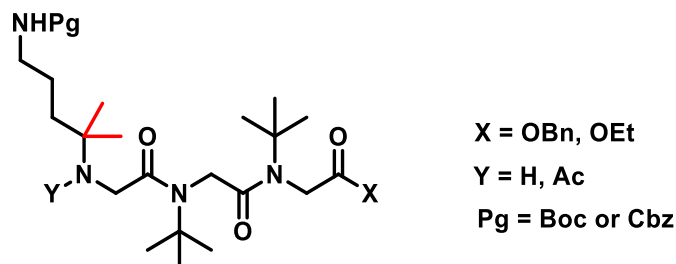
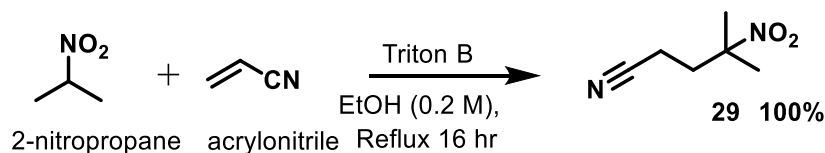


Figure 42 (NgLys-Ntbu-Ntbu)<sub>n</sub> peptoid family IB

To access the key trimer building-block Y-(*NgLys*(Pg)-*Ntbu-Ntbu*)-X, the synthesis of the  $\alpha$ -*gem*-dimethylated primary amine, 5-*N*-Boc-2,5-diamino-2-methylpentane was needed.

#### 3.1 Synthesis of $\alpha$ -*gem*-dimethylated primary amine

The process started with reacting 2-nitropropane with acrylonitrile in the presence of Triton B detergent. It acts as a base for the reaction and helps to form the nitro derivative **29** in 100% yield (Scheme 24).<sup>135</sup> The reflux in the first step was critical as the condensation should be maintained properly to avoid acrylonitrile evaporation from the reaction mixture.

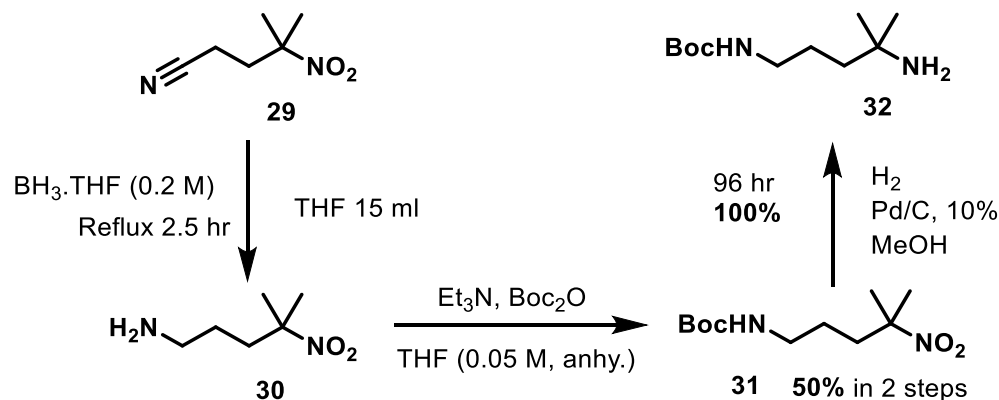


Scheme 24 Synthesis of 4-methyl-4-nitropentanenitrile

The nitrile group of the compound **29** was then reduced in presence of borane tetrahydrofuran complex solution giving the amine **30** which was directly protected with Boc<sub>2</sub>O in the presence of triethylamine as base. The tert-butyl (4-methyl-4-nitropentyl) carbamate **31** was obtained with a yield of 50% over 2 steps after purification by flash chromatography (Scheme 25).<sup>136</sup>

<sup>135</sup> B. A. Helms; S. W. A. Reulen; S. Nijhuis; P. T. H. M. De Graaf-Heuvelmans; M. Merckx; and E. W. Meijer, 'High-Affinity Peptide-Based Collagen Targeting Using Synthetic Phage Mimics: From Phage Display to Dendrimer Display', *Journal of the American Chemical Society*, 131 (2009), 11683–5.

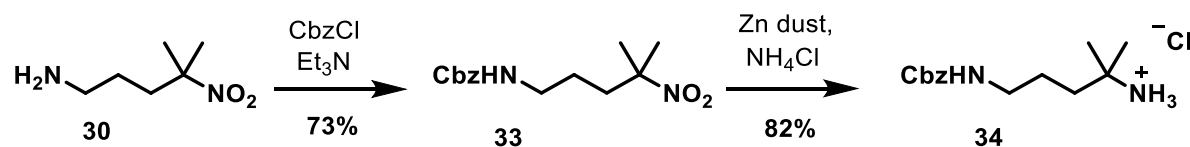
<sup>136</sup> S. Nagarajan and B. Ganem, 'Chemistry of Naturally Occurring Polyamines. 10.1 Nonmetabolizable Derivatives of Spermine and Spermidine', *Journal of Organic Chemistry*, 51 (1986), 4856–61.



Scheme 25 Synthesis of tert-butyl (4-amino-4-methylpentyl)carbamate 32

Finally, the nitro group of the compound **31** was reduced to a primary amine by hydrogenation using Pd/C in methanol to obtain the desired  $\alpha$ -gem-dimethylated primary amine **32** in 100% yield.

Since the cleavage of the Boc may cause problems, the protection by a Cbz group was also done. The primary amine of 1-amino-4-methyl-4-nitropentane **30** was protected using benzyl chloroformate in the presence of triethylamine which led to the formation of benzyl (4-methyl-4-nitropentyl)carbamate **33** in 73% yield (Scheme 26). The nitro group was then reduced in presence of Zinc dust using ammonium chloride as base to furnish benzyl (4-amino-4-methylpentyl)carbamate **34** as a salt in 82% yield.<sup>137</sup>



Scheme 26 Synthesis of benzyl(4-amino-4-methyl pentyl)carbamate 34

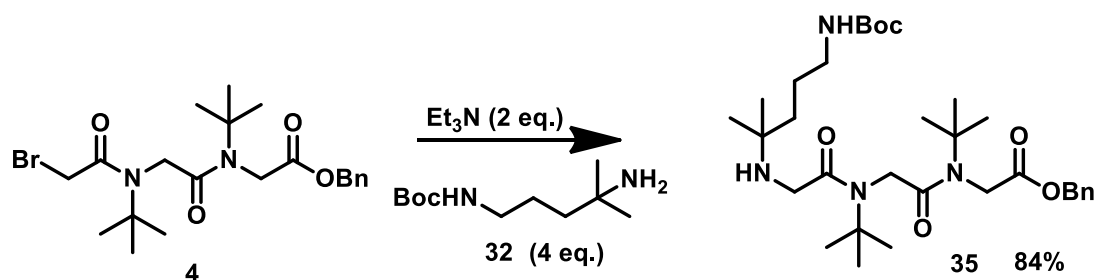
<sup>137</sup> C. Liu; J. Lin; G. V Delucca; D. G. Batt; and Q. Liu, 'Carboline Carboxamide Compounds Useful as Kinase Inhibitors' (Google Patents, 2011).



### 3.2 Synthesis of the trimer H-(NgLys(Pg)-Ntbu-Ntbu)-OR derivatives

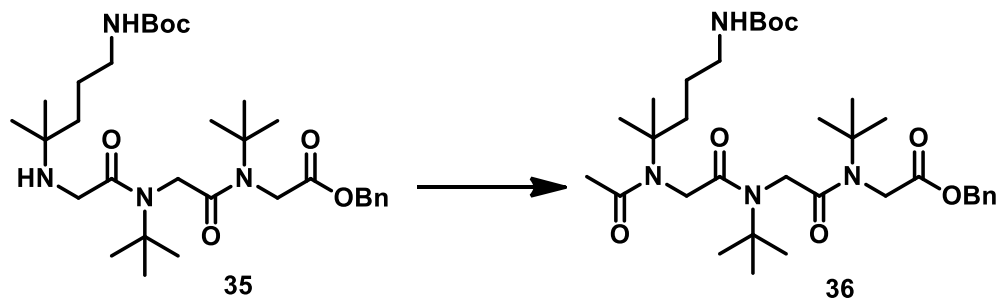
#### 3.2.1 Synthesis of Ac-NgLys(Boc)-Ntbu-Ntbu-OBn

The  $\alpha$ -gem-dimethylated primary amine **32** was then reacted with the bromo derivative **4** in presence of triethylamine as base to furnish the trimer H-NgLys(Boc)-Ntbu-Ntbu-OBn **35** in 84% yield (Scheme 27).



Scheme 27 Synthesis of H-NgLys(Boc)-Ntbu-Ntbu-OBn

The reaction of acetylation of trimer **35** proved to be difficult and was optimised to obtain the best yield of the acetylated trimer (Scheme 28, Table 15). The method using acetyl chloride proved to be shorter in time and more efficient as it produced the capped trimer **36** in 64% yield.



Scheme 28 Acetylation of the trimer block 35

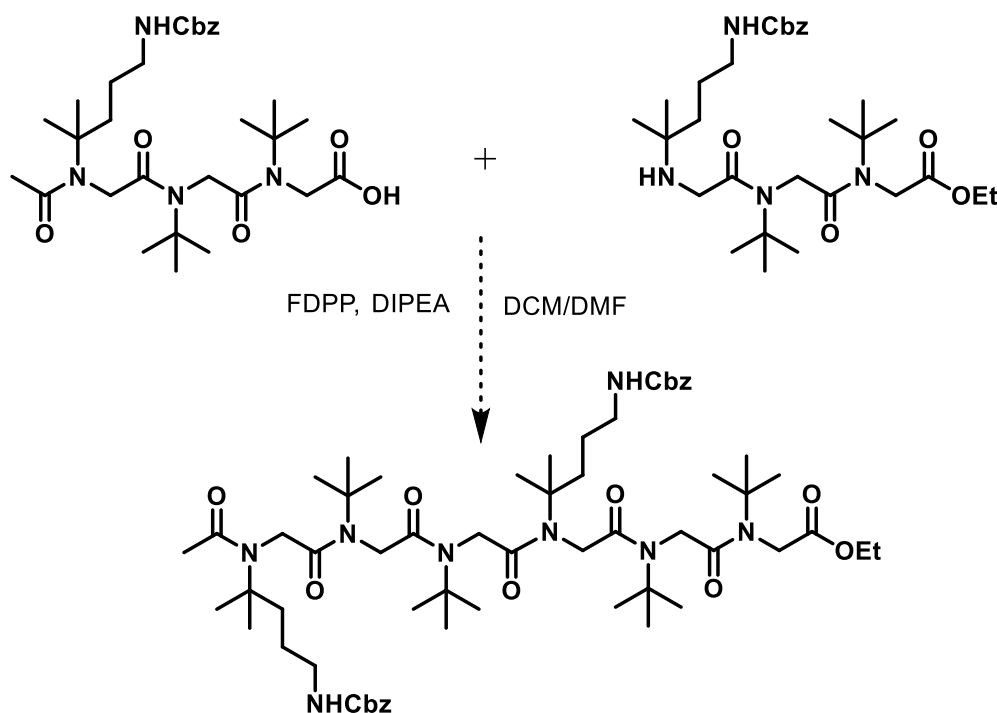
Table 15 Acetylation conditions of trimer 35

Entry	Conditions	Yield
1	1.) Acetic anhydride (4 equiv.), $\text{Et}_3\text{N}$ (2 equiv.), EtOAc (0.2 M), $0^\circ\text{C} \rightarrow 25^\circ\text{C}$ , 18hr	32%
2	2.) AcCl (1.1 equiv.) $\text{Et}_3\text{N}$ (2 equiv.), EtOAc (0.2 M), $0^\circ\text{C} \rightarrow 25^\circ\text{C}$ , 18hr	64%

The deprotection of the Boc group from the trimer **36** was not done as we have already shown on trimer **24** from family I that selective deprotection couldn't be achieved.

### 3.3 Conclusion

In course of this study, we have discovered the evidence for the synthesis of the trimer block Ac-(N<sub>g</sub>Lys(Boc)-N<sub>t</sub>bu-N<sub>t</sub>bu)-OBn using the  $\alpha$ -gem-dimethylated N<sub>L</sub>ys residue successfully. But, we found out that the removal of Boc protecting group alongside of tert-butyl side chain is a very tedious and futile exercise. Therefore, the synthesis of  $\alpha$ -gem-dimethylated N<sub>L</sub>ys side chain with Cbz protection paves the way for the synthesis of long oligomers using optimised coupling protocol developed to access long N<sub>t</sub>bu oligomers (Scheme 29).<sup>122</sup>



Scheme 29 Prospective synthesis of oligomers based on Cbz protected  $\alpha$ -gem-dimethylated N<sub>L</sub>ys side chain.

## 4 Synthesis of (N<sub>x</sub>t<sup>m+</sup>-N<sub>t</sub>bu-N<sub>t</sub>bu)<sub>n</sub> peptoid family II

To synthesise the cationic peptoids belonging to the second family based on tertbutyl and 1,2,3-triazolium-type side chains, we tried accessing long oligomers by submonomer synthesis (Figure 43). Considering the results previously obtained with the first family, we choose to introduce an ethyl ester at the C-terminus. Two types of triazolium side chain have been envisaged, one with an aromatic substituent (benzyl group, btm<sup>+</sup> residue) and the other with an amine moiety (aetm<sup>+</sup>, chtm<sup>+</sup> residue).

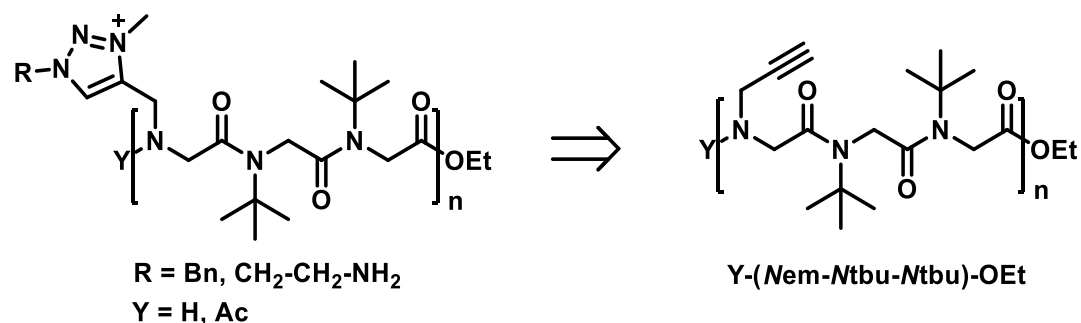
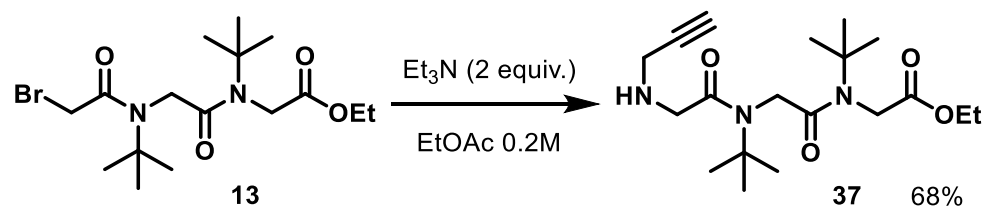


Figure 43 General structure of family II peptoid oligomers

Our strategy entailed the synthesis of linear oligomer sequence including multiple specifically located reactive propargyl group as triazolium precursors.

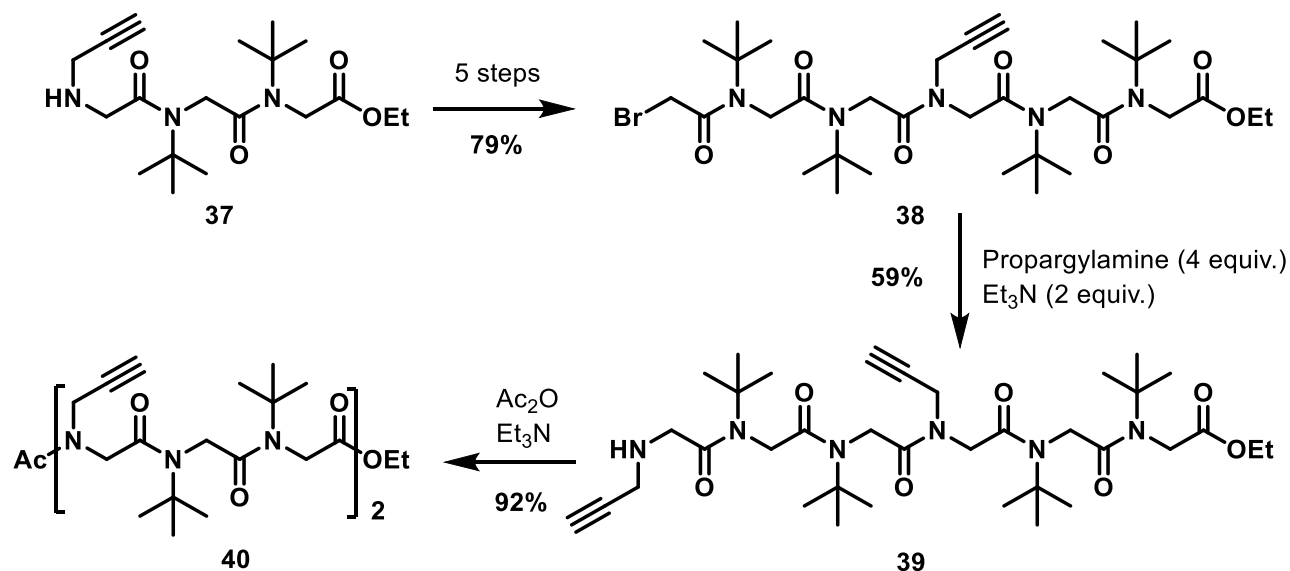
#### 4.1 Synthesis of hexamer $\text{Ac}-(\text{Nem-Ntbu-Ntbu})_2\text{-OEt}$

For the synthesis of the hexamer block with propargyl side chains every three residues, we employed the submonomer strategy. First the trimer  $\text{H}-(\text{Nem-Ntbu-Ntbu})_2\text{-OEt}$  was synthesised from the bromo derivative **13** using the propargylamine as the primary amine in the substitution step (Scheme 30). As for the tert-butyl amine, this primary amine has the advantage to be volatile thus easy to eliminate after the substitution. It is the reason why the synthesis of long oligomers by the submonomer method could be envisaged instead of the block coupling strategy.



Scheme 30 Synthesis of trimer  $\text{H-Nem-Ntbu-Ntbu-OEt}$

The alkyne group is readily incorporated using propargylamine affording the trimer  $\text{H-Nem-Ntbu-Ntbu-OEt}$  **37** in 68% yield. This oligomer is then elongated by iterative synthesis in solution phase to form the hexamer  $\text{H}-(\text{Nem-Ntbu-Ntbu})_2\text{-OEt}$  **39** with 47% yield in 6 steps from trimer **37** (Scheme 31).



Scheme 31 Submonomer synthesis of hexamer  $\text{Ac}-(\text{Nem-Ntbu-Ntbu})_2\text{-OEt}$  **40**

During this synthesis, it was noticed that scale up proved to be difficult for the substitution step. After acetylation, the hexamer  $\text{Ac}-(\text{Nem-Ntbu-Ntbu})_2\text{-OEt}$  **40** was prepared with a global yield of 12% starting from ethyl bromoacetate.

#### 4.2 Post-functionalization of the hexamer $\text{Ac}-(\text{Nem-Ntbu-Ntbu})_2\text{-OEt}$

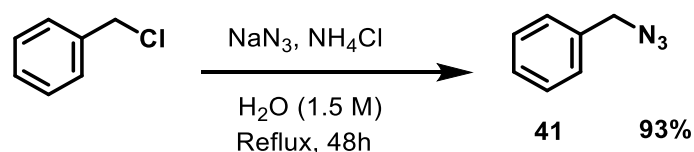
According to the experience of the group, the post-modification of the propargyl into triazole by copper-catalysed azide-alkyne cycloaddition (CuAAC reaction) was less efficient on peptoids with an uncapped *N*-terminus. For this reason, the post-functionalization was performed on acetylated oligomer **40** rather than on free *N*-terminal hexamer **39**.

##### 4.2.1 Oligomer incorporating Nbtm<sup>+</sup> residues (family II, series A)

##### 4.2.1.1 Synthesis of the 1,2,3-triazole-based peptoid oligomer

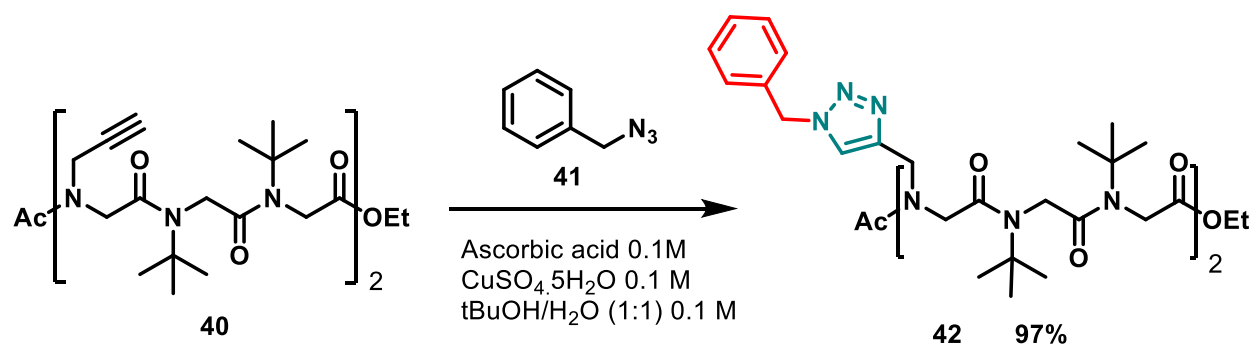
The synthesis of triazole moiety from the propargyl group is carried out by using the benzyl azide **41** synthesised from the benzyl chloride by a method available in the literature (Scheme 32).<sup>138</sup>

<sup>138</sup> A. Maisoniai; P. Serafin; M. Traikia; E. Debiton; V. Théry; D. J. Aitken; P. Lemoine; B. Viossat; and A. Gautier, 'Click Chelators for Platinum-Based Anticancer Drugs', *European Journal of Inorganic Chemistry*, 2008 (**2008**), 298–305.



Scheme 32 Synthesis of benzyl azide **41**

Thereafter, we conjugated the azide partner **41** to the selectively reactive site (alkyne group) on the peptoid scaffold **40**, using copper-catalysed azide-alkyne [3+2] cycloaddition (CuAAC) in solution phase affording oligomer **42** (Scheme 33).<sup>139</sup>



Scheme 33 Post-functionalisation modification by CuAAC

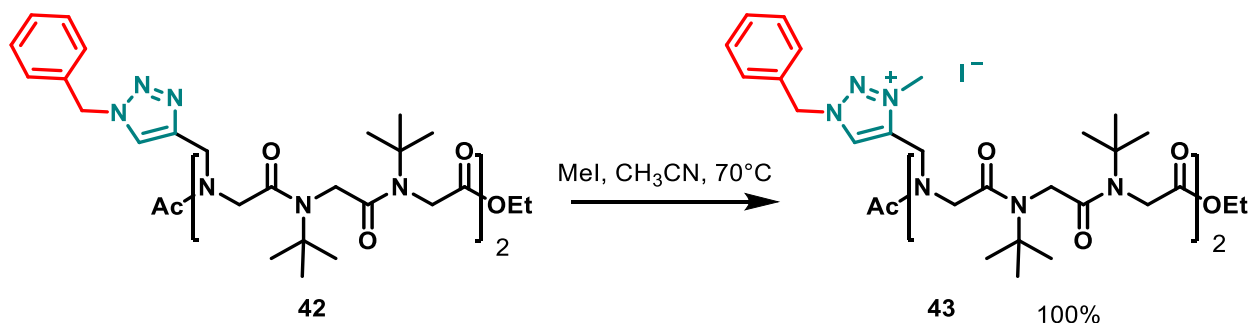
The alkyne groups within the oligomer sequence were modified with good efficiency through click chemistry and the hexamer **42** was obtained in very high yield (97%).

#### 4.2.1.2 Conversion into 1,2,3-triazolium moiety

To access the triazolium moiety, the methylation was performed of the triazole using methyl iodide according to a protocol previously employed in the group to access polytriazolium oligomers (Scheme 34).<sup>140</sup> The 1,2,3-triazolium based cationic oligomer **43** was quantitatively formed.

<sup>139</sup> J. M. Holub and K. Kirshenbaum, 'Tricks with Clicks: Modification of Peptidomimetic Oligomers via Copper-Catalyzed Azide-Alkyne [3 + 2] Cycloaddition.', *Chemical Society Reviews*, 39 (2010), 1325–37.

<sup>140</sup> H. Aliouat; C. Caumes; O. Roy; M. Zouikri; C. Taillefumier; and S. Faure, '1,2,3-Triazolium-Based Peptoid Oligomers', *Journal of Organic Chemistry*, 82 (2017), 2386–98.



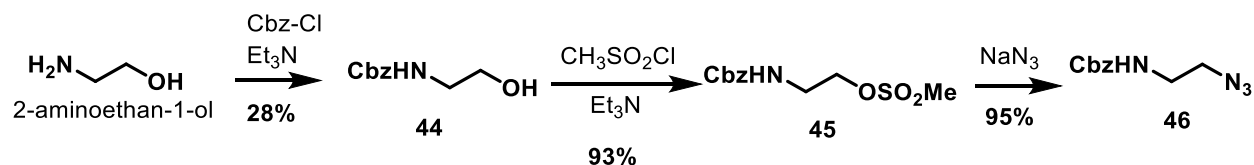
Scheme 34 Methylation of triazole groups to form triazolium cationic groups

The hexamer Ac-(Nbtm<sup>+</sup>-Ntbu-Ntbu)<sub>2</sub>-OEt **43** is ready for the biological studies (see chapter IV).

#### 4.2.2 Oligomer incorporating Naetm<sup>+</sup> residues (family II, series B)

##### 4.2.2.1 Synthesis of N-protected aminoethyl azide

To post modify the propargyl group of oligomer **40** into the 1-aminoethyl-3-methyl-1,2,3-triazolium methyl side chain (Naetm<sup>+</sup> residue), we first needed to synthesise the protected aminoethyl azide using a protocol described in the literature.<sup>141</sup> First, the amine of the 2-aminoethanol was protected using benzyl chloroformate to obtain compound **44** using the previously described strategy.<sup>142</sup> This step was achieved with a modest yield. The protected compound was then reacted with methane sulphonyl chloride to furnish the mesylate **45** in 93% yield<sup>143</sup>, which is then substituted with sodium azide to subsequently form the protected aminoethyl azide **46** in good yield (Scheme 35).



Scheme 35 Synthesis of Cbz-protected aminoethyl azide

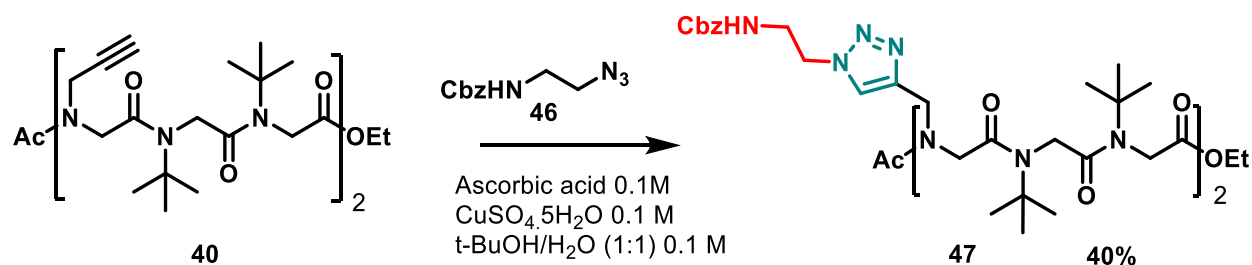
<sup>141</sup> M. S. Abdel-Maksoud; M. I. El-Gamal; M. M. Gamal El-Din; S. S. Kwak; H. Il Kim; and C. H. Oh, 'Broad-Spectrum Antiproliferative Activity of a Series of 6-(4-Fluorophenyl)-5-(2-Substituted Pyrimidin-4-yl)imidazo[2,1-B]thiazole Derivatives', *Medicinal Chemistry Research*, 25 (2016), 824–33.

<sup>142</sup> D. C. Tully; H. Liu; A. K. Chatterjee; P. B. Alper; R. Epple; J. A. Williams; M. J. Roberts; D. H. Woodmansee; B. T. Masick; C. Tumanut; J. Li; G. Spraggon; M. Hornsby; J. Chang; T. Tuntland; T. Hollenbeck; P. Gordon; J. L. Harris; and D. S. Karanewsky, 'Synthesis and SAR of Arylaminoethyl Amides as Noncovalent Inhibitors of Cathepsin S: P3 Cyclic Ethers', *Bioorganic and Medicinal Chemistry Letters*, 16 (2006), 5112–7.

<sup>143</sup> C. A. Townsend and A. Basak, 'Experiments and Speculations on the Role of Oxidative Cyclization Chemistry in Natural Product Biosynthesis', *Tetrahedron*, 47 (1991), 2591–602.

#### 4.2.2.2 Triazole formation by CuAAC using the N-protected aminoethyl azide

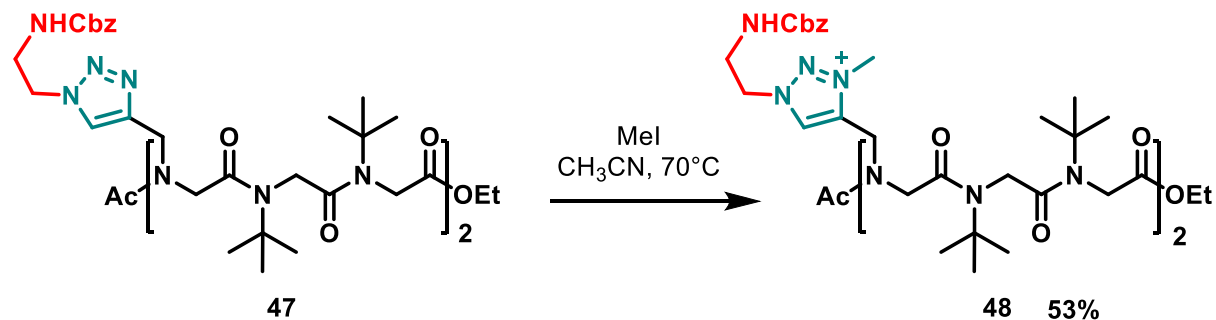
The Cbz-protected aminoethyl azide partner **46** was then conjugated with the peptoid scaffold **40** carrying two propargyl side chains, to produce the 1,2,3-triazole-based hexamer **47** in 40% yield using previously described conditions for the CuAAC (Scheme 36).



Scheme 36 CuAAC between aminoethyl azide and hexamer **40**

#### 4.2.2.3 Conversion into 1,2,3-triazolium moiety

Methylation of the oligomer **47** carrying two triazole moieties, was carried out to furnish the 1,2,3-triazolium-based hexamer **48** in 53% yield with alkylamine substituents (Scheme 37).



Scheme 37 Methylation of the triazoles to form triazolium moieties

Since the alkyl amine substituent on the oligomer **48** was protected with a Cbz group, the amine must be deprotected to obtain the cationic amphipathic oligomer.

## 5 Structural and conformational insights.

In the peptoid field, the determination of the secondary structure of oligomers is a tricky problem. Indeed, due to the absence of intramolecular hydrogen bonding to stabilize the structure as it is the case for  $\alpha$ -,  $\beta$ -peptides and many other peptidomimetics, the NMR approach is not really efficient. In 1998, the Zuckermann group has reported the NMR determination of the major solution conformation of a pentamer carrying various  $\alpha$ -chiral aromatic side chains.<sup>77</sup> Full NMR assignment was really difficult due to the presence of minor conformers and also the very nature of the peptoid; signals of the main chain protons were overlapped. Such a work could not be done routinely on each oligomer synthesised. It is the reason why the circular dichroism is generally preferred to study peptoid structuration.<sup>78</sup> However to perform circular dichroism studies on peptoid, the presence of chiral side chains is mandatory and the peptoid oligomers of family I and II do not contain chirality. Thus, circular dichroism is not applicable.

Another way to determine structuration is the crystallography providing the conformation in the solid state. Unfortunately, crystallisation assays did not provide suitable crystal for X-ray analysis.

Despite the limitations of the NMR technics to study peptoids conformation, analysis of 1D and 2D experiments could give insights on the conformational preferences of these oligomers.

For example, comparison of proton spectra could give information on the homogeneity of the structure. And in certain cases, NMR experiments enable the determination of the backbone amides conformation *cis* or *trans* (global *cis/trans* proportion over the sequence and/or *cis/trans* proportion for a selected amide).

### 5.1 Conformational study of family I oligomers

To access the influence of the  $\alpha$ -*gem*-dimethylated *N*Lys side chain on the conformation of the oligomers, the proton NMR spectra of the two trimers Ac-*N*Lys(Boc)-*N*tbu-*N*tbu-OBn **24** and Ac-*N*gLys(Boc)-*N*tbu-*N*tbu-OBn **36** were compared. We know from previous work that the tert-butyl side chain completely locks the amide in *cis* (Figure 44).

Analysis of the signal of the terminal acetate group in the 2-ppm region allowed for the determination of the *cis/trans* ratio of the *N*-terminal amide carrying the Lys-equivalent side chain or the *gem*-dimethylated side chain (Figure 45). In the proton spectra of trimer **24**, two signals in proportion 73:27 correspond to the acetyl group. According to previous studies, protons of the *trans* acetamide are deshielded and located above 2 ppm and protons from the *cis* acetamide are underneath the 2-ppm value. In the proton spectra of trimer **36**, a major singlet is located at 1.91 ppm indicating a strong preference for the *cis* conformation of the terminal acetamide.



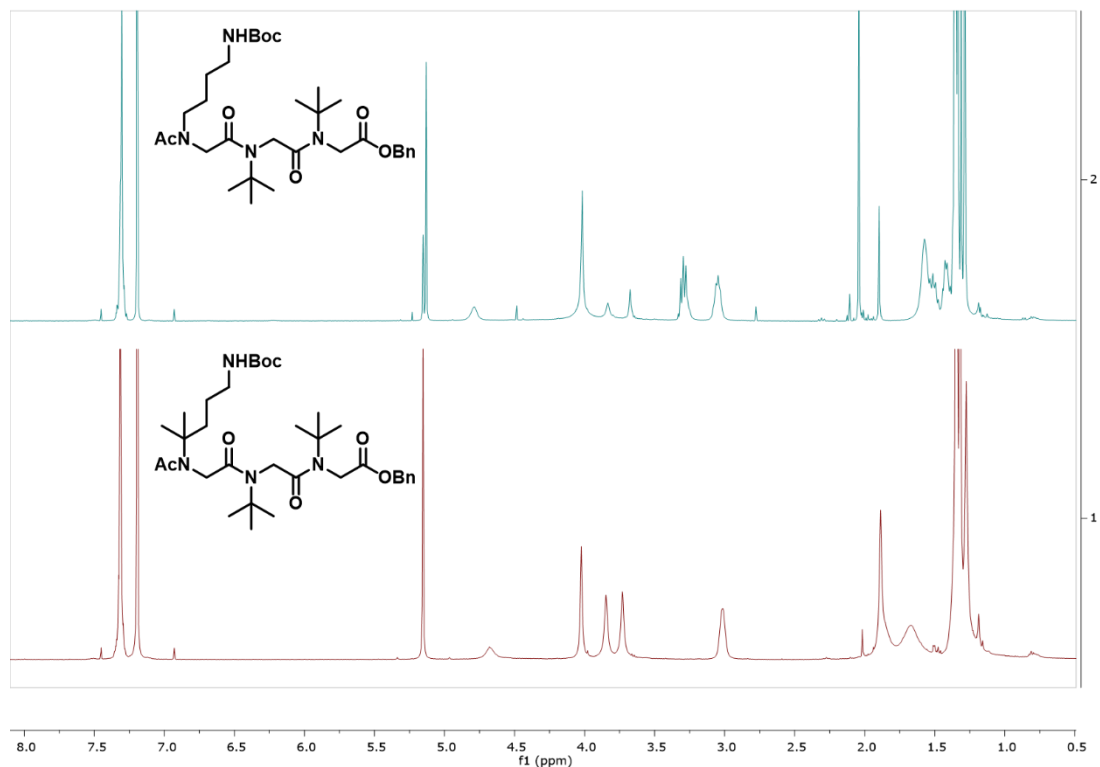


Figure 44 Comparison of  $^1\text{H}$  NMR spectra of trimers **24** (top curve) and **36** (bottom curve) in  $\text{CDCl}_3$

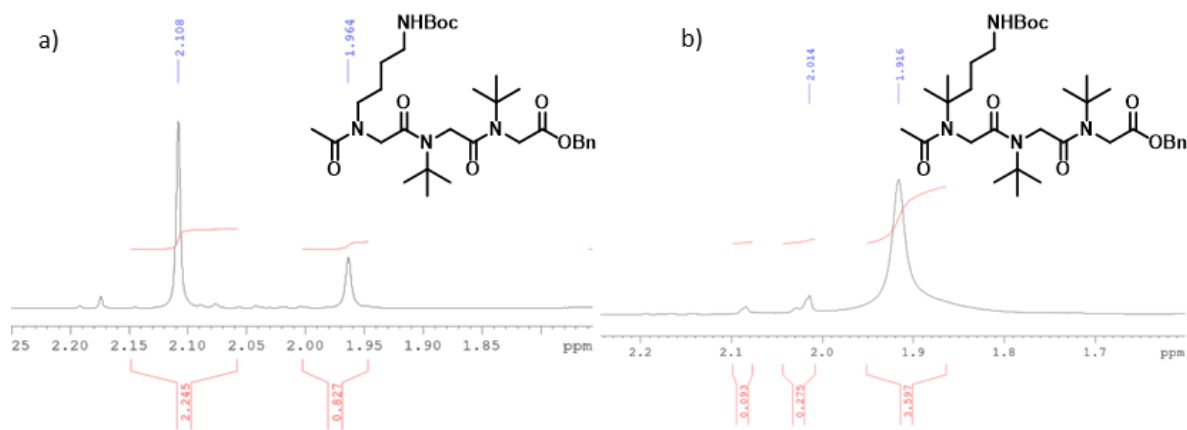


Figure 45 Acetyl proton region of  $^1\text{H}$  NMR spectra of trimers: a) **24** and b) **36** in  $\text{CDCl}_3$

These observations clearly indicate that the  $\alpha$ -gem-dimethylated side chain has the *cis*-directing effect awaited and then reduces the number of conformers of the trimer **36** and provides a robust structure in solution. Moreover, this preliminary NMR study showed that the  $\alpha$ -gem-dimethylated side chain acts as the tert-butyl side chain which can impart the rigidity of the tert-butyl side chain and provide a cationic group for giving an amphipathic nature to the oligomer.

## 5.2 Conformational study of family II oligomers

To access the influence of the triazolium side chain on the conformation of the oligomers, the proton NMR spectra of the two hexamers Ac-(Nbtm-Ntbu-Ntbu)<sub>2</sub>-OEt **42** and Ac-(Nbtm<sup>+</sup>-Ntbu-Ntbu)<sub>2</sub>-OEt **43** were compared (Figure 46). We know from previous work that the triazolium side chain exhibits the high ability for inducing *cis* conformation of the tertiary amide.<sup>121</sup> It was observed in the previous work that monomer units of triazolium showed excellent control over the *cis/trans* ratio by  $n \rightarrow \pi^*_{Ar}$  electronic delocalization.

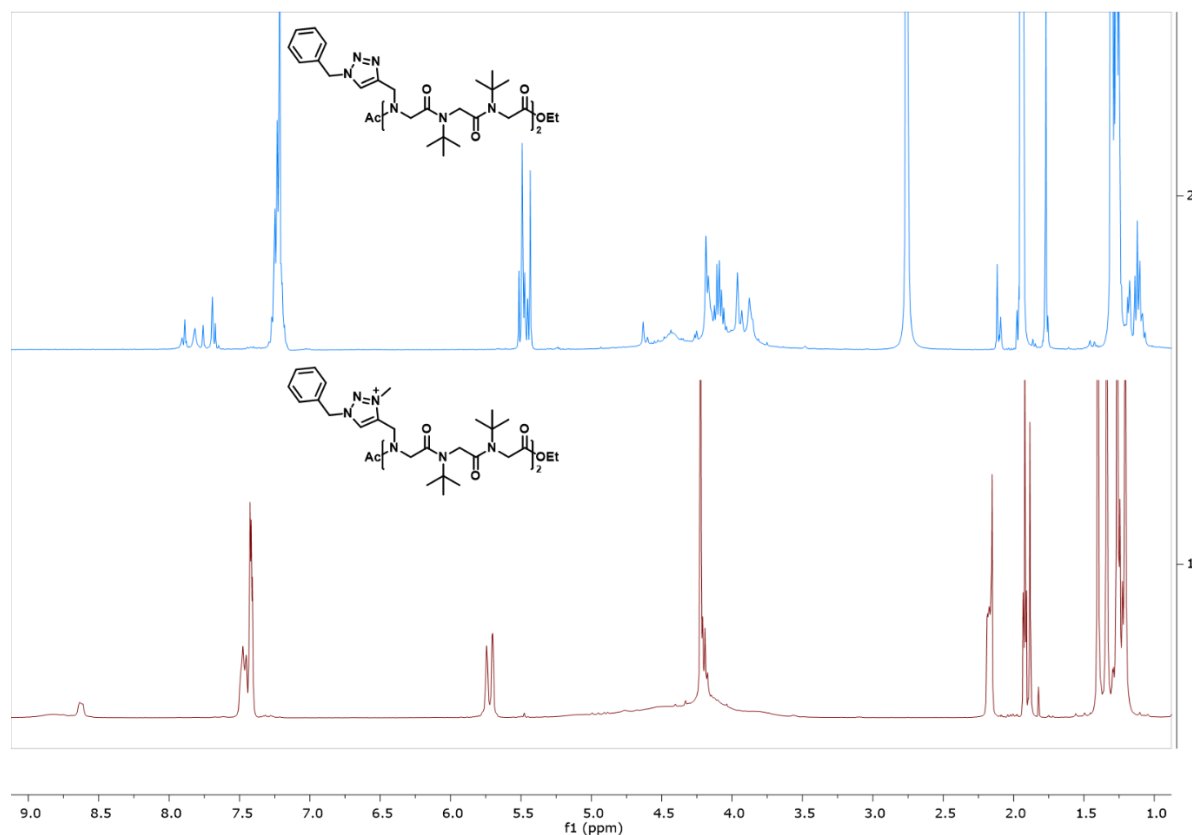


Figure 46 Comparison of <sup>1</sup>H NMR spectra of hexamers **42** (top curve) and **43** (bottom curve) in CD<sub>3</sub>CN

Analysis of the signal of the terminal acetate group in the 1.75 to 2.15 ppm region allows us to determine the *cis/trans* ratio of the *N*-terminal amide carrying the triazolium side chain (Figure 47). In the proton spectra of hexamer **42**, two group of signals in proportion 27:73 correspond to the acetyl group. As discussed before, protons corresponding to a *trans* acetamide are deshielded and located above 2 ppm and protons from the *cis* acetamide are underneath the 2-ppm value. Then according to the proton NMR experiment, the terminal acetamide of hexamer **42** is in a 73:27 *cis/trans* proportion. In the proton spectra of hexamer **43**, peaks corresponding to acetamide protons are all located in 1.82-1.94 area suggesting a strong preference for the *cis* conformation of the terminal acetamide.

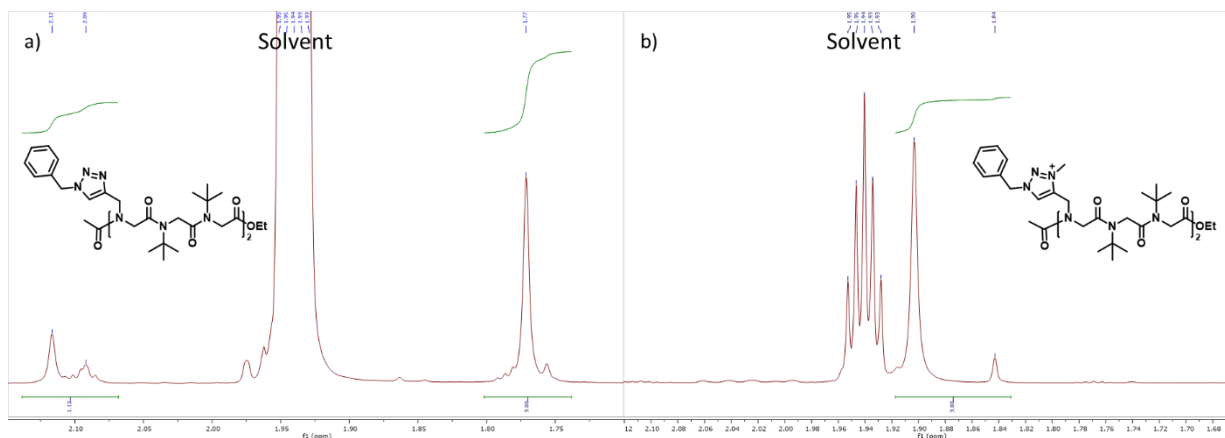


Figure 47 Acetyl proton region of  $^1\text{H}$  NMR spectra of hexamers: a) **42** and b) **43** in  $\text{CD}_3\text{CN}$

Analysis of the acetamide protons region and overall observation of the proton spectra show that the number of conformers of the hexamer **43** is significantly reduced compared to hexamer **42**. This preliminary NMR study suggests that family II oligomers carrying triazolium and tert-butyl side chains adopt a robust structure in solution. The NMR study confirms that the positively charged triazolium type side chain is a strong *cis* inducer. Hence, it is a great tool for diversification of the side chains and producing oligomers with strong amphipathic character.

## 6 Conclusion

The protocol to synthesise the oligomers has been established and it must be exploited in the future to produce longer oligomers.

### 6.1 Family I

Solution phase synthesis of the oligomers based on family I gave insights on the selection of protecting groups. We found out that the oligomers using Cbz protecting groups were easy to deprotect in the presence of a tert-butyl side chain on the oligomer. Therefore, the oligomers synthesized using this approach were used for their biological evaluation (see chapter III).

### 6.2 Family II

Triazolium-based oligomers were synthesised in overall good global yields which paves the way for the synthesis of longer oligomers incorporating the tert-butyl and the triazolium side chains. Also, the oligomers based on aminoethyl side chains on triazolium must be deprotected to produce the rigid cationic amphipathic oligomers.

## **CHAPTER III**

# **Solid-phase synthesis of cationic amphiphilic peptoid oligomers**

## 1 General overview of the solid-phase synthesis

Due to the revolution in genetic engineering in the late eighties, a lot of potential drug targets were being generated. The short peptide oligomers were known to bind to a variety of molecular targets though they lack good pharmacokinetic properties. Therefore, the team at Protos developed peptidomimetics by eliminating the weak points of peptide oligomers and preserving maximum peptidic character.<sup>58</sup> As the first peptoids were being developed it became evident that there was a need for an enhanced strategy for the synthesis of oligomers with high purity.

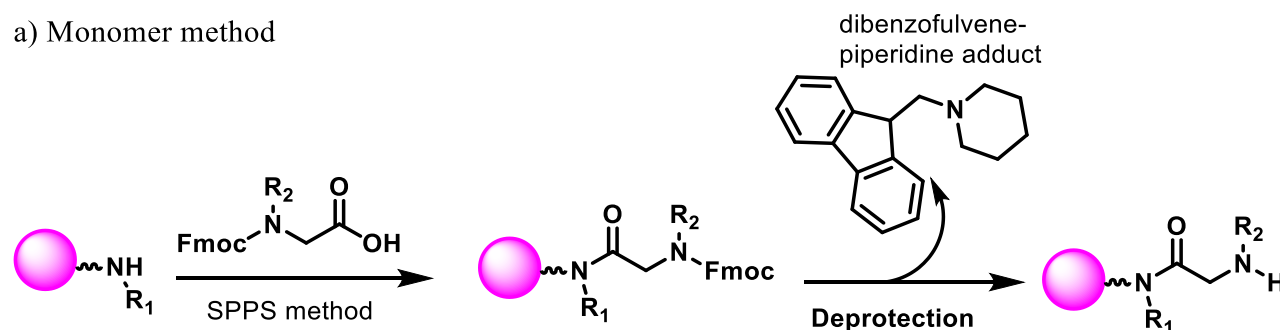
The foremost to appear and subsequently called the monomer approach derives a parallel with Fluorenylmethyloxycarbonyl Solid Phase Peptide Synthesis (Fmoc SPPS).<sup>66</sup> Here, formerly prepared *N*-Fmoc *N*-substituted glycine monomers were successively coupled to create oligomers (Scheme 38). In most of the present-day peptide synthesis, Fmoc-protected amino acids are often used. Therefore, employing Fmoc-protected *N*-substituted glycine derivatives seemed to be a very attractive approach for synthesizing peptoids both in solution and on the solid phase.<sup>144</sup> A practical advantage of using the monomer approach is the easy implementation of the synthesis protocol on commercially automated peptide synthesizers. But as the growing *N*-terminus of the peptoid chain is a secondary amine, which is more hindered compared to primary amines in SPPS, the coupling reaction is slow, and its efficiency depends of the coupling reagent used. However, the coupling reagent PyBop allows to obtain satisfactory results. It is thus possible to prepare peptoids as well as peptide-peptoid hybrids on these apparatus by means of essentially the same peptide synthesis protocol, but using Fmoc-protected *N*-substituted glycine monomers and a powerful coupling agent.<sup>145</sup> Considerable quantities of pure and relatively large peptoids should be accessible while the progress of their synthesis on the solid phase could be monitored by quantifying the dibenzofulvene adduct obtained after cleavage of the Fmoc group (Scheme 38, (a)). Although, the first automated solid phase synthesis of *N*-substituted glycines (NSGs) was done by this method.<sup>57</sup> A disadvantage of this approach, however, is the necessity of preparing suitable quantities of a diverse set of Fmoc-protected *N*-substituted glycine monomers. This point was rapidly a limitation to the development of large libraries of peptoids and to the combinatorial approach. Therefore, the Zuckerman's group quickly developed a more efficient method of supported synthesis adapted to peptoids, which they called "Submonomer solid phase synthesis" (Scheme 38, (b)).

---

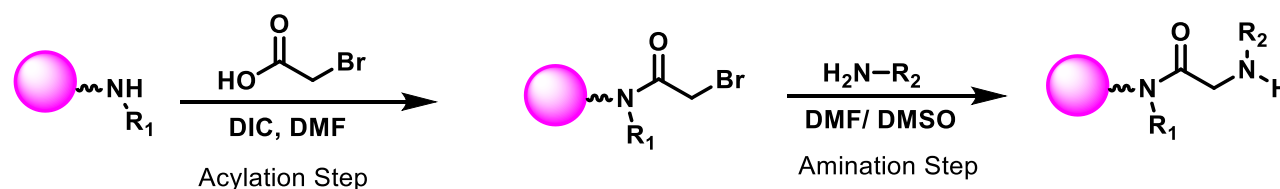
<sup>144</sup> J. A. W. Kruijtzter; L. J. F. Hofmeyer; W. Heerma; C. Versluis; and R. M. J. Liskamp, 'Solid-Phase Syntheses of Peptoids Using Fmoc-Protected *N*-Substituted Substance P', *Chemistry - A European Journal* (1998), 1570–80.

<sup>145</sup> E. Atherton and R. Sheppard, *Solid Phase Peptide Synthesis: A Practical Approach* (Oxford University Press, 1989).

a) Monomer method



b) Submonomer method



Scheme 38 General solid phase monomer and submonomer synthetic routes to NSG's synthesis

The submonomer synthesis cycle consists of two chemical steps starting from resin bound amine; first an acylation step using bromoacetic acid and *N,N'*-diisopropylcarbodiimide (DIC) leads to the formation of the backbone amide, followed by a second nucleophilic substitution step of the intermediate bromoacetamide with a primary amine which makes it possible to introduce a huge diversity of side chains. As in the monomer method, the direction of polymer synthesis occurs in the carboxy to amino direction. Using these two steps, the authors attempted to estimate the coupling efficiency, they synthesised a 25-residue long oligomer with 65% crude purity, indicating a >98% yield per monomer addition cycle. The solid-phase assembly of each monomer, during controlled polymer formation, eliminates the need for *N*-protected monomers and only reactive side-chain functionalities need to be protected which leads to the building of peptoids from readily available materials.<sup>146</sup> In the acylation step, the bromide is preferred; however, if the side-chain functionalities contain unprotected heteroatoms (e.g., heterocycles like- imidazoles, pyridines, pyrazines, and indoles), bromoacetic acid causes undesired side reactions which can be avoided by using chloroacetic acid.<sup>147</sup> The submonomer method can be fine-tuned to gain significant reaction

<sup>146</sup>G. M. Figliozzi; R. Goldsmith; S. C. Ng; S. C. Banville; and R. N. Zuckermann, 'Synthesis of N-Substituted Glycine Peptoid Libraries', *Methods in Enzymology*, Vol. 267 (Academic Press, 1996), 437–47.

<sup>147</sup>T. S. Burkoth; A. T. Fafarman; D. H. Charych; M. D. Connolly; and R. N. Zuckermann, 'Incorporation of Unprotected Heterocyclic Side Chains into Peptoid Oligomers via Solid-Phase Submonomer Synthesis', *Journal of the American Chemical Society*, 125 (2003), 8841–5.

time and purity of the final product by using microwave activation.<sup>148,149</sup> Oligomers up to 50 residues in length could be synthesized by this method with good yields suggesting superior efficiency at each coupling cycle.<sup>150</sup> By the submonomer approach, the oligo-NSGs synthesis is dramatically simplified.

## 2 Synthetic strategy

The submonomer strategy will be used to access cationic amphipathic peptoid oligomers from the family III (Chapter 1 Objectives)

In this section, we will discuss the solid phase synthesis of cationic amphipathic peptoid incorporating 1,2,3-triazolium-type side chains (Figure 48, (a)). The structure of these 1,2,3-triazolium-based peptoids is closely related to those of the potent antimicrobial peptoids (Figure 48, (b)) mimicking magainin-2 developed by Barron.<sup>88</sup>

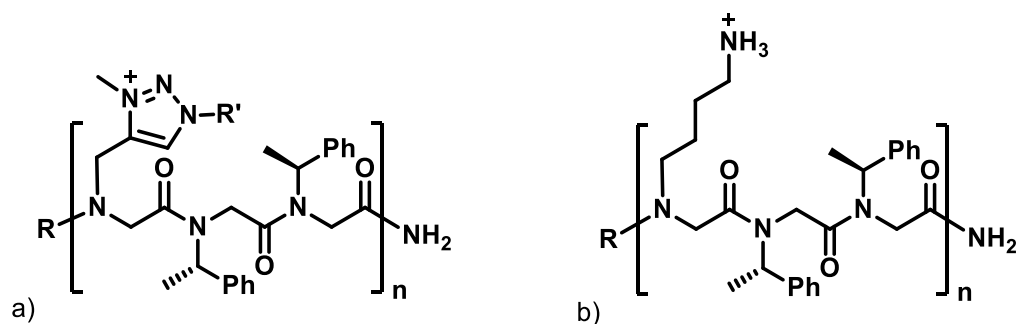


Figure 48 a) Family III cationic amphipathic peptoid incorporating 1,2,3-triazolium-type side chains b) Peptoids mimicking magainin-2 developed by Barron

Based on the rational design of the amphipathic cationic structure, oligomers comprising trimer repeats with two consecutive bulky  $\alpha$ -chiral *spe* side chains and one cationic 1,2,3-triazolium-type side chain should be accessible by synthesis on solid support followed by multivalent post-modification to form the triazolium moieties (Figure 49).

<sup>148</sup>H. J. Olivos; P. G. Alluri; M. M. Reddy; D. Salony; T. Kodadek; Hernando J. Olivos; Prasanna G. Alluri; M. Muralidhar Reddy; A. Derek Salony; T. Kodadek\*; H. J. Olivos; P. G. Alluri; M. M. Reddy; D. Salony; and T. Kodadek, 'Microwave-Assisted Solid-Phase Synthesis of Peptoids', *Organic Letters*, 4 (2002), 4057–8.

<sup>149</sup>M. A. Fara; J. J. Díaz-Mochón; and M. Bradley, 'Microwave-Assisted Coupling with DIC/HOBt for the Synthesis of Difficult Peptoids and Fluorescently Labelled Peptides - A Gentle Heat Goes a Long Way', *Tetrahedron Letters*, 47 (2006), 1011–4.

<sup>150</sup>B. C. Gorske; S. A. Jewell; E. J. Guerard; and H. E. Blackwell, 'Expedient Synthesis and Design Strategies for New Peptoid Construction', *Organic Letters*, 7 (2005), 1521–4.

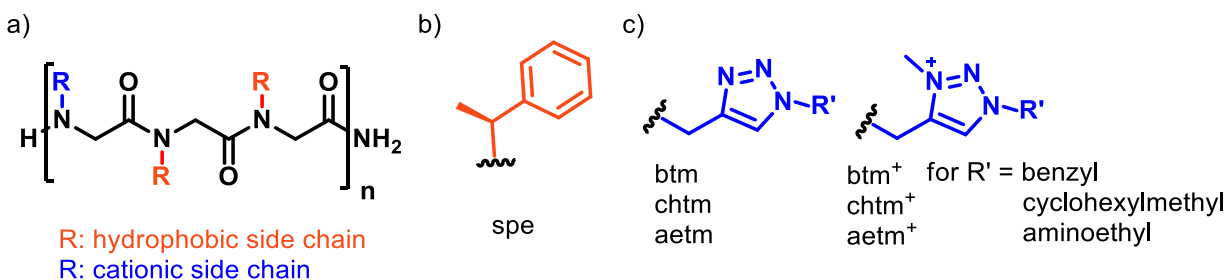
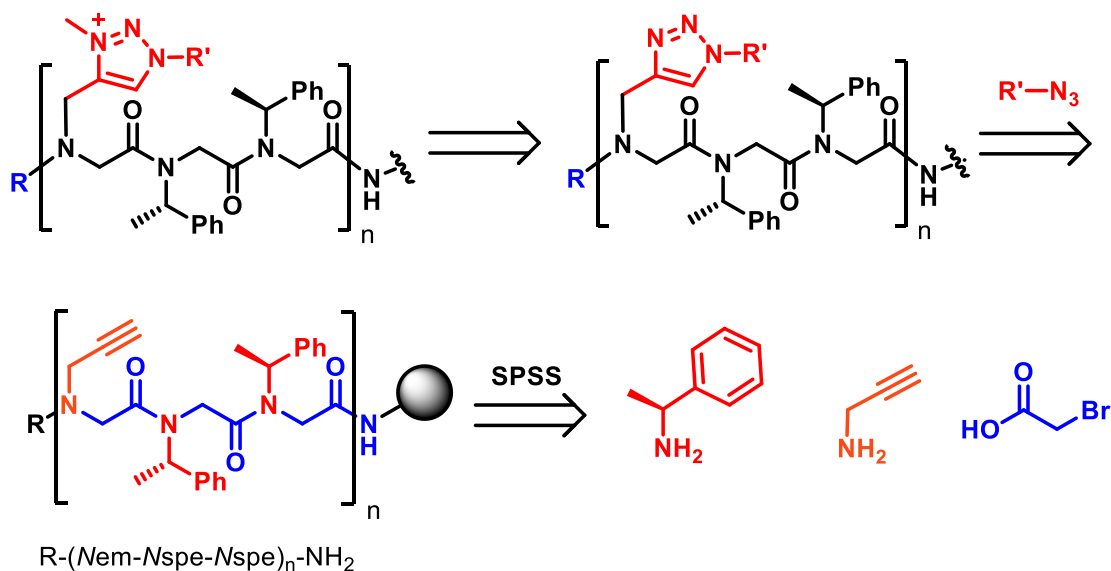


Figure 49 Cationic amphiphilic peptoids: a) Family III generic structure; b) The (S)-phenylethyl aromatic side chain; c) Structure of the 1,2,3-triazolium-type cationic side chains. Abbreviations: Nspe for N-(S)-(1-phenylethyl)glycine, Nchtm for N-(1-cyclohexylmethyl-1,2,3-triazolylmethyl)glycine and Nchtm<sup>+</sup> for N-(1-cyclohexylmethyl-3-methyl-1,2,3-triazolium methyl) glycine, Nbtm for N-(1-benzyl-1,2,3-triazolylmethyl)glycine and Nbtm<sup>+</sup> for N-(1-benzyl-3-methyl-1,2,3-triazolium methyl) glycine, Naetm for N-(1-aminoethyl-1,2,3-triazolylmethyl)glycine and Naetm<sup>+</sup> for N-(1-aminoethyl-3-methyl-1,2,3-triazolium methyl) glycine.

As illustrated in Figure 49, various groups such as benzyl, cyclohexylmethyl and aminoethyl will be introduced on the triazolium moiety to study the outcome of alkyl, aromatic substituents, and additional cationic group on antibacterial activity. The preparation of 1,2,3-triazolium-based amphipathic peptoid oligomers from Family III was envisaged by solid phase submonomer synthesis (SPSS) following the retrosynthetic approach illustrated below (Scheme 39).



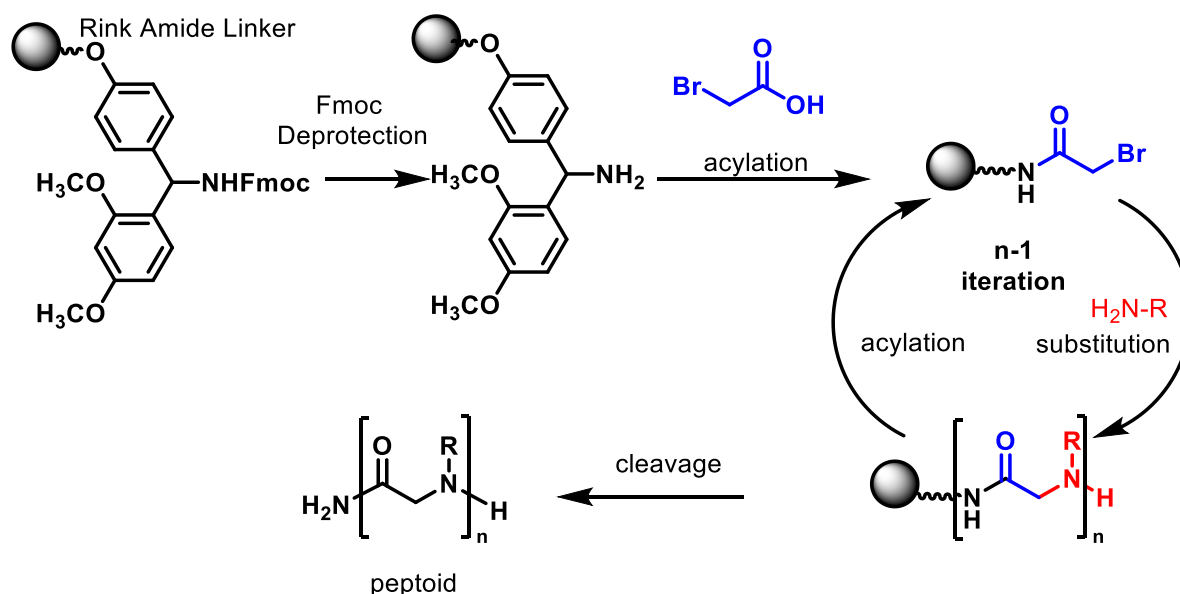
Scheme 39 Retrosynthetic pathway to access 1,2,3-triazolium-type cationic side chains; Abbreviations: Nem for N-(ethynylmethyl)glycine

Using this retrosynthetic approach, the triazolium moiety could be prepared by alkylation of the triazole ring. Triazole ring can, in turn, be accessed by cycloaddition between the alkyne of a propargyl side chain and a complementary azide. Finally, the oligomers R-(Nem-Nspe-Nspe)<sub>n</sub>-NH<sub>2</sub> carrying (S)-phenylethyl and propargyl side chains could be synthesised on the support using classical SPSS.



### 3 Conventional and microwave-assisted solid-phase submonomer synthesis (SPSS)

To perform SPSS, we used the original conditions from Zuckermann<sup>57</sup> adapted by Barron<sup>80</sup> to prepare peptoids (Scheme 40). Some modifications of the protocol have been done in the group to increase the crude purity and to speed up the synthesis. Indeed, a greater efficiency was observed when acylation and substitution steps were performed by heating at 40°C rather than at room temperature. It was also noticed that a short acylation time was beneficial to the crude purity.



Scheme 40 Solid phase submonomer synthesis (SPSS)

#### 3.1 Resin selection and synthesis of reference peptoids

First, the reference peptoid oligomers developed by Barron have been synthesised in order to use these compounds as reference in antimicrobial tests. In this context, different types of rink amide resin were studied in order to select the best one. Most of the reported syntheses have used polystyrene beads functionalized with a rink amide linker leading to C-terminal primary amide analogous to natural peptides.

Both Rink amide resin [4-(2',4'-Dimethoxyphenyl-Fmoc-aminomethyl)-phenoxy resin] and MBHA Rink amide resin [4-(2',4'-Dimethoxyphenyl-Fmoc-aminomethyl)phenoxy-acetamidonorleucyl-4-methylbenzhydrylamine resin] were used to perform the solid phase submonomer synthesis on the model hexamer H-(Nlys-Nspe-Nspe)<sub>2</sub>-NH<sub>2</sub> from Barron (Figure 50).

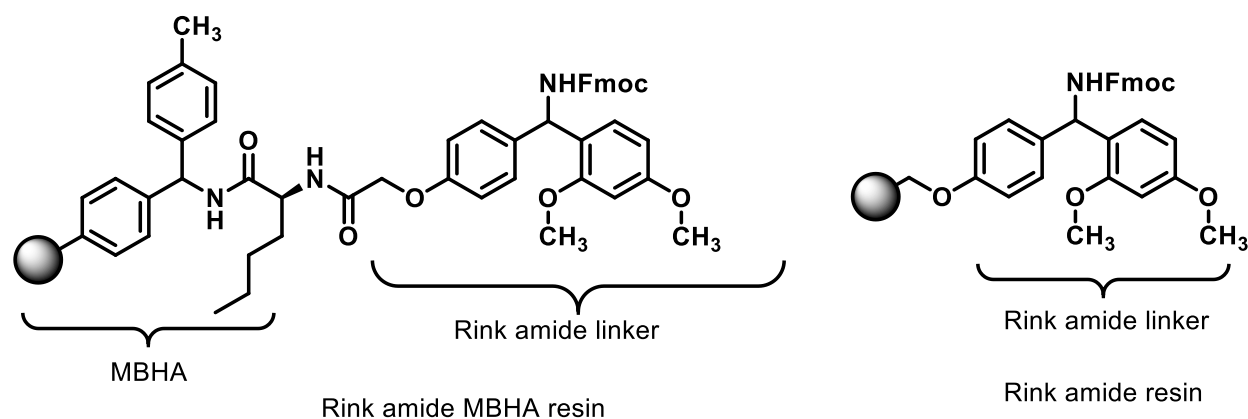


Figure 50 Structures of the Rink amide resin and Rink amide MBHA resin

The reported protocol to synthesise the cationic hexamer from Barron was applied using both resins (Figure 50) and LC-MS experiments of the crudes were performed (Figure 51). These preliminary experiments showed that higher crude purity was obtained using the Rink Amide MBHA resin which is less acid sensitive than the Rink Amide resin. Therefore, the rink amide MBHA resin was selected for further synthesis.

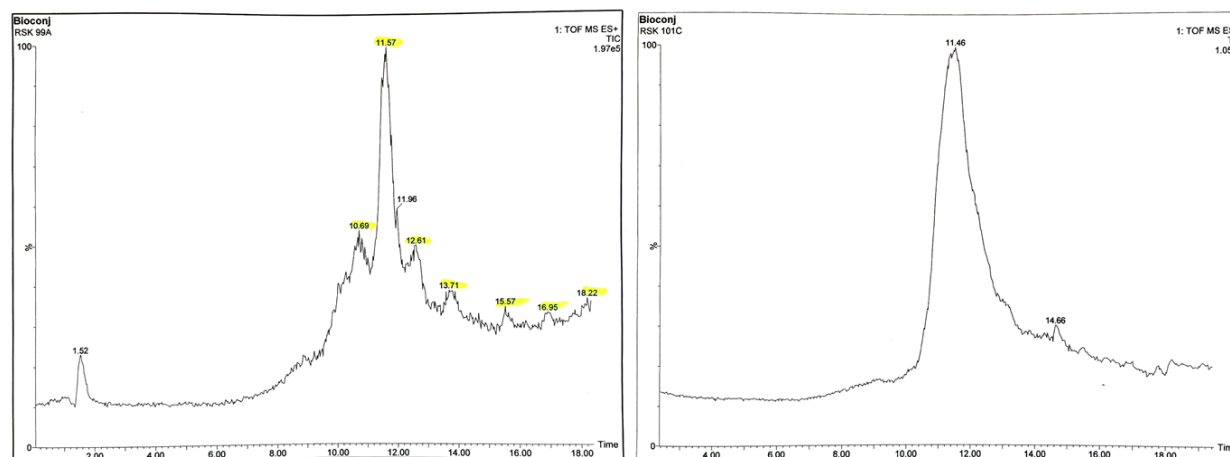
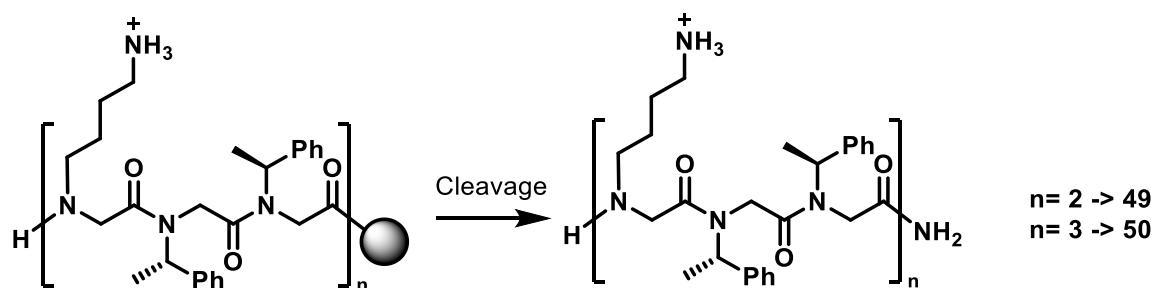


Figure 51 Comparison of LC-MS of the crude hexamer **49** obtained using rink amide (left curve) or MBHA rink amide resin (right curve)

The reference peptoids developed by Barron with the repeating sequence *N*Lys-*N*spe-*N*spe were thus synthesised starting from 100 mg of rink amide MBHA resin (loading 0.78 mmol/g), cleaved from the resin then purified by preparative HPLC (Scheme 41). The hexamer H-(*N*Lys-*N*spe-*N*spe)<sub>2</sub>-NH<sub>2</sub> **49** was obtained with a yield of 72% and the nonamer H-(*N*Lys-*N*spe-*N*spe)<sub>2</sub>-NH<sub>2</sub> **50** was obtained with a yield of 42%.



Scheme 41 Solid-phase synthesis of cationic oligomers developed by Barron

### 3.2 Synthesis of model hexamer H-(Nem-Nspe-Nspe)<sub>2</sub>-NH<sub>2</sub>

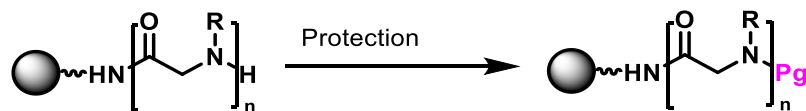
The access to oligomeric precursors of the 1,2,3-triazolium-based amphiphilic peptoids was then studied using Rink Amide MBHA resin. Peptoid oligomers carrying site-specifically positioned (*S*)-1-phenylethyl (*spe*) and propargyl (*em*) side chains as triazolium precursor were prepared by modified solid-phase submonomer strategy by conventional heating or using microwave.<sup>124</sup>

The solid phase synthesis can be carried out by two methods, namely, conventional synthesis and by microwave-assisted synthesis.<sup>148</sup> The conventional synthesis can be done manually by using a benchtop heating shaker (Advanced ChemTech manual organic synthesizer). The microwave assisted synthesis was performed on a microwave CEM Discover equipped with a Discover Bio Manual Peptide Synthesiser. The advantage of using microwave synthesiser is the reduction of time for long oligomers. Indeed, the substitution step can be accomplished in 5 minutes instead of 1 hour. The other highlights of the differences in both methods are detailed below (Table 16).

Table 16 Comparison of conventional SPSS conditions versus Microwave-assisted SPSS conditions

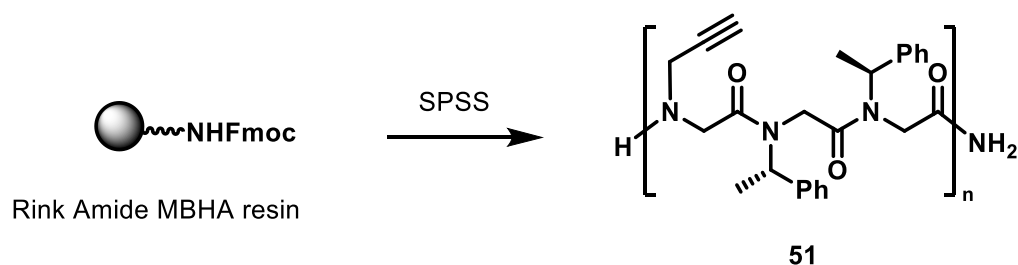
Reaction	Reagents	Conventional		Microwave		
		Time	T°C	Power	Time	T°C
Fmoc deprotection	Piperidine 20% v/v in DMF	2 × 15 min	40°C	20 W	3 min	75°C ± 5°C
Acylation	Bromoacetic acid (6 equiv, 0.4 M in DMF) DIC (8 equiv, 2M in DMF)	5 min	40°C	20 W	1 min	75°C ± 5°C
Substitution	Primary amine (25 equiv, 2 M in DMF)	60 min	40°C	25 W	5 min	75°C ± 5°C
Boc protection	(Boc) <sub>2</sub> O (6 equiv, 0.2 M in DMF), DIPEA (12 equiv)	50 min	40°C			
Acetylation	Ac <sub>2</sub> O (20 equiv, 0.8 M in DMF), Et <sub>3</sub> N (20 equiv)	90 min	25°C			
Cleavage	TFA/TIS/H <sub>2</sub> O (95:2.5:2.5)	2 × 30 min	25°C			

The terminal amine can be protected by a Boc group or capped with acetyl group to reduce the reactivity of the terminal amine and to study the influence of the terminal amine on antibacterial activities (Scheme 42).



Scheme 42 Protection of the terminal amine

Using the conditions reported in Table 16, the model hexamer compound **51** was synthesised (Scheme 43).



Scheme 43 SPSS of model compound  $H-(Nem-Nspe-Nspe)_2-NH_2$  **51**

First,  $H-(Nem-Nspe-Nspe)_2-NH_2$  peptoid **51** was prepared by microwave-assisted<sup>150</sup> SPSS then cleaved from the support using a TFA/TIS/H<sub>2</sub>O mixture.<sup>66</sup> The major impurity detected in the crude product by LC-MS was an oligomer that lacks one *Nspe* residue (Figure 52). After flash column chromatography on silica gel, the peptoid **51** was obtained with a yield of 91%. The main impurity was the pentamer  $H-Nem-Nspe-Nspe-Nem-Nspe-NH_2$ . HPLC separation of these two oligomers revealed difficult to achieve. The presence of this side product means that introduction of the first residue was no as efficient as the introduction of the following ones. This could be due to steric hindrance generated by the close proximity of the polymer resin. During this ongoing study, it was then found that this side product could be avoided doing twice the first acylation and twice the first substitution using *spe* as a primary amine. With this optimization, the peptoid **51** was prepared with a very good LC-MS purity.

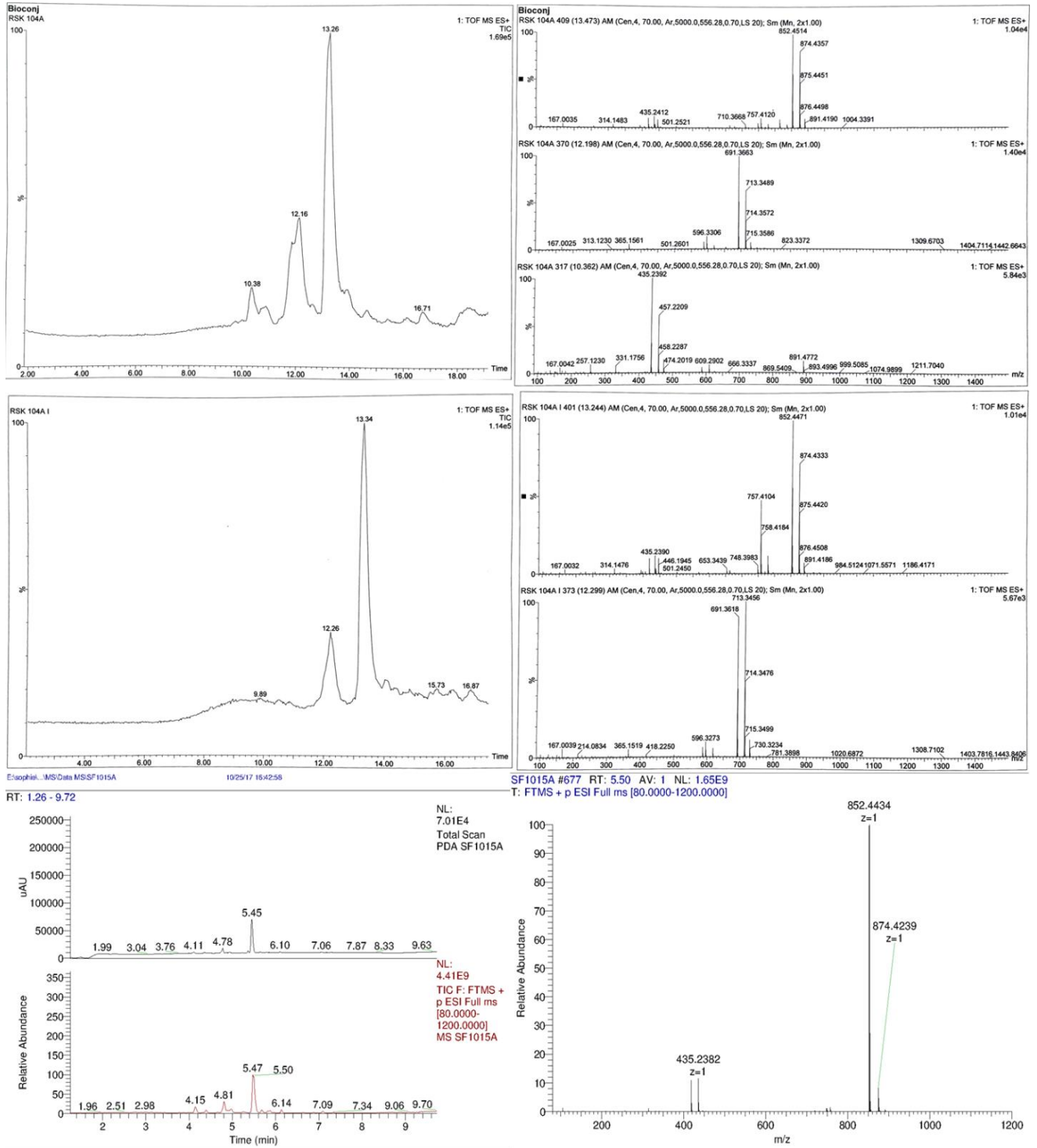


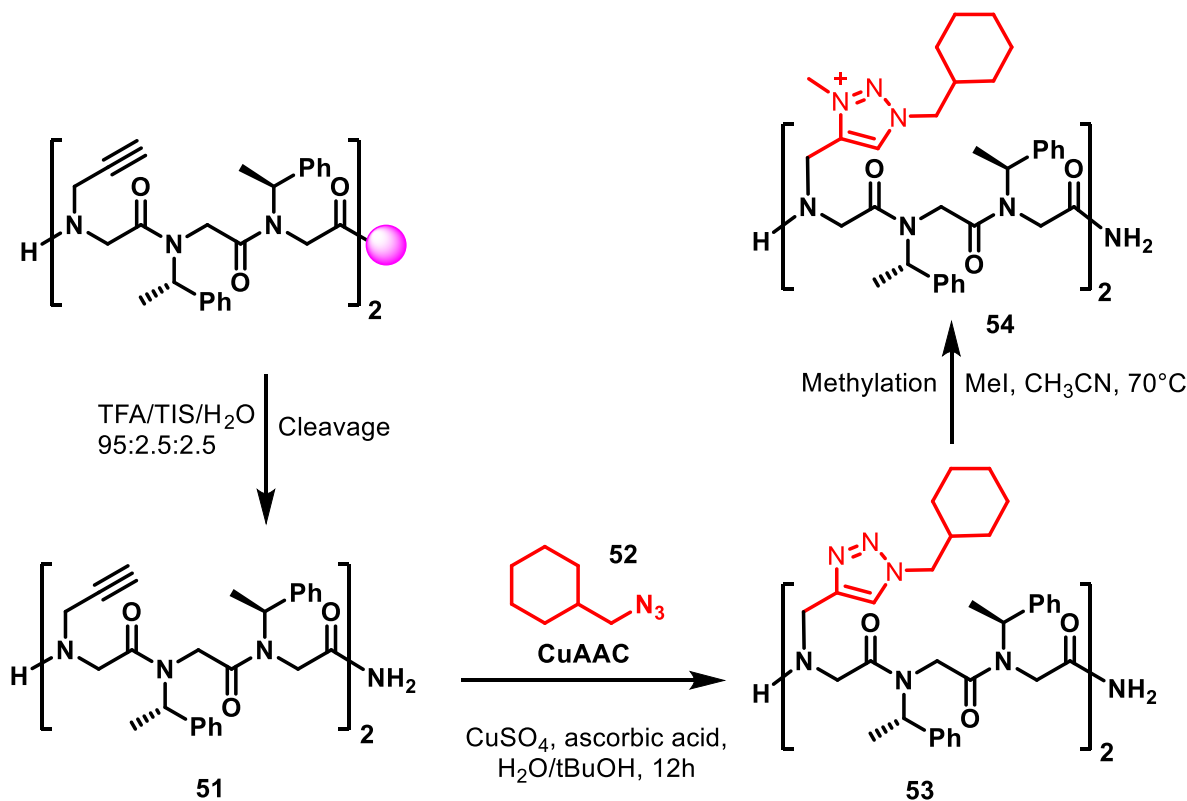
Figure 52 Comparison of LC-MS of crude hexapeptoid (upper spectra), purified hexapeptoid (middle spectra) and hexapeptoid with optimised conditions (bottom spectra).

## 4 Triazolium formation model study

The post-modification of the propargyl side chains into triazoles then triazoliums was studied in both solution phase and solid phase.

### 4.1 Solution phase strategy

To generate the 1,2,3-triazolium moieties, multivalent post-modification in solution has been explored using the hexamer H-(Nchtm<sup>+</sup>-Nspe-Nspe)<sub>2</sub>-NH<sub>2</sub> as a model target (Scheme 44).



Scheme 44 Synthetic strategy on solution phase to access peptid oligomers carrying triazolium side chains.

1,2,3-triazole formation in solution was performed using standard Cu-catalysed azide-alkyne reaction protocol from Sharpless<sup>151</sup> already exploited in the group to prepare polytriazolyl peptoids.<sup>140</sup> Using 1-cyclohexylmethylazide in presence of CuSO<sub>4</sub> and ascorbic acid in a tert-butanol/water mixture, the conversion of alkynyl into 1-cyclohexylmethyl-1,2,3-triazolyl was performed and furnished hexapeptoid with 52% yield after flash chromatography on silica gel. This

<sup>151</sup> H. C. Kolb; M. G. Finn; and K. B. Sharpless, 'Click Chemistry: Diverse Chemical Function from a Few Good Reactions', *Angewandte Chemie - International Edition*, Vol. 40 (WILEY-VCH Verlag GmbH, 2001), 2004–21.

modest yield could be due to the presence of the free *N*-terminus. Indeed, it was already noticed in previous studies that the CuAAc reaction was less efficient when using an uncapped oligoamide.

Conversion of 1,2,3-triazole into 1,2,3-triazolium was tested using methyl iodide in acetonitrile at 70°C for one night,<sup>152,153</sup> a well-established protocol to smoothly prepared polytriazolium peptoids.<sup>140</sup> Unluckily, a complex mixture of compounds was obtained due to reactive primary amide and unprotected terminal-amine groups. This problem of side alkylation by the methyl iodide was expected and can be even more problematic if a functionalized substituent is introduced on triazolium as in the series C of the third family.

This result prompts us to develop a strategy for which the triazolium moiety could be generated on the support without affecting *C*- and *N*-termini of the oligomer and enabling the introduction of functionalised triazolium such as the 1-aminoethyl-3-methyl-1,2,3-triazolium methyl side chain (aetm<sup>+</sup>, Figure 49).

## 4.2 Solid phase strategy

Similarly, to compare the efficiencies of solid phase and solution phase synthesis we synthesised the 1,2,3-triazolium moieties on solid support using the same hexamer H-(*N*chtm<sup>+</sup>-*N*spe-*N*spe)<sub>2</sub>-NH<sub>2</sub> as a model target.

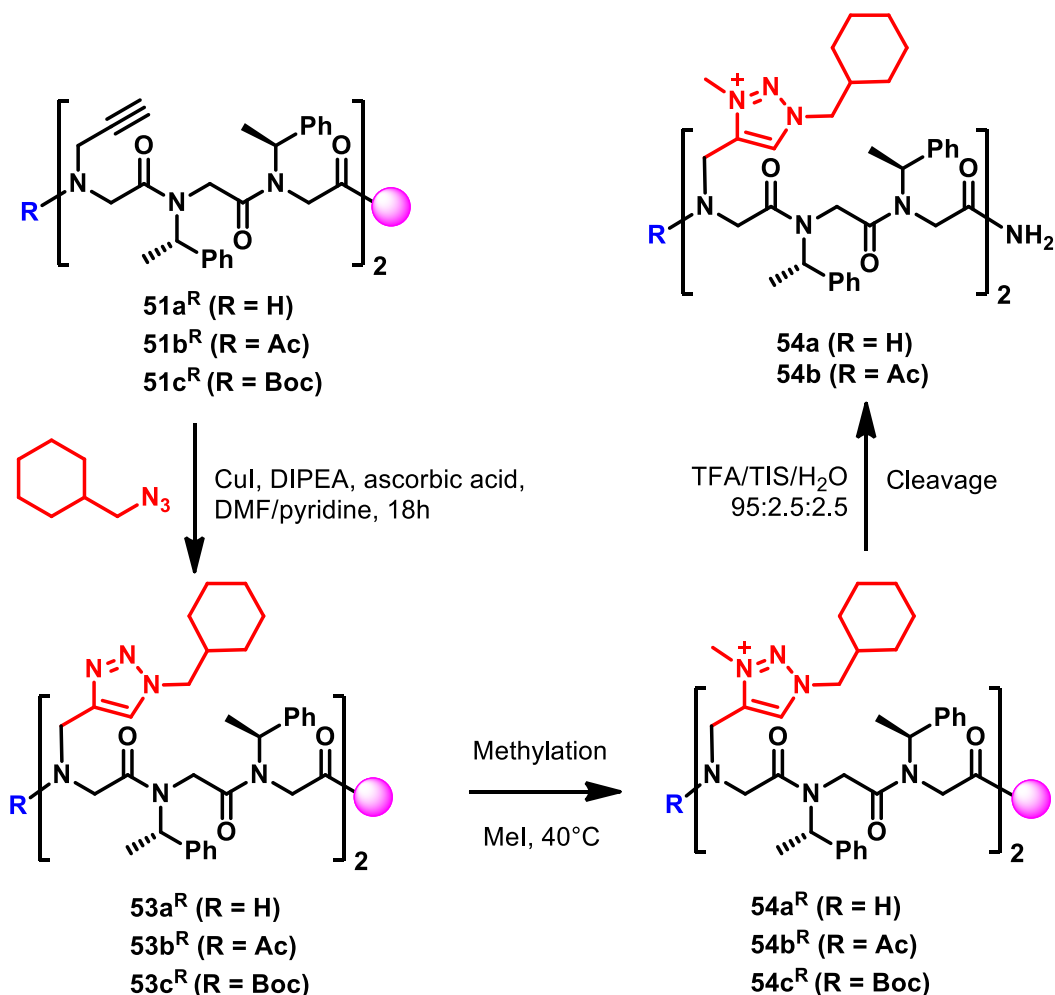
Starting from supported peptoid **51a<sup>R</sup>**, the multiple [3+2] cycloaddition conjugation was performed by the efficient solid-phase protocol using copper iodide, *N,N'*-diisopropylethylamine and ascorbic acid previously used by the Kirshenbaum group on peptoids (Scheme 45).<sup>154</sup>

---

<sup>152</sup> P. Mathew; A. Neels; and M. Albrecht, '1,2,3-Triazolylidenes as Versatile Abnormal Carbene Ligands for Late Transition Metals', *Journal of the American Chemical Society*, 130 (2008), 13534–5.

<sup>153</sup> S. Hanelt and J. Liebscher, 'A Novel and Versatile Access to Task-Specific Ionic Liquids Based on 1,2,3-Triazolium Salts', *Synlett* (2008), 1058–60.

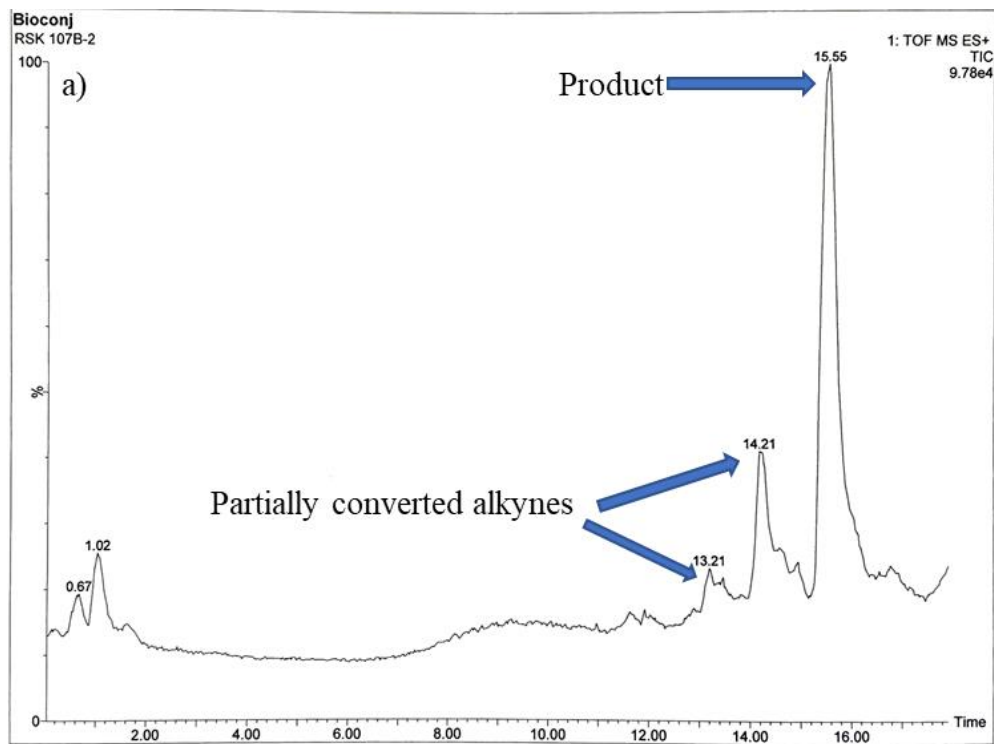
<sup>154</sup> H. Jang; A. Fafarman; J. M. Holub; and K. Kirshenbaum, 'Click to Fit: Versatile Polyvalent Display on a Peptidomimetic Scaffold', *Organic Letters*, 7 (2005), 1951–4.



Scheme 45 Solid-phase strategy on to access peptoid oligomers carrying triazolium side chains.

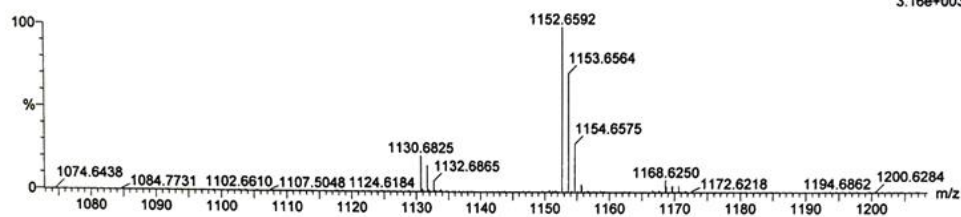
The resin placed in a mixture of DMF/pyridine, was treated with 12 equivalents of Copper iodide, 6 equivalents of ascorbic acid and 15 equivalents of DIPEA overnight at room temperature. After the reaction, the resin was extensively washed with a Cu scavenger cocktail composed of DMF, pyridine and ascorbic acid. Regrettably, cleavage of a sample of **53a** from the resin and LC-MS analysis of the crude showed the only partial conversion of alkynes probably due to the presence of the free *N*-terminus as previously observed (Figure 53, (a)). The LCMS spectra of the crude shows two pics corresponding to hexameric oligomers with one or two remaining propargyl side chains. By contrast, the total conversion proceeded when the *N*-terminal group was masked with an acetyl (**53b<sup>R</sup>**) or Boc-protected (**53c<sup>R</sup>**) (Figure 53, (b)).





RSK 107B-2 481 (15.748) AM (Cen,4, 70.00, Ar,5000.0,556.28,0.70,LS 20); Sm (Mn, 2x1.00)

1: TOF MS ES+  
3.16e+003



Minimum:

Maximum: 5.0 100.0 -1.5

Mass Calc. Mass mDa PPM DBE i-FIT Formula

1130.6825 1130.6668 15.7 13.9 29.5 1.7 C<sub>64</sub> H<sub>84</sub> N<sub>13</sub> O<sub>6</sub>

RT: 0.79 - 9.64

SF10158 #627 RT: 5.09 AV: 1 NL: 1.40E9  
I: FTMS + p ESI Full ms [140.0000-2100.0000]

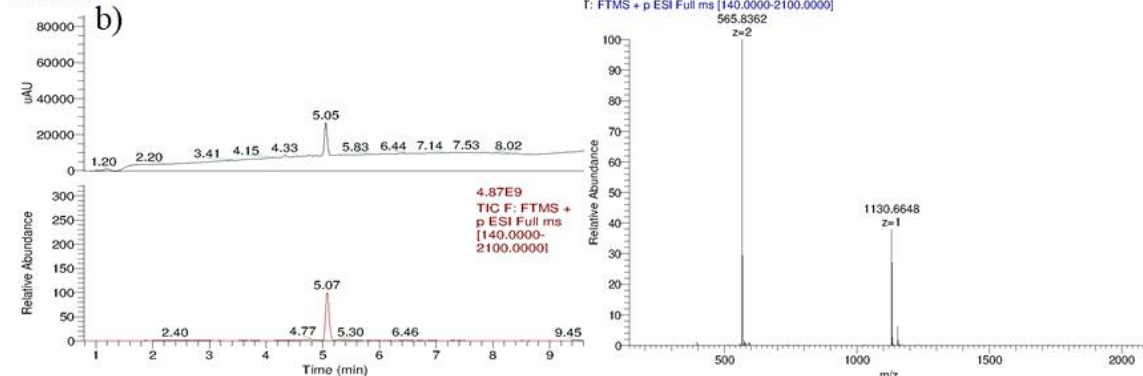


Figure 53 LCMS spectra of a) the crude hexamer 53a; b) the crude hexamer 53c.

Accordingly, the *N*-terminus was protected with a Boc group to improve CuAAC reaction efficiency and prevent from the side-compounds formation during quaternisation of the triazoles

into triazoliums. The Boc protecting group is particularly adapted since the desired free terminal amine will be recovered under resin cleavage conditions. In this work, the Huisgen reaction proceeds at room temperature for 18h. However, Mayaan *et al.* reported that the time for the CuAAc reaction may be reduced using microwaves activation.<sup>155</sup>

The critical step to access the targeted cationic amphipathic oligomers was the quaternisation of the triazoles into triazoliums. To our knowledge, this transformation on resin has never been reported in the literature. Triazoliums formation by methylation of the hexamer **53** was studied on support. Based on previous work,<sup>140</sup> methyl iodide was chosen as alkylating reagent at different concentration (0.1 M, 4 M, 16 M, pure) in diverse solvents (CH<sub>3</sub>CN, DMSO, NMP) and at different temperature (rt, 40°C, 50°C) (Table 2). The method using NMP was chosen based on the work of Amblard's group to synthesise ribbon-like foldamers on resin.<sup>156</sup>

Table 17 Conditions tested for the conversion of triazoles into triazoliums

Entry	Conditions	Time	Results
1	MeI (40 equiv.), 60°C, CH <sub>3</sub> CN (0.1 M), in round bottom flask over magnetic stirrer.	18 h	One methylation
2	MeI (40 equiv.), 40°C, CH <sub>3</sub> CN (0.1 M), in syringe over shaking incubator.	18 h	No triazolium formation
3	[MeI (40 equiv.), 50°C, CH <sub>3</sub> CN (0.1 M)] × 2	5h-> 18 h	No triazolium formation
4	MeI (206 equiv.), 30°C, DMSO (4 M)	20 h	<b>54a</b> as minor product
5	MeI (206 equiv.), 40°C, CH <sub>3</sub> CN (16M)	12 h	Mixture of one methylation, two methylation and other impurities
6	[MeI (102 equiv.), 35°C, NMP (4M)] × 2	2 h	Mixture of one methylation and two methylation
7	MeI (2 ml, pure), 40°C	12 h	Mixture of one methylation and two methylation (major product)
8	[MeI (2 ml, pure), 45°C] × 4	2 h	Complete conversion
9	MeI (2 ml, pure), 50°C	6 h	Complete conversion

<sup>155</sup> T. Zabrodski; M. Baskin; P. J. Kaniraj; and G. Maayan, 'Click to Bind: Microwave-Assisted Solid-Phase Synthesis of Peptoids Incorporating Pyridine-Triazole Ligands and Their copper(II) Complexes', *Synlett*, 25 (2014), 461–6.

<sup>156</sup> L. L. Vezenkov; V. Martin; N. Bettache; M. Simon; A. Messerschmitt; B. Legrand; J. L. Bantignies; G. Subra; M. Maynadier; V. Bellet; M. Garcia; J. Martinez; and M. Amblard, 'Ribbon-like Foldamers for Cellular Uptake and Drug Delivery', *ChemBioChem* (2017).

Most of the time, only one methylation occurred providing a complex mixture of compounds. Complete conversion of triazoles into triazoliums was achieved by exposing the resin to pure methyl iodide at 45°C during 4 x 2h. These conditions were further optimized in order to use less methyl iodide reagent and reduce its handling time. Complete conversion into triazolium was as well obtained by one exposition at 50°C during 6 h. After washing the resin with CH<sub>2</sub>Cl<sub>2</sub> (6 × 2 ml), the hexapeptoid **54a** was cleaved from the support and obtained with a good crude purity evaluated by LC-MS analysis (Figure 54).

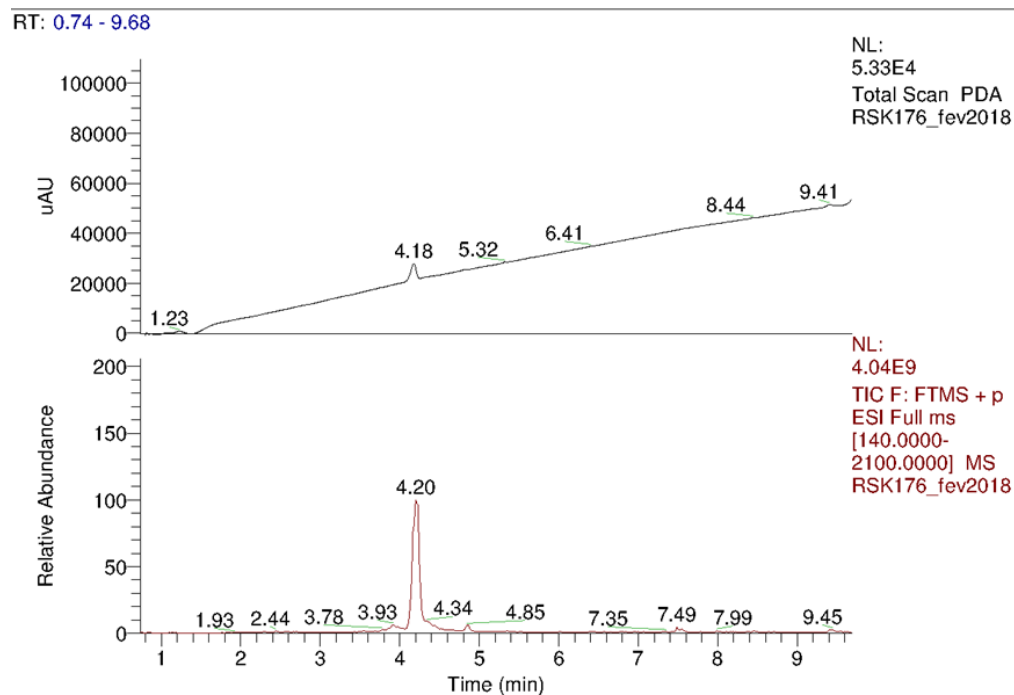


Figure 54 LC-MS of crude hexamer **54a**

## 5 Synthesis of 1,2,3-triazolium-based oligomers

Using the previously described strategy, we were able to generate three series of peptoid oligomers carrying various 1,2,3-triazolium side-chains with a sequence length of 6, 9 or 12 residues (Figure 49). Series A, B and C were designed with different substituents on triazole/triazolium: a cyclohexylmethyl (*N*chtm / *N*chtm<sup>+</sup> residues), a benzyl (*N*btm / *N*btm<sup>+</sup> residues) and an aminoethyl (*N*aetm / *N*aetm<sup>+</sup> residues), respectively.

### 5.1 Series A

The substitution on the triazole with a cyclohexyl residue will show us the effect of the alicyclic moiety on the triazolium (Figure 55). Using cyclohexylmethyl azide for the CuAAC reaction on

resin provided the following oligomers of 6 and 9 residues length (Table 18).

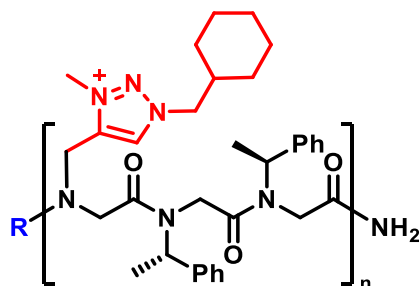


Figure 55 Generic structure of Family III Series A peptoid oligomers

Table 18 Sequences and mass data for peptoid oligomers of Series A

No.	Peptoid sequence	Formula	Exact mass calcd	Exact mass found
<b>53a</b>	H-(Nchtm-Nspe-Nspe) <sub>2</sub> -NH <sub>2</sub>	C <sub>64</sub> H <sub>83</sub> N <sub>13</sub> O <sub>6</sub>	1130.6668	1130.6643
<b>53b</b>	Ac-(Nchtm-Nspe-Nspe) <sub>2</sub> -NH <sub>2</sub>	C <sub>66</sub> H <sub>85</sub> N <sub>13</sub> O <sub>7</sub>	1172.6773	1172.6818
<b>54a</b>	H-(Nchtm <sup>+</sup> -Nspe-Nspe) <sub>2</sub> -NH <sub>2</sub>	C <sub>66</sub> H <sub>89</sub> N <sub>13</sub> O <sub>6</sub> <sup>2+</sup>	579.8524	579.8522
<b>55a</b>	H-(Nchtm-Nspe-Nspe) <sub>3</sub> -NH <sub>2</sub>	C <sub>96</sub> H <sub>123</sub> N <sub>19</sub> O <sub>9</sub>	1686.9829	1686.9850
<b>56a</b>	H-(Nchtm <sup>+</sup> -Nspe-Nspe) <sub>3</sub> -NH <sub>2</sub>	C <sub>99</sub> H <sub>132</sub> N <sub>19</sub> O <sub>9</sub> <sup>3+</sup>	577.0146	577.0146
<b>56b</b>	Ac-(Nchtm <sup>+</sup> -Nspe-Nspe) <sub>3</sub> -NH <sub>2</sub>	C <sub>101</sub> H <sub>134</sub> N <sub>19</sub> O <sub>10</sub> <sup>3+</sup>	591.0181	591.0172

The major problems encountered during the synthesis of series A oligomers was during the purification of the oligomers after the cleavage from the resin. Even after obtaining a clean LCMS of the crude oligomers (see experimental section), the purification using column chromatography or HPLC were not successful. The oligomers were destroyed in the column, leading to complete failure of the purification process. On further investigation, we found that if the terminal amine is masked during the purification process, it is possible to purify the oligomers. One such attempt was the nonamer **56b**, which was masked with acetyl moiety and purified using HPLC to give pure

nonapeptoid. When preparative HPLC purification was not possible, the crude oligomers were intensively triturated in ether to eliminate low molecular weight side-compounds.

## 5.2 Series B

Using the previously prepared, benzyl azide **41** for the CuAAC reaction on resin provided the following oligomers of 6 and 9 residues length (Figure 56,

Table 19).

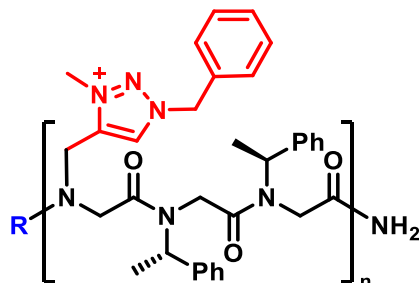


Figure 56 Generic structure of Family III Series B peptoid oligomers

Table 19 Sequences and mass data for peptoid oligomers of Series B

No.	Peptoid sequence	Formula	Exact mass calcd.	Exact mass found
<b>57a</b>	H-(Nbtm <sup>+</sup> -Nspe-Nspe) <sub>2</sub> -NH <sub>2</sub>	C <sub>66</sub> H <sub>77</sub> N <sub>13</sub> O <sub>6</sub> <sup>2+</sup>	573.8054	573.8052
<b>58a</b>	H-(Nbtm <sup>+</sup> -Nspe-Nspe) <sub>3</sub> -NH <sub>2</sub>	C <sub>99</sub> H <sub>114</sub> N <sub>19</sub> O <sub>9</sub> <sup>3+</sup>	570.9678	570.9676
<b>58b</b>	Ac-(Nbtm <sup>+</sup> -Nspe-Nspe) <sub>3</sub> -NH <sub>2</sub>	C <sub>101</sub> H <sub>116</sub> N <sub>19</sub> O <sub>10</sub> <sup>3+</sup>	584.9712	584.9717

The oligomers were synthesised with relatively good purity as evidenced by the LCMS spectra of the crude oligomers (see experimental section), however the purification using either column chromatography or HPLC did not furnish the pure oligomers. Instead it leads to the complete destruction of the cationic peptoids in the column, as observed in the case of series A oligomers. Therefore, similar approach to series A was followed by masking the terminal amine using acetyl moiety to obtain pure oligomer **58b** after HPLC. When preparative HPLC purification was not possible, the crude oligomers were intensively triturated in ether to eliminate low molecular weight side-compounds.

### 5.3 Series C

The introduction of an amino group on the triazolium moieties results in doubling the net positive charge while maintaining a constant length of the oligomer (Figure 57).

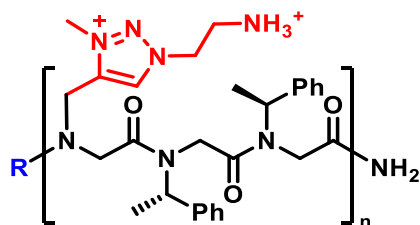
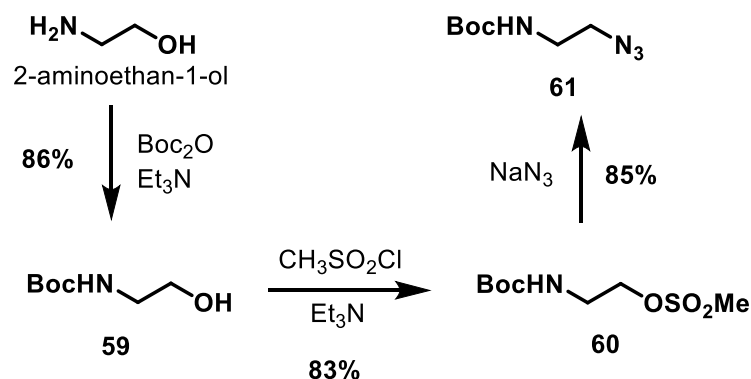


Figure 57 Generic structure of Family III Series C peptoid oligomers

First, the corresponding azide with a Boc-protected amino group was prepared according to a protocol described in the literature (Scheme 46).<sup>157,158</sup> The tert-butyl (2-azidoethyl)carbamate **61** was obtained with a global yield of 61% starting from 2-aminoethanol.



Scheme 46 Synthesis of *N*-Boc-aminoethyl azide

Using *N*-Boc protected aminoethyl azide **61**, the CuAAC reaction on resin provided the following oligomers of 6, 9 and 12 residues length (Table 20).

<sup>157</sup> E. J. F. Prodhomme; C. Ensch; F. B. Bouche; T. Kaminski; S. Deroo; P. Seek; G. Kirsch; and C. P. Muller, 'Synthesis of 4-[2-Aminoethyl(nitrosamino)]-1-Pyridin-3-Yl-Butan-1-One, a New NNK Hapten for the Induction of *N*-Nitrosamine-Specific Antibodies', *Bioconjugate Chemistry*, 18 (2007), 2045–53.

<sup>158</sup> M. Van Dijk; C. F. Van Nostrum; W. E. Hennink; D. T. S. Rijkers; and R. M. J. Liskamp, 'Synthesis and Characterization of Enzymatically Biodegradable Peg and Peptide-Based Hydrogels Prepared by Click Chemistry', *Biomacromolecules*, 11 (2010), 1608–14.

Table 20 Sequences and mass data for peptoid oligomers of Series C

No.	Peptoid sequence	Formula	Exact mass calcd	Exact mass found
62	H-(Naetm-Nspe-Nspe) <sub>2</sub> -NH <sub>2</sub>	C <sub>54</sub> H <sub>69</sub> N <sub>15</sub> O <sub>6</sub>	512.7850	512.7852
63	H-(Naetm <sup>+</sup> -Nspe-Nspe) <sub>2</sub> -NH <sub>2</sub>	C <sub>56</sub> H <sub>75</sub> N <sub>15</sub> O <sub>6</sub> <sup>2+</sup>	526.8006	526.8004
64	Ac-(Nae(Cbz)tm <sup>+</sup> -Nspe-Nspe) <sub>2</sub> -NH <sub>2</sub>	C <sub>74</sub> H <sub>89</sub> N <sub>15</sub> O <sub>11</sub> <sup>2+</sup>	681.8427	681.8427
65	H-(Naetm-Nspe-Nspe) <sub>3</sub> -NH <sub>2</sub>	C <sub>81</sub> H <sub>102</sub> N <sub>22</sub> O <sub>9</sub>	1527.8272	1527.8298
66	H-(Naetm <sup>+</sup> -Nspe-Nspe) <sub>3</sub> -NH <sub>2</sub>	C <sub>84</sub> H <sub>111</sub> N <sub>22</sub> O <sub>9</sub> <sup>3+</sup>	523.9629	523.9631
67	H-(Naetm-Nspe-Nspe) <sub>4</sub> -NH <sub>2</sub>	C <sub>108</sub> H <sub>135</sub> N <sub>29</sub> O <sub>12</sub>	677.7021	677.7009
68	H-(Naetm <sup>+</sup> -Nspe-Nspe) <sub>4</sub> -NH <sub>2</sub>	C <sub>112</sub> H <sub>147</sub> N <sub>29</sub> O <sub>12</sub> <sup>4+</sup>	522.5440	522.5441

Purification of series C oligomers using HPLC was a relatively easy task compared to Series A and B oligomers. However, couple of series C oligomers were synthesised using the non-optimised synthetic strategy. Here, the major impurity detected in the product by LC-MS was an oligomer that lacks one Nspe residue. This lead to the synthesis of oligomers with average purity. However, when the optimised conditions were employed, the oligomers were obtained with excellent purity as evidenced by HPLC spectra (Figure 58).

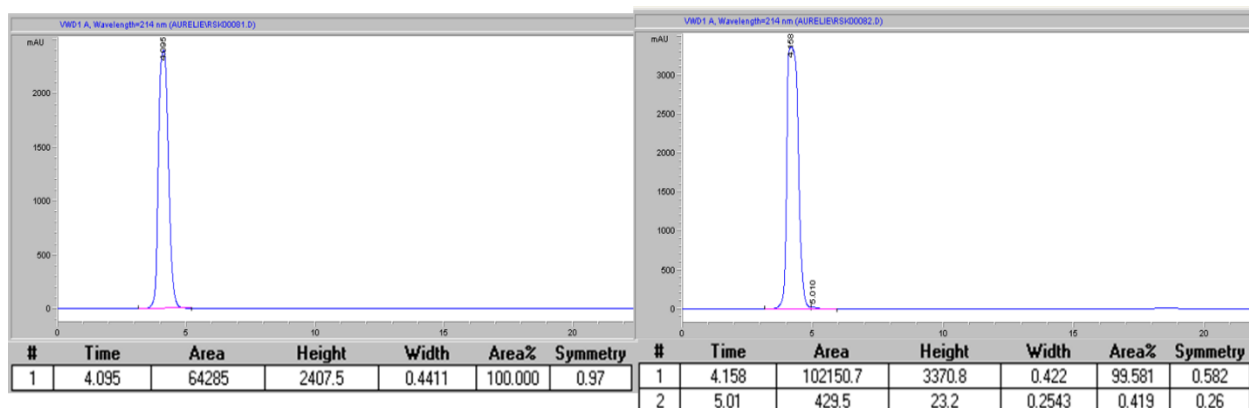


Figure 58 HPLC spectra of dodecapeptides 67 and 68.

## 6 Structural and conformational insights Family III

As we have discussed before, the determination of the secondary structure of peptoid oligomers is not easy. However, in the family III, the presence of  $\alpha$ -chiral *N*spe makes it possible to use circular dichroism to analyse the folding of these oligomers. Also, the oligomers failed to develop suitable crystals for X-ray analysis. Therefore, to have understandings about the conformational aspect of family III oligomers, both NMR determination technique and CD studies have been initiated

### 6.1 NMR study

Using the 1D and 2D NMR techniques (COSY, HSQC) can help us to determine the proportion of *cis/trans* of selected amide or the sequence. In our case, the determination of the overall *cis/trans* proportion for amide carrying spe side chains is possible by simple integration of proton NMR signals in absence of overlapping signals. Otherwise,  $^1\text{H}$ — $^{13}\text{C}$  HSQC experiment enables this determination. But due to the complexity of peptoid NMR, the conformation of the amides carrying the triazolium side chain is not accessible except when the triazolium is located on a terminal acetamide (in the case of *N*-acetylated oligomers).

To start the conformational analysis of the family III oligomers,  $^1\text{H}$ — $^{13}\text{C}$  HSQC experiments were carried out (Figure 59). It helps us to understand the role of triazolium over triazole in the stabilization of the overall sequence.

Analysis of HSQC spectra reveals differences in the chemical shift distribution of the spectral regions that correspond to characteristic carbon-proton cross-peaks for *cis* and *trans* conformers. Analysis of COSY spectra of the triazole based hexamer **53a** shows an overall *cis/trans* ratio of 58:42 and the  $^1\text{H}$ — $^{13}\text{C}$  HSQC spectra showed an overall *cis/trans* ratio of 56:44 for the 4 spe residues. The conversion of triazole to triazolium in the hexamer **54a** tends to favour *cis* conformation of amide carrying the spe as the COSY spectra gives a *cis/trans* ratio of 62:38 and HSQC spectra gives a *cis/trans* ratio of 68:32. This indicates that the influence of the triazolium group that stabilises the *cis* conformation by  $n \rightarrow \pi^*$  electronic delocalization is not limited to the amide carrying it but also contributes to the stabilization of the overall all-*cis* amide sequence. This effect is even more pronounced in the case of nonamer where the *cis/trans* ratio of 72:28 is obtained for **56a**. We can see the higher proportion of *cis* conformation at 5.6 ppm region on the spectra.



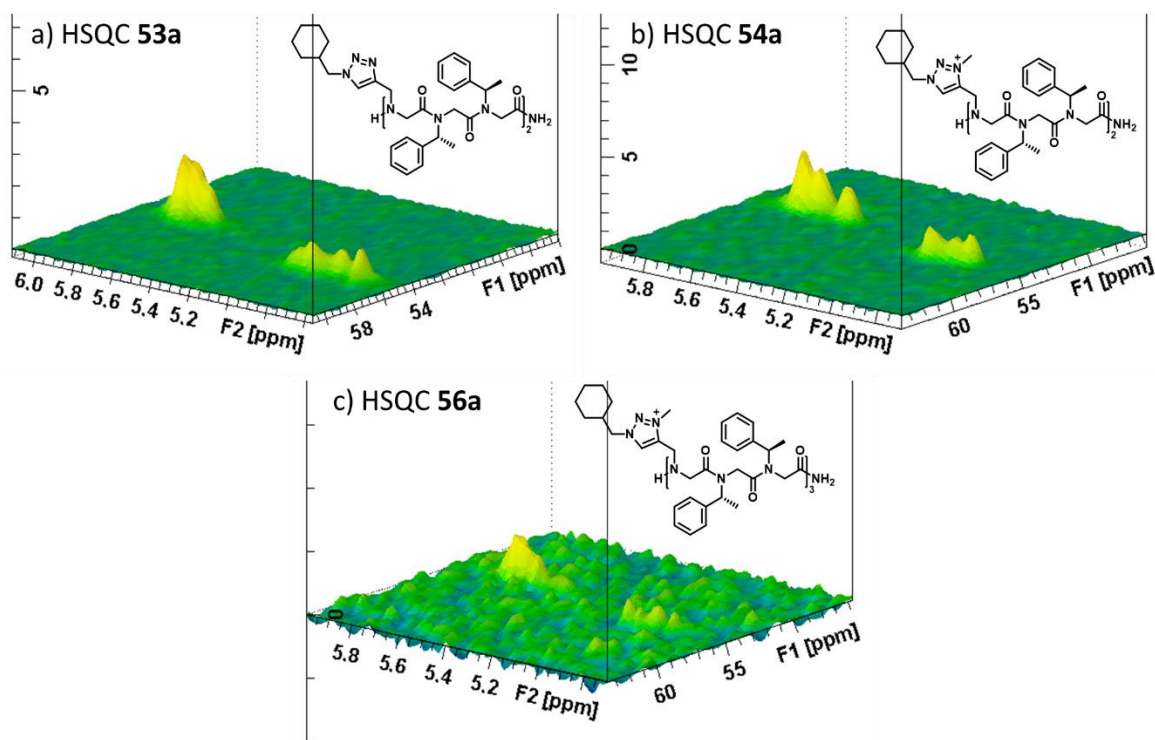


Figure 59 Comparison of HCQC spectra of a) hexamer **53a** with b) hexamer **54a** and c) nonamer **56a** in  $CDCl_3$ .

Similarly, family IIIB with benzyltriazolium based hexamer **57a** and nonamer **58a** favoured *cis* conformations. It is evident from the HSQC spectra of hexamer **57a** and the nonamer **58a** with both having a *cis/trans* ratio of 67:33 (Figure 60).

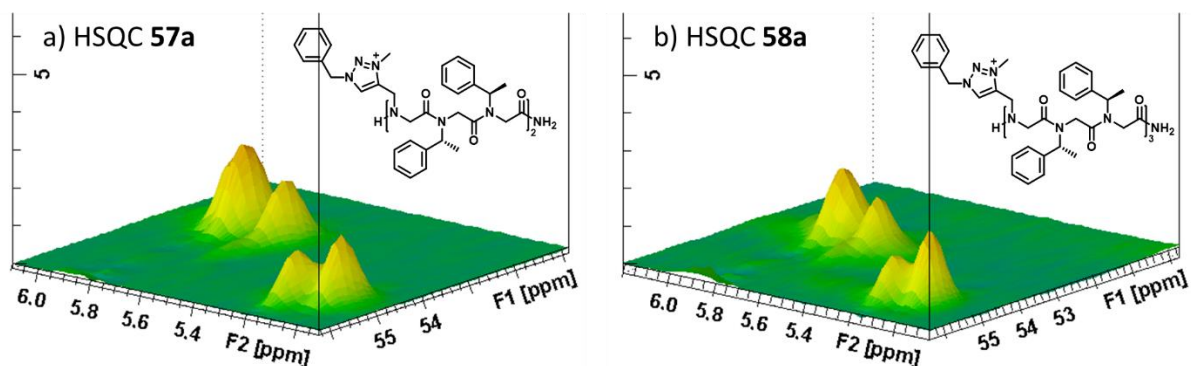


Figure 60 Comparison of HCQC spectra of a) hexamer **57a** with b) nonamer **58a** in  $CDCl_3$ .

Therefore, with the above evidence it can be said that the introduction of triazolium side chain in the *Nspe* dominated oligomer leads to the formation of better rigid structure in solution. It can be further studied with the help of CD signatures.

## 6.2 Circular dichroism study

The circular dichroism of peptoid oligomers containing *spe* side chain has been extensively studied and the CD signature of this type of oligomers adopting polyproline I-type helix is well known (Figure 61).<sup>77</sup>

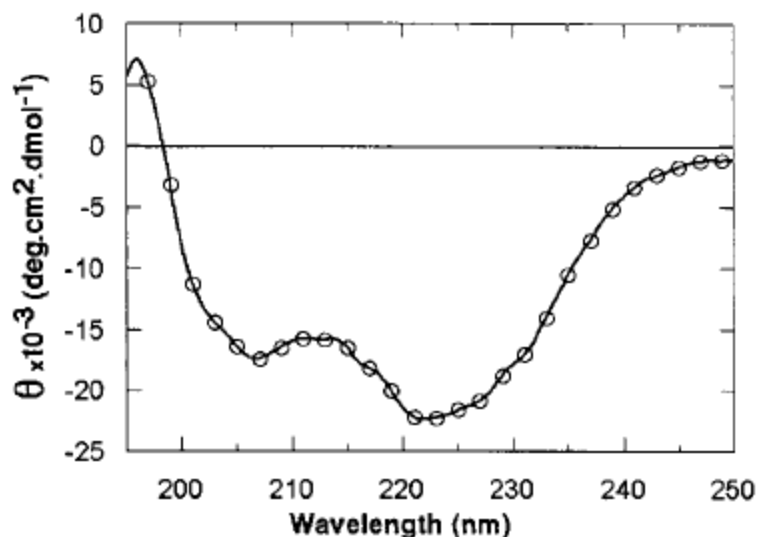


Figure 61 CD signature of peptoid oligomer carrying  $\alpha$ -chiral aromatic side chains.<sup>77</sup>

Common feature of CD curves of peptoid oligomers containing  $\alpha$ -chiral aromatic side chain with a (*S*) configuration is the presence of two minima at approximately 205 and 220 nm. Such oligomers presenting this CD signature were found to adopt a PPI-type helical structure.

Preliminary CD study on the series A of the third family was performed in acetonitrile and methanol. The hexamers **53a** and **54a**, and the nonamer **56a** present the characteristic CD signature of the PPI-like helix of peptoids with two minima at 203 and 220 nm (Figure 62).

The lower band intensity for triazole-based hexapeptoid **53a** compared to the triazolium-based hexapeptoid **54a** is indicative of the helical structure stabilisation by the triazoliums. Besides, a similar CD signature was observed for the hexamer **54a** and the nonamer **56a** suggesting that that the hexamer has already all the elements required for a strong helical nature of the oligomers. The length increase doesn't contribute to the stabilization of the helical structure. Stronger CD signatures were observed for the hexamer **54a** and the nonamer **56a** in acetonitrile with the characteristic minima at 203 and 220 nm (Figure 63).

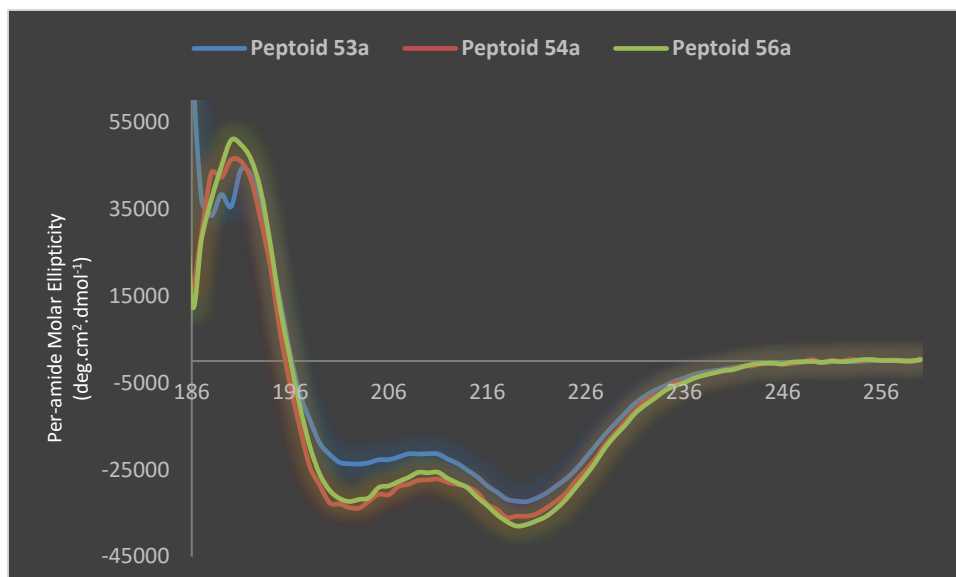


Figure 62 CD curves of triazole- and triazolium-based peptoids at 500  $\mu\text{M}$  in methanol.

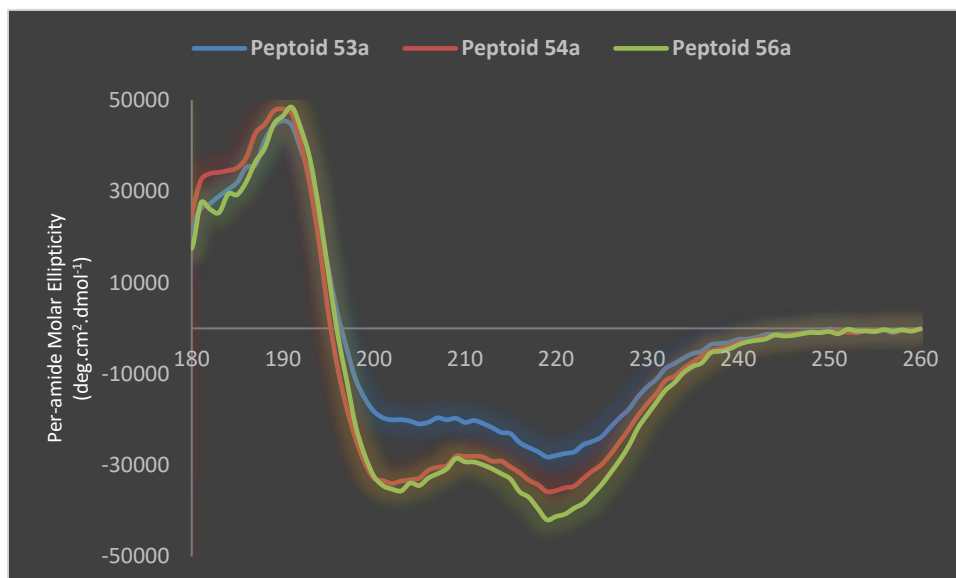


Figure 63 CD analysis of triazole- and triazolium-based peptoids at 500  $\mu\text{M}$  in acetonitrile.

This preliminary CD study need to be completed. The CD curves of all oligomers of the family III have to be recorded. Besides, the CD study has also to be done in other media such as the Tris buffer (pH 7.4) or in presence of anionic liposomes to mimic the bacterial membrane.

## 7 Conclusion:

Using experiences gained in the group from the previous work on the solution-phase synthesis of 1,2,3-triazolium-based oligomers and thanks to our optimized solid-phase strategy developed here, a panel of cationic amphiphilic peptoid oligomers of 6, 9 and 12 residues long and carrying various triazolium moieties were efficiently synthesised on support.

The synthetic strategy developed is very convenient and fully adapted to prepare large library of triazolium-based oligomers. However, the HPLC purification of some of these cationic oligomers revealed difficult. The preparative column used, a C18 Varian Dynamax Microsorb column (C18, 8  $\mu\text{m}$ , 60  $\text{\AA}$ ) wasn't adapted to this type of compounds. A new preparative column Jupiter (C4, 5  $\mu\text{m}$ , 300  $\text{\AA}$ ) has been recently acquired in the group and should enable to solve this problem.

This methodology could also be applied using various alkylating agent instead of methyl iodide in order to increase diversity accessible on the triazolium group (Figure 64).

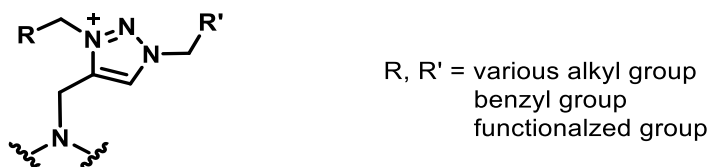


Figure 64 Generic structure of other type of triazolium side chains accessible by the solid-phase strategy

**Chapter IV**  
**Biological evaluation of cationic  
amphipathic peptoids**

## Introduction

The cationic nature of AMPs serves them with two purposes; the interaction with bacteria membrane and selectivity towards mammalian cells. Since the mammalian cells are mostly zwitterionic in nature most of the AMPs are selective towards the bacteria as compared to mammalian cells. Though, the selectivity of the AMPs varies among different types. Therefore, peptidomimetics can serve as a better tool to counter the growing bacterial resistance.

### 1 Selection and design of oligomers:

The reference molecule developed by Barron is based on the repetition of two *N*-(*S*)-(1-phenylethyl) glycine units and one *N*-(4-aminobutyl)glycine unit. Two molecules of the same family were used i.e. hexamer **49** and nonamer **50** as negative and positive reference molecules. These reference molecules contain the three important prerequisites of a good anti-infective agent. The chiral *N*spe acts as helix inducer and also as aromatic block providing the hydrophobic helical face. The *M*lys residue provides the cationic moiety to the oligomer (Figure 65a). All the three combined give a good amphipathic character to the oligomer provided that the sequence is sufficiently long. Indeed, the reference hexamer **49** is inactive on bacteria whereas the nonamer **50** exhibits activity against Gram-positive and Gram-negative bacteria. Based on the reference molecule, we decided to study three families incorporating *N*tbu, *N*tm and *N*tm<sup>+</sup> residues (Figure 65b).

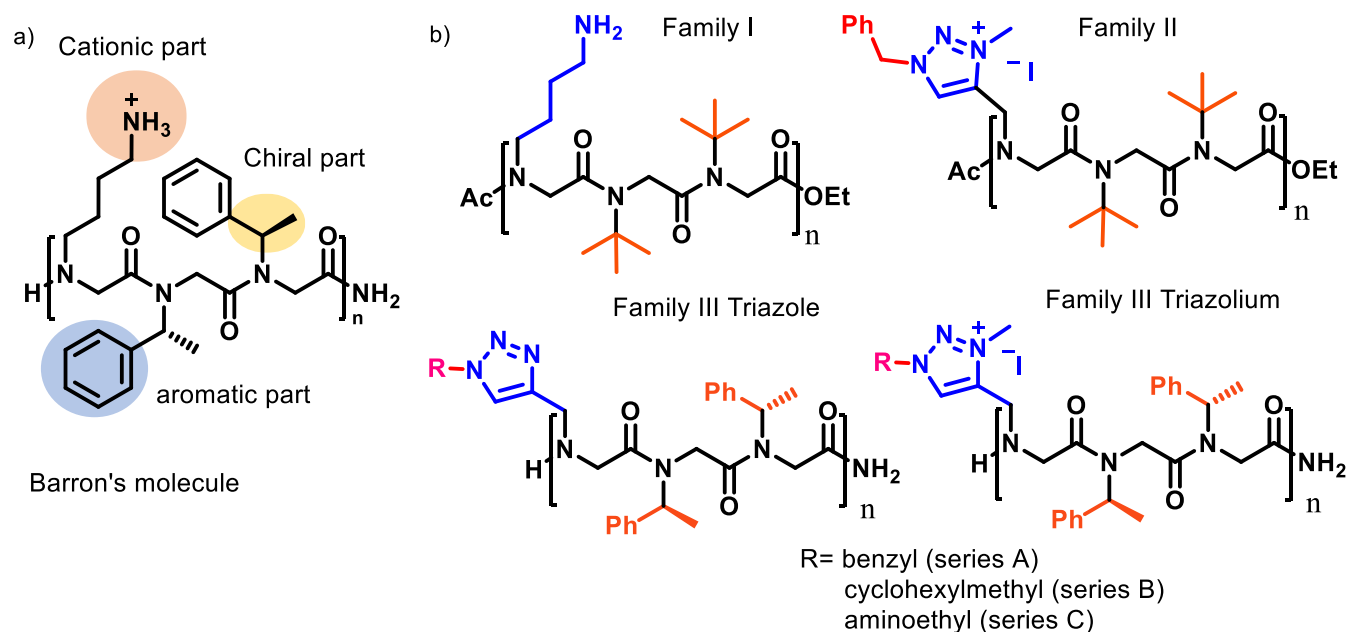


Figure 65 a) Barron's reference Molecule b) General structure of the selected peptoid families for biological evaluation

The synthesis of these three families was presented in Chapter II and III. After many considerations based on the purity of the molecules, the solubility in water, the financial costs and the time required to perform the antimicrobial evaluation of the oligomers, we selected the listed below (Table 21) amphipathic oligomers to test their therapeutic potential.

Table 21 Selected oligomers for antimicrobial evaluation

Peptoid no.	Family	Peptoid sequence	Net charge	Molecular Weight
<b>49</b>	<b>Ref.</b>	H-(Mlys-Nspe-Nspe) <sub>2</sub> -NH <sub>2</sub>	3	1114.25
<b>50</b>		H-(Mlys-Nspe-Nspe) <sub>3</sub> -NH <sub>2</sub>	4	1662.85
<b>27</b>	<b>IA</b>	Ac-(Mlys-Ntbu-Ntbu) <sub>2</sub> -OEt	2	797.09
<b>43</b>	<b>IIA</b>	Ac-(Mbtm <sup>+</sup> -Ntbu-Ntbu) <sub>2</sub> -OEt	2	1027.32
<b>53a</b>	<b>IIIA</b>	H-(Nchtm-Nspe-Nspe) <sub>2</sub> -NH <sub>2</sub>	1	1130.45
<b>54a</b>		H-(Nchtm <sup>+</sup> -Nspe-Nspe) <sub>2</sub> -NH <sub>2</sub>	3	1354.56
<b>56a</b>		H-(Nchtm <sup>+</sup> -Nspe-Nspe) <sub>3</sub> -NH <sub>2</sub>	4	2023.32
<b>58a</b>	<b>IIIB</b>	H-(Nbtm <sup>+</sup> -Nspe-Nspe) <sub>3</sub> -NH <sub>2</sub>	4	2005.17
<b>58b</b>		Ac-(Nbtm <sup>+</sup> -Nspe-Nspe) <sub>3</sub> -NH <sub>2</sub>	4	2047.21
<b>63</b>	<b>IIIC</b>	H-(Naetm <sup>+</sup> -Nspe-Nspe) <sub>2</sub> -NH <sub>2</sub>	5	1248.35
<b>66</b>		H-(Naetm <sup>+</sup> -Nspe-Nspe) <sub>3</sub> -NH <sub>2</sub>	7	1864.00
<b>67</b>		H-(Naetm-Nspe-Nspe) <sub>4</sub> -NH <sub>2</sub>	5	2031.46
<b>68</b>		H-(Naetm <sup>+</sup> -Nspe-Nspe) <sub>4</sub> -NH <sub>2</sub>	9	2479.66

This library of cationic peptoids includes six hexamers with an overall positive charge of +2, +3, +4 or +5, five nonamers with an overall positive charge of +4 or +7 and two dodecamers with an overall positive charge of +5 or +9.

### 1.1 Solubility of peptoid oligomers

The antibacterial tests were carried out by dissolving the peptoids in the Muller Hinton broth which serves as the media to grow the bacteria. A problem of solubility was encountered for a few peptoids due to the high aromatic nature of these oligomers. Therefore 2% of DMSO was added to enhance the solubility. It was checked that it does not have any negative effect on the growth of the bacteria by growing the bacteria in 2% DMSO solution and counting the colony forming units (CFU)/mL. Besides, the first screening was performed with or without DMSO in order to compare MIC values obtained in both conditions.

## 1.2 Peptide control

Melittin (Honey bee 26-amino acid AMP: GIGAVLKVLTTGLPALISWIKRKRQQ) is a  $\alpha$ -helical, cationic, haemolytic component of honey-bee venom with utility in cell lysis and liposome lysis.<sup>159</sup> It has been extensively studied as a model for antimicrobial peptide-membrane interactions. Synthetic melittin and its fragments induce transient pores in membranes at nanomolar concentrations. The Melittin was used as a control in all biological assay.

## 2 Selection of bacteria

The antimicrobial activities of synthesised peptoids have been access on a panel of Gram-negative and Gram-positive bacteria presented in Table 22. The two species of Gram-negative bacteria selected were *Pseudomonas aeruginosa* and *Escherichia coli*. Two strains of *Escherichia coli* were tested; a common laboratory strain and a pathogenic one. Two species of Gram-positive bacteria were selected: *Staphylococcus aureus* and *Enterococcus faecalis*.

Table 22 List of the pathogenic and non-pathogenic bacterial strains tested.

Bacterial strain	Identification	Gram stain	Bio-safety level
<i>Escherichia coli</i>	<b>JM109 (Non-pathogenic)</b>	Negative	BSL-1
<i>Escherichia coli</i>	<b>(ATCC® 25922™)</b>	Negative	BSL-2
<i>Pseudomonas aeruginosa</i>	<b>(ATCC® 27853™)</b>	Negative	BSL-2
<i>Staphylococcus aureus</i>	<b>CIP 6525</b>	Positive	BSL-2
<i>Enterococcus faecalis</i>	<b>(ATCC® 29212™)</b>	Positive	BSL-2

### 2.1 Gram-negative bacteria *Escherichia coli*

*Escherichia coli* forms the most common basis of bloodstream infections and healthcare-associated urinary tract infections worldwide. Antibiotic resistance in *E. coli* requires close attention as the percentages of isolates resistant to commonly used antibiotics continue to increase throughout Europe.<sup>1</sup>

### 2.2 Gram-negative bacteria *Pseudomonas aeruginosa*

*Pseudomonas aeruginosa* is an important cause of infection among patients with impaired immune systems. Multiple drug resistance is common, with 14% of the isolates reported are resistant to at least three antimicrobial classes. *P. aeruginosa* bacteria forms biofilms which make it more

---

<sup>159</sup> W. Shi; C. Li; M. Li; X. Zong; D. Han; and Y. Chen, 'Antimicrobial Peptide Melittin against *Xanthomonas Oryzae* Pv. *Oryzae*, the Bacterial Leaf Blight Pathogen in Rice', *Applied Microbiology and Biotechnology*, 100 (2016), 5059–67.



difficult to treat compared to planktonic bacteria. The current standard of care for the treatment of *P. aeruginosa* infections is long-term use of antibiotics in combination. The frequent use of antibiotics has led to the widespread emergence of multidrug-resistant *Pseudomonas* strains, exacerbating the overall problem.<sup>160</sup>

### 2.3 Gram-positive bacteria *Staphylococcus aureus*

*Staphylococcus* can cause a wide variety of diseases in humans and animals through either toxin production or penetration. Staphylococcal toxins are a common cause of food poisoning, since they can be produced by bacteria growing in improperly stored food items. *S. aureus* is an opportunistic bacterium, it is well known for the nuisance that it causes in hospitals. It has been reported to cause nosocomial infections in hospitals. Its oxacillin-resistant form<sup>161</sup> (methicillin resistant *S. aureus*, MRSA) is one of the most important causes of antimicrobial-resistant healthcare-associated infections worldwide.<sup>162</sup>

### 2.4 Gram-positive bacteria *Enterococcus faecalis*

*Enterococcus* can cause several clinical infections including urinary tract infections, bacteraemia, bacterial endocarditis, diverticulitis, and meningitis. From a medical standpoint, this genus has a high level of intrinsic antibiotic resistance. *E. faecalis* belongs to the normal bacterial flora of the gastrointestinal tract of humans but may also cause a variety of clinical infections including endocarditis, bacteraemia, meningitis, wound and urinary tract infections, and are associated with peritonitis and intra-abdominal abscesses.<sup>163</sup>

### 2.5 Gram Staining

Gram staining is a common technique used to differentiate two large groups of bacteria based on their different cell wall constituents.<sup>164</sup> The Gram stain procedure distinguishes between Gram

---

<sup>160</sup> H. W. Boucher; G. H. Talbot; J. S. Bradley; J. E. Edwards; D. Gilbert; L. B. Rice; M. Scheld; B. Spellberg; and J. Bartlett, 'Bad Bugs, No Drugs: No ESKAPE! An Update from the Infectious Diseases Society of America', *Clinical Infectious Diseases*, 48 (2009), 1–12.

<sup>161</sup> Y. A. Chabbert and J. Fillet, 'Correlation Between "methicillin Resistance" and Serotype in *Staphylococcus*', *Nature*, Vol. 213 (Nature Publishing Group, 1967), 1137.

<sup>162</sup> H. Grundmann; L. M. Schouls; D. M. Aanensen; G. N. Pluister; A. Tami; M. Chlebowicz; C. Glasner; A. J. Sabat; K. Weist; O. Heuer; A. W. Friedrich; O. Denis; D. Nashev; D. S. Blanc; D. Pieridou-Bagatzouni; V. Jakubu; H. Zemlickova; H. Westh; A. R. Larsen; et al., 'The Dynamic Changes of Dominant Clones of *Staphylococcus Aureus* Causing Bloodstream Infections in the European Region: Results of a Second Structured Survey', *Eurosurveillance*, 19 (2014), 1–10.

<sup>163</sup> J. C. S. Kenneth James Ryan, C. George Ray, *Sherris Medical Microbiology: An Introduction to Infectious Diseases*, *Journal of Chemical Information and Modeling*, Vol. 53 (McGraw-Hill, 2004).

<sup>164</sup> T. Brock, 'Milestones in Microbiology 1546 to 1940', Vol. 53 (ASM Press, 1999), 215–8.

positive and Gram-negative groups by colouring these cells red or violet. Gram-positive bacteria stain violet due to the presence of a thick layer of peptidoglycan (50–90% of cell envelope) in their cell walls, which retains the crystal violet these cells are stained with. Alternatively, Gram-negative bacteria stain red, which is attributed to a thinner peptidoglycan wall (10% of cell envelope), which does not retain the crystal violet during the decolouring process and are counter-stained pink-red by fuchsin.

Gram staining was done on the representative bacteria using the well-established procedure of Gram staining.<sup>165</sup> *E. coli* and *S. aureus* were used for the Gram-negative and Gram-positive type respectively. The results are shown below (Figure 66). The Gram-negative bacteria *E. coli* is stained pink, whereas the Gram-positive bacteria *S. aureus* is stained purple.

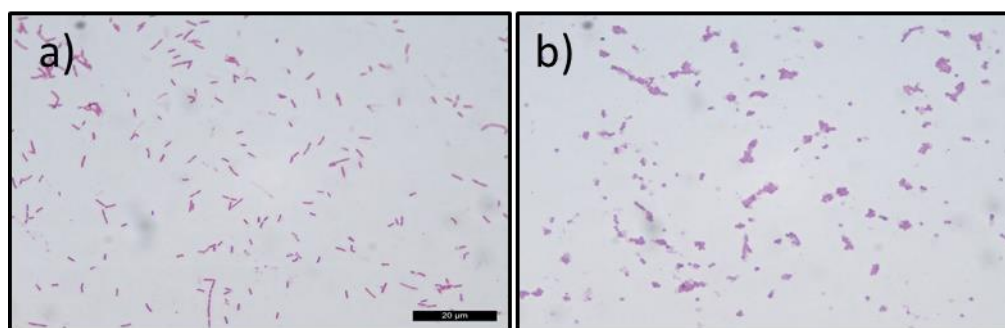


Figure 66 a) Gram-negative *Escherichia coli* b) Gram-positive *Staphylococcus aureus*

### 3 Determination of antimicrobial activity

#### 3.1 Minimal Inhibitory Concentration

Minimum inhibitory concentration (MIC) gives a visible knowledge of the prevention of bacterial growth. It is an important step for *in vitro* activity evaluation of a novel antimicrobial compounds. It is defined as the lowest concentration of an antimicrobial compound that inhibits the visible growth of a bacteria after overnight incubation ( $\approx 18$  h). It was carried out by using the Clinical and Laboratory Standard Institute (CLSI) guidelines for MIC testing<sup>166</sup>. The preferred method was the broth dilution method, where two-fold dilution of the peptoid in MHB growth media was inoculated with bacteria (Figure 67).

---

<sup>165</sup> J. Holt, *Bergey's Manual of Determinative Bacteriology* (Williams & Wilkins, 1994).

<sup>166</sup> CLSI Document, *Methods for Dilution Antimicrobial Susceptibility Tests for Bacteria That Grow Aerobically; Approved Standard — Ninth Edition, Methods for Dilution Antimicrobial Susceptibility Tests for Bacteria That Grow Aerobically; Approved Standard- Ninth Edition*, Vol. 32, ninth edit (2012).

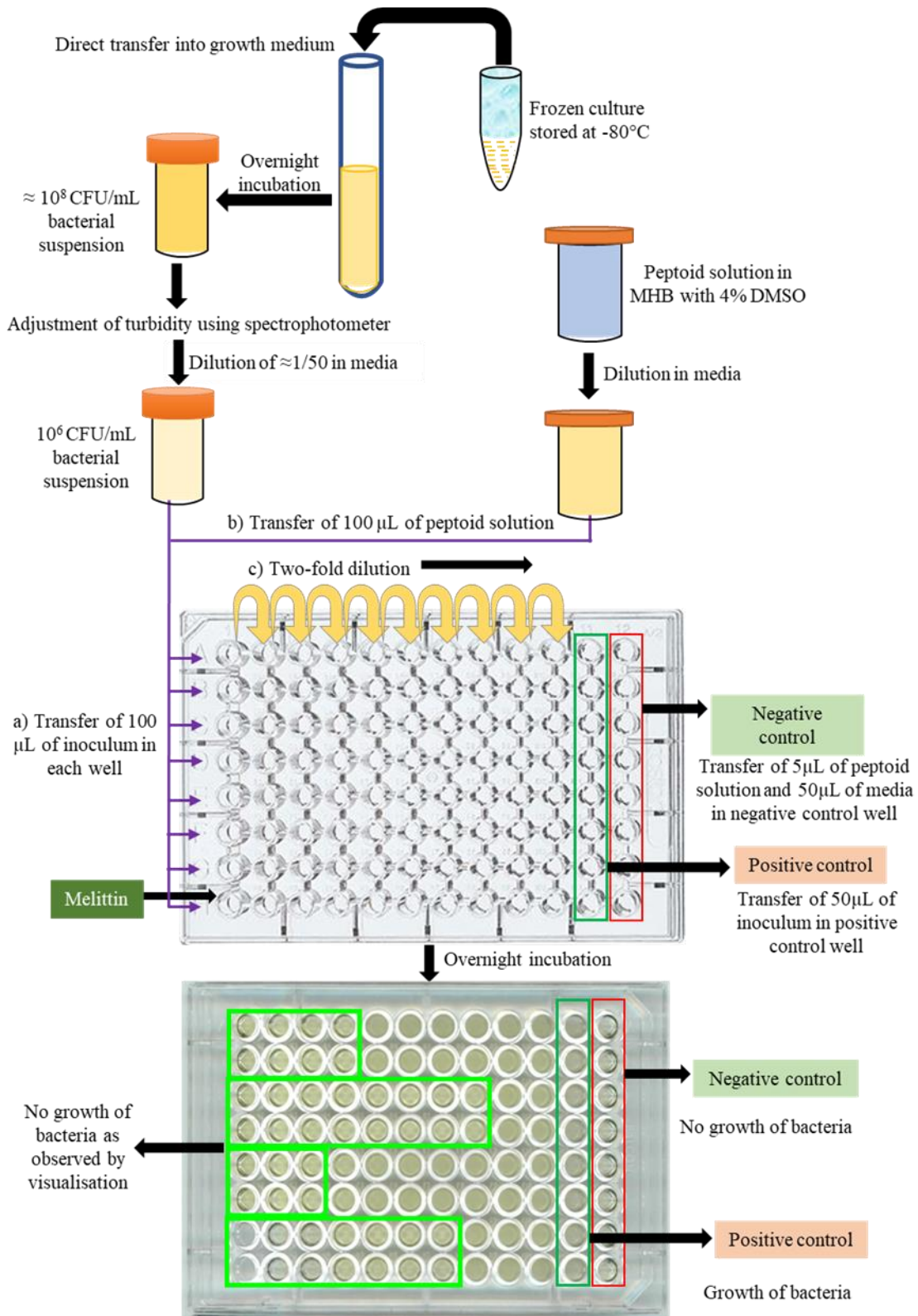


Figure 67 Determination of minimal inhibitory concentration by the broth microdilution method, steps a), b) and c) were carried out sequentially.

### 3.2 Minimal Bactericidal Concentration

The measurement of the minimal bactericidal concentration (MBC) is done by determining the lowest concentration of antibacterial agent that reduces the viability of the initial bacterial inoculum by  $\geq 99.9\%$ .<sup>167</sup> The MBC is complementary to MIC; where MIC denotes the lowest concentration for microbial inhibition, the MBC denotes the lowest concentration for microbial death. The determination of the MBC value enables to determine if the molecule tested has bactericidal or bacteriostatic effect on bacteria at the MIC.

### 3.3 Antibacterial activities of the selected peptoids

The antibacterial activity was assessed against the panel of bacteria (Table 23).

Table 23 Antimicrobial MIC and MBC activities of selected peptoids against Gram-negative and Gram-positive bacteria

No.	Peptoid	<i>E. coli</i> JM109		<i>E. coli</i>		<i>P. aeruginosa</i>		<i>S. aureus</i>		<i>E. faecalis</i>	
		MIC	MBC	MIC	MBC	MIC	MBC	MIC	MBC	MIC	MBC
<b>49</b>	H-(Nlys-Nspe-Nspe) <sub>2</sub> -NH <sub>2</sub>	>200	>200	>200	>200	100	200	>200	>200	>200	>200
<b>50</b>	H-(Nlys-Nspe-Nspe) <sub>3</sub> -NH <sub>2</sub>	50	50	100	100	100	200	25	50	25	25
<b>27</b>	Ac-(Nlys-Ntbu-Ntbu) <sub>2</sub> -OEt	>200	>200	>200	>200	>200	>200	>200	>200	>200	>200
<b>43</b>	Ac-(Nbtm <sup>+</sup> -Ntbu-Ntbu) <sub>2</sub> -OEt	>200	>200	166	>200	>200	>200	6.3	12.5	25	50
<b>53a</b>	H-(Nchtm-Nspe-Nspe) <sub>2</sub> -NH <sub>2</sub>	>200	>200	>200	>200	>200	>200	>200	>200	>200	>200
<b>54a</b>	H-(Nchtm <sup>+</sup> -Nspe-Nspe) <sub>2</sub> -NH <sub>2</sub>	50	50	50	50	>200	>200	3.1	6.3	6.3	12.5
<b>56a</b>	H-(Nchtm <sup>+</sup> -Nspe-Nspe) <sub>3</sub> -NH <sub>2</sub>	25	25	25	25	166.6	>200	3.1	6.3	1.8	3.1
<b>58a</b>	H-(Nbtm <sup>+</sup> -Nspe-Nspe) <sub>3</sub> -NH <sub>2</sub>	12.5	25	12.5	25	>200	>200	1.6	3.1	1.6	3.1
<b>58b</b>	Ac-(Nbtm <sup>+</sup> -Nspe-Nspe) <sub>3</sub> -NH <sub>2</sub>	>200	>200	>200	>200	>200	>200	133.3	>200	100	>200
<b>63</b>	H-(Nactm <sup>+</sup> -Nspe-Nspe) <sub>2</sub> -NH <sub>2</sub>	>200	>200	>200	>200	>200	>200	>200	>200	>200	>200
<b>66</b>	H-(Nactm <sup>+</sup> -Nspe-Nspe) <sub>3</sub> -NH <sub>2</sub>	25	50	100	>200	>200	>200	50	100	50	100
<b>67</b>	H-(Nactm <sup>+</sup> -Nspe-Nspe) <sub>4</sub> -NH <sub>2</sub>	6.3	12.5	12.5	25	37.5	50	10.4	12.5	11.5	25
<b>68</b>	H-(Nactm <sup>+</sup> -Nspe-Nspe) <sub>4</sub> -NH <sub>2</sub>	11.5	12.5	50	100	33.3	50	6.3	12.5	6.3	12.5
	Melittin	6.3	12.5	6.3	12.5	12.5	25	3.1	6.3	6.3	12.5

<sup>167</sup> S. G. B. Amyes, *Antimicrobial Chemotherapy : Pocketbook* (Martin Dunitz, 1996).

The reference oligomers used in this study were developed by Barron, they showed similar activity compared to the work of Barron's group.<sup>89</sup> The hexamer was not active against the bacteria. However, the activity of the nonamer was reduced when compared with the literature, which can be attributed to the purity of the nonamer used in our study. Melittin was used as a control for studies against bacterial strains. It showed similar activity as reported in the literature previously.<sup>168</sup>

Many oligomers showed promising activity against the two strains of *Escherichia coli* and Gram-positive strains. However, they were not very efficient against *P. aeruginosa* strain. Even the longest oligomers, *i.e.*, **67** and **68** showed mild inhibitory activities towards it. It may be attributed to the fact that *P. aeruginosa* produces lot of biofilm to protect itself from the environmental conditions (see section 4).

### 3.3.1 Family I

In family I, the *spe* side chains of the reference peptoids were replaced by the tertbutyl side chain that block the backbone amide conformation in *cis*. In this family, only the hexamer Ac-(Mlys-Ntbu-Ntbu)<sub>2</sub>-OEt **27** was tested since the nonamer **28** was very sensitive and not enough pure to be tested. The hexamer **27** revealed inactive against all the strains of bacteria. However, it was not possible to conclude on the potential of the tertbutyl side chain since the reference hexamer was also inactive on the panel of bacteria except a 100 µM MIC on *Pseudomonas aeruginosa*.

### 3.3.2 Family II

In family II, the *spe* side chains of the reference peptoids were as well replaced by the tertbutyl side chain and cationic triazolium-based residues were incorporated in place of the Mlys residues. It was interesting to found that even a short oligomer such as the hexamer **43** exhibits significant activity against Gram-positive bacteria. Particularly, it shows good activity against *S. aureus* (MIC 6.3 µM) for an oligomer of this length.

It will be interesting to know the activities of longer oligomers Ac-(Nbtm<sup>+</sup>-Ntbu-Ntbu)<sub>n</sub>-OEt with n = 3 and 4. These peptoids have not been synthesised in the course of the PhD work but synthetic methodology is now in place and should enable the access to long oligomers. It would also be interesting to evaluate family II oligomer with a free N-terminus since a capped N-terminus usually decrease the antibacterial activity.

---

<sup>168</sup> T. L. Raguse; E. A. Porter; B. Weisblum; and S. H. Gellman, 'Structure - Activity Studies of 14-Helical Antimicrobial β-Peptides: Probing the Relationship between Conformational Stability and Antimicrobial Potency', *Journal of the American Chemical Society*, 124 (2002), 12774–85.

### 3.3.3 Family III series A

In the family IIIA, like in family II, the net positive charge of the oligomers arises exclusively from the triazolium groups. As expected, compound **53a** carrying the uncharged triazoles was totally inactive on bacteria. However, quaternisation of the two triazoles resulted in the cationic amphiphile **54a** with unprecedented antibacterial activities for a linear peptoid of this length. Indeed, MIC of 6.3 and 3.1  $\mu\text{M}$  were measured against *E. faecalis* and *S. aureus*, respectively. It is important to note that during antimicrobial peptoids design, short oligomers were often poorly active except those incorporating the dehydroabietyl moiety<sup>116,117</sup> or a long alky tail.<sup>169</sup> The lengthened peptoid **56a** showed a two- or a three-fold decrease in the MIC value for all bacteria except for *S. aureus*.

### 3.3.4 Family III series B

In the family IIIB, the only change compared to family IIIA was the substituent on triazolium moiety. The influence of additional aromatic group introduced in place of the aliphatic cyclohexylmethyl on triazolium was studied by comparison of nonamers H-(*N*chtm<sup>+</sup>-*N*spe-*N*spe)<sub>3</sub>-NH<sub>2</sub> **56a** and H-(*N*btm<sup>+</sup>-*N*spe-*N*spe)<sub>3</sub>-NH<sub>2</sub> **58a**.

It is usually noticed in AMP mimetics design that hydrophobic aromatic groups help at improving antibacterial activity but were often detrimental to the specificity.<sup>89</sup> The nonamer **58a** exhibits the best activities over the panel of bacterial strains studied excepted *P. aeruginosa*. A MIC of 1.6  $\mu\text{M}$  was obtained on both Gram-positive bacteria. The family IIIB shows a unique trend when the nonamer **58a** was capped with acetyl group at the *N*-terminus. Using the resulting oligomer Ac-(*N*btm<sup>+</sup>-*N*spe-*N*spe)<sub>3</sub>-NH<sub>2</sub> **58b**, the antibacterial activity was completely lost. This result suggests that the presence of the free terminal amine is important for the activity. However, in the family II, the acetylated hexamer Ac-(*N*btm<sup>+</sup>-*N*tbu-*N*tbu)<sub>2</sub>-OEt **43** was active on Gram-positive bacteria. When comparing the activity of acetylated **43** versus **58b**, it can be hypothesised that the *N*tbu residue has a positive effect on antibacterial activities. This may be due to the specific lipophilic character of the *tert*butyl or its structuring effect providing a better rigid backbone for a short oligomer. In this series, the hexamer has not been tested but its MIC will be measured soon.

### 3.3.5 Family III series C

In the family IIIC, an aminoethyl substituent was introduced on the triazolium resulting in additional cationic group in biological media. This design led to oligomers with a high net positive charge: +5 for hexamer, +7 for nonamer and +9 for dodecamer.

---

<sup>169</sup> J. A. Turkett and K. L. Bicker, 'Evaluating the Effect of Peptoid Lipophilicity on Antimicrobial Potency, Cytotoxicity, and Combinatorial Library Design', *ACS Combinatorial Science*, 19 (2017), 229–33.

Comparison of oligomers **63**, **66** and **68** showed that antimicrobial potency exponentially increased with oligomer length as usually observed for cationic amphiphilic peptoids. The H-(*Naetm*<sup>+</sup>-*Nspe-Nspe*)<sub>2</sub>-NH<sub>2</sub> hexamer **66** has no effect on bacterial strains whereas the dodecamer **68** exhibits high antibacterial activities particularly on Gram-positive bacteria.

To assess the contribution of the triazolium group in the series C of the third family, the activity of dodecamer **68** was compared with that of dodecamer **67** bearing uncharged triazole moieties.

According to our previous work on triazolium-based oligomers, the triazole exert a less marked influence on the amide conformation than the triazolium. This implies a better stabilisation of the peptoid main-chain into a PPI-like helical conformation for triazolium-based oligomers than for triazole-based oligomers. Interestingly, the dodecamer H-(*Naetm-Nspe-Nspe*)<sub>4</sub>-NH<sub>2</sub> **67** was found to have a broad-spectrum activity with potency against *E. coli* and *P. aeruginosa* similar to that of the reference sequence H-(*Mlys-Nspe-Nspe*)<sub>4</sub>-NH<sub>2</sub> from Barron group. In fact, dodecamer **67** was slightly less efficient on Gram-positive bacteria compared to dodecamer **68** but was more potent on *E. coli*. It is important to note that these dodecamers were the only peptoids of this study active on *P. aeruginosa* although with modest MIC values (37-33 μM).

Accordingly, in this series, the incorporation of a triazolium group in between the peptoid backbone and the ammonium cationic moiety mimicking the lysine side chain did not show any beneficial effect on the MIC values. However, we will see later that the incorporation of triazolium has a gain value in term of selectivity and toxicity.

### 3.4 Broad spectrum activity assessment

For the broad spectrum antibacterial activity assessment of the oligomers, the geometric mean (GM) of Gram-negative bacteria: two strains of *E. coli* and Gram-positive bacteria: *E. faecalis* and *S. aureus* was done (Figure 68).

It was observed that the third family has a very good GM score which makes them suitable candidates for broad spectrum antibiotic candidates.

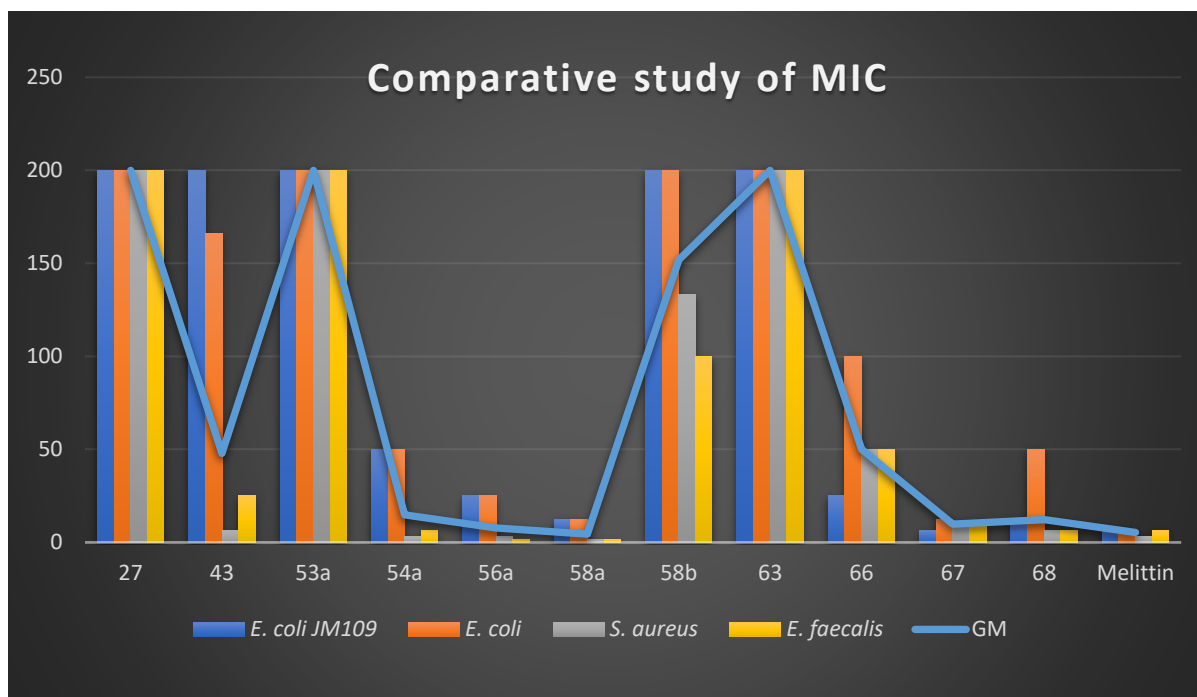


Figure 68 Broad spectrum antibacterial activity; GM= Geometric mean of MIC of four bacterial strains.

### 3.5 Conclusion

After studying the MIC and MBC, we have a promising idea about the activities of the various peptoid families against bacteria. This paves the way to study other biological activities. The selected peptoids and the various planned studies are illustrated below (Table 24).

Table 24 Selected peptoids for complementary biological assays

Family	No.	Peptoid Sequence	AB*	HA <sup>#</sup>	CY <sup>§</sup>
IIA	<b>43</b>	Ac-(Nbtm <sup>+</sup> -Ntbu-Ntbu) <sub>2</sub> -OEt	✓	✓	✓
IIIA	<b>54a</b>	H-(Nchtm <sup>+</sup> -Nspe-Nspe) <sub>2</sub> -NH <sub>2</sub>	✓	✓	✓
IIIA	<b>56a</b>	H-(Nchtm <sup>+</sup> -Nspe-Nspe) <sub>3</sub> -NH <sub>2</sub>	✓	✓	✓
IIIB	<b>58a</b>	H-(Nbtm <sup>+</sup> -Nspe-Nspe) <sub>3</sub> -NH <sub>2</sub>	✓	✓	✓
IIIB	<b>58b</b>	Ac-(Nbtm <sup>+</sup> -Nspe-Nspe) <sub>3</sub> -NH <sub>2</sub>	✓	✗	✗
IIIC	<b>66</b>	H-(Naetm <sup>+</sup> -Nspe-Nspe) <sub>3</sub> -NH <sub>2</sub>	✗	✓	✓
IIIC	<b>67</b>	H-(Naetm-Nspe-Nspe) <sub>4</sub> -NH <sub>2</sub>	✓	✓	✓
IIIC	<b>68</b>	H-(Naetm <sup>+</sup> -Nspe-Nspe) <sub>4</sub> -NH <sub>2</sub>	✓	✓	✓
		Melittin	✓	✓	✗

\*Anti-biofilm study, <sup>#</sup>Haemolytic activity, <sup>§</sup>Cell cytotoxicity



Anti-biofilm formation studies will be done on a selection of 7 peptoid oligomers. To access the therapeutic potential of these antimicrobial agents, their selectivity for bacterial over mammalian cells has to be accessed. Another important indicator is the inherent toxicity of the compounds. To this aim, haemolytic assay on human red blood cells (hRBC) and cell cytotoxicity studies will be carried out on a selection of 7 peptoids.

#### 4 Anti-biofilm studies

Many bacteria grow in the form of biofilms which are also known as biological membranes. Biofilms pose many advantages for the bacteria as it allows them to adapt to the changing environment. They can be communities of single or multiple populations, which are usually embedded on a surface (Figure 69).

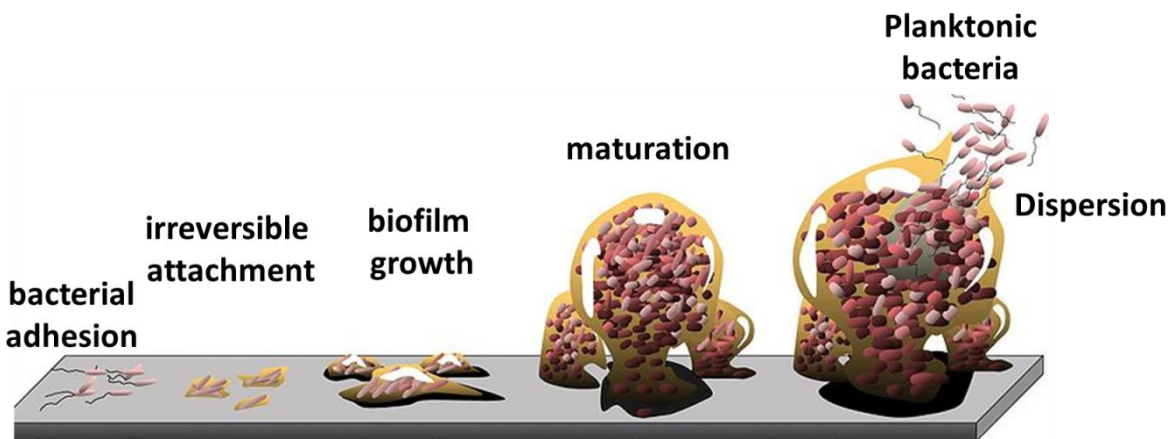


Figure 69 Schematic representation of biofilm formation (picture from [blogs.scientificamerican.com](http://blogs.scientificamerican.com)).

Bacterial growth within biofilms is associated with high tolerance to antibiotics and rapid development of resistance due to slow or incomplete killing. Bacterial cells comprising of biofilms produce extracellular polymeric substances (EPS), which surround them from outside and help protect against harmful external factors.<sup>170</sup> Biofilms are ubiquitous and most of microbial species, bacteria, fungi, yeasts, algae, protozoa, and viruses can adhere to surfaces and/or to each other to form biofilms.<sup>171</sup> Biofilms are found in all the types of environment ranging from natural to anthropogenic origin. Depending on the microbial species and their localization; environmental,

---

<sup>170</sup> I. W. Sutherland, 'The Biofilm Matrix - An Immobilized but Dynamic Microbial Environment', *Trends in Microbiology*, Vol. 9 (Elsevier Current Trends, **2001**), 222–7.

<sup>171</sup> J. Wingender and H. C. Flemming, 'Biofilms in Drinking Water and Their Role as Reservoir for Pathogens', *International Journal of Hygiene and Environmental Health*, 214 (**2011**), 417–23.

biomedical, or industrial, biofilms can be both beneficial and harmful for humans. However, according to the National Institutes of Health, formation and persistence of biofilms promote more than 75% of microbial infections that occur in the human body. Many pathogenic bacteria cause nosocomial infections, especially in urinary tract, genital tract, lower respiratory tract, and surgical site infections.<sup>172</sup> In 2012, RAISIN France (Réseau d'Alerte, d'Investigation et de Surveillance des Infections Nosocomiales) carried out the National Prevalence Survey of nosocomial infections and anti-infective treatments on 1,938 health facilities and 300,330 patients. It reported that most frequent microorganisms associated with nosocomial infections, *Escherichia coli*, *Staphylococcus aureus*, *Pseudomonas aeruginosa* and *Klebsiella pneumoniae*, are also high biofilm producers.<sup>173</sup> Anti-biofilm activity is defined as a natural or induced process, leading to reduction of bacterial biomass through the alteration of biofilm formation, integrity and/or quality.<sup>174</sup>

#### 4.1 Selection of bacteria

Three bacteria were used to grow the biofilm; one Gram-negative bacterium, *P. aeruginosa* and two Gram-positive bacteria, *S. aureus* and *E. faecalis*. The time for the growth of biofilm produced by *S. aureus* and *P. aeruginosa* was 24 hours whereas for *E. faecalis* it was 48 hours.<sup>175</sup> In *P. aeruginosa*, the amount of extracellular matrix is substantially high compared to *S. aureus* and *E. faecalis*. The peptoids were selected based on their minimum inhibitory concentration. The selected peptoids were used to study the reduction of biofilm formation by using preventive anti-biofilm tests. Anti-biofilm activity was assessed on all the selected peptoids at MIC/2 on the respective bacterial strain using two complementary techniques: Crystal violet and colony counting.

#### 4.2 Crystal Violet staining technique

Crystal violet (CV) staining provides total biofilm mass but it does not provide any information about cell viability. To determine if peptoids could be used prophylactically to prevent biofilm formation, we spectrophotometrically tested whether peptoids eliminated the biofilm of selected bacterial strains prior to biofilm formation using CV staining assay. CV imparts a colour which is dissolved using ethanol and can be measure using the spectrophotometer (Figure 70). It can be seen

---

<sup>172</sup> L. Hall-Stoodley and P. Stoodley, 'Biofilm Formation and Dispersal and the Transmission of Human Pathogens', *Trends in Microbiology*, Vol. 13 (Elsevier Current Trends, **2005**), 7–10.

<sup>173</sup> Réseau d'alerte d'investigation et de surveillance des infections Nosocomiales (France), *Enquête Nationale de Prévalence Des Infections Nosocomiales et Des Traitements Anti-Infectieux En Établissements de Santé, France, Mai-Juin 2012. Résultats* (Institut de veille sanitaire, **2013**).

<sup>174</sup> S. Miquel; R. Lagrèfeuille; B. Souweine; and C. Forestier, 'Anti-Biofilm Activity as a Health Issue', *Frontiers in Microbiology*, 7 (**2016**), 1–14.

<sup>175</sup> J. A. Mohamed and D. B. Huang, 'Biofilm Formation by Enterococci', *Journal of Medical Microbiology*, Vol. 56 (Microbiology Society, **2007**), 1581–8.

in the figure that in the replicate wells of peptoid **58b** and **43**, there is less development of violet colour. This shows reduction in biomass of the biofilm produced by *E. faecalis*.

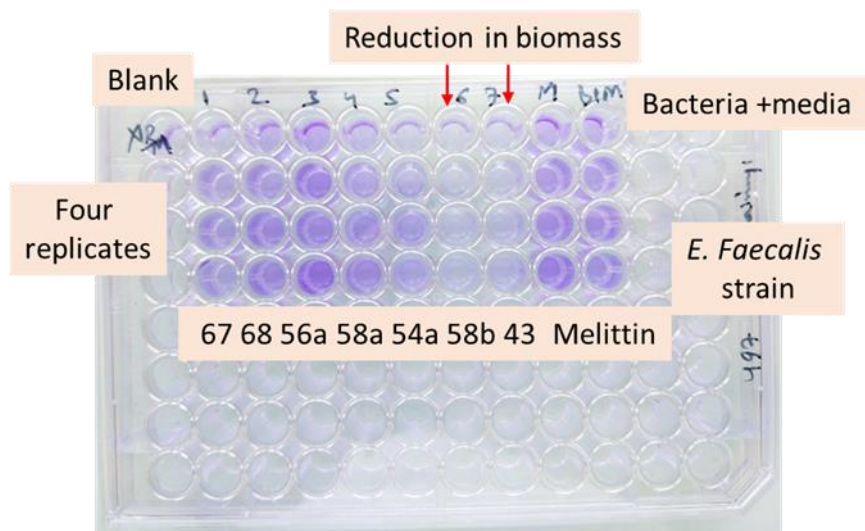


Figure 70 Crystal violet staining on selected oligomers on *E. faecalis* bacterial strain.

The results of the CV assays are summarised in the following table for the three bacteria tested (Table 25).

Table 25 Mean reduction in biomass (%) of selected bacterial strains using CV staining

Family	No.	Peptoid Sequence	<i>P. aeruginosa</i>	<i>S. aureus</i>	<i>E. faecalis</i>
IIA	<b>43</b>	Ac-(Nbtm <sup>+</sup> -Ntbu-Mtbu) <sub>2</sub> -OEt	59	1	57
IIIA	<b>54a</b>	H-(Nchtm <sup>+</sup> -Nspe-Nspe) <sub>2</sub> -NH <sub>2</sub>	0	0	36
IIIA	<b>56a</b>	H-(Nchtm <sup>+</sup> -Nspe-Nspe) <sub>3</sub> -NH <sub>2</sub>	97	0	29
IIIB	<b>58a</b>	H-(Nbtm <sup>+</sup> -Nspe-Nspe) <sub>3</sub> -NH <sub>2</sub>	96	0	52
IIIB	<b>58b</b>	Ac-(Nbtm <sup>+</sup> -Nspe-Nspe) <sub>3</sub> -NH <sub>2</sub>	20	92	90
IIIC	<b>67</b>	H-(Naetm <sup>+</sup> -Nspe-Nspe) <sub>4</sub> -NH <sub>2</sub>	49	3	30
IIIC	<b>68</b>	H-(Naetm <sup>+</sup> -Nspe-Nspe) <sub>4</sub> -NH <sub>2</sub>	64	1	14
		Melittin	32	6	1

The cationic oligomers **56a** and **58a** of family IIIA and IIIB, respectively were very efficient to reduce the biofilm formation in the Gram-negative bacterial strain. However, they were not very effective against the Gram-positive strains. On the contrary, the acetylated nonamer **58b** from the B series inhibits the biofilm formation of Gram-positive bacteria with the same efficiency for *S. aureus* or *E. Faecalis*. This result was quite surprising since this oligomer had no activity on these

bacteria according to MIC measurement. However, it is important to note that the concentration (MIC/2) used for the CV staining was very high compared to those of the other peptoids.

The longer oligomers **67** and **68** of family IIIC reduced the biofilm formation by half for *P. aeruginosa*. Oligomers from family IIA and IIIB with the btm<sup>+</sup> moiety were the best one to prevent the growth of biofilm of *E. faecalis*.

#### 4.3 Colony forming unit plate counting method

Since crystal violet staining gives information about total biomass reduction, it is important to know about the cell viability. Many investigators use plate counting method, but this method is time consuming and requires tedious work. To determine whether peptoids were effective in killing the bacterial cells within biofilms, cell viability was measured by bacterial plating at a concentration of half the MIC. This is a very precise method to know the exact reduction in CFU of bacterial strain (Figure 71).

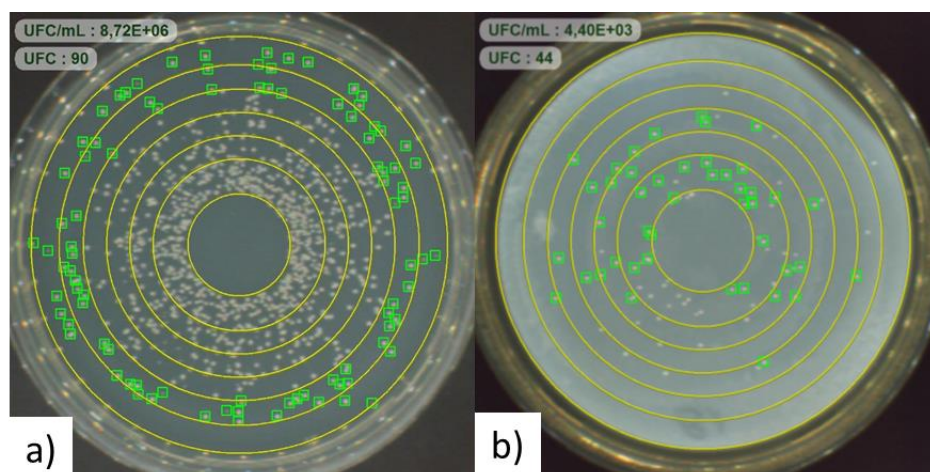


Figure 71 Reduction in the CFU of bacteria (*E. faecalis*); a) 24h incubation without the peptoid and b) 24 h incubation with peptoid at concentration half to the MIC.

The CFU/mL method in biofilm reduction was slightly different in two cases as compared to those obtained by CV staining. First, the hexamer **54a** shows 50% biofilm reduction for *P. aeruginosa* and oligomers from family IIIC lost their ability to reduce the biofilm formation of *E. faecalis*. Interestingly, inhibition of biofilm formation at ½ MIC concentrations was found for all peptoids on Gram-negative bacteria except for the acetylated nonamer **58b**. Other oligomers showed a similar activity as seen in CV staining method for Gram-positive bacteria. This reiterates the results obtained by CV staining (Table 26).

Table 26 Mean reduction in biomass (%) of selected bacterial strains using CFU/mL plate counting method

Family	No.	Peptoid Sequence	<i>P. aeruginosa</i>	<i>S. aureus</i>	<i>E. faecalis</i>
IIA	<b>43</b>	Ac-(Nbtm <sup>+</sup> -Ntbu-Ntbu) <sub>2</sub> -OEt	63	0	59
IIIA	<b>54a</b>	H-(Nchtm <sup>+</sup> -Nspe-Nspe) <sub>2</sub> -NH <sub>2</sub>	51	3	11
IIIA	<b>56a</b>	H-(Nchtm <sup>+</sup> -Nspe-Nspe) <sub>3</sub> -NH <sub>2</sub>	100	0	0
IIIB	<b>58a</b>	H-(Nbtm <sup>+</sup> -Nspe-Nspe) <sub>3</sub> -NH <sub>2</sub>	100	12	5
IIIB	<b>58b</b>	Ac-(Nbtm <sup>+</sup> -Nspe-Nspe) <sub>3</sub> -NH <sub>2</sub>	0	100	95
IIIC	<b>67</b>	H-(Naetm-Nspe-Nspe) <sub>4</sub> -NH <sub>2</sub>	57	14	9
IIIC	<b>68</b>	H-(Naetm <sup>+</sup> -Nspe-Nspe) <sub>4</sub> -NH <sub>2</sub>	57	0	2
		Melittin	0	0	0

## 5 Cell selectivity assays

Cell selectivity, *i.e.*, relative preference for killing bacteria over host cells, is an important property of an antimicrobial agent. We examined the toxicity of the selected peptoids against representative mammalian cell lines to evaluate the potential of peptoids as novel anti-bacterial agents. There are two commonly used ways to assess cellular toxicity of a compound which are discussed below.

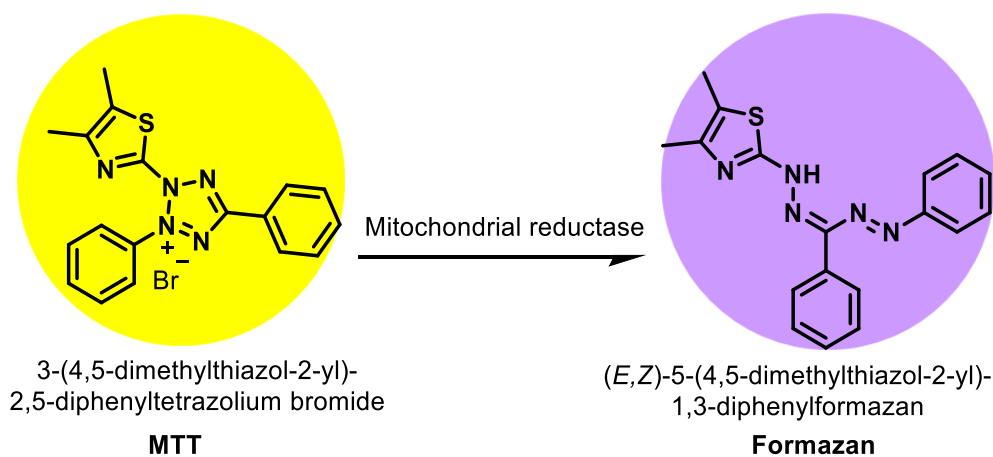
### 5.1 Haemolytic activity:

Haemolytic activity (HA) is a well-known fast screening method to determine the selectivity of peptoids against human erythrocytes. The degree of lysis of human red blood cells (hRBCs) is measured after exposure of hRBCs to the peptoid. The percentage of lysis indicates the tendency of test compounds to disrupt hRBCs by measuring the amount of haemoglobin released from the lysed hRBCs. HA is usually presented as an effective concentration of the compound resulting in 10% (HC<sub>10</sub>) or 50% (HC<sub>50</sub>) lysis of erythrocytes. HA is carried out by incubation of peptoids at different concentrations in phosphate-buffered saline (PBS) with a suspension of freshly drawn red blood cells in PBS at 37°C for 1 h in 96-well microtiter plate. PBS is used as positive control and 0.1% Triton X-100 is used as negative control.<sup>176</sup> Release of haemoglobin is measured on a spectrophotometer at 570 nm. Assessment of haemolysis is useful for screening purposes, however, a non-hemolytic compound can still be toxic towards other cell lines.

<sup>176</sup> X. Zhu; Z. Ma; J. Wang; S. Chou; and A. Shan, 'Importance of Tryptophan in Transforming an Amphipathic Peptide into a Pseudomonas Aeruginosa-Targeted Antimicrobial Peptide', *PLoS ONE*, 9 (2014), 1–19.

## 5.2 Cell Viability:

The best method to determine the selectivity of a compound is by studying the viability of a panel of human cells against the compound. It gives better understanding to estimate its toxicity profile. The cell viability assay is carried out by exposing cells grown in 96-well plates to a manifold concentration of its MIC against bacteria in the medium followed by incubation at 37°C. The easiest way for cell viability studies is by using tetrazolium dyes to stain healthy cells and to provide suitable conditions for spectrophotometric investigation. One of the most common tools for detection of cytotoxicity or cell viability *in vitro* is the MTT ((3-[4,5-dimethylthiazol-2-yl]-2,5-diphenyltetrazolium bromide) assay.<sup>177</sup> MTT is a water-soluble tetrazolium salt, which is reduced by the action of mitochondrial reductase to form an insoluble purple formazan. Formazan lacks the ability to penetrate the cell membrane, and therefore it collects in healthy cells (Scheme 47). The formazan crystals are insoluble in the cell medium, therefore by adding a solubilizing agent (DMSO) prior to the measurement is carried out to release the colour. This method has been successfully used to assess cytotoxicity of AMPs and peptidomimetics.<sup>178</sup>



Scheme 47 Principle of the MTT assay with reduction of MTT into formazan

## 5.3 Results of cell selectivity assays

Haemolytic activity was carried out by standard protocol on human RBCs. The cell viability assays were performed on HeLa (ATCC® CCL2™) cell lines and the more sensitive Jurkat (Clone E61 (ATCC® TIB-152™)) cell lines. The results are given below (Table 27).

<sup>177</sup> T. Mosmann, 'Rapid Colorimetric Assay for Cellular Growth and Survival: Application to Proliferation and Cytotoxicity Assays', *Journal of Immunological Methods*, 65 (1983), 55–63.

<sup>178</sup> X. Dou; X. Zhu; J. Wang; N. Dong; and A. Shan, 'Novel Design of Heptad Amphiphiles To Enhance Cell Selectivity, Salt Resistance, Antibiofilm Properties and Their Membrane-Disruptive Mechanism', *Journal of Medicinal Chemistry*, 60 (2017), 2257–70.



Table 27 Cell selectivity studies

Family	No.	Peptoid Sequence	HC <sub>10</sub> /HC <sub>50</sub> * μM	% Hela cell viability <sup>#</sup>	% Jurkat cell viability <sup>#</sup>
IIA	<b>43</b>	Ac-(Nbtm <sup>+</sup> -Ntbu-Ntbu) <sub>2</sub> -OEt	>200/>200	100	80
IIIA	<b>54a</b>	H-(Nchtm <sup>+</sup> -Nspe-Nspe) <sub>2</sub> -NH <sub>2</sub>	>200/>200	98	51
IIIA	<b>56a</b>	H-(Nchtm <sup>+</sup> -Nspe-Nspe) <sub>3</sub> -NH <sub>2</sub>	50/>75	5	9
IIIB	<b>58a</b>	H-(Nbtm <sup>+</sup> -Nspe-Nspe) <sub>3</sub> -NH <sub>2</sub>	>50/>100	5	10
IIIC	<b>66</b>	H-(Naetm <sup>+</sup> -Nspe-Nspe) <sub>3</sub> -NH <sub>2</sub>	>200/>200	100	86
IIIC	<b>67</b>	H-(Naetm-Nspe-Nspe) <sub>4</sub> -NH <sub>2</sub>	>100/>200	5	7
IIIC	<b>68</b>	H-(Naetm <sup>+</sup> -Nspe-Nspe) <sub>4</sub> -NH <sub>2</sub>	>200/>200	95	44

\*Haemolytic concentrations at which 10% and 50% haemolysis are observed; <sup>#</sup>Cell viability: average percentage of viable HeLa and Jurkat cells after peptoid exposition at 100 μM during 24h determined by MTT assay.

First of all, haemolysis and MTT assays results are in accordance with each other for all tested peptoids. Indeed, the four peptoids **43**, **54a**, **66** and **68** that showed low haemolytic activity on hRBC, were also not cytotoxic on Hela cells and low cytotoxic on Jurkat cells. For other peptoids, higher haemolytic activities were obtained, however acceptable. By contrast, a dramatic effect on cell viability of Hela or Jurkat cells was encountered. The cell selectivity index was calculated (Figure 72).

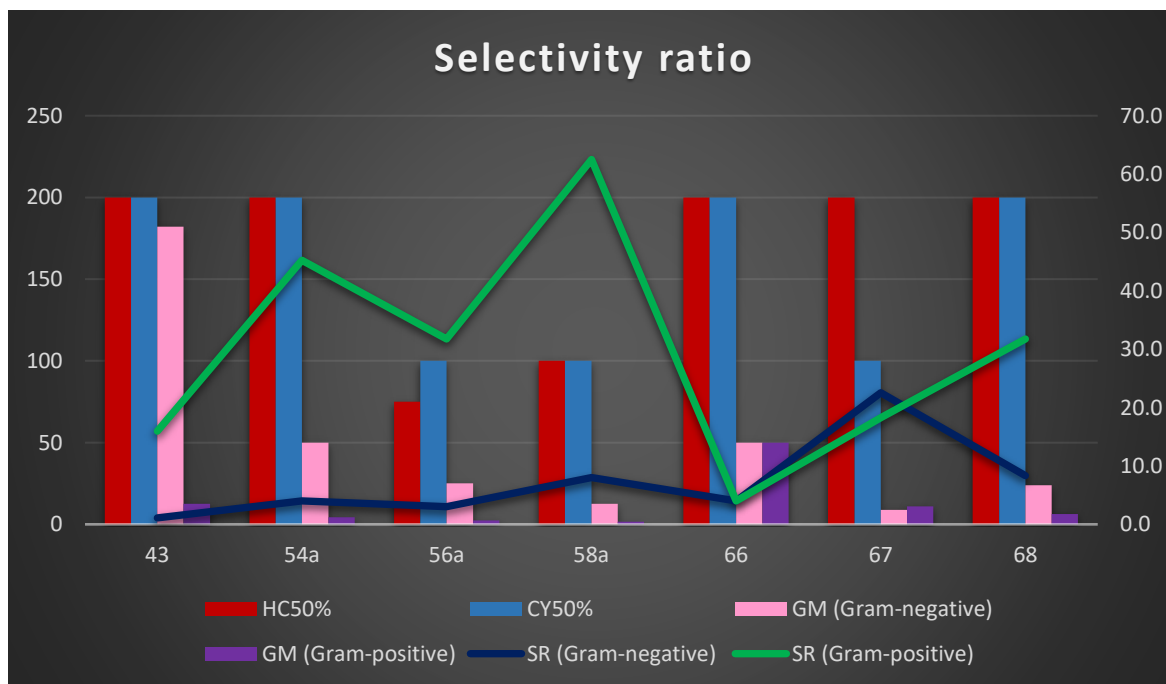


Figure 72 Selectivity ratio based on the geometric mean of two gram-negative and two gram-positive strains; GM (Gram-positive) = Geometric Mean of MIC values of *E. coli* JM109 and *E. coli* ATCC® 25922™; GM (Gram-negative) = Geometric Mean of MIC values of *S. aureus* CIP 6525 and *E. faecalis* ATCC® 29212™; SR= Selectivity Ratio is defined as the ratio of HC<sub>50</sub>% with the GM.

To better understand the cell selectivity, it is required to depict data of cell viability in terms of cell cytotoxicity (CY<sub>50%</sub>) for HeLa cell lines. Here, since the cell viability studies were carried out at only one concentration of peptoids (100 μM), the values for CY<sub>50%</sub> were kept at 200 μM if the cell viability is close to 100% and the values for CY<sub>50%</sub> were kept at <100 μM or <50 μM if the cell viability is close to 5%.

To compare the overall haemolytic activity and cell cytotoxicity of the selected oligomers, it can be said that smaller oligomers were less toxic to the mammalian cells. Indeed, the hexamers **43** of the family II and **54a** of the family IIIA were non-haemolytic nor toxic on studied cells. The haemolytic activity and cell cytotoxicity of the family IIIA increased with the main chain length as HC<sub>50%</sub> and CY<sub>50%</sub> of the nonamer **56a** decreased from >200 μM for the hexamer (both HC<sub>50%</sub> and CY<sub>50%</sub>) to >75 μM and >100 μM, respectively. However, the selectivity ratio (Gram-positive) remained very acceptable. It can be concluded that the hexamer **54a** of family IIIA showed best potency against Gram-positive bacteria with good selectivity ratio (MIC<sub>*S.aureus*</sub> 3.1 μM, MIC<sub>*E.faecalis*</sub> 6.3 μM, HC<sub>10</sub> > 200 μM and CY<sub>50</sub> > 200 μM). The nonamer **56a** of the same series showed slightly better activities but the selectivity dramatically decreased.

The influence of additional aromatic group introduced in place of the aliphatic cyclohexylmethyl on triazolium was studied by comparison of nonamers **56a** and **58a** from family IIIA and family IIIB. It is usually noticed in AMP mimetics design that hydrophobic aromatic groups help at improving antibacterial activity but were often detrimental to the specificity.<sup>89</sup> The nonamer **58a** exhibits the best activities over the panel of bacterial strains studied (best GM values for both Gram-negative and Gram-positive strains) and was surprisingly slightly less haemolytic than nonamer **56a** with a selectivity ratio SR (Gram-positive) greater than 62.5. However, it is important to note that the HeLa or Jurkat cells viability at 100 μM (representing more than 10 times the MIC for Gram-positive bacteria) was very low for both nonamers (**56a** and **58a**).

The family IIIC oligomers presents a peculiar selectivity profile compared to other cationic amphipathic peptoids designed to date. In contrast with previous studies, no increase of haemolytic activity was observed for longer oligomers of family IIIC (**66** versus **68**). Indeed, the dodecamer **68** displayed very low haemolytic activity (HC<sub>10</sub> > 200 μM) and good cells viability (95 % for HeLa and 44% for Jurkat at 100 μM). The selectivity ratio (gram-positive) of 31.7 was obtained for this nonamer. On the contrary, oligomer of the same length but with triazoles instead of triazolium moieties was dramatically less selective. Indeed, treatment of HeLa and Jurkat cells with nonamer **67** at 100 μM resulted in cell viability values of only 5 and 7 %, respectively. To conclude, we can see an increasing trend for the selectivity ratio (Gram-positive) in the triazolium precursors of family IIIC.



## 6 Microscopy

As for AMPs, it is generally accepted that amphipathic cationic peptoids act by bacterial membrane disruption and a few studies have provided evidence for this mechanism.<sup>93,89</sup> However additional modes of action are not excluded.<sup>179</sup>

To investigate the interaction of our peptoids, we decided to perform Scanning Electron Microscopy and field emission gun SEM (FEGSEM) characterisation of bacteria cultures exposed to selected peptoids. Based on the antimicrobial potency and toxicity to the mammalian cells, we selected three oligomers to study their mechanism of action on the bacteria. Dodecamer **68** from family IIIC showed very good potency against *E. Coli* JM109 and *S. aureus* with MIC values of 11.5  $\mu\text{M}$  and 6.3  $\mu\text{M}$ , respectively and showed close to negligible haemolysis and toxicity at 10-fold concentration. Also, the triazolium based hexamers (**43** and **54a**) of Family IIA and IIIA showed excellent potency against *S. aureus* with MIC values of 6.3  $\mu\text{M}$  and 3.1  $\mu\text{M}$ , respectively and showed negligible haemolysis and toxicity at more than 16-fold concentration. The selection of the peptoids **43**, **54** and **68** was done to have the larger sequence diversity and was a compromise between antibacterial activity and selectivity (Figure 73). The effect of peptoid **68** was studied on *E. coli* and the effect of peptoids **43**, **54** and **68** on *S. Aureus*.

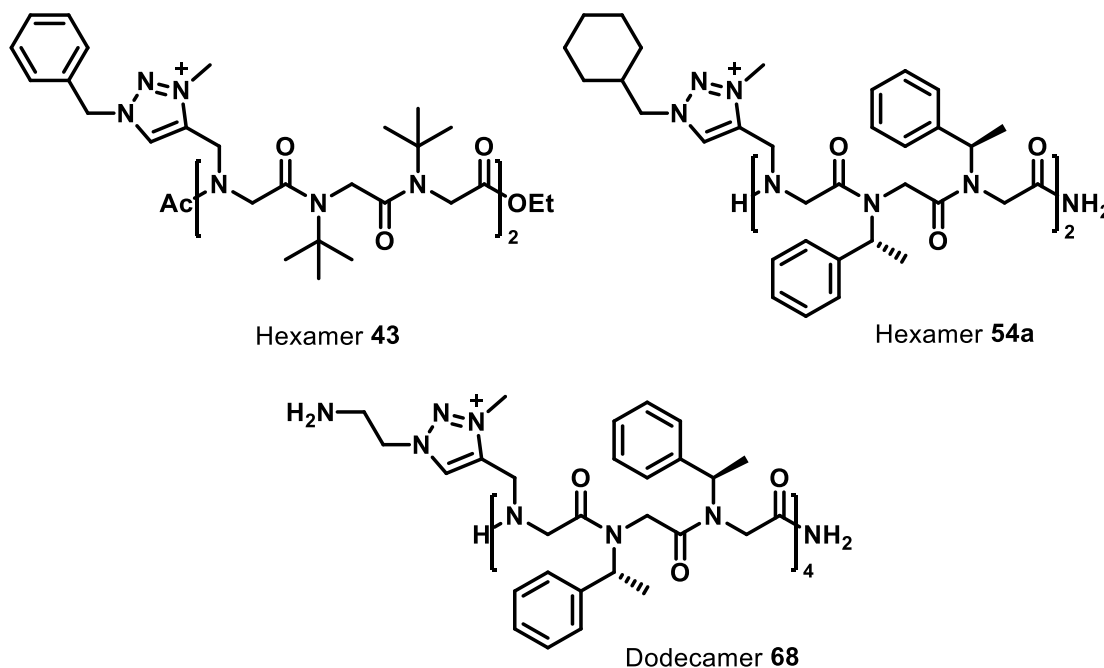


Figure 73 Structures of peptoids selected for microscopy.

<sup>179</sup> N. P. Chongsiriwatana; J. S. Lin; R. Kapoor; M. Wetzler; J. A. C. Rea; M. K. Didwania; C. H. Contag; and A. E. Barron, 'Intracellular Biomass Flocculation as a Key Mechanism of Rapid Bacterial Killing by Cationic, Amphipathic Antimicrobial Peptides and Peptoids', *Scientific Reports*, 7 (2017), 16718.

Changes in membrane morphology of *E. coli* and *S. aureus* bacteria upon peptoid treatment were visualized using Scanning Electron Microscopy.

For dodecamer **68** the longest peptoid from the family IIC, significant damage on the bacterial membrane was observed. Initially at T=0 and after 18h, untreated *E. coli* bacteria appeared as intact rods with no evidence of membrane damage and collapse (Figure 74 a, b). However, upon treatment with the dodecamer **68** at the MIC (11.5  $\mu\text{M}$ ), the bacteria demonstrated strong evidence of membrane disorganisation with great deformation on the surface as compared to the smooth surface of untreated *E. coli* (Figure 74 c, d).

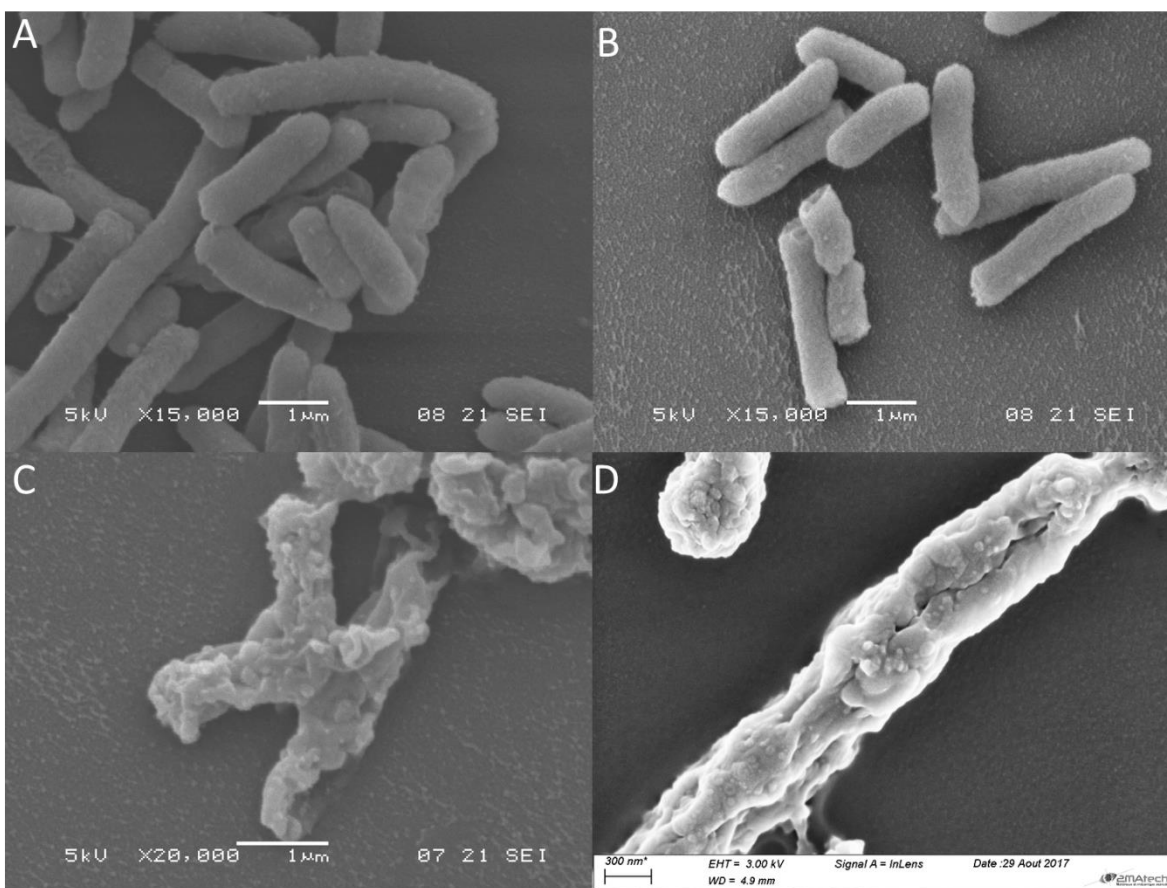


Figure 74 SEM micrographs of *E. coli* cells A) Cultures in log phase at  $10^8$  CFU/ml at  $T = 0$ ; B) untreated after 18h; C) treated with the dodecamer **68** at the MIC (11.5  $\mu\text{M}$ ) after 18h; D) Field emission gun SEM of *E. coli* cells treated with the dodecamer **68**.

The dodecamer **68** showed peculiar effect on *S. aureus* bacteria. In the control samples (untreated *S. aureus*) at T=0 and after 18 h, the cells appeared with round and smooth surfaces in grape-like clusters (Figure 75 a, b). Upon treatment by the peptoid **68** at the MIC (6.3  $\mu\text{M}$ ), cytoplasmic leakage and membrane damage were observed (Figure 75c). Cells showed surface depressions and some of them had holes ( $\approx 70\text{-}80$  nm diameter, measured by FEGSEM) in their cell membrane (Figure 75d). Pore formation has been previously observed on the membrane of MRSA treated by cationic cyclic peptoids.<sup>106</sup>

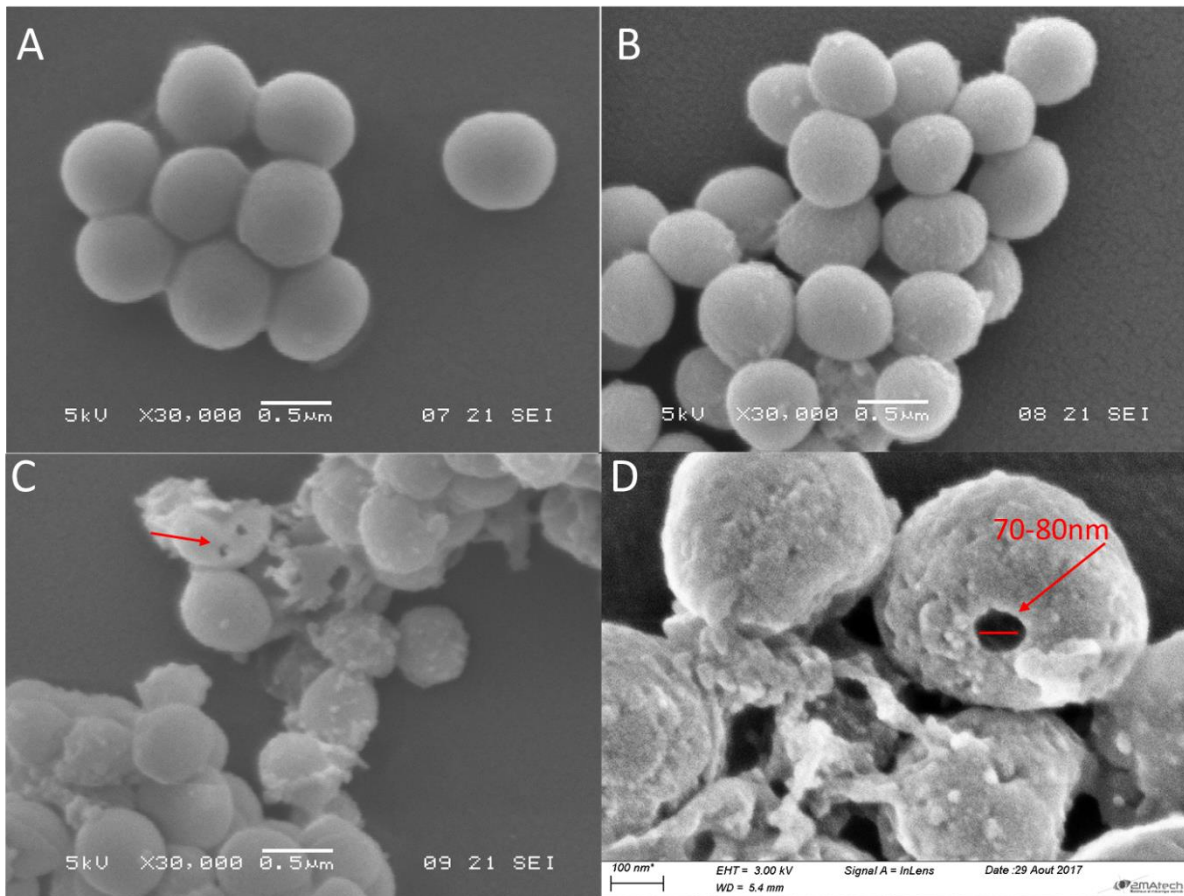


Figure 75 SEM micrographs of *S. aureus* cells A) Cultures in log phase at  $10^8$  CFU/ml at  $T = 0$ ; B) untreated after 18h; C) treated with the dodecamer **68** at the MIC ( $6.3 \mu\text{M}$ ) after 18h; D) Field emission gun SEM of *S. aureus* cells treated with the dodecamer **68**.

SEM micrographs of bacteria treated with hexamer **54a** at the MIC ( $3.1 \mu\text{M}$ ) showed significant morphological alterations of *S. aureus* cells. A major part of the cells presents important membrane corrugation, but no pores have been detected. Fissures were observed near or at the division hemisphere (septum) (Figure 76a). These features were consistently observed in FEGSEM micrographs obtained for antimicrobial treated bacterial cells (Figure 76b). Similarly, SEM of *S. aureus* treated with hexamer **43** showed profound membrane damage and formation of resin like structures (Figure 76c) as compared with the smooth untreated grape like structures (Figure 75 a, b). Complete leakage of the cellular material and the collapse of the membrane are evident from the FEGSEM visualisation (Figure 76d). However, pore formation cannot be ruled out in the case of hexamer **43**, as most of the cells appeared to be shrunk in the volume.

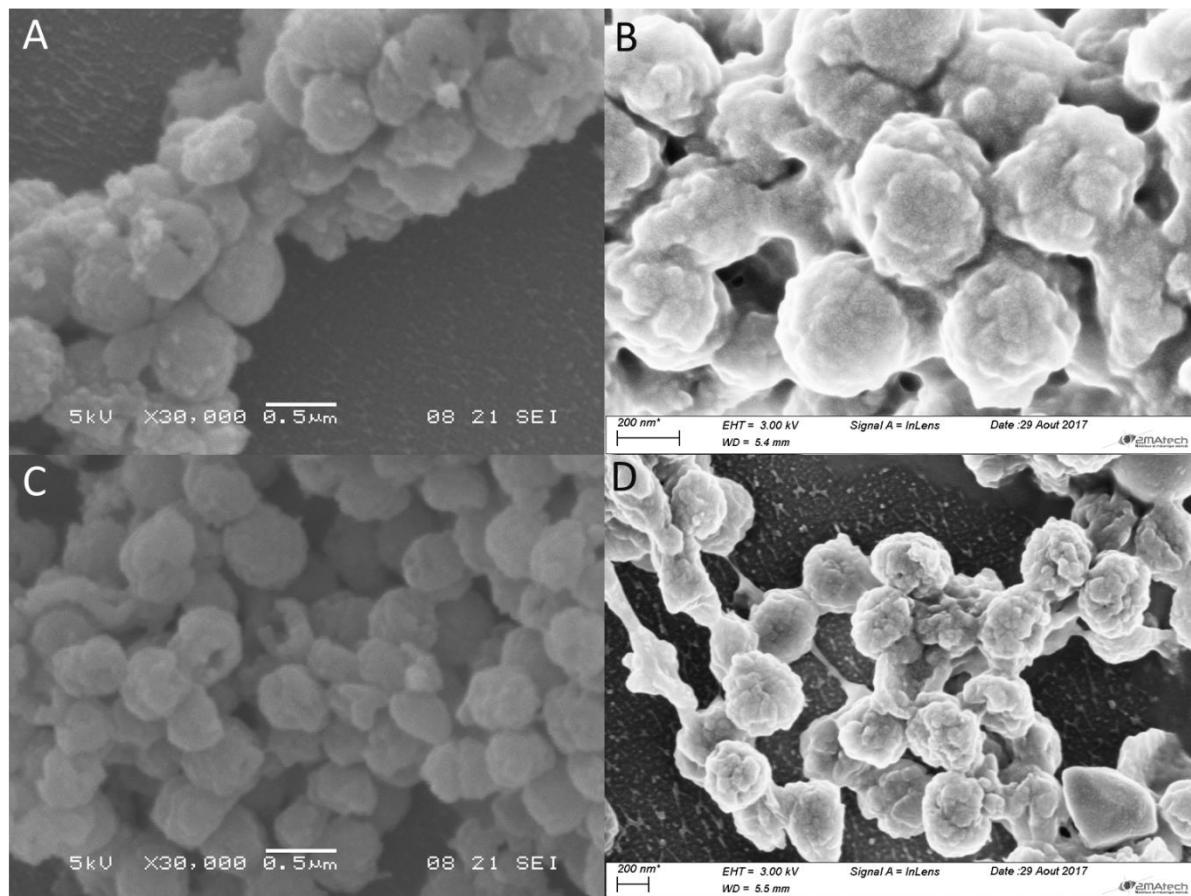


Figure 76 SEM micrographs of *S. aureus* cells A) treated with the hexamer **54a** at the MIC ( $3.1 \mu\text{M}$ ) after 18h; B) Field emission gun SEM of *S. aureus* cells treated with the hexamer **54a**; C) treated with the hexamer **43** at the MIC ( $6.3 \mu\text{M}$ ) after 18h; D) Field emission gun SEM of *S. aureus* cells treated with the hexamer **43**.

By SEM visualization, *S. aureus* cells treated with peptoids **68**, **54a** or **43** revealed severe damaging effects on the cell membrane. Our observations suggested that the longest peptoid **68** acts by pore formation while the smaller hexamers **54a** and **43** seem to cause membrane permeation by another mechanism.

### 6.1 Mode of action hypothesis

It is apparent that triazolium-based peptoids have a promising potential to be used as an antibacterial agent.

However, it was observed that we need higher concentration of peptoids to cause damage to Gram-negative bacteria (*E. coli*) when compared with Gram-positive bacteria (*S. aureus*). This can be explained with three reasons. Firstly, the absence of an outer membrane and the presence of negatively charged teichoic acid molecules within a thick peptidoglycan layer on the surface of *S. aureus* can make them more attractive to the positively charged triazolium-based oligomers as compared with *E. coli*. Secondly, *E. coli* has several small channel porins within the outer

membrane, which can block the entrance of peptoids inside the bacteria, making them more difficult to inhibit than *S. aureus*. Finally, the smaller dimension of *S. aureus* (spherical, ~1 μm) may require less concentration of peptoids, making the antibacterial activity more effective in comparison with *E. coli* (rod, 0.3-1.0 × 1.0-6.0 μm).

Since this work is a first attempt to study the antibacterial activity of triazolium-based peptoid oligomers, not much is known about the mode of action of this type of peptoids on the bacteria. The following (Figure 77) is an attempt to hypothesise the mode of action of triazolium-based peptoids based on the SEM and FEGSEM micrographs. The positively charged triazolium-based oligomers should interact favourably with the negatively charged bacterial cell membrane by electrostatic attraction, causing an increase in membrane permeability and eventual rupture and leakage of the cellular components. In the specific case of *S. aureus*, it can be said that the positively charged triazolium-based oligomers attach to the negatively charged teichoic acid molecules in *S. aureus* (as supported by the reason for why *S. aureus* showed a lower resistance to the antimicrobial effect in comparison to *E. coli*). Disruption of the bacterial membrane can be another possible mode of peptoid action, as it lets the peptoids to go inside the bacteria and damage the inner cellular machinery. Leakage of intracellular material due to the membrane disruption may cause shrinkage of the cell membrane, ultimately leading to the cellular lysis as seen by SEM and FEG SEM images.

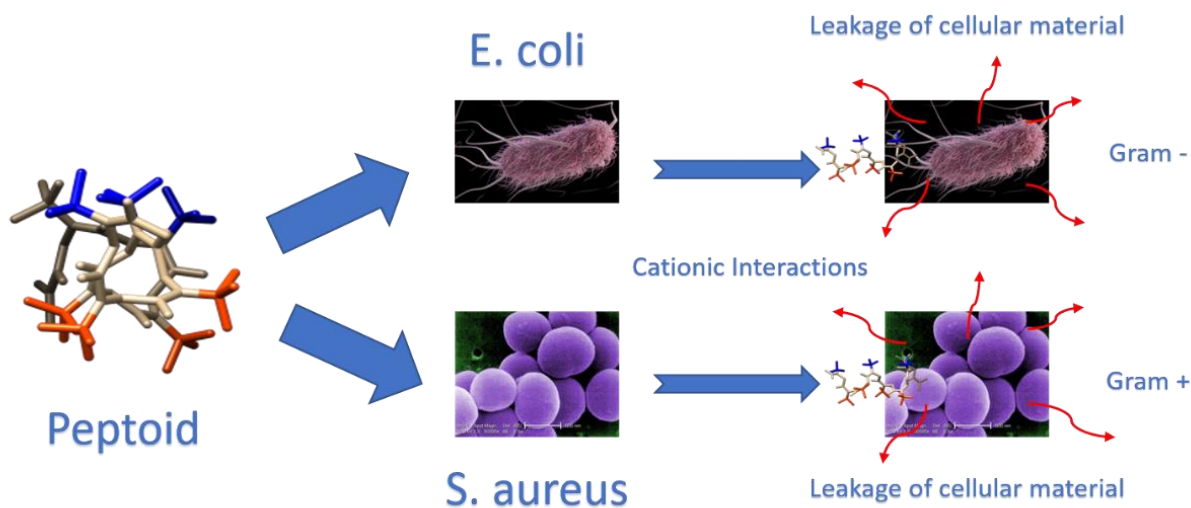


Figure 77 Schematic representation of antibacterial mechanism of triazolium-based peptoids.

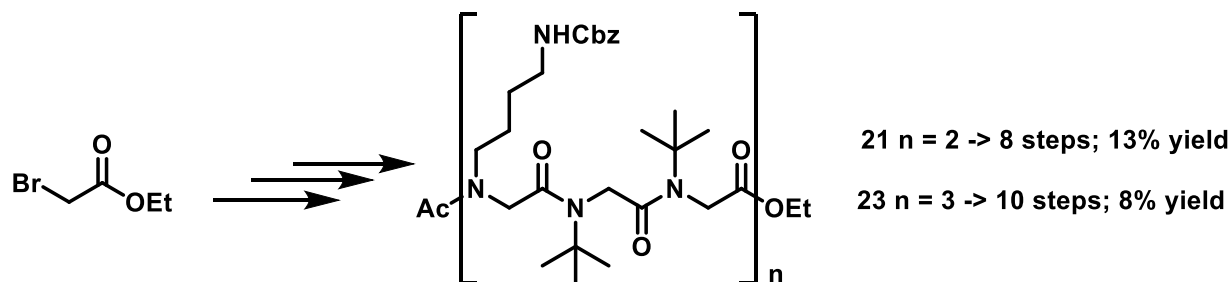
# **General conclusion and perspectives**

## Conclusion and perspectives

The aim of this thesis was to synthesise novel cationic amphipathic oligomers as antimicrobial peptide mimetics. As we know, all the efforts in the past to develop helical peptoid oligomers were done using  $\alpha$ -chiral bulky aromatic side chains like spe and s1npe. However, these helical oligomers have a damaging effect on the haemolytic activity and cytotoxicity. Moreover, these above said side chains limit the chemical diversity among these helix inducers which hampers the development of these foldamers as drug candidates.

Therefore, we designed long oligomers using the side chains developed in the group which work as a better inducer of helix structure in peptoid oligomer. Particularly, tert-butyl and triazolium-based oligomers were a challenge to synthesise using both solution phase and solid phase synthetic strategy. These oligomers are first of this type, which try to create strong amphipathic architecture by stabilising the *cis* conformation of all backbone amides through steric and/or electronic interactions.

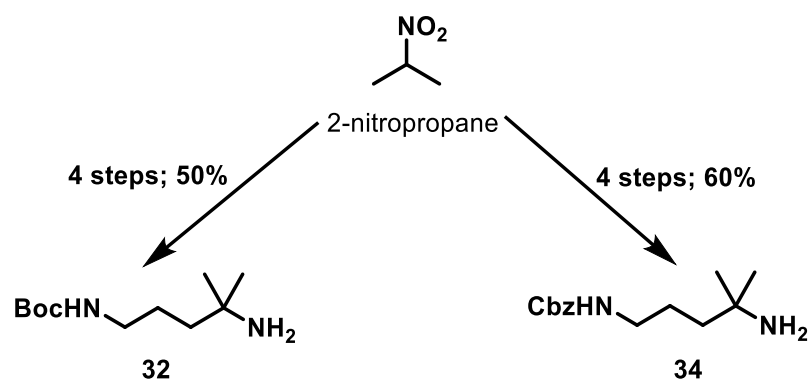
The solution phase synthesis of long oligomers of Family IA was very tedious and numerous hurdles were encountered during the purification of these oligomers. Nevertheless, the hexamer **21** and the nonamer **23** were obtained in global yields of 13% and 8% respectively (Scheme 48).



Scheme 48 Synthesis of oligomers Ac-(Nlys(Cbz)-Ntbu-Ntbu)<sub>n</sub>-OEt.

However, the deprotection and purification of longer oligomer **23** was difficult. That is why only the deprotected hexamer **21** was evaluated against a panel of bacteria. Its failure to produce antibacterial activity led to no further synthetic development of Ac-(Nlys-Ntbu-Ntbu)<sub>n</sub>-OEt family IA oligomers. Nevertheless, now with all the experience it can be said that the deprotected nonamer **23** Ac-(Nlys-Ntbu-Ntbu)<sub>3</sub>-OEt or the dodecamer Ac-(Nlys-Ntbu-Ntbu)<sub>4</sub>-OEt may be active against bacteria.

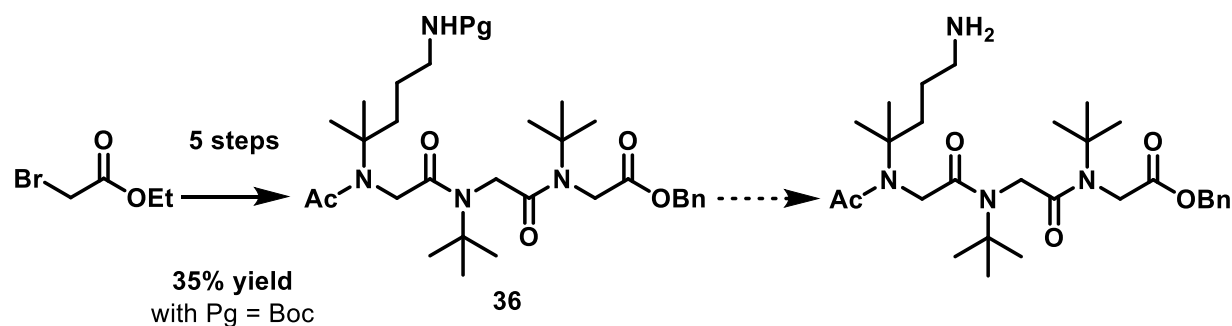
In the synthesis of Family IB based oligomers the crucial step was to develop NgLys,  $\alpha$ -gem-dimethylated Nlys side chain (Scheme 49).



Scheme 49 Development of NgLys side chains.

The side chain was developed by protecting the terminal amine using both Boc and Cbz protecting groups. We obtained the NgLys(Boc) **32** and NgLys(Cbz) **34** side chains in global yield of 50% and 60%, respectively.

This type of trimer was synthesized for the first time and  $\alpha$ -gem-dimethylated MLys side chain works as a functionalised tert-butyl side chain. The trimer block **36** was obtained in global yield of 35% (Scheme 50).

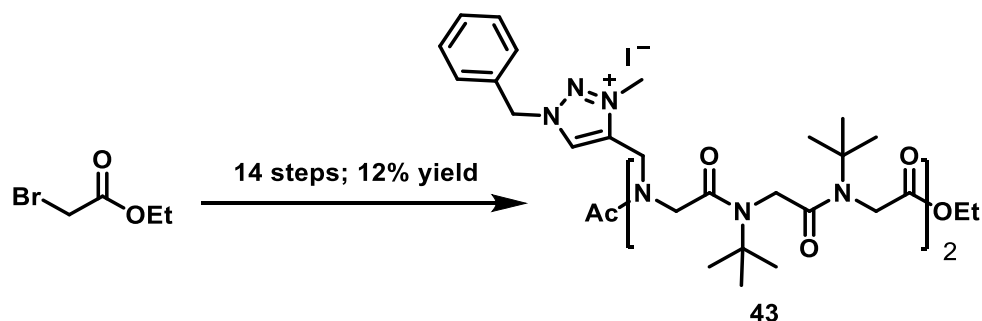


Scheme 50 Synthesis of trimer block with NgLys side chain.

However, since the deprotection of the Boc group is difficult, the synthetic route can now be developed using Cbz protection strategy and synthesise longer oligomers. It can be interesting to see the antimicrobial activity of Ac-(NgLys-Ntbu-Ntbu)<sub>n</sub>-OEt type oligomers..

The synthesis of oligomers based on family II was an easier task, however it is a lengthy process as we cannot use the block coupling strategy for the synthesis of longer oligomers. Yet, the hexamer **43** was obtained in a global yield of 12% in 14 steps (Scheme 51).





Scheme 51 Synthesis of the Family II hexamer  $\text{Ac}-(\text{Nbtm}^+-\text{Ntbu}-\text{Ntbu})_2\text{-OEt}$ .

The most fascinating discovery was the biological activity of family IIA based hexamer **43** which showed peculiar activity for short oligomers against Gram-positive bacteria. Therefore, using the same synthetic strategy longer oligomers like  $\text{Ac}-(\text{Nbtm}^+-\text{Ntbu}-\text{Ntbu})_n\text{-OEt}$  should be synthesised and biological evaluation must be carried out. Moreover, using the same strategy  $\text{chtm}^+$  based oligomers can be synthesised as the oligomers based on  $\text{chtm}^+$  from family IIIA showed high potency for antibacterial activity (Figure 78).

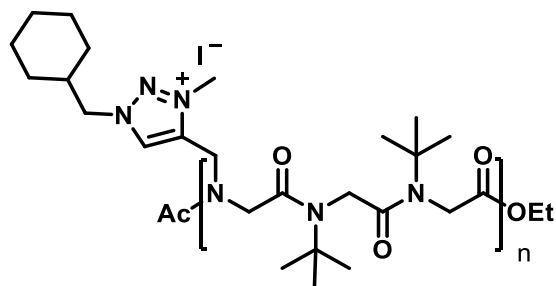
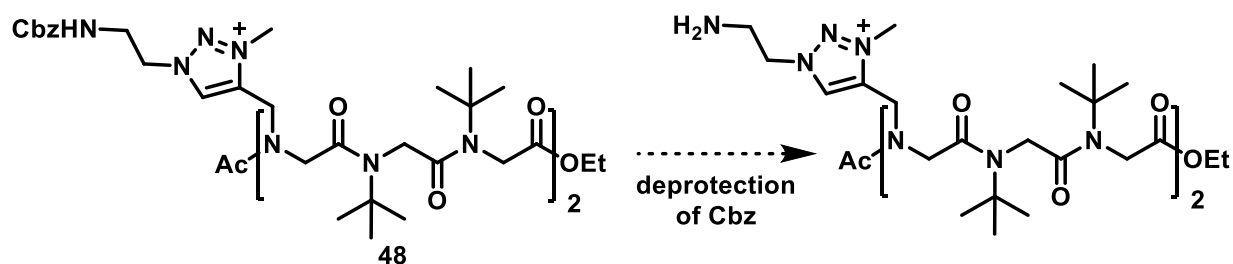


Figure 78 Oligomers based on  $\text{Nchtm}^+$  side chain;  $\text{Ac}-(\text{Nchtm}^+-\text{Ntbu}-\text{Ntbu})_n\text{-OEt}$ .

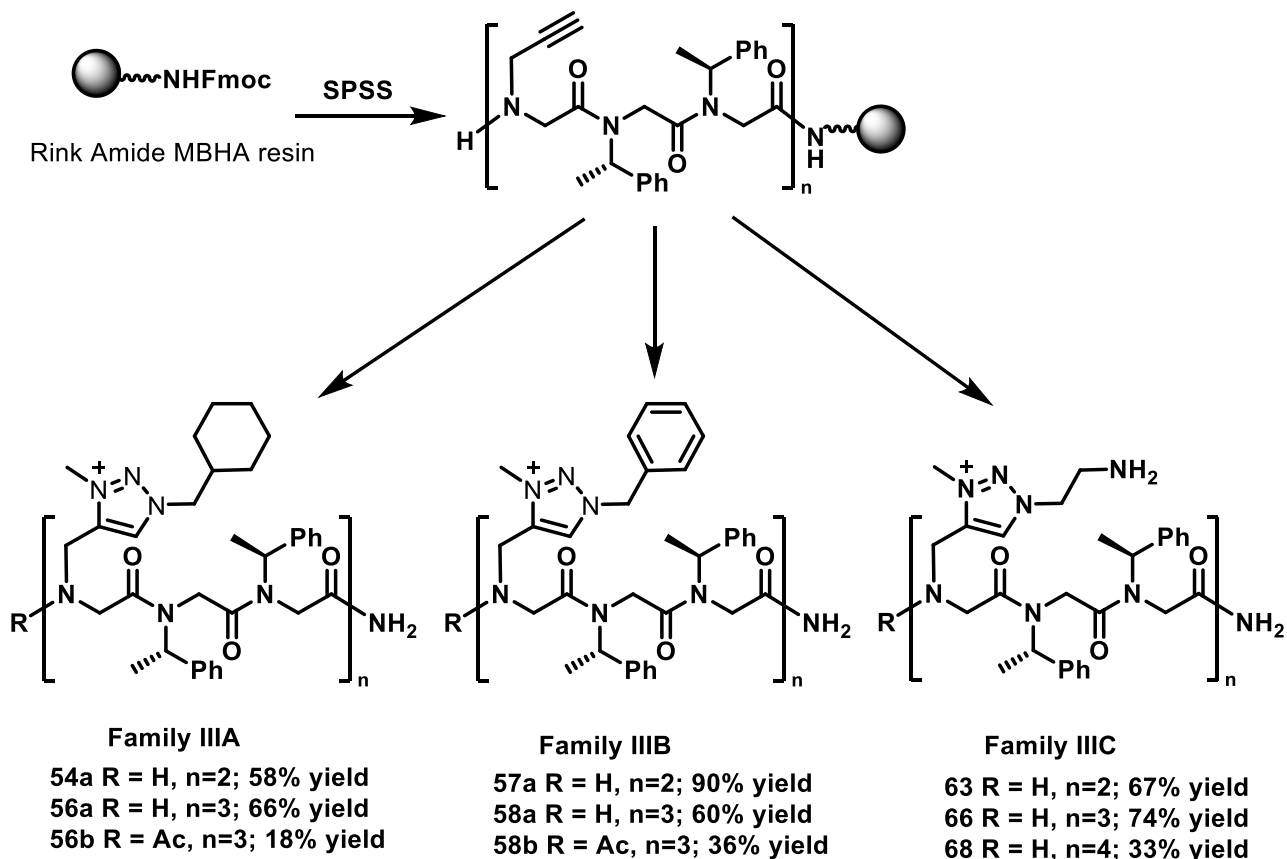
Also, the conditions for synthesis of family IIB were optimised and we developed hexamer **48** with protected  $\text{Naetm}^+(\text{Cbz})$  side chain. This oligomer should be deprotected to obtain the hexamer  $\text{Ac}-(\text{Naetm}^+-\text{Ntbu}-\text{Ntbu})_2\text{-OEt}$  which can be used for the biological evaluation of family IIB (Scheme 52).



Scheme 52 Deprotection of family IIB based hexamer.

It would be very interesting to develop longer oligomer of family II in order to determine and compare their potency and selectivity with those of the family III. Indeed, this will allow evaluating the impact of the *tbu* side chain as hydrophobic group in place of *spe* side chain.

For the synthesis of family III, the SPSS strategy was optimised and we synthesised long oligomers based on R-(Nxtm<sup>+</sup>-Nspe-Nspe)<sub>n</sub>-NH<sub>2</sub>. This methodology is now well in place however the purification process as to be improved. Indeed, the oligomers based on family IIIA and family IIIB with free terminal amines were difficult to purify using the chromatographic techniques. Still, we obtained long oligomers of family III in good overall yields using SPSS strategy (Scheme 53).



Scheme 53 Solid phase synthesis of family III oligomers.

A preliminary circular dichroism has enable to obtain the first CD signature of peptoid oligomer containing triazolium side chains. However, to have a better understanding of the folding of family III oligomers, more work must be done. For example, the CD curves of all oligomers of the family III must be recorded and the CD study can be done in other media such as the Tris buffer (pH 7.4) or in presence of anionic liposomes to mimic the bacterial membrane.

The oligomers from family III showed excellent potential against both Gram-positive and Gram-negative bacteria. Also, not all the oligomers were evaluated for their biological activity; this leaves a room for more biological studies on family III oligomers.

Microscopic studies on the bacteria damaged by the hexamer **43** from family II, hexamer **54a** from family IIIA and dodecamer **68** from family IIIC gave interesting insights in the mode of action of these oligomers against the bacteria. In addition, to have a better understanding of the mechanism

of attack of the oligomers on the bacteria, transmission electron microscopy (TEM) can be done to better see the effect on the bacterial membrane.

A direct perspective of this work is the potency optimization of the most promising amphipathic cationic peptoids while maintaining a good selectivity for prokaryote cells. To reach this purpose different modification strategies are actually explored in the group.

A better comprehension of the mechanism of action of the triazolium-based oligomers is also needed. Indeed, the good activity of the short oligomers **43** and **54a** may be due to an intracellular target of these peptoids. A series of assays could be performed in order to determine if these peptoids act only on the membrane or also interact with cytoplasmic component crucial to proper cellular physiology of bacteria.

To look at the broader perspectives, four oligomers **43**, **54a**, **66** and **68** showed excellent selectivity towards mammalian cells (both HeLa and Jurkat cell lines). Therefore, this type of oligomers can be used to develop cell penetrating peptoids. It can serve two functions, first the oligomers can be tagged with fluorescent dyes which can penetrate the live cells and help to visualise the specific areas inside the tissues; second the oligomers can be used to transport active pharmaceutical ingredient inside mammalian cells (Figure 79).

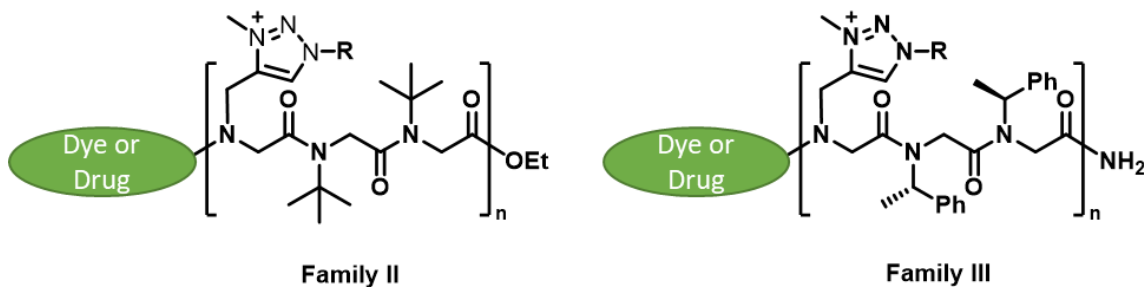


Figure 79 Triazolium-based peptoid oligomers as cell penetrating agents.

# **Chapter V**

## **Experimental Section**

## 1 General Information

**Nuclear magnetic resonance (NMR):** NMR spectra were measured in deuterated solvents ( $\text{CDCl}_3$ ,  $\text{D}_2\text{O}$ , acetone- $d_6$ ,  $\text{CD}_3\text{OD}$  or  $\text{CD}_3\text{CN}$ ) on a Bruker AC-400 spectrometer, operating at 400 MHz for  $^1\text{H}$  and 100 MHz for  $^{13}\text{C}$  J-modulation or a Bruker AC-500 spectrometer operating at 500 MHz for  $^1\text{H}$  and 125 MHz for  $^{13}\text{C}$ . Residual solvent signals were used as internal reference. Chemical shifts ( $\delta$ ) are reported in ppm, coupling constant values ( $J$ ) are given in Hertz (Hz). Abbreviations employed for multiplicity description: s = singlet, d = doublet, t = triplet, q = quadruplet, qu = quintuplet, dd = double doublet, dt = double triplet, ddd = double double doublet, bs = broad singlet, m = multiplet and massif. NMR spectral data often are of rotameric mixture. Where applicable, assignments of  $^1\text{H}$  and  $^{13}\text{C}$  spectra were based on 2D experiments ( $^1\text{H}$ - $^1\text{H}$  COSY,  $^1\text{H}$ - $^{13}\text{C}$  HSQC,  $^1\text{H}$ - $^{13}\text{C}$  HMBC).

**Infrared spectra (IR)** were recorded on a SHIMADZU FTIR-8400S spectrometer equipped with a Pike Technologies MIRacle™ ATR. Only structurally important peaks are presented; wave numbers ( $\bar{\nu}$ ) are expressed in  $\text{cm}^{-1}$ .

**High-resolution mass spectra (HRMS)** are recorded using electrospray ionization in positive mode (ESI+) on or a Q Exactive Quadrupole-Orbitrap Mass Spectrometer or on a Qtof-micro WATERS (3000V) spectrometer.

**Liquid chromatography mass spectroscopy (LC-MS)** were recorded on a Q Exactive Quadrupole-Orbitrap Mass Spectrometer coupled to a UPLC Ultimate 3000 (Kinetex EVO C18; 1,7 $\mu\text{m}$ ; 100mm x 2,1mm column with a flow rate of 0.45  $\text{ml}\cdot\text{min}^{-1}$  with the following gradient: a linear gradient of solvent B from 5% to 95% over 7.5 min (solvent A =  $\text{H}_2\text{O}$  + 0.1% formic acid, solvent B = acetonitrile + 0.1% formic acid) equipped with a DAD UV/VIS 3000 RS detector) or on a Qtof-micro WATERS (3000V) with electrospray ionization coupled to a HPLC ALLIANCE WATERS system with a diode array detector (DAD) using a reverse-phase  $\text{C}_{18}$  Nucleosil column (100 mm x 2.1 mm, 5  $\mu\text{m}$  pore size) with an  $\text{H}_2\text{O}$ /acetonitrile gradient and a flow rate of 0.2  $\text{mL}/\text{min}$ .

**Thin layer chromatography (TLC)** was carried out on silica gel KIESELGEL plates 60 F<sub>254</sub> on alumina (MERCK), visualised by UV fluorescence at 254 nm and revealed with

- Ninhydrin (0.3 % in n-butanol/AcOH) for amine intermediates
- Phosphomolybdic acid for cyclic or acetylated peptoids

**Flash chromatography (FC)** was performed with Merck silica gel 60, 40-63  $\mu\text{m}$  and low pressure of air (300 mbar).

**Analytical high-pressure liquid chromatography (HPLC)** was carried out on a DIONEX (TCC-IOO, 25°C; P580 pumps) coupled to a UVD340U detector equipped with an ACCLAM 120 column (C18, 5  $\mu$ m, 120 Å, 4.6 x 250 mm).

**Preparative HPLC** purifications were carried out on a VARIAN apparatus (Prestar 218 pumps), coupled to a diode array detector VARIAN ProStar 355RI. Analytical: C18, 8  $\mu$ m, 250 x 4.6 mm; preparative: C18, 8  $\mu$ m, 60 Å, 250 x 41.4 mm; scale-up factor: 81.

### Chemicals and solvents

Chemicals obtained from commercial sources were used without further purification unless stated otherwise. All solvents designated as "dry" as well as some liquid reagents were purified as follows:

- CH<sub>3</sub>CN (from HPLC grade bottle) and DMF amine free grade for peptide synthesis were dried and stored over activated molecular sieves 4 Å under argon atmosphere.
- CH<sub>2</sub>Cl<sub>2</sub> and MeOH were distilled from CaH<sub>2</sub> under N<sub>2</sub> atmosphere and stored over activated molecular sieves 4 Å under argon atmosphere.
- THF was distilled from potassium/benzophenone under N<sub>2</sub> atmosphere and stored over activated molecular sieves 4 Å under argon atmosphere.
- Et<sub>2</sub>O was dried and stored over sodium wires.
- Et<sub>3</sub>N was distilled from KOH and stored over molecular sieves 3 Å.

## 2 Solution Phase General procedures

**General procedure A**  $\alpha$ -peptoid residues synthesis: Substitution step.

To a solution of alkyl bromoacetate or crude bromoacetyl amide (1.0 equiv, 0.2 M) in EtOAc or THF at 0°C under Ar, was added Et<sub>3</sub>N (2.0 equiv) followed by the chosen primary amine (4.0 equiv). After stirring overnight at rt, the resulting mixture was diluted with EtOAc (10 mL per mmol starting material) and filtered, washing the solids with EtOAc. The filtrate was then concentrated under reduced pressure. EtOAc was added to the residue, remaining salts were eliminated by filtration and the filtrate was concentrated under reduced pressure. The residue was dried in vacuo, yielding the desired crude secondary amine.

**General procedure B**  $\alpha$ -peptoid residues synthesis: Acylation step using bromoacetic anhydride.

To a solution of the crude secondary amine (1.0 equiv, 0.2 M) in EtOAc or THF at 0°C under Ar, was added Et<sub>3</sub>N (1.2 equiv) and then a solution of freshly made bromoacetic anhydride (1.2 equiv) in EtOAc. After stirring for 2 h at rt the resulting mixture was filtered washing the solids with

EtOAc. The filtrate was then concentrated and dried *in vacuo*, flash chromatography yielding the bromoacetyl amide.

Bromoacetic anhydride preparation:<sup>126</sup> DCC (1.2 equiv.) was added to a solution of bromoacetic acid (2.4 equiv.) in CH<sub>2</sub>Cl<sub>2</sub> (0.5 mL per mmol of bromoacetic acid). After stirring for 30 min at room temperature, the solution was filtered to remove the dicyclohexylurea solid. Evaporation of the filtrate gave bromoacetic anhydride as a colourless oily residue which was directly used in the acylation protocol.

**General procedure C** Acetylation of *N*-terminal peptoid using acetic anhydride.

To a solution of a peptoid (1 equiv) and Et<sub>3</sub>N (2 equiv) in EtOAc (0.2 M) at 0°C under Ar, was added Ac<sub>2</sub>O (4 equiv). After stirring overnight at rt, the mixture was filtered washing the solids with EtOAc. The filtrate was then concentrated and dried *in vacuo*, yielding the crude *N*-acylated compound.

**General procedure D** Acetylation of *N*-terminal peptoid using acetyl chloride.

To a solution of a peptoid (1 equiv) and Et<sub>3</sub>N (1.4 equiv) in THF or EtOAc (0.2 M) at 0°C under Ar, was added AcCl (1.2 equiv). After stirring for 1 hour at 0°C, the mixture was filtered washing the solids with EtOAc. The filtrate was then concentrated and dried *in vacuo*, yielding the crude *N*-acylated compound.

**General procedure E** tert-butyl carbamate removal.

The protected compound (1 equiv) was dissolved in CH<sub>2</sub>Cl<sub>2</sub> (0.05-0.1 M) at 0°C under an argon atmosphere and TFA (equal volume of that of CH<sub>2</sub>Cl<sub>2</sub>) was added. After stirring 30 minutes at 0°C, the mixture is concentrated under reduced pressure. The residue was dissolved and concentrated in Et<sub>2</sub>O or CH<sub>2</sub>Cl<sub>2</sub> (three times) to afford evaporation of TFA and furnish the trifluoroacetate salt.

**General procedure F** Solution-phase copper-catalysed alkyne-azide cycloaddition (CuAAC).

To a solution of a peptoid (1 equiv) in tert-BuOH (0.1 M) at rt under Ar were added freshly prepared 0.1 M aq. ascorbic acid (0.24 equiv), 0.1 M aq. CuSO<sub>4</sub> (0.08 equiv) and the chosen azide (2 equiv per alkyne group). After stirring for 4 h at rt, water (16 mL) was added and the product was extracted with CH<sub>2</sub>Cl<sub>2</sub> (5x 10 mL). The combined organic layer was washed twice with a basic aqueous solution of EDTA (0.1 M, pH = 9), then dried over MgSO<sub>4</sub>, filtered, and concentrated under reduced pressure yielding the crude triazole product.

**General procedure G** Methylation of triazole using methyl iodide.

To a solution of a peptoid (1 equiv) in anhydrous MeCN (0.1 M) was added MeI (15 equiv). The resulting mixture was stirred at 70°C for 24 h then evaporated under reduced pressure yielding the crude triazolium product.

### 3 Solid Phase General Procedures

**General Procedure H:** Solid phase submonomer synthesis with conventional heating.

Oligomer synthesis was performed on a bench top Advanced ChemTech Europe incubator. Rink amide resin (100-200 mesh; 0.74 mmol/g; Novabiochem S5135901 151 lot) or Rink amide MBHA resin (100-200 mesh; 0.78 mmol/g; Novabiochem S6789403 504 lot) were swelled for 2×10 min in DMF. First, the 9-fluorenylmethoxycarbonyl (Fmoc) protecting group was removed by treatment with 20% piperidine solution in DMF (2×15 min). The resin was then washed with DMF (5×2 ml). Acylation reactions were performed by addition of bromoacetic acid (6 equiv., 0.4 M) in DMF and diisopropylcarbodiimide (8 equiv., 2 M) in DMF (5 min at 40°C). Next, the resin was rinsed with DMF (5×2 ml). Substitution reaction was performed by addition of the primary amine (25 equiv., 2 M) in DMF to react with the resin bound bromoacetyl moiety, displacing bromide for 1 hr at 40°C. The resin was then rinsed again with DMF (5×2 ml). Peptoids were elongated by this iterative acylation/substitution method until the desired chain length was attained.

**General Procedure H':** Optimized solid phase submonomer synthesis with conventional heating.

General procedure H with the following modification: The first acylation and substitution reactions were repeated twice.

**General Procedure I:** Microwave-assisted solid phase submonomer synthesis.

Oligomer synthesis was performed on a microwave CEM Discover Bio Manual Peptide Synthesiser. The Rink amide MBHA resin (100-200 mesh) Novabiochem (S6789403 504 lot), with 0.078 mmol/g loading was swelled for 2×10 min in DMF with nitrogen bubbling. First, the 9-fluorenylmethoxycarbonyl (Fmoc) protecting group was removed by treatment with 20% piperidine solution in DMF (3 min at 75°C ± 5°C and 20W power). The resin was then washed with DMF (5×2 ml). Acylation reactions were performed by addition of bromoacetic acid (6 equiv., 0.4 M) in DMF and diisopropylcarbodiimide (8 equiv., 2 M) in DMF (1 min at 75°C ± 5°C and 20W power). Next, the resin was rinsed with DMF (5×2 ml). Substitution reaction was performed by addition of the primary amine (25 equiv., 2 M) in DMF reacted with the resin bound bromoacetyl moiety, displacing bromide (5 min at 75°C ± 5°C and 25W power). The resin was then rinsed again with DMF (5×2 ml). Peptoids were elongated by this iterative acylation/substitution method until the desired chain length was attained.

**General Procedure I':** Optimized microwave-assisted Solid phase submonomer synthesis.

General procedure I with the following modification: The first acylation and substitution reactions were repeated twice.

**General Procedure J:** Boc protection of terminal amine on resin.



To the resin swelled in DMF (2 ml), Boc<sub>2</sub>O (6 equiv.) and DIPEA (12 equiv.) were added. After shaking it for 50 minutes at 40°C on benchtop shaker, the resin was washed with DMF (5×2ml).

**General Procedure K:** Capping of the terminal amine on resin using acetic anhydride.

To the resin swelled in DMF (2 ml), acetic anhydride (20 equiv.) and Et<sub>3</sub>N (20 equiv.) were added. After shaking it for 90 minutes on benchtop shaker, the resin was washed with DMF (5×2ml).

**General Procedure L:** Solid-phase copper-catalysed azide-alkyne cycloaddition (CuAAC).

To the resin swelled in DMF/Pyridine (7:3), azide (4 equiv. per alkyne group), ascorbic acid (6 equiv.), CuI (12 equiv.) and DIPEA (15 equiv.) were added. After shaking it overnight on benchtop shaker at rt, the resin was washed seven times with a scavenger solution (3 ml of 0.02 g/ml solution of ascorbic acid in DMF/pyridine 6:5), followed by washing with DMF (3×2 ml).

**General Procedure M:** Methylation of triazole using methyl iodide on the resin.

To the resin rinsed with CH<sub>2</sub>Cl<sub>2</sub> (4×2 ml), pure MeI (2 ml) was added. After shaking it for 2 hours at 45°C, the solution was drained, and the process was repeated 2 to 4 times to complete the methylation. Finally, the solution was drained, and the resin was washed with CH<sub>2</sub>Cl<sub>2</sub> (6×2 ml) to yield the crude triazolium product.

**or**

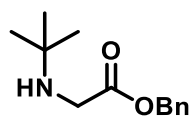
To the resin rinsed with CH<sub>2</sub>Cl<sub>2</sub> (4×2 ml), pure MeI (2 ml) was added. After shaking it for 6 hours at 50°C, the solution was drained washed with CH<sub>2</sub>Cl<sub>2</sub> (6×2 ml) to yield the crude triazolium product.

**General Procedure N:** Cleavage of oligomer from resin and tert-butyl carbamate removal.

Peptoid oligomers were cleaved from the resin, by treatment with 2×2.5 ml of TFA/triisopropylsilane/water (95:2.5:2.5 by volume) for 30 min. The cleavage mixture was then diluted with acetonitrile (4×2 ml) and evaporated under reduced pressure to get rid of TFA. The resulting concentrate was diluted with 50% aqueous acetonitrile (1.5 ml), frozen and lyophilized.

## 4 Experimental procedures and compounds characterisations Chapter II

### Benzyl *N*-*tert*-butylglycinate **1**



C<sub>13</sub>H<sub>19</sub>NO<sub>2</sub>  
MW: 221.30

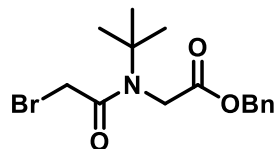
Compound **1** was synthesised starting from benzyl bromoacetate (4.57 g, 20.0 mmol) by application of the **General Procedure A** using *tert*-butyl amine as primary amine. The compound **1** was obtained as a yellow liquid (3.76 g, 17.0 mmol, 85%).

TLC R<sub>f</sub> = 0.33 (Cyclohexane/EtOAc, 8:2)

<sup>1</sup>H NMR (400 MHz, CDCl<sub>3</sub>) δ (ppm): 1.09 (s, 9H, *t*Bu), 1.85 (bs, 1H, NH), 3.44 (s, 2H, NCH<sub>2</sub>), 5.16 (s, 2H, PhCH<sub>2</sub>), 7.33-7.36 (m, 5H, Ph).

Spectroscopic data are consistent with the previous characterisation carried out in the group.<sup>180</sup>

### Benzyl *N*-(2-bromoacetyl)-*N*-(*tert*-butyl) glycinate **2**



C<sub>15</sub>H<sub>20</sub>BrNO<sub>3</sub>  
MW: 342.23

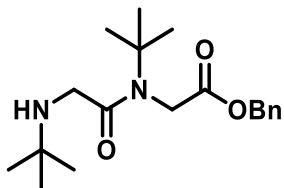
Compound **2** was synthesised by starting from compound **1** (3.76 g, 17.0 mmol) by application of the **General Procedure B**. The compound **2** was obtained after filtration on silica gel (eluent cyclohexane/AcOEt 8:2) as a yellow viscous liquid (3.68 g, 10.7 mmol, 63%).

TLC R<sub>f</sub> = 0.58 (Cyclohexane/EtOAc, 1:1)

<sup>1</sup>H NMR (400 MHz, CDCl<sub>3</sub>) δ (ppm): 1.37 (s, 9H, *t*Bu), 3.72 (s, 2H, NCH<sub>2</sub>CO), 4.21 (s, 2H, BrCH<sub>2</sub>CO), 5.21 (s, 2H, CH<sub>2</sub>Ph), 7.36-7.38 (m, 5H, Ph).

Spectroscopic data are consistent with the previous characterisation carried out in the group.<sup>180</sup>

### Benzyl *N*-(*tert*-butyl)-*N*-(*N*-*tert*-butyl glycy) glycinate **3**



C<sub>19</sub>H<sub>30</sub>N<sub>2</sub>O<sub>3</sub>  
MW: 334.46

Compound **3** was synthesised starting from compound **2** (3.68 g, 10.7 mmol) by application of the **General Procedure A** using *tert*-butyl amine as primary amine. The compound **3** was obtained as a yellow liquid (3.40 g) and was used directly for the next step.

TLC R<sub>f</sub> = 0.43 (Cyclohexane/EtOAc, 8:2)

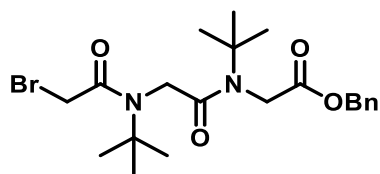
<sup>1</sup>H NMR (400 MHz, CDCl<sub>3</sub>) δ (ppm): 1.07-1.10 (m, 9H, *t*Bu), 1.35-1.44 (m, 9H, *t*Bu), 2.20 (bs, 1H, NH), 3.30 (s, 2H, CH<sub>2</sub>N), 4.14 (s, 2H, ), 5.20 (s, 2H, CH<sub>2</sub>Ph), 7.35-7.37 (m, 5H, Ph).

---

<sup>180</sup> Yannick Esvan, 'Préparation de Peptoides Présentant Des Amides Cis : Vers Des Hélices Polyprolines de Type I (PPI)' (Rapport de stage Master 1, Université Blaise Pascal, 2012).

Spectroscopic data are consistent with the previous characterisation carried out in the group.<sup>180</sup>

#### Benzyl *N*-(*N*-(2-bromoacetyl)-*N*-(*tert*-butyl)glycyl)-*N*-(*tert*-butyl) glycinate **4**



$C_{21}H_{31}BrN_2O_4$   
MW: 455.39

Compound **4** was synthesised by starting from compound **3** (crude, 10.7 mmol, 1.0 equiv.) by application of the **General Procedure B**. The compound **4** was obtained after filtration on silica

gel (eluent cyclohexane/AcOEt 8:2) as a yellow viscous liquid (3.72 g, 8.17 mmol, 76%).

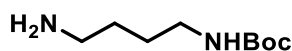
**TLC**  $R_f$  = 0.28 (Cyclohexane/EtOAc, 8:2)

**<sup>1</sup>H NMR** (400 MHz,  $CDCl_3$ )  $\delta$  (ppm) : 1.38 (s, 9H, *t*Bu), 1.40 (s, 9H, *t*Bu), 1.68 (bs, 1H, *NH*), 3.61 (s, 2H,  $NCH_2O$ ), 4.07 (s, 2H,  $NCH_2O$ ), 4.09 (s, 2H,  $CH_2Br$ ), 5.23 (s, 2H,  $CH_2Ph$ ), 7.38 (m, 5H, Ph).

**<sup>13</sup>C NMR** (100 MHz,  $CDCl_3$ )  $\delta$  (ppm): 26.0 (6  $CH_3$ , *Nt*Bu), 27.6 ( $CH_2$ ,  $CH_2Br$ ), 42.0 (2 $CH_2$ , 2 $\times NCH_2CO$ ), 59.1 (2C, *t*Bu), 69.0 ( $CH_2$ ,  $OCH_2Ph$ ), 128.8, 129.1 (5CH, Ph), 140.1 (1C, Ph), 166.7 (1C,  $NC=O$ ), 169.3 (1C,  $NC=O$ ), 170.3 (1C,  $NC=O$ ).

Spectroscopic data are consistent with the previous characterisation carried out in the group.<sup>180</sup>

#### *N*-Boc-1,4-diaminobutane **5**



$C_9H_{20}N_2O_2$   
MW: 188.27

To a solution of 1,4-diaminobutane (5.26 g, 59.7 mmol, 5 equiv.) in  $CHCl_3$  (60 mL) at 0°C was added dropwise a solution of  $Boc_2O$  (2.61 g, 11.9 mmol, 1.0 equiv) in  $CHCl_3$  (15 mL) over 120 minutes at 0°C. The resulting mixture was stirred at room temperature overnight then filtered. The filtrate was concentrated under reduced pressure. The residue was dissolved in EtOAc (100 mL) and washed with brine (2x15 mL). The combined aqueous layers were back-extracted with EtOAc (20 mL). The combined organic layers were dried over  $Na_2SO_4$ , filtered, concentrated, and dried in vacuo yielding **5** (2.10 g, 11.1 mmol, 87%\*) as a colourless oil.

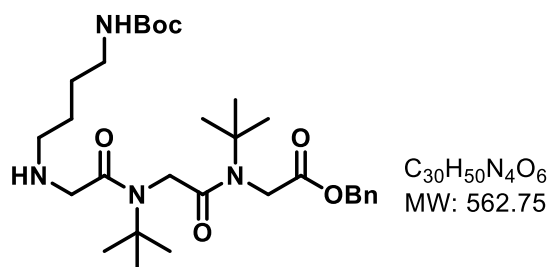
**TLC**  $R_f$  = 0.33 ( $CH_2Cl_2/MeOH$ , 8:2)

**<sup>1</sup>H NMR** (400 MHz,  $CDCl_3$ )  $\delta$  (ppm): 1.43 (s, 9H, *t*Bu), 1.43-1.46 (m, 4H,  $CH_2CH_2$ ), 1.82 (ls, 2H,  $NH_2$ ), 2.67 (t, 2H,  $J = 6.6$  Hz,  $CH_2NH_2$ ), 3.06-3.07 (m, 2H,  $CH_2NHBoc$ ), 4.70 (bs, 1H, *NH*).

\*This yield considers the proportion of mono- and di-protected compounds determined by proton NMR (ratio: 9/1).

Spectroscopic data are consistent with those reported in the literature.<sup>127</sup>

### H-(NLys(Boc)-Ntbu-Ntbu)OBn 6



Compound **6** was synthesised starting from compound **4** (2.74 g, 6.03 mmol, 1.0 equiv.) by application of the **General Procedure A** using compound **5** (4.54 g, 24.1 mmol, 4.0 equiv) as a primary amine. Purification by flash chromatography on silica gel (eluent:  $CH_2Cl_2/MeOH$  9:1) gave the

compound **6** as a yellow liquid (2.22 g, 3.95 mmol, 66%).

**TLC**  $R_f$  = 0.44 (EtOAc /MeOH, 9:1)

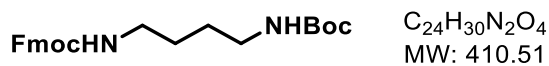
**IR** (ATR)  $\bar{\nu}$  ( $cm^{-1}$ ): 3015, 2978, 1744, 1690, 1667, 1651, 1633, 1500, 1455, 1435, 1392, 1365, 1320, 1249, 1242, 1184, 1173, 1144, 1000, 836, 750, 740.

**$^1H$  NMR** (400 MHz,  $CDCl_3$ )  $\delta$  (ppm): 1.32 (s, 9H, *t*Bu), 1.37 (s, 9H, *t*Bu), 1.39 (s, 9H, *t*Bu), 1.49-1.55 (m, 2H, BocNHCH<sub>2</sub>CH<sub>2</sub>CH<sub>2</sub>), 1.57-1.67 (m, 2H, BocNHCH<sub>2</sub>CH<sub>2</sub>CH<sub>2</sub>), 2.79 (t,  $J$  = 7.4 Hz, 2H, NHCH<sub>2</sub>), 3.09-3.10 (m, 2H, BocNHCH<sub>2</sub>), 3.42 (bs, 2H, COCH<sub>2</sub>NH), 4.03 (s, 2H, COCH<sub>2</sub>N), 4.13 (s, 2H, COCH<sub>2</sub>N), 5.06 (bs, 1H, BocNH), 5.13 (bs, 1H, NH), 5.19 (s, 2H, PhCH<sub>2</sub>), 7.28-7.37 (m, 5H, Ph).

**$^{13}C$  NMR** (100 MHz,  $CDCl_3$ )  $\delta$  (ppm): 25.1 (CH<sub>2</sub>, NHCH<sub>2</sub>CH<sub>2</sub>CH<sub>2</sub>), 27.2 (CH<sub>2</sub>, NHCH<sub>2</sub>CH<sub>2</sub>CH<sub>2</sub>), 28.2 (3CH<sub>3</sub>, *O**t*Bu), 28.5 (6 CH<sub>3</sub>, *Nt*Bu), 40.0 (CH<sub>2</sub>, BocNHCH<sub>2</sub>CH<sub>2</sub>), 46.4 (CH<sub>2</sub>, NCH<sub>2</sub>CO), 48.3 (CH<sub>2</sub>, CH<sub>2</sub>COOBn), 48.6 (CH<sub>2</sub>, NHCH<sub>2</sub>CH<sub>2</sub>), 50.6 (CH<sub>2</sub>, NHCH<sub>2</sub>CO), 58.6 (2C, *t*Bu), 67.7 (CH<sub>2</sub>, OCH<sub>2</sub>Ph), 78.9 (1C, *t*Bu, Boc), 128.7, 128.8, 128.8 (5CH, Ph), 135.0 (1C, Ph), 156.1 (1C, OC=O), 168.9 (1C, NC=O), 169.1 (1C, NC=O), 170.3 (1C, Boc).

**HRMS** (TOF MS ES<sup>+</sup>):  $m/z$  calculated for  $C_{30}H_{51}N_4O_6$   $[M+H]^+$ : 563.3809; found: 563.3806 (-0.5 ppm)

### 1-N-Boc-4-N-Fmoc-1,4-diaminobutane 7



The protected compound 1-*N*-Boc-1,4-diaminobutane **5** (1.00 g, 5.31 mmol, 1 equiv) was dissolved in a mixture of equal volume (20 ml each)  $CH_2Cl_2/NaHCO_3$  (aq.) at room temperature and FmocCl (1.44 g, 5.58 mmol, 1.05 equiv) was added. After stirring overnight at room temperature, the aqueous layer from the mixture was removed by separating funnel. The organic layer was washed thrice with water, then dried over  $MgSO_4$ , filtered, and concentrated under reduced pressure yielding **7** as a white solid (1.84 g, 4.48 mmol, 84%).

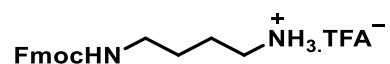
**TLC**  $R_f$  = 0.43 (Cyclohexane/EtOAc, 6:4)

**$^1H$  NMR** (400 MHz,  $CDCl_3$ )  $\delta$  (ppm): 1.47 (s, 9H, *t*Bu), 1.49-1.60 (bs, 4H, CH<sub>2</sub>CH<sub>2</sub>), 2.97-3.44 (m, 4H, 2×CH<sub>2</sub>NH<sub>2</sub>), 4.24 (t,  $J$  = 6.9 Hz, 1H, CH, Fmoc), 4.43 (d,  $J$  = 7.0 Hz, 2H, CH<sub>2</sub>OC=O;

Fmoc), 4.88 (bs, 1H, *NHBoc*) 5.32 (s, 1H, *NHFmoc*), 7.34 (td,  $J = 7.4, 1.2$  Hz, 2H, Ph), 7.43 (tt,  $J = 7.5, 0.9$  Hz, 2H, Ph), 7.62 (d,  $J = 7.5$  Hz, 2H, Ph), 7.79 (d,  $J = 7.5$  Hz, 2H, Ph).

Spectroscopic data are consistent with those reported in the literature.<sup>127</sup>

### (9H-fluoren-9-yl)methyl (4-aminobutyl)carbamate.TFA **8**

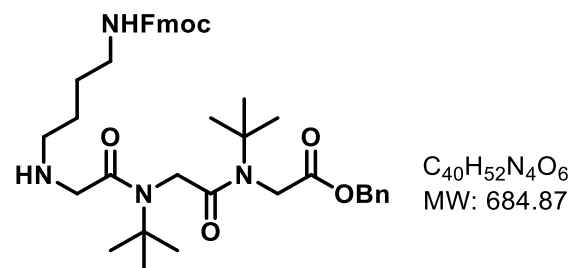
  $\text{C}_{21}\text{H}_{23}\text{F}_3\text{N}_2\text{O}_3^+$  Compound **8** was synthesised starting from compound **7** (0.80 g, 1.95 mmol) by application of the **General Procedure E** and it was let to stir for 2 hours. The compound **8** was obtained as white solid (0.33 g, 0.76 mmol, 40%).  
MW: 408.42

**TLC**  $R_f = 0.11$  (Cyclohexane/EtOAc, 8:2)

**<sup>1</sup>H NMR** (400 MHz, MeOD)  $\delta$ (ppm): 1.52 – 1.62 (m, 2H,  $\text{CH}_2\text{CH}_2$ ), 1.63-1.67 (m, 2H,  $\text{CH}_2\text{CH}_2$ ), 2.93 (t,  $J = 7.4$  Hz, 2H,  $\text{CH}_2\text{NH}_2$ ), 3.15 (t,  $J = 6.6$  Hz, 2H,  $\text{CH}_2\text{NH}_2$ ), 4.20 (t,  $J = 6.7$  Hz, 1H, *CH*, Fmoc), 4.37 (d,  $J = 6.8$  Hz, 2H,  $\text{CH}_2\text{OC}=\text{O}$ , Fmoc), 5.49 (s, 1H, *NHFmoc*), 7.26 – 7.44 (m, 4H, *CHAr*), 7.64 (d,  $J = 7.3$  Hz, 2H, *CHAr*), 7.80 (d,  $J = 7.5$  Hz, 2H, *CHAr*).

Spectroscopic data are consistent with those reported in the literature.<sup>127</sup>

### H-(NLys(Fmoc)-NtBu-NtBu)-OBn **9**



To a solution of compound **8** (373 mg, 0.88 mmol, 4 equiv) in THF at 0°C under Ar was added DIPEA (2.0 equiv). After stirring for 30 min at rt, the mixture was filtered to remove the precipitate. Compound **4** (100 mg, 0.22 mmol, 1 equiv) was added to the filtrate at 0°C followed by DIPEA (2.0

equiv). After stirring overnight at rt, the resulting mixture was diluted with EtOAc (10 mL per mmol starting material) and filtered, washing the solids with EtOAc. The filtrate was then concentrated under reduced pressure. Purification by flash chromatography on silica gel (eluent:  $\text{CH}_2\text{Cl}_2/\text{MeOH}$  95:5 then 93:7) gave the residue, which was dried in vacuo, yielding the desired Compound **9** as a yellow viscous liquid (68 mg, 0.10 mmol, 45 %).

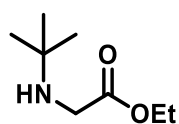
**TLC**  $R_f = 0.22$  ( $\text{CH}_2\text{Cl}_2/\text{MeOH}$ , 95:5)

**<sup>1</sup>H NMR** (400 MHz,  $\text{CDCl}_3$ )  $\delta$ (ppm): 1.36 (s, 9H, *tBu*), 1.37 (s, 9H, *tBu*), 1.49 – 1.64 (m, 2H,  $\text{FmocNHCH}_2\text{CH}_2\text{CH}_2$ ), 1.63 – 1.87 (m, 2H,  $\text{FmocNHCH}_2\text{CH}_2\text{CH}_2$ ), 2.76-2.80 (bt, 2H,  $\text{NHCH}_2$ ), 3.18-3.21 (bt, 2H,  $\text{FmocNHCH}_2\text{CH}_2\text{CH}_2$ ), 3.43 (bs, 2H,  $\text{NHCH}_2\text{CO}$ ), 3.98 (s, 2H,  $\text{NCH}_2\text{CO}$ ), 4.08 (s, 2H,  $\text{NCH}_2\text{COOBn}$ ), 4.19 (t,  $J = 7.1$  Hz, 1H, *CH*, Fmoc), 4.34 (d,  $J = 7.1$  Hz, 2H,  $\text{CH}_2\text{OC}=\text{O}$ , Fmoc), 4.76 (bs, 1H,  $\text{CH}_2\text{NHCH}_2$ ), 5.18 (s, 2H,  $\text{PhCH}_2$ ), 5.45 (bs, 1H,  $\text{CH}_2\text{NHCO}$ ), 7.27 – 7.43 (m, 9H, *CHAr*), 7.52-7.63 (m, 2H, *CHAr*), 7.68-7.75 (m, 2H, *CHAr*).

**<sup>13</sup>C NMR** (100 MHz, CDCl<sub>3</sub>)  $\delta$ (ppm): 25.5 (CH<sub>2</sub>, NHCH<sub>2</sub>CH<sub>2</sub>CH<sub>2</sub>), 27.3 (CH<sub>2</sub>, NHCH<sub>2</sub>CH<sub>2</sub>CH<sub>2</sub>), 28.3 (3CH<sub>3</sub>, *Ot*Bu), 28.4 (3CH<sub>3</sub>, *Ot*Bu), 40.6 (CH<sub>2</sub>, FmocNHCH<sub>2</sub>CH<sub>2</sub>), 46.3 (CH<sub>2</sub>, NCH<sub>2</sub>CO), 47.4 (1C, CH, Fmoc), 48.2 (CH<sub>2</sub>, NCH<sub>2</sub>COOBn), 48.8 (CH<sub>2</sub>, NHCH<sub>2</sub>CH<sub>2</sub>), 50.9 (CH<sub>2</sub>, NHCH<sub>2</sub>CO), 58.6 (2C, *t*Bu), 66.7 (CH<sub>2</sub>, CH<sub>2</sub>OC=O, Fmoc), 67.8 (CH<sub>2</sub>, OCH<sub>2</sub>Ph), 119.9, 120.0 (3CH, Ph), 125.3 (2CH, Ph), 127.2, 127.7 (3CH, Ph), 128.8, 128.9, 128.9 (5CH, Ph), 135.0 (1C, Ph), 141.4 (2C, Fmoc), 144.2 (2C, Fmoc), 156.7 (1C, OC=O), 169.1 (1C, NC=O), 169.5 (1C, NC=O), 170.3 (1C, BnOC=O).

**HRMS** (TOF MS ES<sup>+</sup>): *m/z* calculated for C<sub>40</sub>H<sub>53</sub>N<sub>4</sub>O<sub>6</sub> [M+H]<sup>+</sup>: 685.3959; found: 685.3961 (0.14 ppm)

### Ethyl *N*-*tert*-butylglycinate **10**



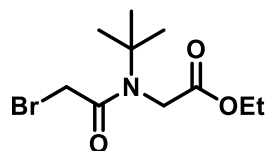
C<sub>8</sub>H<sub>17</sub>NO<sub>2</sub>  
MW: 159.22

Compound **10** was synthesised starting from ethyl bromoacetate (3.34 g, 20,0 mmol) by application of the **General Procedure A** using *tert*-butyl amine as primary amine. The compound **10** was obtained as a yellow liquid (2.73 g, 17.1 mmol, 86%).

**TLC** R<sub>f</sub> = 0.44 (Cyclohexane/EtOAc, 1:1)

**<sup>1</sup>H NMR** (400 MHz, CDCl<sub>3</sub>)  $\delta$ (ppm): 1.10 (s, 9H, *t*Bu), 1.27 (t, *J* = 7.1 Hz, 3H, CH<sub>2</sub>CH<sub>3</sub>), 1.95 (bs, NH), 3.39 (s, 2H, NHCH<sub>2</sub>CO), 4.18 (q, *J* = 7.2 Hz, 2H, CH<sub>2</sub>CH<sub>3</sub>).

### Ethyl *N*-(2-bromoacetyl)-*N*-(*tert*-butyl)glycinate **11**



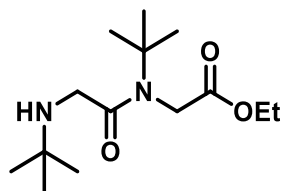
C<sub>10</sub>H<sub>18</sub>BrNO<sub>3</sub>  
MW: 280.16

Compound **11** was synthesised by starting from compound **10** (2.73 g, 17.1 mmol) by application of the **General Procedure B**. After filtration on silica gel (eluent: cyclohexane/AcOEt 8:2), the compound **11** was obtained as a yellow viscous liquid (4.80 g) and was used directly for the next step.

**TLC** R<sub>f</sub> = 0.49 (Cyclohexane/EtOAc, 8:2)

**<sup>1</sup>H NMR** (400 MHz, CDCl<sub>3</sub>)  $\delta$ (ppm):  $\delta$  1.31 (t, *J* = 7.2 Hz, 3H, CH<sub>2</sub>CH<sub>3</sub>), 1.43 (s, 9H, *t*Bu), 3.76 (s, 2H, CH<sub>2</sub>*Nt*Bu), 4.17 (s, 2H, CH<sub>2</sub>Br), 4.24 (q, *J* = 7.1 Hz, 2H, CH<sub>2</sub>CH<sub>3</sub>).

### Ethyl *N*-(*tert*-butylglycyl)-*N*-(*tert*-butyl)glycinate **12**



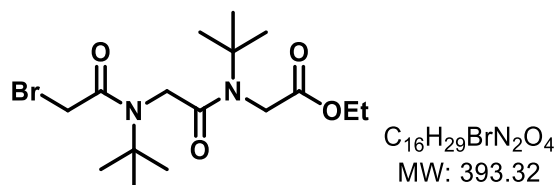
C<sub>14</sub>H<sub>28</sub>N<sub>2</sub>O<sub>3</sub>  
MW: 272.38

Compound **12** was synthesised starting from compound **11** (crude, 17.1 mmol) by application of the **General Procedure A** using *tert*-butyl amine as primary amine. The compound **12** was obtained as a yellow liquid (4.66 g) and was used directly for the next step.

**TLC** R<sub>f</sub> = 0.13 (Cyclohexane/EtOAc, 8:2)

**<sup>1</sup>H NMR** (400 MHz, CDCl<sub>3</sub>)  $\delta$ (ppm): 1.17 (s, 9H, <sup>t</sup>Bu), 1.31 (t,  $J = 7.1$  Hz, 3H, CH<sub>2</sub>CH<sub>3</sub>), 1.43 (s, 9H, <sup>t</sup>Bu), 2.04 (s, 1H, NH), 3.40 (s, 2H, CH<sub>2</sub>N<sup>t</sup>Bu), 4.09 (s, 2H, CH<sub>2</sub>NH<sup>t</sup>Bu), 4.24 (q,  $J = 7.2$  Hz, 2H, CH<sub>2</sub>CH<sub>3</sub>).

### Ethyl *N*-[*N*-(2-bromoacetyl)-*N*-(*tert*-butyl)glycyl]-*N*-(*tert*-butyl)glycinate **13**



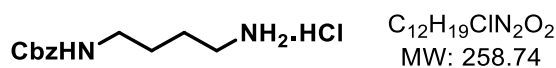
Compound **13** was synthesised by starting from compound **12** (crude, 17.1 mmol, 1.0 equiv.) by application of the **General Procedure B**. Purification by flash chromatography on silica gel (eluent cyclohexane/AcOEt 8:2) gave the compound

**13** as yellow viscous liquid (3.27 g, 8.31 mmol, 49% for three steps).

**TLC** R<sub>f</sub> = 0.28 (Cyclohexane/EtOAc, 6:4)

**<sup>1</sup>H NMR** (400 MHz, CDCl<sub>3</sub>)  $\delta$ (ppm): 1.33 (t,  $J = 7.1$  Hz, 3H, OCH<sub>2</sub>CH<sub>3</sub>), 1.42 (s, 9H, <sup>t</sup>Bu), 1.43 (s, 9H, <sup>t</sup>Bu), 3.68 (s, 2H, CH<sub>2</sub>Br), 4.05 (s, 2H, CH<sub>2</sub>N<sup>t</sup>Bu), 4.11 (s, 2H, CH<sub>2</sub>N<sup>t</sup>Bu), 4.27 (q,  $J = 7.2$  Hz, 2H, OCH<sub>2</sub>CH<sub>3</sub>).

### Benzyl (4-aminobutyl) carbamate.HCl **14**



To a solution of 1,4-diaminobutane (1.75 g, 19.9 mmol, 5 equiv.) in CH<sub>2</sub>Cl<sub>2</sub> (50 mL) at 0°C was added dropwise a solution of benzyl chloroformate (0.68 g, 4.00 mmol, 1.0 equiv) in CH<sub>2</sub>Cl<sub>2</sub> (15 ml) over 120 minutes at 0°C. The resulting mixture was stirred at room temperature overnight then filtered. The filtrate was concentrated under reduced pressure. The residue was dissolved in EtOAc (90 mL) and washed with brine (3x15 ml). The combined organic layers were dried over Na<sub>2</sub>SO<sub>4</sub>, filtered, concentrated, and dried in vacuo yielding **14** (788 mg, 3.05 mmol, 76 %) as a white powder.

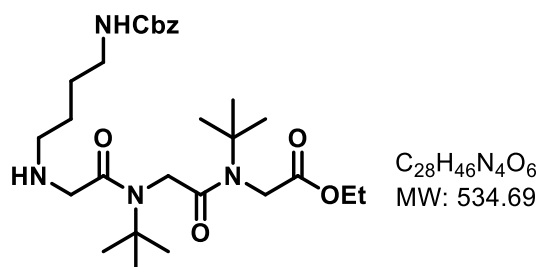
**TLC** R<sub>f</sub> = 0.15 (DCM/MeOH, 9:1)

**<sup>1</sup>H NMR** (400 MHz, MeOD)  $\delta$ (ppm) 1.51-1.58 (m, 4H, CH<sub>2</sub>CH<sub>2</sub>), 2.72 (bt, 2H, CH<sub>2</sub>NH<sub>2</sub>), 3.05 – 3.19 (m, 2H, CH<sub>2</sub>NHCbz), 5.06 (s, 2H, CH<sub>2</sub>Ph), 7.22 – 7.45 (m, 5H, CHAr).

Spectroscopic data are consistent with those reported in the literature.<sup>181</sup>

<sup>181</sup> G. J. Atwell and W. A. Denny, 'Monoprotection of  $\omega$ -Alkanediamines with the *N*-Benzyloxycarbonyl Group', *Synthesis* (1984), 1032–3.

### H-(NLys(Cbz)-NtBu-NtBu)-OEt **15**



To a solution of compound **14** (900 mg, 4.06 mmol, 4 equiv) in EtOAc at 0°C under Ar was added DIPEA (4.0 equiv). After stirring for 10 min at rt, the compound **13** (0.40 g, 1.02 mmol, 1 equiv) was added to it at 0°C followed by DIPEA (0.26 g, 2.03 mmol, 2.0 equiv). After stirring overnight at rt, the resulting

mixture was diluted with EtOAc (10 mL per mmol starting material) and filtered, washing the solids with EtOAc. The filtrate was then concentrated under reduced pressure. Purification by flash chromatography on silica gel (eluent: CH<sub>2</sub>Cl<sub>2</sub>/MeOH 95:5 then 93:7) yielded the desired compound **15** as a yellow viscous liquid (343 mg, 0.64 mmol, 63%).

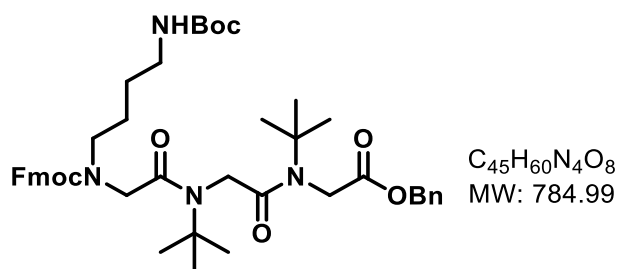
TLC  $R_f$  = 0.52 (Cyclohexane/EtOAc, 1:1)

<sup>1</sup>H NMR (400 MHz, MeOD)  $\delta$  (ppm): 1.30 (t,  $J$  = 7.0 Hz, 3H, OCH<sub>2</sub>CH<sub>3</sub>), 1.42 (s, 9H, *t*Bu), 1.43 (s, 9H, *t*Bu), 1.49 – 1.66 (m, 2H, CbzNHCH<sub>2</sub>CH<sub>2</sub>CH<sub>2</sub>), 1.63 – 1.74 (m, 2H, CbzNHCH<sub>2</sub>CH<sub>2</sub>CH<sub>2</sub>), 2.88 (t,  $J$  = 7.6 Hz, 2H, NHCH<sub>2</sub>), 3.15 (t,  $J$  = 6.8 Hz, 2H, CbzNHCH<sub>2</sub>), 3.60 (bs, 2H, COCH<sub>2</sub>NH), 4.19 (bs, 2H, COCH<sub>2</sub>NtBu), 4.24 (q,  $J$  = 7.0 Hz, 2H, OCH<sub>2</sub>CH<sub>3</sub>), 4.25 (s, 2H, COCH<sub>2</sub>NtBu), 5.06 (s, 2H, PhCH<sub>2</sub>), 7.34 (m, 5H, Ph).

<sup>13</sup>C NMR (100 MHz, MeOD)  $\delta$  (ppm): 14.5 (CH<sub>3</sub>, CH<sub>2</sub>CH<sub>3</sub>), 25.2 (CH<sub>2</sub>, NHCH<sub>2</sub>CH<sub>2</sub>CH<sub>2</sub>), 28.0 (CH<sub>2</sub>, NHCH<sub>2</sub>CH<sub>2</sub>CH<sub>2</sub>), 28.5 (3 CH<sub>3</sub>, *t*Bu), 28.6 (3 CH<sub>3</sub>, *t*Bu), 41.1 (CH<sub>2</sub>, CbzNHCH<sub>2</sub>CH<sub>2</sub>), 47.2 (CH<sub>2</sub>, NCH<sub>2</sub>CO), 48.9 (CH<sub>2</sub>, NCH<sub>2</sub>CO), 49.4 (CH<sub>2</sub>, NHCH<sub>2</sub>CH<sub>2</sub>), 51.1 (CH<sub>2</sub>, NHCH<sub>2</sub>CO), 59.5 (C, *t*Bu), 59.7 (C, *t*Bu), 62.9 (CH<sub>2</sub>, CH<sub>2</sub>CH<sub>3</sub>), 67.3 (CH<sub>2</sub>, CH<sub>2</sub>Ph), 128.7, 128.9, 129.4 (5CH, Ph), 138.3 (1C, Ph), 158.8 (1C, BnOC=O), 169.2 (1C, NC=O), 171.2 (1C, NC=O), 172.3 (1C, EtOC=O).

HRMS (TOF MS ES<sup>+</sup>):  $m/z$  calculated for C<sub>28</sub>H<sub>47</sub>N<sub>4</sub>O<sub>6</sub> [M+H]<sup>+</sup>: 535.3496; found: 535.3500 (0.7 ppm).

### Fmoc-(NLys(Boc)-NtBu-NtBu)-OBn **16**



To a solution of compound **6** (150 mg, 0.26 mmol, 1 equiv) and Et<sub>3</sub>N (54 mg, 0.53 mmol, 2 equiv) in anhydrous THF (2 ml) at 0 °C under Ar was added FmocCl (72 mg, 0.27 mmol, 1.05 equiv). After stirring for 1 h at room temperature, the mixture was filtered. The

filtrate was concentrated under reduced pressure to yield the crude. The crude was subjected to flash chromatography on silica gel (EtOAc 100 %) to yield the trimer **16** (196 mg, 0.25 mmol, 94%).



**TLC**  $R_f = 0.6$  (EA/MeOH, 98:2)

**IR** (ATR)  $\tilde{\nu}$  ( $\text{cm}^{-1}$ ): 2980, 1743, 1700, 1669, 1508, 1479, 1451, 1430, 1392, 1365, 1318, 1247, 1182, 1144, 987, 955, 752, 740.

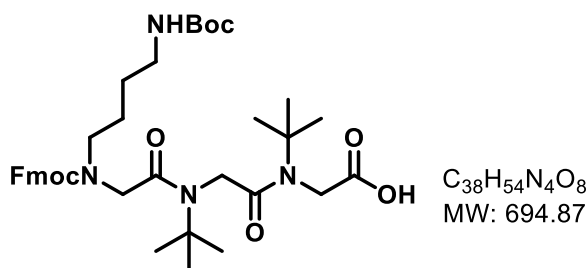
2 conformers are observed by NMR in a 68/32 ratio.

**$^1\text{H}$  NMR** (400 MHz,  $\text{CDCl}_3$ )  $\delta$  (ppm): 1.35 (s, 9H, *t*Bu), 1.39 (m, 9H, *t*Bu), 1.43 (m, 9H, *t*Bu), 1.30-1.65 (m, 4H,  $\text{NHCH}_2\text{CH}_2\text{CH}_2$ ), 3.01-3.40 (m, 4H,  $\text{NHCH}_2\text{CH}_2\text{CH}_2$ ,  $\text{CH}_2\text{CH}_2\text{CH}_2\text{N}$ ), 3.68-3.88 (m, 2H,  $\text{NCH}_2\text{COOBn}$ ), 4.00 (s, 2H,  $\text{NCH}_2\text{CO}$ ), 4.09 (s, 2H,  $\text{FmocNCH}_2\text{CO}$ ), 4.23-4.24 (2 $\times$ t, 1H,  $J = 6.0$  Hz and 5.6 Hz, CH, Fmoc, 2 conformers), 4.40 and 4.50 (2 $\times$ d, 2H,  $J = 6.0$  Hz,  $\text{CH}_2\text{OC}=\text{O}$ , 2 conformers), 4.80-5.00 (m, 1H, NH, 2 conformers), 5.19-5.21 (2s, 2H,  $\text{PhCH}_2$ , 2 conformers), 7.28-7.41 (m, 9H, Ar), 7.57-7.74 (m, 4H, Ar).

**$^{13}\text{C}$  NMR** (100 MHz,  $\text{CDCl}_3$ )  $\delta$  24.3 ( $\text{CH}_2$ ,  $\text{FmocNCH}_2\text{CH}_2\text{CH}_2$ ), 25.4 ( $\text{CH}_2$ ,  $\text{FmocNCH}_2\text{CH}_2\text{CH}_2$ ), 28.4 (3 $\text{CH}_3$ , *Ot*Bu), 28.6 (6  $\text{CH}_3$ , *Nt*Bu), 40.4 ( $\text{CH}_2$ ,  $\text{FmocNCH}_2\text{CH}_2$ ), 46.4 ( $\text{CH}_2$ ,  $\text{BocNHCH}_2\text{CH}_2$ ), 47.5 (1C, CH, Fmoc), 47.7 ( $\text{CH}_2$ ,  $\text{FmocNCH}_2\text{CO}$ ), 50.9 (2 $\times$  $\text{CH}_2$ , 2 $\times$  $\text{NCH}_2\text{CO}$ ), 55.7 (2C, *t*Bu), 67.2 ( $\text{CH}_2$ ,  $\text{CH}_2\text{OC}=\text{O}$ , Fmoc), 67.9 ( $\text{CH}_2$ ,  $\text{PhCH}_2$ ), 79.7 (1C, *t*Bu), 120.1 (2CH, Ph), 125.0 (2CH, Ph), 127.2 (2CH, Ph), 127.8 (2CH, Ph), 128.9, 128.9, 129.0, 129.1, 129.1 (5CH, Ph), 135.8 (1C, Ph), 141.5 (2C, Ph), 144.2 (2C, Ph), 147.6 (1C,  $\text{OC}=\text{O}$ ), 149.3 (1C,  $\text{OC}=\text{O}$ ), 169.7 (1C,  $\text{NC}=\text{O}$ ), 169.8 (1C,  $\text{NC}=\text{O}$ ), 170.2 (1C, Boc).

**HRMS** (TOF MS ES<sup>+</sup>):  $m/z$  calculated for  $\text{C}_{45}\text{H}_{61}\text{N}_4\text{O}_8$   $[\text{M}+\text{H}]^+$ : 785.4514; found: 785.4489 (3.2 ppm).

### Fmoc-(*N*Lys(Boc)-*Nt*bu-*Nt*bu)-OH **17**



To a solution of benzyl ester **16** (80 mg, 0.10 mmol) dissolved in THF/EtOH (5:2) at 30°C was added Pd/BaSO<sub>4</sub> 10% (5 mg) stirring under the atmosphere of hydrogen overnight. 5 mg of Pd/BaSO<sub>4</sub> 10% was added twice after 24h. End of deprotection was confirmed by TLC. The resulting

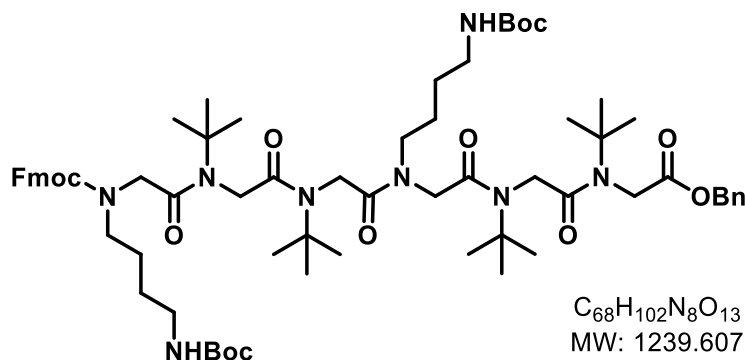
mixture was then filtered using celite pad and then concentrated under reduced pressure to obtain the compound **17** (75 mg, 0.10 mmol, 100%)

**TLC**  $R_f = 0.24$ , Cyclohexane/EtOAc, 1:1)

**$^1\text{H}$  NMR** (400 MHz, MeOD)  $\delta$  1.43 (2 $\times$ s, 18H, *t*Bu), 1.45 (s, 9H, *t*Bu), 1.49 – 1.54 (m, 2H,  $\text{NHCH}_2\text{CH}_2\text{CH}_2$ ), 1.58-1.64 (m, 2H,  $\text{NHCH}_2\text{CH}_2\text{CH}_2$ ), 2.80 (t,  $J = 7.5$  Hz, 2H,  $\text{NHCH}_2\text{CH}_2\text{CH}_2$ ), 3.06 (t,  $J = 6.7$  Hz, 2H,  $\text{CH}_2\text{CH}_2\text{CH}_2\text{N}$ ), 3.53 (s, 2H,  $\text{FmocNCH}_2\text{CO}$ ), 3.88 (s, 2H,  $\text{NCH}_2\text{CO}$ ), 3.88-3.93 (m, 2H,  $\text{CH}_2$ , Fmoc), 4.16 (s, 2H,  $\text{NCH}_2\text{CO}$ ), 4.38 (m, 1H, CH, Fmoc), 7.24 – 7.38 (m, 4H, Ar), 7.51 (m, 2H, Ar), 7.72 – 7.79 (m, 2H, Ar).

**<sup>13</sup>C NMR** (100 MHz, MeOD)  $\delta$  25.9 (CH<sub>2</sub>, FmocNCH<sub>2</sub>CH<sub>2</sub>CH<sub>2</sub>), 28.2 (CH<sub>2</sub>, FmocNCH<sub>2</sub>CH<sub>2</sub>CH<sub>2</sub>), 28.6 (3CH<sub>3</sub>, *Ot*Bu), 28.7 (3CH<sub>3</sub>, *Ot*Bu), 28.8 (3CH<sub>3</sub>, *Ot*Bu), 40.8 (CH<sub>2</sub>, FmocNCH<sub>2</sub>CH<sub>2</sub>CH<sub>2</sub>), 43.5 (1C, CH, Fmoc), 49.2 (2×CH<sub>2</sub>, 2×NCH<sub>2</sub>CO), 49.6 (CH<sub>2</sub>, BocNHCH<sub>2</sub>CH<sub>2</sub>), 51.5 (CH<sub>2</sub>, FmocNCH<sub>2</sub>CO), 59.2 (3C, 3×*t*Bu), 59.5 (CH<sub>2</sub>, CH<sub>2</sub>OC=O, Fmoc), 120.7 (2CH, Ph), 125.0 (2CH, Ph), 128.0 (4CH, Ph), 141.7 (2C, Ph), 150.3 (2C, Ph), 170.3 (2C, Boc, OC=O), 171.3 (2C, 2×NC=O), 176.5 (1C, COOH).

**Fmoc-(NLys(Boc)-Ntbu-Ntbu)<sub>2</sub>-OBn 18**



To a solution of the free acid **17** (70 mg, 0.10 mmol, 1 equiv.) in DMF at rt under Ar was added free amine **6** (57 mg, 0.10 mmol, 1 equiv.) dissolved in CH<sub>2</sub>Cl<sub>2</sub> and the resulting mixture was placed at 0°C under Ar. DIPEA (66 mg, 0.51 mmol, 5 equiv.) and HATU (47 mg, 0.12 mmol, 1.2

equiv.) was added and the resulting mixture was stirred for 18h at rt. The solvents were evaporated under reduced pressure and the residue was taken up in EtOAc. The organic layer was washed with water (2 x) and the aqueous layer was extracted with EtOAc (×1). The combined organic layers were dried over MgSO<sub>4</sub>, filtered, and concentrated under reduced pressure. Flash chromatography (Cy/EA 6:4) of the residue yielded oligomer **18** (90 mg, 0.074 mmol, 73%).

**TLC** R<sub>f</sub> = (0.56, CY/EA, 3:7)

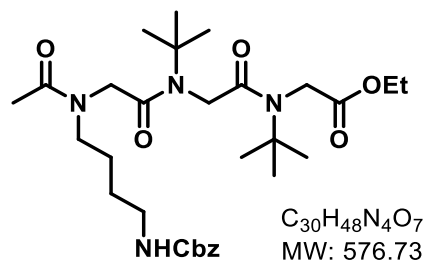
**IR** (ATR)  $\bar{\nu}$  (cm<sup>-1</sup>): 2984, 2930, 1701, 1668, 1479, 1451, 1447, 1437, 1430, 1393, 1365, 1316, 1249, 1246, 1242, 1236, 1218, 1195, 1189, 1186, 1174, 1150, 1137, 842, 838, 835, 832, 765, 759.

**<sup>1</sup>H NMR** (400 MHz, CDCl<sub>3</sub>)  $\delta$  0.93 – 1.83 (m, 62H, 6×*t*Bu, 2×CH<sub>2</sub>CH<sub>2</sub>), 2.76 – 3.54 (m, 8H, 2×BocNHCH<sub>2</sub>, 2×NCH<sub>2</sub>CH<sub>2</sub>CH<sub>2</sub>), 3.54 – 4.60 (m, 15H, 6×NCH<sub>2</sub>CO, CH, CH<sub>2</sub>OC=O), 4.97 (bs, 2H, 2×NH), 5.19 (m, 2H, PhCH<sub>2</sub>), 7.11 – 7.43 (m, 9H, Ar), 7.50 (m, 2H, Ar), 7.71 (m, 2H, Ar).

**<sup>13</sup>C NMR** (100 MHz, CDCl<sub>3</sub>)  $\delta$  24.8 (CH<sub>2</sub>, FmocNCH<sub>2</sub>CH<sub>2</sub>CH<sub>2</sub>), 25.4 (CH<sub>2</sub>, NCH<sub>2</sub>CH<sub>2</sub>CH<sub>2</sub>), 27.2 (2CH<sub>2</sub>, 2×BocNHCH<sub>2</sub>CH<sub>2</sub>CH<sub>2</sub>), 28.3, 28.4, 28.5 (18CH<sub>3</sub>, 6×*Ot*Bu), 40.2 (2CH<sub>2</sub>, FmocNCH<sub>2</sub>, NCH<sub>2</sub>), 46.3 (2CH<sub>2</sub>, 2×BocNHCH<sub>2</sub>), 47.1 (1CH, CH, Fmoc), 47.9, 48.4, 50.7, 51.0, (6CH<sub>2</sub>, 6×NCH<sub>2</sub>CO), 58.1, 58.5, 58.6, 58.8 (4C, 4×*t*Bu), 67.4 (CH<sub>2</sub>, PhCH<sub>2</sub>) 67.9 (CH<sub>2</sub>, Fmoc), 78.7, 78.9 (2C, 2×*t*Bu), 119.6, 119.8 (2CH, Ph), 124.9 (2CH, Ph), 125.7 (2CH, Ph), 127.4, 127.6 (2CH, Ph), 128.6, 128.7, 128.8, 128.9 (5CH, Ph), 135.0 (1C, Ph), 141.1, 141.3 (2C, Ph), 144.0, 144.4 (2C, Ph), 156.2, 156.3, 157.2 (3C, 2×Boc, Fmoc), 168.8, 169.5, 170.1, 170.5 (5C, 5×NC=O), 170.6 (1C, OC=O).

**HRMS** (TOF MS ES<sup>+</sup>):  $m/z$  calculated for C<sub>68</sub>H<sub>103</sub>N<sub>8</sub>O<sub>13</sub> [M+H]<sup>+</sup>: 1239.7645; found: 1239.7714 (5.6 ppm).

### Ac-(NLys(Cbz)-NtBu-NtBu)-OEt **19**



Compound **19** was synthesised starting from compound **15** (68 mg, 0.13 mmol, 1 equiv) by application of **General Procedure C** using EtOAc as solvent. The crude was subjected to flash chromatography (EtOAc 100 %) to yield compound **19** (60 mg, 0.104 mmol, 82%).

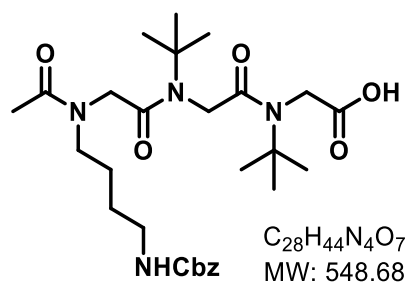
**TLC** R<sub>f</sub> = 0.29 (EtOAc)

**<sup>1</sup>H NMR** (400 MHz, CDCl<sub>3</sub>) δ 1.27 (t,  $J$  = 7.0 Hz, 3H, CH<sub>2</sub>CH<sub>3</sub>), 1.36-1.39 (m, 18H, 2×*t*Bu), 1.50-1.58 (m, 4H, NHCH<sub>2</sub>CH<sub>2</sub>CH<sub>2</sub>), 1.97, 2.09 (2×s, 3H, Ac, 2 conformers), 3.18 (t,  $J$  = 6.8 Hz, 2H, NHCH<sub>2</sub>CH<sub>2</sub>), 3.35 (t,  $J$  = 7.4 Hz, 2H, AcNCH<sub>2</sub>), 3.53 – 4.15 (m, 6H, 3×NCH<sub>2</sub>CO), 4.20 (q,  $J$  = 7.0 Hz, 2H, CH<sub>2</sub>CH<sub>3</sub>), 5.05 (s, 2H, PhCH<sub>2</sub>), 5.31 (s, 1H, NH), 7.27 – 7.39 (m, 5H, Ar).

**<sup>13</sup>C NMR** (100 MHz, CDCl<sub>3</sub>) δ 14.2 (CH<sub>3</sub>, CH<sub>2</sub>CH<sub>3</sub>), 21.2, 21.7 (CH<sub>3</sub>, Ac, 2 conformers), 24.8, 25.3 (CH<sub>2</sub>, AcNCH<sub>2</sub>CH<sub>2</sub>CH<sub>2</sub>, 2 conformers), 27.0, 27.1 (CH<sub>2</sub>, AcNCH<sub>2</sub>CH<sub>2</sub>CH<sub>2</sub>, 2 conformers), 28.3 (3 CH<sub>3</sub>, *Nt*Bu), 28.4 (3 CH<sub>3</sub>, *Nt*Bu), 40.5, 40.7 (CH<sub>2</sub>, CbzNHCH<sub>2</sub>CH<sub>2</sub>, 2 conformers), 46.2, 47.1 (CH<sub>2</sub>, AcNCH<sub>2</sub>CH<sub>2</sub>, 2 conformers), 48.0, 48.6, 48.8, 49.1 (2×CH<sub>2</sub>, 2×NHCH<sub>2</sub>CO), 52.4 (CH<sub>2</sub>, AcNCH<sub>2</sub>CO), 58.2, 58.4 (2C, *t*Bu), 62.0, 62.2 (CH<sub>2</sub>, CH<sub>2</sub>CH<sub>3</sub>, 2 conformers), 66.4, 66.6 (CH<sub>2</sub>, CH<sub>2</sub>Ph, 2 conformers), 128.0, 128.1, 128.2, 128.5 (5CH, Ph), 136.8, (1C, Ph), 156.6, 156.7 (1C, NHOC=O), 168.9, 169.1, 169.7, 170.0, 170.4, 171.0 (3C, 2×NC=O, CH<sub>3</sub>CO), 172.4 (1C, EtOC=O).

**HRMS** (TOF MS ES<sup>+</sup>):  $m/z$  calculated for C<sub>30</sub>H<sub>49</sub>N<sub>4</sub>O<sub>7</sub> [M+H]<sup>+</sup>: 577.3601 ; found: 577.3624 (4.0 ppm)

### Ac-(NLys(Cbz)-NtBu-NtBu)OH **20**



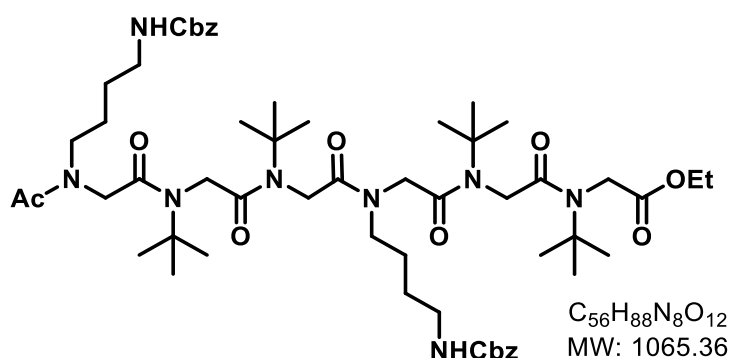
To a homogeneous solution of **19** (110 mg, 0.19 mmol, 1 equiv) in THF/H<sub>2</sub>O/MeOH (4:1:1) solvent system was added LiOH·H<sub>2</sub>O (24 mg, 0.57 mmol, 3 equiv) at rt. After stirring for 4 hours at rt, the solution was hydrolysed with water (3 ml) and acidified (pH = 4) with HCl (1 N). The solution is then extracted with EtOAc to yield crude compound **20** (104 mg, 0.19 mmol, 100%).

**TLC** R<sub>f</sub> = 0.3 (EtOAc/MeOH, 95:5)

**<sup>1</sup>H NMR** (400 MHz, MeOD)  $\delta$  1.40 – 1.44 (m, 18H, *t*Bu), 1.46-1.59 (m, 4H, NHCH<sub>2</sub>CH<sub>2</sub>CH<sub>2</sub>), 1.97, 2.13 (2×s, 3H, Ac, 2 conformers), 3.09-3.15 (m, 2H, AcNCH<sub>2</sub>), 3.32-3.33 (m, 2H, NHCH<sub>2</sub>CH<sub>2</sub>), 4.00-4.20 (m, 6H, 3×NCH<sub>2</sub>CO), 5.05 (s, 2H, PhCH<sub>2</sub>), 7.17 – 7.44 (m, 5H, Ar).

**HRMS** (TOF MS ES<sup>+</sup>): *m/z* calculated for C<sub>28</sub>H<sub>45</sub>N<sub>4</sub>O<sub>7</sub> [M+H]<sup>+</sup>: 549.3288 ; found: 549.3286 (-0.4 ppm).

#### Ac-(NLys(Cbz)-N*t*bu-N*t*bu)<sub>2</sub>-OEt **21**



To a solution of the free acid **20** (108 mg, 0.19 mmol, 1 equiv.) in CH<sub>2</sub>Cl<sub>2</sub> (2 ml) at rt under Ar was added free amine **15** (106 mg, 0.19 mmol, 1 equiv.) dissolved in CH<sub>2</sub>Cl<sub>2</sub> (2 ml) and the resulting mixture was placed at 0°C under Ar. DIPEA (76.8 mg, 0.59 mmol, 3 equiv.), DMF (1 ml) and FDPP (91

mg, 0.24 mmol, 1.2 equiv.) was added. After stirring for 18h at rt the resulting mixture was washed with 5% citric acid solution (×2). The combined organic layers were washed with saturated NaHCO<sub>3</sub> (×2) followed by water (×1) and finally with brine (×2). The combined organic layers were dried over NaSO<sub>4</sub>, filtered, and concentrated under reduced pressure. Flash chromatography (EtOAc/MeOH, 95:5) of the residue yielded oligomer **21** (128 mg, 0.12 mmol, 61%).

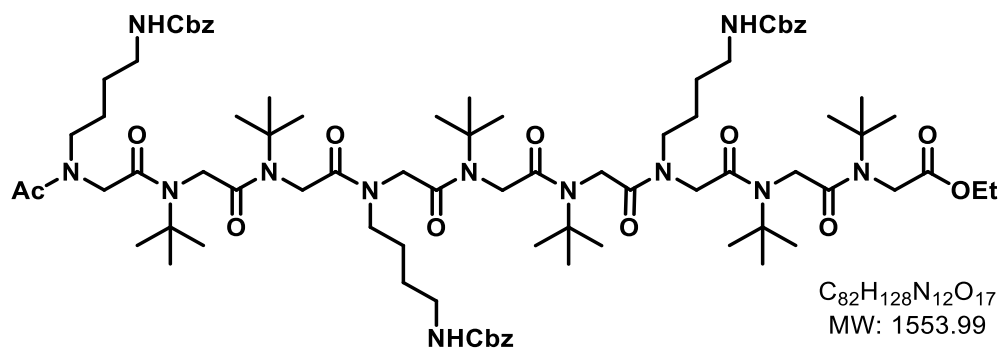
**TLC** R<sub>f</sub> = 0.4 (EtOAc/MeOH, 95:5)

**<sup>1</sup>H NMR** (400 MHz, CDCl<sub>3</sub>)  $\delta$  (ppm): 1.18 (t, *J* = 7.1 Hz, 3H, CH<sub>2</sub>CH<sub>3</sub>), 1.22 – 1.39 (m, 36H, 4×*t*Bu), 1.39 – 1.60 (m, 8H, 2×CbzNHCH<sub>2</sub>CH<sub>2</sub>CH<sub>2</sub>), 1.93-2.05 (m, 3H, Ac, 4 conformers), 3.07 – 3.25 (m, 8H, 2×CbzNHCH<sub>2</sub>CH<sub>2</sub>CH<sub>2</sub>CH<sub>2</sub>N), 3.52 – 4.11 (m, 12H, 6×NCH<sub>2</sub>CO), 4.12 – 4.31 (m, 2H, CH<sub>2</sub>CH<sub>3</sub>), 5.02, 5.03, 5.04 (3×s, 4H, 2×PhCH<sub>2</sub>, 4 conformers), 5.27, 5.58, (2×bs, 2H, 2×NH), 7.26-7.31 (m, 10H, Ar).

**<sup>13</sup>C NMR** (100 MHz, CDCl<sub>3</sub>)  $\delta$  (ppm): 14.2 (CH<sub>3</sub>, CH<sub>2</sub>CH<sub>3</sub>), 21.1, 21.8 (CH<sub>3</sub>, Ac, 2 conformers), 23.7, 24.8, 25.0, 25.3, 25.4 (2CH<sub>2</sub>, 2×NCH<sub>2</sub>CH<sub>2</sub>CH<sub>2</sub>, 2 conformers), 26.8, 27.0, 27.3 (2CH<sub>2</sub>, 2×NCH<sub>2</sub>CH<sub>2</sub>CH<sub>2</sub>, 2 conformers), 28.3 (6CH<sub>3</sub>, 6×N*t*Bu), 28.4 (6CH<sub>3</sub>, 6×N*t*Bu), 40.2, 40.8 (2CH<sub>2</sub>, 2×CbzNHCH<sub>2</sub>CH<sub>2</sub>, 2 conformers), 46.2 (2CH<sub>2</sub>, 2×NCH<sub>2</sub>CH<sub>2</sub>), 46.9, 48.1, 51.0, 52.3, 55.1 (6CH<sub>2</sub>, 6×NCH<sub>2</sub>CO), 58.1, 58.7 (2C, *t*Bu), 58.9, 60.5 (2C, *t*Bu), 62.3 (CH<sub>2</sub>, CH<sub>2</sub>CH<sub>3</sub>), 66.3, 66.4, 66.5 (2CH<sub>2</sub>, 2×CH<sub>2</sub>Ph, 2 conformers), 127.9, 127.9, 128.1, 128.1, 128.5, 128.5, 128.6 (10CH, Ph), 136.7, 136.8 (2C, Ph), 156.7 (2C, 2×NHOC=O), 168.2, 168.5, 169.0, 169.3, 170.3, 170.5 (6C, 5×NC=O, CH<sub>3</sub>CO) 172.5 (1C, EtOC=O).

**HRMS** (TOF MS ES<sup>+</sup>): *m/z* calculated for C<sub>56</sub>H<sub>89</sub>N<sub>8</sub>O<sub>12</sub> [M+H]<sup>+</sup>: 1065.6600 ; found: 1065.6534 (-6.2 ppm).

### Ac-(NLys(Cbz)-NtBu-NtBu)<sub>3</sub>-OEt **23**



To a homogeneous solution of **21** (85 mg, 0.08 mmol, 1 equiv) in THF/H<sub>2</sub>O/MeOH (4:1:1) solvent system was added LiOH·H<sub>2</sub>O (10 mg, 0.24 mmol, 3 equiv) at rt. After stirring for 4 hours at rt, the solution was hydrolysed with water (3 ml) and acidified (pH = 4) with HCl (1 N). The solution is then extracted with EtOAc to yield crude compound **22** (79 mg, 0.08 mmol, 100%). To a solution of the free acid **22** (79 mg, 0.08 mmol, 1 equiv.) in CH<sub>2</sub>Cl<sub>2</sub> (1 ml) at rt under Ar was added FDPP (91 mg, 0.24 mmol, 1.2 equiv.). Then the free amine **15** (43 mg, 0.08 mmol, 1 equiv.) dissolved in CH<sub>2</sub>Cl<sub>2</sub> (1ml) and DIPEA (76.8 mg, 0.59 mmol, 3 equiv) were added. After stirring for 18h at rt the resulting mixture was concentrated under reduced pressure. Flash chromatography (EtOAc/MeOH, 95:5) of the residue yielded oligomer **23** (76 mg, 0.48 mmol, 61%).

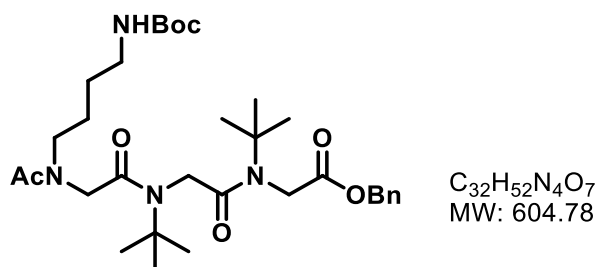
**TLC** R<sub>f</sub> = 0.46 (EtOAc/MeOH, 95:5)

**<sup>1</sup>H NMR** (400 MHz, CDCl<sub>3</sub>) δ (ppm): 1.25 – 1.51 (m, 69H, CH<sub>2</sub>CH<sub>3</sub>, 6×*t*Bu, 3×CbzNHCH<sub>2</sub>CH<sub>2</sub>, 3×NCH<sub>2</sub>CH<sub>2</sub>), 1.99 (m, 3H, Ac), 3.16 (m, 12H, 3×CbzNHCH<sub>2</sub>, 3×NCH<sub>2</sub>), 3.83 – 4.27 (m, 20H, 9×NCH<sub>2</sub>CO, CH<sub>2</sub>CH<sub>3</sub>), 5.03 – 5.06 (m, 6H, 3×PhCH<sub>2</sub>), 5.23 – 6.00 (m, 3H, 3×NH), 7.28 – 7.31 (m, 15H, Ar).

**<sup>13</sup>C NMR** (100 MHz, CDCl<sub>3</sub>) δ (ppm): 14.2 (CH<sub>3</sub>, CH<sub>2</sub>CH<sub>3</sub>), 21.0, 21.6 (CH<sub>3</sub>, Ac, two conformers), 24.7, 24.8, 25.2, 25.6, (3CH<sub>2</sub>, 3×NCH<sub>2</sub>CH<sub>2</sub>CH<sub>2</sub>, conformers), 26.7, 27.0, 27.3, (3CH<sub>2</sub>, 3×NCH<sub>2</sub>CH<sub>2</sub>CH<sub>2</sub>, conformers), 28.2 (6CH<sub>3</sub>, 6×*Nt*Bu), 28.4 (6CH<sub>3</sub>, 6×*Nt*Bu), 28.6 (6CH<sub>3</sub>, 6×*Nt*Bu), 40.6, 40.7 (3CH<sub>2</sub>, 3×CbzNHCH<sub>2</sub>CH<sub>2</sub>, conformers), 46.2 (3CH<sub>2</sub>, 3×NCH<sub>2</sub>CH<sub>2</sub>), 46.4, 47.0, 48.1, 50.3, 51.0, 52.3 (9CH<sub>2</sub>, 9×NCH<sub>2</sub>CO), 58.7, 58.9 (6C, 6×*t*Bu), 62.1, 62.3, (CH<sub>2</sub>, CH<sub>2</sub>CH<sub>3</sub>, conformers), 66.3, 66.5 (3CH<sub>2</sub>, 3×CH<sub>2</sub>Ph, conformers), 127.8, 128.0, 128.0, 128.4, 128.4, 128.5, 129.4, (15CH, Ph), 135.6, 136.6, 136.7, 136.9, 137.4, (3C, Ph), 156.7 (3C, 3×NHOC=O), 169.2, 169.8, 170.5, 171.3, (9C, 8×NC=O, CH<sub>3</sub>CO) 172.7 (1C, EtOC=O).

**HRMS** (TOF MS ES<sup>+</sup>): *m/z* calculated for C<sub>82</sub>H<sub>129</sub>N<sub>12</sub>O<sub>17</sub> [M+H]<sup>+</sup>: 1553.9593; found: 1553.9595 (0.1 ppm).

### Ac-(NLys(Boc)-Ntbn-Ntbn)OBn 24



To a solution of **15** (400 mg, 0.71 mmol, 1 equiv) and  $Et_3N$  (143 mg, 1.42 mmol, 2 equiv.) in EtOAc (3.5 ml) at 0 °C under Ar was added anhydride acetic acid (290 mg, 2.84 mmol, 4 equiv.). After stirring for 18 h at room temperature the mixture was filtered. The filtrate was concentrated under

reduced pressure to yield crude. The crude was subjected to flash chromatography (EtOAc 100 %) to yield the compound **24** (374 mg, 0.61 mmol, 87%).

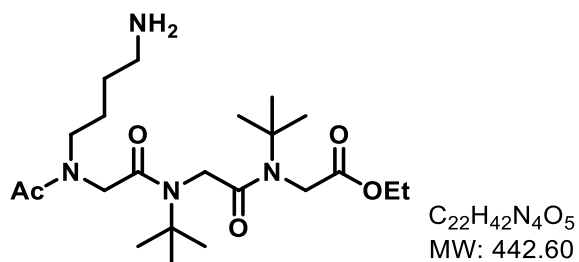
TLC  $R_f$  = 0.52 (EtOAc, 100)

IR (ATR)  $\tilde{\nu}$  ( $cm^{-1}$ ): 2978, 2933, 1743, 1740, 1701, 1695, 1668, 1663, 1651, 1644, 1634, 1500, 1457, 1437, 1393, 1365, 1316, 1265, 1245, 1237, 1176, 1003, 816, 758, 752, 747.

2 conformers are observed by NMR in a 7/3 ratio.

$^1H$  NMR (400 MHz,  $CDCl_3$ )  $\delta$  1.33 – 1.39 (m, 9H, *t*Bu), 1.39 – 1.45 (m, 18H, 2×*t*Bu), 1.43 – 1.56 (m, 4H,  $NHCH_2CH_2CH_2$ ), 2.01 – 2.15 (m, 3H, Ac), 2.98 – 3.22 (m, 2H,  $NHCH_2$ ), 3.25 – 3.45 (m, 2H,  $AcNCH_2CH_2$ ), 3.74 (ls, 2H,  $NCH_2C=O$ ), 3.87 (ls, 2H,  $NCH_2C=O$ ), 4.11 (ls, 2H,  $NCH_2C=O$ ), 4.86 (s, 1H, NH), 5.20, 5.22 (2s, 2H,  $PhCH_2$ , 2 conformers), 7.32 – 7.43 (m, 5H, Ph).

### Ac-(NLys-Ntbn-Ntbn)-OEt 26



To a solution of ethyl ester **19** (74 mg, 0.13 mmol) dissolved in EtOH (2.5 ml) at rt was added Pd/Carbon 10% (5 mg) stirring under the atmosphere of hydrogen overnight. End of deprotection was confirmed by TLC. The resulting mixture was then filtered using celite pad and then

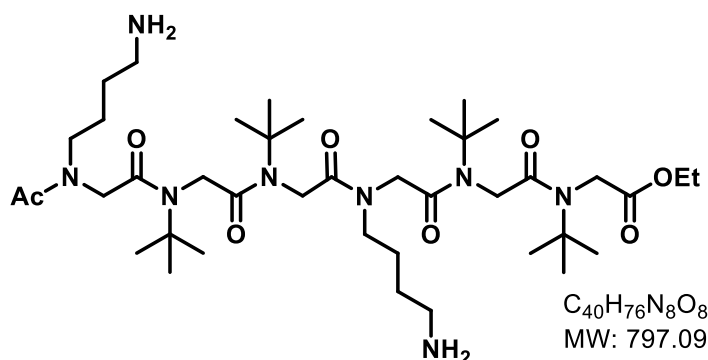
concentrated under reduced pressure to obtain the compound **26** (55.4 mg, 0.10 mmol, 79%)

TLC  $R_f$  = 0.06 (EtOAc/MeOH, 9:1)

$^1H$  NMR (400 MHz, MeOD)  $\delta$  (ppm): 1.27 – 1.33 (m, 3H,  $CH_2CH_3$ ), 1.39 – 1.50 (m, 18H, 2×*t*Bu), 1.53 – 1.62 (m, 4H,  $NH_2CH_2CH_2CH_2$ ), 1.98, 2.15 (3H, Ac, 2 conformers), 2.80-2.85 (m, 2H,  $NH_2CH_2$ ), 3.34-3.39 (m, 2H,  $AcNCH_2$ ), 4.02 - 4.28 (m, 6H, 2× $NCH_2CO$ ,  $CH_2CH_3$ ).

HRMS (TOF MS ES<sup>+</sup>):  $m/z$  calculated for  $C_{22}H_{43}N_4O_5$  [ $M+H$ ]<sup>+</sup>: 443.3233 ; found: 443.3266 (7.4 ppm).

### Ac-(NLys-NtBu-NtBu)<sub>2</sub>-OH **27**



To a solution of ethyl ester **21** (70 mg, 0.065 mmol) dissolved in EtOH (3 ml) at rt was added Pd/Carbon 10% (5 mg) stirring under the atmosphere of hydrogen overnight. End of deprotection was confirmed by TLC. The resulting mixture was then filtered using celite pad and then concentrated under reduced

pressure to obtain the compound **27** (44 mg, 0.055 mmol, 84%)

**TLC**  $R_f = 0.07$  (EtOAc/MeOH, 9:1)

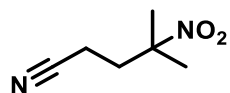
4 conformers are observed by NMR in a 61/29 (*cis/trans*) ratio.

**<sup>1</sup>H NMR** (400 MHz, MeOD)  $\delta$  (ppm): 1.27 – 1.35 (m, 3H, CH<sub>2</sub>CH<sub>3</sub>), 1.41, 1.42, 1.44, 1.45, 1.46 (5×s, 36H, 4×*t*Bu), 1.38 – 1.56 (m, 8H, 2×NH<sub>2</sub>CH<sub>2</sub>CH<sub>2</sub>CH<sub>2</sub>), 1.95, 1.97, 1.98, 2.16 (4×s, 3H, Ac, 4 conformers), 2.62 – 2.78 (m, 4H, 2×NH<sub>2</sub>CH<sub>2</sub>), 3.25 – 3.44 (m, 4H, 2×NCH<sub>2</sub>), 3.80-4.30 (m, 14H, 6×NCH<sub>2</sub>CO, CH<sub>2</sub>CH<sub>3</sub>).

**<sup>13</sup>C NMR** (100 MHz, CDCl<sub>3</sub>)  $\delta$ (ppm): 14.2 (CH<sub>3</sub>, CH<sub>2</sub>CH<sub>3</sub>), 21.2, 21.8 (CH<sub>3</sub>, Ac, conformers), 24.6, 24.9, 25.5 (4CH<sub>2</sub>, 2×NCH<sub>2</sub>CH<sub>2</sub>CH<sub>2</sub>), 28.3, 28.4 (12CH<sub>3</sub>, 4×*t*Bu), 30.9, 40.9, 41.6, 41.8 (2CH<sub>2</sub>, 2×NH<sub>2</sub>CH<sub>2</sub>CH<sub>2</sub>), 46.2 (2CH<sub>2</sub>, 2×NCH<sub>2</sub>CH<sub>2</sub>), 47.1, 48.0, 48.1, 48.4, 49.3, 52.0 (6CH<sub>2</sub>, 6×NCH<sub>2</sub>CO), 58.0, 58.6 (4C, 4×*t*Bu), 61.9, 62.0, 62.2 (CH<sub>2</sub>, CH<sub>2</sub>CH<sub>3</sub>, conformers), 168.9, 170.2, 170.3, 170.3, 170.4 (7C, 5×NC=O, CH<sub>3</sub>CO, EtOC=O).

**HRMS** (TOF MS ES<sup>+</sup>):  $m/z$  calculated for C<sub>40</sub>H<sub>77</sub>N<sub>8</sub>O<sub>8</sub> [M+H]<sup>+</sup>: 797.5864 ; found: 797.5870 (0.8 ppm).

### 4-methyl-4-nitropentanenitrile **29**



$C_6H_{10}N_2O_2$   
MW: 142.15

To a mixture of 2-nitropropane (1g, 11.23 mmol) and acrylonitrile (0.88 ml, 13.48 mmol) dissolved in EtOH (5 ml) was added Triton B (65  $\mu$ l, 0.37 mmol). The mixture

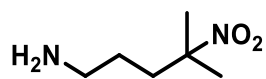
was then refluxed for 16 h. It was then concentrated under reduced pressure to obtain the crude. The crude was filtered using column (eluent, cyclohexane/AcOEt 7:3) The filtrate was concentrated under reduced pressure to obtain compound **29** (1.62 g, 11.2 mmol, 100%)

**TLC**  $R_f = 0.61$ (Cyclohexane/EtOAc, 7:3)

**<sup>1</sup>H NMR** (400 MHz, CDCl<sub>3</sub>)  $\delta$  1.63 (s, 6H, C(CH<sub>3</sub>)<sub>2</sub>), 2.30-2.34 (m, 2H, NCCH<sub>2</sub>CH<sub>2</sub>), 2.38-2.44 (m, 2H, NCCH<sub>2</sub>CH<sub>2</sub>).

Spectroscopic data are consistent with those reported in the literature.<sup>135</sup>

### 4-methyl-4-nitropentan-1-amine **30**



$C_6H_{14}N_2O_2$   
MW: 146.19

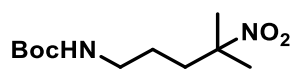
To a solution of **29** (1.62 g, 11.2 mmol) dissolved in anhydrous THF (6 ml) was added  $BH_3 \cdot THF$  (22.8 ml, 1 M) in hexane. It was refluxed for 1.5 hrs. The solution was then cooled under ice bath and hydrolysed with a solution of HCl (6 N, 15 ml). Then the bulk of THF was removed in vacuum. The mixture was basified using NaOH pellets followed by extraction using  $CH_2Cl_2$  (3 x 30ml). The combined organic layers were dried over  $MgSO_4$  and concentrated to obtain a pale green oil **30** (1.75 g) which was directly used for the next step.

TLC  $R_f = 0.65$  (Cyclohexane/EtOAc, 7:3)

$^1H$  NMR (400 MHz,  $CDCl_3$ )  $\delta$  1.37 – 1.45 (m, 2H,  $CH_2$ ), 1.59-1.62 (m, 8H, 2 $CH_3$ ,  $NH_2$ ), 1.93 (m, 2H,  $NO_2C(CH_3)_2CH_2CH_2$ ), 2.71 (t,  $J = 7.0$  Hz, 2H,  $CH_2NH_2$ ).

Spectroscopic data are consistent with those reported in the literature.<sup>136</sup>

### tert-butyl (4-amino-4-methylpentyl)carbamate **31**



$C_{11}H_{22}N_2O_4$   
MW: 246.30

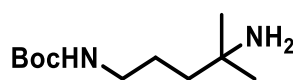
To a solution of **30** (1.75 g, 11.23 mmol) and  $Et_3N$  (2.53 ml, 18.04 mmol, 1.5 equiv.) dissolved in anhydrous THF (45 ml) was added  $(Boc)_2O$  (2.88 g, 13.23 mmol). It was then stirred for 60h. THF was removed under reduced pressure. The residue was dissolved in EtOAc (150 ml) and washed with solution of NaOH (1 M, 3 x 15ml). The combined organic layers were then dried over  $MgSO_4$  and concentrated to obtain the crude. The expected compound was purified by Flash chromatography on silica gel (eluent, cyclohexane/EtOAc, 8:2) to yield **31** (1.38 g, 5.61 mmol, 50% (2 steps)).

TLC  $R_f = 0.68$  (Cyclohexane/EtOAc, 7:3)

$^1H$  NMR (400 MHz,  $CDCl_3$ )  $\delta$  (ppm): 1.41-1.49 (m, 11H, *t*Bu and  $CH_2CH_2CH_2$ ), 1.58 (s, 6H,  $C(CH_3)_2$ ), 1.91 (m, 2H,  $NO_2C(CH_3)_2CH_2$ ), 3.15 (m, 2H,  $NHCH_2$ ), 4.54 (s, 1H,  $NH$ ).

$^{13}C$  NMR (100 MHz,  $CDCl_3$ )  $\delta$  (ppm): 25.0 (3C, *t*Bu), 30.5 ( $CH_2$ ,  $CH_2CH_2CH_2$ ), 37.9 ( $CH_2$ ,  $CH_2C(CH_3)_2$ ), 40.2 ( $CH_2$ ,  $NHCH_2$ ), 82.5 (1C, *t*Bu), 87.9 (1C,  $C(CH_3)_2$ ), 155.9 (1C,  $OC(O)NH$ ).

### tert-butyl (4-amino-4-methylpentyl)carbamate **32**



$C_{11}H_{24}N_2O_2$   
MW: 216.32

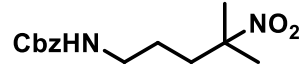
To a solution of compound **31** (2.55 g, 10.35 mmol, 1 equiv) dissolved in anhydrous MeOH (100 ml) at rt was added Pd/Carbon 10% (50 mg) stirring under the atmosphere of hydrogen overnight. 50 mg of Pd/ $BaSO_4$  10% was added thrice after 24h. End of reduction was confirmed by TLC. The resulting mixture was then filtered using celite pad and then concentrated under reduced pressure to obtain the compound **32** (2.23 g, 10.35 mmol, 100%)

TLC  $R_f = 0.52$  (Cyclohexane/EtOAc, 7:3)



**<sup>1</sup>H NMR** (400 MHz, CDCl<sub>3</sub>) δ(ppm): 1.10 (s, 6H, C(CH<sub>3</sub>)<sub>2</sub>), 1.22 – 1.60 (m, 4H, NH<sub>2</sub>, CH<sub>2</sub>CH<sub>2</sub>CH<sub>2</sub>), 1.43 (s, 9H, *t*Bu), 1.66 – 2.18 (m, 2H, C(CH<sub>3</sub>)<sub>2</sub>CH<sub>2</sub>), 3.11 (m, 2H, NHCH<sub>2</sub>), 4.64 (bs, 1H, NH).

### Benzyl (4-methyl-4-nitropentyl)carbamate **33**

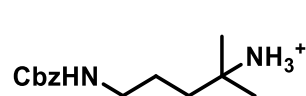
  $\text{C}_{14}\text{H}_{20}\text{N}_2\text{O}_4$  To a solution of **30** (100 mg, 0.68 mmol) and Et<sub>3</sub>N (104 mg, 1.03 mmol, 1.5 equiv.) dissolved in anhydrous THF (4 ml) was added Cbz-Cl (128 mg, 0.75 mmol). It was then stirred for 48h. THF was removed under reduced pressure. The residue was washed with EtOAc (150 ml) and concentrated to obtain the crude. The expected compound was purified by Flash chromatography on silica gel (eluent, cyclohexane/EtOAc, 8:2) to yield **33** (142 mg, 0.5 mmol, 73%).  
MW: 280.32

**TLC** R<sub>f</sub> = 0.53 (Cyclohexane/EtOAc, 8:2)

**<sup>1</sup>H NMR** (400 MHz, CDCl<sub>3</sub>) δ(ppm): 1.43 – 1.52 (m, 2H, NHCH<sub>2</sub>CH<sub>2</sub>CH<sub>2</sub>), 1.58 (s, 6H, C(CH<sub>3</sub>)<sub>2</sub>), 1.81 – 2.00 (m, 2H, NHCH<sub>2</sub>CH<sub>2</sub>), 3.20 (m, 2H, NHCH<sub>2</sub>), 4.76 (s, 1H, NH), 5.10 (s, 2H, PhCH<sub>2</sub>), 7.29 – 7.44 (m, 5H, Ph).

**<sup>13</sup>C NMR** (100 MHz, CDCl<sub>3</sub>) δ(ppm): 25.0 (CH<sub>2</sub>, CH<sub>2</sub>CH<sub>2</sub>CH<sub>2</sub>), 25.9 (2×CH<sub>3</sub>, CH<sub>2</sub>C(CH<sub>3</sub>)<sub>2</sub>NO<sub>2</sub>), 37.8 (CH<sub>2</sub>, CH<sub>2</sub>CH<sub>2</sub>CH<sub>2</sub>), 40.7 (CH<sub>2</sub>, CH<sub>2</sub>CH<sub>2</sub>CH<sub>2</sub>), 66.8 (CH<sub>2</sub>, CH<sub>2</sub>Ph), 89.5, 89.5 (1C, CH<sub>2</sub>C(CH<sub>3</sub>)<sub>2</sub>NO<sub>2</sub>), 128.1, 128.2, 128.6 (5CH, Ph), 139.4 (1C, Ph), 159.9 (1C, OC=O).

### Benzyl (4-amino-4-methylpentyl)carbamate.HCl **34**

  $\text{C}_{14}\text{H}_{22}\text{N}_2\text{O}_2$  A mixture of compound **33** (139 mg, 0.5 mmol), zinc dust (486 mg, 7.44 mmol), and ammonium chloride (397 mg, 7.44 mmol) in tetrahydrofuran (7.5 mL) and methanol (7.5 mL) was stirred at room temperature for 4 hr. The residue was removed by suction filtration through filter paper. The filtrate was concentrated under vacuum. The residue was diluted with ethyl acetate (50 mL), washed with 10% NaHCO<sub>3</sub> solution (5 mL) and brine (5 mL), and dried over MgSO<sub>4</sub>. Removal of solvent under vacuum provided the desired product **34** (100.5 mg, 0.41 mmol, 82%) as a pale white solid.  
MW: 250.34

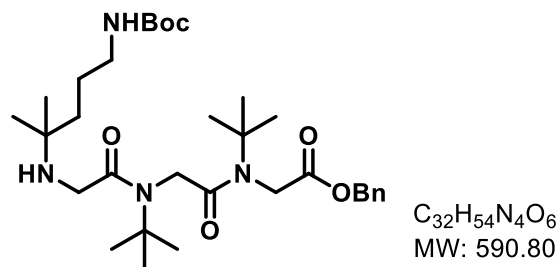
**TLC** R<sub>f</sub> = 0.2 (CH<sub>2</sub>Cl<sub>2</sub>/MeOH, 94:6)

**<sup>1</sup>H NMR** (400 MHz, CDCl<sub>3</sub>) δ(ppm): 1.24 – 1.30 (m, 6H, C(CH<sub>3</sub>)<sub>2</sub>), 1.48-1.65 (m, 4H, NHCH<sub>2</sub>CH<sub>2</sub>CH<sub>2</sub>), 3.20 (m, 2H, NHCH<sub>2</sub>), 5.06 (s, 2H, PhCH<sub>2</sub>), 5.26 - 5.44 (m, 1H, NH), 5.50 – 6.60 (s, 3H, NH<sub>3</sub><sup>+</sup>), 7.20 – 7.37 (m, 5H, Ph).

**<sup>13</sup>C NMR** (100 MHz, CDCl<sub>3</sub>) δ(ppm): 22.3 (2×CH<sub>3</sub>, CH<sub>2</sub>C(CH<sub>3</sub>)<sub>2</sub>NH<sub>2</sub>), 24.1 (CH<sub>2</sub>, CH<sub>2</sub>CH<sub>2</sub>CH<sub>2</sub>), 33.8 (CH<sub>2</sub>, CH<sub>2</sub>CH<sub>2</sub>CH<sub>2</sub>), 41.1 (CH<sub>2</sub>, CH<sub>2</sub>CH<sub>2</sub>CH<sub>2</sub>), 61.6 (1C, CH<sub>2</sub>C(CH<sub>3</sub>)<sub>2</sub>NH<sub>2</sub>), 66.7 (CH<sub>2</sub>, PhCH<sub>2</sub>), 127.1, 128.1, 128.4, 128.6 (5CH, Ph), 136.7 (1C, Ph), 156.7 (1C, OC=O).

**HRMS** (TOF MS ES<sup>+</sup>):  $m/z$  calculated for C<sub>14</sub>H<sub>23</sub>N<sub>2</sub>O<sub>2</sub> [M+H]<sup>+</sup>: 251.1754; found: 251.1754 (-0.2 ppm).

### H-NgLys(Boc)-Ntbu-Ntbu-OBn 35



Compound **28** was synthesised starting from compound **4** (1.20 g, 2.63 mmol, 1.0 equiv.) by application of the **General Procedure A** using compound **32** (2.28 g, 10.35 mmol, 4.0 equiv) as primary amine. Purification by flash chromatography on silica gel (eluent: CH<sub>2</sub>Cl<sub>2</sub>/MeOH 95:05) gave the compound **35** as a yellow liquid (1.31 g, 2.21 mmol, 84%).

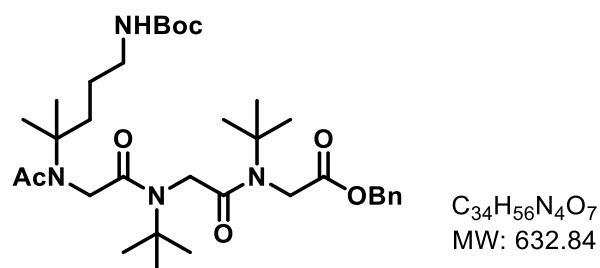
**TLC** R<sub>f</sub> = 0.37 (Cyclohexane/EtOAc, 8:2)

**<sup>1</sup>H NMR** (400 MHz, CDCl<sub>3</sub>)  $\delta$ (ppm): 1.25 (s, 6H, C(CH<sub>3</sub>)<sub>2</sub>), 1.33, 1.37, 1.39 (3×s, 27H, 3×*t*Bu), 1.44-1.67 (m, 4H, NH CH<sub>2</sub>CH<sub>2</sub>CH<sub>2</sub>), 3.10 (m, 2H, NHCH<sub>2</sub>CH<sub>2</sub>), 3.54 (bs, 2H, NHCH<sub>2</sub>CO), 4.05 (s, 2H, NCH<sub>2</sub>CO), 4.13 (s, 2H, NCH<sub>2</sub>CO), 4.94 (s, 1H, NHCH<sub>2</sub>), 5.19 (s, 2H, PhCH<sub>2</sub>), 6.84 (bs, 1H, BocNH), 7.34-7.36 (m, 5H, Ph).

**<sup>13</sup>C NMR** (100 MHz, CDCl<sub>3</sub>)  $\delta$ (ppm): 24.2 (CH<sub>2</sub>, CH<sub>2</sub>CH<sub>2</sub>CH<sub>2</sub>), 24.2 (2CH<sub>3</sub>, CH<sub>2</sub>C(CH<sub>3</sub>)<sub>2</sub>NH), 28.1, 28.2, 28.4 (9 CH<sub>3</sub>, *t*Bu), 36.5 (CH<sub>2</sub>, CH<sub>2</sub>CH<sub>2</sub>CH<sub>2</sub>C(CH<sub>3</sub>)<sub>2</sub>), 40.6 (CH<sub>2</sub>, CH<sub>2</sub>CH<sub>2</sub>CH<sub>2</sub>C(CH<sub>3</sub>)<sub>2</sub>), 44.0, 46.4, 48.2 (3 CH<sub>2</sub>, 3×NCH<sub>2</sub>C=O), 58.7, 59.0 (3C, NC(CH<sub>3</sub>)<sub>3</sub>, 2×C(CH<sub>3</sub>)<sub>2</sub>), 67.8 (CH<sub>2</sub>, PhCH<sub>2</sub>), 79.0 (1C, *t*Bu), 128.7, 128.7, 128.8 (5CH, Ph), 134.9 (1C, Ph), 156.0 (1C, OC=ONH), 167.9, 168.7, 170.3 (3C, 2×NC=O, BnOC=O).

**HRMS** (TOF MS ES<sup>+</sup>):  $m/z$  calculated for C<sub>32</sub>H<sub>54</sub>N<sub>4</sub>O<sub>6</sub> [M+H]<sup>+</sup>: 591.4122 ; found: 591.4141 3.2 ppm).

### Ac-NgLys(Boc)-Ntbu-Ntbu-OBn 36



Compound **36** was synthesised starting from compound **35** (100 mg, 0.17 mmol, 1 equiv) by application of **General Procedure D** using EtOAc as solvent. The crude was subjected to flash chromatography (EtOAc 100 %) to yield compound **36** (68 mg, 0.108 mmol, 64%).

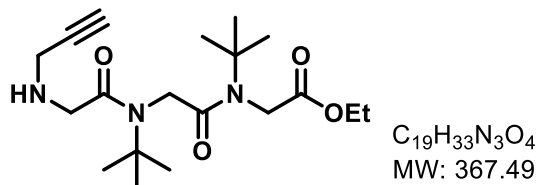
**TLC** R<sub>f</sub> = 0.6 (EtOAc 100 %)

**<sup>1</sup>H NMR** (400 MHz, CDCl<sub>3</sub>)  $\delta$ (ppm): 1.31 (s, 6H, C(CH<sub>3</sub>)<sub>2</sub>), 1.36, 1.38 (2×s, 27H, 3×*t*Bu), 1.24 – 1.50 (m, 4H, NHCH<sub>2</sub>CH<sub>2</sub>CH<sub>2</sub>), 1.92 (s, 3H, Ac), 3.06 (m, 2H, NHCH<sub>2</sub>), 3.77 (s, 2H, NCH<sub>2</sub>C=O), 3.90 (s, 2H, NCH<sub>2</sub>C=O), 4.08 (s, 2H, NCH<sub>2</sub>C=O), 4.80 (s, 1H, NHCH<sub>2</sub>), 5.19 (s, 2H, PhCH<sub>2</sub>), 7.36 (s, 5H, Ph).

**<sup>13</sup>C NMR** (100 MHz, CDCl<sub>3</sub>)  $\delta$ (ppm): 25.0 (CH<sub>2</sub>, CH<sub>2</sub>CH<sub>2</sub>CH<sub>2</sub>), 25.2 (CH<sub>3</sub>, Ac), 26.9 (2CH<sub>3</sub>, CH<sub>2</sub>C(CH<sub>3</sub>)<sub>2</sub>NH), 28.4, 28.5 (9 CH<sub>3</sub>, 3×*t*Bu), 37.1 (CH<sub>2</sub>, CH<sub>2</sub>CH<sub>2</sub>CH<sub>2</sub>C(CH<sub>3</sub>)<sub>2</sub>), 41.0 (CH<sub>2</sub>, CH<sub>2</sub>CH<sub>2</sub>CH<sub>2</sub>C(CH<sub>3</sub>)<sub>2</sub>), 46.3, 48.1, 50.5 (3CH<sub>2</sub>, 3×NCH<sub>2</sub>C=O), 58.1, 58.7, 60.1 (3C, 2×*t*Bu, C(CH<sub>3</sub>)<sub>2</sub>), 67.8 (CH<sub>2</sub>, PhCH<sub>2</sub>), 78.9 (1C, Boc), 128.7, 128.9, 129.0 (5CH, Ph), 134.9 (1C, Ph), 156.2 (1C, OC=ONH), 169.1, 169.8, 170.3 (3C, 2×NC=O, NC=OCH<sub>3</sub>), 172.7 (1C, BnOC=O).

**HRMS** (TOF MS ES<sup>+</sup>): *m/z* calculated for C<sub>34</sub>H<sub>57</sub>N<sub>4</sub>O<sub>7</sub> [M+H]<sup>+</sup>: 633.4227; found: 633.4224 (-0.5 ppm).

### H-(Nem-NtBu-NtBu)-OEt **37**



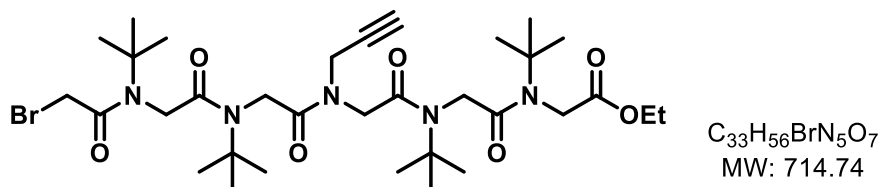
Compound **37** was synthesised starting from compound **4** (1 g, 2.54 mmol, 1.0 equiv.) by application of the **General Procedure A** using propargyl amine (0.56 g, 10.16 mmol, 4.0 equiv) as primary amine. The compound **37** was obtained as

yellow liquid (0.64 g, 1.72 mmol, 68%).

**TLC** R<sub>f</sub> = 0.52 (EtOAc/MeOH, 95:5)

**<sup>1</sup>H NMR** (400 MHz, CDCl<sub>3</sub>)  $\delta$ (ppm): 1.32 (t, *J* = 7.1 Hz, 3H, OCH<sub>2</sub>CH<sub>3</sub>), 1.43 (s, 18H, 2×*t*Bu), 2.20 (s, 1H, C≡CH), 3.34 (s, 2H, CH<sub>2</sub>C≡CH), 3.48 (s, 2H, NHCH<sub>2</sub>CO), 4.01 (s, 2H, NCH<sub>2</sub>CO), 4.04 (s, 2H, NCH<sub>2</sub>CO), 4.25 (q, *J* = 7.1 Hz, 2H, OCH<sub>2</sub>CH<sub>3</sub>).

### BrCH<sub>2</sub>OC(NtBu-NtBu-Nem-NtBu-NtBu)OEt **38**



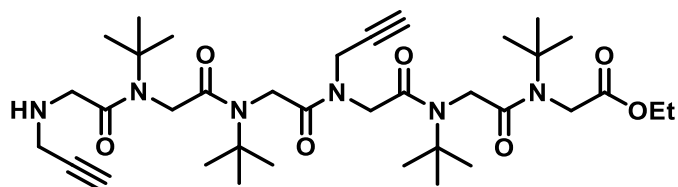
Compound **38** was synthesised by starting from compound **37** (0.64 g, 1.73 mmol) by repetitive application of the **General**

**Procedure A** using tert-butyl as primary amine and **General Procedure B** to elongate the oligomer until the bromo derivative **38**. The compound **38** was obtained as yellow viscous liquid (0.97 g, 1.36 mmol, 79%).

**TLC** R<sub>f</sub> = 0.42 (Cyclohexane/EtOAc, 1:1)

**<sup>1</sup>H NMR** (400 MHz, CDCl<sub>3</sub>)  $\delta$ (ppm): 1.26 (t, *J* = 7.1 Hz, 3H, OCH<sub>2</sub>CH<sub>3</sub>), 1.36 – 1.47 (m, 36H, 4×*t*Bu), 2.22 (t, *J* = 2.5 Hz, 0.5H, C≡CH, 1 conformer), 2.35 (t, *J* = 2.3 Hz, 0.5H, C≡CH, 1 conformer), 3.72 – 4.30 (m, 16H, 6×NCH<sub>2</sub>CO, OCH<sub>2</sub>CH<sub>3</sub>, CH<sub>2</sub>C≡CH).

### H-(Nem-Ntbu-Ntbu)<sub>2</sub>-OEt 39



C<sub>36</sub>H<sub>60</sub>N<sub>6</sub>O<sub>7</sub>

MW: 688.91

Compound **39** was synthesised starting from compound **37** (0.97 g, 1.36 mmol, 1.0 equiv.) by application of the **General**

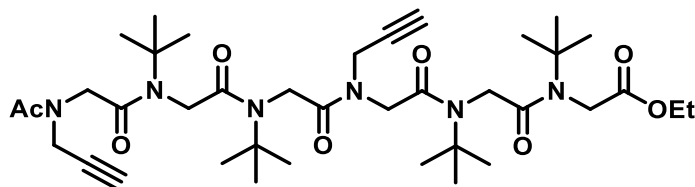
**Procedure A** using propargylamine (0.30 g, 5.46 mmol, 4.0 equiv) as primary amine. Purification by flash chromatography on silica gel (eluent: AcOEt/MeOH 95:05) gave the compound **39** as a yellow liquid (0.56 g, 0.80 mmol, 59%).

**TLC** R<sub>f</sub> = 0.53 (EtOAc/MeOH, 95:5).

**<sup>1</sup>H NMR** (400 MHz, CDCl<sub>3</sub>) δ(ppm): 1.33 (t, *J* = 7.1 Hz, 3H, OCH<sub>2</sub>CH<sub>3</sub>), 1.36 – 1.50 (m, 36H, 4×*t*Bu), 2.15 (s, 1H, NH), 2.22 (t, *J* = 2.6 Hz, 0.8H, C≡CH, 1 conformer), 2.35 (t, *J* = 2.5 Hz, 0.2H, C≡CH, 1 conformer), 3.28 (s, 2H, NHCH<sub>2</sub>C≡CH), 3.41 (s, 2H, NHCH<sub>2</sub>CO), 3.89 – 4.20 (m, 12H, 5×NCH<sub>2</sub>CO, NCH<sub>2</sub>C≡CH), 4.22 – 4.37 (m, 2H, OCH<sub>2</sub>CH<sub>3</sub>).

**HRMS** (TOF MS ES<sup>+</sup>): *m/z* calculated for C<sub>36</sub>H<sub>61</sub>N<sub>6</sub>O<sub>7</sub> [M+H]<sup>+</sup>: 689.4596; found: 689.4596 (-0.04 ppm).

### Ac-(Nem-Ntbu-Ntbu)<sub>2</sub>-OEt 40



C<sub>38</sub>H<sub>62</sub>N<sub>6</sub>O<sub>8</sub>

MW: 730.94

Compound **40** was synthesised starting from compound **39** (250 mg, 0.36 mmol, 1 equiv) by application of

**General Procedure C** using EtOAc as solvent. The crude was subjected to flash chromatography (EtOAc 100 %) to yield compound **36** (242 mg, 0.33 mmol, 92%).

3 conformers are observed by NMR in a 42/29/29 (*cis/trans/trans*) ratio

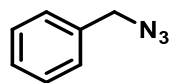
**TLC** R<sub>f</sub> = 0.53 (EtOAc 100 %)

**<sup>1</sup>H NMR** (400 MHz, CDCl<sub>3</sub>) δ(ppm): 1.23 (2×t, *J* = 7.1 Hz, 3H, OCH<sub>2</sub>CH<sub>3</sub>, conformers), 1.30 – 1.44 (m, 36H, 4×*t*Bu), 1.99/2.02/2.13 (3×s, 3H, NAc, conformers), 2.15 – 2.36 (m, 2H, 2×C≡CH), 3.82-4.20 (m, 16H, 2×NCH<sub>2</sub>C≡CH, 6×NCH<sub>2</sub>CO), 4.22-4.34 (m, 2H, OCH<sub>2</sub>CH<sub>3</sub>).

**<sup>13</sup>C NMR** (100 MHz, CDCl<sub>3</sub>) δ(ppm): 14.1, 14.2 (CH<sub>3</sub>, OCH<sub>2</sub>CH<sub>3</sub>), 21.1, 21.5 (CH<sub>3</sub>, Ac), 28.2, 28.2, 28.3, 28.4 (12 CH<sub>3</sub>, 4×*t*Bu), 35.4, 36.5 (2CH<sub>2</sub>, 2×NCH<sub>2</sub>C≡CH), 46.1, 48.1, 48.6, 50.2 (6 CH<sub>2</sub>, 6×NCH<sub>2</sub>CO), 58.0, 58.2, 58.6, 58.9 (4C, 4×NC(CH<sub>3</sub>)<sub>3</sub>), 62.2 (CH<sub>2</sub>, OCH<sub>2</sub>CH<sub>3</sub>), 71.9, 73.0 (2CH, 2×NCH<sub>2</sub>C≡CH), 78.7, 79.4 (2C, 2×NCH<sub>2</sub>C≡CH), 168.6, 169.4, 169.6, 170.4 (5C, 5×NC=O), 171.2 (1C, CH<sub>3</sub>C=O), 171.8 (1C, EtOC=O).

**HRMS** (TOF MS ES<sup>+</sup>):  $m/z$  calculated for C<sub>38</sub>H<sub>63</sub>N<sub>6</sub>O<sub>8</sub> [M+H]<sup>+</sup>: 731.4702; found: 731.4700 (-0.22 ppm).

### Benzyl azide **41**



C<sub>7</sub>H<sub>7</sub>N<sub>3</sub>  
MW: 133.15

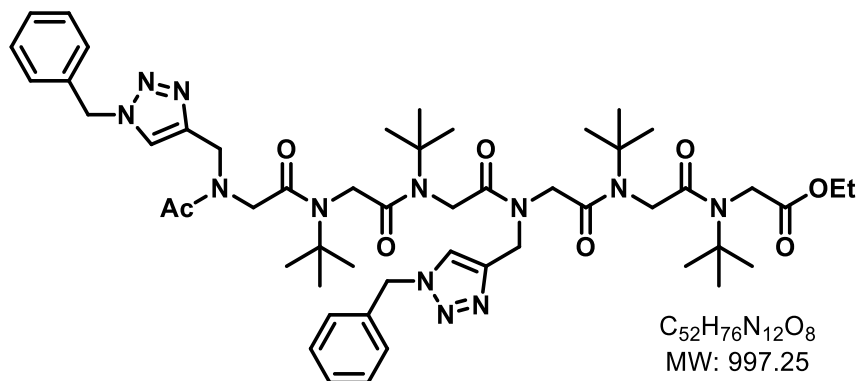
To a suspension of benzyl chloride (1.00 g, 7.9 mmol, 1 equiv) in water (1.5 M) were added NaN<sub>3</sub> (0.54 g, 8.3 mmol, 1.05 equiv) and NH<sub>4</sub>Cl (0.85 g, 15.8 mmol, 2 equiv) and the resulting mixture was stirred vigorously at 70°C for 48h. After cooling to rt, the aqueous layer was extracted with Et<sub>2</sub>O (3x10 mL). The combined organic layers were dried over MgSO<sub>4</sub>, filtered, and concentrated carefully under reduced pressure at room temperature. The remaining Et<sub>2</sub>O was evaporated overnight under a fume hood yielding benzyl azide (0.98 g, 7.8 mmol, 94 %) as a colourless liquid.

**TLC** R<sub>f</sub> = 0.55 (pentane).

**<sup>1</sup>H NMR** (400 MHz, CDCl<sub>3</sub>) δ(ppm): 4.34 (s, 2H, PhCH<sub>2</sub>N<sub>3</sub>), 7.29-7.44 (m, 5H, C<sub>6</sub>H<sub>5</sub>).

Spectroscopic data are consistent with those reported in the literature.<sup>127</sup>

### Ac-(Nbtm-Ntbu-Ntbu)<sub>2</sub>-OEt **42**



C<sub>52</sub>H<sub>76</sub>N<sub>12</sub>O<sub>8</sub>  
MW: 997.25

Compound **42** was synthesised starting from compound **40** (100 mg, 0.136 mmol, 1 equiv) by application of the **General Procedure F** using compound **41** as azide (55 mg, 0.41 mmol, 3 equiv). The crude was subjected to

flash chromatography (EtOAc/MeOH 90:10) to yield compound **42** was obtained as a white foam (133 mg, 0.132 mmol, 97%).

**TLC** R<sub>f</sub> = 0.63 (EtOAc/MeOH, 9:1)

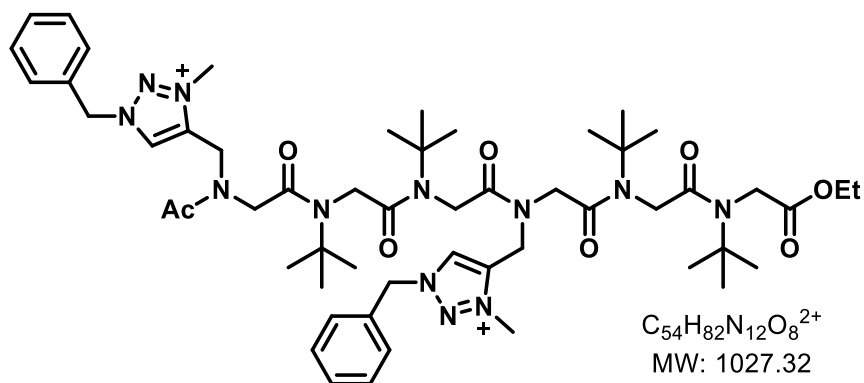
**<sup>1</sup>H NMR** (400 MHz, MeOD) δ(ppm): 1.13 – 1.45 (m, 39H, CH<sub>2</sub>CH<sub>3</sub> and 4×*t*Bu), 1.94/1.98/2.25/2.28 (4×s, 3H, NAc, 4 conformers), 4.06 – 4.81 (m, 18H, 6×NCH<sub>2</sub>CO, CH<sub>2</sub>CH<sub>3</sub> and 2×NCH<sub>2</sub>-triazole), 5.45 – 5.61 (m, 4H, 2×PhCH<sub>2</sub>), 7.23 – 7.39 (m, 10H, 2×Ar), 7.80 – 8.06 (m, 2H, 2×C=CHN).

**<sup>13</sup>C NMR** (100 MHz, CDCl<sub>3</sub>) δ(ppm): 14.2 (CH<sub>3</sub>, OCH<sub>2</sub>CH<sub>3</sub>), 21.5, 21.6, 21.9 (CH<sub>3</sub>, Ac), 28.2, 28.3, 28.3, 29.7 (12CH<sub>3</sub>, 4×*t*Bu), 42.5, 42.6, 42.6 (2CH<sub>2</sub>, 2×NCH<sub>2</sub>-triazole), 46.1, 46.2, 46.3, 48.0, 48.1, 50.0, 52.2, 52.3 (6CH<sub>2</sub>, 6×NCH<sub>2</sub>CO), 53.5, 53.9, 54.0, 54.1, 54.3 (2CH<sub>2</sub>, 2×NCH<sub>2</sub>C<sub>6</sub>H<sub>5</sub>),

57.9, 58.0, 58.0, 58.2, 58.3, 58.4, 58.5, 58.7, 58.7 (4C, 4×NC(CH<sub>3</sub>)<sub>3</sub>), 61.9, 62.3 (1CH<sub>2</sub>, OCH<sub>2</sub>CH<sub>3</sub>), 123.3, 123.8 (2CH, 2×C=CHN), 127.8, 128.0, 128.0, 128.1, 128.3, 128.5, 128.6, 128.6, 128.9, 128.9, 129.0, 129.0, 129.1, 129.2 (10CH, 2×NCH<sub>2</sub>C<sub>6</sub>H<sub>5</sub>), 134.4, 134.6, 134.8 (2C, 2×NCH<sub>2</sub>C<sub>6</sub>H<sub>5</sub>), 143.0, 145.0 (2C, 2×C=CHN), 168.2, 168.4, 168.9, 169.1, 169.4, 170.2 (5C, 5×NC=O), 171.3 (1C, CH<sub>3</sub>C=O), 172.3 (1C, EtOC=O).

**HRMS** (TOF MS ES<sup>+</sup>): *m/z* calculated for C<sub>52</sub>H<sub>77</sub>N<sub>12</sub>O<sub>8</sub> [M+H]<sup>+</sup>: 997.5981; found: 997.5955 (-2.67 ppm).

**Ac-(Nbtm<sup>+</sup>-Ntbu-Ntbu)<sub>2</sub>-OEt 43**



Compound **43** was synthesised starting from compound **42** (97 mg, 0.097 mmol, 1 equiv) by application of the **General Procedure G**. The crude was subjected to flash chromatography (CH<sub>2</sub>Cl<sub>2</sub>/MeOH 9:1) to yield

compound **43** was obtained as a white foam (114 mg, 0.097 mmol, 100%).

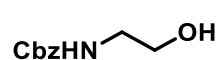
**TLC** R<sub>f</sub> = 0.22 (EtOAc/MeOH, 95:5)

**<sup>1</sup>H NMR** (400 MHz, CD<sub>3</sub>CN) δ(ppm): 1.22 (s, 9H, *t*Bu), 1.24 (m, 3H, CH<sub>2</sub>CH<sub>3</sub>), 1.27 (s, 9H, *t*Bu), 1.31 (s, 9H, *t*Bu), 1.42 (s, 9H, *t*Bu), 1.90/2.11 (2×s, 3H, NAc, conformer), 3.67 – 4.51 (m, 24H, 6×NCH<sub>2</sub>CO, CH<sub>2</sub>CH<sub>3</sub>, 2×NCH<sub>2</sub>-triazolium and 2×NCH<sub>3</sub>), 5.69 (s, 2H, PhCH<sub>2</sub>), 5.72 (s, 2H, PhCH<sub>2</sub>), 7.45 (s, 10H, 2×Ar), 8.38 – 8.67 (m, 2H, 2×C=CHN).

**<sup>13</sup>C NMR** (100 MHz, CD<sub>3</sub>CN) δ(ppm): 14.3, 14.5 (CH<sub>3</sub>, CH<sub>2</sub>CH<sub>3</sub>), 21.6, 23.3 (CH<sub>3</sub>, Ac), 28.3, 28.4, 28.5, 29.6, 29.7, 30.0, 30.1, 30.2 (12 CH<sub>3</sub>, 4×*t*Bu), 39.5, 39.7, 40.9, 41.0 (2CH<sub>3</sub>, 2×N<sup>+</sup>CH<sub>3</sub>), 47.8, 49.7, 53.1 (8CH<sub>2</sub>, 6×NCH<sub>2</sub>CO, 2×NCH<sub>2</sub>-triazolium), 53.8, 55.3 (2CH<sub>2</sub>, 2×NCH<sub>2</sub>C<sub>6</sub>H<sub>5</sub>), 57.7, 58.7, 58.8, 59.0, 59.1 (4C, 4×NC(CH<sub>3</sub>)<sub>3</sub>), 62.5 (1CH<sub>2</sub>, CH<sub>2</sub>CH<sub>3</sub>), 130.0, 130.1, 130.1, 130.5 (10CH, 2×NCH<sub>2</sub>C<sub>6</sub>H<sub>5</sub>), 131.5, 131.5 (2CH, 2×C=CHN), 133.0, 133.1 (2C, 2×NCH<sub>2</sub>C<sub>6</sub>H<sub>5</sub>), 141.4, 141.6 (2C, 2×C=CHN), 169.4, 169.7, 170.9, 171.6 (5C, 5×NC=O), 172.5 (1C, CH<sub>3</sub>C=O), 173.5 (1C, EtOC=O).

**HRMS** (TOF MS ES<sup>+</sup>): *m/z* calculated for C<sub>51</sub>H<sub>82</sub>N<sub>12</sub>O<sub>8</sub><sup>2+</sup> [M]<sup>2+</sup>: 513.3183; found: 513.3179 (-0.87 ppm).

### Benzyl 2-hydroxyethylcarbamate **44**



$C_{10}H_{13}NO_3$   
MW: 195.21

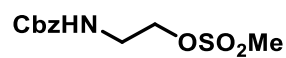
To a stirred solution of 2-aminoethanol (5.05 g, 82.67 mmol, 1 equiv) in  $CH_2Cl_2$  (50 mL) at  $0^\circ C$ , triethylamine (16.31 g, 161.2 mmol, 1.95 equiv) was added dropwise. Benzyloxy carbonyl chloride (18.34 g, 106.42 mmol, 1.3 equiv) was added dropwise over 30 min. After completion of the addition, the mixture was stirred at  $0^\circ C$  for 1 h. The mixture was quenched with water (50 mL) and extracted with  $CH_2Cl_2$  ( $3 \times 50$  mL). The combined organic layers were washed with brine, dried over anhydrous  $MgSO_4$ , filtered, and concentrated under reduced pressure. The residue was purified by flash column chromatography (eluent, cyclohexane/EtOAc 1:1). The desired product **44** was obtained as white solid (4.54 g, 23 mmol, 28 %).

TLC  $R_f = 0.14$  (Cyclohexane/EtOAc, 6:4)

$^1H$  NMR (400 MHz,  $CDCl_3$ )  $\delta$ (ppm): 1.83 (s, 1H, OH), 3.36 (t,  $J = 6.1$  Hz, 2H,  $NHCH_2$ ), 3.71 (t,  $J = 5.0$  Hz, 2H,  $NHCH_2CH_2$ ), 5.10 (s, 2H,  $PhCH_2$ ), 5.24 (s, 1H, NH), 7.27 – 7.41 (m, 5H, Ar).

The spectroscopic data was found in accordance with the literature.<sup>142</sup>

### 2-(Benzyloxycarbonylamino)ethyl methanesulfonate **45**



$C_{11}H_{15}NO_5S$   
MW: 273.30

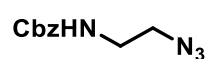
To a stirred solution of compound **44** (4.54 g, 23.25 mmol, 1 equiv) in  $CH_2Cl_2$  (60 mL) at  $0^\circ C$ , triethylamine (3.53 g, 34.88 mmol, 1.5 equiv) was added dropwise. Methane sulfonyl chloride (3.19 g, 27.9 mmol, 1.2 equiv) was then added dropwise to the reaction mixture over 30 min. After completion of the addition, the mixture was stirred at  $0^\circ C$  for 1 h. The mixture was quenched with water (60 mL) and extracted with  $CH_2Cl_2$  ( $3 \times 60$  mL). The combined organic layer extracts were washed with brine, dried over anhydrous  $MgSO_4$ , filtered, and concentrated under reduced pressure. The residue was purified by flash column chromatography (eluent, cyclohexane/EtOAc 1:1). The desired product **45** was obtained (5.90 g, 22 mmol, 93%).

TLC  $R_f = 0.48$  (Cyclohexane/EtOAc, 1:1)

$^1H$  NMR (400 MHz,  $CDCl_3$ )  $\delta$ (ppm): 2.99 (s, 3H,  $CH_3$ ), 3.55 (q,  $J = 5.4$  Hz, 2H,  $NHCH_2$ ), 4.30 (t,  $J = 5.1$  Hz, 2H,  $NHCH_2CH_2$ ), 5.12 (s, 2H,  $PhCH_2$ ), 5.20 (bs, 1H, NH), 7.28 – 7.42 (m, 5H, Ar).

The spectroscopic data was found in accordance with the literature.<sup>143</sup>

### Benzyl (2-azidoethyl)carbamate **46**



$C_{10}H_{12}N_4O_2$   
MW: 220.23

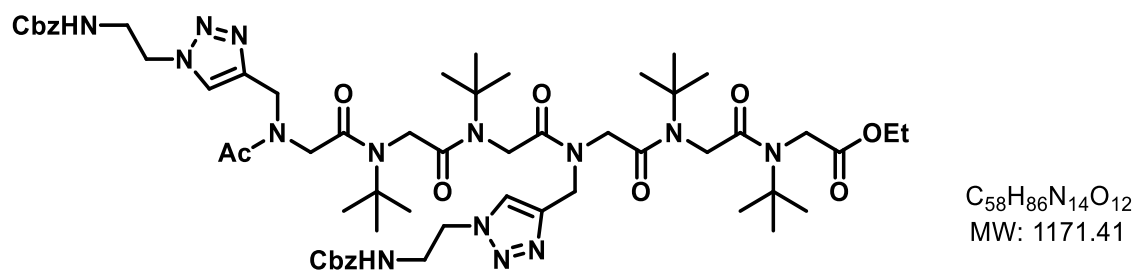
A mixture of sodium azide (1.90 g, 29.27 mmol, 4 equiv) and compound **45** (2 g, 7.32 mmol, 1 equiv) in DMSO (20 mL) was stirred at  $70^\circ C$  for 2 h. The mixture was cooled to room temperature, quenched with water (80 mL), and then extracted with ethyl acetate ( $3 \times 80$  mL). The combined organic layer extracts were

washed with brine, dried over anhydrous  $\text{MgSO}_4$ , filtered, and concentrated carefully under reduced pressure. The desired product **46** was obtained as a colourless oil (1.53 g, 7 mmol, 95 %).

$^1\text{H NMR}$  (400 MHz,  $\text{CDCl}_3$ )  $\delta$ (ppm): 3.37 (t,  $J = 5.6$  Hz, 2H,  $\text{NHCH}_2$ ), 3.45 (t,  $J = 5.6$  Hz, 2H,  $\text{NHCH}_2\text{CH}_2$ ), 5.06 (s, 1H,  $\text{NH}$ ), 5.11 (s, 2H,  $\text{PhCH}_2$ ), 7.29 – 7.41 (m, 5H, Ar).

The spectroscopic data was found in accordance with the literature.<sup>141</sup>

#### Ac-(Naetm(Cbz)-NtBu-NtBu)<sub>2</sub>-OEt **47**



Compound **47** was synthesised starting from compound **40** (100 mg, 0.136 mmol, 1 equiv) by application of the **General Procedure F** using compound **46** as azide (90 mg, 0.41 mmol, 3 equiv). The crude was subjected to flash chromatography (EtOAc/MeOH 95:5, then 9:1) to yield compound **47** was obtained as a white foam (63 mg, 0.054 mmol, 40%).

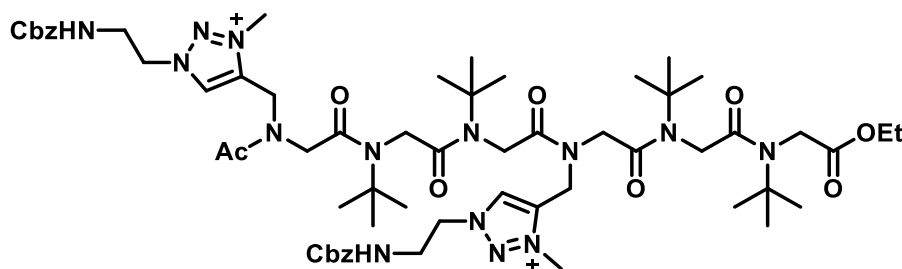
**TLC**  $R_f = 0.1$  (EtOAc, 100%)

$^1\text{H NMR}$  (400 MHz,  $\text{CD}_3\text{CN}$ )  $\delta$ (ppm): 1.20 (m, 3H,  $\text{OCH}_2\text{CH}_3$ ), 1.22 – 1.40 (m, 36H,  $4 \times t\text{Bu}$ ), 1.86/1.88/2.18/2.20 (4 $\times$ s, 3H, NAc, conformers), 3.32 – 3.63 (m, 4H,  $2 \times \text{CbzNHCH}_2\text{CH}_2$ ), 3.75 – 4.27 (m, 14H,  $6 \times \text{NCH}_2\text{CO}$  and  $\text{OCH}_2\text{CH}_3$ ), 4.27 – 4.76 (m, 8H,  $2 \times \text{CbzNHCH}_2\text{CH}_2$  and  $2 \times \text{NCH}_2$ -triazole), 5.01 (s, 4H,  $2 \times \text{PhCH}_2$ ), 5.94 (s, 2H,  $2 \times \text{NH}$ ), 7.22 – 7.43 (m, 10H,  $2 \times \text{Ar}$ ), 7.56 – 7.80 (m, 2H,  $2 \times \text{C}=\text{CHN}$ ).

$^{13}\text{C NMR}$  (100 MHz,  $\text{CD}_3\text{CN}$ )  $\delta$ (ppm): 14.4 ( $\text{CH}_3$ ,  $\text{CH}_2\text{CH}_3$ ), 21.8 ( $\text{CH}_3$ , Ac), 28.3, 28.5, 28.5, 28.5, 28.6, 28.6, 28.6, 28.7 (12 $\text{CH}_3$ ,  $4 \times t\text{Bu}$ ), 38.5, 39.2 ( $2\text{CH}_2$ ,  $2 \times \text{CbzNHCH}_2\text{CH}_2$ ), 41.7, 41.8, 41.8, 42.2, 42.3, 43.2, 43.3, 43.9, 43.9 ( $2\text{CH}_2$ ,  $2 \times \text{NCH}_2$ -triazole), 46.3, 47.1, 47.2, 48.9, 49.1, 49.1, 50.4, 50.4, 50.4 (8 $\text{CH}_2$ ,  $6 \times \text{NCH}_2\text{CO}$ ,  $2 \times \text{CbzNHCH}_2\text{CH}_2$ ), 56.5, 58.4, 58.5, 58.5, 58.5, 58.9 (4C,  $4 \times \text{NC}(\text{CH}_3)_3$ ), 62.6 ( $1\text{CH}_2$ ,  $\text{CH}_2\text{CH}_3$ ), 66.9, 67.0, 67.0 ( $2\text{CH}_2$ ,  $2 \times \text{NCH}_2\text{C}_6\text{H}_5$ ), 124.7, 125.2 ( $2\text{CH}$ ,  $2 \times \text{C}=\text{CHN}$ ), 128.7, 128.9, 129.5 (10 $\text{CH}$ ,  $2 \times \text{NCH}_2\text{C}_6\text{H}_5$ ), 130.7, 132.0, 134.3, 135.1 ( $2\text{C}$ ,  $2 \times \text{NCH}_2\text{C}_6\text{H}_5$ ), 138.2, 139.6 ( $2\text{C}$ ,  $2 \times \text{C}=\text{CHN}$ ), 157.3, 157.3, 157.4, 158.0 ( $2\text{C}$ ,  $2 \times \text{BnOC}=\text{ONH}$ ), 165.6, 170.7, 170.8, 170.8, 170.9, 171.5, 171.6 (5C,  $5 \times \text{NC}=\text{O}$ ), 172.3, 172.4 (1C,  $\text{CH}_3\text{C}=\text{O}$ ), 172.8 (1C,  $\text{EtOC}=\text{O}$ ).



**Ac-(Naetm<sup>+</sup>(Cbz)-Ntbu-Ntbu)<sub>2</sub>-OEt 48**



C<sub>60</sub>H<sub>92</sub>N<sub>14</sub>O<sub>12</sub><sup>2+</sup>  
MW: 1201.48

Compound **48** was synthesised starting from compound **47** (54 mg, 0.046 mmol, 1 equiv) by application of the **General Procedure G**. The crude was purified by using flash chromatography (CH<sub>2</sub>Cl<sub>2</sub>/MeOH, 9:1). The compound **48** was obtained as a white foam (30 mg, 0.024 mmol, 53%).

**TLC** R<sub>f</sub> = 0.4 (DCM/MeOH, 9:1)

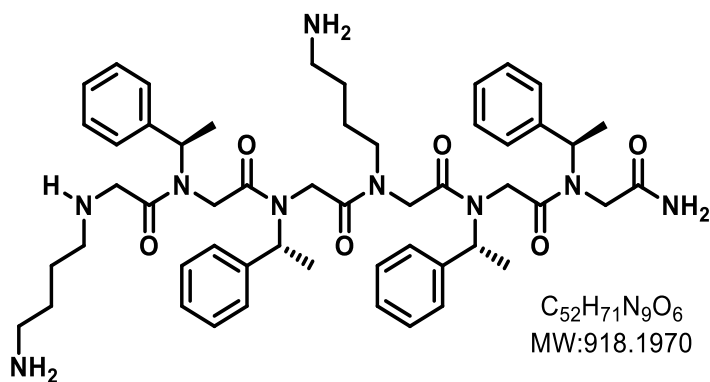
**<sup>1</sup>H NMR** (400 MHz, CD<sub>3</sub>CN) δ(ppm): 1.17 – 1.50 (m, 39H, CH<sub>2</sub>CH<sub>3</sub> and 4×*t*Bu), 2.20 (s, 3H, NAc), 3.62 – 3.72 (m, 4H, 2×CbzNHCH<sub>2</sub>CH<sub>2</sub>), 3.76 – 4.89 (m, 28H, 6×NCH<sub>2</sub>CO, 2×CbzNHCH<sub>2</sub>CH<sub>2</sub>, CH<sub>2</sub>CH<sub>3</sub>, 2×N<sup>+</sup>CH<sub>3</sub> and 2×NCH<sub>2</sub>-triazolium), 5.02 – 5.10 (m, 4H, 2×PhCH<sub>2</sub>), 6.03 – 6.44 (m, 2H, NH), 7.20 – 7.52 (m, 10H, 2×Ar), 8.42 – 8.78 (m, 2H, 2×C=CHN).

**<sup>13</sup>C NMR** (100 MHz, CDCl<sub>3</sub>) δ(ppm): 13.1 (CH<sub>3</sub>, CH<sub>2</sub>CH<sub>3</sub>), 20.2 (CH<sub>3</sub>, Ac), 27.1, 27.3, 27.3 (12CH<sub>3</sub>, 4×*t*Bu), 37.8, 37.8 (2CH<sub>2</sub>, 2×CbzNHCH<sub>2</sub>CH<sub>2</sub>), 39.2, 39.8, 39.8, 40.9 (2CH<sub>3</sub>, 2×N<sup>+</sup>CH<sub>3</sub>), 42.5, 42.5, 42.6, 42.6, 42.7 (2CH<sub>2</sub>, 2×NCH<sub>2</sub>-triazolium), 47.0, 47.2, 47.4, 47.6, 47.8, 48.0, 48.2 (8CH<sub>2</sub>, 6×NCH<sub>2</sub>CO, 2×CbzNHCH<sub>2</sub>CH<sub>2</sub>), 53.5, 53.7, 58.3, 58.3, 58.3, 58.5, 58.6 (4C, 4×NC(CH<sub>3</sub>)<sub>3</sub>), 64.8 (1CH<sub>2</sub>, CH<sub>2</sub>CH<sub>3</sub>), 66.3 (2CH<sub>2</sub>, 2×NCH<sub>2</sub>C<sub>6</sub>H<sub>5</sub>), 124.2, 124.4 (2CH, 2×C=CHN), 127.5, 127.8, 127.8, 128.2 (10CH, 2×NCH<sub>2</sub>C<sub>6</sub>H<sub>5</sub>), 131.2, 131.4, 131.8 (2C, 2×NCH<sub>2</sub>C<sub>6</sub>H<sub>5</sub>), 139.8, 140.3 (2C, 2×C=CHN), 157.3, 158.3 (2C, 2× BnOC=ONH), 167.2, 168.1, 168.3, 168.4, 168.7, 169.5 (5C, 5×NC=O), 170.2, 171.1 (2C, CH<sub>3</sub>C=O, EtOC=O).

**HRMS** (TOF MS ES<sup>+</sup>): *m/z* calculated for C<sub>60</sub>H<sub>92</sub>N<sub>14</sub>O<sub>12</sub><sup>2+</sup> [M]<sup>2+</sup>: 600.3504; found: 600.3512(1.31 ppm).

## 5 Experimental procedures and compounds characterisations Chapter III

### Hexapeptoid H-(Nlys-Nspe-Nspe)<sub>2</sub>-NH<sub>2</sub> **49**



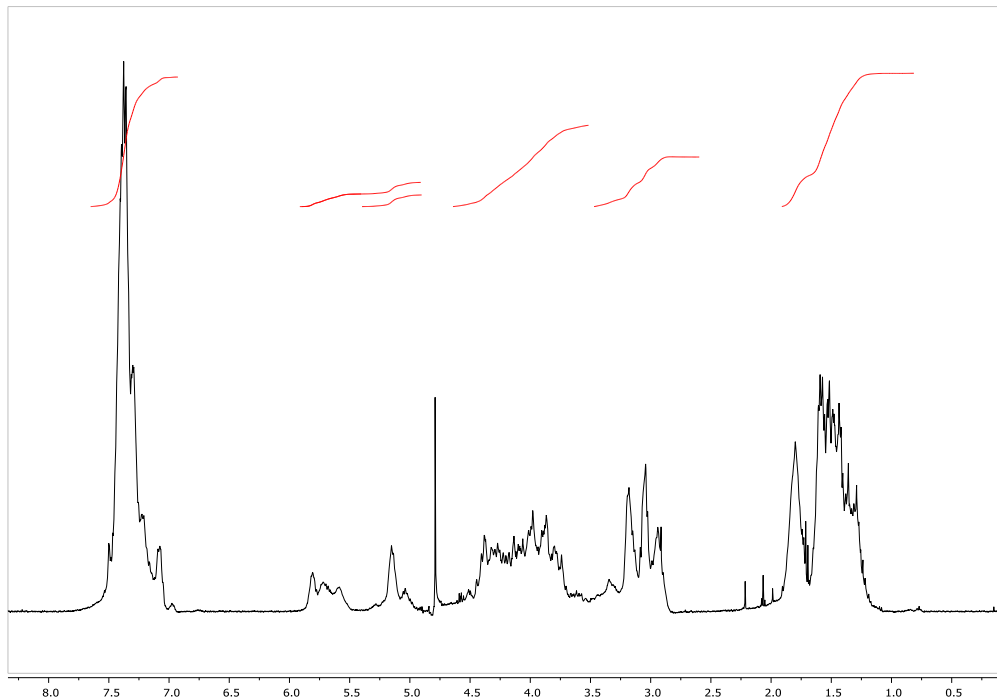
The hexapeptoid **49** was synthesised by the application of **General Procedure H** on 100 mg Rink amide resin by using successively as primary amines: (*S*)-1-phenylethylamine (2x), 1-*N*-Boc-1,4-diaminobutane **5** (1x), (*S*)-1-phenylethylamine (2x), then 1-*N*-Boc-1,4-diaminobutane **5** (1x). The hexapeptoid **49** was cleaved from the

resin by the application of **General Procedure N**. The crude mixture was analysed by LC-MS. Purification by preparative HPLC yielded hexapeptoid **49** (49 mg, 0.05 mmol, 72%).

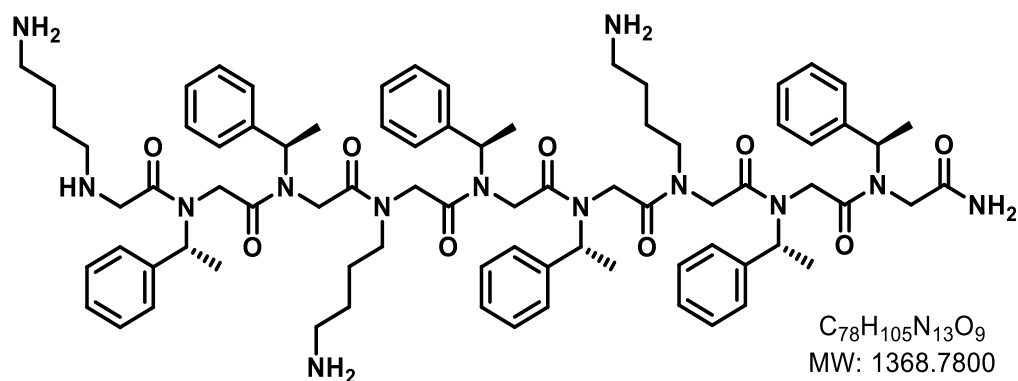
**<sup>1</sup>H NMR** (400 MHz, D<sub>2</sub>O)  $\delta$ (ppm): 0.71 – 1.95 (m, 20H, 4×CH<sub>3</sub>, 2×NCH<sub>2</sub>CH<sub>2</sub>CH<sub>2</sub>), 2.59 – 3.50 (m, 8H, 2×CH<sub>2</sub>NH<sub>2</sub>, 2×NCH<sub>2</sub>CH<sub>2</sub>), 3.51 – 4.58 (m, 12H, 6×NCH<sub>2</sub>CO), 4.75 – 5.25 (m, 1.88H, NCH, *trans* conformers), 5.35 – 5.85 (m, 2.12H, NCH, *cis* conformers), 6.90 – 7.82 (m, 20H, Ph).

**HRMS** (TOF MS ES<sup>+</sup>): *m/z* calculated for C<sub>52</sub>H<sub>72</sub>N<sub>9</sub>O<sub>6</sub> [M + H]<sup>+</sup>: 918.5606, found 918.5611 (0.5 ppm).

#### Copy of <sup>1</sup>H NMR in D<sub>2</sub>O of hexapeptoid **49**:



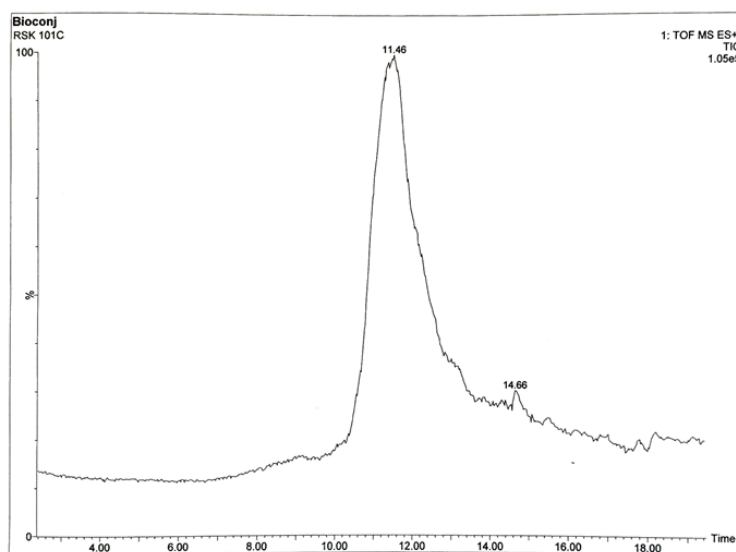
### Nonapeptoid H-(Nlys-Nspe-Nspe)<sub>3</sub>-NH<sub>2</sub> **50**

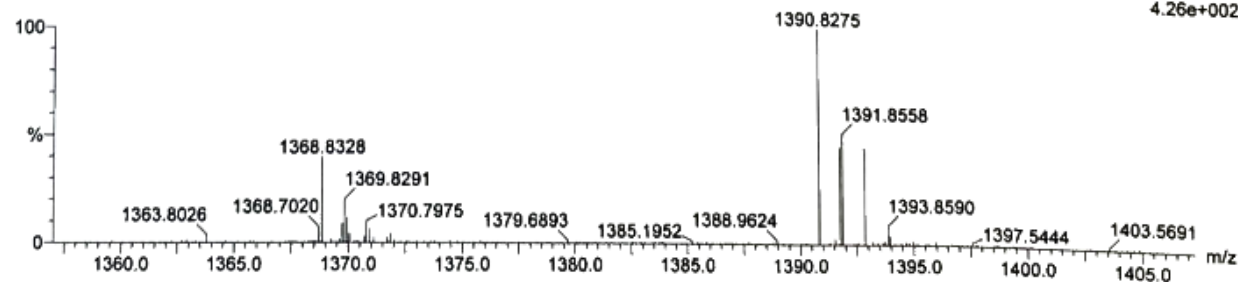


The nonapeptoid **50** was synthesised by the application of **General Procedure I** on 100 mg Rink amide MBHA resin by using successively as primary amines: (*S*)-1-phenylethylamine (2x), 1-*N*-Boc-1,4-diaminobutane **5** (1x), (*S*)-1-phenylethylamine (2x), 1-*N*-Boc-1,4-diaminobutane **5** (1x), (*S*)-1-phenylethylamine (2x), then 1-*N*-Boc-1,4-diaminobutane **5** (1x). The nonapeptoid **50** was cleaved from the resin by the application of **General Procedure N**. The crude mixture was analysed by LC-MS. Purification by preparative HPLC yielded hexapeptoid **50** (45 mg, 0.03 mmol, 42%).

**HRMS** (TOF MS ES<sup>+</sup>): *m/z* calculated for  $C_{78}H_{106}N_{13}O_9$  [M+H]<sup>+</sup>: 1368.8231; found: 1368.8234 (0.19 ppm)

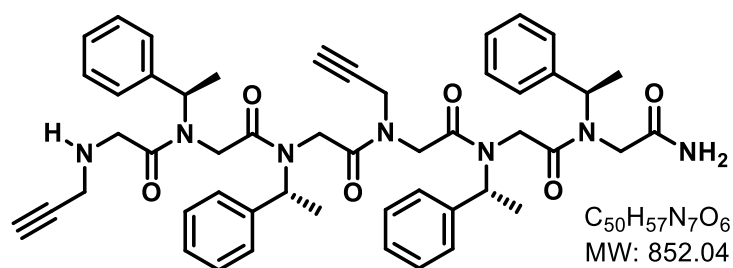
#### Copy of LCMS of nonapeptoid **50**:





Mass	Calc. Mass	mDa	PPM	DBE	i-FIT	Formula
1368.8328	1368.8236	9.2	6.7	32.5	12.8	C78 H106 N13 O9

### Hexapeptoid H-(Nem-Nspe-Nspe)<sub>2</sub>-NH<sub>2</sub> **51**



The hexapeptoid **51** was synthesised by the application of **General Procedure H'** on 100 mg Rink amide MBHA resin by using successively as primary amines: (*S*)-1-phenylethylamine (2x), propargylamine (1x), (*S*)-1-

phenylethylamine (2x), then propargylamine (1x). The hexapeptoid **51** was cleaved from the resin by the application of **General Procedure N**. The crude mixture was analysed by LC-MS. Purification by flash chromatography (CH<sub>2</sub>Cl<sub>2</sub>/MeOH, 9:1) yielded the hexapeptoid **51** (36 mg, 0.04 mmol, 55%) as a pale-yellow foam.

**TLC** R<sub>f</sub> = 0.6 (CH<sub>2</sub>Cl<sub>2</sub>/MeOH, 9:1); 0.37 (AcOEt/MeOH 95:5).

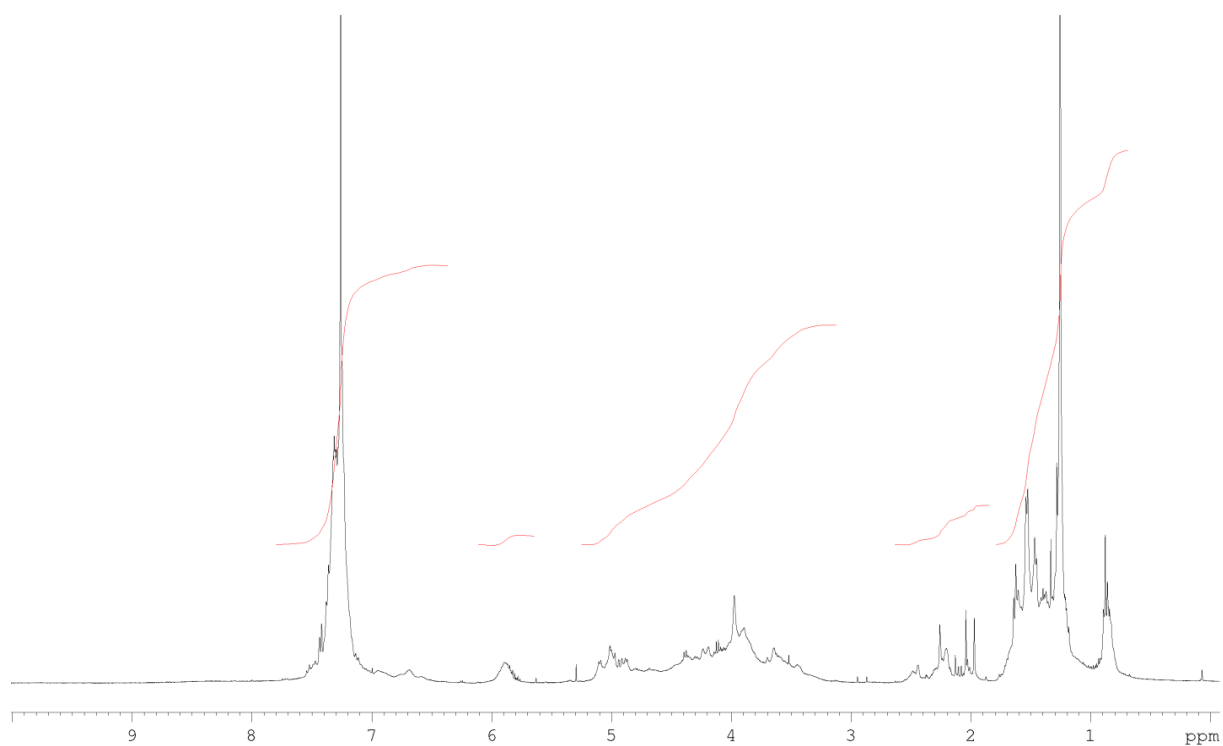
**IR** (ATR) ν (cm<sup>-1</sup>): 3307, 2930, 2854, 1662, 1653, 1437, 1419, 1285, 1203, 1179, 1029, 700.

**<sup>1</sup>H NMR** (400 MHz, CDCl<sub>3</sub>) δ (ppm): 0.62 – 1.81 (m, 12H, 4×CH<sub>3</sub>), 1.89 – 2.62 (m, 2H, 2×C≡CH), 3.15 – 5.15 (m, 16H, 2×NCH<sub>2</sub>C≡CH, 6×NCH<sub>2</sub>CO), 5.51 – 6.12 (m, 4H, 4×NCH), 6.48 – 8.21 (m, 20H, 4×Ph).

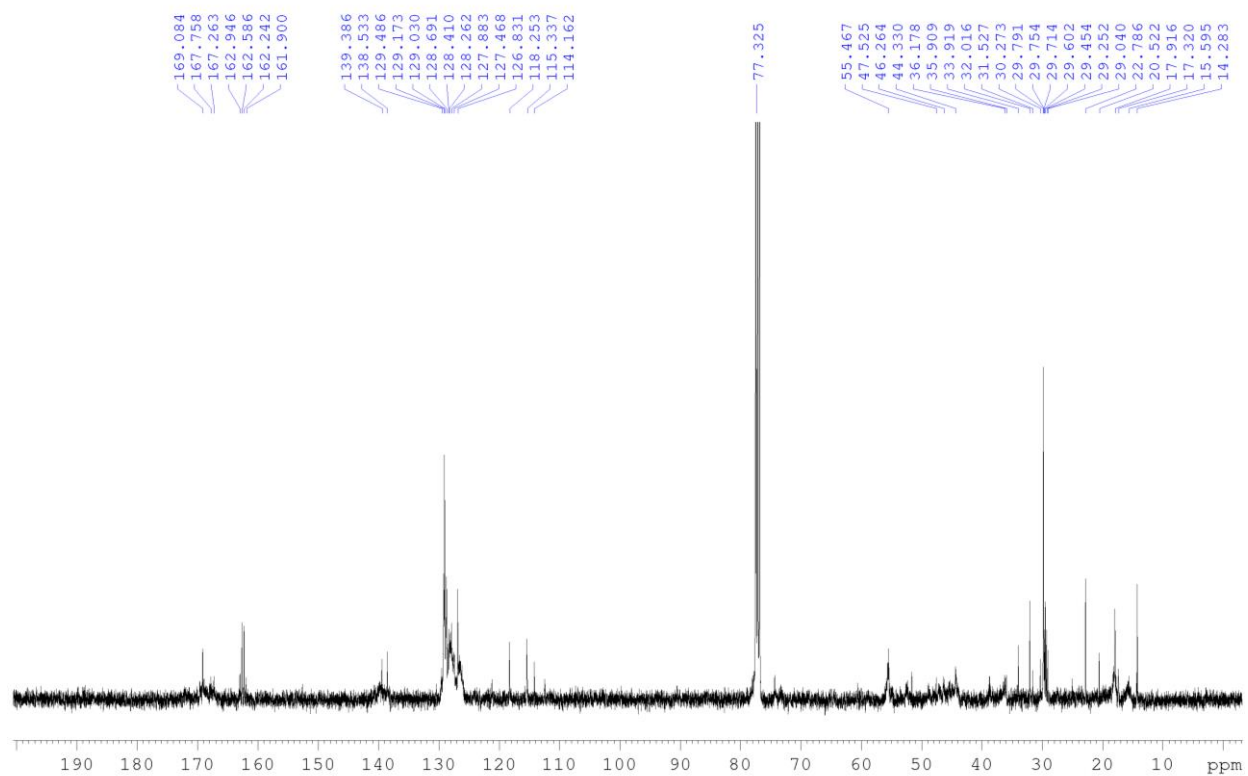
**<sup>13</sup>C NMR** (100 MHz, CDCl<sub>3</sub>) δ (ppm): 14.3, 17.3, 20.5, 22.8 (4CH<sub>3</sub>, 4×NCHCH<sub>3</sub>), 29.0, 29.3, 29.5, 29.6, 29.7, 29.8, 29.9, 30.3, (6CH<sub>2</sub>, 6×NCH<sub>2</sub>CO) 35.9, 36.2 (4CH<sub>2</sub>, 4×NCH<sub>2</sub>C≡CH), 44.3, 46.3, 47.5, 55.5 (4CH, 4×NCHCH<sub>3</sub>), 76.6, 76.9 (2CH, 2×NCH<sub>2</sub>C≡CH), 77.2, 77.6 (2C, 2×NCH<sub>2</sub>C≡CH), 126.8, 127.4, 127.9, 128.2, 128.4, 128.7, 129.0, 129.2, 129.5 (20CH, Ph), 138.5, 139.4 (4C, Ph), 161.9, 162.2, 162.6, 162.9, 167.3, 167.8, 169.1 (6C, 6×NC=O).

**HRMS** (TOF MS ES<sup>+</sup>): *m/z* calculated for C<sub>50</sub>H<sub>58</sub>N<sub>7</sub>O<sub>6</sub> [M+H]<sup>+</sup>: 852.4449; found: 852.4435 (-1.6 ppm).

Copy of  $^1\text{H}$  NMR in  $\text{CDCl}_3$  of hexapeptoid 51:

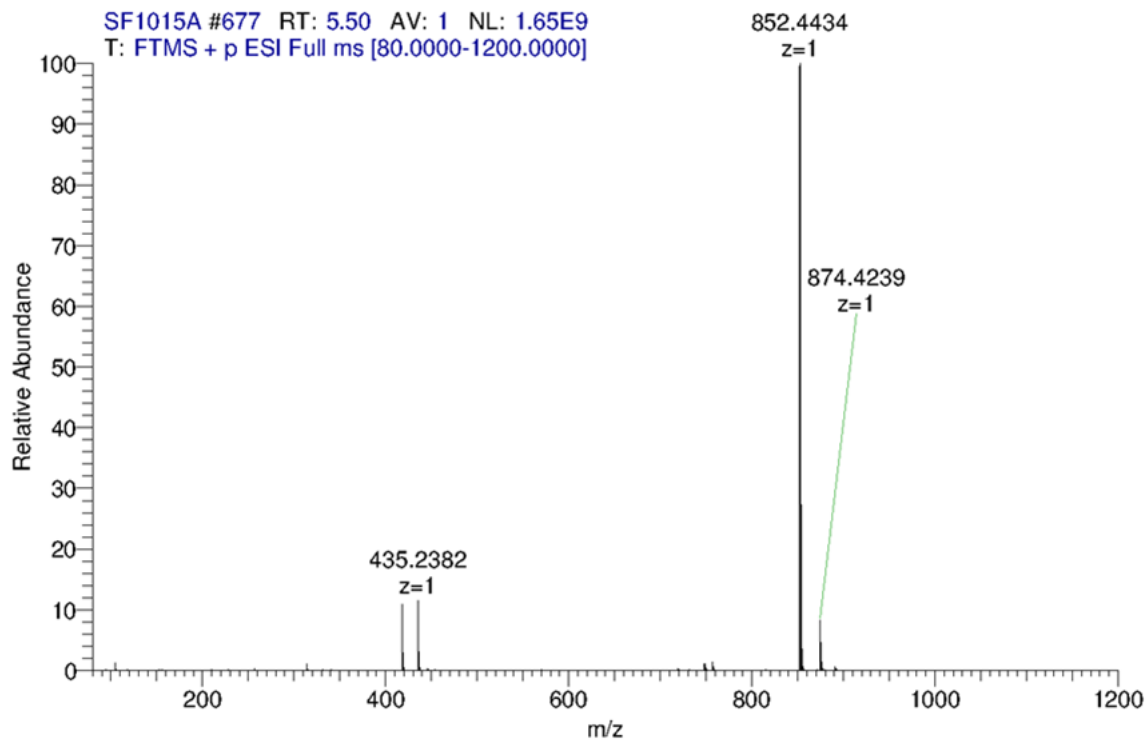
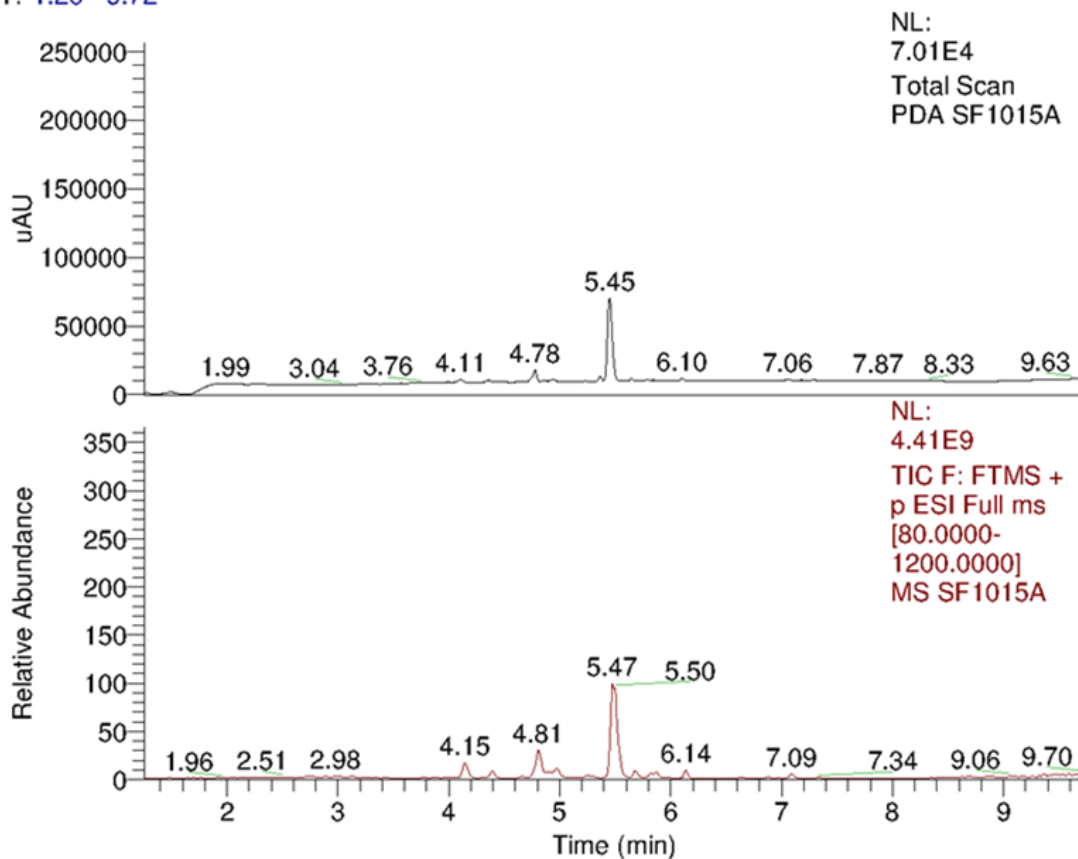


Copy of  $^{13}\text{C}$  NMR in  $\text{CDCl}_3$  of hexapeptoid 51:

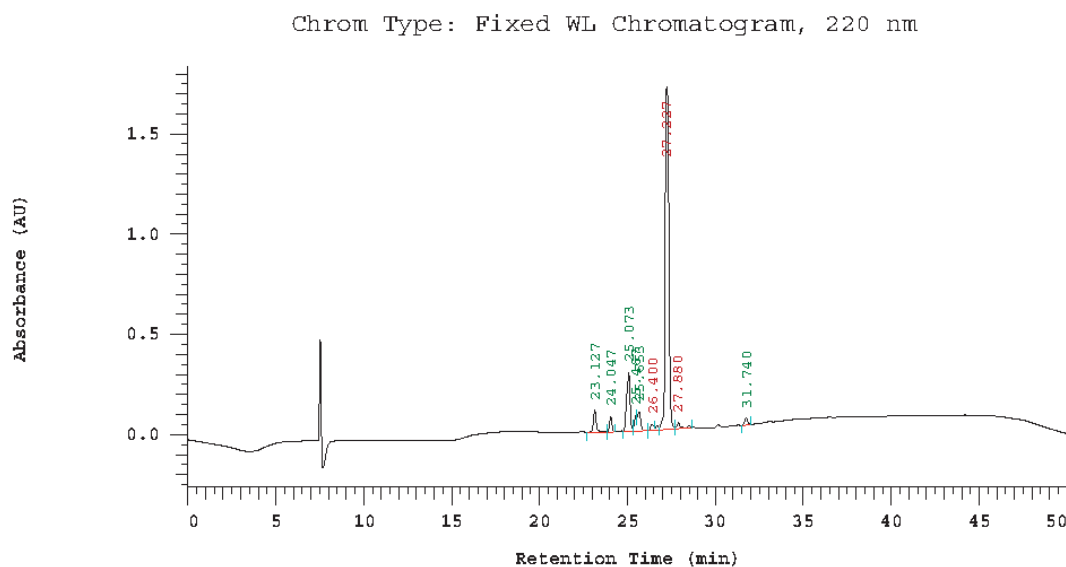


LCMS of hexapeptoid 51 obtained using optimized protocol H':

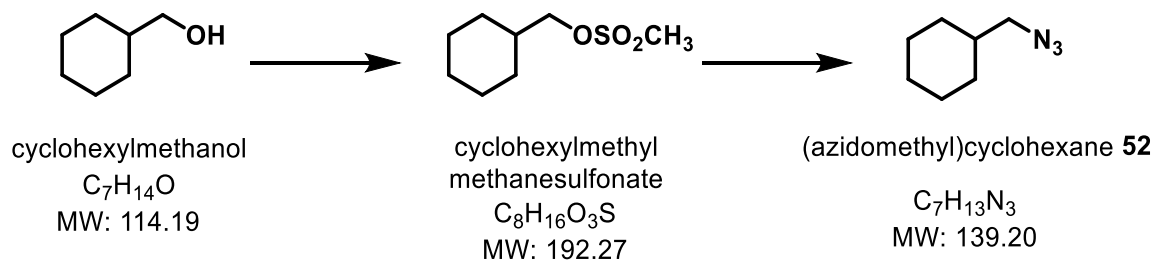
RT: 1.26 - 9.72



## HPLC chromatogram of hexapeptoid **51** (Jupiter column C<sub>4</sub>, 5 μm, 300Å):



## Cyclohexylmethyl azide **52**



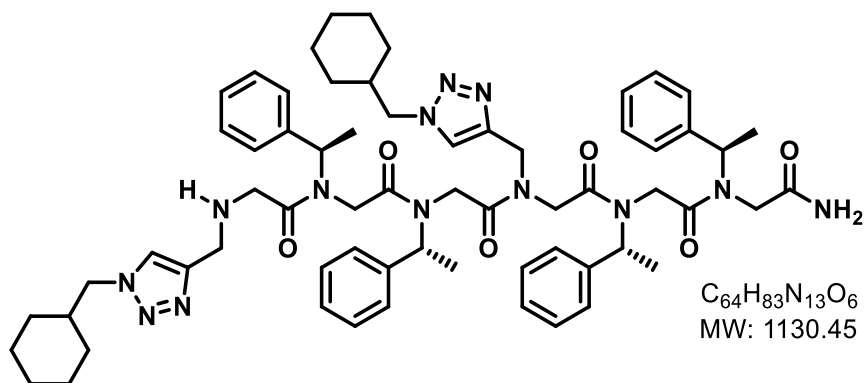
To a solution of cyclohexyl methanol (1.00 g, 8.78 mmol, 1 equiv.) and Et<sub>3</sub>N (1.35 mL, 9.66 mmol, 1.1 equiv.) in anhydrous CH<sub>2</sub>Cl<sub>2</sub> (18 mL, 0.5 M) under Ar atmosphere at 0°C was added slowly mesylchloride (0.75 mL, 9.66 mmol, 1.1 equiv.). The resulting mixture was stirred for 1 hour at rt then diluted with CH<sub>2</sub>Cl<sub>2</sub> (9 mL) and washed with NaOH 1M (3×30 mL). The organic layer was dried over Na<sub>2</sub>SO<sub>4</sub>, filtered, and concentrated under reduced pressure. The resulting mesylate (1.81 g, yellow liquid) was dissolved in DMF (9 mL) and NaN<sub>3</sub> (0.83, 12.72 mmol, 1.5 equiv.) was added. The mixture was stirred at 65°C overnight then allowed to cool at rt, diluted with H<sub>2</sub>O (18 mL), and extracted with Et<sub>2</sub>O/pentane 50:50 (2×20 mL). The combined organic layers were dried over MgSO<sub>4</sub>, filtered, and concentrated carefully under reduced pressure without heating. The remaining Et<sub>2</sub>O was evaporated overnight under a fume hood yielding cyclohexylmethyl azide **52** (1.05 g, 8.59 mmol, 89%) as a pale yellowish liquid.

TLC R<sub>f</sub> = 0.42 (Cyclohexane/EtOAc 1:1)

<sup>1</sup>H NMR (400 MHz, CDCl<sub>3</sub>) δ (ppm): 0.87-1.02 (m, 2H, CH<sub>2</sub>), 1.06-1.32 (m, 4H, 2×CH<sub>2</sub>) 1.45-1.60 (m, 1H, N<sub>3</sub>CH<sub>2</sub>CH), 1.61-1.80 (m, 4H, 2×CH<sub>2</sub>), 3.09 (d, J = 6.7 Hz, 2H, N<sub>3</sub>CH<sub>2</sub>CH).

Spectroscopic data are consistent with those reported in the literature.<sup>182</sup>

### Hexapeptoid H-(Nchtm-Nspe-Nspe)<sub>2</sub>-NH<sub>2</sub> 53a



The hexapeptoid **53a** was synthesised by the application of **General Procedure H'** on 100 mg Rink amide MBHA resin by using successively as primary amines: (*S*)-1-phenylethylamine (2x), propargylamine (1x), (*S*)-1-

phenylethylamine (2x), then propargylamine (1x). The protection of the terminal amine was carried out by the application of **General Procedure J**. The triazoles were generated using **General Procedure E** using cyclohexylmethyl azide **52** (87 mg, 0.62 mmol, 8 equiv.). The hexapeptoid **53a** was cleaved from the resin by the application of **General Procedure N**. The crude mixture was analysed by LC-MS. Purification by flash chromatography on silica gel (CH<sub>2</sub>Cl<sub>2</sub>/MeOH 9:1 then 8:2) yielded the hexapeptoid **53a**\* (42 mg, 0.037 mmol, 60%)\*\* as a beige foam. \* After evaporation of the fractions, the compound was dissolved in CH<sub>2</sub>Cl<sub>2</sub> and filtered to eliminate remaining silica gel. \*\*The yield considers a sample of resin taken for intermediate characterization.

**TLC** R<sub>f</sub> = 0.27 (CH<sub>2</sub>Cl<sub>2</sub>/MeOH 90:10)

**IR** (ATR)  $\nu$  (cm<sup>-1</sup>): 2926, 2852, 1664, 1662, 1653, 1450, 1437, 1206, 1184, 1052, 1029, 700.

**<sup>1</sup>H NMR** (400 MHz, CDCl<sub>3</sub>)  $\delta$ (ppm): 0.62 – 2.39 (m, 34H, 4×CH<sub>3</sub>, CH<sub>2</sub>(cyclohexyl) and CH(cyclohexyl)), 2.95 – 5.45 (m, 24H, 2×NCH<sub>2</sub>-triazole, 2×NCH<sub>2</sub>cyclohexyl, 6×NCH<sub>2</sub>CO) 5.65 – 6.18 (m, 4H, 4×NCHCH<sub>3</sub>), 6.62 – 7.45 (m, 20H, 4×Ph), 7.51– 8.12 (m, 2H, 2×C=CHN).

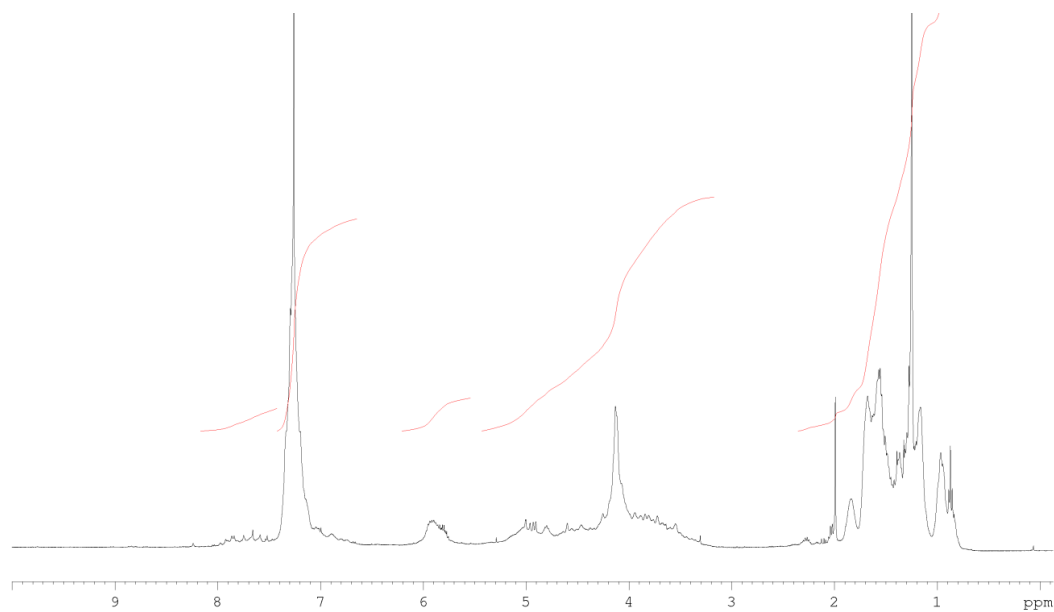
**<sup>13</sup>C NMR** (100 MHz, CDCl<sub>3</sub>)  $\delta$ (ppm): 14.2, 16.1, 16.3, 21.1 (4CH<sub>3</sub>, 4×NCHCH<sub>3</sub>), 22.7, 25.5, 26.1, 29.4, 29.7, 29.7, 30.4, 31.9 (10CH<sub>2</sub>, CH<sub>2</sub>(cyclohexyl)), 38.7 (2CH, 2×CH(cyclohexyl)), 42.5, 43.1, 44.3, 45.0, 46.6, 47.9, 48.4 (8CH<sub>2</sub>, 6×NCH<sub>2</sub>CO and 2×NCH<sub>2</sub>-triazole), 52.2, 52.5, 55.2, 55.3 (4CH, 4×NCHCH<sub>3</sub>), 56.5 (2CH<sub>2</sub>, 2×NCH<sub>2</sub>cyclohexyl), 127.1, 127.6, 127.6, 127.7, 127.7, 128.3, 128.4, 128.7, 128.8, 128.8, 128.9, 129.0, 129.0 (22CH, 20×Ph and 2×C=CHN), 139.1, 139.7, 139.8, 140.1, 140.5, 142.2, 143.1 (6C, 4×Ph and 2×C=CHN), 166.2, 168.2, 168.6, 168.9, 169.0, 169.3, 169.4, 170.1, 170.8 (6C, 6×NC=O).

<sup>182</sup> Keillor, J.; Lubell, W.; Pardin, C. Cinnamoyl Inhibitors of Transglutaminase 2008, W02008/144933A1.

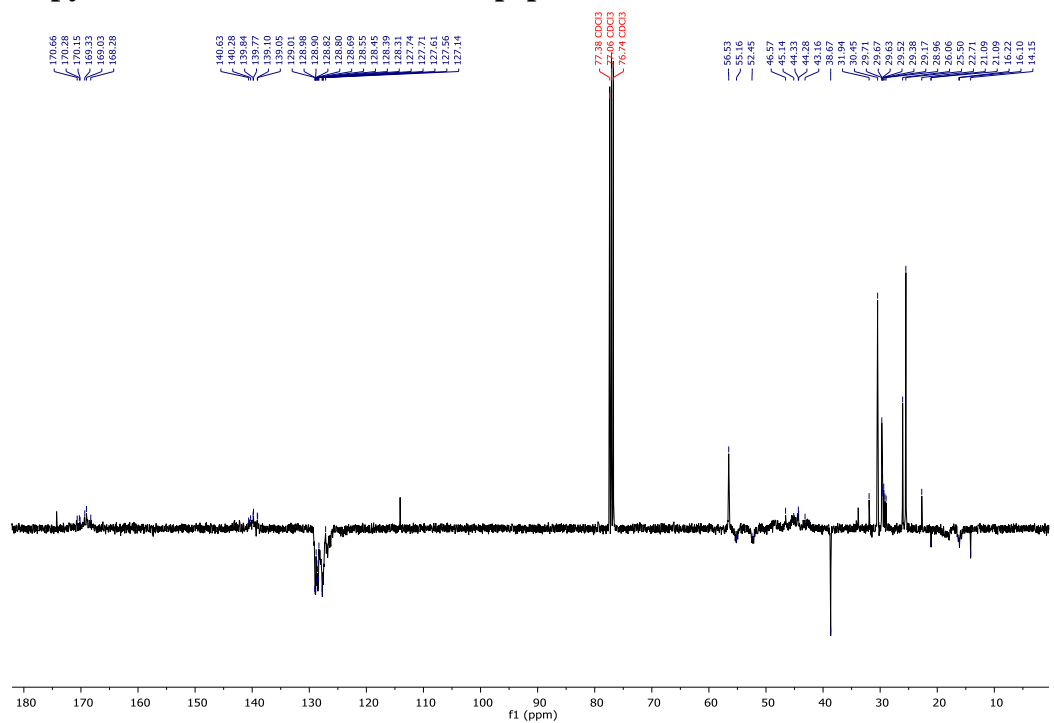


**HRMS (TOF MS ES+):**  $m/z$  calculated for  $C_{64}H_{84}N_{13}O_6 [M+H]^+$ : 1130.6668; found: 1130.6643 (-2.2 ppm)

**Copy of  $^1H$  NMR in  $CDCl_3$  of hexapeptoid 53a:**

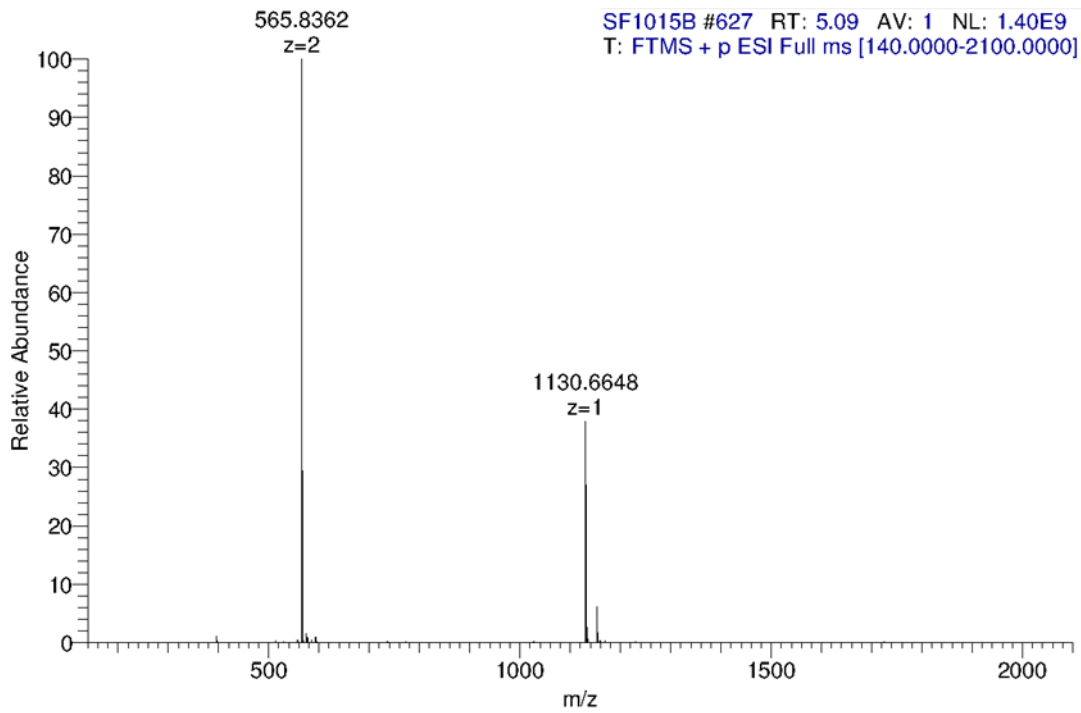
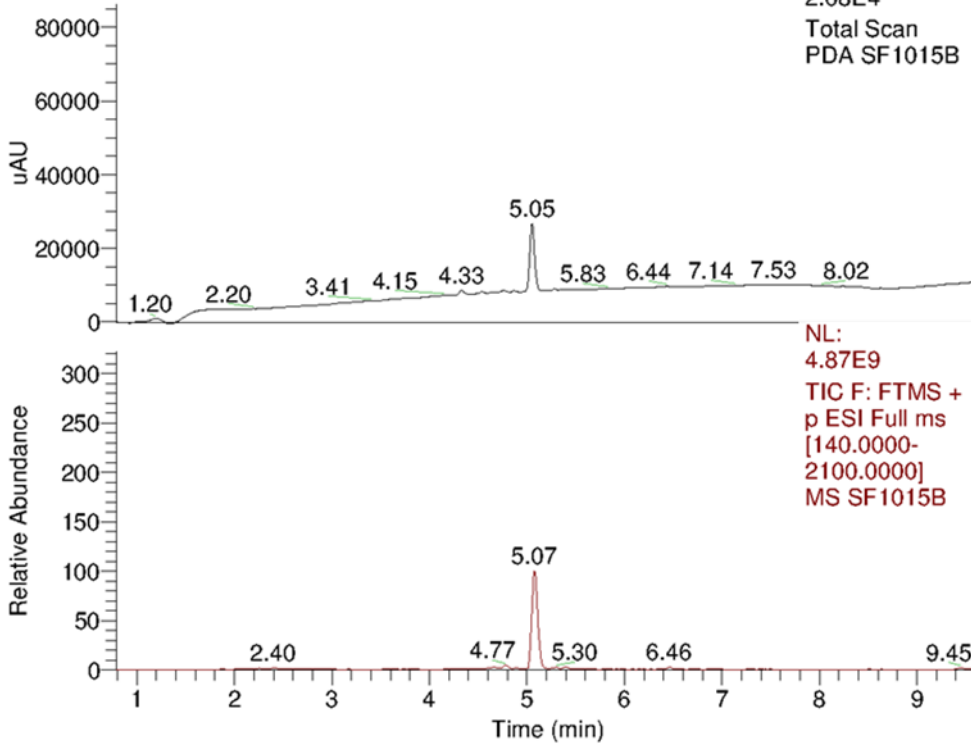


**Copy of  $^{13}C$  NMR in  $CDCl_3$  of hexapeptoid 53a:**



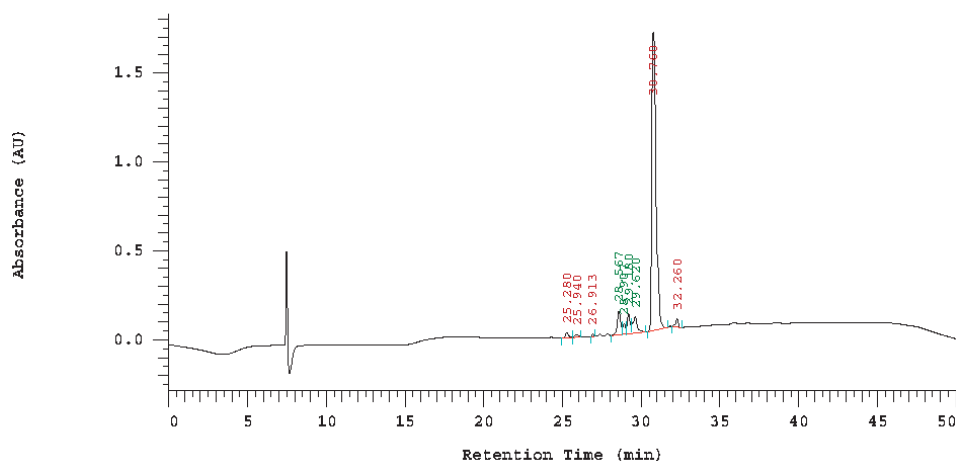
**Copy of LCMS of hexapeptoid 53a:**

RT: 0.79 - 9.64



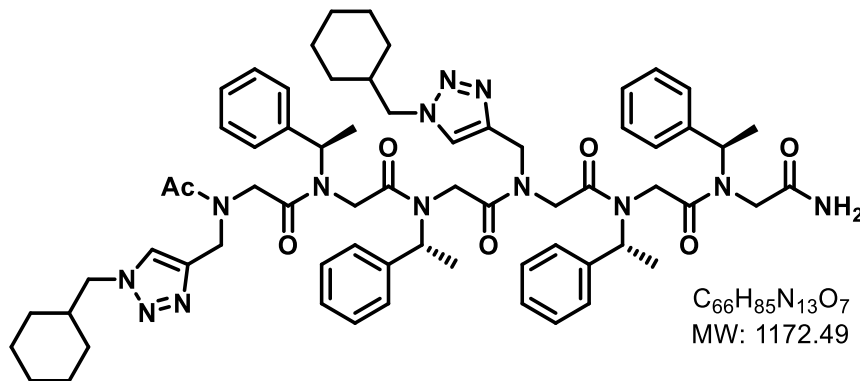
**HPLC chromatogram of hexapeptoid 53a (Jupiter column C<sub>4</sub>, 5 μm, 300Å):**

Chrom Type: Fixed WL Chromatogram, 220 nm



No.	RT	Area	Conc 1
1	25.280	194146	1.038
2	25.940	109335	0.585
3	26.913	47340	0.253
4	28.567	967378	5.173
5	28.907	331469	1.772
6	29.180	699607	3.741
7	29.620	932232	4.985
8	30.760	15150727	81.013
9	32.260	269289	1.440
			100.000

### Hexapeptoid Ac-(Nchtm-Nspe-Nspe)<sub>2</sub>-NH<sub>2</sub> **53b**



The hexapeptoid **53b** was synthesised by the application of **General Procedure I** on 100 mg Rink amide MBHA resin by using successively as primary amines: (*S*)-1-phenylethylamine (2x), propargylamine (1x), (*S*)-1-

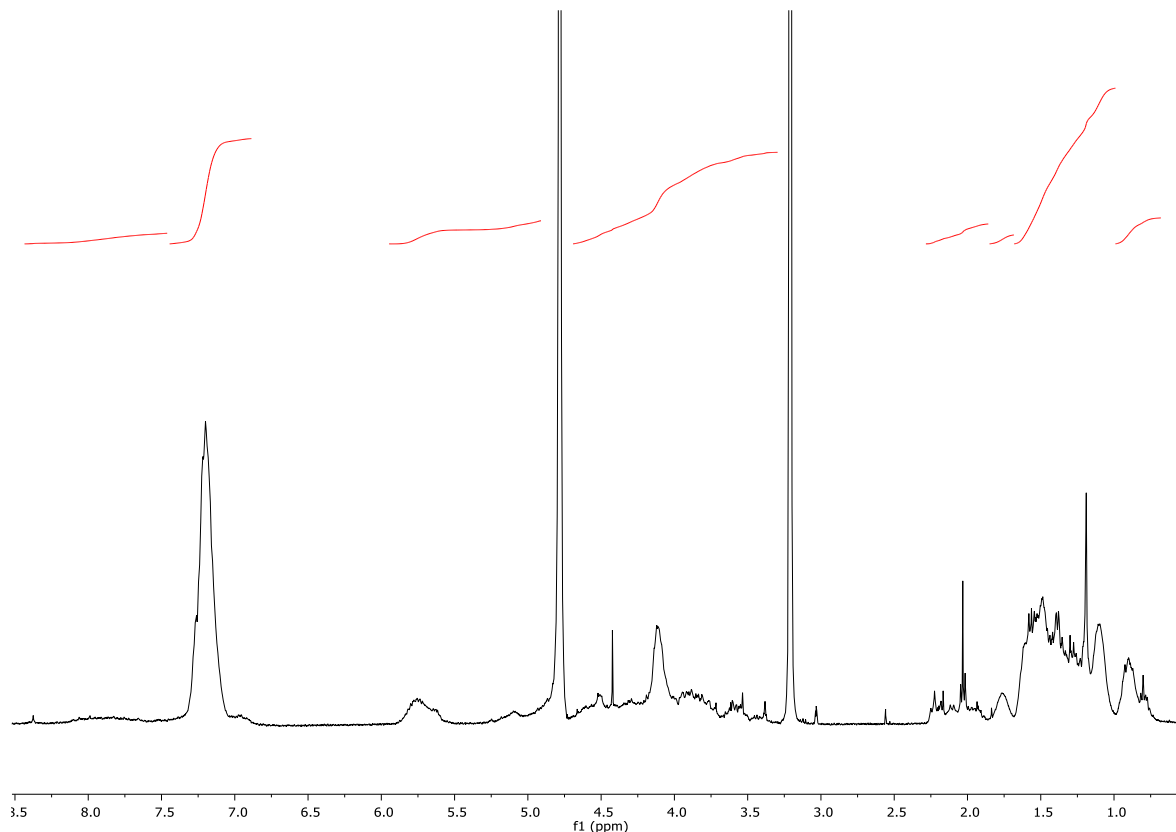
phenylethylamine (2x), then propargylamine (1x). The capping of the terminal amine was carried out by the application of **General Procedure K**. The triazoles were generated using **General Procedure L** using cyclohexylmethyl azide **52** (87 mg, 0.62 mmol, 8 equiv.). The hexapeptoid **53b** was cleaved from the resin by the application of **General Procedure N**. The crude mixture was analysed by LC-MS. Purification by flash chromatography on silica gel (CH<sub>2</sub>Cl<sub>2</sub>/MeOH 94:06) yielded the hexapeptoid **53b** (35 mg, 0.03 mmol, 38%).

**TLC** R<sub>F</sub> = 0.46 (CH<sub>2</sub>Cl<sub>2</sub>/MeOH, 94:6)

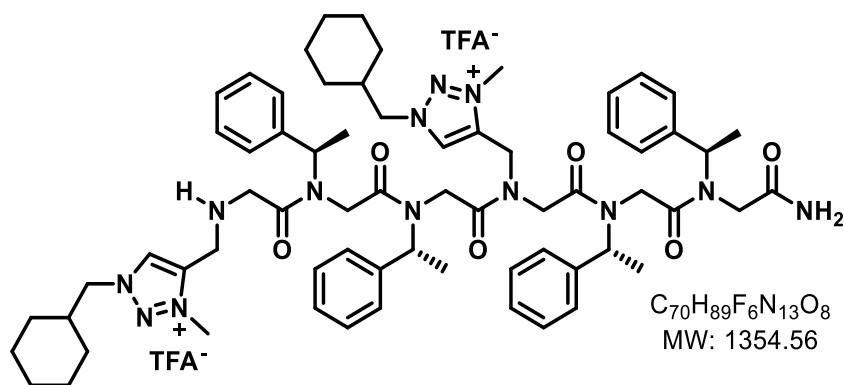
**$^1\text{H}$  NMR** (400 MHz,  $\text{CD}_3\text{OD}$ )  $\delta$ (ppm): 0.89 – 1.68 (m, 34H,  $4\times\text{CH}_3$ ,  $\text{CH}_2$ (cyclohexyl) and  $\text{CH}$ (cyclohexyl)), 1.86 – 2.28 (m, 3H,  $\text{CH}_3\text{CO}$ ), 3.30 – 4.69 (m, 20H,  $2\times\text{NCH}_2$ -triazole,  $2\times\text{NCH}_2$ cyclohexyl,  $6\times\text{NCH}_2\text{CO}$ ), 5.00-6.00 (m, 4H,  $4\times\text{NCHCH}_3$ ), 6.89 – 7.44 (m, 20H,  $4\times\text{Ph}$ ), 7.52 – 8.44 (m, 2H,  $2\times\text{C}=\text{CHN}$ ).

**HRMS** (TOF MS ES<sup>+</sup>):  $m/z$  calculated for  $\text{C}_{66}\text{H}_{86}\text{N}_{13}\text{O}_7$   $[\text{M}+\text{H}]^+$ : 1172.6773; found: 1172.6818 (3.8 ppm).

**Copy of  $^1\text{H}$  NMR in  $\text{CDCl}_3$  of hexapeptoid 53b:**



**Hexapeptoid H-(Nchtm<sup>+</sup>-Nspe-Nspe)<sub>2</sub>-NH<sub>2</sub> 54a**



The hexapeptoid **54a** was synthesised by the application of **General Procedure I** on 100 mg Rink amide MBHA resin by using successively as primary amines: (*S*)-1-phenylethylamine (2x), propargylamine (1x), (*S*)-1-phenylethylamine (2x), then propargylamine (1x). The protection of the terminal amine was carried out by the application of

**General Procedure J.** The triazoles were generated using **General Procedure L** using cyclohexylmethyl azide **52** (87 mg, 0.62 mmol, 8 equiv.). The conversion of triazoles into triazoliums was performed using **General Procedure M**. The hexapeptoid **54a** was cleaved from the resin by the application of **General Procedure N**. The crude mixture was analysed by LC-MS. The crude was triturated in ether to yield hexapeptoid **54a** (62 mg, 0.05 mmol, 58% crude yield). Hexapeptoid **54a** was sufficiently pure to be used for biological evaluation.

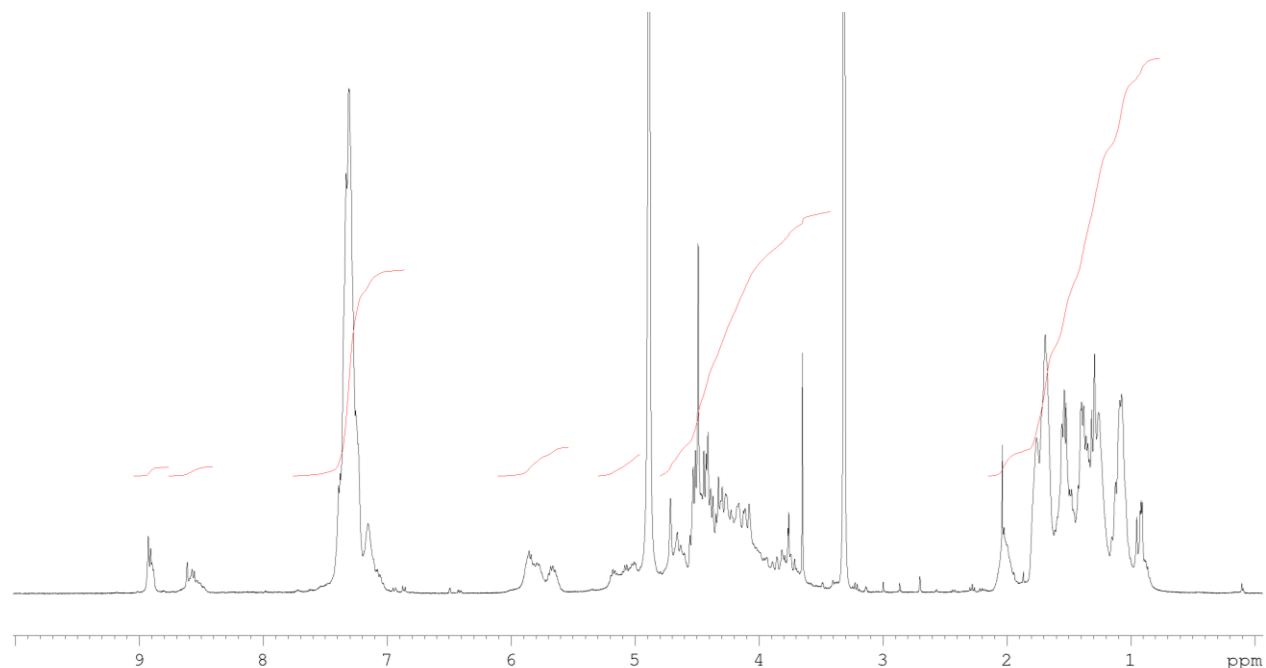
**IR** (ATR)  $\tilde{\nu}$  (cm<sup>-1</sup>): 2935, 2869, 1702, 1686, 1652, 1457, 1412, 1201, 1184, 1127, 720, 700

**<sup>1</sup>H NMR** (400 MHz, MeOD)  $\delta$ (ppm): 0.79 – 2.12 (m, 34H, 4×CH<sub>3</sub>, CH<sub>2</sub>(cyclohexyl) and CH(cyclohexyl)), 3.46 – 4.80 (m, 26H, 2×NCH<sub>2</sub>-triazolium, 2×NCH<sub>2</sub>cyclohexyl, 2×N<sup>+</sup>CH<sub>3</sub>, 6×NCH<sub>2</sub>CO) 4.90 – 6.04 (m, 4H, 4×NCHCH<sub>3</sub>), 6.97 – 7.62 (m, 20H, 4×Ph), 8.31 – 8.72 (m, 1H, C=CHN), 8.85 – 9.01 (m, 1H, C=CHN).

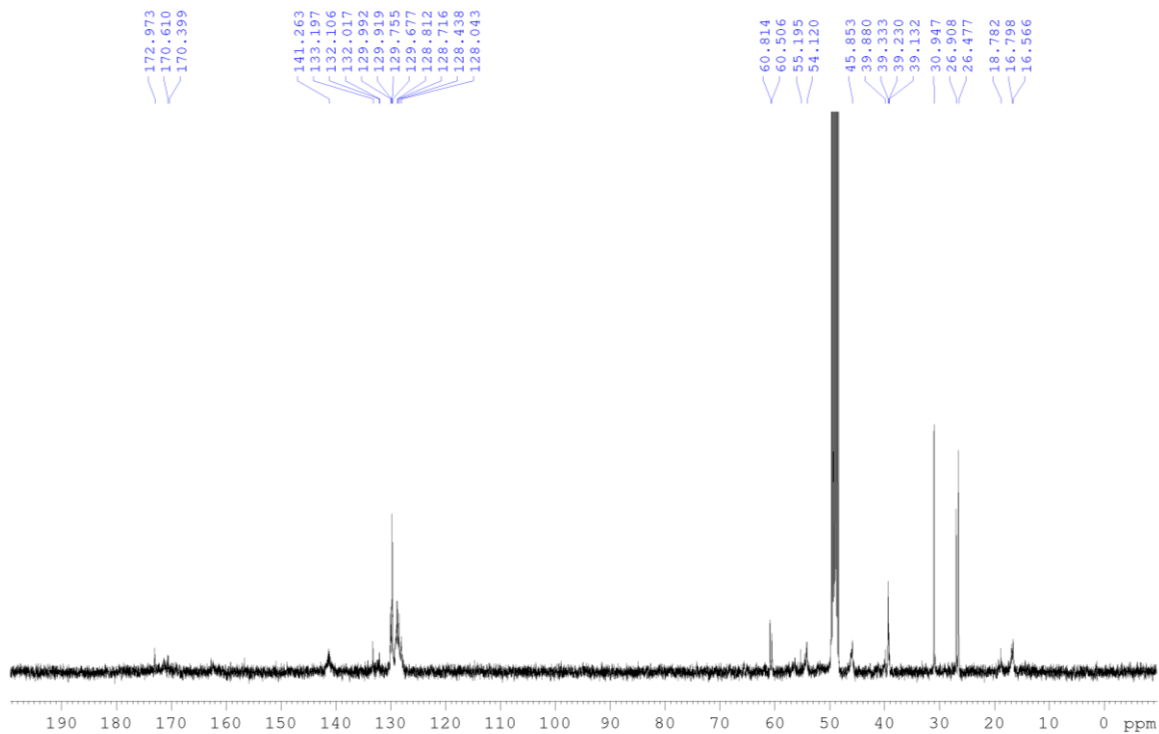
**<sup>13</sup>C NMR** (100 MHz, MeOD)  $\delta$ (ppm): 16.6, 16.8, 18.8 (4CH<sub>3</sub>, 4×NCHCH<sub>3</sub>), 26.5, 26.9, 31.0 (10CH<sub>2</sub>, CH<sub>2</sub>(cyclohexyl)), 39.1, 39.2 (2CH, 2×CH(cyclohexyl)), 39.3, 39.9 (2CH<sub>3</sub>, 2×N<sup>+</sup>CH<sub>3</sub>), 45.7, 45.8, 45.9, 45.9, 46.1, 46.2 49.1, 49.3, 49.5, 49.7, 49.8 (8CH<sub>2</sub>, 6×NCH<sub>2</sub>CO and 2×NCH<sub>2</sub>-triazolium) 54.1 (4CH, 4×NCHCH<sub>3</sub>), 55.2, 60.5, 60.8 (2CH<sub>2</sub>, 2×NCH<sub>2</sub>cyclohexyl), 128.0, 128.4, 128.7, 128.8, 129.7, 129.8, 129.9, 130.0 (22CH, 20×Ph and 2×C=CHN) 132.0, 132.1, 133.2, 141.3 (6C, 4×Ph and 2×C=CHN), 170.4, 170.6, 173.0 (6C, 6×NC=O).

**HRMS** (TOF MS ES<sup>+</sup>):  $m/z$  calculated for C<sub>66</sub>H<sub>89</sub>N<sub>13</sub>O<sub>6</sub><sup>2+</sup> [M]<sup>2+</sup>: 579.8524, found 579.8522.

**Copy of <sup>1</sup>H NMR in MeOD of hexapeptoid 54a:**

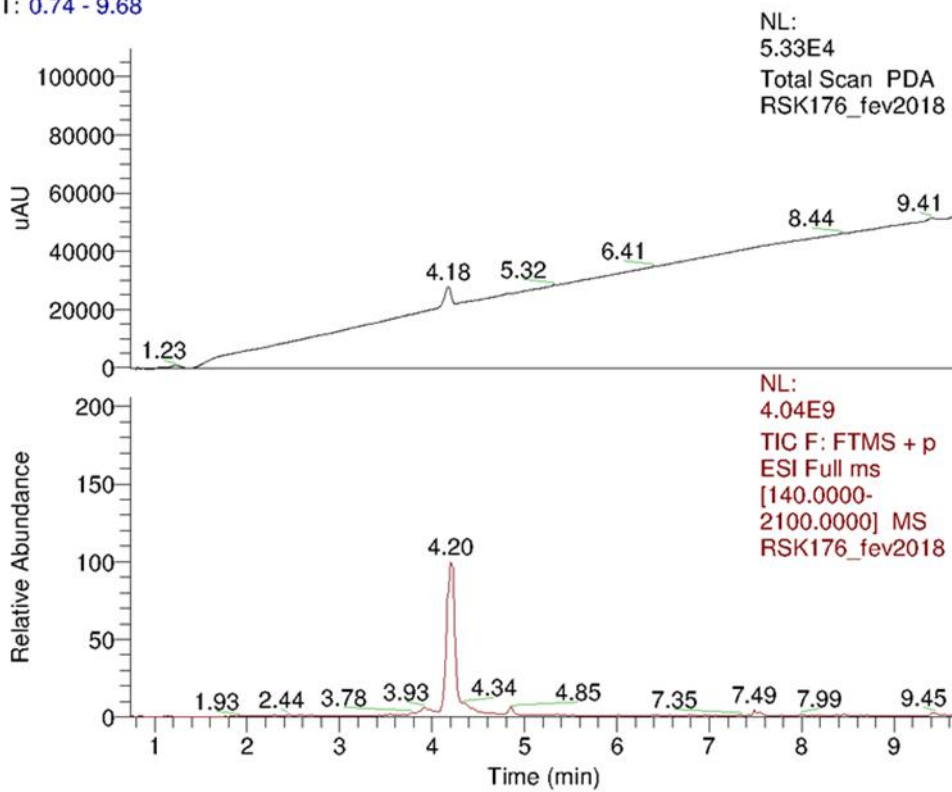


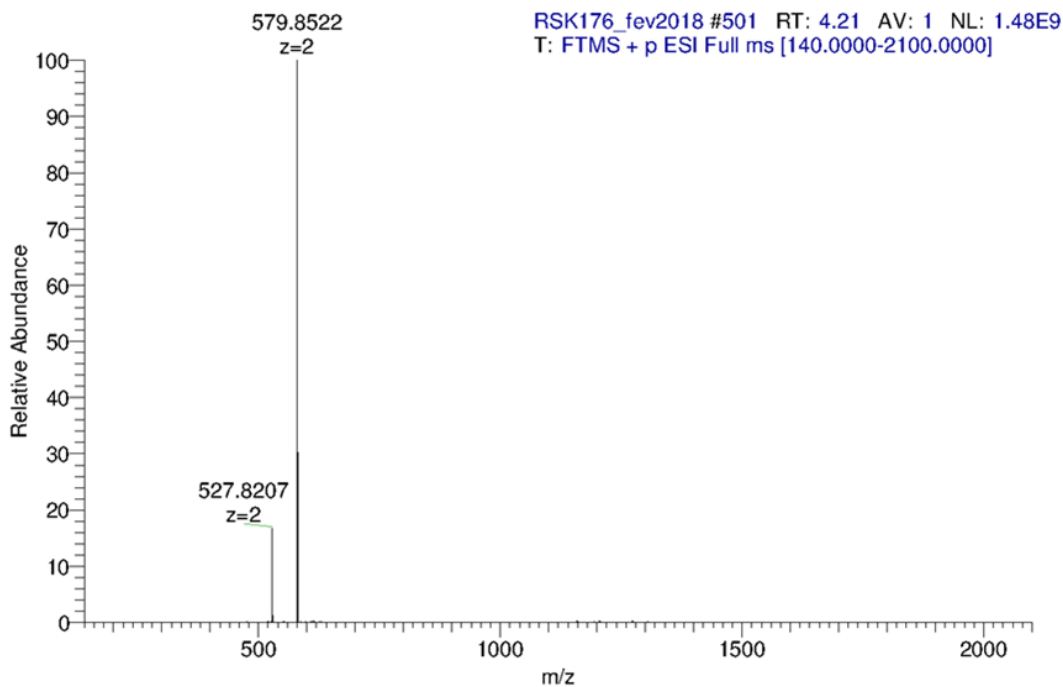
**Copy of <sup>13</sup>C NMR in MeOD of hexapeptoid 54a:**



**Copy of LCMS of hexapeptoid 54a:**

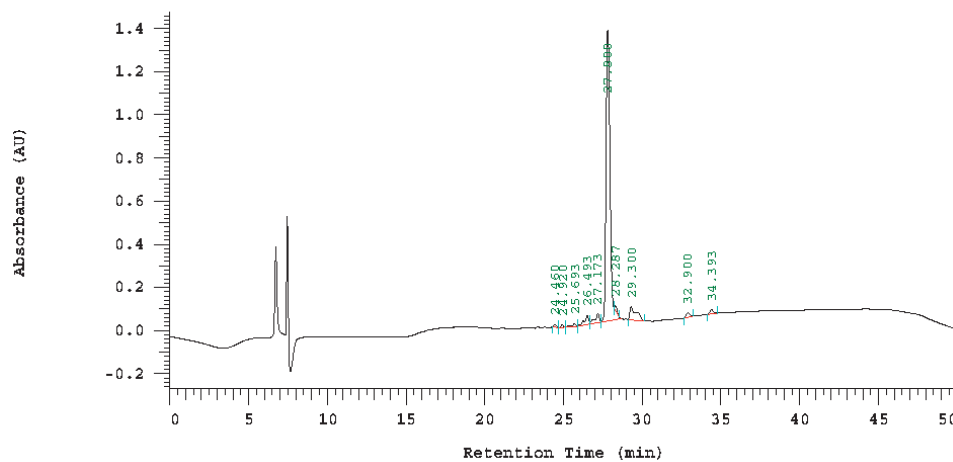
RT: 0.74 - 9.68





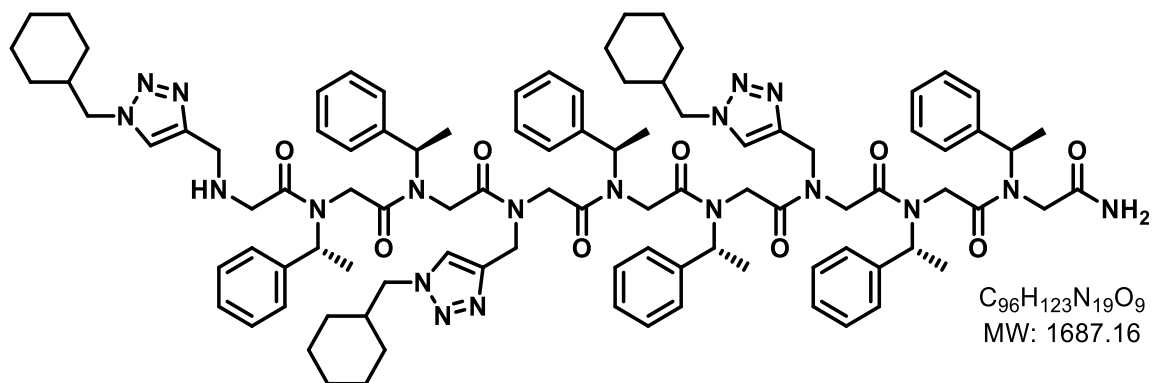
**HPLC chromatogram of hexapeptoid 54a (Jupiter column C<sub>4</sub>, 5 μm, 300Å):**

Chrom Type: Fixed WL Chromatogram, 220 nm



No.	RT	Area	Conc 1
1	24.460	62985	0.457
2	24.920	56546	0.410
3	25.693	103032	0.747
4	26.493	391104	2.836
5	27.173	398181	2.887
6	27.800	11511029	83.469
7	28.287	109242	0.792
8	29.300	881224	6.390
9	32.900	150038	1.088
10	34.393	127393	0.924
		13790774	100.000

### Nonapeptoid H-(Nchtm-Nspe-Nspe)<sub>3</sub>-NH<sub>2</sub> **55a**



The nonapeptoid **55a** was synthesised by the application of **General Procedure I** on 100 mg Rink amide MBHA resin by using successively as primary amines: (*S*)-1-phenylethylamine (2x), propargylamine (1x), (*S*)-1-phenylethylamine (2x), propargylamine (1x), (*S*)-1-phenylethylamine (2x), then propargylamine (1x). The protection of the terminal amine was carried out by the application of **General Procedure J**. The triazoles were generated using **General Procedure L** using cyclohexylmethyl azide **52** (130 mg, 0.93 mmol, 12 equiv.). The nonapeptoid **55a** was cleaved from the resin by the application of **General Procedure N**. The crude mixture was analysed by LC-MS. Purification by flash chromatography on silica gel (CH<sub>2</sub>Cl<sub>2</sub>/MeOH 93:7) yielded the hexapeptoid **55a** (53 mg, 0.03 mmol, 40%).

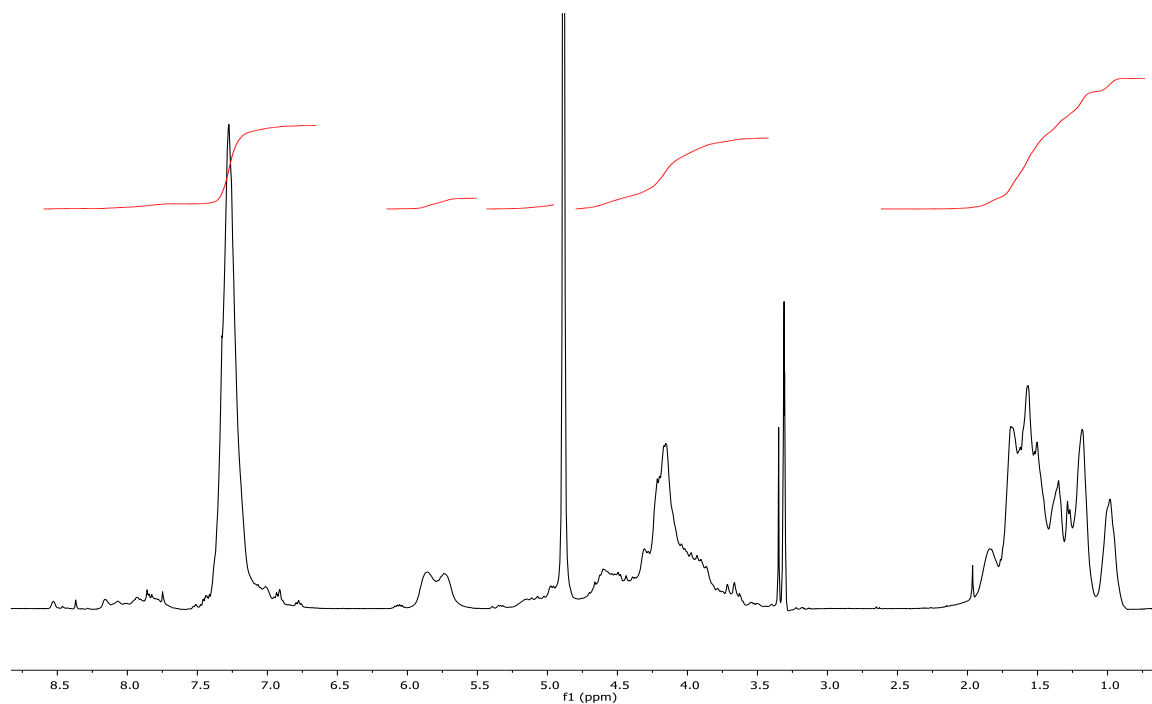
**TLC** R<sub>f</sub> = 0.12 (CH<sub>2</sub>Cl<sub>2</sub>/MeOH, 98:2).

**<sup>1</sup>H NMR** (400 MHz, MeOD) δ(ppm): 0.73 – 2.62 (m, 51H, 6×CH<sub>3</sub>, 15×CH<sub>2</sub>(cyclohexyl) and 3×CH(cyclohexyl)), 3.42 – 4.75 (m, 30H, 3×NCH<sub>2</sub>-triazole, 3×NCH<sub>2</sub>cyclohexyl, 9×NCH<sub>2</sub>CO) 4.80 – 6.26 (m, 6H, 6×NCHCH<sub>3</sub>), 6.65 – 7.60 (m, 30H, 6×Ph), 7.62 – 8.60 (m, 3H, 3×C=CHN).

**HRMS** (TOF MS ES<sup>+</sup>): *m/z* calculated for C<sub>96</sub>H<sub>124</sub>N<sub>19</sub>O<sub>9</sub> [M+H]<sup>+</sup>: 1686.9829; found: 1686.9850 (1.2 ppm).

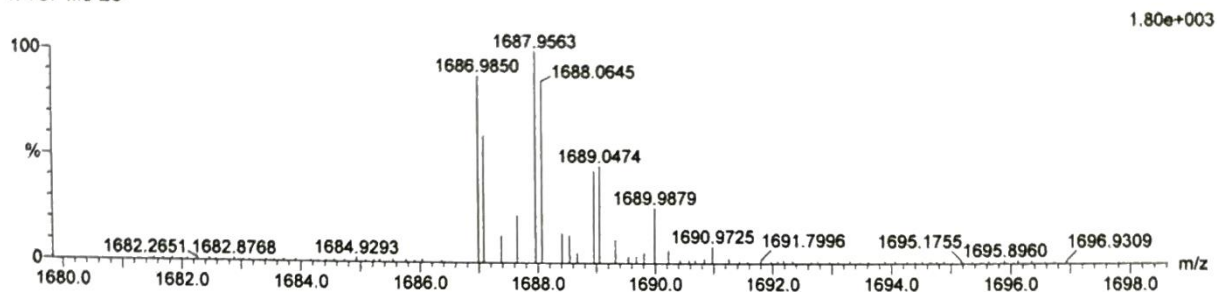


**Copy of <sup>1</sup>H NMR in MeOD of nonapeptoid 55a:**



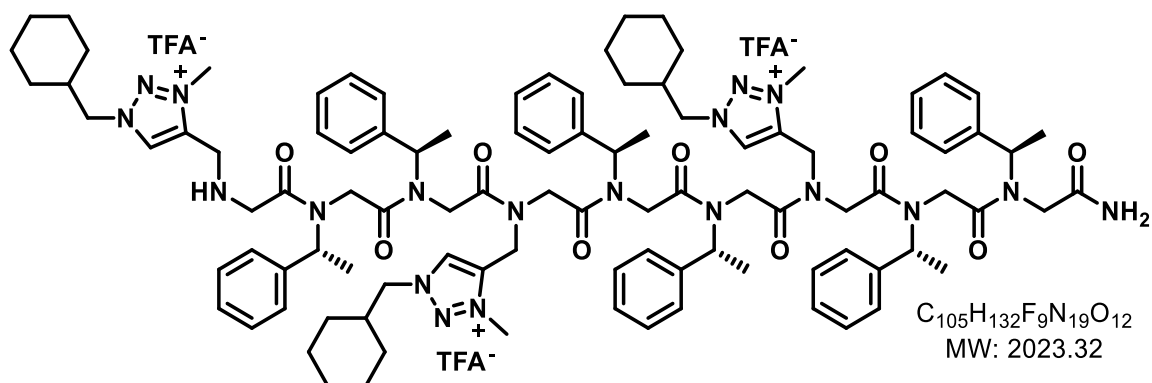
**Copy of HRMS of nonapeptoid 55a:**

RSK121A0-d50b 20 (0.649) AM (Cen,4, 70.00, Ar,5000.0,556.28,0.70,LS 20); Sm (Mn, 2x1.00)  
1: TOF MS ES+



Mass	Calc. Mass	mDa	PPM	DBE	i-FIT	Formula
1686.9850	1686.9829	2.1	1.2	44.5	41.4	C <sub>96</sub> H <sub>124</sub> N <sub>19</sub> O <sub>9</sub>

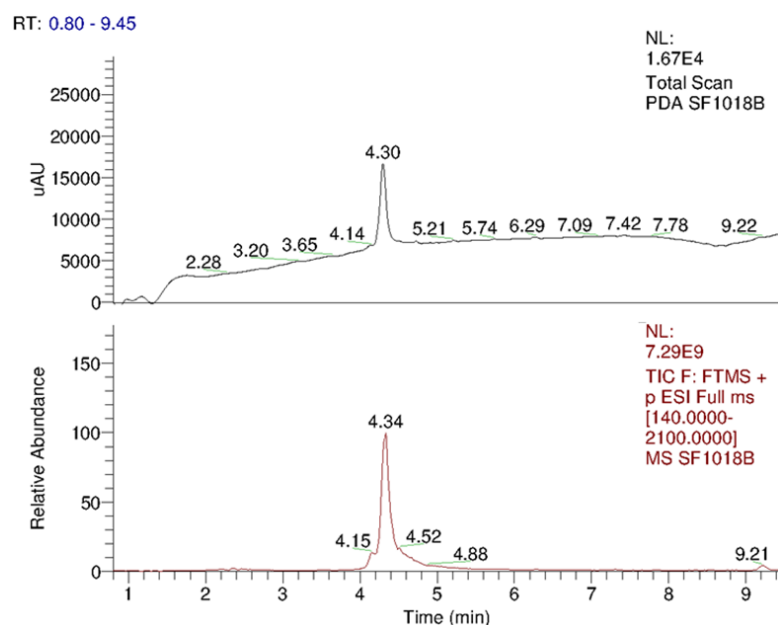
## Nonapeptoid H-(Nchtm<sup>+</sup>-Nspe-Nspe)<sub>3</sub>-NH<sub>2</sub> 56a

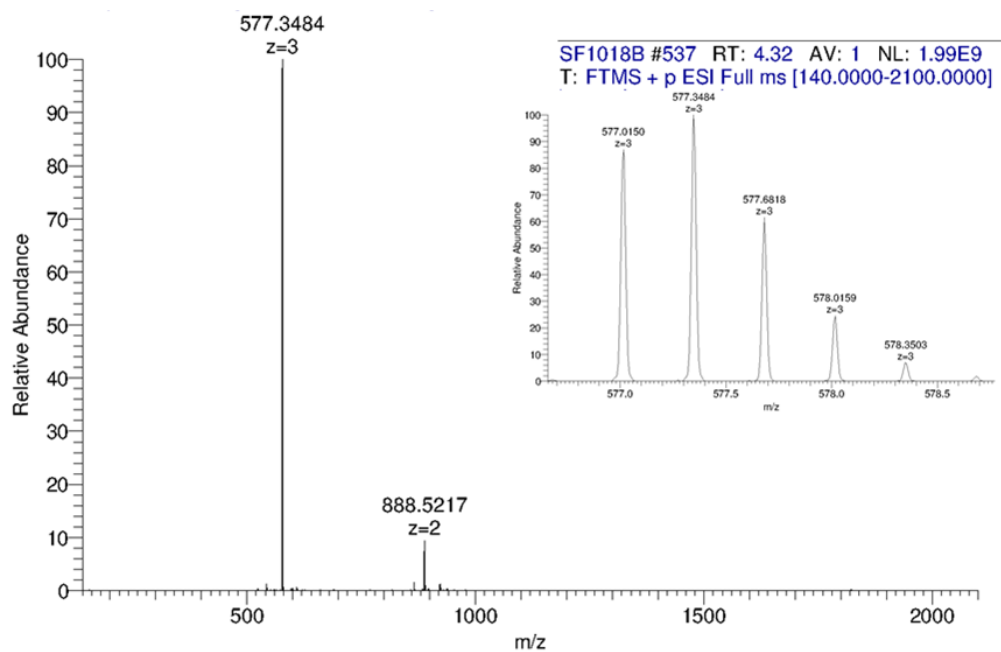


The nonapeptoid **56a** was synthesised by the application of **General Procedure H'** on 100 mg Rink amide MBHA resin by using successively as primary amines: (*S*)-1-phenylethylamine (2x), propargylamine (1x), (*S*)-1-phenylethylamine (2x), propargylamine (1x), (*S*)-1-phenylethylamine (2x), then propargylamine (1x). The protection of the terminal amine was carried out by the application of **General Procedure J**. The triazoles were generated using **General Procedure L** using cyclohexylmethyl azide **52** (130 mg, 0.93 mmol, 12 equiv.). The conversion of triazoles into triazoliums was performed using **General Procedure M**. The nonapeptoid **56a** was cleaved from the resin by the application of **General Procedure N**. The crude mixture was analysed by LC-MS. The crude was triturated in ether to yield nonapeptoid **56a** (104 mg, 0.05 mmol, 66%). Nonapeptoid **56a** was sufficiently pure to be used for biological evaluation.

**HRMS** (TOF MS ES<sup>+</sup>): *m/z* calculated for C<sub>99</sub>H<sub>132</sub>N<sub>19</sub>O<sub>9</sub><sup>3+</sup> [M]<sup>3+</sup>: 577.0146; found: 577.0146 (-0.08 ppm).

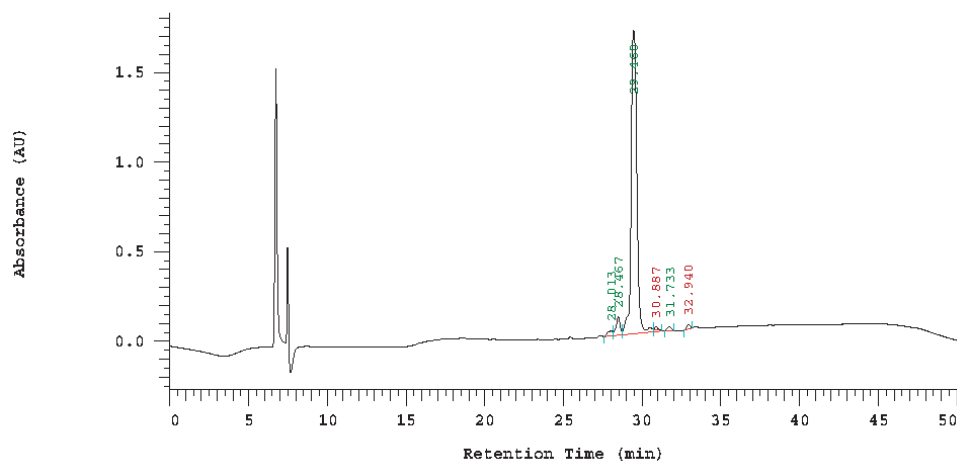
### Copy of LCMS of nonapeptoid 56a:





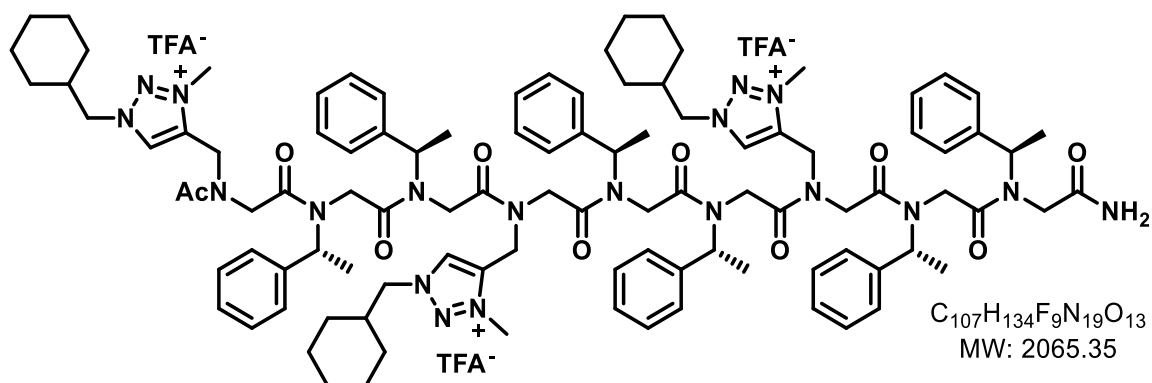
**HPLC chromatogram of nonapeptoid 56a (Jupiter column C<sub>4</sub>, 5 μm, 300Å):**

Chrom Type: Fixed WL Chromatogram, 220 nm



No.	RT	Area	Conc 1
1	28.013	319959	1.415
2	28.467	879557	3.889
3	29.460	20948563	92.626
4	30.887	109119	0.482
5	31.733	187791	0.830
6	32.940	171203	0.757
		22616192	100.000

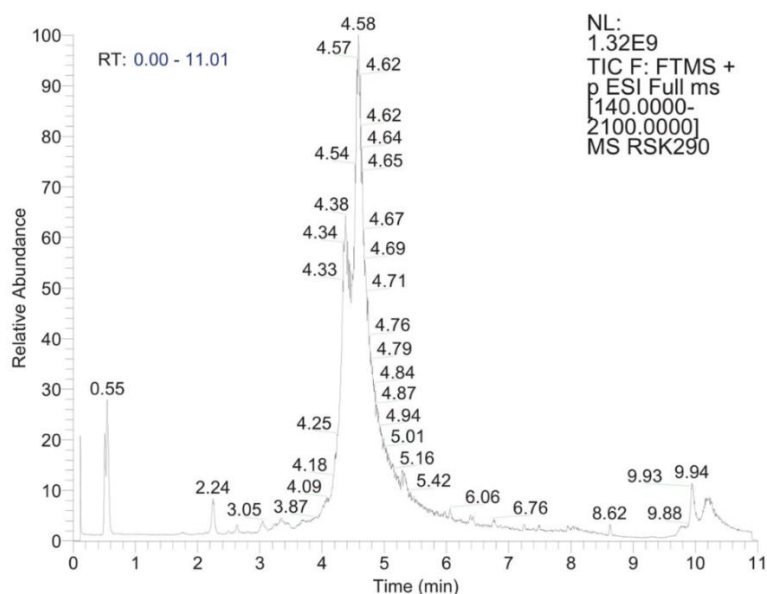
## Nonapeptoid Ac-(Nchtm<sup>+</sup>-Nspe-Nspe)<sub>3</sub>-NH<sub>2</sub> **56b**

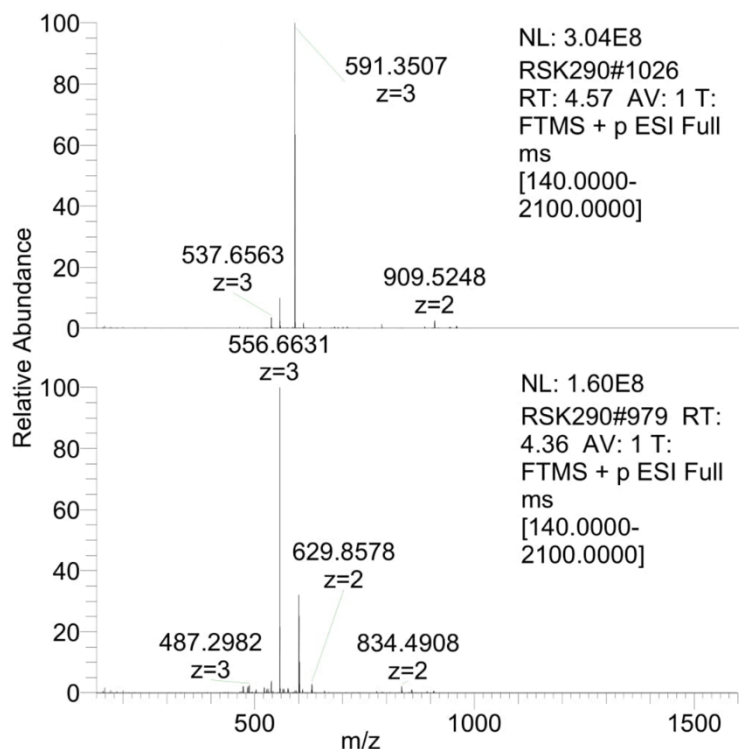


The nonapeptoid **56b** was synthesised by the application of **General Procedure I'** on 100 mg Rink amide MBHA resin by using successively as primary amines: (*S*)-1-phenylethylamine (2x), propargylamine (1x), (*S*)-1-phenylethylamine (2x), propargylamine (1x), (*S*)-1-phenylethylamine (2x), then propargylamine (1x). The capping of the terminal amine was carried out by the application of **General Procedure K**. The triazoles were generated using **General Procedure L** using cyclohexylmethyl azide **52** (130 mg, 0.93 mmol, 12 equiv.). The conversion of triazoles into triazoliums was performed using **General Procedure M**. The nonapeptoid **56a** was cleaved from the resin by the application of **General Procedure N**. The crude mixture was analysed by LC-MS. Purification by preparative HPLC furnished the nonapeptoid **56b** (29 mg, 0.014 mmol, 18%).

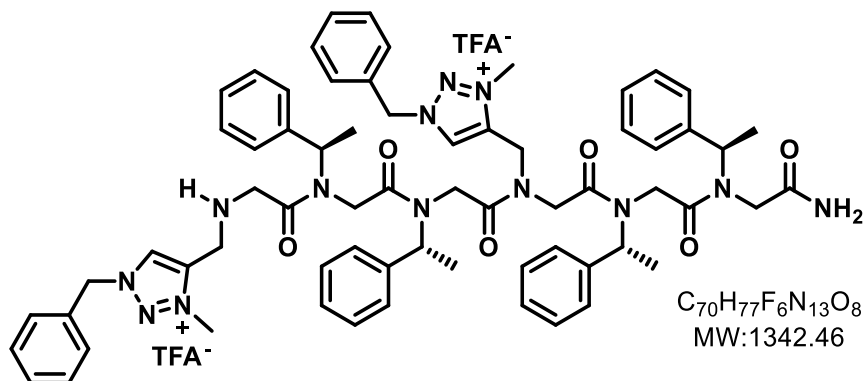
**HRMS** (TOF MS ES<sup>+</sup>): *m/z* calculated for  $C_{101}H_{134}N_{19}O_{10}^{3+}$  [M]<sup>3+</sup>: 591.0181; found: 591.0172 (-1.59 ppm).

### Copy of LCMS spectra of crude nonapeptoid **56b**:





### Hexapeptoid H-(Nbtm<sup>+</sup>-Nspe-Nspe)<sub>2</sub>-NH<sub>2</sub> **57a**



The hexapeptoid **57a** was synthesised by the application of **General Procedure I'** on 100 mg Rink amide MBHA resin by using successively as primary amines: (*S*)-1-phenylethylamine (2x), propargylamine (1x), (*S*)-1-

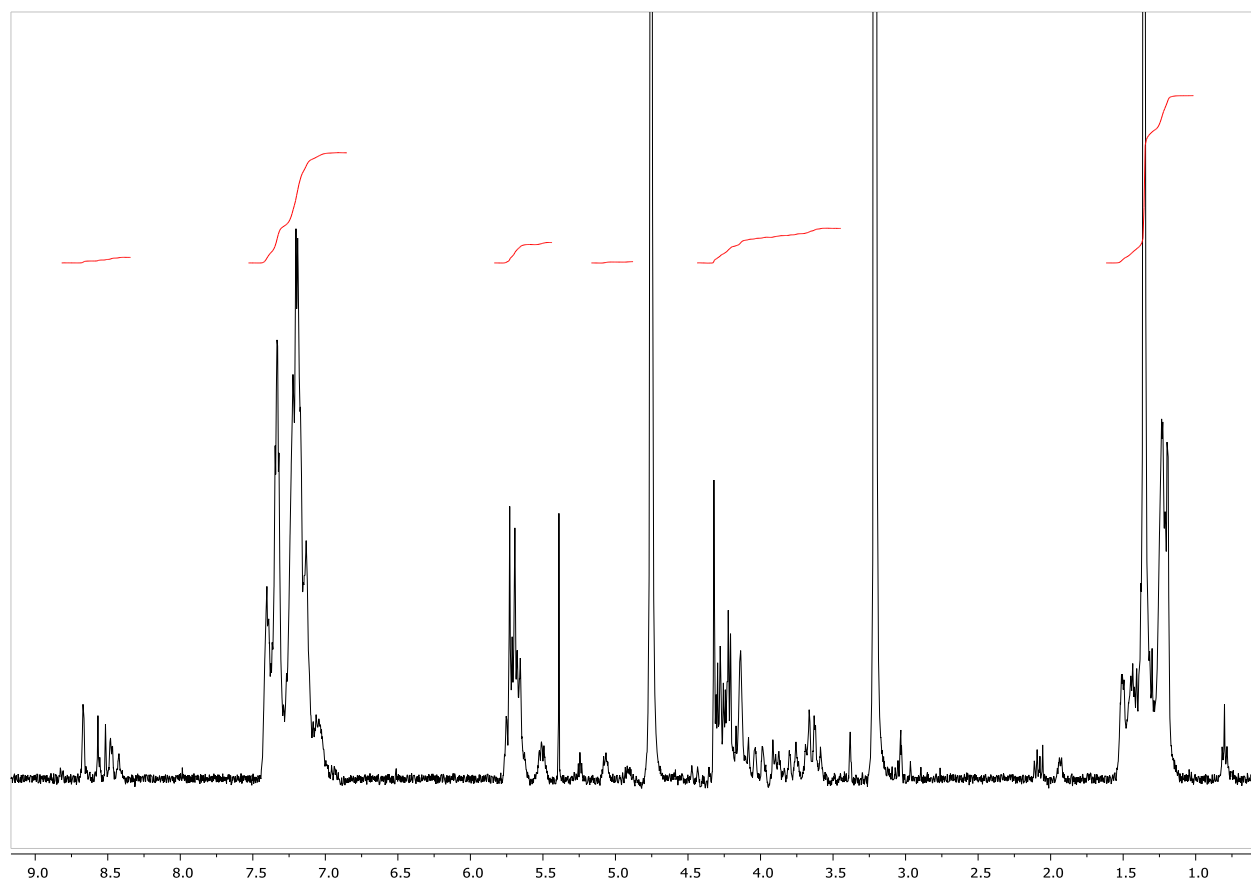
phenylethylamine (2x), then propargylamine (1x). The protection of the terminal amine was carried out by the application of **General Procedure J**. The triazoles were generated using **General Procedure L** using azide **41** (84 mg, 0.62 mmol, 8 equiv.). The conversion of triazoles into triazoliums was performed using **General Procedure M**. The hexapeptoid **57a** was cleaved from the resin by the application of **General Procedure N**. The crude mixture was analysed by LC-MS. The crude was triturated in ether to yield hexapeptoid **57a** (94 mg, 0.07 mmol, 90%). Hexapeptoid **57a** was sufficiently pure to be used for biological evaluation.

**<sup>1</sup>H NMR** (400 MHz, CD<sub>3</sub>OD)  $\delta$ (ppm): 0.66 – 1.92 (m, 12H, 4×CH<sub>3</sub>), 2.78 – 5.26 (m, 26H, 2×NCH<sub>2</sub>-triazolium, 2×N<sup>+</sup>CH<sub>3</sub>, 6×NCH<sub>2</sub>CO, 4×NCHCH<sub>3</sub>), 5.42 – 6.18 (m, 4H, 2×PhCH<sub>2</sub>), 6.80 – 7.90 (m, 30H, 6×Ph), 8.66 (s, 1H, C=CHN), 8.99 (s, 1H, C=CHN).

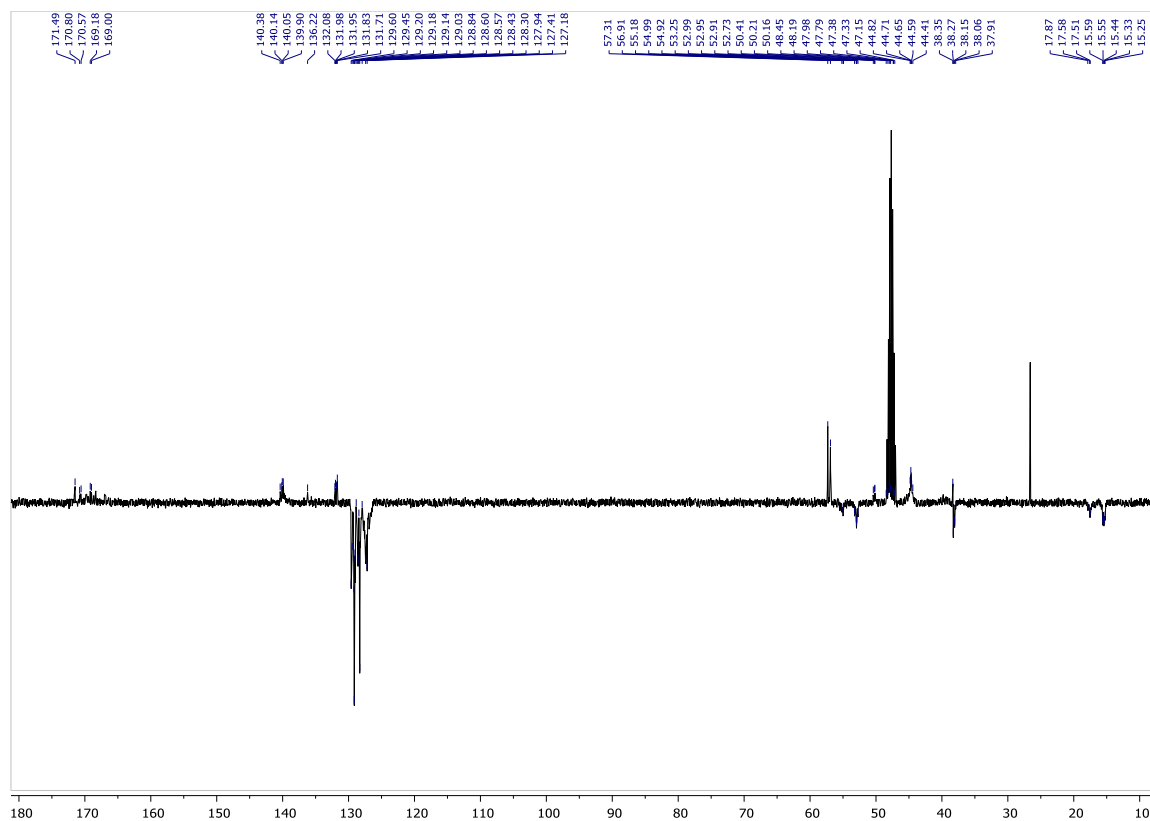
**<sup>13</sup>C NMR** (100 MHz, CD<sub>3</sub>OD)  $\delta$ (ppm): 15.4, 15.6, 17.5, 17.6 (4CH<sub>3</sub>, 4×NCHCH<sub>3</sub>), 37.9, 38.1 (2CH<sub>3</sub>, 2×N<sup>+</sup>CH<sub>3</sub>), 38.3 (2CH<sub>2</sub>, 2×NCH<sub>2</sub>-triazolium) 44.4, 44.6, 44.7, 44.8, 50.2, 50.2, 50.4 (6CH<sub>2</sub>, 6×NCH<sub>2</sub>CO), 53.0, 53.3, 54.9, 55.0 (4CH, 4×NCHCH<sub>3</sub>), 56.9, 57.3 (2CH<sub>2</sub>, 2×NCH<sub>2</sub>C<sub>6</sub>H<sub>5</sub>), 127.2, 127.4, 127.9, 128.3, 128.4, 128.6, 128.6, 128.8, 129.0, 129.1, 129.2, 129.2, 129.4, 129.6, (32CH, 30×Ph and 2×C=CHN), 131.7, 131.8, 132.0, 132.0, 132.1, 136.2, 139.9, 140.1, 140.1, 140.4 (8C, 6×Ph and 2×C=CHN), 169.0, 169.2, 170.6, 170.8, 171.5 (6C, 6×NC=O).

**HRMS** (TOF MS ES<sup>+</sup>): *m/z* calculated for C<sub>66</sub>H<sub>77</sub>N<sub>13</sub>O<sub>6</sub><sup>2+</sup> [M+H]<sup>+</sup>: 573.8054; found: 573.8052 (-0.35 ppm)

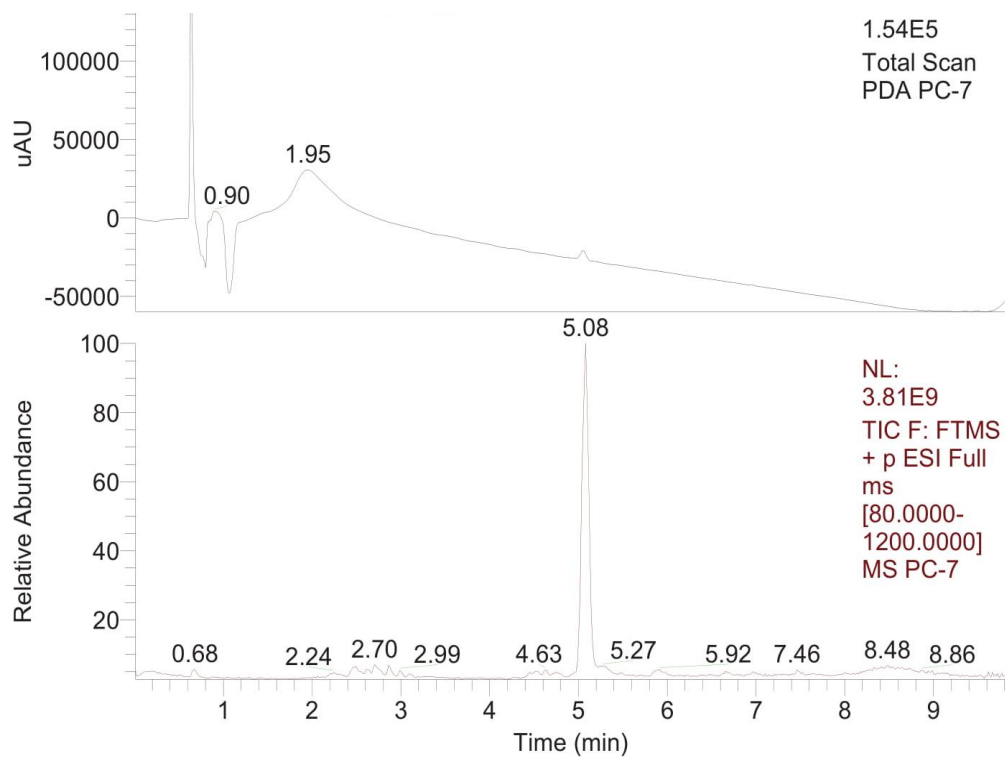
**Copy of <sup>1</sup>H NMR in MeOD of hexapeptoid 57a:**

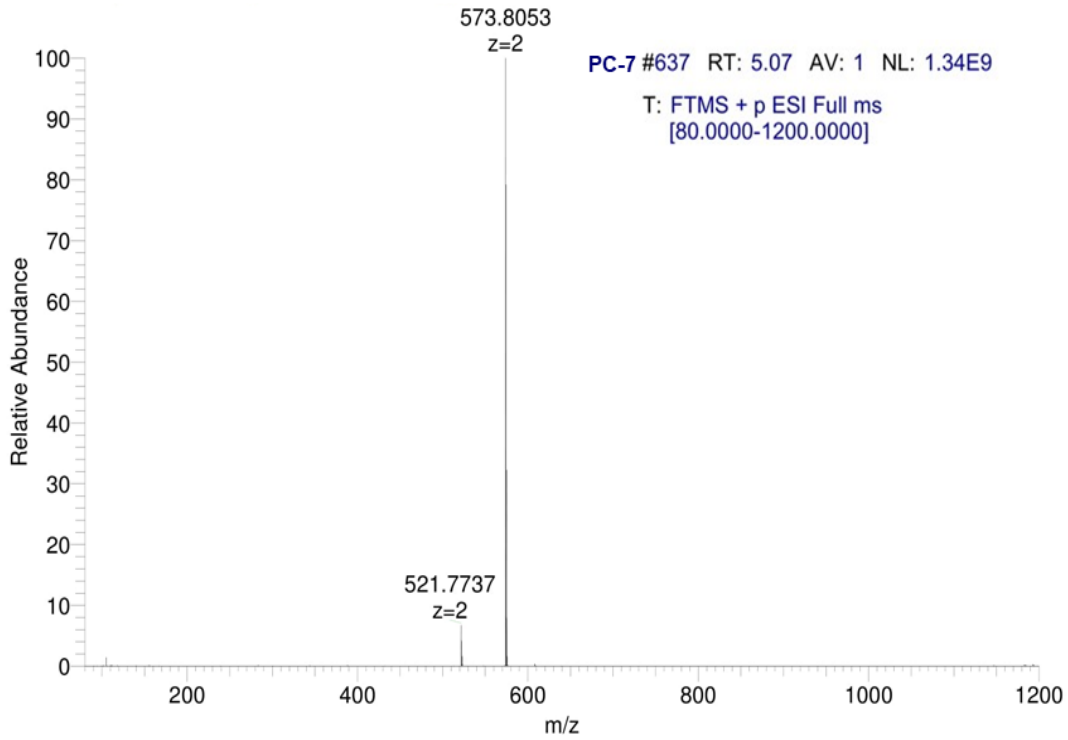


Copy of  $^{13}\text{C}$  NMR in MeOD of hexapeptoid 57a:



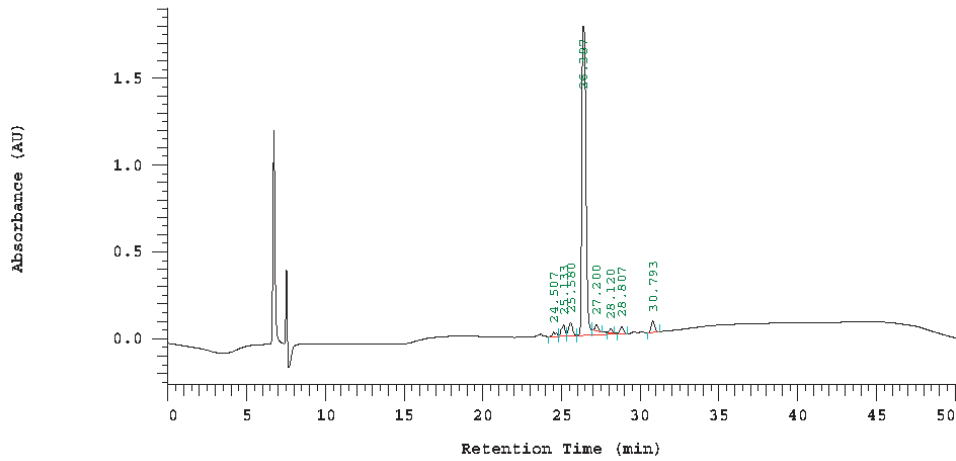
Copy of LCMS spectra of hexapeptoid 57a:





**HPLC chromatogram of hexapeptoid 57a (Jupiter column C<sub>4</sub>, 5 μm, 300Å):**

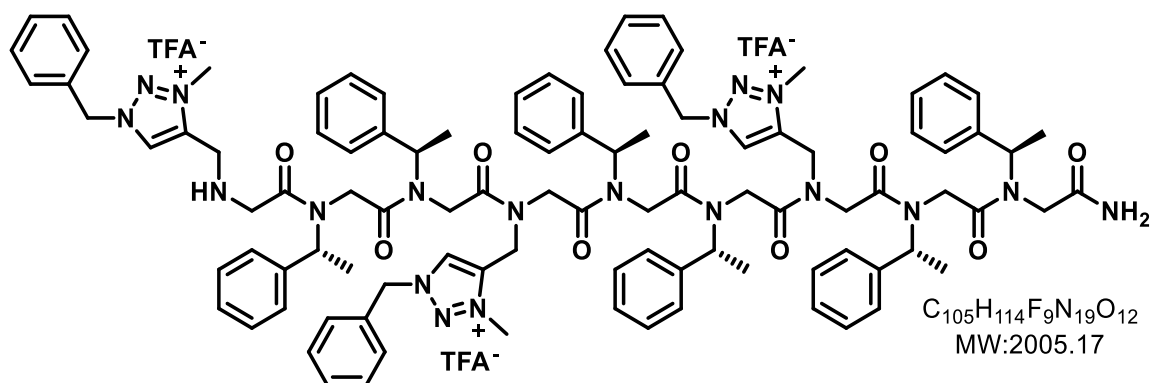
Chrom Type: Fixed WL Chromatogram, 220 nm



No.	RT	Area	Conc 1
1	24.507	215253	1.136
2	25.133	508765	2.685
3	25.580	680297	3.590
4	26.387	16368796	86.370
5	27.200	255896	1.350
6	28.120	147267	0.777
7	28.807	280894	1.482
8	30.793	494720	2.610
		18951888	100.000



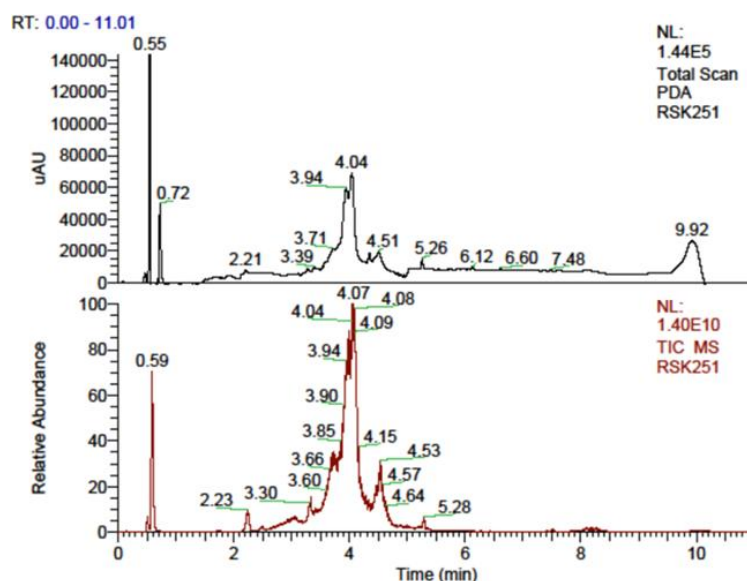
## Nonapeptoid H-(Nbtm<sup>+</sup>-Nspe-Nspe)<sub>3</sub>-NH<sub>2</sub> **58a**

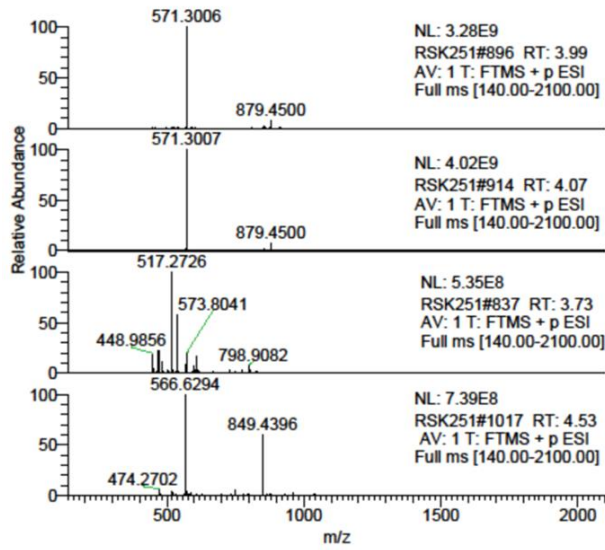


The nonapeptoid **58a** was synthesised by the application of **General Procedure I'** on 100 mg Rink amide MBHA resin by using successively as primary amines: (*S*)-1-phenylethylamine (2x), propargylamine (1x), (*S*)-1-phenylethylamine (2x), propargylamine (1x), (*S*)-1-phenylethylamine (2x), then propargylamine (1x). The protection of the terminal amine was carried out by the application of **General Procedure J**. The triazoles were generated using **General Procedure L** using azide **41** (126 mg, 0.93 mmol, 12 equiv.). The conversion of triazoles into triazoliums was performed using **General Procedure M**. The nonapeptoid **58a** was cleaved from the resin by the application of **General Procedure N**. The crude mixture was analysed by LC-MS. The crude was triturated in ether to yield nonapeptoid **58a** (94 mg, 0.05 mmol, 60%). Nonapeptoid **58a** was sufficiently pure to be used for biological evaluation.

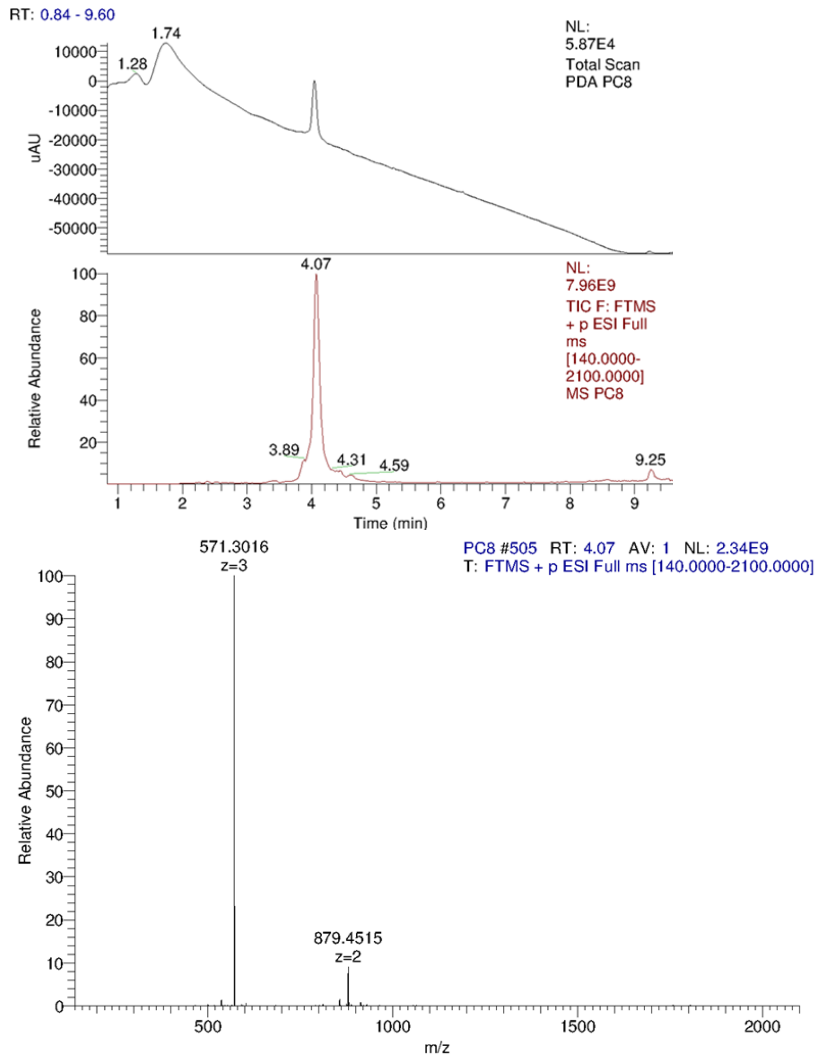
**HRMS** (TOF MS ES<sup>+</sup>):  $m/z$  calculated for  $C_{99}H_{114}N_{19}O_9^{3+}$   $[M]^{3+}$ : 570.9678; found: 570.9676 (-0.16 ppm)

### Copy of LCMS spectra of crude nonapeptoid **58a** synthesized by non-optimized protocol:

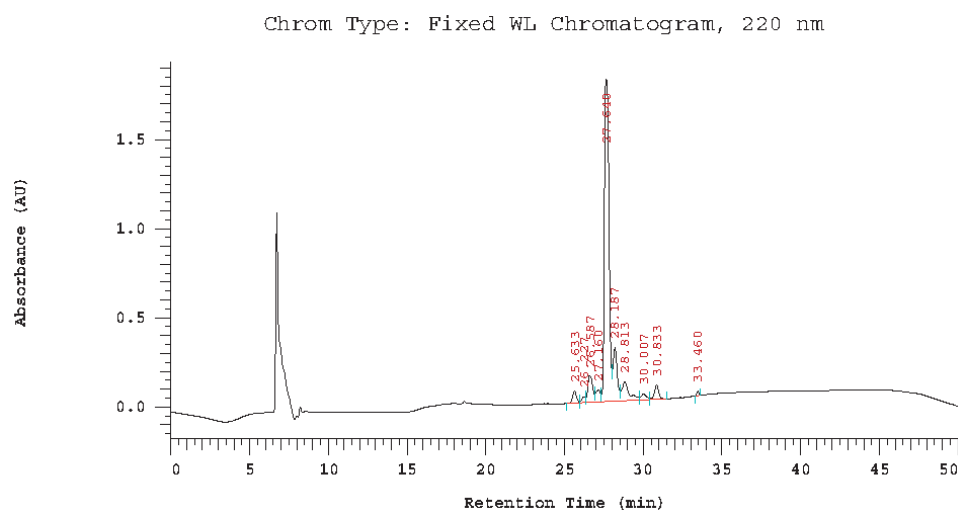




**Copy of LCMS spectra of crude nonapeptoid 58a synthesized by optimized protocol:**

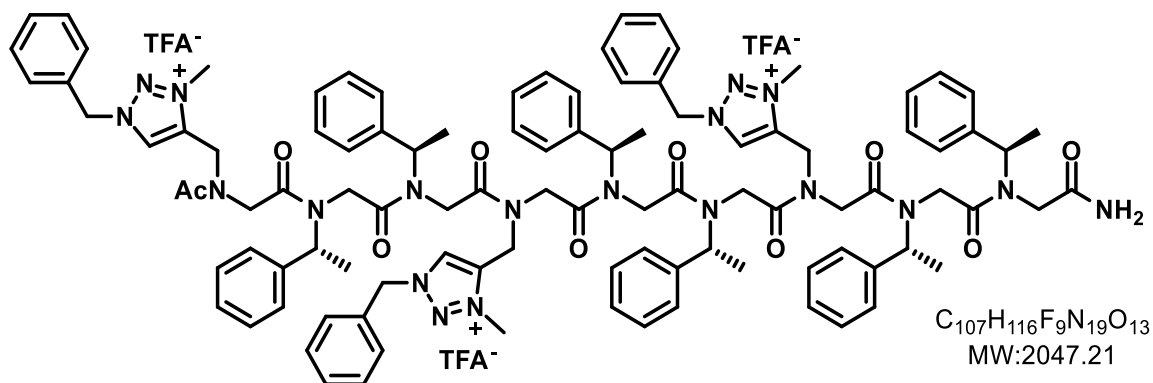


## HPLC chromatogram of nonapeptoid **58a** (Jupiter column C<sub>4</sub>, 5 μm, 300Å):



No.	RT	Area	Conc 1
1	25.633	538649	2.026
2	26.227	254570	0.958
3	26.587	1538073	5.786
4	27.160	708407	2.665
5	27.640	17768529	66.840
6	28.187	2837120	10.672
7	28.813	1683356	6.332
8	30.007	398387	1.499
9	30.833	748688	2.816
10	33.460	107867	0.406
		26583646	100.000

## Nonapeptoid H-(Nbtm<sup>+</sup>-Nspe-Nspe)<sub>3</sub>-NH<sub>2</sub> **58b**



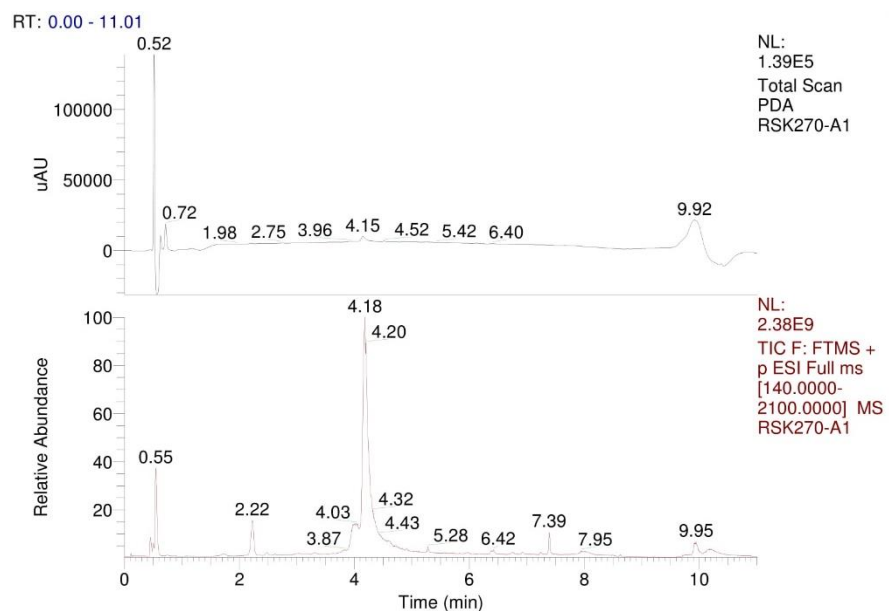
The nonapeptoid **58b** was synthesised by the application of **General Procedure I'** on 100 mg Rink amide MBHA resin by using successively as primary amines: (*S*)-1-phenylethylamine (2x), propargylamine (1x), (*S*)-1-phenylethylamine (2x), propargylamine (1x), (*S*)-1-phenylethylamine (2x), then propargylamine (1x). The capping of the terminal amine was carried out by the application of **General Procedure K**. The triazoles were generated using **General Procedure L**

using azide **41** (126 mg, 0.93 mmol, 12 equiv.). The conversion of triazoles into triazoliums was performed using **General Procedure M**. The nonapeptoid **58b** was cleaved from the resin by the application of **General Procedure N**. The crude mixture was analysed by LC-MS. Purification by preparative HPLC furnished the nonapeptoid **58b** (58 mg, 0.03 mmol, 36%).

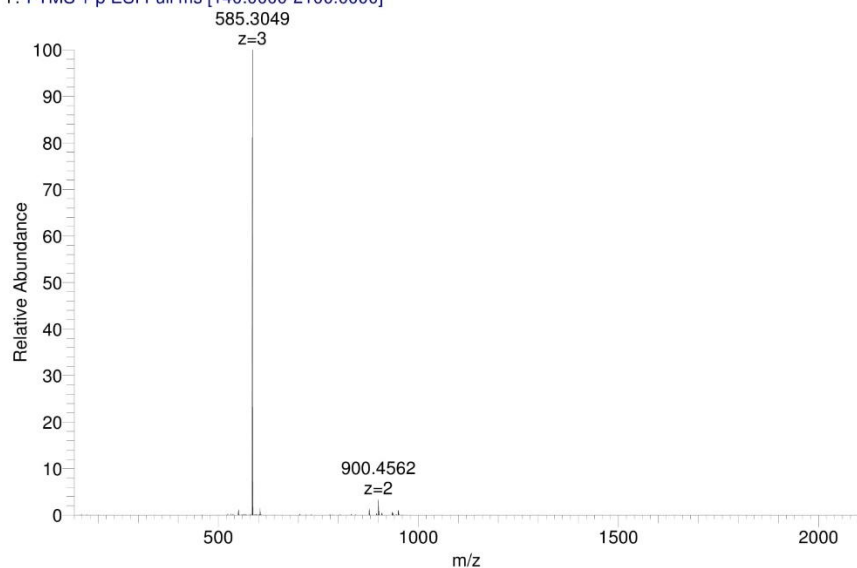
**TLC**  $R_f = 0.6$  ( $\text{CH}_2\text{Cl}_2/\text{MeOH}$ , 8:2)

**HRMS** (TOF MS ES+):  $m/z$  calculated for  $\text{C}_{101}\text{H}_{116}\text{N}_{19}\text{O}_{10}^{3+}$   $[\text{M}]^{3+}$ : 584.9712; found: 584.9717 (0.81 ppm).

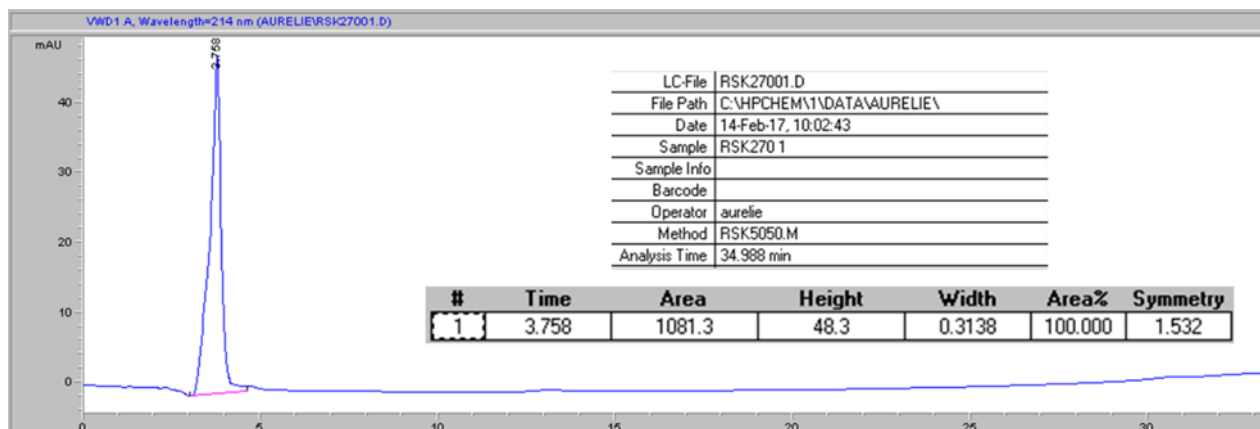
### Copy of LCMS of nonapeptoid **58b**:



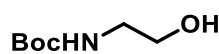
RSK270-A1 #937 RT: 4.17 AV: 1 NL: 6.78E8  
T: FTMS + p ESI Full ms [140.0000-2100.0000]



## Copy of HPLC chromatogram of nonapeptoid **58b** (Acclaim Column C<sub>18</sub>, 5 μm, 120Å):



### Tert-butyl (2-hydroxyethyl)carbamate **59**



C<sub>7</sub>H<sub>15</sub>NO<sub>3</sub>  
MW: 161.20

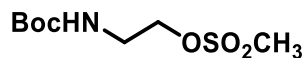
To a solution of 2-aminoethanol (2.74 g, 44.90 mmol, 1 equiv.) in 100 mL dry CH<sub>2</sub>Cl<sub>2</sub>, was added Et<sub>3</sub>N (6.99 g, 69.07 mmol, 1.53 equiv.) at r. t. and after 30 min the solution was cooled to 0°C. Then a solution of Boc<sub>2</sub>O (9.8 g, 44.9 mmol, 1 equiv.) in 50 mL of dry CH<sub>2</sub>Cl<sub>2</sub> was slowly added. The mixture was stirred at r. t. for 15 h and then quenched with a saturated aqueous NH<sub>4</sub>Cl solution. The aqueous phase was extracted 3 times with 50 mL CH<sub>2</sub>Cl<sub>2</sub> and the combined organic extracts were washed with brine, dried over anhydrous Na<sub>2</sub>SO<sub>4</sub>, and concentrated under reduced pressure to give the crude product **59** as a colourless oil (8.42 g, 38.6 mmol, 86%).

TLC R<sub>f</sub> = 0.36 (CH<sub>2</sub>Cl<sub>2</sub>/MeOH, 95:5).

<sup>1</sup>H NMR (400 MHz, CDCl<sub>3</sub>) δ (ppm): 1.44 (s, 9H, 3×CH<sub>3</sub>), 2.51 (s, 1H, OH), 3.28 (dt, J = 5.3 Hz, 2H, CH<sub>2</sub>NH), 3.70 (dt, J = 5.1 Hz, 2H, CH<sub>2</sub>OH), 4.96 (s, 1H, NH).

Spectroscopic data are consistent with those reported in the literature.<sup>157</sup>

### 2-((tert-butoxycarbonyl)amino)ethyl methanesulfonate **60**



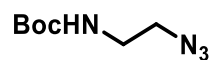
C<sub>8</sub>H<sub>17</sub>NO<sub>5</sub>S  
MW: 239.28

To the Boc protected compound **59** (8.42 g, 52.23 mmol, 1 equiv.) in 120 mL dry CH<sub>2</sub>Cl<sub>2</sub> was added Et<sub>3</sub>N (5.81 g, 57.45 mmol, 1.1 equiv.) and after 30 min the solution was cooled to 0 °C. Then the mesyl chloride (6.58 g, 57.45 mmol, 1.1 equiv.) was added. The resulting mixture was stirred for 1 hour at rt then diluted with CH<sub>2</sub>Cl<sub>2</sub> (60 mL) and washed with NaOH 1M (3x40 mL). The organic layer was dried over Na<sub>2</sub>SO<sub>4</sub>, filtered, and concentrated under reduced pressure to yield the crude mesylate. It was then purified by using column chromatography (Cyclohexane/EtOAc, 6:4) to yield the pure mesylate **60** (10.35 g, 43.35 mmol, 83%).

R<sub>f</sub> = 0.46 (Cyclohexane/EtOAc, 6:4).

<sup>1</sup>H NMR (400 MHz, CDCl<sub>3</sub>): δ 1.45 (s, 9H, 3×CH<sub>3</sub>), 3.03 (s, 3H, CH<sub>3</sub>), 3.47 (m, 2H, CH<sub>2</sub>NH), 4.29 (t, *J* = 5.1 Hz, 2H, CH<sub>2</sub>OH), 4.90 (s, 1H, NH).

### tert-butyl (2-azidoethyl)carbamate **61**



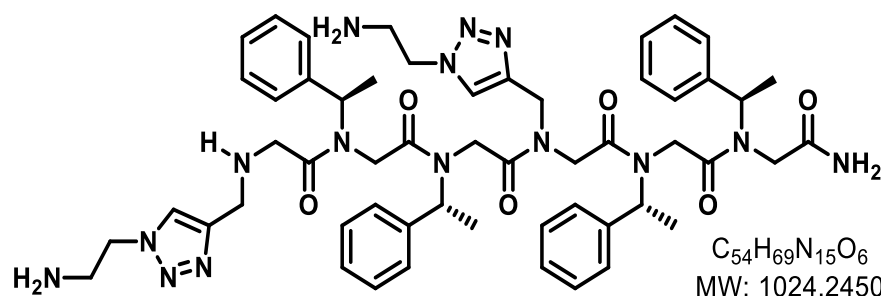
C<sub>7</sub>H<sub>14</sub>N<sub>4</sub>O<sub>2</sub>  
MW: 186.21

The resulting mesylate **60** (1.00 g, 4.18 mmol, 1 equiv.) was dissolved in DMF (6 mL) and NaN<sub>3</sub> (0.41 g, 6.26 mmol, 1.5 equiv.) was added. The mixture was stirred at 65°C overnight then allowed to cool at rt, diluted with H<sub>2</sub>O (9 mL), and extracted with Et<sub>2</sub>O/pentane 50:50 (2×10 mL). The combined organic layers were dried over MgSO<sub>4</sub>, filtered, and concentrated carefully under reduced pressure without heating. The remaining Et<sub>2</sub>O was evaporated overnight under a fume hood yielding tert-butyl (2-azidoethyl)carbamate **61** (0.66 g, 3.55 mmol, 85%) as a white solid.

<sup>1</sup>H NMR (400 MHz, CDCl<sub>3</sub>) δ (ppm): 1.39 (s, 9H, (CH<sub>3</sub>)<sub>3</sub>), 3.28 (t, 2H, CH<sub>2</sub>), 3.36 (t, 2H, CH<sub>2</sub>), 4.81 (bs, 1H, NH).

Spectroscopic data are consistent with those reported in the literature.<sup>158</sup>

### Hexapeptoid H-(Naetm-Nspe-Nspe)<sub>2</sub>-NH<sub>2</sub> **62**



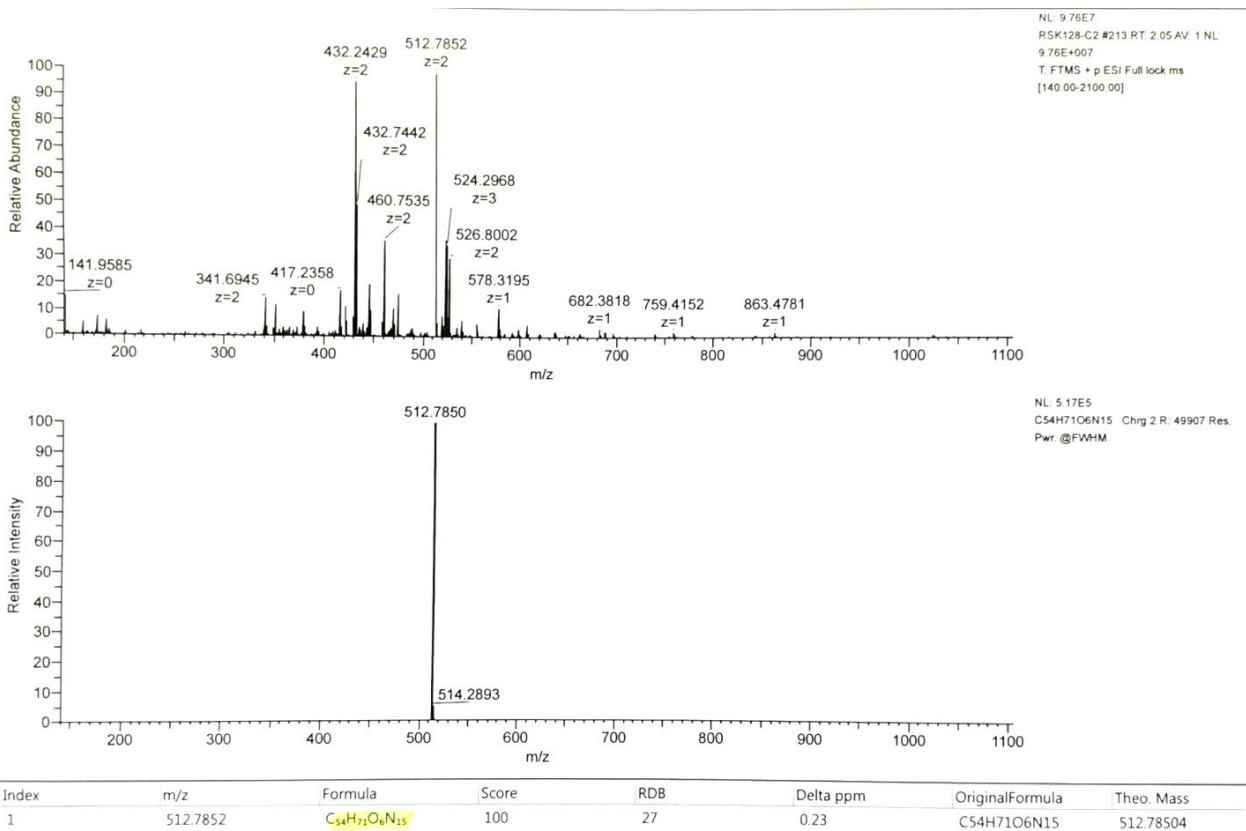
The hexapeptoid **62** was synthesised by the application of **General Procedure I** on 100 mg Rink amide MBHA resin by using successively as primary amines: (*S*)-1-phenylethylamine (2x), propargylamine (1x), (*S*)-1-phenylethylamine (2x), then propargylamine (1x). The protection of the terminal amine was carried out by the application of **General Procedure J**. The triazoles were generated using **General Procedure L** using azide **61** (116 mg, 0.62 mmol, 8 equiv.). The hexapeptoid **62** was cleaved from the resin by the application of **General Procedure N**. The crude mixture was analysed by LC-MS. Purification by preparative HPLC (eluent H<sub>2</sub>O/CH<sub>3</sub>CN 40:60, flow 0.5 ml/min) furnished the hexapeptoid **62** (42 mg) in mixture with the pentapeptoid H-Naetm-Nspe-Nspe-Naetm-Nspe-NH<sub>2</sub>.

The hexapeptoid **62** was synthesised by the application of **General Procedure I** on 100 mg Rink amide MBHA resin by using successively as primary amines: (*S*)-1-phenylethylamine (2x), propargylamine (1x), (*S*)-1-phenylethylamine (2x), then propargylamine (1x). The protection of the terminal amine was carried out by the application of **General Procedure J**. The triazoles were generated using **General Procedure L** using azide **61** (116 mg, 0.62 mmol, 8 equiv.). The hexapeptoid **62** was cleaved from the resin by the application of **General Procedure N**. The crude mixture was analysed by LC-MS. Purification by preparative HPLC (eluent H<sub>2</sub>O/CH<sub>3</sub>CN 40:60, flow 0.5 ml/min) furnished the hexapeptoid **62** (42 mg) in mixture with the pentapeptoid H-Naetm-Nspe-Nspe-Naetm-Nspe-NH<sub>2</sub>.

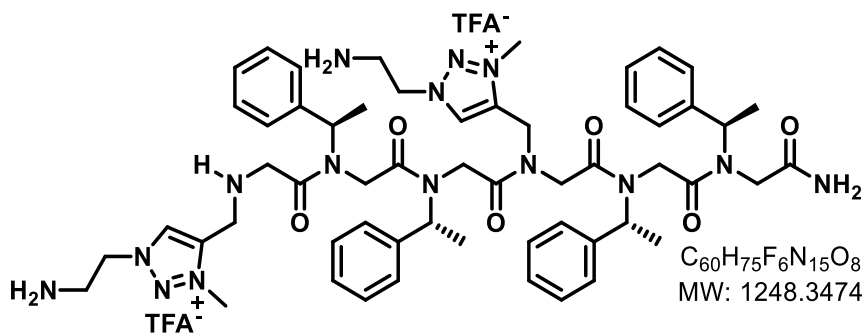
TLC R<sub>f</sub> = 0.51 (CH<sub>2</sub>Cl<sub>2</sub>/MeOH, 93:7)

HRMS (TOF MS ES<sup>+</sup>): *m/z* calculated for C<sub>54</sub>H<sub>69</sub>N<sub>15</sub>O<sub>6</sub> [M]<sup>2+</sup>: 512.7850; found: 512.7852 (0.23 ppm).

## Copy of HRMS of hexapeptoid **62**:



## Hexapeptoid H-(Naetm<sup>+</sup>-Nspe-Nspe)<sub>2</sub>-NH<sub>2</sub> **63**



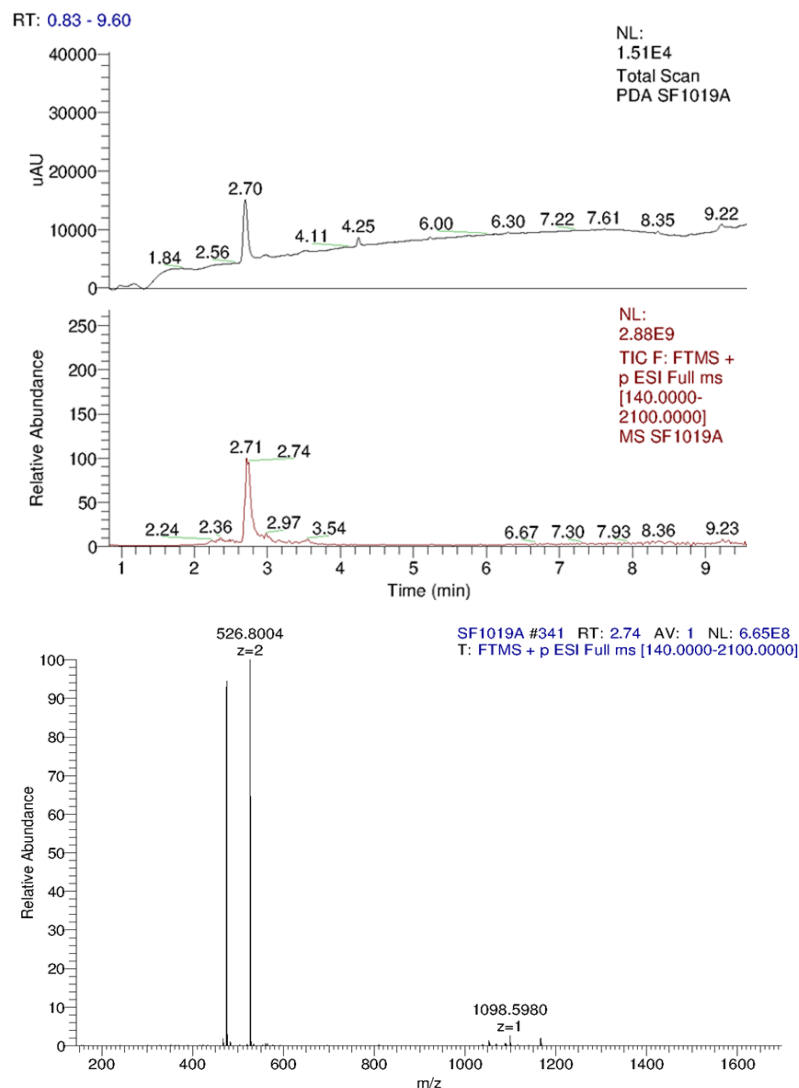
The hexapeptoid **63** was synthesised by the application of **General Procedure I** on 100 mg Rink amide MBHA resin by using successively as primary amines: (*S*)-1-phenylethylamine (2x),

propargylamine (1x), (*S*)-1-phenylethylamine (2x), then propargylamine (1x). The protection of the terminal amine was carried out by the application of **General Procedure J**. The triazoles were generated using **General Procedure L** using azide **61** (116 mg, 0.62 mmol, 8 equiv.). The conversion of triazoles into triazoliums was performed using **General Procedure M**. The hexapeptoid **63** was cleaved from the resin by the application of **General Procedure N**. The crude mixture was analysed by LC-MS. Purification by preparative HPLC (eluent H<sub>2</sub>O/CH<sub>3</sub>CN 65:35) yielded hexapeptoid **63** (33 mg) in mixture with the pentapeptoid H-Naetm<sup>+</sup>-Nspe-Nspe-Naetm<sup>+</sup>-Nspe-NH<sub>2</sub>.

**HRMS** (TOF MS ES+):  $m/z$  calculated for  $C_{56}H_{77}N_{15}O_6^{2+}$   $[M+2H]^{2+}$ : 526.8006; found: 526.8004 (-0.64 ppm)

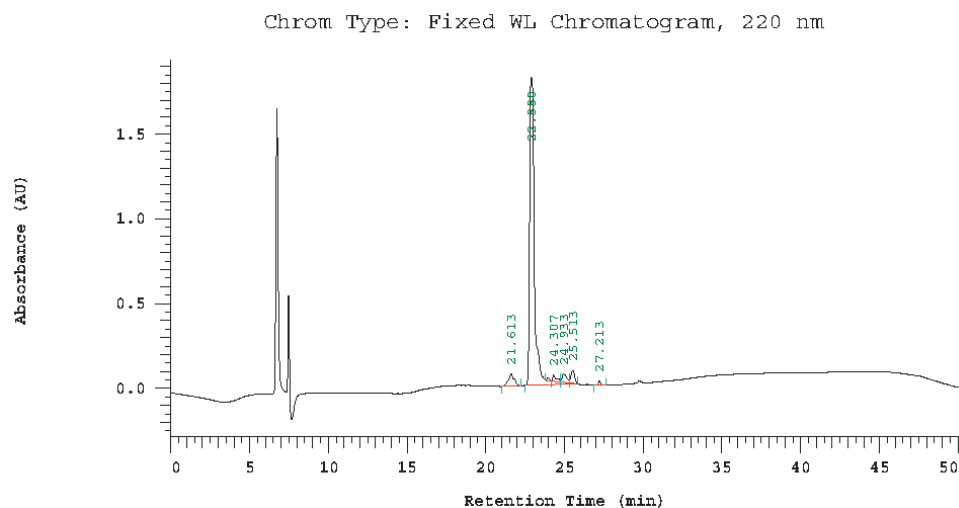
The hexapeptoid **63** was synthesised by the application of **General Procedure H'** on 100 mg Rink amide MBHA resin by using successively as primary amines: (*S*)-1-phenylethylamine (2x), propargylamine (1x), (*S*)-1-phenylethylamine (2x), then propargylamine (1x). The protection of the terminal amine was carried out by the application of **General Procedure J**. The triazoles were generated using **General Procedure L** using azide **61** (116 mg, 0.62 mmol, 8 equiv.). The conversion of triazoles into triazoliums was performed using **General Procedure M**. The hexapeptoid **63** was cleaved from the resin by the application of **General Procedure N**. The crude mixture was analysed by LC-MS. The crude was triturated in ether to yield hexapeptoid **63** (50 mg, 0.04 mmol, 64%\*). \*The yield considers a sample of resin (20%) taken for intermediate characterization.

### Copy of LCMS of hexapeptoid **63** obtained using optimized protocol H':



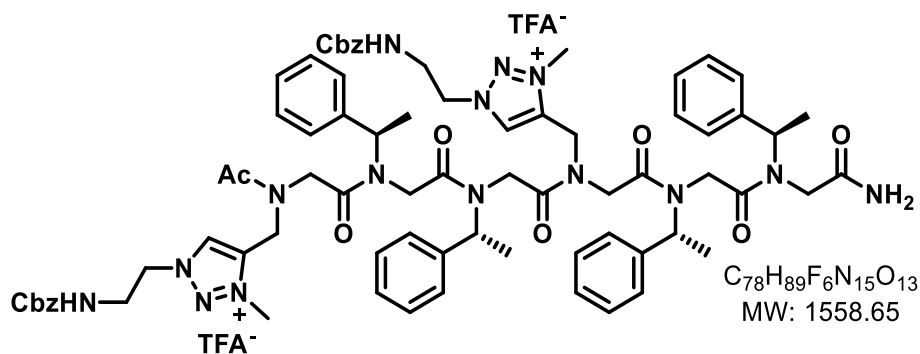


**Copy of HPLC chromatogram of hexapeptoid 63** (Jupiter column C<sub>4</sub>, 5 μm, 300Å):



No.	RT	Area	Conc 1
1	21.613	922460	4.357
2	22.880	18731344	88.475
3	24.307	315096	1.488
4	24.933	500916	2.366
5	25.513	596719	2.819
6	27.213	104737	0.495
		21171272	100.000

**Hexapeptoid Ac-(Naetm<sup>+</sup>(Cbz)-Nspe-Nspe)<sub>2</sub>-NH<sub>2</sub> 64**



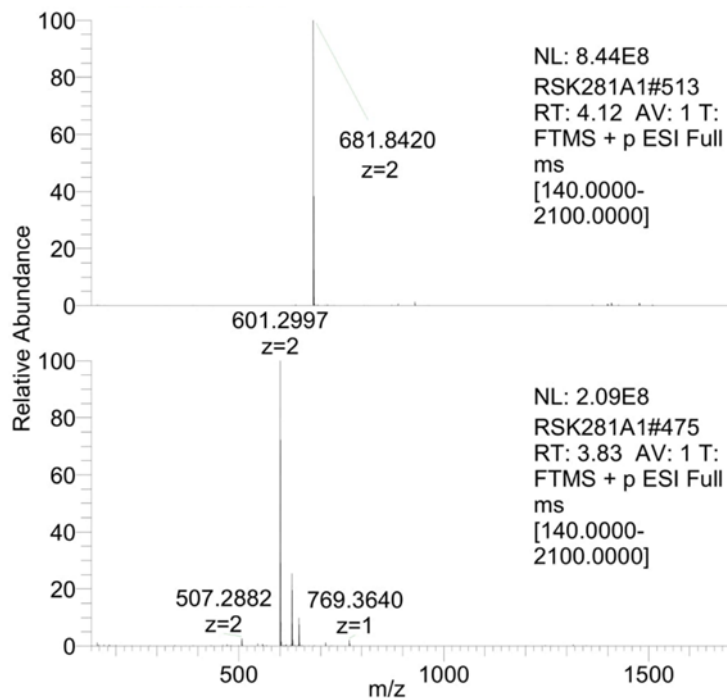
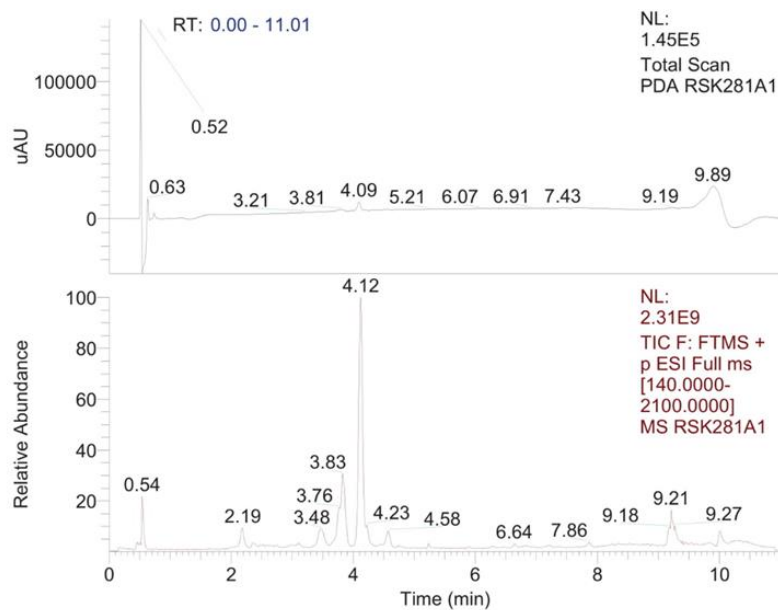
The hexapeptoid **64** was synthesised by the application of **General Procedure I'** on 100 mg Rink amide MBHA resin by using successively as primary amines: (S)-1-

phenylethylamine (2x), propargylamine (1x), (S)-1-phenylethylamine (2x), then propargylamine (1x). The capping of the terminal amine was carried out by the application of **General Procedure K**. The triazoles were generated using **General Procedure L** using azide **46** (137 mg, 0.62 mmol, 8 equiv.). The conversion of triazoles into triazoliums was performed using **General Procedure M**. The hexapeptoid **64** was cleaved from the resin by the application of **General Procedure N**. The crude mixture was analysed by LC-MS. Purification by preparative HPLC (eluent H<sub>2</sub>O/CH<sub>3</sub>CN 70:30) yielded the hexapeptoid **64** (61 mg, 0.04 mmol, 50%).

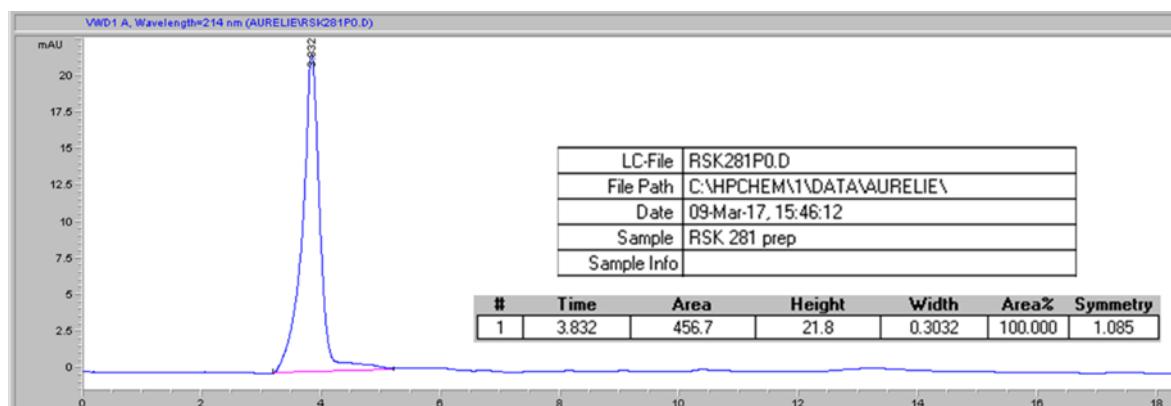
**TLC** R<sub>f</sub> = 0.57 (CH<sub>2</sub>Cl<sub>2</sub>/MeOH, 8:2)

**HRMS (TOF MS ES+):**  $m/z$  calculated for  $C_{74}H_{89}N_{15}O_{11}^{2+}$   $[M]^{2+}$ : 681.8427; found: 681.8427 (-0.15 ppm).

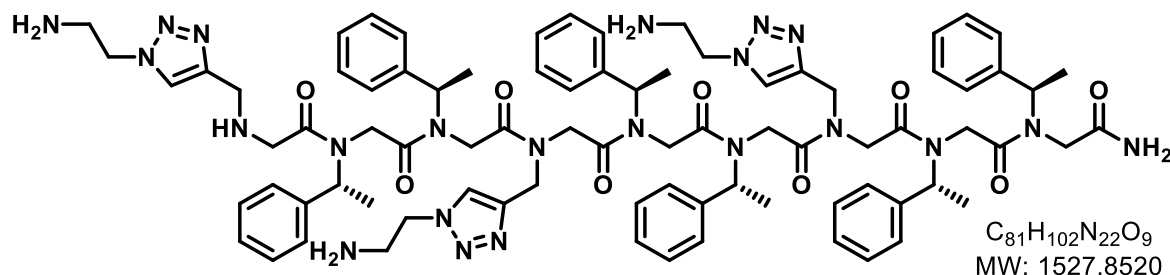
**Copy of LCMS of hexapeptoid 64:**



## Copy of HPLC chromatogram of hexapeptoid **64** (Acclaim Column C<sub>18</sub>, 5 μm, 120Å)



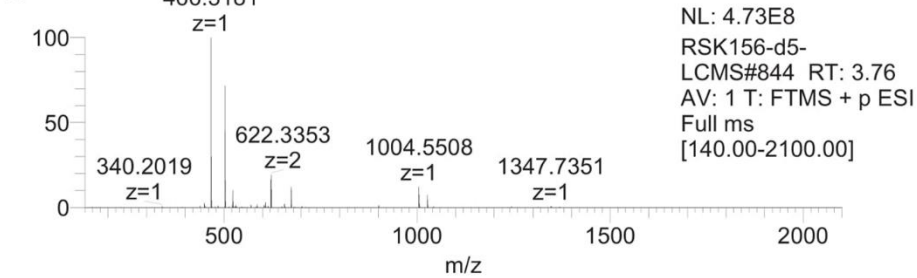
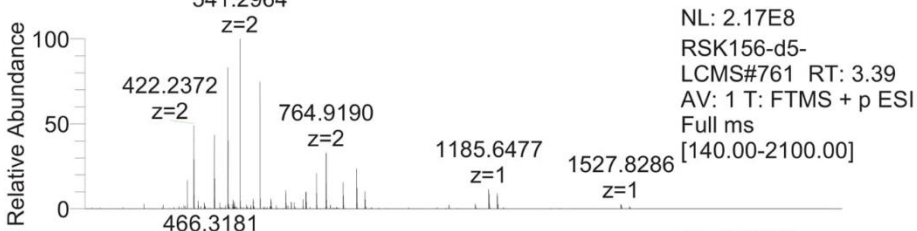
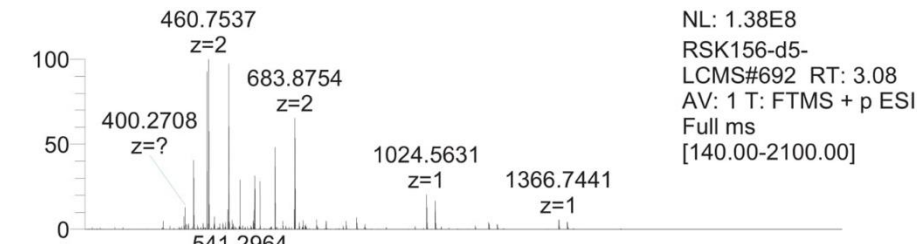
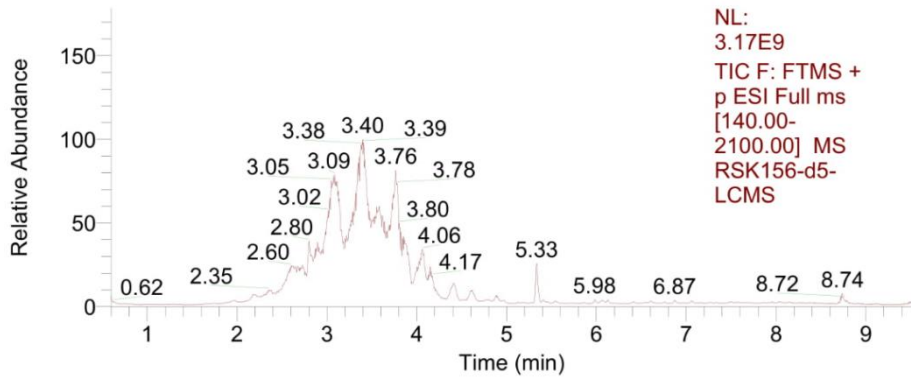
## Nonapeptoid H-(Naetm-Nspe-Nspe)<sub>3</sub>-NH<sub>2</sub> **65**



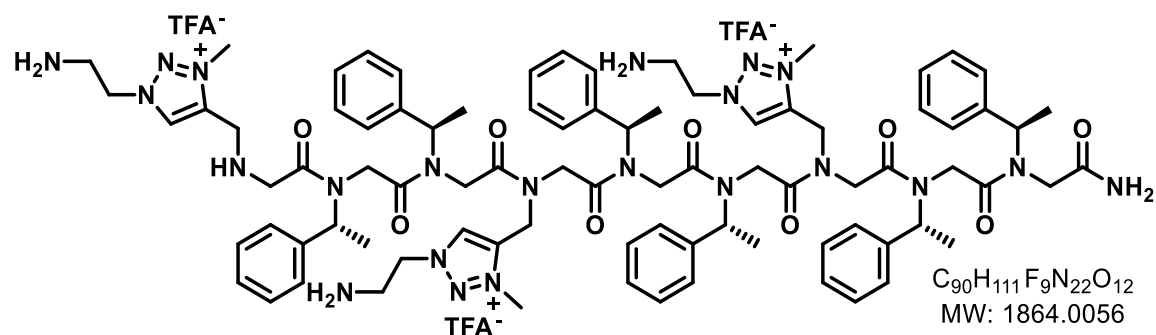
The nonapeptoid **65** was synthesised by the application of **General Procedure I** on 100 mg Rink amide MBHA resin by using successively as primary amines: (*S*)-1-phenylethylamine (2x), propargylamine (1x), (*S*)-1-phenylethylamine (2x), propargylamine (1x), (*S*)-1-phenylethylamine (2x), then propargylamine (1x). The protection of the terminal amine was carried out by the application of **General Procedure J**. The triazoles were generated using **General Procedure L** using azide **61** (174 mg, 0.93 mmol, 12 equiv.). The nonapeptoid **65** was cleaved from the resin by the application of **General Procedure N**. The crude mixture was analysed by LC-MS. Purification by preparative HPLC (eluent H<sub>2</sub>O/CH<sub>3</sub>CN 60:40) did not furnish the desired pure nonapeptoid **65**.

**HRMS** (TOF MS ES<sup>+</sup>): *m/z* calculated for C<sub>81</sub>H<sub>102</sub>N<sub>22</sub>O<sub>9</sub> [M+3H]<sup>3+</sup>: 1527.8272; found: 1527.8298 (1.67 ppm).

**Copy of LCMS of nonapeptoid 65:**



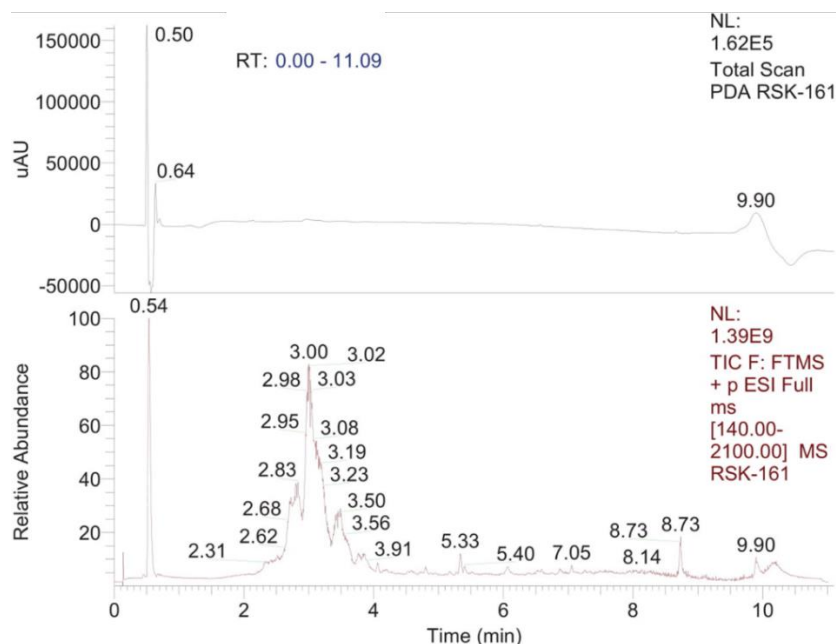
## Nonapeptoid H-(*Naetm*<sup>+</sup>-*Nspe*-*Nspe*)<sub>3</sub>-NH<sub>2</sub> **66**

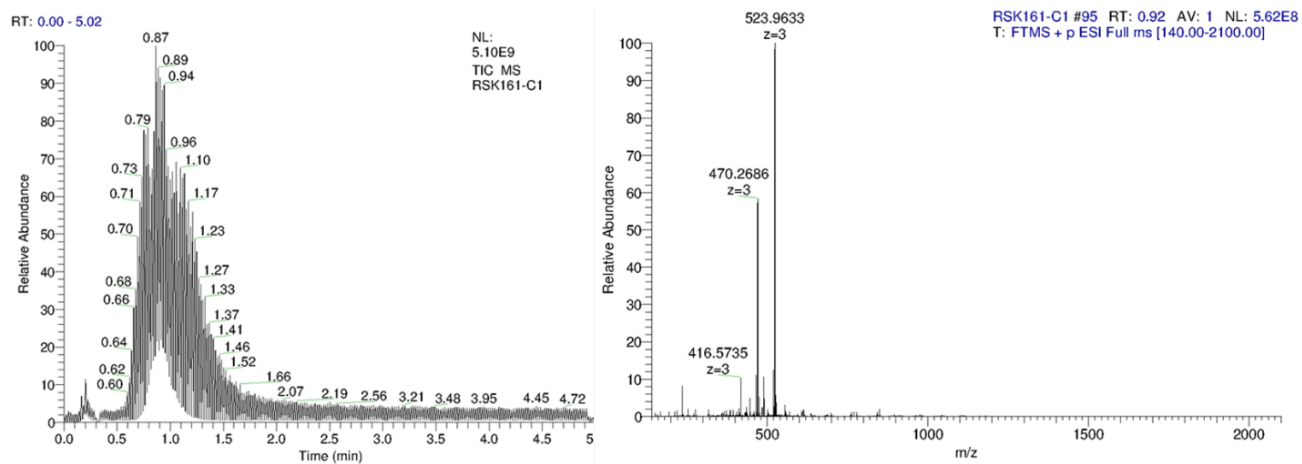
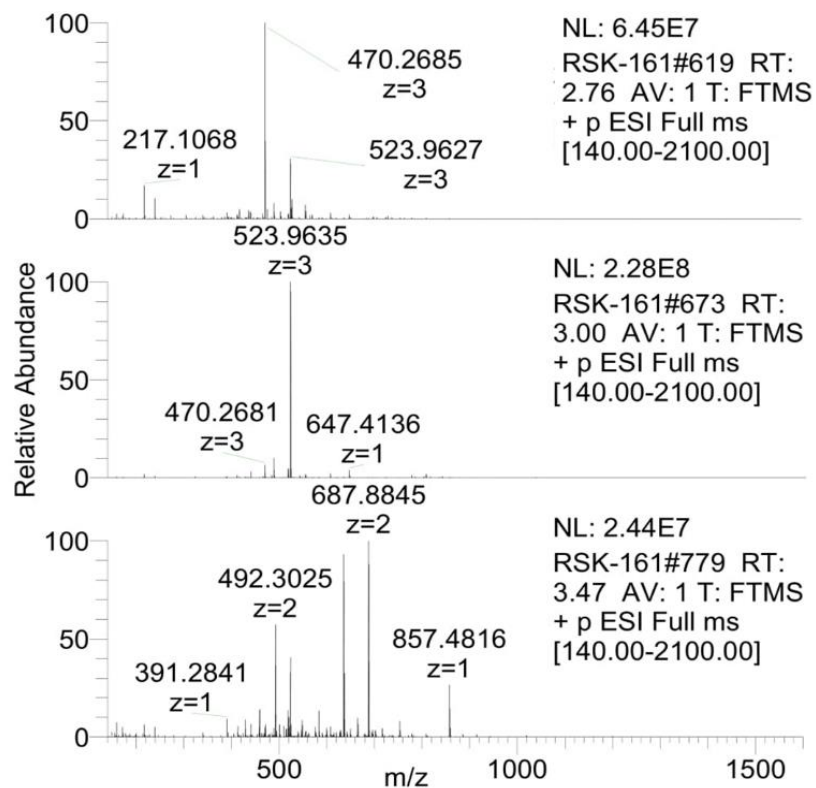


The nonapeptoid **66** was synthesised by the application of **General Procedure I** on 100 mg Rink amide MBHA resin by using successively as primary amines: (*S*)-1-phenylethylamine (2x), propargylamine (1x), (*S*)-1-phenylethylamine (2x), propargylamine (1x), (*S*)-1-phenylethylamine (2x), then propargylamine (1x). The protection of the terminal amine was carried out by the application of **General Procedure J**. The triazoles were generated using **General Procedure L** using azide **61** (174 mg, 0.93 mmol, 12 equiv.). The conversion of triazoles into triazoliums was performed using **General Procedure M**. The nonapeptoid **66** was cleaved from the resin by the application of **General Procedure N**. The crude mixture was analysed by LC-MS. Purification by preparative HPLC (eluent H<sub>2</sub>O/CH<sub>3</sub>CN 60:40) yielded the desired nonapeptoid **66** (90 mg, 0.06 mmol, 74%) contaminated with the octapeptoid H-(*Naetm*<sup>+</sup>-*Nspe*-*Nspe*)<sub>2</sub>-*Naetm*<sup>+</sup>-*Nspe*-NH<sub>2</sub>.

**HRMS** (TOF MS ES<sup>+</sup>): *m/z* calculated for C<sub>84</sub>H<sub>111</sub>N<sub>22</sub>O<sub>9</sub><sup>3+</sup> [M]<sup>3+</sup>: 523.9629; found: 523.9631 (0.39 ppm).

### Copy of LCMS of nonapeptoid **66**:

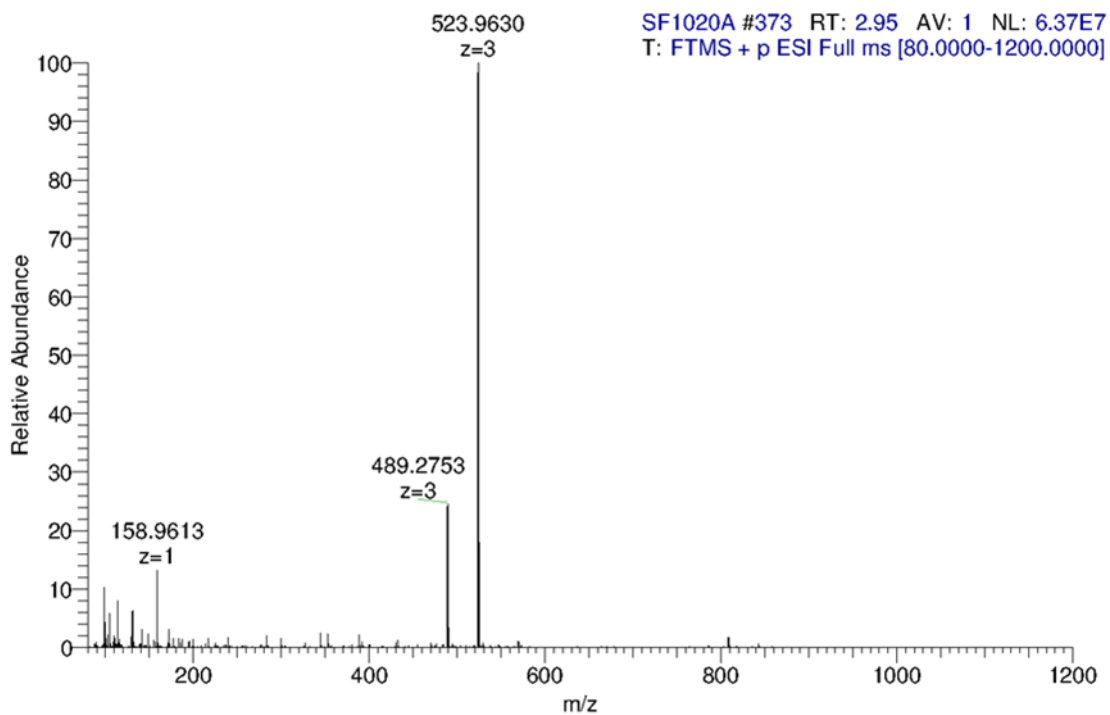
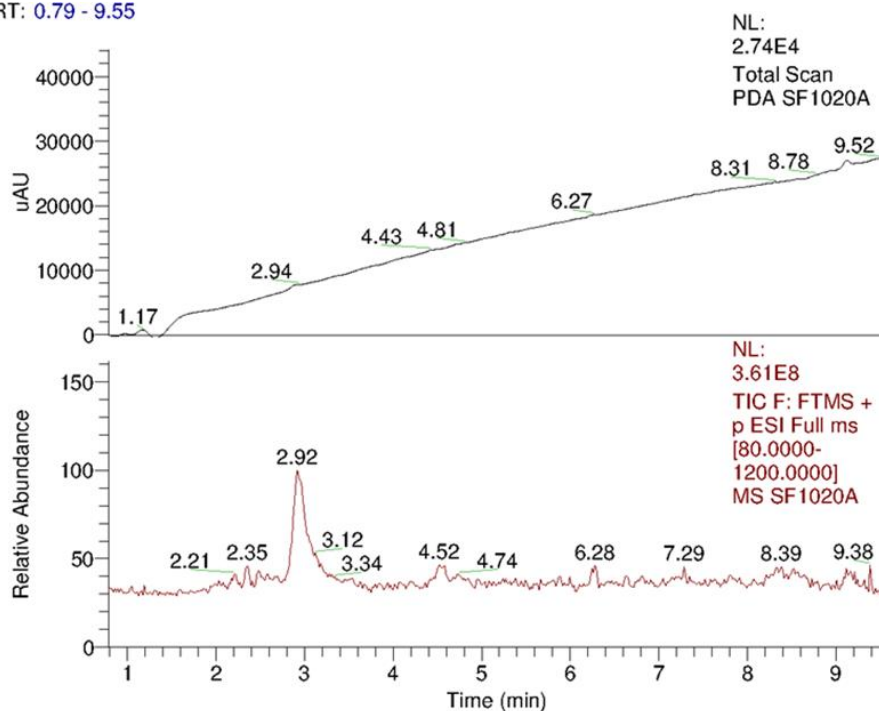




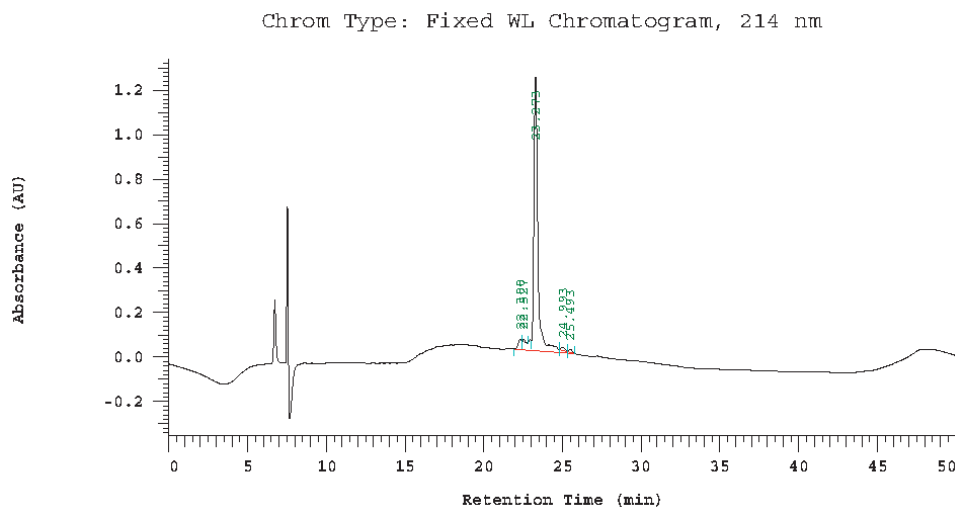
Using **optimized protocol H'**, the nonapeptoid **66** was obtained with a good purity after trituration in ether.

# LCMS of nonapeptoid 66 obtained using optimized protocol H':

RT: 0.79 - 9.55

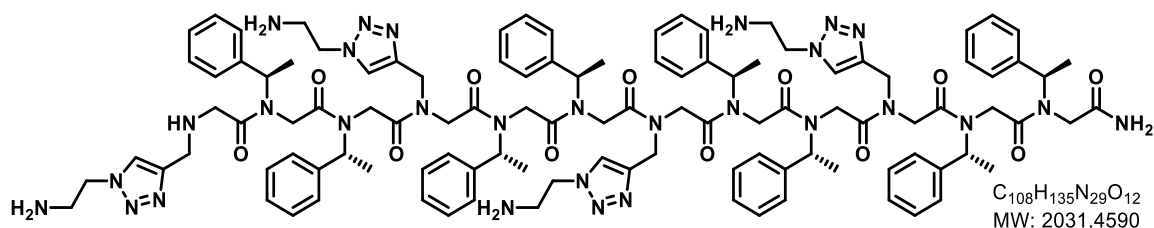


## Copy of HPLC chromatogram of hexapeptoid **63** (Jupiter column C<sub>4</sub>, 5 μm, 300Å):



No.	RT	Area	Conc 1
1	22.300	350267	2.975
2	22.527	403535	3.427
3	23.273	10807987	91.791
4	24.993	122743	1.042
5	25.493	90017	0.765
		11774549	100.000

## Dodecapeptoid H-(*Naetm-Nspe-Nspe*)<sub>4</sub>-NH<sub>2</sub> **67**



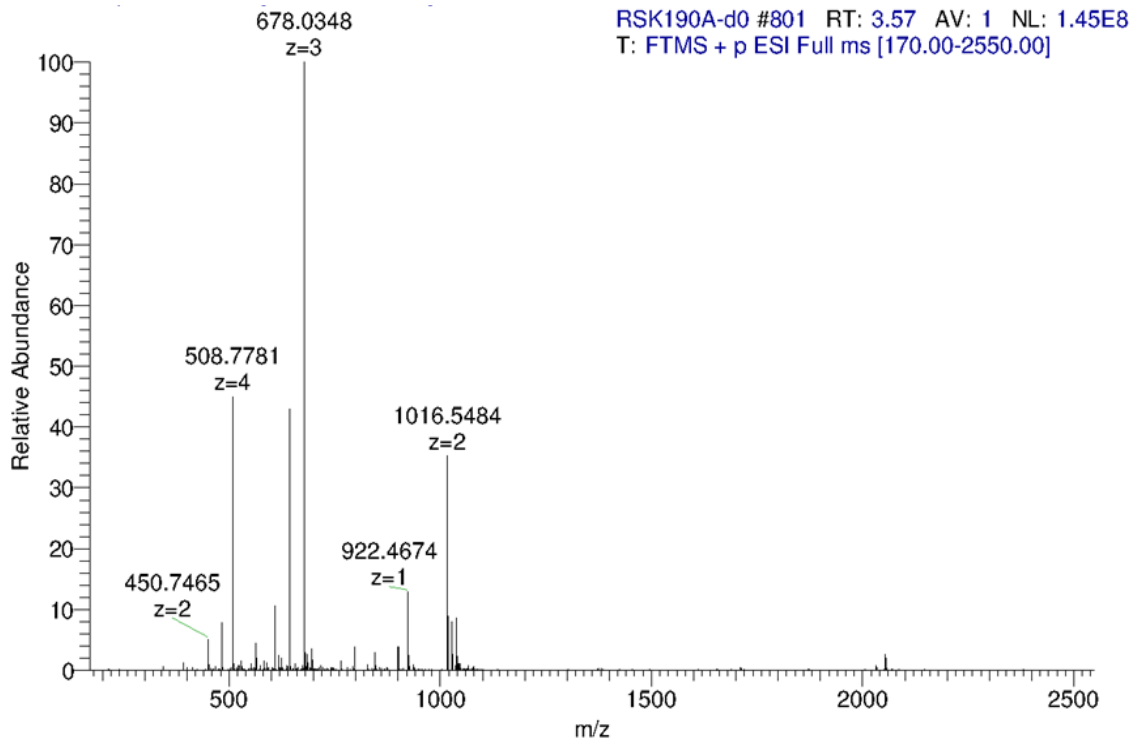
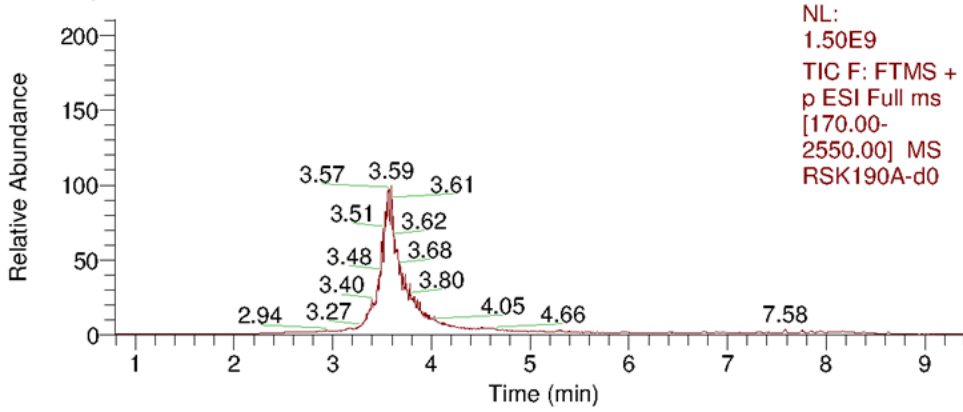
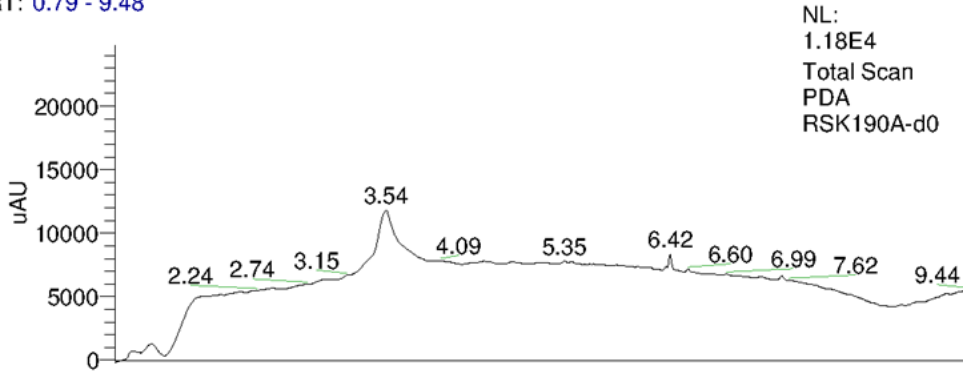
The dodecapeptoid **67** was synthesised by the application of **General Procedure I'** on 100 mg Rink amide MBHA resin by using successively as primary amines: (*S*)-1-phenylethylamine (2x), propargylamine (1x), (*S*)-1-phenylethylamine (2x), propargylamine (1x), (*S*)-1-phenylethylamine (2x), propargylamine (1x), (*S*)-1-phenylethylamine (2x), then propargylamine (1x). The protection of the terminal amine was carried out by the application of **General Procedure J**. The triazoles were generated using **General Procedure L** using azide **61** (232 mg, 1.24 mmol, 16 equiv.). The dodecapeptoid **67** was cleaved from the resin by the application of **General Procedure N**. The crude mixture was analysed by LC-MS. Purification by preparative HPLC (eluent H<sub>2</sub>O/CH<sub>3</sub>CN 65:35) furnished the desired dodecapeptoid **67** (91 mg, 0.05 mmol, 57%).



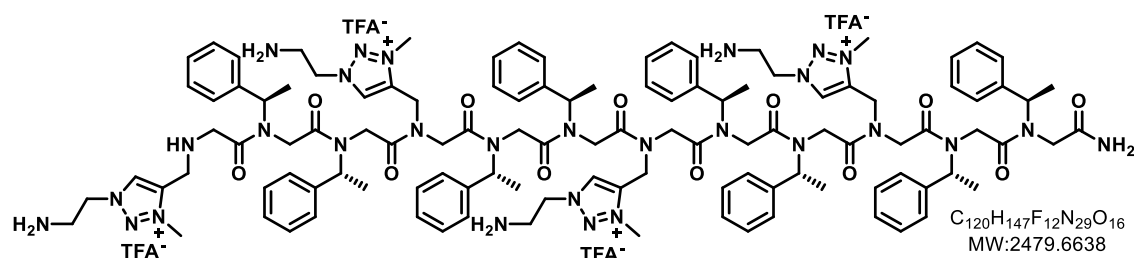
**HRMS (TOF MS ES+):**  $m/z$  calculated for  $C_{108}H_{135}N_{29}O_{12} [M+3H]^{3+}$ : 677.7021; found: 677.7009 (-1.74 ppm).

**Copy of LCMS of dodecapeptoid 67:**

RT: 0.79 - 9.48



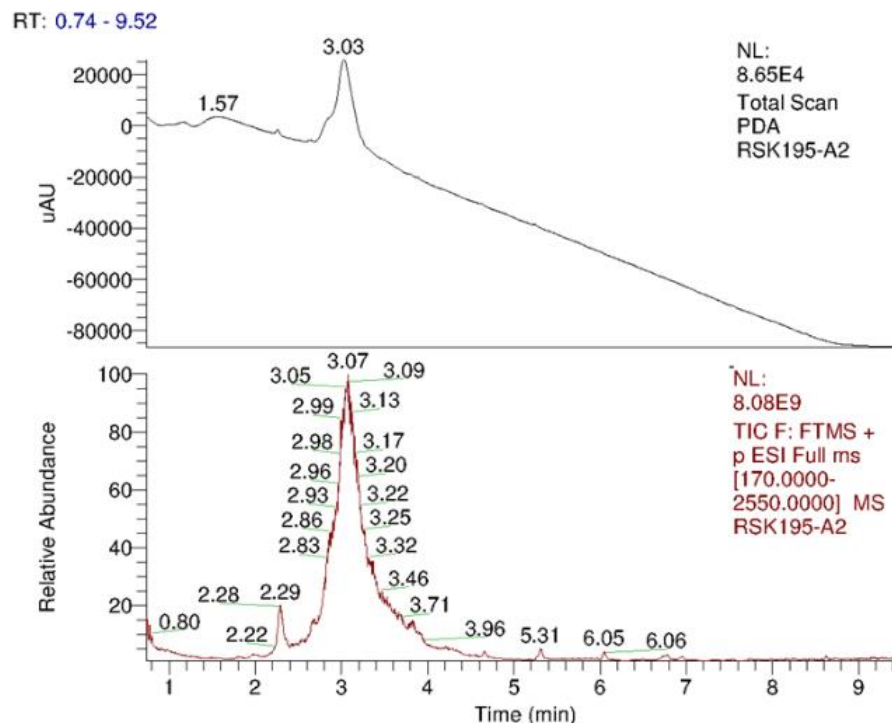
## Dodecapeptoid H-(*N*aetm<sup>+</sup>-*N*spe-*N*spe)<sub>4</sub>-NH<sub>2</sub> **68**

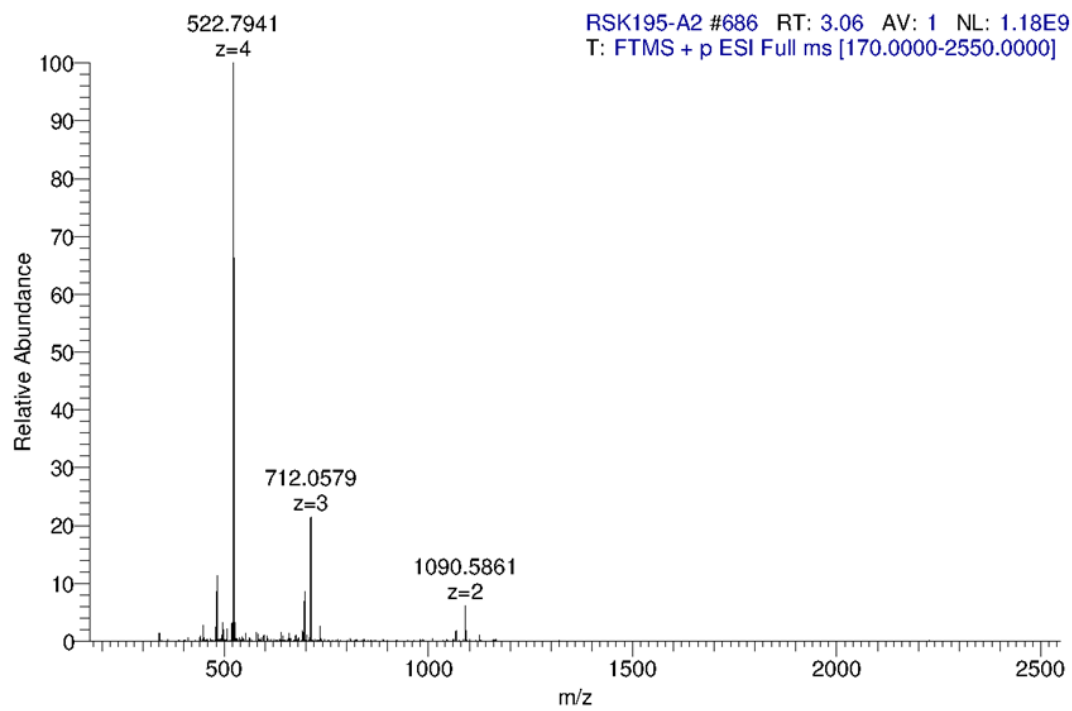


The dodecapeptoid **68** was synthesised by the application of **General Procedure I'** on 100 mg Rink amide MBHA resin by using successively as primary amines: (*S*)-1-phenylethylamine (2x), propargylamine (1x), (*S*)-1-phenylethylamine (2x), propargylamine (1x), (*S*)-1-phenylethylamine (2x), propargylamine (1x), (*S*)-1-phenylethylamine (2x), then propargylamine (1x). The protection of the terminal amine was carried out by the application of **General Procedure J**. The triazoles were generated using **General Procedure L** using azide **61** (232 mg, 1.24 mmol, 16 equiv.). The conversion of triazoles into triazoliums was performed using **General Procedure M**. The dodecapeptoid **67** was cleaved from the resin by the application of **General Procedure N**. The crude mixture was analysed by LC-MS. Purification by preparative HPLC (eluent H<sub>2</sub>O/CH<sub>3</sub>CN 65:35) furnished the desired dodecapeptoid **68** (63 mg, 0.03 mmol, 33%).

**HRMS** (TOF MS ES<sup>+</sup>): *m/z* calculated for C<sub>112</sub>H<sub>147</sub>N<sub>29</sub>O<sub>12</sub><sup>4+</sup> [M]<sup>4+</sup>: 522.5440; found: 522.5441 (0.03 ppm).

### Copy of LCMS of dodecapeptoid **68**:





## 6 General information Biological assays

Peptoids were dissolved in Muller Hinton broth (MHB) with 4% of DMSO at a concentration of 400  $\mu$ M, filtered using 0.45  $\mu$ M sterile, non-pyrogenic hydrophilic filter, and were stored at -20 °C before subsequent assessments. Bacterial strains *E. coli* JM109, *E. coli* ATCC® 25922™, *P. aeruginosa* ATCC® 27853™, *S. aureus* CIP6525, and *E. faecalis* ATCC® 29212™ were stored at -80 °C in 15% glycerol. Melittin was purchased from Iscabiochemicals, United Kingdom and stored in fridge and it was dissolved in MHB and stored at -20°C. MHB powder was purchased from Difco™, Becton-Dickinson™ France and used to prepare the culture medium according to the manufacturer's instructions. Triton X-100, EDTA, dimethyl sulfoxide (DMSO) were purchased from Sigma-Aldrich. Ethanol, acetone, tertiary butanol, and glutaraldehyde were all analytical grade. 3-(4,5-dimethylthiazol-2-yl)-2,5-diphenyltetrazolium bromide (MTT) was purchased from Sigma-Aldrich. Fresh human red blood cells (hRBCs) were collected by ZenBio (USA) reference number (w36981700775500) and stored in Acid Citrate Dextrose Solution (ACD). The HeLa (ATCC® CCL2™) and Jurkat Clone E6-1 (ATCC® TIB-152™) cells were purchased from American Type Cell Culture (ATCC). The MEM with Earle's Salts, with stabilized Glutamine; RPMI 1640 with stabilized Glutamine; Trypsin-EDTA 1X in PBS without calcium, without magnesium, with phenol red; Dulbecco's Phosphate Buffered Saline without magnesium, without calcium; and Bovine Serum Albumin (BSA) Fraction V were purchased from Dominique Dutscher.

## EXPERIMENTAL PROCEDURES CHAPTER IV

### 7 Antimicrobial activity

#### 7.1 Bacterial cell culture:

Overnight cultures were made by transferring a colony (~half a loop) from the frozen cultures of bacteria (e.g. *E. coli* ATCC 25922) to culture tubes containing sterilized Muller Hilton broth (7 ml) in a sterile environment. Bacterial cultures were incubated overnight at 37 °C with aeration and with agitation at 150 rotations per minute using New Brunswick Scientific's C25 Incubator Shaker.

##### 7.1.1 Gram Staining:

Transfer a drop of the suspended culture to be examined on a slide with inoculation loop. Note that only a very small amount of culture is needed. Spread the culture with an inoculation loop to an even thin film over a circle of 1.5 cm in diameter, approximately the size of a 1 cm<sup>2</sup>. Air-dry the culture, while moving the slide in a circular for the cell adhesion on the glass. Add crystal violet stain over the fixed culture. Let stand for 10 to 60 seconds. Pour off the stain and gently rinse the excess stain with a stream of water from a plastic water bottle. Add the Gram's iodine solution on the smear, enough to cover the fixed culture. Let stand for 10 to 60 seconds. Pour off the iodine solution and rinse the slide with running water. Shake off the excess water from the surface. Add a few drops of decolourizer (95% ethanol) so the solution trickles down the slide. Rinse it off with

water after 5 seconds. Counter stain with 0.1% basic fuchsin solution for 40 to 60 seconds. Wash off the solution with water. Blot with bibulous paper to remove the excess water and air-dry the slide. Examine the finished slide under a microscope. Look at areas that are one cell thick only; observation of thick areas will give variable and often incorrect results.

## 7.2 Minimum inhibitory concentration (MIC) measurement:

After culturing, bacterial cells were measured for optical density (OD) using Thermo Scientific's GENESYS 30 visible spectrophotometer at 470 nm and were diluted in media (MHB) to have the cell density of  $1 \times 10^6$  CFU/mL by appropriate dilution factor as described. (Table 28).

Table 28 Inoculum preparation from bacterial stock culture.

Bacteria	Factor
<i>E. coli</i> JM109	Optical density $\times 5 \times 10^8$
<i>E. coli</i>	Optical density $\times 10^9$
<i>P. aeruginosa</i>	Optical density $\times 10^9$
<i>S. aureus</i>	Optical density $\times 1.8 \times 10^8$
<i>E. faecalis</i>	Optical density $\times 10^9$

To verify the cell density of  $1 \times 10^6$  CFU/mL for each bacterium, the inoculum was plated on a petri plate with Muller Hinton agar media using Interscience's easySpiral® Dilute (Automatic serial diluter and plater) and the cells were counted using Interscience's Scan® 500 automatic colony counter. The results are given below in the following tables.

Table 29 *E. coli* JM109 with  $10^{-3}$  dilution

Sample No.	1	2	3	4	5	6	7
No. of CFU	50	47	86	56	54	38	47
Sensibility	26	28	51	40	27	30	26
CFU/mL	$1.6 \times 10^6$	$1.3 \times 10^6$	$0.9 \times 10^6$	$0.6 \times 10^6$	$2.7 \times 10^6$	$1.9 \times 10^6$	$0.9 \times 10^6$

Table 30 *E. coli* with  $10^{-3}$  dilution

Sample No.	1	2	3	4	5	6	7
No. of CFU	50	43	42	55	36	51	49
Sensibility	25	30	19	28	36	28	26
CFU/mL	$1.4 \times 10^6$	$1.2 \times 10^6$	$1.2 \times 10^6$	$1.5 \times 10^6$	$1.0 \times 10^6$	$1.4 \times 10^6$	$1.6 \times 10^6$

Table 31 *P. aeruginosa* with  $10^{-3}$  dilution

Sample No.	1	2	3	4	5	6	7
No. of CFU	50	63	53	61	54	49	59
Sensibility	28	28	21	39	33	26	26
CFU/mL	$1.6 \times 10^6$	$1.8 \times 10^6$	$0.5 \times 10^6$	$1.0 \times 10^6$	$1.5 \times 10^6$	$1.0 \times 10^6$	$1.2 \times 10^6$

Table 32 *S. aureus* with 10<sup>-3</sup> dilution

Sample No.	1	2	3	4	5	6	7
No. of CFU	72	61	71	54	53	62	63
Sensibility	28	28	28	26	39	46	26
CFU/mL	3.5×10 <sup>6</sup>	3.0×10 <sup>6</sup>	3.9×10 <sup>6</sup>	5.3×10 <sup>6</sup>	5.1×10 <sup>6</sup>	1.0×10 <sup>6</sup>	3.5×10 <sup>6</sup>

Table 33 *E. faecalis* with 10<sup>-3</sup> dilution

Sample No.	1	2	3	4	5	6	7
No. of CFU	69	90	67	57	62	37	58
Sensibility	28	46	36	33	30	26	26
CFU/mL	6.7×10 <sup>6</sup>	8.7×10 <sup>6</sup>	3.3×10 <sup>6</sup>	5.5×10 <sup>6</sup>	1.0×10 <sup>6</sup>	2.1×10 <sup>6</sup>	1.9×10 <sup>6</sup>

MICs were determined according to CLSI M7-A9 protocols in a Falcon® 96-well Clear Flat Bottom microtiter plate.<sup>166</sup> A dilution series of each peptoid was made by 1:2 serially diluting test compound stock (400 µM) in media (MHB) to a desired range of concentrations (ranging from 200 µM to 0.35 µM) and a final volume of 100 µL in each well of a 96-well microtiter plate. 100 µL of 1×10<sup>6</sup> CFU/mL bacteria solution (prepared according to Table 28) was added to each well. The 96-well plate was then incubated at 37 °C for overnight. Positive control was made by adding 50 µL of MHB and 50 µL of the 10<sup>6</sup> CFU of bacterial culture. Negative control was made by adding 100 µL of the MHB and 5 µL of peptoid. The Melittin (100 µM stock) was used as control. The measurement of MIC was done by the visual inspection of the microtiter plate after overnight incubation. The wells with transparent media were marked as the inhibitory concentrations of the peptoid giving us the last concentration with transparent media as the MIC of the peptoid. A minimum of three independent experiments (biological replicates) of the assay were conducted, and two technical replicates (parallel) were used in each experiment for each bacterium, peptoid and concentration.

### 7.3 Minimal Bactericidal Concentration (MBC) measurement:

MBC is obtained by sub-culturing an inoculum (10 µL aliquots) from all the wells showing no growth into Falcon® square petri dish containing Muller Hinton agar. For each well, microbial solution was diluted with saline (0.9% sodium chloride solution) using an appropriate dilution factor (1:2 serial dilution). The agar plates were incubated for 1h at room temperature with aeration and then for overnight at 37 °C in an anaerobic chamber. The last of the wells yielding no growth on that agar indicates the MBC of the peptoid. A minimum of three independent experiments (biological replicates) of the assay were conducted, and two technical replicates (parallel) were used in each experiment for each bacterium, peptoid and concentration.

Table 34 MIC and MBC values of 3 families of peptoid oligomers

	Peptoid	Conc.		<i>E. coli</i> JM109		<i>E. coli</i>		<i>P. aeruginosa</i>		<i>S. aureus</i>		<i>E. faecalis</i>	
		MIC	MBC	MIC	MBC	MIC	MBC	MIC	MBC	MIC	MBC	MIC	MBC
<b>49</b>	H-(Nlys-Nspe-Nspe) <sub>2</sub> -NH <sub>2</sub>	μM	>200	>200	>200	>200	>200	100	200	>200	>200	>200	>200
		μg/ml	>184	>184	>184	>184	92	184	>184	>184	>184	>184	>184
		μM	50	50	100	100	100	200	25	50	25	25	25
<b>50</b>	H-(Nlys-Nspe-Nspe) <sub>3</sub> -NH <sub>2</sub>	μg/ml	68.5	68.5	137	137	137	137	274	34.3	68.5	14.3	34.3
		μM	>200	>200	>200	>200	>200	>200	>200	>200	>200	>200	>200
		μg/ml	>159	>159	>159	>159	>159	>159	>159	>159	>159	>159	>159
<b>IA</b>	Ac-(Nlys-Mbu-Mtbu) <sub>2</sub> -OEt	μM	200	>200	166	200	>200	>200	>200	6.3	12.5	25	50
		μg/ml	256	>256	213	256	>256	>256	>256	8	16	32	64.1
		μM	>200	>200	>200	>200	>200	>200	>200	>200	>200	>200	>200
<b>IIA</b>	Ac-(Nbtm <sup>+</sup> -Ntbu-Ntbu) <sub>2</sub> -OEt	μM	200	>200	166	200	>200	>200	>200	6.3	12.5	25	50
		μg/ml	256	>256	213	256	>256	>256	>256	8	16	32	64.1
		μM	>200	>200	>200	>200	>200	>200	>200	>200	>200	>200	>200
<b>IIIA</b>	H-(Nchtm-Nspe-Nspe) <sub>2</sub> -NH <sub>2</sub>	μM	>274	>274	>274	>274	>274	>274	>274	>274	>274	>274	>274
		μg/ml	>274	>274	>274	>274	>274	>274	>274	>274	>274	>274	>274
		μM	50	50	50	50	>200	>200	>200	3.1	6.3	6.3	12.5
<b>54a</b>	H-(Nchtm <sup>+</sup> -Nspe-Nspe) <sub>2</sub> -NH <sub>2</sub>	μg/ml	69.3	69.3	69.3	69.3	>277	>277	>277	3.5	7.1	7.1	14.1
		μM	25	25	25	25	166.6	200	3.1	6.3	1.8	3.1	
		μg/ml	51.8	51.8	51.8	51.8	344.5	414.2	6.5	12.9	3.8	6.5	
<b>58a</b>	H-(Nbtm <sup>+</sup> -Nspe-Nspe) <sub>3</sub> -NH <sub>2</sub>	μM	12.5	25	12.5	25	>200	>200	>200	1.6	3.1	1.6	3.1
		μg/ml	25.7	51.3	25.7	51.3	>410.6	>410.6	3.2	6.4	3.2	6.4	
		μM	>200	>200	>200	>200	>200	>200	133.3	>200	100	>200	
<b>58b</b>	Ac-(Nbtm <sup>+</sup> -Nspe-Nspe) <sub>3</sub> -NH <sub>2</sub>	μg/ml	>419	>419	>419	>419	>419	>419	>419	>279	>419	>209	>419
		μM	>200	>200	>200	>200	>200	>200	>200	>200	>200	>200	>200
		μg/ml	>256	>256	>256	>256	>256	>256	>256	>256	>256	>256	>256
<b>66</b>	H-(Naetm <sup>+</sup> -Nspe-Nspe) <sub>3</sub> -NH <sub>2</sub>	μM	25	50	100	200	>200	>200	>200	50	100	50	100
		μg/ml	47.8	95.6	191.2	382.4	>382	>382	>382	95.6	191.2	95.6	191.2
		μM	6.3	12.5	12.5	25	37.5	50	10.4	12.5	11.5	25	
<b>67</b>	H-(Naetm-Nspe-Nspe) <sub>4</sub> -NH <sub>2</sub>	μg/ml	12.7	25.4	25.4	50.8	76.2	101.6	21.6	25.4	23.2	50.8	
		μM	11.5	12.5	50	100	33.3	50	6.3	12.5	6.3	12.5	
		μg/ml	29.2	31.8	127.2	254.4	84.8	127.2	15.9	31.8	15.9	31.8	
<b>68</b>	Melittin <sup>a</sup>	μM	6.3	12.5	6.3	12.5	12.5	25	3.1	6.3	6.3	12.5	
		μg/ml	6.3	12.5	6.3	12.5	12.5	25	3.1	6.3	6.3	12.5	
		μM	6.3	12.5	6.3	12.5	12.5	25	3.1	6.3	6.3	12.5	

<sup>a</sup>Honey bee 26-amino acid peptide: GIGAVLKVLTTGLPALISWIKRKRQQ

## 8 Preventive Anti-Biofilm activity

### 8.1 Growing the biofilm:

Grow a culture of the *Pseudomonas aeruginosa* and *Staphylococcus aureus* and *Enterococcus faecalis* overnight in a rich medium (i.e. Muller Hinton Broth). From the freshly prepared bacterial culture, prepare the 96 well microtiter plates with 100 $\mu$ L of bacterial culture of  $5 \times 10^6$  CFU/mL cell density. Add 100  $\mu$ L of the peptoids (1/2 MIC) per well in a 96 well flat bottom dish. For quantitative assays, we typically use 4 replicate wells for each treatment. Incubate the microtiter plate with bacteria and peptoids for 24 hrs for *P. aeruginosa* and *S. aureus* and 48 hrs for *E. faecalis* at 37°C.

### 8.2 Crystal-violet staining <sup>183</sup>

Grow and incubate the biofilm as described above (section 8.1). After incubation to stain the plates, dump out cells by turning the plate over and shaking out the liquid. Repeat this process a second time. This step helps remove unattached cells and media components that can be stained in the next step and significantly lowers background staining. Add 100  $\mu$ L of a 0.1% solution of crystal violet in water to each well of the microtiter plate. Wear gloves and a lab coat while making the solution. Use caution when weighing out the CV as the powder is hygroscopic and readily stains clothing, skin, etc. Incubate the microtiter plate at room temperature for 10-15 min. Rinse the plate 3-4 times with water by submerging in a tub of water, shake out and blot vigorously on a stack of paper towels to rid the plate of all excess cells and dye. Turn the microtiter plate upside down and dry it for significant time. For qualitative assays, the wells can be photographed when dry. To quantify the biofilm, add 100  $\mu$ L of ethanol to each well of the microtiter plate to solubilize the CV. Incubate the microtiter plate at room temperature for 10-15 min. Transfer 125  $\mu$ L of the solubilized CV to a new flat-bottomed microtiter plate. Quantify absorbance in a plate reader (MULTISKAN SPECTRUM type 1500 from Thermo Electron Corporation) at 595 nm using ethanol as the blank.

---

<sup>183</sup> C. Forestier, 'Anti-Biofilm Activity: A Function of Klebsiella Pneumoniae Capsular Polysaccharide', José A. Bengoechea (ed.), *PloS One*, 9 (2014), e99995.



Table 35 Results of anti-biofilm activity performed on selected peptoid oligomers at ½ MIC levels.

No.	Peptoid	% Biofilm reduction								
		<i>E. faecalis</i>			<i>P. aeruginosa</i>			<i>S. aureus</i>		
		A	B	C	A	B	C	A	B	C
<b>43</b>	Ac-(Nbtm <sup>+</sup> -Ntbu-Ntbu) <sub>2</sub> -OEt	86	27	-	52	77	48	0	0	2
<b>54a</b>	H-(Nchtm <sup>+</sup> -Nspe-Nspe) <sub>2</sub> -NH <sub>2</sub>	61	47	0	0	0	0	0	0	0
<b>56a</b>	H-(Nchtm <sup>+</sup> -Nspe-Nspe) <sub>3</sub> -NH <sub>2</sub>	0	40	46	93	99	99	0	0	0
<b>58a</b>	H-(Nbtm <sup>+</sup> -Nspe-Nspe) <sub>3</sub> -NH <sub>2</sub>	37	95	23	90	98	99	0	0	0
<b>58b</b>	Ac-(Nbtm <sup>+</sup> -Nspe-Nspe) <sub>3</sub> -NH <sub>2</sub>	96	100	71	43	17	0	75	100	100
<b>67</b>	H-(Naetm-Nspe-Nspe) <sub>4</sub> -NH <sub>2</sub>	52	9	-	37	61	50	0	0	10
<b>68</b>	H-(Naetm <sup>+</sup> -Nspe-Nspe) <sub>4</sub> -NH <sub>2</sub>	28	-	0	71	62	60	0	0	2
	melittin	2	-	0	47	27	23	4	15	0

### 8.3 Colony forming units (CFU) enumeration:

Grow and incubate the biofilm as described above (section 8.1). After incubation, remove the non-adherent bacteria by turning the plate over and shaking out the liquid. Repeat this process a second time. This step helps remove unattached cells and media components. Then biofilm was washed with saline, suspended in 100 µl of saline and disrupted by ultrasonicator (3×5 minutes). Resulting biofilm suspensions were serially diluted and plated into media using Interscience's easySpiral® Dilute (Automatic serial diluter and plater). The plates were incubated at 37°C for 24 h. To determine the number of CFU/mL, the colonies were counted using Interscience's Scan® 500 automatic colony counter.

## 9 Cell selectivity tests

### 9.1 Haemolytic assays

Fresh human red blood cells (hRBCs) were collected by ZenBio (USA) reference number (w36981700775500) and stored in Acid Citrate Dextrose Solution (ACD). It was diluted 10-fold in phosphate buffered saline (PBS) (pH 7.4). Then 100 µL of hRBCs was added to each tube containing an equal volume (100 µL) of peptoid in Muller Hinton Broth in 2 ml Eppendorf vials. After incubation at 37 °C for 1 h using Grant-bio incubator, the suspension was centrifuged at 1000 × g for 5 min using Eppendorf Centrifuge 5417R, and the supernatants were transferred to wells of

a 96-well plate. Release of haemoglobin was monitored by measuring the absorbance at 570 nm. The hRBCs in PBS and 0.1% Triton X-100 were employed as negative and positive controls, respectively.<sup>176</sup> The percent haemolysis was calculated using the following formula:  $[(A-A_0)/(A_t-A_0)] \times 100$  where A represents the absorbance of the peptoid sample at 570 nm (MULTISKAN SPECTRUM type 1500 from Thermo Electron Corporation, Reference- 51118500), and A<sub>0</sub> and A<sub>t</sub> represent the absorbance at 0% (positive control) and 100% (negative control) haemolysis as determined in 10 mM PBS and 0.1% Triton X-100, respectively. Each test was reproduced at least three times using two technical replicates.

Table 36 Results of haemolytic assays performed on selected peptoid oligomers at different concentrations

Exp.		PBS	43	54a	56a	58a	66	67	68	Melittin	Triton-X
1	[c] (μM)	blank	200	200	100	50	200	50	200	50	control
	%haemolysis	0	-0.2	-0.2	69.7	0.2	0	3.1	0.8	106	100
2	[c] (μM)	blank	200	200	50	100	200	100	200	50	control
	%haemolysis	0	0.2	0.2	10.9	0.5	0.3	30.5	5.4	48.7	100
3	[c] (μM)	blank	200	200	75	200	200	125	200	50	control
	%haemolysis	0	0.1	0.4	25.8	4	0.3	56.2	1.5	51.4	100
4	[c] (μM)	blank	200	200	75	200	200	100	200	50	control
	%haemolysis	0	0.1	0.3	45.6	24	0.6	58.8	1.2	74.5	100
5	[c] (μM)	blank	200	200	75	200	200	125	200	50	control
	%haemolysis	0	0.5	1.1	41.7	28	0.2	85.3	1.6	72.6	100

## 9.2 Cytotoxic assays:

The HeLa (ATCC® CCL2™) and Jurkat Clone E6-1 (ATCC® TIB-152™) cell lines was purchased from ATCC bank, and cells were grown in media as described below.<sup>184</sup>

### 9.2.1 Protocol for the culturing of cells

#### 9.2.1.1 *Preparation of sterile environment*

The following is a general guideline for culturing of cell lines. All cell culture must be undertaken in microbiological safety cabinet using aseptic technique to ensure sterility. Prepare an aseptic environment in a laminar hood. Close the hood sash to a proper position to maintain laminar air flow and avoid cluttering. Spray the working area with 70% ethanol. All the pipette tips should be DNase and RNase free (autoclaved or can be purchased pre-autoclaved). Autoclave 9” glass Pasteur pipettes. All media, supplement and reagents must be sterile to prevent microbial growth in the cell culture. Some reagents and supplements will require filter sterilization if they are not provided sterile. Culture media and supplements should always be sterile. Purchase sterile reagents when possible, only use under aseptic conditions in a culture hood to ensure they remain sterile. Use 75 cm<sup>2</sup> Falcon® tissue culture treated flasks with vented cap and canted neck for culturing the cell lines.

#### 9.2.1.2 *Preparation of cell growth medium*

For HeLa cell lines use MEM with Earle's Salts, with stabilized Glutamine supplied with 10% Foetal Bovine Serum (FBS) and for Jurkat cell lines use RPMI 1640 with stabilized Glutamine supplied with 10% Foetal Bovine Serum (FBS).

#### 9.2.1.3 *Splitting*

When the cells are approximately 80% confluent (80% of surface of flask covered by cell monolayer) they should still be in the log phase of growth and will require sub-culturing. (Do not let cells become over confluent as they will start to die off and may not be recoverable). To sub-culture, first warm the fresh culture medium at 37°C water bath or incubator for at least 30 minutes. Make sure flasks are labelled with the cell line, passage number, split ratio, date, operator initials and the vial number of the cells. Place flask(s) straight into 37°C incubator with 95% air and 5% CO<sub>2</sub>. Write down the details of the sub-culturing in the culture record log sheet. There should be a separate log sheet for each vial of cells resuscitated and in use.

---

<sup>184</sup> ‘Mammalian Cell Tissue Culture Techniques Protocol | Abcam [Http://www.abcam.com/protocols/mammalian-Cell-Tissue-Culture-Techniques-Protocol](http://www.abcam.com/protocols/mammalian-Cell-Tissue-Culture-Techniques-Protocol)’ (n.d.).

#### 9.2.1.4 *Checking cells*

Cells should be checked microscopically daily to ensure they are healthy and growing as expected. Attached cells should be mainly attached to the bottom of the flask, round and plump or elongated in shape and refracting light around their membrane. Suspension cells should look round and plump and refracting light around their membrane. Some suspension cells may clump. Media should be pink orange in colour. Discard cells if: They are detaching in large numbers (attached lines) and/or look shrivelled and grainy/dark in colour. They are in quiescence (do not appear to be growing at all).

#### 9.2.1.5 *Changing media*

If cells have been growing well for a few days but are not yet confluent (e.g. if they have been split 1:10) then they will require media changing to replenish nutrients and keep correct pH. If there are a lot of cells in suspension (attached cell lines) or the media is starting to go orange rather than pink orange, then change the media of them as soon as possible. To change the media, warm up fresh culture media at 37°C in water bath or incubator for at least 30 mins. Carefully pour out the media from the flask into a waste pot containing some disinfectant. Immediately replace the media with 100 mL of fresh pre-warmed culture media and return to 37°C incubator with 95% air and 5% CO<sub>2</sub>.

#### 9.2.1.6 *Passage number*

The passage number is the number of sub-cultures the cells have gone through. Passage number should be recorded and not get too high. This is to prevent use of cells undergoing genetic drift and other variations.

#### 9.2.1.7 *Preparation of primary HeLa cell line culture*

The frozen sample of HeLa cells was taken from the deep freezer. It was kept in sterile conditions as discussed above. The vial is rubbed between the palms to melt the media of sample. Add 1 mL of the MEM to it and mix it using the micropipette. Transfer the cells to a 10 mL vial and then add 3 mL MEM to it. Centrifuge at 501 × g for 10 minutes at 20°C using Jouan BR4i centrifuge. After centrifugation remove the excess supernatant (leave 0.5 mL of the supernatant) by taking a sterile Pasteur pipette using aspirator pump. Shake the vial to mix the adherent cells in it. Transfer the contents of vial in a 20 mL vial and add 14 mL MEM to it and mix well. Divide it into two equal parts and distribute it into Falcon® canted neck flasks. Incubate the cells in 37°C incubator with 95% air and 5% CO<sub>2</sub>.

#### 9.2.1.8 *Sub-culturing attached cell lines requiring trypsin (HeLa cell line)*

Using aspirator pump, carefully remove excess media from flask of the required cells into waste pot (containing 100 mL 10% sodium hypochlorite) taking care not to increase contamination risk with any drips. Using aseptic technique, pipette enough sterile PBS into the flask to give cells a wash and get rid of any FBS in the residual culture media. Tip flask gently a few times to rinse the cells and carefully pipette the PBS back out into waste pot. This may be repeated another one or

two times if necessary. Using pipette, add enough trypsin EDTA ( $\approx 5$  mL for  $75\text{ cm}^2$  flask) to cover the cells at the bottom of the flask. Roll flask gently to ensure trypsin contact with all cells. Place flask in  $37^\circ\text{C}$  incubator with 95% air and 5%  $\text{CO}_2$ . As soon as cells have detached (the flask may require a few gentle taps) add some culture media to the flask (the FBS in this will inactivate the trypsin). Using this cell suspension, pipette required volume of cells into new flasks at required split ratio. These flasks should then be topped up with culture media to required volume (10-30 mL for  $75\text{ cm}^2$  flask). Leave cells overnight to recover and settle. Change media every two days.

#### 9.2.1.9 *Sub-culturing of suspension cell lines (Jurkat cell line)*

Take out required amount of cell suspension from the flask using pipette and place into new flask. Add required amount of pre-warmed cell culture media to fresh flask. For 1:5 split from 50 mL add 40mL of fresh media to 10 mL cell suspension.

#### 9.2.2 Mammalian cell culture and cytotoxicity assay using MTT

Cytotoxicity against HeLa cells and Jurkat cells were measured using a tetrazolium salt (MTT)-based colorimetric assay as previously described.<sup>177</sup> Cells were counted using Cellometer<sup>®</sup> automated cell counting chamber to prepare  $5 \times 10^5$  cells/mL with the help of trypan blue stain to visualise cells. Aliquots of 100  $\mu\text{L}$  media containing  $5 \times 10^5$  HeLa cells and Jurkat cells were distributed into each well of a 96-well plate (Falcon<sup>®</sup> Clear Flat Bottom), and these cells were grown in a humidified atmosphere of 5%  $\text{CO}_2$  in air at  $37^\circ\text{C}$ . The following day, when cell density reaches about 70% confluency, the peptoids were added to the cell culture at final concentrations on 100  $\mu\text{M}$  and incubated for 24 h at  $37^\circ\text{C}$  with 95% air and 5%  $\text{CO}_2$ . Then 22  $\mu\text{L}$  (0.5 mg/mL) of the Cell Proliferation Kit I (MTT) (Sigma-aldrich) reagent which contains a tetrazolium compound, -(4,5-dimethylthiazol-2-yl)- 2,5-diphenyltetrazolium bromide inner salt; MTT] was added to each well, and the plate was incubated for 2 h (4h for Jurkat cell lines) at  $37^\circ\text{C}$  to metabolize. The cell cultures were centrifuged at  $1,000 \times g$  for 5 min at  $20^\circ\text{C}$ , and the supernatants were discarded. Subsequently, 150  $\mu\text{L}$  of DMSO was added to dissolve the MTT-formazan formed crystals. Transfer 100  $\mu\text{L}$  of the solubilized formazan crystals to a new flat-bottomed microtiter plate and the absorbance was measured at 590 nm using microplate reader (MULTISKAN SPECTRUM type 1500 from Thermo Electron Corporation) and compared with untreated cells. Percentage of cell viability =  $(A - A_{\text{testblank}})/(A_{\text{control}} - A_{\text{blank}}) \times 100$ , where  $A$  is the absorbance of the test well and  $A_{\text{control}}$  the average absorbance of wells with cells not treated with peptoids (negative control).  $A_{\text{testblank}}$  (media, MTS, and diluted peptoids) and  $A_{\text{blank}}$  (media and MTS) were background absorbances measured in the absence of cells. The negative control for the cell cytotoxicity was the average absorbance of wells with cells not treated with peptoids. The positive control for the cell cytotoxicity was sanguinarine chloride hydrate (SCH) of  $12\mu\text{M}$  concentration. A minimum of three independent experiments (biological replicates) of the assay

were conducted, and four technical replicates (parallel) were used in each experiment for each peptoid and concentration.

Table 37 Results of cell viability assays performed on selected peptoid oligomers at 100  $\mu$ M concentration.

No	Peptoid	% cell viability					
		HeLa cells			Jurkat Cells		
		A	B	C	A	B	C
43	Ac-(Nbtm <sup>+</sup> -Ntbu-Ntbu) <sub>2</sub> -OEt	112.7	104.6	112.0	78.4	83.9	78.9
54a	H-(Nchtm <sup>+</sup> -Nspe-Nspe) <sub>2</sub> -NH <sub>2</sub>	116	93.1	126.2	39.2	38.7	74.7
56a	H-(Nchtm <sup>+</sup> -Nspe-Nspe) <sub>3</sub> -NH <sub>2</sub>	-9.8	7.4	8.7	-14.0	22.6	3.1
58a	H-(Nbtm <sup>+</sup> -Nspe-Nspe) <sub>3</sub> -NH <sub>2</sub>	-10.7	6.2	9.7	2.3	24.4	4.0
66	H-(Naetm <sup>+</sup> -Nspe-Nspe) <sub>3</sub> -NH <sub>2</sub>	120.3	100.5	132.2	88.3	97.0	72.4
67	H-(Naetm-Nspe-Nspe) <sub>4</sub> -NH <sub>2</sub>	-10.7	6.7	7.0	-2.1	19.0	3.1
68	H-(Naetm <sup>+</sup> -Nspe-Nspe) <sub>4</sub> -NH <sub>2</sub>	86.2	102.2	126.7	26.3	64.8	40.0

## 10 Scanning Electron Microscopy (SEM) Imaging

For scanning electron microscopy, bacteria were washed in PHEM buffer pH 8 (PIPES 60mM, HEPES 25 mM, EGTA 10 mM, MgCl<sub>2</sub> 2 mM) and fixed 4 hours at 4°C in same buffer contained 1.6% glutaraldehyde and 0.05 % ruthenium red. Bacteria were then washed 20 minutes in PHEM buffer pH 8 and post-fixed 1 hour with 1% osmium tetroxide at room temperature. After 20 minutes rinsed in distilled water, dehydration by graded ethanol were performed from 25° to 100° (10 minutes each) to finish in hexamethyldisilazane (HMDS) 10 minutes. Bacteria were deposited on Thermanox slides and placed under Sorbonne overnight. After drying, samples were mounted on stubs using adhesive carbon tabs and sputter-coated with gold-palladium (JFC-1300 JEOL, Japan).

Morphology analysis was carried out using a scanning electron microscope JSM-6060 LV (Jeol, Japan) at 5kV in high-vacuum mode at the Centre Imagerie Cellulaire Santé (CICS) platform, University Clermont Auvergne. Field Emission Gun scanning electron microscopy (FEG SEM) was performed at 2MATech by Madame Anne-Marie Gelinaud.

10.1 Supplementary images from Microscopy

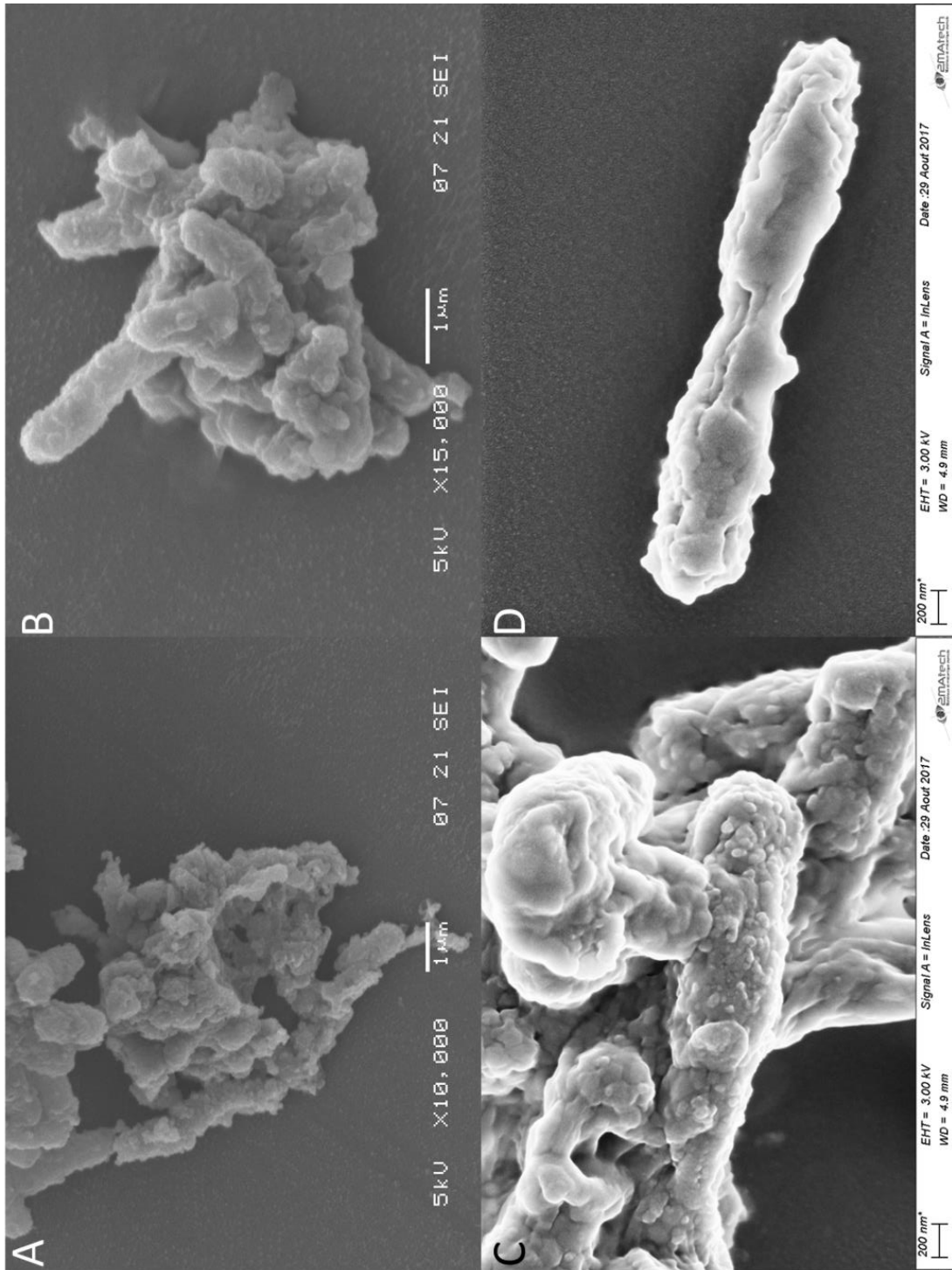


Figure 80 (A, B) SEM micrographs of *E. coli* cells treated with the dodecamer 68 at the MIC (11.5 μM) after 18h; (C, D) FEGSEM micrographs of *E. coli* cells treated with the dodecamer 68 at the MIC (11.5 μM) after 18h. (A&B: CICS platform, UCA; C&D: 2MATech, Aubiere)

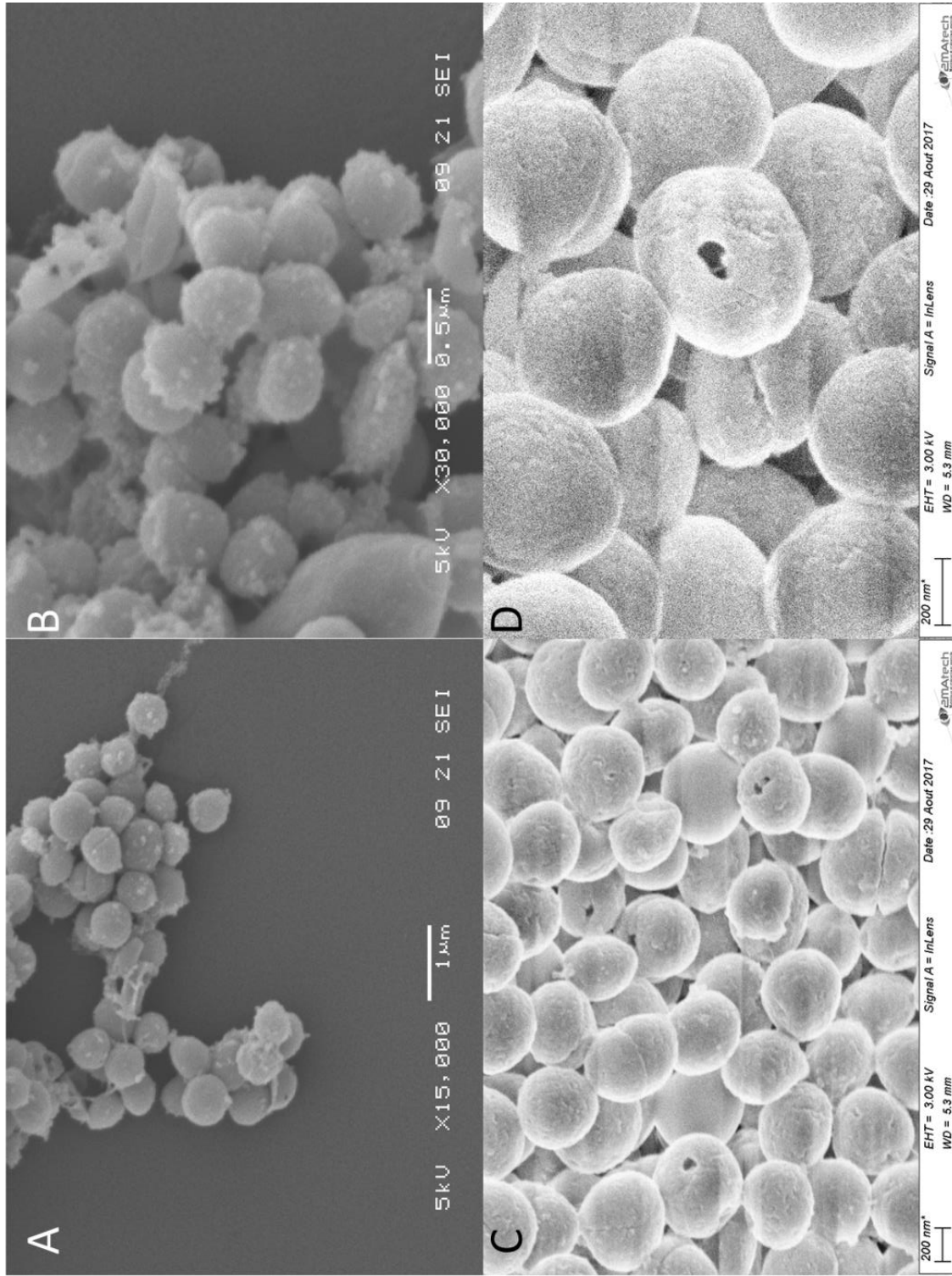


Figure 81 (A, B) SEM micrographs of *S. aureus* cells treated with the dodecamer 68 at the MIC (6.3 μM) after 18h; (C, D) FEGSEM micrographs of *S. aureus* cells treated with the dodecamer 68 at the MIC (6.3 μM) after 18h. (A&B: CICS platform, UCA; C&D: 2MATech, Aubiere)



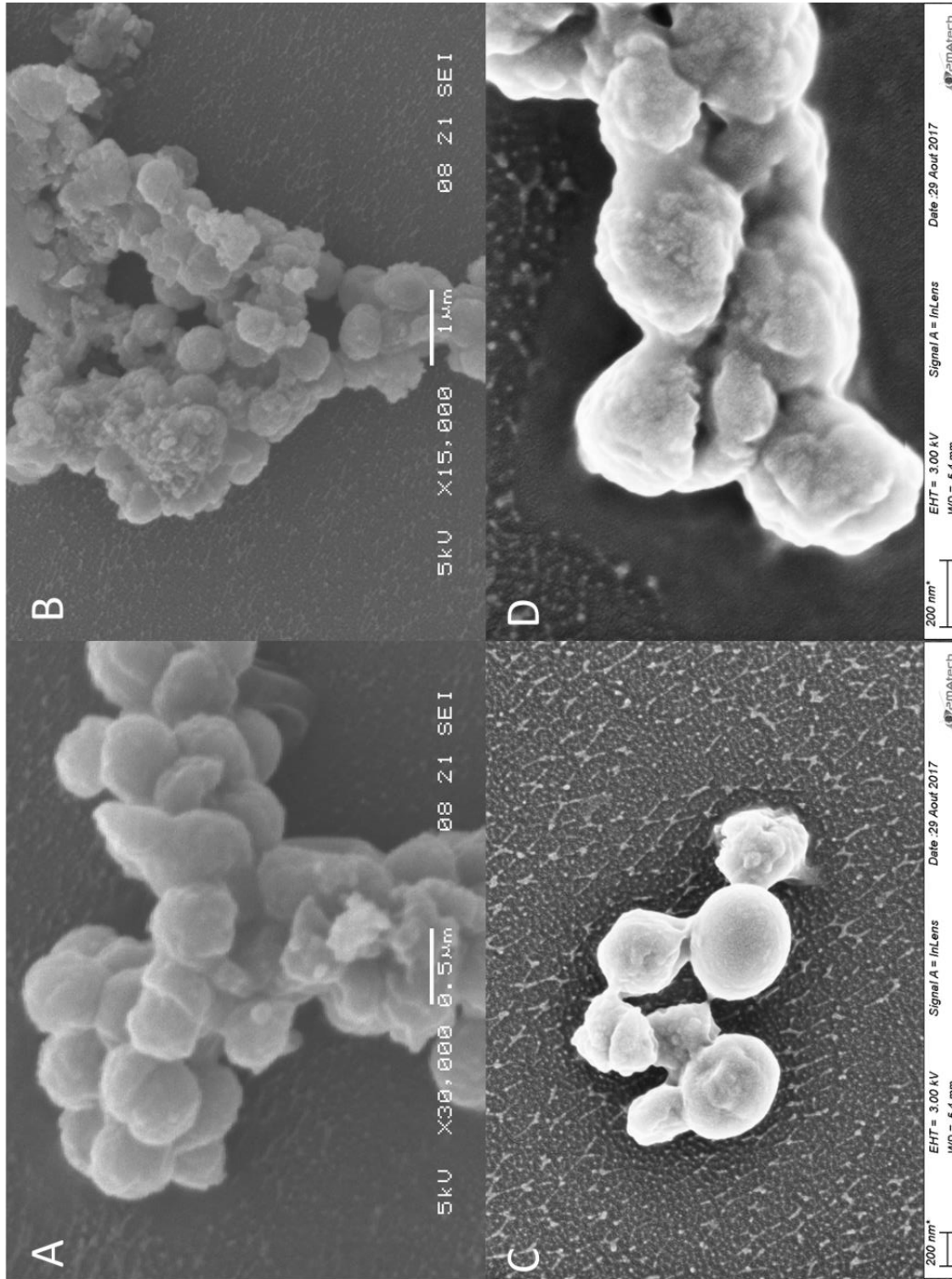


Figure 82 (A, B) SEM micrographs of *S. aureus* cells treated the hexamer 54a at the MIC (3.1 μM) after 18h; (C, D) FEGSEM micrographs of *S. aureus* cells treated with the hexamer 54a at the MIC (3.1 μM) after 18h. (A&B: CICS platform, UCA; C&D: 2MATech, Aubiere)

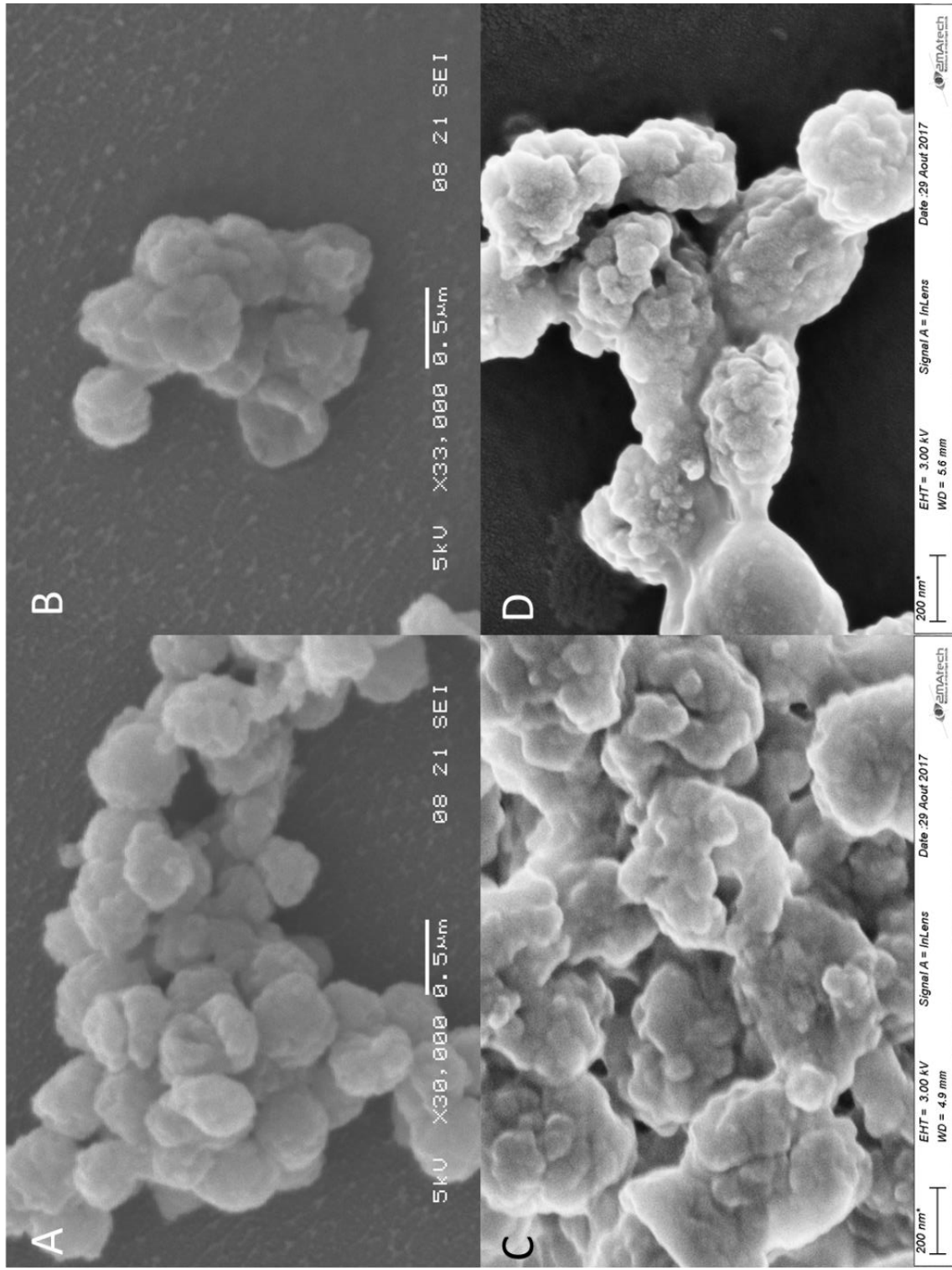


Figure 83 (A, B) SEM micrographs of *S. aureus* cells treated the hexamer 43 at the MIC (6.3  $\mu$ M) after 18h; (C, D) FEGSEM micrographs of *S. aureus* cells treated with the hexamer 43 at the MIC (6.3  $\mu$ M) after 18h. (A&B: CICS platform, UCA; C&D: 2MAtech, Aubiere)

# **Bibliography**

1. European Centre for Disease Prevention and Control. Antimicrobial resistance surveillance in Europe 2016. Annual Report of the European Antimicrobial Resistance Surveillance Network (EARS-Net). *European Centre for Disease Prevention and Control* 1–88 (2017).
2. Fjell, C. D., Hiss, J. A., Hancock, R. E. W. & Schneider, G. Designing antimicrobial peptides: Form follows function. *Nature Reviews Drug Discovery* **11**, 37–51 (2012).
3. Hancock, R. E. W. & Sahl, H. G. Antimicrobial and host-defense peptides as new anti-infective therapeutic strategies. *Nature Biotechnology* **24**, 1551–1557 (2006).
4. Reddy, K. V. R., Yedery, R. D. & Aranha, C. Antimicrobial peptides: Premises and promises. *International Journal of Antimicrobial Agents* **24**, 536–547 (2004).
5. Brahmachary, M. *et al.* ANTIMIC: a database of antimicrobial sequences. *Nucleic Acids Res.* **32**, D586-9 (2004).
6. Wang, Z. & Wang, G. The Antimicrobial Peptide Database. *Nucleic Acids Res.* **32**, D590–D592 (2004).
7. Tossi, A., Sandri, L. & Giangaspero, A. Amphipathic, alpha-helical antimicrobial peptides. *Biopolymers* **55**, 4–30 (2000).
8. Zasloff, M. Antimicrobial peptides of multicellular organisms. *Nature* **415**, 389–395 (2002).
9. Peters, B. M., Shirliff, M. E. & Jabra-Rizk, M. A. Antimicrobial peptides: Primeval molecules or future drugs? *PLoS Pathog.* **6**, e1001067 (2010).
10. Wang, G., Xia Li & Michael Zasloff. *Antimicrobial peptides: discovery, design and novel therapeutic strategies*. (CABI, 2010).
11. Matsuzaki, K. Control of cell selectivity of antimicrobial peptides. *Biochim. Biophys. Acta - Biomembr.* **1788**, 1687–1692 (2009).
12. Matsuzaki, K. Why and how are peptide-lipid interactions utilized for self-defense? Magainins and tachyplesins as archetypes. *Biochimica et Biophysica Acta - Biomembranes* **1462**, 1–10 (1999).
13. Yeaman, M. R. & Yount, N. Y. Mechanisms of antimicrobial peptide action and resistance. *Pharmacol. Rev.* **55**, 27–55 (2003).
14. Hancock, R. E. W. & Rozek, A. Role of membranes in the activities of antimicrobial cationic peptides. *FEMS Microbiol. Lett.* **206**, 143–149 (2002).
15. Shai, Y. Mechanism of the binding, insertion and destabilization of phospholipid bilayer membranes by  $\alpha$ -helical antimicrobial and cell non-selective membrane-lytic peptides. *Biochimica et Biophysica Acta - Biomembranes* **1462**, 55–70 (1999).
16. Yang, L., Weiss, T. M., Lehrer, R. I. & Huang, H. W. Crystallization of antimicrobial pores in membranes: Magainin and protegrin. *Biophys. J.* **79**, 2002–2009 (2000).
17. Mahlapuu, M., Håkansson, J., Ringstad, L. & Björn, C. Antimicrobial Peptides: An Emerging Category of Therapeutic Agents. *Front. Cell. Infect. Microbiol.* **6**, 194 (2016).
18. Phoenix, D. A., Dennison, S. R. & Harris, F. Cationic Antimicrobial Peptides. in *Antimicrobial Peptides* 39–81 (Wiley-VCH Verlag GmbH & Co. KGaA, 2013).
19. Marsh, E. N. G., Buer, B. C. & Ramamoorthy, A. Fluorine—a new element in the design of membrane-active peptides. *Mol. Biosyst.* **5**, 1143 (2009).

20. Hemshekhar, M., Anaparti, V. & Mookherjee, N. Functions of cationic host defense peptides in immunity. *Pharmaceuticals* **9**, 40 (2016).
21. Mansour, S. C., Pena, O. M. & Hancock, R. E. W. Host defense peptides: Front-line immunomodulators. *Trends in Immunology* **35**, 443–450 (2014).
22. Hancock, R. E. Cationic peptides: effectors in innate immunity and novel antimicrobials. *Lancet Infect. Dis.* **1**, 156–164 (2001).
23. Peschel, A. & Sahl, H. G. The co-evolution of host cationic antimicrobial peptides and microbial resistance. *Nature Reviews Microbiology* **4**, 529–536 (2006).
24. O'Neill, J. Tackling drug-resistant infections globally: final report and recommendations. *Rev. Antimicrob. Resist.* 84 (2016).
25. Dawson, R. M., Fox, M. A., Atkins, H. S. & Liu, C. Q. Potent antimicrobial peptides with selectivity for *Bacillus anthracis* over human erythrocytes. *Int. J. Antimicrob. Agents* **38**, 237–242 (2011).
26. Moore, A. The big and small of drug discovery. Biotech versus pharma: Advantages and drawbacks in drug development. *EMBO Rep.* **4**, 114–117 (2003).
27. Fosgerau, K. & Hoffmann, T. Peptide therapeutics: Current status and future directions. *Drug Discovery Today* **20**, 122–128 (2015).
28. Breijl, A. de *et al.* The antimicrobial peptide SAAP-148 combats drug-resistant bacteria and biofilms. *Sci. Transl. Med.* **10**, eaan4044 (2018).
29. Kosikowska, P. & Lesner, A. Antimicrobial peptides (AMPs) as drug candidates: a patent review (2003–2015). *Expert Opinion on Therapeutic Patents* **26**, 689–702 (2016).
30. Wang, S., Zeng, X., Yang, Q. & Qiao, S. Antimicrobial peptides as potential alternatives to antibiotics in food animal industry. *International Journal of Molecular Sciences* **17**, 603 (2016).
31. Epan, R. M. *Host Defense Peptides and Their Potential as Therapeutic Agents*. (Springer International Publishing, 2016).
32. Mojsoska, B. & Jenssen, H. Peptides and peptidomimetics for antimicrobial drug design. *Pharmaceuticals* **8**, 366–415 (2015).
33. Molchanova, N., Hansen, P. R. & Franzyk, H. Advances in development of antimicrobial peptidomimetics as potential drugs. *Molecules* **22**, 1430 (2017).
34. Gellman, S. H. Foldamers: A Manifesto. *Acc. Chem. Res.* **31**, 173–180 (1998).
35. Gabriel, G. J. & Tew, G. N. Conformationally rigid proteomimetics: a case study in designing antimicrobial aryl oligomers. *Org. Biomol. Chem.* **6**, 417–423 (2008).
36. Guichard, G. & Seebach, D. Solid-Phase Synthesis of  $\beta$ -Oligopeptides. *Chim. Int. J. Chem.* **51**, 315–318 (1997).
37. Seebach, D. *et al.*  $\beta$ -Peptides: Synthesis by Arndt-Eistert homologation with concomitant peptide coupling. Structure determination by NMR and CD spectroscopy and by X-ray crystallography. Helical secondary structure of a  $\beta$ -hexapeptide in solution and its stability towards pe. *Helv. Chim. Acta* **79**, 913–941 (1996).
38. Appella, D. H., Christianson, L. A., Karle, I. L., Powell, D. R. & Gellman, S. H.  $\beta$ -Peptide foldamers: Robust helix formation in a new family of  $\beta$ -amino acid oligomers. *J. Am. Chem. Soc.* **118**, 13071–13072 (1996).

39. Le Grel, P. & Guichard, G. Foldamers Based on Remote Intrastrand Interactions. in *Foldamers: Structure, Properties, and Applications* 35–74 (Wiley-VCH Verlag GmbH & Co. KGaA, 2007).
40. Seebach, D. & Matthews, J. L.  $\beta$ -Peptides: a surprise at every turn. *Chem. Commun.* 2015–2022 (1997).
41. Hamuro, Y., Schneider, J. P. & DeGrado, W. F. De Novo Design of Antibacterial  $\beta$ -Peptides. *J. Am. Chem. Soc.* **121**, 12200–12201 (1999).
42. Arvidsson, P. I. *et al.* On the antimicrobial and hemolytic activities of amphiphilic beta-peptides. *Chembiochem* **2**, 771–773 (2001).
43. Porter, E. A., Wang, X., Lee, H. S., Weisblum, B. & Gellman, S. H. Non-haemolytic beta-amino-acid oligomers. *Nature* **404**, 565 (2000).
44. Porter, E. A., Weisblum, B. & Gellman, S. H. Mimicry of host-defense peptides by unnatural oligomers: Antimicrobial  $\beta$ -peptides. *J. Am. Chem. Soc.* **124**, 7324–7330 (2002).
45. Karlsson, A. J., Pomerantz, W. C., Weisblum, B., Gellman, S. H. & Palecek, S. P. Antifungal activity from 14-helical  $\beta$ -peptides. *J. Am. Chem. Soc.* **128**, 12630–12631 (2006).
46. Mowery, B. P., Lindner, A. H., Weisblum, B., Stahl, S. S. & Gellman, S. H. Structure-activity relationships among random nylon-3 copolymers that mimic antibacterial host-defense peptides. *J. Am. Chem. Soc.* **131**, 9735–9745 (2009).
47. Liu, R. *et al.* Tuning the biological activity profile of antibacterial polymers via subunit substitution pattern. *J. Am. Chem. Soc.* **136**, 4410–4418 (2014).
48. Semetey, V. *et al.* Stable Helical Secondary Structure in Short-Chain N,N'-Linked Oligoureas Bearing Proteinogenic Side Chains. *Angew. Chemie Int. Ed.* **41**, 1893–1895 (2002).
49. Violette, A. *et al.* Mimicking Helical Antibacterial Peptides with Nonpeptidic Folding Oligomers. *Chem. Biol.* **13**, 531–538 (2006).
50. Claudon, P. *et al.* Consequences of isostructural main-chain modifications for the design of antimicrobial foldamers: Helical mimics of host-defense peptides based on a heterogeneous amide/urea backbone. *Angew. Chemie - Int. Ed.* **49**, 333–336 (2010).
51. Antunes, S. *et al.* Effect of replacing main-chain ureas with thiourea and guanidinium surrogates on the bactericidal activity of membrane active oligourea foldamers. *Bioorganic Med. Chem.* **25**, 4245–4252 (2017).
52. Tew, G. N. *et al.* De novo design of biomimetic antimicrobial polymers. *Proc. Natl. Acad. Sci. U. S. A.* **99**, 5110–4 (2002).
53. Liu, D. *et al.* Nontoxic membrane-active antimicrobial arylamide oligomers. *Angew. Chemie - Int. Ed.* **43**, 1158–1162 (2004).
54. Choi, S. *et al.* De novo design and in vivo activity of conformationally restrained antimicrobial arylamide foldamers. *Proc. Natl. Acad. Sci.* **106**, 6968–6973 (2009).
55. Tang, H., Doerksen, R. J. & Tew, G. N. Synthesis of urea oligomers and their antibacterial activity. *Chem. Commun. (Camb).* **0**, 1537–9 (2005).

56. Tew, G. N., Clements, D., Tang, H., Arnt, L. & Scott, R. W. Antimicrobial activity of an abiotic host defense peptide mimic. *Biochim. Biophys. Acta - Biomembr.* **1758**, 1387–1392 (2006).
57. Simon, R. J. *et al.* Peptoids: a modular approach to drug discovery. *Proc. Natl. Acad. Sci. U. S. A.* **89**, 9367–71 (1992).
58. Simon, R. J., Bartlett, P. A. & Santi, D. V. Modified peptide and peptide libraries with protease resistance, derivatives thereof and methods of producing and screening such. (1999).
59. Hamper, B. C., Kolodziej, S. A., Scates, A. M., Smith, R. G. & Cortez, E. Solid Phase Synthesis of beta-Peptoids: N-Substituted beta-Aminopropionic Acid Oligomers. *J. Org. Chem.* **63**, 708–718 (1998).
60. Hjelmgard, T. *et al.* Convenient solution-phase synthesis and conformational studies of novel linear and cyclic alpha,beta-alternating peptoids. *Org. Lett.* **11**, 4100–4103 (2009).
61. Zuckermann, R. N. Peptoid origins. *Biopolymers* **96**, 545–55 (2011).
62. Zuckermann, R. N. *et al.* Efficient Method for the Preparation of Peptoids [Oligo(N-substituted glycines)] by submonomer solid-phase synthesis. *J. Am. Chem. Soc.* **114**, 10646–10647 (1992).
63. Sui, Q., Borchardt, D. & Rabenstein, D. L. Kinetics and equilibria of cis/trans isomerization of backbone amide bonds in peptoids. *J. Am. Chem. Soc.* **129**, 12042–12048 (2007).
64. Miller, S. M. *et al.* Proteolytic studies of homologous peptide and N-substituted glycine peptoid oligomers. *Bioorganic Med. Chem. Lett.* **4**, 2657–2662 (1994).
65. Miller, S. M. *et al.* Comparison of the proteolytic susceptibilities of homologous L-amino acid, D-amino acid, and N-substituted glycine peptide and peptoid oligomers. *Drug Dev. Res.* **35**, 20–32 (1995).
66. Fields, G. B. & NOBLE, R. L. Solid phase peptide synthesis utilizing 9-fluorenylmethoxycarbonyl amino acids. *Int. J. Pept. Protein Res.* **35**, 161–214 (1990).
67. Zuckermann, R. N., KERR, J. M., SIANI, M. A. & BANVILLE, S. C. Design, construction and application of a fully automated equimolar peptide mixture synthesizer. *Int. J. Pept. Protein Res.* **40**, 497–506 (1992).
68. Shin, A. *et al.* Peptoid-Substituted Hybrid Antimicrobial Peptide Derived from Papiliocin and Magainin 2 with Enhanced Bacterial Selectivity and Anti-inflammatory Activity. *Biochemistry* **54**, 3921–3931 (2015).
69. Chen, X. *et al.* Expanded polyglutamine-binding peptoid as a novel therapeutic agent for treatment of Huntington's disease. *Chem. Biol.* **18**, 1113–1125 (2011).
70. Luo, Y. *et al.* A $\beta$ 42-binding peptoids as amyloid aggregation inhibitors and detection ligands. *ACS Chem. Neurosci.* **4**, 952–962 (2013).
71. Turner, J. P. *et al.* Rationally designed peptoids modulate aggregation of amyloid-beta 40. *ACS Chem. Neurosci.* **5**, 552–558 (2014).
72. Turner, J. P., Chastain, S. E., Park, D., Moss, M. A. & Servoss, S. L. Modulating amyloid- $\beta$  aggregation: The effects of peptoid side chain placement and chirality. *Bioorganic Med. Chem.* **25**, 20–26 (2017).

73. Kamimura, K., Suda, T., Zhang, G. & Liu, D. Advances in Gene Delivery Systems. *Pharmaceut. Med.* **25**, 293–306 (2012).
74. Murphy, J. E. *et al.* A combinatorial approach to the discovery of efficient cationic peptoid reagents for gene delivery. *Proc. Natl. Acad. Sci. U. S. A.* **95**, 1517–22 (1998).
75. Huang, C.-Y. Y. *et al.* Lipitoids--novel cationic lipids for cellular delivery of plasmid DNA in vitro. *Chem. Biol.* **5**, 345–354 (1998).
76. Armand, P. *et al.* Chiral N-substituted glycines can form stable helical conformations. *Fold. Des.* **2**, 369–375 (1997).
77. Armand, P. *et al.* NMR determination of the major solution conformation of a peptoid pentamer with chiral side chains. *Proc. Natl. Acad. Sci. U. S. A.* **95**, 4309–4314 (1998).
78. Kirshenbaum, K. *et al.* Sequence-specific polypeptoids: a diverse family of heteropolymers with stable secondary structure. *Proc. Natl. Acad. Sci. U. S. A.* **95**, 4303–4308 (1998).
79. Wu, C. W., Sanborn, T. J., Huang, K., Zuckermann, R. N. & Barron, A. E. Peptoid oligomers with  $\alpha$ -chiral, aromatic side chains: Sequence requirements for the formation of stable peptoid helices. *J. Am. Chem. Soc.* **123**, 6778–6784 (2001).
80. Wu, C. W., Sanborn, T. J., Zuckermann, R. N. & Barron, A. E. Peptoid oligomers with  $\alpha$ -chiral, aromatic side chains: Effects of chain length on secondary structure. *J. Am. Chem. Soc.* **123**, 2958–2963 (2001).
81. Wu, C. W. *et al.* Structural and Spectroscopic Studies of Peptoid Oligomers with  $\alpha$ -Chiral Aliphatic Side Chains. *J. Am. Chem. Soc.* **125**, 13525–13530 (2003).
82. Sanborn, T. J., Wu, C. W., Zuckermann, R. N. & Barron, A. E. Extreme stability of helices formed by water-soluble poly-N-substituted glycines (polypeptoids) with  $\alpha$ -chiral side chains. *Biopolymers* **63**, 12–20 (2002).
83. Shin, H.-M., Kang, C.-M., Yoon, M.-H. & Seo, J. Peptoid helicity modulation: precise control of peptoid secondary structures via position-specific placement of chiral monomers. *Chem. Commun.* **50**, 4465–4468 (2014).
84. Stringer, J. R., Crapster, J. A., Guzei, I. A. & Blackwell, H. E. Extraordinarily robust polyproline type i peptoid helices generated via the incorporation of  $\alpha$ -chiral aromatic N-1-naphthylethyl side chains. *J. Am. Chem. Soc.* **133**, 15559–15567 (2011).
85. Roy, O. *et al.* Homogeneous and Robust Polyproline Type i Helices from Peptoids with Nonaromatic  $\alpha$ -Chiral Side Chains. *J. Am. Chem. Soc.* **139**, 13533–13540 (2017).
86. Rosenfeld, Y. & Shai, Y. Lipopolysaccharide (Endotoxin)-host defense antibacterial peptides interactions: Role in bacterial resistance and prevention of sepsis. *Biochimica et Biophysica Acta - Biomembranes* **1758**, 1513–1522 (2006).
87. Jenssen, H., Hamill, P. & Hancock, R. E. W. Peptide antimicrobial agents. *Clinical Microbiology Reviews* **19**, 491–511 (2006).
88. Patch, J. A. & Barron, A. E. Helical peptoid mimics of magainin-2 amide. *J. Am. Chem. Soc.* **125**, 12092–12093 (2003).
89. Chongsiriwatana, N. P. *et al.* Peptoids that mimic the structure, function, and mechanism of helical antimicrobial peptides. *Proc. Natl. Acad. Sci. U. S. A.* **105**, 2794–9 (2008).
90. Statz, A. R., Park, J. P., Chongsiriwatana, N. P., Barron, A. E. & Messersmith, P. B. Surface-immobilised antimicrobial peptoids. *Biofouling* **24**, 439–448 (2008).



91. Lee, J. *et al.* Effect of side chain hydrophobicity and cationic charge on antimicrobial activity and cytotoxicity of helical peptoids. *Bioorganic Med. Chem. Lett.* **28**, 170–173 (2018).
92. Mojsoska, B., Zuckermann, R. N. & Jenssen, H. Structure-activity relationship study of novel peptoids that mimic the structure of antimicrobial peptides. *Antimicrob. Agents Chemother.* **59**, 4112–20 (2015).
93. Mojsoska, B., Carretero, G., Larsen, S., Mateiu, R. V. & Jenssen, H. Peptoids successfully inhibit the growth of gram negative E. coli causing substantial membrane damage. *Sci. Rep.* **7**, 1–12 (2017).
94. Czyzewski, A. M. *et al.* In vivo, in vitro, and in silico characterization of peptoids as antimicrobial agents. *PLoS One* **11**, 1–17 (2016).
95. Tang, Y. C. & Deber, C. M. Hydrophobicity and helicity of membrane-interactive peptides containing peptoid residues. *Biopolymers* **65**, 254–262 (2002).
96. Bolt, H. L. *et al.* Log D versus HPLC derived hydrophobicity: The development of predictive tools to aid in the rational design of bioactive peptoids. *Biopolymers* **108**, 1–7 (2017).
97. Bolt, H. L. *et al.* Exploring the links between peptoid antibacterial activity and toxicity. *Med. Chem. Commun.* **8**, 886–896 (2017).
98. Driggers, E. M., Hale, S. P., Lee, J. & Terrett, N. K. The exploration of macrocycles for drug discovery - An underexploited structural class. *Nature Reviews Drug Discovery* **7**, 608–624 (2008).
99. Yoo, B., Shin, S. B. Y., Huang, M. L. & Kirshenbaum, K. Peptoid macrocycles: making the rounds with peptidomimetic oligomers. *Chem. - A Eur. J.* **16**, 5527–5537 (2010).
100. Shin, S. B. Y., Yoo, B., Todaro, L. J. & Kirshenbaum, K. Cyclic peptoids. *J. Am. Chem. Soc.* **129**, 3218–3225 (2007).
101. Blankenstein, J. & Zhu, J. Conformation-directed macrocyclization reactions. *European J. Org. Chem.* **2005**, 1949–1964 (2005).
102. Scherer, G., Kramer, M. L., Schutkowski, M., Reimer, U. & Fischer, G. Barriers to rotation of secondary amide peptide bonds. *J. Am. Chem. Soc.* **120**, 5568–5574 (1998).
103. Maulucci, N. *et al.* Synthesis, structures, and properties of nine-, twelve-, and eighteen-membered N-benzyloxyethyl cyclic  $\alpha$ -peptoids. *Chem. Commun.* **0**, 3927 (2008).
104. Comegna, D., Benincasa, M., Gennaro, R., Izzo, I. & De Riccardis, F. Design, synthesis and antimicrobial properties of non-hemolytic cationic  $\alpha$ -cyclopeptoids. *Bioorg. Med. Chem.* **18**, 2010–2018 (2010).
105. Huang, M. L., Shin, S. B. Y., Benson, M. A., Torres, V. J. & Kirshenbaum, K. A comparison of linear and cyclic peptoid oligomers as potent antimicrobial agents. *ChemMedChem* **7**, 114–122 (2012).
106. Huang, M. L., Benson, M. A., Shin, S. B. Y., Torres, V. J. & Kirshenbaum, K. Amphiphilic cyclic peptoids that exhibit antimicrobial activity by disrupting Staphylococcus aureus membranes. *European J. Org. Chem.* 3560–3566 (2013).
107. Andreev, K. *et al.* Cyclization Improves Membrane Permeation by Antimicrobial Peptoids. *Langmuir* **32**, 12905–12913 (2016).

108. Olsen, C. A. Peptoid-peptide hybrid backbone architectures. *ChemBioChem* **11**, 152–160 (2010).
109. Goodman, M., Melacini, G. & Feng, Y. Collagen-like triple helices incorporating peptoid residues. *J. Am. Chem. Soc.* **118**, 10928–10929 (1996).
110. Ryge, T. S. & Hansen, P. R. Potent antibacterial lysine-peptoid hybrids identified from a positional scanning combinatorial library. *Bioorganic Med. Chem.* **14**, 4444–4451 (2006).
111. Olsen, C. A. *et al.*  $\alpha$ -Peptide/ $\beta$ -Peptoid Chimeras. *Org. Lett.* **9**, 1549–1552 (2007).
112. Olsen, C. A. *et al.* Antimicrobial, hemolytic, and cytotoxic activities of  $\beta$ -peptoid-peptide hybrid oligomers: Improved properties compared to natural AMPs (ChemBioChem (2010) 11, (152-160)). *ChemBioChem* **11**, 1630 (2010).
113. Jahnsen, R. D., Frimodt-Møller, N. & Franzyk, H. Antimicrobial activity of peptidomimetics against multidrug-resistant *Escherichia coli*: A comparative study of different backbones. *J. Med. Chem.* **55**, 7253–7261 (2012).
114. Jahnsen, R. D. *et al.* Tailoring Cytotoxicity of Antimicrobial Peptidomimetics with High Activity against Multidrug-Resistant *Escherichia coli*. *J. Med. Chem.* **57**, 2864–2873 (2014).
115. Lin, H. *et al.* Statistical design, structural analysis, and in vitro susceptibility assay of antimicrobial peptoids to combat bacterial infections. *J. Chemom.* **30**, 369–376 (2016).
116. Goodson, B. *et al.* Characterization of novel antimicrobial peptoids. *Antimicrob. Agents Chemother.* **43**, 1429–34 (1999).
117. Schneider, A. C. *et al.* Microwave-Facilitated SPOT-Synthesis of Antibacterial Dipeptoids. *ACS Comb. Sci.* **19**, 715–737 (2017).
118. Gopalakrishnan, R., Frolov, A. I., Knerr, L., Drury, W. J. & Valeur, E. Therapeutic potential of foldamers: From chemical biology tools to drug candidates? *J. Med. Chem.* **59**, 9599–9621 (2016).
119. Gorske, B. C., Stringer, J. R., Bastian, B. L., Fowler, S. A. & Blackwell, H. E. New strategies for the design of folded peptoids revealed by a survey of noncovalent interactions in model systems. *J. Am. Chem. Soc.* **131**, 16555–16567 (2009).
120. Roy, O. *et al.* The tert-butyl side chain: A powerful means to lock peptoid amide bonds in the cis conformation. *Org. Lett.* **15**, 2246–2249 (2013).
121. Caumes, C., Roy, O., Faure, S. & Taillefumier, C. The click triazolium peptoid side chain: A strong cis-amide inducer enabling chemical diversity. *J. Am. Chem. Soc.* **134**, 9553–9556 (2012).
122. Angelici, G. *et al.* Weak backbone CH  $\cdots$  O=C and side chain tBu  $\cdots$  tBu London interactions help promote helix folding of achiral NtBu peptoids. *Chem. Commun.* **52**, 4573–4576 (2016).
123. Murphy, J. E. *et al.* A combinatorial approach to the discovery of efficient cationic peptoid reagents for gene delivery. *Proc. Natl. Acad. Sci. U. S. A.* **95**, 1517–22 (1998).
124. Culf, A. S. & Ouellette, R. J. Solid-phase synthesis of N-substituted glycine oligomers ( $\alpha$ -peptoids) and derivatives. *Molecules* **15**, 5282–5335 (2010).

125. Caumes, C., Hjelmgaard, T., Remuson, R., Faure, S. & Taillefumier, C. Highly convenient gram-scale solution-phase peptoid synthesis and orthogonal side-chain post-modification. *Synthesis (Stuttg)*. **2**, 257–264 (2011).
126. Calas, B., Mery, J. & Parello, J. SYNTHESIS OF THE FRAGMENT 14-21 OF THE AMINO ACID. *Tetrahedron* **41**, 5331–5339 (1985).
127. Schmuck, C. & Dudaczek, J. Ion pairing between the chain ends induces folding of a flexible zwitterion in methanol. *European J. Org. Chem.* **3**, 3326–3330 (2007).
128. Carpino, L. A. & Han, G. Y. 9-Fluorenylmethoxycarbonyl amino-protecting group. *J. Org. Chem.* **37**, 3404–3409 (1972).
129. Shendage, D. M., Fröhlich, R. & Haufe, G. Highly efficient stereoconservative amidation and deamidation of  $\alpha$ -amino acids. *Org. Lett.* **6**, 3675–3678 (2004).
130. He, J., Bawiec, J., Liu, W., Liang, G. B. & Yang, L. Substituted bicyclic amines for the treatment of diabetes. (2010).
131. De Santis, E. *et al.* Effect of capping groups at the N- and C-termini on the conformational preference of  $\alpha,\beta$ -peptoids. *Org. Biomol. Chem.* **10**, 1108–1122 (2012).
132. Hwu, J. R., Jain, M. L., Tsay, S. C. & Hakimelahi, G. H. Ceric ammonium nitrate in the deprotection of tert-butoxycarbonyl group. *Tetrahedron Lett.* **37**, 2035–2038 (1996).
133. Gibson, F. S., Bergmeier, S. C. & Rapoport, H. Selective Removal of an N-BOC Protecting Group in the Presence of a tert-Butyl Ester and Other Acid-Sensitive Groups. *J. Org. Chem.* **59**, 3216–3218 (1994).
134. Stahl, G. L., Walter, R. & Smith, C. W. General Procedure for the Synthesis of Mono-N-acylated 1,6-Diaminohexanes. *J. Org. Chem.* **43**, 2285–2286 (1978).
135. Helms, B. A. *et al.* High-affinity peptide-based collagen targeting using synthetic phage mimics: From phage display to dendrimer display. *J. Am. Chem. Soc.* **131**, 11683–11685 (2009).
136. Nagarajan, S. & Ganem, B. Chemistry of Naturally Occurring Polyamines. 10.1 Nonmetabolizable Derivatives of Spermine and Spermidine. *J. Org. Chem.* **51**, 4856–4861 (1986).
137. Liu, C., Lin, J., Delucca, G. V, Batt, D. G. & Liu, Q. Carboline carboxamide compounds useful as kinase inhibitors. (2011).
138. Maisonial, A. *et al.* Click Chelators for Platinum-Based Anticancer Drugs. *Eur. J. Inorg. Chem.* **2008**, 298–305 (2008).
139. Holub, J. M. & Kirshenbaum, K. Tricks with clicks: modification of peptidomimetic oligomers via copper-catalyzed azide-alkyne [3 + 2] cycloaddition. *Chem. Soc. Rev.* **39**, 1325–1337 (2010).
140. Aliouat, H. *et al.* 1,2,3-Triazolium-Based Peptoid Oligomers. *J. Org. Chem.* **82**, 2386–2398 (2017).
141. Abdel-Maksoud, M. S. *et al.* Broad-spectrum antiproliferative activity of a series of 6-(4-fluorophenyl)-5-(2-substituted pyrimidin-4-yl)imidazo[2,1-b]thiazole derivatives. *Med. Chem. Res.* **25**, 824–833 (2016).
142. Tully, D. C. *et al.* Synthesis and SAR of arylaminoethyl amides as noncovalent inhibitors of cathepsin S: P3 cyclic ethers. *Bioorganic Med. Chem. Lett.* **16**, 5112–5117 (2006).

143. Townsend, C. A. & Basak, A. Experiments and speculations on the role of oxidative cyclization chemistry in natural product biosynthesis. *Tetrahedron* **47**, 2591–2602 (1991).
144. Kruijtzter, J. A. W., Hofmeyer, L. J. F., Heerma, W., Versluis, C. & Liskamp, R. M. J. Solid-Phase Syntheses of Peptoids using Fmoc-Protected N -Substituted Substance P. *Chem. - A Eur. J.* 1570–1580 (1998).
145. Atherton, E. & Sheppard, R. *Solid Phase Peptide Synthesis: A Practical Approach*. (Oxford University Press, 1989).
146. Figliozzi, G. M., Goldsmith, R., Ng, S. C., Banville, S. C. & Zuckermann, R. N. Synthesis of N-substituted glycine peptoid libraries. in *Methods in Enzymology* **267**, 437–447 (Academic Press, 1996).
147. Burkoth, T. S., Fafarman, A. T., Charych, D. H., Connolly, M. D. & Zuckermann, R. N. Incorporation of unprotected heterocyclic side chains into peptoid oligomers via solid-phase submonomer synthesis. *J. Am. Chem. Soc.* **125**, 8841–8845 (2003).
148. Olivos, H. J. *et al.* Microwave-assisted solid-phase synthesis of peptoids. *Org. Lett.* **4**, 4057–4058 (2002).
149. Fara, M. A., Díaz-Mochón, J. J. & Bradley, M. Microwave-assisted coupling with DIC/HOBt for the synthesis of difficult peptoids and fluorescently labelled peptides - A gentle heat goes a long way. *Tetrahedron Lett.* **47**, 1011–1014 (2006).
150. Gorske, B. C., Jewell, S. A., Guerard, E. J. & Blackwell, H. E. Expedient synthesis and design strategies for new peptoid construction. *Org. Lett.* **7**, 1521–1524 (2005).
151. Kolb, H. C., Finn, M. G. & Sharpless, K. B. Click Chemistry: Diverse Chemical Function from a Few Good Reactions. *Angewandte Chemie - International Edition* **40**, 2004–2021 (2001).
152. Mathew, P., Neels, A. & Albrecht, M. 1,2,3-Triazolylidenes as versatile abnormal carbene ligands for late transition metals. *J. Am. Chem. Soc.* **130**, 13534–13535 (2008).
153. Hanelt, S. & Liebscher, J. A novel and versatile access to task-specific ionic liquids based on 1,2,3-triazolium salts. *Synlett* 1058–1060 (2008).
154. Jang, H., Fafarman, A., Holub, J. M. & Kirshenbaum, K. Click to fit: Versatile polyvalent display on a peptidomimetic scaffold. *Org. Lett.* **7**, 1951–1954 (2005).
155. Zabrodski, T., Baskin, M., Kaniraj, P. J. & Maayan, G. Click to bind: Microwave-assisted solid-phase synthesis of peptoids incorporating pyridine-triazole ligands and their copper(II) complexes. *Synlett* **25**, 461–466 (2014).
156. Vezenkov, L. L. *et al.* Ribbon-like Foldamers for Cellular Uptake and Drug Delivery. *ChemBioChem* (2017). doi:10.1002/cbic.201700455
157. Prodhomme, E. J. F. *et al.* Synthesis of 4-[2-aminoethyl(nitrosamino)]-1-pyridin-3-ylbutan-1-one, a new NNK hapten for the induction of N-nitrosamine-specific antibodies. *Bioconjug. Chem.* **18**, 2045–2053 (2007).
158. Van Dijk, M., Van Nostrum, C. F., Hennink, W. E., Rijkers, D. T. S. & Liskamp, R. M. J. Synthesis and characterization of enzymatically biodegradable peg and peptide-based hydrogels prepared by click chemistry. *Biomacromolecules* **11**, 1608–1614 (2010).

159. Shi, W. *et al.* Antimicrobial peptide melittin against *Xanthomonas oryzae* pv. *oryzae*, the bacterial leaf blight pathogen in rice. *Appl. Microbiol. Biotechnol.* **100**, 5059–5067 (2016).
160. Boucher, H. W. *et al.* Bad Bugs, No Drugs: No ESKAPE! An Update from the Infectious Diseases Society of America. *Clin. Infect. Dis.* **48**, 1–12 (2009).
161. Chabbert, Y. A. & Fillet, J. Correlation between ‘methicillin resistance’ and serotype in staphylococcus. *Nature* **213**, 1137 (1967).
162. Grundmann, H. *et al.* The dynamic changes of dominant clones of *Staphylococcus aureus* causing bloodstream infections in the European region: Results of a second structured survey. *Eurosurveillance* **19**, 1–10 (2014).
163. Kenneth James Ryan, C. George Ray, J. C. S. *Sherris medical microbiology: an introduction to infectious diseases. Journal of Chemical Information and Modeling* **53**, (McGraw-Hill, 2004).
164. Brock, T. Milestones in microbiology 1546 to 1940. in **53**, 215–218 (ASM Press, 1999).
165. J. Holt. *Bergey’s Manual of Determinative Bacteriology*. (Williams & Wilkins, 1994).
166. CLSI Document. *Methods for Dilution Antimicrobial Susceptibility Tests for Bacteria That Grow Aerobically; Approved Standard — Ninth Edition. Methods for Dilution Antimicrobial Susceptibility Tests for Bacteria That Grow Aerobically; Approved Standard- Ninth Edition* **32**, (2012).
167. Amyes, S. G. B. *Antimicrobial chemotherapy : Pocketbook*. (Martin Dunitz, 1996).
168. Raguse, T. L., Porter, E. A., Weisblum, B. & Gellman, S. H. Structure - Activity studies of 14-helical antimicrobial  $\beta$ -peptides: Probing the relationship between conformational stability and antimicrobial potency. *J. Am. Chem. Soc.* **124**, 12774–12785 (2002).
169. Turkett, J. A. & Bicker, K. L. Evaluating the Effect of Peptoid Lipophilicity on Antimicrobial Potency, Cytotoxicity, and Combinatorial Library Design. *ACS Comb. Sci.* **19**, 229–233 (2017).
170. Sutherland, I. W. The biofilm matrix - An immobilized but dynamic microbial environment. *Trends in Microbiology* **9**, 222–227 (2001).
171. Wingender, J. & Flemming, H. C. Biofilms in drinking water and their role as reservoir for pathogens. *Int. J. Hyg. Environ. Health* **214**, 417–423 (2011).
172. Hall-Stoodley, L. & Stoodley, P. Biofilm formation and dispersal and the transmission of human pathogens. *Trends in Microbiology* **13**, 7–10 (2005).
173. Réseau d’alerte d’investigation et de surveillance des infections Nosocomiales (France). *Enquête nationale de prévalence des infections nosocomiales et des traitements anti-infectieux en établissements de santé, France, mai-juin 2012. Résultats*. (Institut de veille sanitaire, 2013).
174. Miquel, S., Lagrèfeuille, R., Souweine, B. & Forestier, C. Anti-biofilm activity as a health issue. *Front. Microbiol.* **7**, 1–14 (2016).
175. Mohamed, J. A. & Huang, D. B. Biofilm formation by enterococci. *Journal of Medical Microbiology* **56**, 1581–1588 (2007).
176. Zhu, X., Ma, Z., Wang, J., Chou, S. & Shan, A. Importance of Tryptophan in Transforming an Amphipathic Peptide into a *Pseudomonas aeruginosa*-Targeted Antimicrobial Peptide. *PLoS One* **9**, 1–19 (2014).

177. Mosmann, T. Rapid colorimetric assay for cellular growth and survival: Application to proliferation and cytotoxicity assays. *J. Immunol. Methods* **65**, 55–63 (1983).
178. Dou, X., Zhu, X., Wang, J., Dong, N. & Shan, A. Novel Design of Heptad Amphiphiles To Enhance Cell Selectivity, Salt Resistance, Antibiofilm Properties and Their Membrane-Disruptive Mechanism. *J. Med. Chem.* **60**, 2257–2270 (2017).
179. Chongsiriwatana, N. P. *et al.* Intracellular biomass flocculation as a key mechanism of rapid bacterial killing by cationic, amphipathic antimicrobial peptides and peptoids. *Sci. Rep.* **7**, 16718 (2017).
180. Yannick Esvan. Préparation de peptoïdes présentant des amides cis : vers des hélices Polyprolines de type I (PPI). (Rapport de stage Master 1, Université Blaise Pascal, 2012).
181. Atwell, G. J. & Denny, W. A. Monoprotection of  $\alpha,\omega$ -Alkanediamines with the N - Benzyloxycarbonyl Group. *Synthesis (Stuttg)*. 1032–1033 (1984).
182. Forestier, C. Anti-biofilm activity: a function of *Klebsiella pneumoniae* capsular polysaccharide. *PLoS One* **9**, e99995 (2014).
183. Mammalian cell tissue culture techniques protocol | Abcam <http://www.abcam.com/protocols/mammalian-cell-tissue-culture-techniques-protocol>. Available at: <http://www.abcam.com/protocols/mammalian-cell-tissue-culture-techniques-protocol>. (Accessed: 20th March 2017)

## Résumé en Français

L'inquiétude mondiale à propos de la résistance aux antibiotiques est aggravée par le fait que la découverte de nouveaux antibiotiques est à son plus bas niveau. Cela fait 30 ans qu'une nouvelle classe d'antibiotiques a été introduite. Le réseau européen de surveillance de la résistance aux antimicrobiens (EARS-Net) observe une augmentation croissante de la résistance aux antimicrobiens dans les traitements d'infections bactériennes à Gram négatif. Il est donc urgent de mettre en place de nouvelles stratégies pour lutter contre l'antibiorésistance.<sup>1</sup> Les sociétés pharmaceutiques explorent de nouvelles stratégies telles que les anticorps thérapeutiques, les immunomodulateurs, les probiotiques, les thérapies à base de bactériophages et les peptides antimicrobiens.

### Chapitre I Introduction bibliographique

Les peptides antimicrobiens naturels (PAMs) ont montré un potentiel novateur en tant qu'agents antimicrobiens.<sup>2</sup> Les peptides antibactériens sont produits par les organismes vivants en tant que partie intégrante du système de défense immunitaire innée. Ils aident les êtres vivants à se protéger contre divers agents pathogènes. Ils présentent une activité antibactérienne à large spectre contre les bactéries à Gram-positif et à Gram-négatif, ce qui en fait des candidats puissants pour remplacer les antibiotiques classiques. Sur la base de leur structure, ils sont divisés en quatre groupes, à savoir les PAMs structurés en hélice  $\alpha$ , en feuillet  $\beta$ , les PAM contenant à la fois des structures secondaires en hélice et en feuillet et enfin les PAMs n'adoptant pas de structure secondaire particulière.<sup>3</sup> Dans ce manuscrit, nous allons nous concentrer sur la principale classe de PAMs, celle structurée en hélice.

La Magainine II est un excellent exemple de PAMs de type hélicoïdal amphiphile cationique. La magainine II est un peptide de 23 acides aminés sécrété par la peau d'une rainette africaine à griffes appelée *Xenopus laevis*. Les magainines sont de nature sélective car leur nature cationique permet d'interagir sélectivement avec les parois bactériennes en raison des différences dans la composition membranaire des cellules procaryotes et eucaryotes. Les phospholipides acides présents dans la membrane externe des micro-organismes en font de

---

<sup>1</sup> European Centre for Disease Prevention and Control, 'Antimicrobial Resistance Surveillance in Europe 2016. Annual Report of the European Antimicrobial Resistance Surveillance Network (EARS-Net)', *European Centre for Disease Prevention and Control* (2017), 1-88.

<sup>2</sup> R. M. Epand, *Host Defense Peptides and Their Potential as Therapeutic Agents*, Richard M. Epand (ed.) (SpringerInternational Publishing, 2016).

<sup>3</sup> Z. Wang and G. Wang, 'The Antimicrobial Peptide Database', *Nucleic Acids Research*, 32 (2004), D590-2.

bonnes cibles pour les peptides antimicrobiens amphiphiles cationiques. Par exemple, la magainine adopte en structure hélicoïdale à la surface de la membrane bactérienne et interagit avec les phospholipides chargés négativement, ce qui entraîne la pénétration de la magainine qui provoque la rupture de la membrane ou agit éventuellement sur des cibles internes, tuant ainsi la bactérie.<sup>4</sup>

Le mécanisme d'action principal des PAMs par rupture de la membrane cellulaire bactérienne implique une faible apparition de résistance. Cependant, leur coût de fabrication élevé et leur faible stabilité en milieu biologique entravent leur utilisation thérapeutique. Par conséquent, certaines modifications de la structure sont nécessaires pour améliorer leur stabilité et leur biodisponibilité. De nombreux peptides antimicrobiens synthétiques sont actuellement en essais cliniques.<sup>5</sup> Cependant, même après plus de vingt-cinq ans de développement, aucune avancée décisive n'a été réalisée. Une autre façon de contourner les faiblesses thérapeutiques des PAMs naturels consiste à développer des mimes synthétiques présentant l'activité antibactérienne des PAMs naturels avec une stabilité protéolytique et une biodisponibilité améliorée.

Depuis dix ans, cette question revêt un intérêt majeur pour les chimistes du domaine des foldamères.<sup>6</sup> De nombreux groupes ont travaillé sur des foldamères conçus pour présenter la structure hélicoïdale amphiphile cationique des PAMs naturels, qui est le facteur déterminant de leur activité par perméation membranaire. Les mimes d'antimicrobiens amphiphiles cationiques offrent la possibilité de développer une approche thérapeutique alternative pour lutter contre la résistance aux antibiotiques. Dans cette optique, des  $\beta$ -peptides ont été développés indépendamment par Seebach<sup>7</sup> et Gellman<sup>8</sup> en 1996. Les oligourées ont été

---

<sup>4</sup> K. Matsuzaki, 'Why and How Are Peptide-Lipid Interactions Utilized for Self-Defense? Magainins and Tachyplesins as Archetypes', *Biochimica et Biophysica Acta - Biomembranes*, Vol. 1462 (Elsevier, **1999**), 1-10.

<sup>5</sup> P. Kosikowska and A. Lesner, 'Antimicrobial Peptides (AMPs) as Drug Candidates: A Patent Review (2003-2015)', *Expert Opinion on Therapeutic Patents*, Vol. 26 (**2016**), 689-702.

<sup>6</sup> S. H. Gellman, 'Foldamers: A Manifesto', *Accounts of Chemical Research*, 31 (**1998**), 173-80.

<sup>7</sup> D. Seebach; M. Overhand; F. N. M. Kühnle; B. Martinoni; L. Oberer; U. Hommel; and H. Widmer, ' $\beta$ -Peptides: Synthesis by Arndt-Eistert Homologation with Concomitant Peptide Coupling. Structure Determination by NMR and CD Spectroscopy and by X-Ray Crystallography. Helical Secondary Structure of a  $\beta$ -Hexapeptide in Solution and Its Stability towards Pe', *Helvetica Chimica Acta*, 79 (**1996**), 913-41.

<sup>8</sup> D. H. Appella; L. A. Christianson; I. L. Karle; D. R. Powell; and S. H. Gellman, ' $\beta$ -Peptide Foldamers: Robust Helix Formation in a New Family of  $\beta$ -Amino Acid Oligomers', *Journal of the American Chemical Society*, 118 (**1996**), 13071-2.



développées en 2002 par le groupe de Guichard.<sup>9</sup> De plus, quelques protéomimétiques optimisés de manière appropriée ont montré une activité antimicrobienne puissante, tels que les arylurées et les arylamides développés par Tew et DeGrado en 2002.<sup>10</sup>

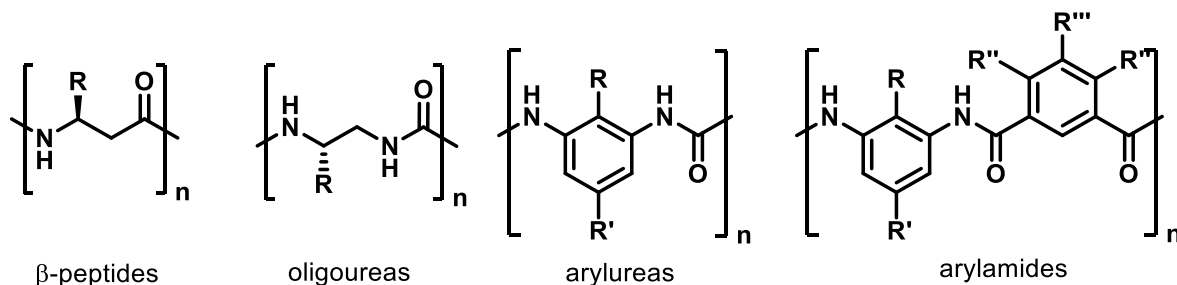


Figure 1 Structure des peptidomimétiques et des protéomimétiques utilisés pour concevoir des mimes de PAMs.

Une autre classe de peptidomimétiques importante qui a été largement étudiée est celle des peptoïdes amphipathiques cationiques. Les peptoïdes sont des peptidomimétiques dont la chaîne latérale est connectée à l'azote du squelette au lieu du carbone  $\alpha$  comme dans les peptides. Ils ont été développés par Zuckermann en 1992.<sup>11</sup> Plus tard en 1998, Hamper a synthétisé les  $\beta$ -peptoïdes.<sup>12</sup> Le groupe de Taillefumier a mis au point la synthèse de  $\alpha,\beta$ -peptoïdes en 2009.<sup>13</sup>

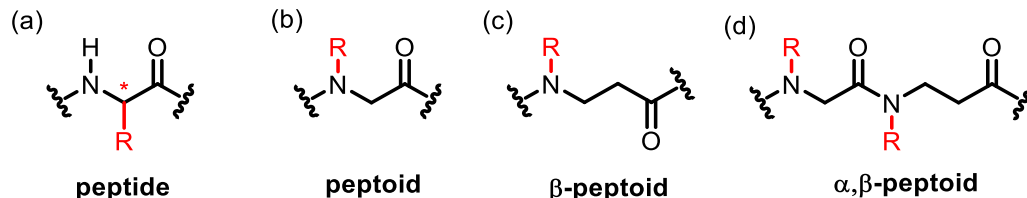


Figure 2: a) Peptide, b)  $\alpha$ -Peptoïde (Zukermann 1992), c)  $\beta$ -peptoïde (Hamper 1998), d)  $\alpha,\beta$ -peptoïde (Taillefumier 2009)

Les peptoïdes (oligomères de glycine *N*-substitués) représentent une classe prometteuse de mimes d'AMPs. Les peptoïdes possèdent plusieurs avantages tels que la stabilité vis à vis de

<sup>9</sup> V. Semetey; D. Rognan; C. Hemmerlin; R. Graff; J.-P. Briand; M. Marraud; and G. Guichard, 'Stable Helical Secondary Structure in Short-Chain *N,N'*-Linked Oligoureas Bearing Proteinogenic Side Chains', *Angewandte Chemie International Edition*, 41 (2002), 1893-5.

<sup>10</sup> G. N. Tew; D. Liu; B. Chen; R. J. Doerksen; J. Kaplan; P. J. Carroll; M. L. Klein; and W. F. DeGrado, 'De Novo Design of Biomimetic Antimicrobial Polymers.', *Proceedings of the National Academy of Sciences of the United States of America*, 99 (2002), 5110-4.

<sup>11</sup> R. J. Simon; R. S. Kania; R. N. Zuckermann; V. D. Huebner; D. A. Jewell; S. Banville; S. Ng; L. Wang; S. Rosenberg; and C. K. Marlowe, 'Peptoids: A Modular Approach to Drug Discovery.', *Proceedings of the National Academy of Sciences of the United States of America*, 89 (1992), 9367-71

<sup>12</sup> B. C. Hamper; S. A. Kolodziej; A. M. Scates; R. G. Smith; and E. Cortez, 'Solid Phase Synthesis of Beta-Peptoids: *N*-Substituted Beta-Aminopropionic Acid Oligomers.', *The Journal of Organic Chemistry*, 63 (1998), 708-18.

<sup>13</sup> B. C. Hamper; S. A. Kolodziej; A. M. Scates; R. G. Smith; and E. Cortez, 'Solid Phase Synthesis of Beta-Peptoids: *N*-Substituted Beta-Aminopropionic Acid Oligomers.', *The Journal of Organic Chemistry*, 63 (1998), 708-18.

protéase, une synthèse peu coûteuse et une grande diversité accessible. Cependant, les peptoïdes présentent certains inconvénients. Ils ont un squelette achiral et sont dépourvus de donneurs de liaison hydrogène. En outre, ils présentent une isomérisation *cis/trans* des amides *N,N*-disubstitués. Mais cet inconvénient peut être rendu avantageux en utilisant des chaînes latérales spécifiques pour contrôler cette isomérisation. En fonction des chaînes latérales utilisées, les peptoïdes peuvent adopter des structures secondaires particulières comme des hélices. La structuration est basée principalement sur la conformation des amides *N,N*-disubstitués du squelette. Par exemple, les amides *cis* conduisent à une structure secondaire en hélice de type PolyProline I (PPI). Armand et Zuckermann ont démontrés par modélisation et RMN l'adoption d'une structure en hélice de type PPI d'un octamère portant des chaînes volumineuses (*S*)-phényléthyle.<sup>14</sup> Plus tard, la première structure rayons X d'un pentamère a été élucidée par Wu et Kirshenbaum avec des unités *N*-(*R*)-cyclohexylethyl glycines.<sup>15</sup> Cependant, la structure était hétérogène en solution avec la présence de conformères minoritaires. De la même façon, lorsque les amides sont en *trans*, une structuration en hélice de type PolyProline 2 (PPII) est préférée. Par exemple, les oligomères de *N*-aryl glycines adoptent une structure hélicoïdale de type PPII homogène en solution.

Pour avoir une structure homogène de type PolyProline 1 (PPI), le groupe de Blackwell a développé des oligomères portant des chaînes latérales naphthyléthyles.<sup>16</sup> Récemment, notre groupe a étudié des chaînes latérales *N*- $\alpha$ -chirales mais en s'affranchissant de groupement aromatique présent dans les chaînes actuellement utilisées (1-phenylethyl et 1-naphtylethyl). Les études de RMN et dichroïsme circulaire ont montré une structuration en hélice de type PolyProline I (PPI) d'une grande stabilité, confirmé par la structure cristallographique d'un pentamère de *Ns1tbe*. De plus, la construction d'oligomères mixtes comportant les chaînes *t*Bu et *s*1tbe a permis d'obtenir la structure RX du plus long oligomère reporté à ce jour, un

---

<sup>14</sup> P. Armand; K. Kirshenbaum; A. Falicov; R. L. Dunbrack; K. a Dill; R. N. Zuckermann; and F. E. Cohen, 'Chiral *N*-Substituted Glycines Can Form Stable Helical Conformations', *Folding and Design*, 2 (1997), 369–75.

<sup>15</sup> C. W. Wu; K. Kirshenbaum; T. J. Sanborn; J. A. Patch; K. Huang; K. A. Dill; R. N. Zuckermann; and A. E. Barron, 'Structural and Spectroscopic Studies of Peptoid Oligomers with  $\alpha$ -Chiral Aliphatic Side Chains', *Journal of the American Chemical Society*, 125 (2003), 13525–30

<sup>16</sup> J. R. Stringer; J. A. Crapster; I. A. Guzei; and H. E. Blackwell, 'Extraordinarily Robust Polyproline Type I Peptoid Helices Generated via the Incorporation of  $\alpha$ -Chiral Aromatic *N*-1-Naphthylethyl Side Chains', *Journal of the American Chemical Society*, 133 (2011), 15559–67.

octamère dont l'hélice est d'une remarquable régularité et parfaitement superposable avec le modèle PPI.<sup>17</sup>

Dans le domaine des mimes de peptides antibactériens, des peptoïdes amphiphiles cationiques ont été développés par Barron en 2003. Puis des peptoïdes cycliques ont été développés par De Riccardis en 2010 et Kirshenbaum en 2014. Des hybrides  $\beta$ -peptoïdes/ $\alpha$ -peptides ont été développés par Olsen en 2007, suivis du développement d'hybrides  $\alpha$ -peptoïde/peptides par Franzyk en 2014.

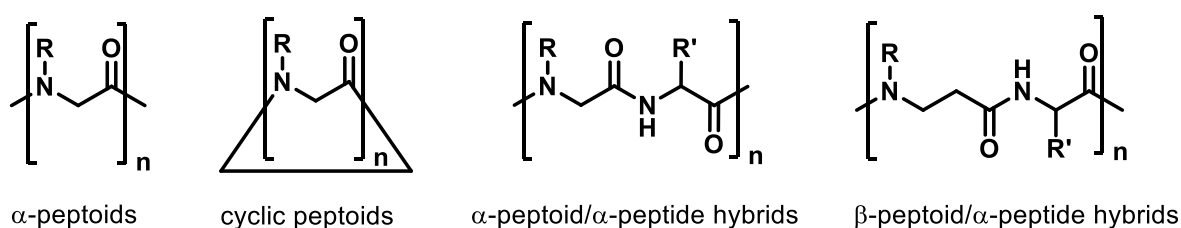


Figure 3 Structure des peptoïdes amphiphiles cationiques utilisés pour concevoir des mimes de PAMs

Le groupe de Barron a montré que la périodicité de l'hélice de type PPI permet de mimer la structure amphiphile cationique en hélice de la magainine. Comme on peut le voir dans la représentation schématique du peptoïde amphipathique, un côté est composé de chaînes latérales cationiques et les deux autres positions portent des chaînes latérales hydrophobes.<sup>18</sup>

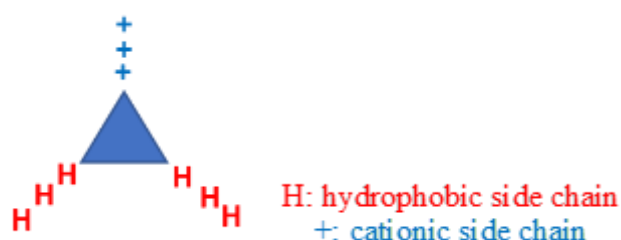


Figure 4 Représentation schématique de la structure hélicoïdale amphipathique des peptoïdes.

L'hélice amphipathique est construite par incorporation périodique d'une chaîne latérale cationique tous les trois résidus, les positions restantes étant occupées par la chaîne latérale aromatique  $\alpha$ -chirale (S)-phényléthyle qui favorise la formation de l'hélice et fournit une face hélicoïdale hydrophobe. En utilisant cette approche, le groupe de Barron a développé plusieurs séries d'oligomères de longueur, hydrophobie, chiralité, séquence et terminaisons variées. Cette étude a permis de développer un dodécamère (NLys-Nspe-Nspe)<sub>4</sub> possédant

<sup>17</sup> O. Roy; G. Dumonteil; S. Faure; L. Jouffret; A. Kriznik; and C. Taillefumier, 'Homogeneous and Robust Polyproline Type I Helices from Peptoids with Nonaromatic  $\alpha$ -Chiral Side Chains', *Journal of the American Chemical Society*, 139 (2017), 13533–40

<sup>18</sup>N. P. Chongsiriwatana; J. A. Patch; A. M. Czyzewski; M. T. Dohm; A. Ivankin; D. Gidalevitz; R. N. Zuckermann; and A. E. Barron, 'Peptoids That Mimic the Structure, Function, and Mechanism of Helical Antimicrobial Peptides.', *Proceedings of the National Academy of Sciences of the United States of America*, 105 (2008), 2794–9

d'excellentes activités antibactériennes à large spectre. Cependant ce composé a également fait preuve d'une cytotoxicité puissante vis-à-vis des cellules de carcinome. Les paramètres pouvant influencer sur les activités (longueur d'oligomère, charge, hydrophobicité, chiralité, structure secondaire et nature des chaînes latérales), le mode d'action de ces peptidomimétiques et leur sélectivité pour les bactéries par rapport aux cellules de mammifères ont été examinés au cours des dix dernières années.<sup>19</sup>

Par ailleurs, le groupe de Janssen a développé des oligomères riches en chaînes latérales mimes de lysine et de tryptophane et a découvert qu'ils présentaient une activité antimicrobienne prometteuse avec des profils de sélectivité comparables.<sup>20</sup> Ils ont également mené des études de microscopie sur les cellules de *E. coli* et ont observé des dommages à la membrane.<sup>21</sup>

Il a été démontré que la cyclisation augmente l'activité de peptoïdes vis-à-vis des membranes bactériennes, ce qui entraîne une inhibition supérieure de la croissance bactérienne *in vitro*.<sup>22</sup> Kirshenbaum a étudié la comparaison des peptoïdes linéaires et cycliques et a découvert que les peptoïdes cycliques sont plus puissants que leurs homologues linéaires acétylés. Un dodécacyclopeptoïde portant des chaînes latérales aminopropyle et phenylméthyle présente une CMI faible contre *E. coli*.<sup>23</sup> Ils ont également sélectionné l'hexacyclopeptoïde portant des chaînes latérales aminopropyle et diphenyléthyle pour des études de microscopie électronique à balayage afin de déterminer les dommages causés à la membrane bactérienne. La formation de pores a été observée à la surface de la bactérie *S. aureus*.<sup>24</sup>

### **Objectifs de ce projet de thèse:**

Malgré le grand nombre d'oligomères peptoïdes cationiques amphiphiles étudiés, la diversité chimique des chaînes latérales cationiques est limitée à ce jour à des équivalents de chaînes latérales protéinogènes chargées positivement c'est-à-dire ammonium, guanidinium ou imidazolium. Ces chaînes latérales apportent la charge positive mais n'exercent aucun rôle sur

---

<sup>19</sup>A. M. Czyzewski; H. Jenssen; C. D. Fjell; M. Waldbrook; N. P. Chongsiriwatana; E. Yuen; R. E. W. W. Hancock; and A. E. Barron, 'In Vivo, in Vitro, and in Silico Characterization of Peptoids as Antimicrobial Agents', *PLoS ONE*, 11 (2016), 1–17.

<sup>20</sup>B. Mojsoska; R. N. Zuckermann; and H. Jenssen, 'Structure-Activity Relationship Study of Novel Peptoids That Mimic the Structure of Antimicrobial Peptides.', *Antimicrobial Agents and Chemotherapy*, 59 (2015), 4112–20.

<sup>21</sup>B. Mojsoska; G. Carretero; S. Larsen; R. V. Mateiu; and H. Jenssen, 'Peptoids Successfully Inhibit the Growth of Gram-Negative *E. coli* Causing Substantial Membrane Damage', *Scientific Reports*, 7 (2017), 1–12.

<sup>22</sup>E. M. Driggers; S. P. Hale; J. Lee; and N. K. Terrett, 'The Exploration of Macrocycles for Drug Discovery - An Underexploited Structural Class', *Nature Reviews Drug Discovery*, Vol. 7 (2008), 608–24.

<sup>23</sup>M. L. Huang; S. B. Y. Shin; M. A. Benson; V. J. Torres; and K. Kirshenbaum, 'A Comparison of Linear and Cyclic Peptoid Oligomers as Potent Antimicrobial Agents', *ChemMedChem*, 7 (2012), 114–22.

<sup>24</sup>M. L. Huang; M. A. Benson; S. B. Y. Shin; V. J. Torres; and K. Kirshenbaum, 'Amphiphilic Cyclic Peptoids That Exhibit Antimicrobial Activity by Disrupting *Staphylococcus aureus* Membranes', *European Journal of Organic Chemistry* (2013), 3560–6.

le repliement en hélice amphipathique. L'utilisation de chaînes latérales cationiques impliquées dans la stabilisation de l'hélice pourrait fournir des oligomères amphiphiles courts présentant des propriétés antimicrobiennes intéressantes. Comme nous l'avons vu dans l'introduction, le repliement en hélice des peptoïdes, mimes d'AMPs, n'est pas nécessaire pour obtenir de puissantes activités antimicrobiennes. En outre, les séquences présentant une propension plus élevée à adopter une structure hélicoïdale se sont révélées plus toxiques que les oligomères non structurés, probablement dues à la nature des chaînes latérales aromatiques utilisées pour induire la structuration en hélice. Dans un contexte plus général, à ce jour, tous les oligomères peptoïdes conçus pour adopter des structures hélicoïdales visant une application biologique particulière, ont été construits en utilisant une proportion élevée (> 50%) de chaînes latérales  $\alpha$ -chiral aromatiques, en particulier des (S)-phényléthyles (spe) et dans une moindre mesure des (S)-naphtyléthyle (snpe).<sup>25</sup> Cependant, la nature et le nombre de ces chaînes structurantes entravent le développement de ces foldamères comme candidats-médicaments.

Conscient de ce problème, notre groupe s'emploie depuis dix ans à améliorer les propriétés foldamériques des peptoïdes en développant des chaînes latérales spécifiques capables de contrôler efficacement l'isomérisation *cis/trans* des amides par le biais d'interactions locales entre la chaîne latérale et le squelette. L'hélice de type PPI peut être générée à l'aide de chaînes latérales qui stabilisent la conformation *cis* des amides du squelette par le biais d'interactions stériques et/ou électroniques. Par exemple, la chaîne latérale tert-butyle exerce un contrôle total via des effets stériques.<sup>26</sup> La chaîne latérale de type 1,2,3-triazolium présente un fort effet *cis* directeur grâce à une interaction électronique  $n \rightarrow \pi^*_{Ar}$  forte.<sup>27</sup> De plus, la chaîne latérale du triazolium permet l'introduction d'une grande variété de substituants (groupe R), cette diversité chimique étant cruciale pour leurs applications en tant que peptidomimétiques, foldamères ou matériaux. En raison de ces propriétés, l'introduction de la chaîne latérale triazolium est d'un grand intérêt potentiel pour la stabilisation de la structure des oligopeptoïdes pour diverses applications. Dans le contexte de la conception des peptoïdes amphiphiles cationiques, cette chaîne latérale chargée positivement pourrait permettre de cibler la membrane bactérienne tout en favorisant le repliement en hélice.

Pour atteindre cet objectif, différentes familles d'oligomères peptoïdes amphiphiles cationiques imitant la structure hélicoïdale amphiphile de la magainine ont été conçues. Les structures de ces oligomères sont étroitement liées à celles développées par Barron. Afin

---

<sup>25</sup>B. C. Gorske; J. R. Stringer; B. L. Bastian; S. A. Fowler; and H. E. Blackwell, 'New Strategies for the Design of Folded Peptoids Revealed by a Survey of Noncovalent Interactions in Model Systems', *Journal of the American Chemical Society*, 131 (2009), 16555–67.

<sup>26</sup>O. Roy; C. Caumes; Y. Esvan; C. Didierjean; S. Faure; and C. Taillefumier, 'The Tert-Butyl Side Chain: A Powerful Means to Lock Peptoid Amide Bonds in the Cis Conformation', *Organic Letters*, 15 (2013), 2246–9

<sup>27</sup>C. Caumes; O. Roy; S. Faure; and C. Taillefumier, 'The Click Triazolium Peptoid Side Chain: A Strong Cis-Amide Inducer Enabling Chemical Diversity', *Journal of the American Chemical Society*, 134 (2012), 9553–6.

d'étudier l'influence des chaînes latérales *cis* inductrices récemment développées (hydrophobes ou cationiques) sur les activités antibactériennes ainsi que sur la sélectivité, nous avons conçu plusieurs familles d'oligomères peptoïdes.

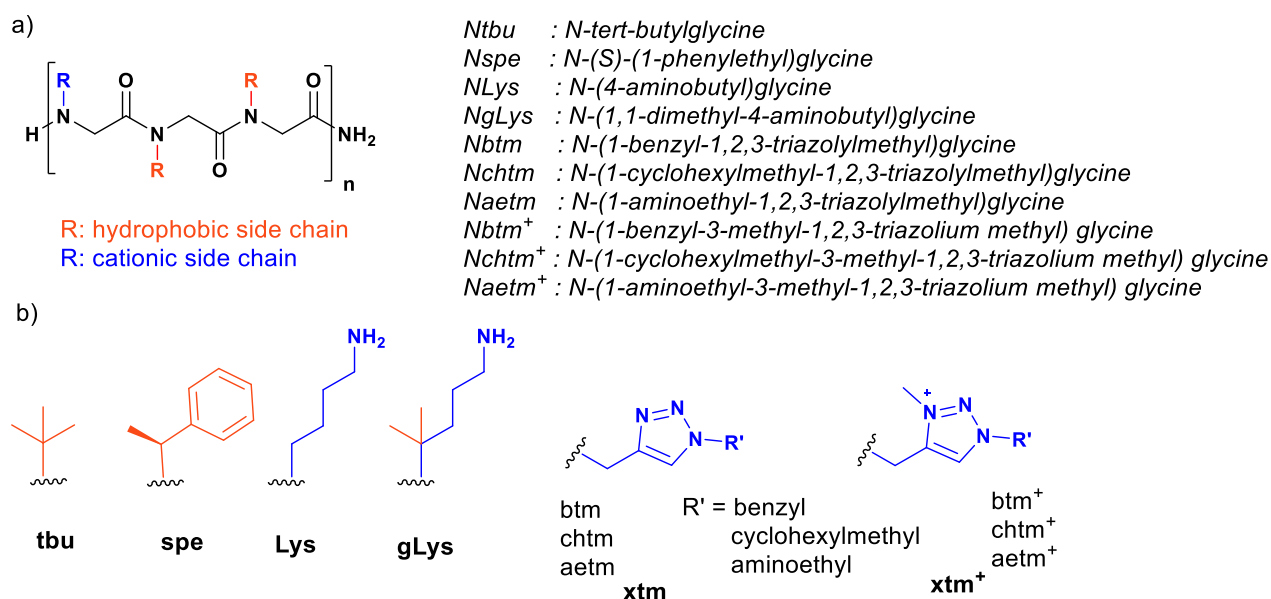


Figure 5 Peptoïdes amphiphiles cationiques : a) Structure générale ; b) Structure des chaînes latérales hydrophobes et cationiques.

Le présent travail est divisé en trois chapitres, deux consacrés à la synthèse en solution ou en phase solide des différentes familles de peptoïdes amphiphiles cationiques et un chapitre consacré à l'évaluation biologique de ces composés.

## Chapitre II Synthèse en solution des oligomères amphiphiles cationiques

Le chapitre II présente la mise au point de méthodes de synthèse en solution pour accéder aux peptoïdes incorporant des chaînes latérales *tert*-butyle (familles I et II). Dans la famille I, la première série est basée sur la répétition de deux résidus *Ntbu* et un *Nlys* (série A). La deuxième série est basée sur la modification supplémentaire de *NLys* en *NgLys*, équivalent de *Nlys*  $\alpha,\alpha$ -diméthylé (série B) (Figure 4).

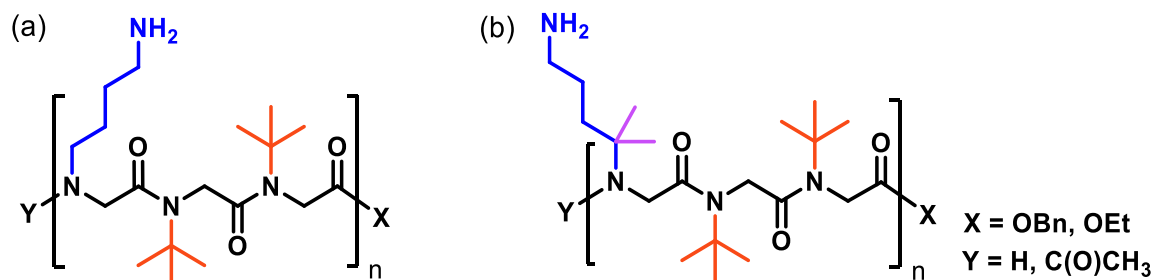
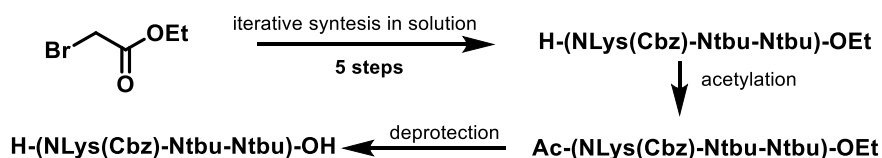


Figure 4 Structures de la famille I (a) série A:  $Y-(NLys-Ntbu-Ntbu)_n-X$ ; (b) Série B:  $Y-(NgLys-Ntbu-Ntbu)_n-X$  avec *Ntbu* pour la *N*-(*tert*-butyl)glycine et *NgLys* pour les résidus *N*-(1,1-diméthyl-4-aminobutyl)glycine.

La chaîne latérale  $\alpha$ -gem diméthylée pourrait être considérée comme une chaîne latérale tert-butyle fonctionnalisée. Par effet stérique, cette chaîne latérale induit une géométrie *cis* complète de l'amide du squelette. De manière générale, la stratégie submonomère en phase solide est utilisée pour la synthèse de peptoïdes. Les résidus peptoïdes sont créés en deux étapes : une acylation de l'extrémité *N*-terminale du peptoïde, suivie de la substitution de l'intermédiaire bromé avec une amine primaire. L'utilisation d'amine primaire permet ainsi l'introduction d'une très grande diversité de chaînes latérales sur les peptoïdes.<sup>28</sup> Une limitation de la synthèse supportée est l'incapacité à produire une grande quantité du composé final. Par conséquent, la méthode submonomère en solution a été développée pour produire des quantités à l'échelle du gramme d'oligomère<sup>29</sup> mais également pour permettre l'utilisation d'amines primaires très encombrées comme la *tert*-butylamine par exemple. La principale différence est l'élongation du squelette : étape d'acylation. En solution, ceci est accompli par réaction de l'amine *N*-terminale avec un halogénure d'acide plutôt que par couplage d'acide bromoacétique à l'aide d'un réactif de couplage.

- Synthèse et étude des oligomères de la Famille I

Pour synthétiser la première famille, nous avons synthétisé le trimère *N*Lys-*N*tbu-*N*tbu par un protocole de synthèse submonomère en solution, puis avons accédé à des oligomères plus longs par couplage de blocs.



Scheme 1 Synthèse submonomère en solution du bloc trimère

Différentes stratégies ont été étudiées pour la protection orthogonale de l'ester, de l'amine terminale et des amines des chaînes latérales. La synthèse en solution des oligomères de la famille I a permis de mieux comprendre le choix des groupes protecteurs. Nous avons découvert que les oligomères utilisant des groupes protecteurs Cbz étaient faciles à déprotéger en présence d'une chaîne latérale tert-butyle sur l'oligomère. Par conséquent, les oligomères synthétisés en utilisant cette approche ont été sélectionnés pour les évaluations biologiques (voir chapitre III).

Le trimère de la famille IB Ac-(*N*gLys(Boc)-*N*tbu-*N*tbu)-OBn a été obtenu par synthèse itérative en solution. Pour cette synthèse, l'amine primaire  $\alpha$ -gem-diméthylée a tout d'abord

<sup>28</sup>A. S. Culf and R. J. Ouellette, 'Solid-Phase Synthesis of *N*-Substituted Glycine Oligomers ( $\alpha$ -Peptoids) and Derivatives', *Molecules*, 15 (2010), 5282–335.

<sup>29</sup>C. Caumes; T. Hjelmgaard; R. Remuson; S. Faure; and C. Taillefumier, 'Highly Convenient Gram-Scale Solution-Phase Peptoid Synthesis and Orthogonal Side-Chain Post-Modification', *Synthesis*, 2 (2011), 257–64.

été préparée puis incorporée dans le trimère. Au cours de cette étude, nous avons pu accéder au bloc trimère Ac-(NgLys(Boc)-Ntbu-Ntbu)-OBn comportant le résidu NgLys. Mais nous avons découvert que l'élimination du groupe protecteur Boc en présence de la chaîne latérale tert-butyle est un exercice très fastidieux. Par conséquent, la synthèse de la chaîne latérale NLys  $\alpha$ -gem-diméthylée avec une protection Cbz est plus prometteuse pour accéder à des oligomères de la famille IB plus longs.

Pour comprendre l'influence de la chaîne latérale  $\alpha$ -gem-diméthylée sur la conformation des oligomères, les spectres de RMN du proton des deux trimères Ac-NLys(Boc)-Ntbu-Ntbu-OBn et Ac-NgLys(Boc)-Ntbu-Ntbu-OBn ont été analysés et comparés. Ces observations indiquent clairement que la chaîne latérale  $\alpha$ -gem-diméthylée a l'effet *cis* directeur attendu et donc réduit le nombre de conformères présents en solution. Cette étude préliminaire montre que la chaîne  $\alpha$ -gem-diméthylée permet d'apporter la même contrainte que la chaîne tert-butyle tout en permettant l'introduction d'un groupe cationique ammonium conférant un caractère amphiphile à l'oligomère.

- Synthèse et étude des oligomères de la Famille II

Dans la famille II, les résidus NLys cationiques sont remplacés par des chaînes latérales de type 1,2,3-triazolium tout en conservant la chaîne latérale tert-butyle pour la partie hydrophobe (Figure 5). La substitution des NLys par un groupe cationique de type 1,2,3-triazolium, nous donne l'avantage de contrôler la géométrie *cis* des amides pour conduire à une architecture hélicoïdale amphiphile.

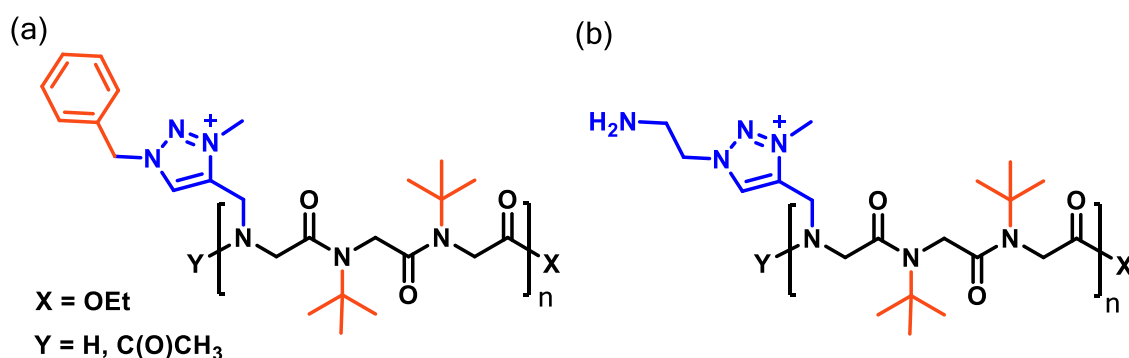


Figure 5 Structures de la famille II (a) série A: Y-(Nbtm<sup>+</sup>-Ntbu-Ntbu)<sub>n</sub>-X; et b) série B: Y-(Naetm<sup>+</sup>-Ntbu-Ntbu)<sub>n</sub>-X avec Nbtm<sup>+</sup> pour le N-(1-benzyl-3-méthyl-1,2,3-triazolium méthyl)glycine, Ntbu pour le N-(tert-butyle)glycine et Naetm<sup>+</sup> pour les résidus N-(1-aminoéthyl-3-méthyl-1,2,3-triazolium méthyl)glycine.

Pour synthétiser les peptoides cationiques appartenant à cette deuxième famille à base de chaînes latérales tertbutyle et de type 1,2,3-triazolium, nous avons essayé d'accéder à de longs oligomères par synthèse submonomère. Compte tenu des résultats précédemment obtenus avec la première famille, nous avons choisi d'introduire un ester éthylique au niveau C-terminal. Deux types de chaînes latérales de triazolium ont été synthétisés, l'un avec un



substituant aromatique (groupe benzyle,  $\text{btm}^+$ ) :  $\text{Ac}-(\text{Nbtm}^+-\text{Ntbu}-\text{Ntbu})_2\text{-OEt}$  et l'autre avec un groupement amine ( $\text{aetm}^+$ ) :  $\text{Ac}-(\text{Naetm}^+-\text{Ntbu}-\text{Ntbu})_2\text{-OEt}$ .

Les oligomères à base de triazolium ont été synthétisés avec de bons rendements globaux ouvrant la voie à la synthèse d'oligomères plus longs incorporant les chaînes latérales tert-butyle et triazolium. Par conséquent, les oligomères synthétisés en utilisant cette approche ont été sélectionnés pour les évaluations biologiques (voir chapitre IV).

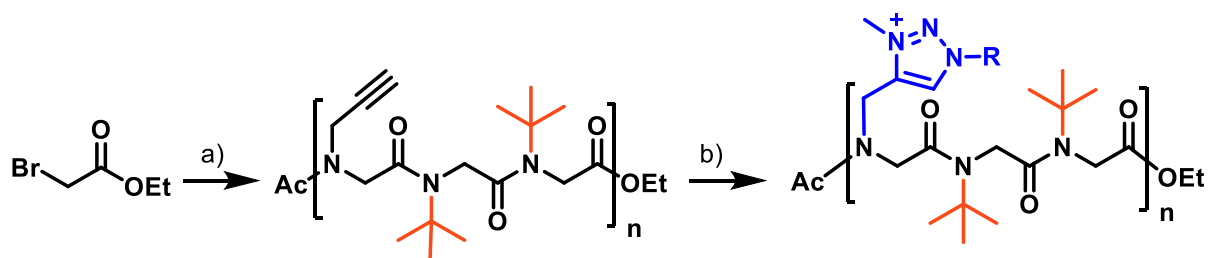


Figure 6 Synthèse d'oligomères ( $n = 1$  et  $2$ ) de la famille II a) Synthèse itérative b) Post-fonctionnalisation

Les spectres de RMN des deux hexamères de la famille II à base de triazole et un autre à base de triazolium ont été comparés pour étudier l'influence du triazolium sur la structuration de ces oligomères. Cette étude préliminaire par RMN suggère que les oligomères de la famille II portant des chaînes latérales triazolium et tert-butyle adoptent une structure définie et robuste en solution. L'étude par RMN confirme que la chaîne latérale de type triazolium chargée positivement est un puissant inducteur d'amide *cis*. C'est donc un excellent outil pour la diversification des chaînes latérales et la production d'oligomères à fort caractère amphiphile.

### Chapitre III Synthèse sur support des oligomères amphiphiles cationiques

Ce chapitre concerne la préparation des oligomères de la famille III, en utilisant la synthèse submonomère supportée.<sup>30</sup> De nouveaux oligomères à la fois cationiques et hydrophobes ont été synthétisés sur support en utilisant diverses chaînes latérales. La synthèse sur support par chauffage conventionnel ou par micro-ondes<sup>31</sup> a été optimisée pour obtenir des peptoides à base de 1,2,3-triazolium.

Cette troisième famille est basée sur l'utilisation de résidus  $\text{N}_{\text{spe}}$  employés par Barron en tant que promoteur d'hélice et de groupe hydrophobe, et l'introduction de diverses chaînes latérales du type 1,2,3-triazolium en tant que groupe cationique. Trois séries d'oligomères

<sup>30</sup>T. S. Burkoth; A. T. Fafarman; D. H. Charych; M. D. Connolly; and R. N. Zuckermann, 'Incorporation of Unprotected Heterocyclic Side Chains into Peptoid Oligomers via Solid-Phase Submonomer Synthesis', *Journal of the American Chemical Society*, 125 (2003), 8841–5.

<sup>31</sup>H. J. Olivos; P. G. Alluri; M. M. Reddy; D. Salony; T. Kodadek; Hernando J. Olivos; Prasanna G. Alluri; M. Muralidhar Reddy; A. Derek Salony; T. Kodadek\*; H. J. Olivos; P. G. Alluri; M. M. Reddy; D. Salony; and T. Kodadek, 'Microwave-Assisted Solid-Phase Synthesis of Peptoids', *Organic Letters*, 4 (2002), 4057–8.

peptoïdes portant des chaînes latérales 1,2,3-triazole ou 1,2,3-triazolium ont été conçues en fonction du substituant sur le triazole/triazolium: un cyclohexylméthyle pour la série A (résidus *Nchtm* ou *Nchtm+*), un benzyle pour série B (résidus *Nbtm* ou *Nbtm+*) et un aminoéthyle pour la série C (résidus *Naetm* ou *Naetm+*).

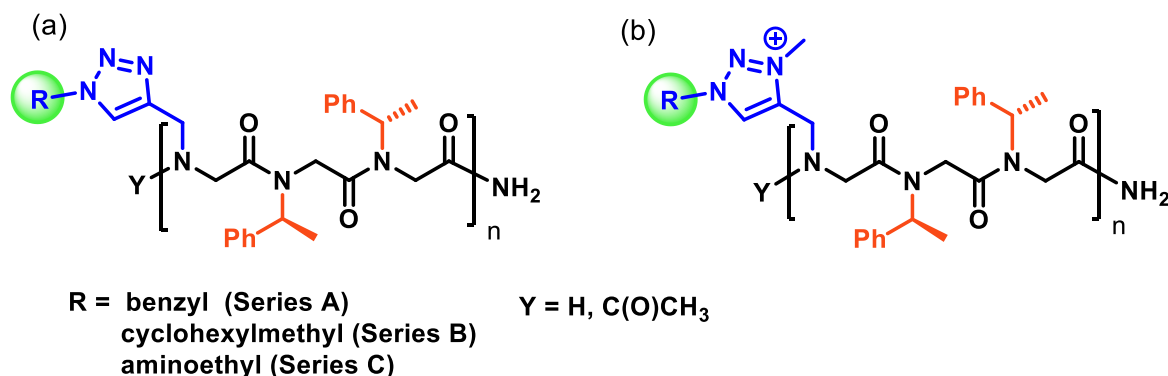
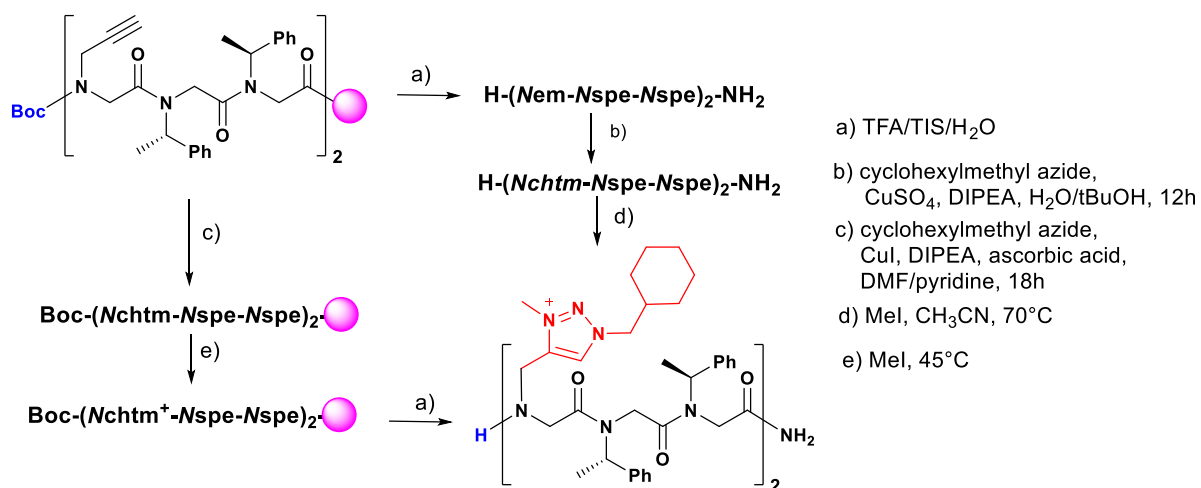


Figure 7 Structures de la famille III (a) incorporant des résidus de type triazole:  $Y-(Nxtm-Nspe-Nspe)_n-NH_2$  et (b) incorporant des résidus de type triazolium:  $Y-(Nxtm^+-Nspe-Nspe)_n-NH_2$  avec *Nbtm* pour *N*-(1-benzyl-1,2,3-triazolylméthyl)glycine, *Nbtm+* pour *N*-(1-benzyl-3-méthyl-1,2,3-triazolium méthyl)glycine, *Nchtm* pour *N*-(1-cyclohexylméthyle-1,2,3-triazolylméthyl)glycine, *Nchtm+* pour le *N*-(1-cyclohexylméthyle-3-méthyl-1,2,3-triazolium méthyl)glycine, *Naetm* pour le *N*-(1-aminoéthyl-1,2,3-triazolylméthyle)glycine et *Naetm+* pour la *N*-(1-aminoéthyl-3-méthyl-1,2,3-triazolium méthyl)glycine.

Le meilleur moyen de formation multivalente de groupes 1,2,3-triazolium a été initialement évalué en synthétisant le modèle hexamère  $H-(Nchtm^+-Nspe-Nspe)_2-NH_2$  en solution ou sur support. Tout d'abord, l'hexamère modèle portant les chaînes latérales spe et les chaînes latérales propargyle (*em*) localisées spécifiquement en tant que précurseurs des groupements triazolium a été préparé par synthèse submonomère standard en phase solide assistée par micro-ondes. La formation de triazole en solution a été obtenue en utilisant un protocole standard de cycloaddition azoture-alcyne catalysée au cuivre (CuAAC). En utilisant de l'azoture de cyclohexylméthyle, la conversion des fonctions alcynes en triazoles a été réalisée pour créer l'hexapeptoid  $H-(Nchtm-Nspe-Nspe)_2-NH_2$ . La conversion des triazoles en triazolium a été testée selon un protocole bien établi (CuSO<sub>4</sub>, acide ascorbique, *tert*-butanol/eau). Un mélange complexe de composés a été obtenu probablement due de la présence de l'amide primaire et de l'amine *N*-terminal non protégé. Ce résultat nous a incité à développer une nouvelle stratégie consistant à former le groupement triazolium directement sur la résine après une protection préalable de l'amine *N*-terminale. Par conséquent, la peptoïde  $H-(Nem-Nspe-Nspe)_2-NH_2$  supporté a été protégé avec un groupement Boc, sensible aux conditions de décrochage de la résine. La conjugaison multiple de CuAAC a ensuite été réalisée sur support en utilisant de l'iodure de cuivre, une base de Hünig et de l'acide ascorbique.<sup>32</sup>

<sup>32</sup>H. Jang; A. Fafarman; J. M. Holub; and K. Kirshenbaum, 'Click to Fit: Versatile Polyvalent Display on a Peptidomimetic Scaffold', *Organic Letters*, 7 (2005), 1951–4.



Scheme 2 Accès aux oligomères à base de 1,2,3-triazolium selon deux stratégies

Enfin, la formation du triazolium a été étudiée sur support pour conduire aux oligomères amphiphiles cationiques. Sur la base de travaux antérieurs, l'iodure de méthyle a été choisi comme réactif d'alkylation à différentes concentrations dans divers solvants et à différentes températures. Dans la plupart des cas, une méthylation partielle est observée, conduisant à un mélange complexe de composés. La conversion complète des triazoles en triazoliums a finalement été obtenue en exposant la résine à de l'iodure de méthyle pur à 45 °C pendant 5h. Ensuite, l'hexapeptide H-(Nchtm<sup>+</sup>-Nspe-Nspe)<sub>2</sub>-NH<sub>2</sub> a été décroché du support et obtenu avec une bonne pureté évaluée par analyse LC-MS. En utilisant l'expérience acquise dans le groupe lors des travaux précédents sur la synthèse en solution d'oligomères à base de 1,2,3-triazolium et grâce à notre stratégie optimisée en phase solide développée ici, un panel d'oligomères peptidés amphiphiles cationiques de 6, 9 et 12 résidus de longueur et portant différentes chaînes latérales de type triazolium ont été synthétisés efficacement sur support. La stratégie de synthèse développée est très pratique et parfaitement adaptée à la préparation d'une grande banque d'oligomères.

Une étude préliminaire de dichroïsme circulaire de cette série d'oligomères a montré que les peptidés H-(Nchtm-Nspe-Nspe)<sub>2</sub>-NH<sub>2</sub>, H-(Nchtm<sup>+</sup>-Nspe-Nspe)<sub>2</sub>-NH<sub>2</sub> et H-(Nchtm<sup>+</sup>-Nspe-Nspe)<sub>3</sub>-NH<sub>2</sub> présentent la signature caractéristique de l'hélice de type PPI des peptidés portant des chaînes spe avec deux minima à 203 et 220 nm.<sup>33</sup> L'intensité inférieure de l'hexapeptide H-(Nchtm-Nspe-Nspe)<sub>2</sub>-NH<sub>2</sub> à base de triazole par rapport à l'hexapeptide à base de triazolium H-(Nchtm<sup>+</sup>-Nspe-Nspe)<sub>2</sub>-NH<sub>2</sub> est révélatrice de la stabilisation de la structure hélicoïdale par les chaînes de type triazolium. En outre, une signature CD similaire a été observée pour l'hexamère H-(Nchtm<sup>+</sup>-Nspe-Nspe)<sub>2</sub>-NH<sub>2</sub> et le nonamère H-(Nchtm<sup>+</sup>-

<sup>33</sup>P. Armand; K. Kirshenbaum; R. A. Goldsmith; S. Farr-Jones; A. E. Barron; K. T. V Truong; K. A. Dill; D. F. Mierke; F. E. Cohen; R. N. Zuckermann; and E. K. Bradley, 'NMR Determination of the Major Solution Conformation of a Peptoid Pentamer with Chiral Side Chains', *Proceedings of the National Academy of Sciences of the United States of America*, 95 (1998), 4309–14

*Nspe-Nspe*)<sub>3</sub>-NH<sub>2</sub>, ce qui suggère que l'oligomère court a déjà une structure hélicoïdale bien définie et donc le caractère amphiphile nécessaire pour l'activité antibactérienne.

### Chapitre IV Evaluation biologique

Dans ce chapitre, nous décrivons l'évaluation biologique des différentes familles d'oligomères amphiphiles cationiques synthétisés précédemment (Tableau 1). L'évaluation biologique comprendra l'étude de l'activité antibactérienne, de l'activité hémolytique et de la viabilité cellulaire. Pour mieux comprendre le mode d'action de ces peptoïdes, l'observation par microscopie électronique des bactéries traitées avec une sélection d'oligomères peptoïdes sera présentée.

Table 1 Oligomères sélectionnés pour l'évaluation de l'activité antibactérienne

Peptoïde n°.	Famille	sequence	Charge nette	Masse molaire
<b>27</b>	<b>IA</b>	Ac-( <i>Nlys-Ntbu-Ntbu</i> ) <sub>2</sub> -OEt	2	797.09
<b>43</b>	<b>IIA</b>	Ac-( <i>Nbtm<sup>+</sup>-Ntbu-Ntbu</i> ) <sub>2</sub> -OEt	2	1027.32
<b>53a</b>	<b>IIIA</b>	H-( <i>Nchtm-Nspe-Nspe</i> ) <sub>2</sub> -NH <sub>2</sub>	1	1130.45
<b>54a</b>		H-( <i>Nchtm<sup>+</sup>-Nspe-Nspe</i> ) <sub>2</sub> -NH <sub>2</sub>	3	1354.56
<b>56a</b>		H-( <i>Nchtm<sup>+</sup>-Nspe-Nspe</i> ) <sub>3</sub> -NH <sub>2</sub>	4	2023.32
<b>58a</b>	<b>IIIB</b>	H-( <i>Nbtm<sup>+</sup>-Nspe-Nspe</i> ) <sub>3</sub> -NH <sub>2</sub>	4	2005.17
<b>58b</b>		Ac-( <i>Nbtm<sup>+</sup>-Nspe-Nspe</i> ) <sub>3</sub> -NH <sub>2</sub>	4	2047.21
<b>63</b>	<b>IIIC</b>	H-( <i>Naetm<sup>+</sup>-Nspe-Nspe</i> ) <sub>2</sub> -NH <sub>2</sub>	5	1248.35
<b>66</b>		H-( <i>Naetm<sup>+</sup>-Nspe-Nspe</i> ) <sub>3</sub> -NH <sub>2</sub>	7	1864.00
<b>67</b>		H-( <i>Naetm-Nspe-Nspe</i> ) <sub>4</sub> -NH <sub>2</sub>	5	2031.46
<b>68</b>		H-( <i>Naetm<sup>+</sup>-Nspe-Nspe</i> ) <sub>4</sub> -NH <sub>2</sub>	9	2479.66

L'activité antibactérienne des amphiphiles conçus a été évaluée contre deux bactéries à Gram-négatif : deux souches d'*Escherichia coli* et une souche de *P. aeruginosa*, et deux bactéries à Gram-positif : *Enterococcus faecalis* et *Staphylococcus aureus*. La sélectivité pour les cellules bactériennes sur les mammifères a été évaluée en testant les activités hémolytiques sur les globules rouges humains (hRBC) et la toxicité sur les cellules HeLa.

Table 2 CMI, activité hémolytique et cytotoxicité des peptoïdes amphiphiles cationiques

No.	CMI ( $\mu\text{M}$ ) <sup>a</sup>					HC <sub>10</sub> /HC <sub>50</sub> <sup>b</sup> ( $\mu\text{M}$ )	CV <sup>c</sup> (%)	SR <sup>d</sup>
	<i>E. coli</i> *	<i>E. coli</i> **	<i>P. aeruginosa</i>	<i>E. faecalis</i>	<i>S. aureus</i>			
ref	3.5 <sup>18</sup>	14-24 <sup>18</sup>	-	-	-	21/100 <sup>18</sup>	-	-
27	>200.0	>200.0	>200.0	>200.0	>200.0	-	-	-
43	>200.0	166.0	>200.0	25.0	6.3	>200/>200	100	>31
53a	>200.0	>200.0	>200.0	>200.0	>200.0	-	-	-
54a	50.0	50.0	>200.0	6.3	3.1	>200/>200	100	>64
56a	25.0	25.0	166.6	1.8	1.6	50/>75	7	31
58a	12.5	12.5	>200.0	1.6	1.6	>50/>100	7	>31
63	>200.0	>200.0	>200.0	>200.0	>200.0	-	-	-
66	25.0	100.0	>200.0	50.0	50.0	>200/>200	100	>4
67	6.3	12.5	37.5	11.5	10.4	>100/>200	6	>9
68	11.5	50.0	33.3	6.3	6.3	>200/>200	100	>31
Melittine <sup>e</sup>	6.3	6.3	25.0	6.3	3.1	-	-	-

<sup>a</sup>Concentration minimale inhibitrice (CMI) a été déterminée comme étant la plus faible concentration de peptoïde inhibant la croissance bactérienne de *Escherichia coli* \* JM109 et \*\* ATCC® 25922 <sup>TM</sup>, *Pseudomonas aeruginosa* ATCC® 27853 <sup>TM</sup>, *Enterococcus faecalis* ATCC® 29212 <sup>TM</sup>, *Staphylococcus aureus* CIP 6525. Les données sont représentatives de trois expériences indépendantes ; <sup>b</sup>Concentrations hémolytiques au cours desquelles on observe une hémolyse à 10% et à 50%; Viabilité de la cellule (CV): pourcentage moyen de cellules HeLa viables ATCC® CCL2 <sup>TM</sup> après exposition au peptoïde à 100  $\mu\text{M}$  pendant 24 h (dosage au MTT); <sup>d</sup>Selectivité SR = HC<sub>10</sub>/CMI<sub>S.aureus</sub>; <sup>e</sup>Peptide GIGAVLKVLTTGLPALISWIKRKRQQ.

Dans la famille I, l'hexamère **27** s'est révélé inactif contre toutes les souches de bactéries. Cependant, dans la famille II, il était intéressant de constater que même un oligomère court tel que l'hexamère **43** présentait une activité significative contre les bactéries à Gram positif. En particulier, cet hexamère présente une bonne activité contre *S. aureus* (CMI 6,3  $\mu\text{M}$ ) pour un oligomère de cette longueur. Dans la famille IIIA, la puissance antimicrobienne a augmenté de manière exponentielle avec la longueur de l'oligomère, comme cela est habituellement observé pour les peptoïdes amphiphiles cationiques développés par d'autres groupes.<sup>11</sup> Dans les séries A et B, la charge positive nette des oligomères provient exclusivement des groupes triazolium. Comme prévu, le composé **53a** avec les triazoles non chargés est inactif sur les bactéries et la quaternarisation des deux triazoles conduit à l'hexamère amphiphile cationique **54a** aux activités antibactériennes sans précédent pour un

peptoïde linéaire de cette longueur. En effet, des CMI de 6,3 et 3,1  $\mu\text{M}$  ont été mesurées contre *E. faecalis* et *S. aureus*, respectivement. L'activité du peptoïde **54a** peut être due à l'effet structurant du triazolium.<sup>20</sup>

Le peptoïde **56a**, un nonamère a montré une diminution de deux ou trois fois la valeur de la CMI pour toutes les bactéries. Malheureusement, ce nonamère s'est également révélé plus hémolytique que l'hexamère **54a** (HC<sub>10</sub> 50  $\mu\text{M}$ ) cependant la sélectivité demeure très acceptable. Enfin, l'influence de groupes aromatiques supplémentaires a été étudiée par comparaison des nonamères **56a** et **58a**. Il est généralement observé dans la conception des mimes d'AMP que les groupes aromatiques hydrophobes aident à améliorer l'activité antibactérienne mais sont souvent préjudiciables à la spécificité. Le nonamère **58a** présente les meilleures activités sur l'ensemble des souches bactériennes étudiées et est étonnamment légèrement moins hémolytique que le nonamère **56a** avec une sélectivité SR supérieure à 31.

L'hexamère **63** n'a aucun effet sur les souches bactériennes tandis que le dodécamère **68** présente une activité antibactérienne élevée, en particulier sur les bactéries à Gram-positif. Contrairement aux études précédentes, aucune augmentation de l'activité hémolytique n'a été observée pour les oligomères plus longs (**66** contre **68**). Contrairement au triazolium, le triazole a peu d'influence sur l'adoption de structure secondaire en hélice de type PPI. Cependant, le dodécamère **67** portant les chaînes triazoles non chargées s'est avéré avoir une activité à large spectre avec une puissance similaire à celle de la séquence de référence contre *E. coli*. Il est important de noter que ces dodécamères **67** et **68** sont les seuls peptoïdes de cette étude actifs sur *P. aeruginosa* cependant avec des valeurs de CMI modestes (37-33  $\mu\text{M}$ ). En conséquence, dans cette série IIC, l'incorporation d'un groupe triazolium entre le squelette peptoïde et le fragment cationique ammonium n'a montré aucun effet particulier sur les valeurs de CMI. Toutefois ces peptoïdes à base de triazolium se sont révélés moins hémolytiques et toxiques que leurs précurseurs à base de triazoles et la séquence de référence (**68** contre **67** et réf).

En ce qui concerne les mimes d'AMPs, des études ont démontré que les peptoïdes cationiques amphiphiles agissent principalement en perturbant la membrane bactérienne.<sup>34</sup> Les modifications de la morphologie membranaire des bactéries *S. aureus* lors du traitement par une sélection de peptoïdes, ont été visualisées par microscopie électronique à balayage (figure 11). Le dodécamère **68**, le plus long peptoïde de la série C et l'hexamère **54a** de la série A ont été sélectionnés. Dans les échantillons de contrôle (*S. aureus* non traité), les cellules sont apparues avec des surfaces rondes et lisses en grappes ressemblant à du raisin

---

<sup>34</sup>K. Andreev; M. W. Martynowycz; A. Ivankin; M. L. Huang; I. Kuzmenko; M. Meron; B. Lin; K. Kirshenbaum; and D. Gidalevitz, 'Cyclization Improves Membrane Permeation by Antimicrobial Peptoids', *Langmuir*, 32 (2016), 12905–13.

(figures 11A, B). Lors du traitement avec le peptoïde **68** à la CMI, une fuite cytoplasmique et des dommages à la membrane ont été observés (figure 11C). Les cellules présentent des dépressions superficielles et certaines d'entre elles montrent des trous (diamètre d'environ 70 à 80 nm) dans leur paroi cellulaire. La formation de pores a déjà été observée sur une membrane de *S. aureus* traité avec des peptoïdes cycliques.<sup>27</sup> Des micrographies MEB de bactéries traitées avec l'hexamère **54a** à la CMI ont montré des altérations morphologiques importantes telles qu'une ondulation de la membrane, mais aucun pore n'a été observé (figure 11D).

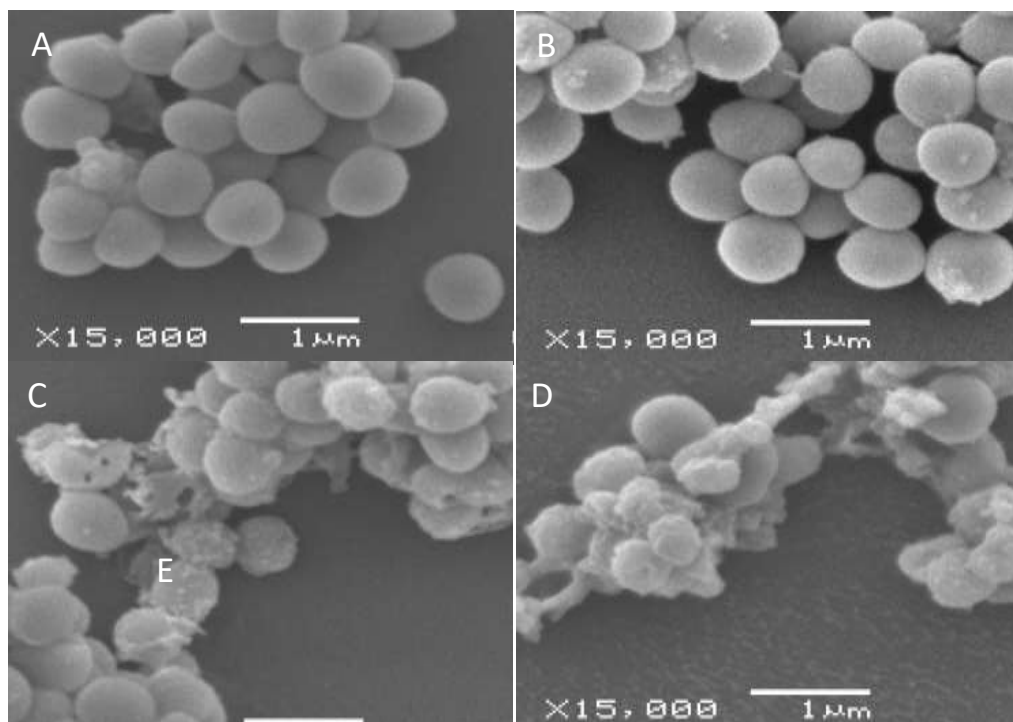


Figure 8 Micrographies MEB de cellules de *S. aureus* A) Cultures à  $10^8$  UFC / ml à  $T = 0$ ; B) non traité après 18h; C) traité avec le dodécamère **68** à la CMI ( $6,3 \mu\text{M}$ ) après 18h; D) traité avec l'hexamère **54a** à la CMI ( $3,1 \mu\text{M}$ ) après 18h.

En résumé, les peptoïdes amphiphiles présentant les meilleures activités ont été trouvés dans la famille III. Notamment, les nonamères **67** et **56a** ont montré des activités puissantes ( $\text{CMI} \leq 3 \mu\text{M}$ ), en particulier contre les souches *E. faecalis* et *S. aureus*, et une bonne sélectivité. En outre, un oligomère court, l'hexamère **54a** est également actif contre les bactéries à Gram-positif et non hémolytique et non cytotoxique sur les cellules Hela. Par visualisation par microscopie, les cellules de *S. aureus* traitées avec les peptoïdes **54a** ou **68** ont révélé un effet extrêmement dommageable sur la membrane. Nos observations suggèrent que le plus long peptoïde agit par la formation de pores tandis que l'hexamère **54a** semble provoquer une perméation de la membrane par un autre mécanisme.

## Conclusion

Le but de cette thèse était de synthétiser de nouveaux oligomères amphiphiles cationiques en tant que mimes de peptides antimicrobiens. Comme nous le savons, tous les efforts dans le passé pour développer des oligomères peptoïdes hélicoïdaux ont été réalisés en utilisant des chaînes latérales  $\alpha$ -chirales aromatiques volumineuses comme spe et slnpe. Cependant, ces oligomères hélicoïdaux ont un effet néfaste sur l'activité hémolytique et la cytotoxicité. De plus, ces chaînes latérales ci-dessus limitent la diversité chimique accessible, ce qui entrave le développement de ces foldamères comme candidats médicaments.

Par conséquent, nous avons conçu des oligomères utilisant les chaînes latérales directrices développées dans le groupe qui permettent l'adoption de structure en hélice des oligomères peptoïdes. Les différents oligomères (Famille I, II et III) ont été synthétisés en solution ou sur support. Ces oligomères sont les premiers de ce type, qui tentent de créer une architecture amphiphile robuste en stabilisant la conformation *cis* de tous les amides du squelette par le biais d'interactions stériques et/ou électroniques. Les activités antibactériennes et sélectivités de ces nouveaux oligomères se sont révélées très prometteuses.

Une perspective directe de ce travail est l'optimisation de la puissance des peptoïdes cationiques amphiphiles les plus prometteurs tout en maintenant une bonne sélectivité pour les cellules procaryotes. Pour atteindre cet objectif, différentes stratégies de modification pourraient être explorées dans le groupe.



## Cationic Amphipathic Peptoid Oligomers as Antimicrobial Peptide Mimics

Living organisms produce antimicrobial peptides (AMPs) to protect themselves against microbes. The growing problem of antimicrobial resistance calls for new therapeutic strategies and the natural AMPs have shown ground-breaking potential to address that issue. They show broad-spectrum activity and their main mechanism of action by bacterial cell membrane disruption implies low emergence of resistance which makes them potent candidates for replacing conventional antibiotics. Nevertheless, few hurdles are impeding their use, notably poor bioavailability profile. Some of these limitations can be overcome by developing peptidomimetics of AMPs which exhibit antibacterial activities together with enhanced therapeutic potential. Peptoids (*i.e.* *N*-alkyl glycine oligomers) adopting cationic amphipathic helical structures are mostly competent AMP mimetics. From a conformational point of view, peptoids are fundamentally more flexible than peptides primarily due to the *cis/trans* isomerism of *N,N*-disubstituted amides but studies in this area have shown that *cis* amide conformation can be controlled by careful choice of side-chain to set a PolyProline I-type helical structure of peptoids. In this thesis, the genesis of novel amphipathic cationic peptoids carrying *cis*-directing tert-butyl and/or triazolium-type side-chains and their untapped potential to act against bacteria will be discussed comprehensively. First, the solution-phase synthesis of tert-butyl-based oligomers was developed. Second, novel method of solid-phase submonomer synthesis was optimised to access 1,2,3-triazolium-based oligomers. Then, the synthesised cationic oligomers were evaluated for their antibacterial potential, followed by antibiofilm activity and cell selectivity assays. In the end, to have insights on the mode of action of amphipathic peptoids, microscopy was carried out.

Keywords: Peptidomimetics, antimicrobial peptides, peptoids, 1,2,3-triazolium, cationic amphipathic helical structure, submonomer synthesis, antibacterial activity.

## Peptoïdes Cationiques Amphiphiles comme Mîmes de Peptides Antibactériens

Les organismes vivants produisent des peptides antimicrobiens (PAMs) pour se protéger contre les microbes. La résistance croissante aux antibiotiques nécessite le développement de nouvelles stratégies thérapeutiques et les PAMs sont des candidats prometteurs pour résoudre ce problème. Ils possèdent une activité à large spectre et leur principal mécanisme d'action par perméation de la membrane engendre peu de phénomènes de résistance. Néanmoins, leur faible biodisponibilité empêche leur utilisation. Certaines limitations peuvent être surmontées en développant des mîmes de PAMs qui conservent leur activité mais avec un potentiel thérapeutique accru. Les peptoïdes (oligomères de *N*-alkylglycine) structurés en hélice cationique amphiphile sont de bons mîmes de PAMs. Les peptoïdes sont plus flexibles que les peptides en raison de l'isomérisation *cis/trans* des amides *N,N*-disubstitués ; cependant la conformation des amides peut être contrôlée par un choix judicieux des chaînes latérales. Le but de cette thèse est d'étudier l'influence de chaînes latérales (hydrophobes ou cationiques) bloquant la conformation des amides en *cis* et induisant une structure hélicoïdale de type PolyProline I (PPI) robuste, sur l'activité antibactérienne et la sélectivité de peptoïdes. La conception, la synthèse et l'étude conformationnelle de nouveaux oligomères peptoïdes cationiques portant des chaînes latérales de type tert-butyle et/ou triazolium ont été réalisées. Dans un premier temps, la synthèse en solution d'oligomères à base de tert-butyle a été développée puis une stratégie de synthèse en phase solide a été mise en place pour accéder aux oligomères à base de 1,2,3-triazolium. Ensuite, ces nouveaux oligomères ont été évalués pour leur activité vis à vis d'un panel de bactéries Gram-positives et Gram-négatives, leur l'activité antibiofilm et leur sélectivité cellulaire. Enfin, pour visualiser les effets des peptoïdes amphiphiles sur les bactéries, une étude de microscopie a été réalisée.

Mots-clés : Peptidomimétiques, peptides antimicrobiens, peptoïdes, 1,2,3-triazolium, hélice amphiphile cationique, synthèse submonomère, activité antibactérienne.